

**Multi-objective Optimal Design and Assessment Framework of Freeform
Timber Structure oriented by Robotic Automation Construction**

Yiping Meng

A thesis submitted in partial fulfilment of the requirements for the degree of
Doctor of Philosophy

The University of Sheffield
Faculty of Social Science
School of Architecture

Submission Date

25/01/2023



The
University
Of
Sheffield.

Multi-objective Optimal Design and Assessment Framework of Freeform Timber Structure oriented by Robotic Automation Construction

Yiping Meng

A thesis submitted in partial fulfilment of the requirements for the degree of
Doctor of Philosophy

The University of Sheffield
Faculty of Social Science
School of Architecture

Submission Date

30/01/2022

Acknowledgements

Throughout the writing of this thesis, I have received a great deal of support and assistance from different people.

First and foremost, I would first like to express my deepest gratitude to my supervisor, Dr. Wen-shao Chang, whose expertise helps me a lot in formulating the research aims and questions. Your valuable feedback always pushed me to reconsider my ways of thinking critically and brought my research to higher level. I could not imagine my progress in conducting independent research without the oversight from you. You gave me enough freedom to conduct my own research and to learn many new skills which I thought I would not get in touch with before my PhD study.

I would particularly like to acknowledge the teammate that I met in Rob|Arch workshop and conference in ETH Zurich. The collaboration and the results helped me to have better understanding for my research and the experience broadened my view of new technology.

I would like to thank our School of Architecture of University of Sheffield. The strong academic atmosphere and the sufficient doctoral trainings help me to strengthen the research skills. The academic seminars held within our apartment let us share our research experience which helped me to learn from others to improve myself continuously. I would also like to thank Dr Luis Hernan, Dr Catalina Mejia Moreno and Dr Emma Cheatle of our department. They gave me chances to become the graduate teaching assistant. These teaching experiences let me share my experience with undergraduate and graduate students which also helped me to enhance the research skills to understand new knowledge.

I would particularly like to thank my current colleagues in Department of Architecture of University of Cambridge. The research experience in this institute helps me to complete my research topics. I would also like to express my thanks to Construction Robotics to accept the paper to give me opportunities to present my research results and to communicate with peers to improve.

In addition, I would like to thank my parents for their unconditional spiritual and material support through my whole PhD research and study. You are always there for me.

I could not have completed this dissertation without the support of my husband Yiming Sun, who provided valuable technical experience and information. He was always being patient to listen to my thoughts and gave me enough confidence to learn much new knowledge to finish the research by myself.

Finally, I would like to express my thanks to our lovely cat Fibonacci. He accompanied us from the pandemic to ease my mind from anxiety and gave me enough distraction to keep me away from my research.

Abstract

Although robotic fabrication has been successfully applied to non-standard geometry structure forms using various materials, there has not been enough research on detailed design guidance for design under the use of robotic arm for construction based on the impact of the technique on design with a higher level of rationality and reliability. And freeform structures are one-of-a-kind, which means that specific working space, tools, and tool paths can only be used for the required design. These are the primary impediments to robotic automation in mass production. As a result, the purpose of this study is to describe the benefits and limitations of robotic timber automation techniques in order to create a comprehensive design system that includes geometry form generation, mesh generation, material, structural performance, modularisation, fabrication, and assessment. Six hypotheses are proposed in this study and will be tested in the following sections.

This study transformed a complex system into a multi-objective optimisation system. The impact factors of robotic automation in fabrication and construction are identified through a review of the literature and the use of the self-organizing maps (SOM) text clustering method to provide reference for the indicators. Fuzzy-Analytic Hierarchy Process (F-AHP) and Fuzzy Comprehensive Evaluation (FCE) methods are chosen based on these factors to determine the weights of these impact factors and to evaluate the impact level of robotic technology on design, fabrication, construction, and management aspects using a Multi-input and Multi-output (MIMO) assessment framework.

Taking the impact factors into consideration, this thesis chooses complex geometry & particle method, biometrics & reverse engineering method, and machine learning method to generate rational and complex geometry forms. Non-Uniform Rational B-Spline (NURBS) are used to extract variables to optimise the strain energy and mass of the structure describe by numerical finite element analysis method. The mesh of the optimal surfaces is generated and optimised in triangular, quadrilateral or hexagon forms to achieve planar and homogeneous grids. After the whole building information model is complete, the working space for the robotic automation construction system would be set, and the initial trajectories for the fabrication tasks would be generated and optimised in operating time and travel distance.

Indicators are selected to build the assessment framework for geometry rationality, structure robustness, automation automaticity, and modular standardisation, information management criteria. 12 plans are put forward by combing different form-finding and mesh modularisation methods. The assessment framework applies the kernel principal component analysis (KPCA) method to determine the weights and grey relation analysis (GRA) together with grey clustering (GC) assess the relations of different indicators on different design plans. In the end, fuzzy c-means clustering (FCM) predicts the level of different plans to support decision making.

The results show the initial geometry forms generated by three design methods are more rational in material aspect. The NURBS geometry models provided detailed geometry information on control points, weight factors to optimise the strain energy and robustness by adjusting the morphology. The structural performance of the structure is remarkably improved while giving more substantial rationality to the freeform surfaces. The optimisation results for robotic trajectory planning show that the travel distance and operating time are shortened significantly to enhance motion control stability and to improve the automaticity of fabrication. The assessment framework for the impact level of robotic automation technique provides quantitative results and the assessment framework for design system performance gives qualitative and quantitative evaluation for the plan decision-making.

The final conclusion section discusses the six hypotheses and summarise the accomplishments and limitations. Following that, further research topics are discussed briefly.

List of contents

Acknowledgements	i
Abstract	ii
List of contents	iv
List of Tables	xii
List of Figures	xiv
Terms	xxiii
List of Abbreviation	xxiv
Declaration	xxvi
Chapter 1	1
Introduction	1
1.1 Research background	1
1.1.1 Digital architecture design	1
1.1.2 Timber as construction material.....	2
1.1.3 Robotics in automation construction.....	4
1.1.4 multi-objective Design and assessment	5
1.2 Research question	5
1.3 Aims and objectives	6
1.4 Hypotheses	7
1.5 Research Content and Focus	8
1.6 Scope and boundary of the research	10
1.7 Structure of this thesis	12
Chapter 2.....	15
State-of-the-Art Review	15
2.1 Design methods for freeform morphology generation and optimisation	15
2.1.1 From Euclidean Geometry to Advanced Geometry	15
2.1.2 Computational Design for freeform surface.....	20
2.1.3 Machine Learning.....	23
2.1.4 Biomimetic Design	25

2.2 Timber as a construction material for freeform structure	27
2.2.1 Typologies of Timber products.....	27
2.2.2 Freeform design concepts for timber structure.....	30
2.2.3 Joints design	31
2.3 Robotic automation for timber freeform structure.....	32
2.3.1 Robotic timber fabrication	33
2.3.2 Robotic automation construction design concepts	37
2.3.3 Robotics technical system related to automation construction	39
2.4 Assessment for freeform structure under RTAC.....	43
2.5 Conclusion.....	44
Chapter 3.....	47
Framework of the Multi-Objective Optimal Design and Assessment System for Freeform Timber Structure (FTS) Oriented by Robotic Automation Construction (RAC)	47
3.1 Theoretical basis and method of RAC-FTS design based on multi-objective dynamic optimisation system	47
3.1.1 multi-objective optimisation problem.....	47
3.1.2 MOO workflow for RAC-FTS.....	49
3.1.3 Dynamic robotic-oriented workflow.....	50
3.2 Non-linear interaction between multiple indicators of the RAC-FTS system.....	52
3.2.1 Multiple indicators.....	52
3.2.2 Nexus between design and material, structure	54
3.2.3 Nexus between material, structure, and RAC	55
3.2.4 Nexus between design and robotic fabrication.....	56
3.3 Multi-objective design and optimisation principles oriented by robotic automation	58
3.3.1 Standardisation and Modularisation.....	58
3.3.2 Automaticity	59
3.3.3 Rationalisation.....	59
3.3.4 Robustness.....	60
3.3.5 Digitalisation	60
3.4 Design strategies of the RAC-FTS.....	60

3.4.1 Comprehensive geometric form evaluation method.....	60
3.4.2 Fitted design of components	61
3.4.3 Highly efficient timber fabrication	61
3.4.4 Smooth Robotic Trajectories	62
3.5 Synergetic methodology for RAC-FTS system	62
3.5.1 Digital design method.....	62
3.5.2 Digital design process.....	62
3.5.3 Building Information Model Platform Environment.....	63
3.5.4 Digital software environment	63
3.6 Assessment and decision-making system of RAC-FTS.....	64
3.6.1 Assessment framework and methodology.....	64
3.6.2 Decision-making Support System.....	66
3.7 Conclusion.....	67
Chapter 4.....	68
Robotic Timber Fabrication-Case Study.....	68
4.1 Robot arm and industrial robot	69
4.1.1 Self-assembly robot and control system.....	69
4.1.2 Examples and questions.....	72
4.2 Robotic timber chainsaw cutting.....	75
4.2.1 Preparation for the geometry and fabrication	76
4.2.2 Information transformation.....	79
4.2.3 Important input information.....	81
4.2.4 Practical Questions	83
4.3 The initial process for robotic fabrication	84
4.3.1 Robot system	85
4.3.2 Workspace setting.....	87
4.3.3 Software platforms and roadmaps.....	91
4.4 The characteristics and Potential of RAC	98
4.4.1 Rationality in performance	99

4.4.2 Complexity in design methodology and of the theory	100
4.4.3 Diversification of design materials	101
4.4.4 Increased efficiency of data exchange	102
4.4.5 New types of fabrication.....	103
4.4.6 Limitations.....	104
4.5 Conclusion.....	106
Chapter 5.....	108
Hierarchy impact model of Robotic-automation Oriented Design System (RAOD).....	108
5.1 Impact factor identification for RAC Impact Model on FTS through Text Clustering	108
5.1.1 Text dataset for Robotic Automation Construction and Freeform Structure	109
5.1.2 Impact factor identification method (Impact factor and output factor analysis) for RAOD	113
5.1.3 Character of impact factor and impact factor analysis system	118
5.2 AHP method to determine the hierarchies and factor weights	120
5.2.1 The principles and characters of AHP	121
5.2.2 The steps for AHP	122
5.3 Multi-level fuzzy comprehensive evaluation model	126
5.3.1 Characteries of Fuzzy comprehensive evaluation	126
5.3.2 Principles of the fuzzy comprehensive evaluation method	127
5.3.3 Steps for the fuzzy comprehensive evaluation method	128
5.4 Fuzzy-AHP evaluation method for impact factor from RAC on FTS design	130
5.4.1 Establishment of Fuzzy-AHP Assessment System	130
5.4.2 Determination of indicator weights.....	133
5.4.3 Impact level of RAC on FTS	136
5.5 Conclusion.....	138
Chapter 6.....	140
Robotic-automation Oriented Design (RAOD) for Initial Freeform Timber Structure Morphology.....	140
6.1 Basic concepts for RAOD for Freeform Timber Morphology (FF-TM)	140
6.1.1 Surface classification	142

6.1.2 Form-find of Morphology of Freeform surface.....	147
6.1.3 RAC-FTS form-finding methods.....	148
6.2 Complex geometry in RAC-FTS morphogenesis	150
6.2.1 Complex geometry together with mathematics.....	150
6.2.2 Minimal surface in RAC-FTS.....	153
6.2.3 Construction feasibility analysis	154
6.3 Biomimetic and construction feasibility analysis	156
6.3.1 The relationship between bionics and freeform biomorphism	156
6.3.2 Reconfiguration Bionics: A bionic design approach combined with reverse engineering	159
6.4 Machine learning form finding and construction feasibility analysis.....	161
6.4.1 LSTM workflow for curve prediction.....	162
6.4.2 Data Transformation.....	164
6.4.3 Train and test	164
6.5 Conclusion.....	167
Chapter 7.....	170
Multi-objectives Optimisation for Morphology of Freeform Timber Structure based on NURBS	170
7.1 Numerical method for structural morphogenesis	170
7.2 Numerical description of the geometry and optimisation.....	172
7.2.1 Basic knowledge of B-spline	172
7.2.2 NURBS curve and surface	174
7.2.3 Determine parameters of NURBS.....	176
7.3 Strain energy evaluation methods for structural rationality.....	177
7.3.1 Strain Energy formulation for grid shell	178
7.3.2 Stiffness matrix for grid thin shell element.....	181
7.3.3 The morphogenesis optimisation method for freeform surface.....	181
7.4 Robustness evaluation for structure rationality	187
7.4.1 Robustness system based on H^∞ theory	187
7.4.2 The morphology optimisation based on robustness	190

7.5 Example of multi-optimisation	191
7.6 Conclusion	198
Chapter 8.....	201
Optimisation for Trajectory and Motion Control to Minimize Travel Length and Operation Time	201
8.1 Process of robotic simulation in Grasshopper	201
8.1.1 The working principle of industrial robotic arms	202
8.1.2 Movement mechanisms of industrial robotic arms	203
8.2 Spatial posture of the robot	203
8.2.1 Spatial description and coordinate system	203
8.2.2 Posture analysis of jointed robots	207
8.2.3 Establishment of the robot coordinate system.....	209
8.2.4 Establishment of the robot coordinate system.....	210
8.2.5 Inverse kinematic solutions	211
8.3 Principle of trajectory planning	213
8.3.1 Trajectory planning in joint space.....	213
8.3.2 Joint space trajectory interpolation	214
8.3.3 End-to-end Cartesian spatial trajectory planning	215
8.4 Singularity avoidance and optimisation algorithms	218
8.4.1 Six-axis robot singularity analysis	218
8.4.2 Jacobi matrix solutions	219
8.4.3 Singularity generation mechanism.....	220
8.5 Optimisation of robotic arms	220
8.6 Algorithm simulation and analysis	222
8.7 Conclusion	229
Chapter 9.....	231
Rationalisation and Modularisation of Freeform Timber Structure Components	231
9.1 Overview of modularity	231
9.1.1 The Theory and Aim of Modularity.....	232
9.1.2 Features of Modularity	234

9.1.3 Analysis of the Applicability of Modularity to FTS.....	235
9.2 Modular FTS Design	237
9.2.1 Characteristics of Modular FTS.....	237
9.2.2 Standardisation of components	238
9.2.3 Modular Mesh Design for FTS	239
9.3 Mesh optimisation methods	243
9.3.1 Geometry optimisation	243
9.3.2 Mesh smoothness optimisation	243
9.3.3 Structure Optimisation	244
9.3.4 Example.....	245
9.4 Evaluation of the quality of modular mesh.....	248
9.4.1 Criteria for evaluation.....	248
9.4.2 Determination of fabrication errors.....	251
9.5 Conclusion.....	255
Chapter 10.....	257
Multi-criteria Assessment and Decision-making Support System for Robotic Automation Construction-Freeform Timber Structure (RAC-FTS).....	257
10.1 Establishment of evaluation systems and decision-making systems	257
10.1.1 Purpose and process of evaluation	258
10.1.2 Choice of evaluation indicators.....	259
10.1.3 Choice of evaluation method	260
10.1.4 Decision Support Systems	261
10.2 Integrated evaluation method modelling	261
10.2.1 Calculation of weights	261
10.2.2 Comprehensive evaluation model.....	262
10.3 Establishment of the evaluation system	263
10.3.1 Establishment of the framework	263
10.3.2 Extraction of evaluation support information	265
10.3.3 Determination of weights based on KPCA	270
10.3.4 Comprehensive evaluation of indicators using grey correlation.....	273

10.4 Decision-making and forecasting systems	275
10.4.1 Prediction systems	275
10.4.2 Rank clustering by FCM.....	278
10.4.3 Decision-making systems	280
10.5 Conclusion	283
Chapter 11	286
Conclusion	286
11.1 Discussion and conclusion for the results	286
11.2 Main Contribution	289
11.2.1 Non-linear design system model.....	289
11.2.2 Software ecosystem for digitalisation of RAC-FTSS.....	290
11.2.3 Architectural Artificial Intelligence for freeform morphology design	290
11.2.4 Standardisation for RAC-FTS.....	291
11.3 Limitations	291
11.4 Further development	292
11.4.1 Dynamic system modelling through digital twin	292
11.4.2 Net Zero Target	293
Appendices-1 Figures	294
Appendices-2 Tables	298
Appendices – 3 Equations	319
Appendices – 4 Publications	321
References	350

List of Tables

Table 4-1 Advantages and Disadvantages of ROS	96
Table 4-2 Comparison between Matlab and Mathematica	97
Table 4-3 Comparison of different software of plugin for robotic simulation and visualisation ...	98
Table 5-1 Summary of rough search details	111
Table 5-2 Risk identification method	114
Table 5-3 Assignment standard of Elements in the Judgement Matrix	123
Table 5-4 Assignment standard of Elements in the Judgement Matrix	123
Table 5-5 Value of R.I with different matrix order	124
Table 5-6 Weight synthesise method.....	126
Table 5-7 Hierarchy Structure between the criterion layer and indicator layer	133
Table 5-8 Judgement Matrix of Criterion $U-U_i$ for Design O_1 (CR=0.0530)	134
Table 5-9 Judgement Matrix of Criterion U_1-U_{1i} for Design O_1 (CR=0.0797)	134
Table 5-10 Judgement Matrix of Criterion U_2-U_{2i} for Design O_1 (CR=0.0768)	134
Table 5-11 Judgement Matrix of Criterion U_3-U_{3i} for Design O_1 (CR=0.0611)	135
Table 5-12 Judgement Matrix of Criterion U_4-U_{4i} for Design O_1 (CR=0.0038)	135
Table 5-13 Weights of the Impact Level Evaluation Indicators.....	135
Table 5-14 Evaluation level assignment	136
Table 5-15 Comprehensive values of impact levels.....	136
Table 10-1 Index framework of an assessment system for RAC-FTS	264
Table 10-2 Extraction methods for qualitative and quantitative indicators - design performance (B1)	265
Table 10-3 Extraction Methods for Qualitative and Quantitative Indicators - Building Information Performance (B_2)	266
Table 10-4 Extraction Methods for Qualitative and Quantitative Indicators - Technical performance (B_3)	267
Table 10-5 Extraction Methods for Qualitative and Quantitative Indicators - Fabrication performance (B_4)	267
Table 10-6 Extraction Methods for Qualitative and Quantitative Indicators - Construction performance (B_5)	268
Table 10-7 Extraction Methods for Qualitative and Quantitative Indicators - Sustainability performance (B6).....	269

Table 10-8 Extraction Methods for Qualitative and Quantitative Indicators - Information transmission (B7)	269
Table 10-9 Values of each evaluation indicator for each design method ($\sigma = 25$).....	271
Table 10-10 Kernel principal component data processing	272
Table 10-11 Matrix of grey relational coefficients	273
Table 10-12 Grey correlation degree	274
Table 10-13 Grey Clustering	275
Table 10-14 Grading of evaluation indicators	279
Table 10-15 FCM Affiliation Matrix	279
Table 10-16 Design plans affiliation	280

List of Figures

Figure 1.1 Example CE certificate.....	3
Figure 1.2 Construction Productivity compared with Manufacturing over time	4
Figure 1.3 The logic for the hypothesis	8
Figure 1.4 Keywords of from Six research fields	9
Figure 1.5 Hierarchy of the research concepts.....	11
Figure 1.6 Research Roadmap for Chapter 4-10.....	13
Figure 1.7 Roadmap of the thesis	14
Figure 2.1 Oriente Station, Lisbon. Santiago Calatrava.....	19
Figure 2.2 German Pavilion by Frei Otto	20
Figure 2.3 Venn diagram for the relations of PD, AD, and GD.....	22
Figure 2.4 Common Raw wood material forms.....	27
Figure 2.5 The macroscopic and microstructure of wood.....	28
Figure 2.6 Industrial process turning log into engineering timber products.....	29
Figure 2.7 Defects of timber products	29
Figure 2.8 Robotic milling	34
Figure 2.9 Multi-task workspace setting.....	35
Figure 2.10 a three-axis CNC saw	36
Figure 2.11 Robotic fabrication setup for timber layer assembly	36
Figure 2.12 Robotic assembly prototype	38
Figure 2.13 Robotic fabricated biometric design.....	38
Figure 2.14 Milestones of industrial robots, 1950s-1970s	40
Figure 2.15 Connection between RAC and FTS.....	46
Figure 2.16 Concept map between the principles of robotics and freeform structure	46
Figure 3.1 Information transformation in MOO for RAC-FTS	50
Figure 3.2 Dynamic loop within the workflow.....	51
Figure 3.3 Multi-objective robotic oriented model.....	51
Figure 3.4 Workflow of dynamic MOO for RAC-FTS.....	52
Figure 3.5 Concept map of RAC-FTS	53

Figure 3.6 Interaction between different indicators	57
Figure 3.7 Computational digital design system.....	63
Figure 3.8 Software for data transformation	65
Figure 3.9 Function of Assessment.....	66
Figure 4.1 Roadmap for Chapter 4	68
Figure 4.2The layout of Arduino IDE	69
Figure 4.3 One example of Arduino program.....	69
Figure 4.4 Essential kits for operating the robot	70
Figure 4.5 Control the servomotor through Arduino	70
Figure 4.6 A four-axis robot arm.....	71
Figure 4.7 A six-axis robot arm.....	71
Figure 4.8 Three servo motors connect to the Arduino board.....	71
Figure 4.9 Simple connection of the control board and 4-DOF robot arm.....	71
Figure 4.10 Schematic of the Arduino board to control the robot by buttons	72
Figure 4.11 Circular movement of single joint movement	72
Figure 4.12 Simplified two-link model shown in two-dimension.....	73
Figure 4.13 Reachable space of the two-link robot.....	73
Figure 4.14 o-xy Coordinate for the robot arm.....	73
Figure 4.15 Two-link model built in processing	74
Figure 4.16 Diagram for 3D two-link robot arm.....	74
Figure 4.17 Steps for controlling the robot to move from a to b.....	75
Figure 4.18 Robotic Chainsaw cutting working space.....	75
Figure 4.19 Wood joint cutting by the robotic chainsaw from the log.....	76
Figure 4.20 Views for working space organization	77
Figure 4.21 Coordinate systems of the working space.....	77
Figure 4.22 8-point calibration	78
Figure 4.23 Orientation of the tool coordinate system.....	78
Figure 4.24 Calibrated system for working space.....	79
Figure 4.25 Views for 3D scanning using robot	80

Figure 4.26 3D scan results	80
Figure 4.27 Design and modelling of the joinery	81
Figure 4.28 the tool path of the robot arm within one cutting surface	81
Figure 4.29 Cutting surface set for the timber fabrication	82
Figure 4.30 positions of cutting points	83
Figure 4.31 Singularity of robot arm when operating	83
Figure 4.32 Software of robot simulation and visualisation.....	85
Figure 4.33 industrial robot and controller	86
Figure 4.34 Example of subroutine language for robot control	87
Figure 4.35 Different workspace setting.....	89
Figure 4.36 Robotic working space setting for welding process.....	89
Figure 4.37 Robotic working space setting for cutting process	89
Figure 4.38 References of robotic mechanism.....	90
Figure 4.39 References of robotic mechanism.....	90
Figure 4.40 The setting for a synchronized process.....	91
Figure 4.41 A synchronized welding process	91
Figure 4.42 KUKA robot types supported in KUKA prc	93
Figure 4.43 Robot models supported by HAL.....	93
Figure 4.44 Controller options.....	93
Figure 4.45 Controller configuration	93
Figure 4.46 Solve component of KUKA prc.....	94
Figure 4.47 Solve component of HAL.....	94
Figure 4.48 Main components for KUKA prc solver.....	94
Figure 4.49 Main components for HAL solver.....	95
Figure 4.50 Part of execution of the process.....	96
Figure 4.51 ROS Operating System	97
Figure 4.52 Structural form find and translation.....	100
Figure 4.53 MOCAPE Museum	101
Figure 4.54 Sewing the connections between components	102

Figure 4.55 Lightweight, Long Span Fibrous Construction.....	104
Figure 4.56 Connection to Hypothesis	106
Figure 4.57 Connection with other chapters	107
Figure 5.1 Roadmap for Chapter 5	108
Figure 5.2 RAOD system composed by Input, output, and impact.....	109
Figure 5.3 Text Clustering Process.....	110
Figure 5.4 Level of literature research.....	110
Figure 5.5 Example of Original Text Dataset	112
Figure 5.6 Example of Cleaned Text Dataset	112
Figure 5.7 Bilinear chart for the count of the research areas and categories	113
Figure 5.8 RAOD for RAC-FTS design system	114
Figure 5.9 A two-dimensional model	116
Figure 5.10 The process of SOM cluster	117
Figure 5.11 Keywords cluster.....	119
Figure 5.12 Hierarchy Chart.....	122
Figure 5.13 Fuzzy-AHP Assessment Process	131
Figure 5.14 Multiple input multiple output assessment model	132
Figure 5.15 Hierarchy Structure between the goal layer and criterion layer of MIMO.....	132
Figure 5.16 Distribution of manipulated data	134
Figure 5.17 Connection to the Hypothesis.....	138
Figure 5.18 Connection to other chapters	139
Figure 6.1 Roadmap for Chapter 6	140
Figure 6.2 Structure and fabrication involved in different stage of design	141
Figure 6.3 Swiss Insurance Headquarters Building with the prototype of the revolving surface	142
Figure 6.4 The Japan Pavilion at the Hannover Expo.....	143
Figure 6.5 Generation of ruled surfaces.....	143
Figure 6.6 Hyperbolic paraboloid construction	143
Figure 6.7 YSIOS Brewery	144
Figure 6.8 Walt Disney Concert Hall in Los Angeles.....	144

Figure 6.9 Serpentine Gallery in London	145
Figure 6.10 Planar free grid spatial structure	145
Figure 6.11 The roof of British Museum	146
Figure 6.12 The roof of Yas Island of Abu Dhabi	146
Figure 6.13 The spatial structure of Water Cube	146
Figure 6.14 The spatial structure of Federation Square	146
Figure 6.15 British Pavilion at Milan Expo	146
Figure 6.16 Centre Pompidou Metz.....	147
Figure 6.17 Nine Bridges Golf Club.....	147
Figure 6.18 Radiolarian project of Christian Troche	151
Figure 6.19 5000 steps of Chaos Game of different shapes	151
Figure 6.20 Egypt Museum	152
Figure 6.21 Danmark Pavilion Shanghai Expo.....	152
Figure 6.22 Origami Pavilion	153
Figure 6.23 Minimal surface example	154
Figure 6.24 Radius of Osculating circle and curvature of curve	155
Figure 6.25 Curvature of surface	155
Figure 6.26 continuity of curved surfaces.....	156
Figure 6.27 Fuller Molecular Structure and American Pavilion	157
Figure 6.28 Honeycomb Speculation.....	158
Figure 6.29 Process of reverse engineering	159
Figure 6.30 Biometrics with reverse engineering	159
Figure 6.31 Original surface and point cloud	160
Figure 6.32 Point cloud mapping.....	160
Figure 6.33 Generative Design Process	161
Figure 6.34 Fitted new surface	161
Figure 6.35 Classification and Regression of ML	162
Figure 6.36 Workflow of the LSTM prediction for Curve of Freeform Surface	163
Figure 6.37 Centre Pompidou-Metz	163

Figure 6.38 Geometric Model	164
Figure 6.39 Geometric information for the model	164
Figure 6.40 Process to transfer geometric data into sequential data.....	165
Figure 6.41 Learning and Prediction Process for LSTM	166
Figure 6.42 Training results with 21 points	166
Figure 6.43 Test results with 21 points	166
Figure 6.44 Histogram of the MSE of the prediction.....	167
Figure 6.45 Comparison of the generated curve and the tested curve	168
Figure 6.46 Connection to hypothesis	169
Figure 6.47 Connection to other chapters	169
Figure 7.1 Roadmap for Chapter 7	170
Figure 7.2 Formation of cubic B-spline.....	173
Figure 7.3 Example of NURBS Surface	174
Figure 7.4 NURBS curve and surface with control points	176
Figure 7.5 plate shell element.....	179
Figure 7.6 Element stiff matrix for thin shell element	181
Figure 7.7 Flow chart of structural morphology using gradient decent for strain energy.....	186
Figure 7.8 Example surface	191
Figure 7.9 Optimisation results compared with the original values	192
Figure 7.10 Geometry comparison of evolution steps	193
Figure 7.11 Displacement of original morphology	193
Figure 7.12 Displacement of 60-step evolution	194
Figure 7.13 The utilisation of original morphology	195
Figure 7.14 The utilisation of 60-step evolution.....	195
Figure 7.15 the principal stress of the original morphology	196
Figure 7.16 The principal stress of 60-step evolution.....	197
Figure 7.17 The second principal stress of the original morphology	197
Figure 7.18 The second principal stress of 60-step evolution	198
Figure 7.19 Connection to the hypothesis.....	199

Figure 7.20 Connection to other chapters	200
Figure 8.1 Roadmap for Chapter 8	201
Figure 8.2 The motion of the robot arm.....	202
Figure 8.3 The visualisation of the simulation process	202
Figure 8.4 The kinematic chain of a robot arm.....	203
Figure 8.5 the translational transformation	205
Figure 8.6 the rotation transformation	205
Figure 8.7 The position of Point P and two coordinate system.....	205
Figure 8.8 The position of point P, three coordinate systems	206
Figure 8.9 Rotation transformation for two coordinate systems	207
Figure 8.10 Schematic diagram of space link (Craig, 2009).....	208
Figure 8.11 Joint linkage of two axes (Craig, 2009).....	209
Figure 8.12 The D-H coordinate system of the linkage (Craig, 2009).....	210
Figure 8.13 Space linear interpolation	216
Figure 8.14 Three-point arc	217
Figure 8.15 Circular interpolation	217
Figure 8.16 Singularity locations of the robot arm	219
Figure 8.17 Kinematic singularities.....	222
Figure 8.18 KUKA KR-90 Robotic arm model.....	224
Figure 8.19 Tool path from Rhino.....	224
Figure 8.20 Tool path in Matlab	224
Figure 8.21 Working space limits.....	225
Figure 8.22 Modified PSO model for path planning.....	225
Figure 8.23 Trajectories of 66 tool paths.....	226
Figure 8.24 The initial tool path and the optimised tool path	226
Figure 8.25 The optimised travel distance	227
Figure 8.26 Initial trajectories and optimised trajectories of six-joints	227
Figure 8.27 The evolution results of AGA of six joints of four tool paths.....	228
Figure 8.28 Fitness value after 100 generation	228

Figure 8.29 Time value after 100 generation	228
Figure 8.30 Comparisons between the original and the optimal value for time and distance.....	229
Figure 8.31 Connection to Hypothesis	230
Figure 8.32 Connection to other chapters	230
Figure 9.1 Roadmap for Chapter 9	231
Figure 9.2 Research concept of chapter 9	232
Figure 9.3 Modularisation of freeform structure.....	233
Figure 9.4 Comparison between modular design and conventional forward design	239
Figure 9.5 Mapping	241
Figure 9.6 Process of AFT.....	242
Figure 9.7 Delaunay triangle and Voronoi	242
Figure 9.8 The merging and splitting of mesh	243
Figure 9.9 Interchange of edges.....	243
Figure 9.10 The mesh optimisation at half-volcano position	244
Figure 9.11 Quad mesh for minimal surface.....	245
Figure 9.12 Point deviation between the mesh and the fitted surface of first optimisation	246
Figure 9.13 Point deviation between the mesh and fitted surface of second optimisation	246
Figure 9.14The comparison between two optimisations	247
Figure 9.15 Planarity of different panels	247
Figure 9.16 Triangular mesh	250
Figure 9.17 Quadrilateral mesh	250
Figure 9.18 Optimisation for quad and triangular mesh	251
Figure 9.19 The fabrication error of the fabricated surface.....	252
Figure 9.20 Process of Rebuild of the NURBS surface	252
Figure 9.21 The shortest distance between point and surface	253
Figure 9.22 Error measurement	254
Figure 9.23 Symbols for tolerance control	254
Figure 9.24 Connection to Hypothesis	255
Figure 9.25 Connection to other chapters	256

Figure 10.1 Roadmap of Chapter 10.....	257
Figure 10.2 The evaluation and decision-making system	258
Figure 10.3 Indicators of technology within sustainability	264
Figure 10.4 Indicators for flexibility for BIM.....	264
Figure 10.5 Example for Plan 7	271
Figure 10.6 Example for Plan 8.....	271
Figure 10.7 Norm fit of first three rows.....	272
Figure 10.8 The contribution rate of the eigenvalues.....	273
Figure 10.9 Grey correlation degree	274
Figure 10.10 Pedigree chart of grey clustering	275
Figure 10.11 Workflow of FCM.....	276
Figure 10.12 Iterations of the objective function	279
Figure 10.13 Affiliation of FCM	280
Figure 10.14 Three-layer DSS system	281
Figure 10.15 Multi-agent Decision Support System	283
Figure 10.16 Agent-based Collaborative Design Decision-making Workflow	284
Figure 10.17 Connection to other chapters	285
Figure 11.1 Product life cycle stages	289
Figure 11.2 Further step on system modelling.....	292
Figure 11.3 ‘Bathtub Curve ‘Hazard function	293

Terms

Chapter 1

MMC: Modern Methods of Construction is a range of approaches which spans off-site, near site and on-site pre-manufacturing, process improvements and technology applications. The framework of MMC is divided into 7 categories for both structural, and non-structural systems for different building

Chapter 2

Raw material: Raw wood materials are made from forest trees, including hardwood and softwood, e.g., pine compared to processed engineering timber products like Glulam Timber (GLT). Raw wood materials consist of chunks or logs which are ready for further processing for industrial products. The qualities of raw wood materials vary depending on different physical, chemical and mechanical properties.

Chapter 6

Curvature: a measurement that indicates how curved a geometry is, such as the deviation of a curved surface from a plane or the deviation of a curve from a straight line. The precise definition of curvature differs between fields of geometry. Curvature is classified as either extrinsic or intrinsic, with significant differences between the two. The former requires the geometry to be embedded in Euclidean space, whereas the latter is defined directly on the Riemannian manifold.

Ruled Surface: In geometry, a surface is said to be ruled if there is at least one straight line passing through it at any point on the surface. Another common expression is that a surface is said to be a straight surface if it can be formed by a straight line passing through continuous motion. The famous Möbius ring is a ruled surface.

Chapter 8

Kinematics: Kinematics is a branch of mechanics that specialises in describing the movement of objects, i.e., the change in position of an object in space as it evolves in time, without regard to factors such as forces or masses that affect movement.

List of Abbreviation

Chapter 1

CNC: computer numerical control

MMC: Modern Methods of Construction

RAC-FTS: Robotic Automation Construction for Freeform Timber Structure

Chapter 2

RAC: Robotic Automation Construction

RTA: Robotic timber automation construction

RAC-FTS: Robotic Automation Construction for Freeform Timber Structure

FCE: Fuzzy Comprehensive Evaluation

RAOD: Robotic-automation Oriented Design

RA: Robotic automation

Chapter 3

MOO: Multi-Objective Optimisation

POS: Pareto optimal solution

MOP: multi-objective optimisation problem

Chapter 4

IDE: integrated development environment

TCP: tool centre point

DOF: Degree of freedom

KRL: KUKA ROBOTLANGUAGE

Chapter 5

PCA: principal component analysis

C.I: consistency index

R.I: random index

C.R: consistency ratio

FTA: Fault Tree Analysis

WBS: Work Breakdown Structure

IFA: impact factor analysis

SRA: Systematic review analysis

MIMO: multiple input multiple output

SOM: self-organizing maps

VSM: vector space model

WOS: Web of science

FCE: Fuzzy comprehensive evaluation

MCS: Monte Carlo simulation method

Chapter 9

FE: fabrication error

GTS: Geometric Tolerancing Symbols

Chapter 10

GRA: Grey relation analysis

GC: Grey clustering

KPCA: Kernal principal component analysis

FCM: Fuzzy c-means evaluation method

DSS: Decision support system

Chapter 11

SDG: Sustainability development goals

Declaration

I, the author, confirm that the Thesis is my own work. I am aware of the University's Guidance on the Use of Unfair Means (www.sheffield.ac.uk/ssid/unfair-means). This work has not previously been presented for an award at this, or any other, university.

Chapter 1

Introduction

This thesis begins with the assertion that future design is digitalisation, and the automation techniques are applied to construction industry to improve the working efficiency, reducing the energy and material waste and management. More and more complex forms appeared in the current construction industry, followed by new design and construction concepts, for example, digital design, parametric design, algorithm and script design, generative design, and computer numerical control (CNC). For the new digital design, new manufacturing methods are needed to control the fabrication and construction process better to ensure its accuracy and constructability to reduce the deviation between the design and the fabricated (or constructed) products.

Automation construction is one technique that could meet the demands of digital construction, widely used since the 1960s, and in recent years, automation construction has been redeveloped based on CAD, CAM, and BIM techniques. The robotic construction technique is one of these applied in architecture fields. The robotic technique could combine design, fabrication, and construction to make the construction process visible. Thus, robotic has better potential in non-linear structure compared with CNC. Furthermore, the demands for the variety of architecture design have grown, and robotic could fully satisfy the freeform shape fabrication and construction to fulfil it.

As the design and fabrication techniques are combined in this research, the technique could bring different demands for the design, from material, shape form, to joint design. So, this research tries to figure out what form of the shape and joints would fit? Moreover, how to assess structure from design, structure behaviour, fabrication efficiency, three perspectives quantitatively?

This chapter sets out the research background and motivation for this thesis. Secondly, the research questions are introduced. Thirdly, the aims and objectives are put forward. Finally, the research methods are described, and the structure of the thesis is presented.

1.1 Research background

1.1.1 Digital architecture design

The current standard form of architecture could not meet the variety of demands of human aesthetic needs. Non-standard and freeform architecture becomes more and more acceptable. Under the advancement of computer science and technology, the development of construction technology and the improvement of architectural aesthetics, especially since the beginning of the 21st century, freeform surface structures have increasingly appeared in people's vision with their creative shapes. Different form-finding measures are taken to achieve the geometry space forms different from the traditional Euclid ones like the digital design. Digital design means developing computer-aided design (CAD) techniques based on digital theory, taking the dataset, computer graphics, visual reality as main techniques, dealing with two or three-dimensional image processing to build geometry models. Digital

architecture design is the application of digital design, including parametric design, algorithm design, building information models. Digital architecture design is a valuable design tool, including the geometry information needed in later fabrication and construction processes. Also, the geometry model is easy to adjust the form by controlling geometry parameters to meet the demands of users. With the help of the designing tools like Rhino or Revit, the space form becomes more complex and extensive.

Compared with the spatial structure of traditional architecture, the freeform surface grid structure has smoother lines, more various shape, which can better express the meaning of the building and is favoured by many architects. However, it is easy to build the model in software. To achieve this kind of spatial form would confront some main challenges: logical rationality, material, structure form and construction methods. One of the main challenges is that current digital design cares more about form or morphology if more precise than the restrictions of material, structure form optimisation, and standardization of components, so the information of these factors is neglected from the beginning of the design. The other problem is the gap between the geometry model and the technique used in construction, which means that in some cases, traditional approaches are used to build complex non-linear structures and may cause imperfection or deviation from the initial design.

If following the life cycle stages of construction product, including construction process, operation and end-of-life stages, (Buyle, Braet, & Audenaert, 2013) to achieve the constructability and extend the life span of digital design, the following requirements needs to be meet.

- (a) constructability: This means that the design can be achieved by current existed manufacturing (including fabrication and construction) methods;
- (b) rational: This means that the design results need to be rational either following the restriction of the material of the structural behaviours;
- (c) robust: This means that the design results need robustness in both structure and the manufacturing process;

To meet the mentioned requirements, there is knowledge gap between the rational design and the material or structural or manufacturing methods, which would be discussed in the following chapters.

1.1.2 Timber as construction material

Timber is an ancient kind of material that has been used for an extended period. Based on the attention paid to sustainable environmental design, timber is a perfect building material to meet the measurements for environmental construction efficiency. Compared with other traditional building materials like bricks, steel, or concrete, the lower the energy consumption to produce raw material, the lower carbon dioxide impact from construction, the higher level of reusing the material and degradable properties make the timber a potential material to be used more widely. Especially when the logging and utilization of timber enter a virtuous cycle, advantages of environmental protection will become more and more prominent to avoid the waste of resources and environmental deterioration.

However, there are some disadvantages like becoming rotted quickly, wood nodes, cracking, and deformation hampered the natural timber to be widely used in the construction industry, which would cause uneven strength of mechanics of material. The significant components from raw material are hard to get restricted to the cross-sectional area of trunks from natural growth. Correspondingly, the raw material of timber has limited usage in construction, only used on a small scale. Large-scale standardised production could produce standard engineered timber products, like glulam or wood composites. When these industrial products could avoid the disadvantages mentioned to have enough durability, then engineering timber could be applied in various architectural designs.

Besides, glulam breaks through the size limit of natural logs and can be made into large-scale structural sections according to actual needs. Moreover, in terms of shape, glulam is not limited by the cross-sectional form and can not only be moulded into various cross-sectional shapes such as rectangles and cones. It can also form various arches, shells, and other curvilinear architectural components, which provides a greater degree of freedom in shapes. Accordingly, using timber in large-scale public space has become cutting-edge research, construction, and design.

Many pavilions or large span roof practices using timber have been put into these years. These practices showed good examples in exploring the workflow of combining digital architecture design as new design methods, using a new type of engineering timber products, and taking new construction methods. However, the connections between each part of the workflow are neglected; that is to say, to complete a curvilinear timber architecture, the relationship between design tools, structure form, connection type and final fabrication process need to identify. The method to make the typology fit the properties of the material, choose connection types to get the stable structure, and the design of the components limited by fabrication tools need further and more detailed discussion. There are some standards for engineering timber to assess the strength to be applied in different construction scenarios. For example, for the softwood supply chain in Europe, “CE” is one required product label following different standards including EN 14081, EN 14080, EN 14915 and EN 15497.



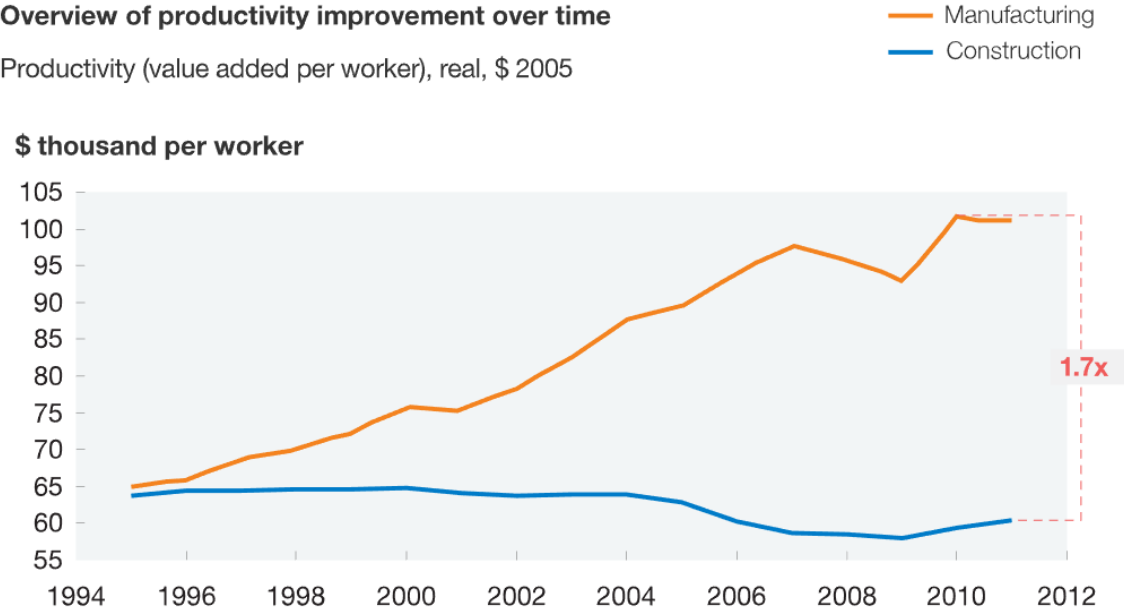
Source: Wood grades - Swedish <https://www.swedishwood.com/wood-facts/about-wood/wood-grades/Wood>
 Figure 1.1 Example CE certificate

In Figure 1.1 of CE, it presented the name of the producer (ABC Trä AB X), sorting class (T2) and standards (SS 230120 in Sweden) and strength class (C24). The certificate provides material transparency for the engineering timber products.

1.1.3 Robotics in automation construction

Efficiency is highly valued to achieve production sustainability and economic growth. However, as the productivity of the whole industry grew, especially for the manufacturing industry, the construction industry's productivity has declined in recent years (Figure 1.2). Conventional construction is a complicated system involving a variety of products, diversity of dimensions and compound construction sites so that traditional technique has reached its performance limits due to the material waste, overrunning cost and non-environmental sustainability. Under the notion of "Industry 4.0" called for a highly automated, autonomous, flexible manufacturing system, some universities and governmental institutions try to explore new construction processes and techniques, which could be summarized as "automation construction". The new automation construction technology like computer numerical control (CNC), 3d print, laser scanning and robot system promotes the efficiency of production and, at the same time, facilitate the freedom of architecture design.

The new automation construction technology could increase productivity and bring breakthroughs to the non-linear space form of architecture. The digital architecture design is combined closely with the construction techniques, which means the intricate design relies on the techniques fabricated to numerous shapes and various built-in sites. Moreover, correspondingly, along with all the geometry information in the whole fabrication and construction process, the design could be more complex or use new materials without being confined to the common practice.



Source: Expert Interview; HIS Global Insight (Belgium, France, Germany, Italy, Spain, United Kingdom, United States); World Input-Output Database
 Figure 1.2 Construction Productivity compared with Manufacturing over time

Robotic arms with multiple tool heads are one fitted choice to complete gripping, drilling, milling, cutting, or 3d printing. Also, compared with other automatic techniques like CNC, the flexibility of robotic arm to be used in on-site or off-site tasks, working in three-dimensional space, cooperation between different robotic arms, the direct translation from geometry information to fabrication and construction process make robotic arm appropriate for the non-linear design especially.

Under the more and more practices using robotic arms to build non-linear structures, the limitation of the tools and the impact on design need to be defined explicitly despite the advantages of robotic arms. Also, the discussion about optimisation of control of robotic arms in performing the tasks is not highly paid attention to. The theory of robotics has developed in the engineering area, and in the architecture area, the robotic arm is used as a tool, and more systematic knowledge about it need to be introduced to digital design and automation construction.

1.1.4 multi-objective Design and assessment

To date, the evaluation of most architecture designs is qualitative or objective. For large scale adoption of any new construction techniques, subjective and detailed performance, operation, and management assessment are needed. A qualitative assessment is not enough, especially for the advanced digital architecture robotic automation (DARC), focused on large-scale applications. For example, some digital architecture designs on a small scale could be finished by traditional fabrication method using raw material and by building it through manual work, where the inaccuracy would not lead to failure. However, on a large scale, the quantitative assessment is needed to give the DARC an exhaustive evaluation from multi-discipline to have systematic guidance to enhance performance and prevent DARC failure.

As robotic construction is expensive and not replaceable in the construction industry, some experts explained the superiority of sustainability in adopting robotics in construction compared to traditional construction techniques. So, there are some investigate of the impacts of using construction automation and robotics in the context of sustainability performance (M. Pan, Linner, Pan, Cheng, & Bock, 2018b). Moreover, most of the research scopes are bounded to building construction sustainability or life-cycle assessment on the energy of prefabrication (Hong, Shen, Mao, Li, & Li, 2016). To fully access the technical capabilities of the DARC, a completely new workflow assessment needs to be built to ameliorate the current building assessment system that is to allow experts from different research backgrounds (design, material, structure, robotics), who evaluate the whole process from their concepts, to compare their criteria to come to a definitive evaluation conclusion.

1.2 Research question

To summarize, one trend for robotics automation today is to complete the digital architecture design on a large scale. Some practices have already explored the workflow to combine design, structure, and construction; some focused on the construction-oriented design, some on the enforcement of material, and some on the development of tool heads of robotic arms, which will be discussed in detail within Chapter 2. These practices are completed based on introducing the new technique to traditional

construction and are succeeded in finishing the non-linear building tasks instead of manual work. Inside the architecture design and construction field, there remains a crucial knowledge gap in structure behaviour and robotics motion control. Therefore, an appropriate explanation for the logical rationality for the design form and structure system and optimisation for the robotic arm should be considered by applying the comprehensive quantitative assessment system.

To build the workflow to transfer the information among different stage (space form design, structure optimisation, robotic fabrication, and construction) and to have an overall assessment, this study put forward the research questions:

- (1) How should a design model system be reformed for robotic-oriented design?
 - What are the system's guiding principles?
 - What are the workflow's strategies?
 - How can data from different disciplines be used synergistically?
- (2) How can the system be evaluated to help make decisions? How can the impact of robotic techniques on design be quantified?
 - What are the criteria and what factors having an impact?
 - What methods are used to assess the level of impact?
- (3) How can the best design for a freeform timber structure be achieved while taking material, structure, and fabrication methods into account?
 - How to improve the conventional methods to achieve the robotic-oriented design for freeform timber structure?
 - How to optimise the structural morphology including the parameters selection, algorithms, and restrictions?
 - How to generate and optimise the mesh of freeform surface considering the robotic technique?
- (4) How to achieve the automaticity level of robotic automation in freeform timber structure?
 - What is the combination of a robotic automation system?
 - What are the principles of controlling the robotic procedure for fabrication?
 - How to improve the stability and efficiency of robotic automation?

1.3 Aims and objectives

The aim of this thesis is to develop appropriate design and optimal methodology and assessment framework for freeform structure with complex geometry taking the robotic automation construction technique as the main driven factor and timber as the material restriction to achieve rationality, reliability, automaticity to meet the objectives of digitalisation, standardisation as sustainable national goals¹. Robotic fabrication has been successfully applied to non-standard geometry structure form using various materials, but to date, no further research on the impact of the technique on design. For this reason, this research aims at describing the advantages and limitations of robotic timber fabrication to develop a comprehensive design system including geometry form generation, mesh generation,

¹ The goals are emphasised in Green Book- Central Government Guidance on Appraisal and Evaluation (2022).

structural performance, materialisation with building information, modularisation, and fabrication planning. The whole workflow would be assessed by a multi-criteria framework and a decision-making support system would be developed.

The lack of knowledge of systematic guidance and appropriate starting points for different stages of the whole process from design, structure to robotic construction is the main obstacle. Therefore, the main aim of the study is to investigate the four main aspects of the whole system and to establish a quantitative assessment for the performance of the whole process.

This aim is satisfied through the following key objectives:

- (1) Develop the principals, strategies and framework for the conceptual multi-objective optimal design and assessment methodology and workflow. Determine a multi-criteria assessment framework for the “design-construction” systems to evaluate the plan quantitatively for different stakeholders to support decision-making.
- (2) Operate text data analysis to determine the main impact factors. Choose the criteria for impact factors of robotic system to build an impact model and evaluate the impact level of robotic automation technique in complex design system using qualitative and quantitative methods.
- (3) Develop appropriate methodologies for generating the morphology for freeform timber structure based on cutting edge morphology design methods. Determine the parameters and objectives for structural morphology optimisation. Choose the appropriate methods for meshing the freeform surface to obtain the standardised components for industrialisation and materialisation with planar or linear engineering timber products.
- (4) Determine the step to build a robotic automation construction system including hardware and software. Develop the workflow to simulate the construction process to generate tool path. Optimise the tool path from optimise motion control and trajectory planning perspective by determining the optimisation objectives, variables, restrictions to get smooth trajectories and time saving tool path to achieve the goal of energy efficiency, time efficiency and productivity.

1.4 Hypotheses

Because of the anisotropy of a timber product's mechanical properties, it can be used as a compressive material. If the freeform structure is composed by timber as the main building material, apart from the foundation and connections, and if the main off-site prefabrication and on-site procedures like assembly, scanning, etc are operated by robotic arm, then there are some limitations from the tools and the materials themselves posed to the whole process from design to construction. To be more specific, the application of robotic arm in construction industry needs the development for the tools, e.g., sewing machine mounted on robotic arm. There are new types of engineering timber products with higher strength and curved shapes. Still, timber cannot be made into products with any shapes like concrete under the process like 3D printing. Based on the characteristics and limitations of robotic automation construction technique and engineering timber products, the research comes with the following hypothesis:

- (1) Non-standard freeform structure can be composed by regular and standard timber components which are in planar or linear shape.
- (2) The standard timber structure components (linear & planar) can be prefabricated by simple robotic fabrication tasks like cutting with no need to develop or design new tools mounted on the robotic arm;
- (3) The standard structure components can be achieved by appropriate design and optimisation methods to achieve high level of standardisation.
- (4) Robotic Automation Construction (RAC) would have impact on freeform surface design and optimisation methods to achieve:
 - a. **Structure Rationality:** The shape of freeform surface has structure stability and stiffness.
 - b. **Material Rationality:** The design of freeform surface can be materialised by using timber as main building material.
 - c. **Fabrication Rationality:** The components of the optimal design can be fabricated within the working space limits of robotic arm.
- (5) For each freeform structure component, the corresponding robotic tool path can be generated automatically following the restrictions of simple robotic fabrication operations.
- (6) The tool path can be optimised through trajectory and motion control optimisation to achieve higher level of automaticity without singularities, higher productivity and time efficiency.

These hypotheses are in progressive relationship which means each depending on others (Figure 1.3). For example, if selecting cutting as the main fabrication process, then the form of the products would be the planar ones. Based on this premise, the design and optimisation method for the freeform surface need to be easy to be planarization. Then the generation and optimisation for the tool path and motion control would be taken out afterwards.

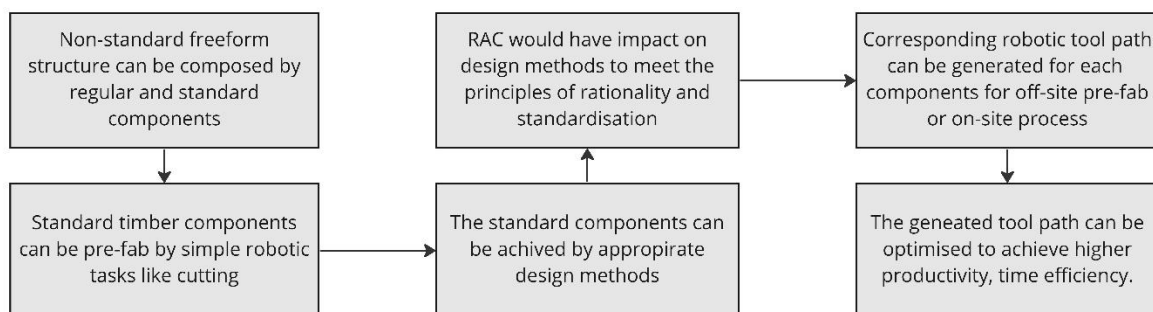


Figure 1.3 The logic for the hypothesis

1.5 Research Content and Focus

Based on the hypothesis, the research would be taken from four main aspects: geometry design methods, structure analysis, materialisation and component standardisation, and robotic simulation; and three main steps: design, optimisation and assessment. To figure out the main research packages with different activities and the corresponding research content, the key words for the six main fields are listed to sort out the connections between different research fields. In Figure 1.4, there are six main fields, one composite system as “Robotic Automation Construction” (RAC) and one material type "Timber". The

"Automation construction" is one technique within the context of Industry 4.0 which provides the guidelines for RAC and principles for optimisation with different objectives. "Robotics" is a discipline works on computer science and engineering. This interdisciplinary branch can provide technical knowledge on construction industry. There are three main steps to have a freeform structure which are morphology generation and optimisation, mesh generation and mesh optimisation for homogenisation. To operate the optimisation process, objective determination, parameters selection, restriction definition and appropriate algorithms are the main procedures. The current widely used design methods for freeform surface can provide rationality for freeform morphology generation. "Timber" works as a material selection premise to freeform structure and puts constraints on design methods as timber cannot be manufactured into products with any shapes. Besides, "Timber" impacts the fabrication tool selection e.g., 3D printing is not applicable for RAC for timber products.

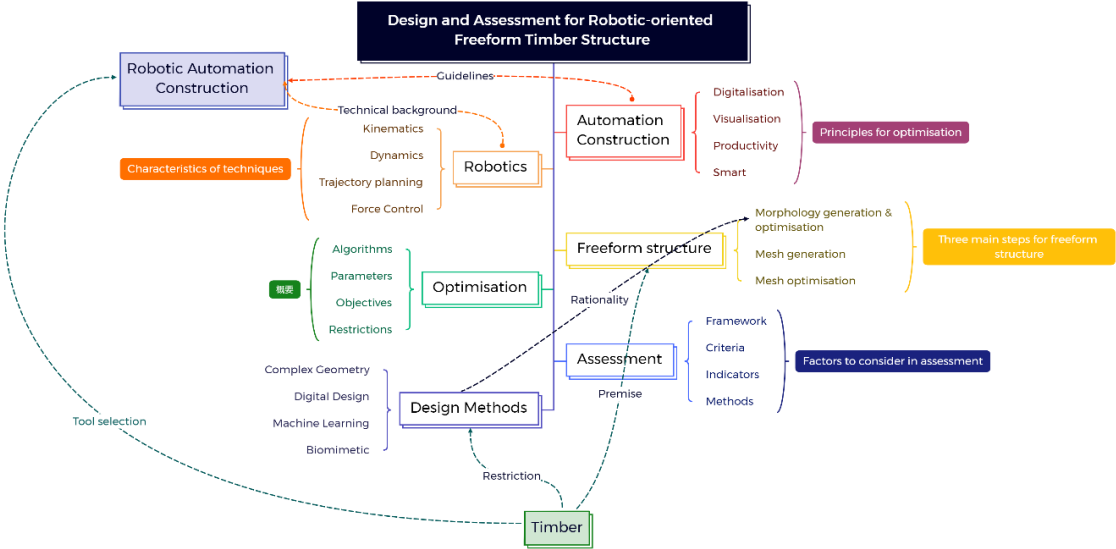


Figure 1.4 Keywords of from Six research fields

After listing the relevant keywords from different research fields or disciplines, the next step is to rearrange these keywords to classify the hierarchy of these words, shown in Figure 1.5. The keywords are organised into three main hierarchies: basic concepts, developed concepts and main parts. Construction, material and design are the three main keywords for the basic concepts as robotic automation construction is the trend for construction industry development; application and market growth of engineering timber products gives more opportunities for timber structure with more complex and non-standard form; digital design is the way to achieve the rational geometry design and to generate digital information to connect all different parts together. In more details, the three main concepts are narrowed down into six main fields: *Robotics*, *Freeform Geometry*, *Timber*, *Fabrication*, *Component*, and *Assessment*. To have a comprehensive understanding for the freeform timber structure and robotic automation construction, the up-to-date knowledge or research results from these field are essential to find the appropriate starting point to connect multi-discipline to establish the system containing design, optimisation and assessment. Then the main parts to fulfil the objectives of the whole research are developed to meet the research aim and to test the research hypothesis.

- (1) **Framework of dynamic RAC-FTS design system.** A dynamic framework with interactions between different research contents would be developed by putting forward principles and strategies.
- (2) **Robotic Automation Construction system.** To identify the essential parts to establish a automation construction system using robotic as the main driven factors including both hardware arrangement and software platform for information exchange.
- (3) **Impact level model of RAC for construction industry.** Whether robotic as a new construction technique has impacts on the geometry design and optimisation would be analysed by establishing an impact level assessment framework to operate quantitative analysis.
- (4) **Morphology design methods development.** Consider the principles and strategies of the overall framework to define the characteristics for appropriate methods. Develop the appropriate morphology design methods considering robotic technique and timber as the main constraints to achieve rational design based on the up-to-date complex design methods.
- (5) **Optimise the structural morphology.** Structure reliability is one main concern for the freeform structure. The morphology achieved from the developed design methods would be optimised to increase the stiffness and robustness of the structure.
- (6) **Generate optimal robotic tool path.** The optimal tool path would be achieved through trajectory planning and motion control with higher level of automaticity, time efficiency and productivity.
- (7) **Standardisation for structure component.** Each component would have one corresponding tool path. To reduce the complexity of the pre-fabrication task, the freeform surface would be optimised to achieve homogenised structure components.
- (8) **Assessment and decision-making support system.** There are different design and component form selections to construction a freeform timber structure. To help different stakeholders to make decisions on different combination options, a multi-criteria assessment and decision-making system would be developed.

1.6 Scope and boundary of the research

This research is based on the architecture design field, to have a thoroughly investigation and to build a workflow framework on freeform timber structure from design strategy to construction process through simulation, and to have a quantitative assessment system. The research is related to the basic knowledge of architecture design, structure behaviour, optimisation, and robotics.

Correspondingly, the research boundary and specific definition are defined according to research contents mentioned above.

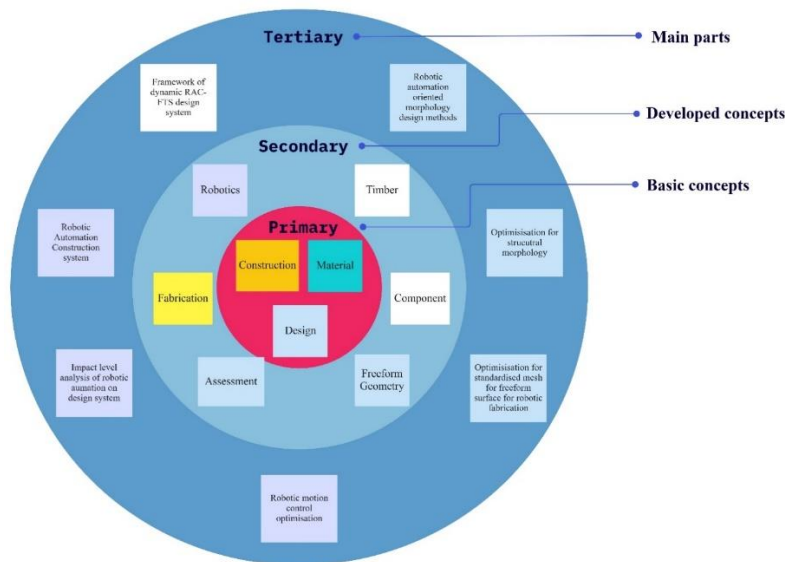


Figure 1.5 Hierarchy of the research concepts

(1) Robotic Automation Construction:

According to Modern Methods of Construction (MMC) definition framework² aiming at innovation and productivity, robotic technique is within this definition framework. MMC is a range of approaches which spans off-site pre-fabrication, near site product design and on-site process like scanning and surveying. According to the definition and the research focus on freeform timber structure, robotic automation technique can be applied to off-site prefabrication and on-site construction process like assembly. When robotic automation construction is mentioned in this research, it could be either the general concept as a construction technology or specific pre-fabrication operation depending on the context. Robot arm in this research is stationary rather than with mobility, then the research content for robotics is focused on motion control and trajectory optimisation when taking the components fabrication tasks.

(2) Timber structure:

In this research timber structure refers to a structure constructed with various engineering timber panels or processed logs as structural materials, with timber or steel components as connecting materials. The architectural form is diverse, not limited to traditional ones. In this research, the timber structures are no longer limited to pure wood structures, the structures are composite that combine two or more forms with modern materials such as steel, glass, and reinforced concrete.

(3) Freeform surface and structure:

Generally, the surfaces of traditional curved space structures are planar surface or simple curved function surfaces like spherical surface, ellipsoid surface that can be expressed by analytical functions. "Freeform surface" refers to a surface that cannot be expressed by a single or several analytic functions and can also be understood as those surfaces that are clearly different from traditional architectural

²MMC Developing Definition Framework is the document published by UK Ministry of Housing, Communities and local government aiming at Fixing the Broken Housing Market following the commitment of housing white paper in 2017.

modelling. Freeform surfaces are usually described in the form of rational B-splines or non-uniform rational B-splines (non-uniform B-splines, NURBS). The surface itself is controlled by its control points, knot vectors and weight factors. This control and expression give the surface a great degree of freedom, allowing the designer to achieve arbitrary surface modelling by adjusting control points or weight factors. In this research, NURBS is chosen to describe the freeform surface. According to the point of view in the book "Space Grid Structures" by John Chilton (Chilton, 2007), spatial grid structure refers to the general term of space truss. The contents in research about freeform would be divided into three-parts: 1) form generating; 2) meshing; 3) mesh optimisation. op

According to the research, the scope of the thesis is limited to:

(1) Concept design: All the process is focused on conceptual design stage which means detailed design like connection design or foundation design are out of the research scope.

(2) Design methods and optimisation algorithms: New freeform morphology design methods and optimisation algorithms would not be focused on, the appropriated methods and optimisation are developed or applied based on the current widely used or up-to-date methods like Particle Swarm Optimisation.

(3) Structure analysis: The structure analysis would be based on simulation rather than statics or dynamic tests as there are many cases mentioned in the whole research. Single experiment would not give provide enough details to cover all the different types of freeform structure cases.

(4) Robotic tool: New tool heads development for robotic arms would not be discussed as the hypothesis of this research is limited to simple robotic fabrication tasks e.g., cutting. CNC is another option for numerical control for fabrication.

(5) Material: Timber is selected as the material premise for this research. The detailed material research like new engineering timber products, material mechanical experiments would not be operated in this research. The anisotropy of a timber product's mechanical properties makes it suitable for use as a compressive material. And because the tensile strength of timber depends on whether it is along-grained or not, which means timber cannot be manufactured into shapes like concrete. Based on this limitation, the hypotheses for the structural components are put forward as planar panels or linear rods which are easy to be manufactured.

1.7 Structure of this thesis

This thesis is composed of eleven chapters. In Chapter 2, the state-of-the-art research and practices of freeform structure generation and optimisation, timber joints and robotics control and optimisation are reviewed. The principles and strategies of synergetic workflow of the complex " design-optimisation-fabrication" are established in Chapter 3. In Chapter 4, cases of operating the simplified robotic arm and industrial robot to conduct cutting task are introduced to summarize the basic environment setting for robotic automation as well as the characteristics of robotic automation. Chapter 5 operate the qualitative and quantitative assessment of robotic automation on the comprehensive design system based on the determination of impact factors. Morphology design methods are developed considering the characteristics of robotic fabrication and timber as a construction material in Chapter 6. Chapter 7

discussed the optimisation for morphology taking the structural behaviour into consideration including the optimisation methods, the parameters, the optimisation objectives. Techniques for optimizing trajectories of single cutting task and path planning are presented in Chapter 8 by choosing the appropriate algorithms, restrictions, and parameters. The methods of generating and optimising the mesh for freeform surface are introduced in Chapter 9. Chapter 10 introduces the framework of criterial for assessment the whole process and decision-making support workflow. Finally, Chapter 11 concludes the thesis by summarizing the main contributions and the shortages as well as putting forward the future work. Figure 1.6 shows the roadmaps for chapter 4-6 and Figure 1.7 shows the whole roadmap.

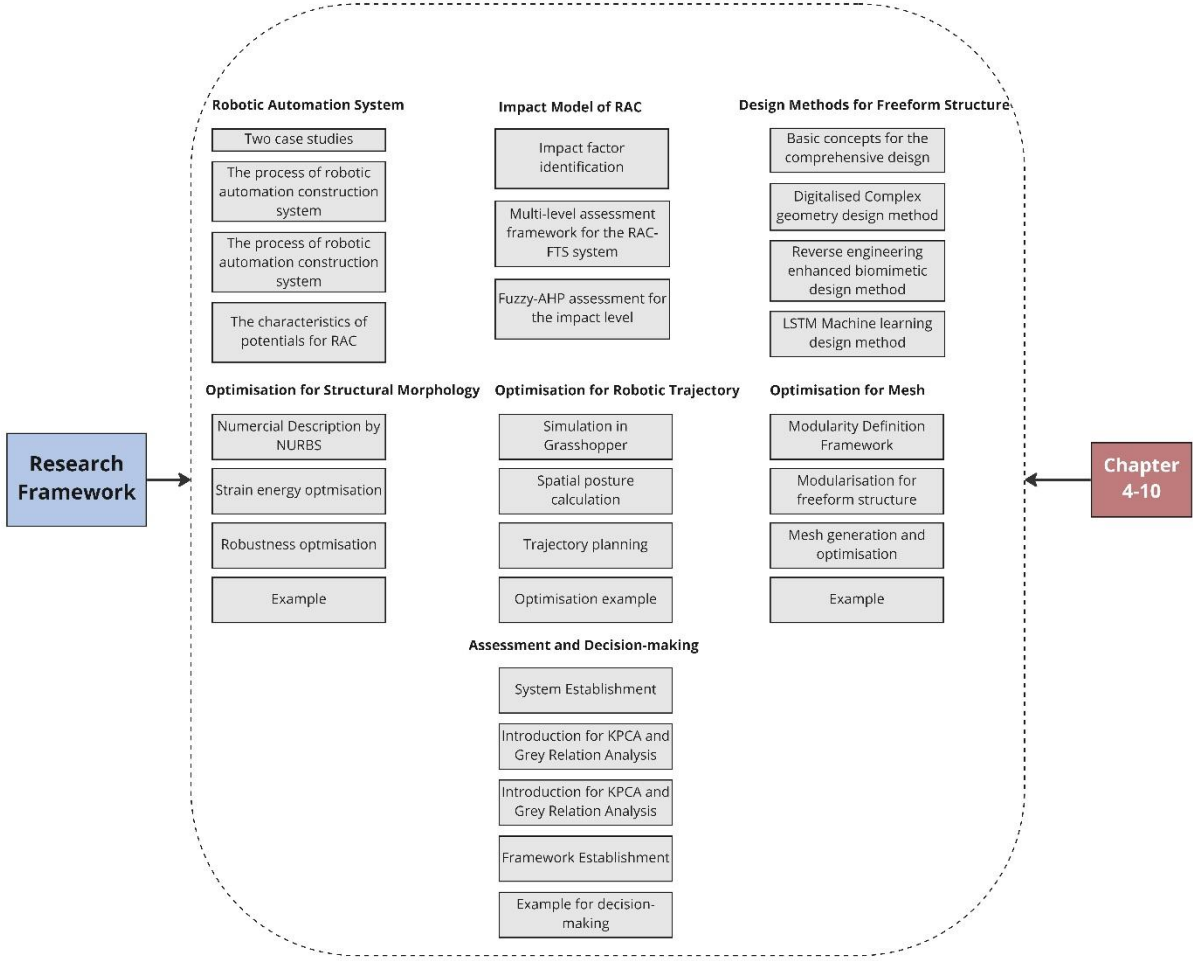


Figure 1.6 Research Roadmap for Chapter 4-10

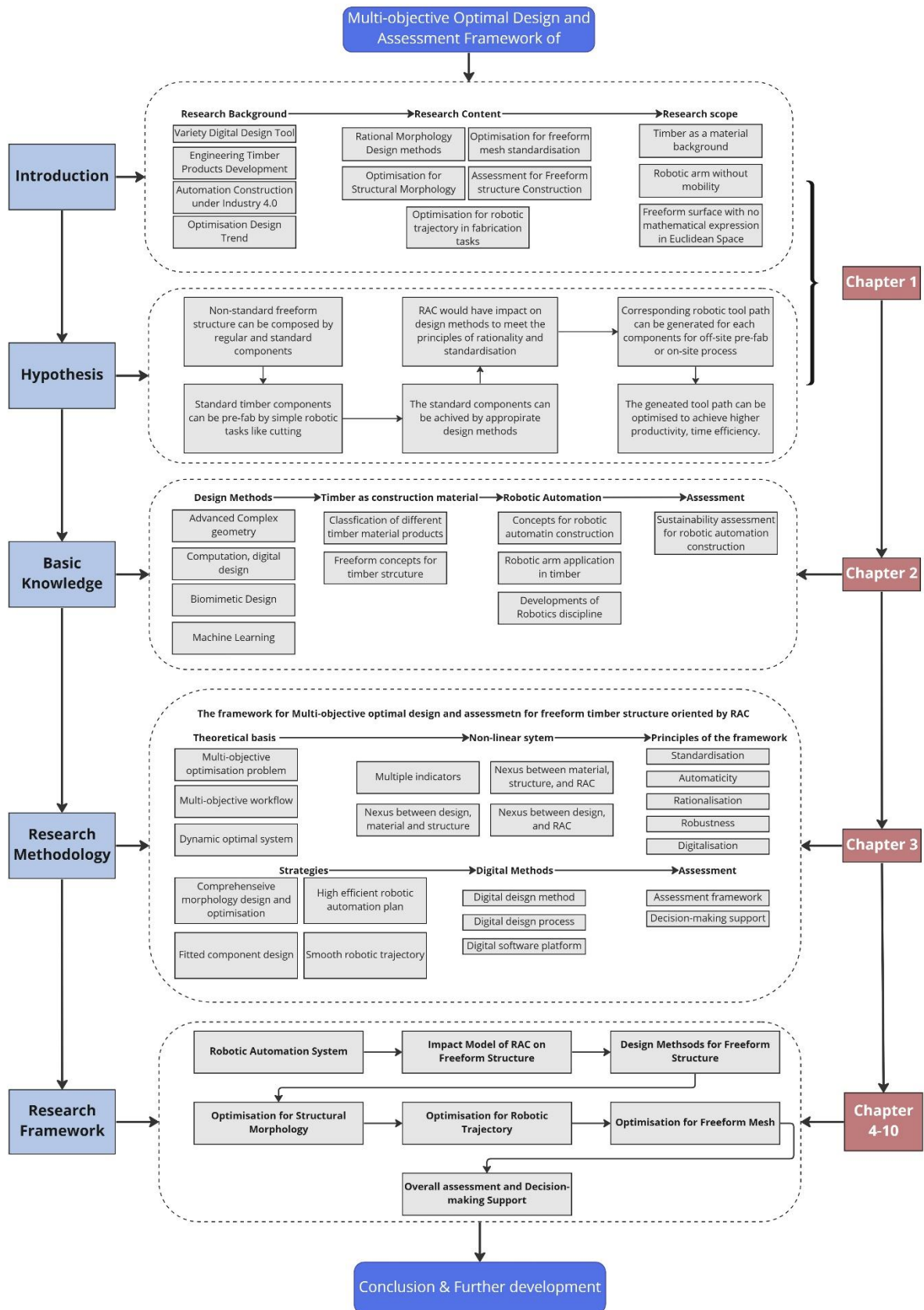


Figure 1.7 Roadmap of the thesis

Chapter 2

State-of-the-Art Review

2.1 Design methods for freeform morphology generation and optimisation

Researches on architectural freeform surface design focuses on the form design and optimisation (Q.-s. Wang, Ye, Wu, Gao, & Shepherd, 2019). As the regular architecture form could not meet the up-to-date aesthetic requirements, the irregular forms put forward new challenges for the conventional design paradigms from design method to design tools. To achieve the complex form and realizing the freeform skins, there are some new criteria needed to be met compared with traditional regular architectural design, such as smoothness, dimensions. In addition, the deviation of the real project from the original design needs to be decreased if taken manufacturing into consideration, which means that additional knowledge about geometry are essential in the optimum design (Wallner & Pottmann, 2011).

2.1.1 From Euclidean Geometry to Advanced Geometry

2.1.1.1 Concepts of advanced geometry

Some mathematicians and a structural engineer argued that there is not closed relationships between pure mathematics and architecture (Salvadori, 2015). Architectural Geometry (AG) is a research field that combines applied geometry and architecture. It focuses on the design, analysis, and construction process of architecture. As the core of architectural design, this concept is proposed to face the challenges of architectural design practice in the current digital age. This concept was first proposed in 2007 by Helmut Pottmann in his book "Architectural Geometry" published by the Bentley Institute (Pottmann, 2007). Then in 2008 and 2010, two "Advances in Architectural Geometry" academic conferences were held in Vienna (Adriaenssens, Gramazio, Kohler, Menges, & Pauly, 2016; Block, Knippers, Mitra, & Wang, 2015; Ceccato, Hesselgren, Pauly, Pottmann, & Wallner, 2016). In the exchange of architects and scholars and engineers in many other fields, this interdisciplinary subject has basically taken shape and is the current digital Architectural practice provides a solid scientific and technological foundation.

Throughout history, geometry and architecture are strongly connected, and when architects take mathematics as the tool to complete design, geometry has always provided the spatial shapes for them to choose from (Scheer, 2014). As a kind of objective reality and basic theory, architectural geometry is always related to the logic, form, and construction method of the building (Hillier, 2007). The development of geometry can basically be divided into three periods: ancient Greek, analytic geometry and Non-Euclidean geometry (Rosenfeld, 2012; Ryan, 1986).

The third critical period in the development of geometry was the advent of Non-Euclidean Geometry in the 19th century (Bonola, 1955). The complexity of nature has caused people to rethink the limitations of Euclidean geometry. Non-Euclidean geometry has brought profound conceptual changes to geometry, which has since expanded the connotation and extension of geometry (Eisenhart, 1997). Non-Euclidean

has provided architect inspirations for diverse spatial form and the development of digital tools facilitated the complex geometry design with rational structure (Gawell, 2013). When seeking inspiration for the development of spatial architectural structures, it is vital to analyse the interplay of individual structural elements in space. Dynamic growth of digital tools supporting the application of non-Euclidean geometry enables architects to develop organic but at the same time, structurally sound forms. The birth of new geometric theories such as Riemannian geometry, Roche's geometry, algebraic geometry, differential geometry, topological geometry, fractal geometry, etc. marks the entry of geometry into the era of complex science, and they have also penetrated the current design and practice of complex buildings. Balmond once said that geometry liberates architecture (Balmond, 1997). It is precise with these emerging advanced geometries as the design source and technical foundation that architecture has moved towards a broader and profound world.

2.1.1.2 Discrete Differential Geometry

Freeform structure constitutes one of the most conspicuous trends in the up to date architecture field (Pottmann, Eigensatz, Vaxman, & Wallner, 2015). As for the application of non-Euclidean geometry on free-form structure, one argument is that the research started from Frank Gehry, who employed digital techniques, which is developed for aviation industry, to complete the freeform surface design and construction task in early stage, such as the Guggenheim Museum from 1991 to 1997 (Shelden, 2002). Differential Geometry, as a branch of mathematics, uses the theory of differential calculus, integral calculus, linear algebra and multilinear algebra to study the properties of a curve or surface in its neighbourhood (Wolfram, 2002). Discrete Differential Geometry (DDG) is a discipline combined discrete geometry and differential geometry to use of meshes, polygons, and simple complexes to describe smooth surfaces (Bobenko, Sullivan, Schröder, & Ziegler, 2008). It is widely used in computer graphics, geometry processing and topological combinatorics (Crane & Wardetzky, 2017). This discipline can be used to determine the normal vector, Gaussian curvature, mean curvature, principal direction vector and geodesic analysis, to realise the process of fitting complex curved surfaces with polygonal planes (Crane, 2018).

When taking fabrication of freeform surface into consideration, the process of breaking the whole surface into small panels to realise a freeform surface called *rationalisation*, which is well-known as *panelization* (Pottmann et al., 2015). One way to achieve panelization is to transform the freeform surface into polyhedral surface at first and to take quads as the base polygons. This method has been widely used in roof structures in 20th century because of meeting the requirement of aesthetic and construction (Pottmann et al., 2015). Although triangle meshes could describe any freeform shape (Holgate, 1997), they are less economical compared with planar quadrilateral (PQ), because of the complexity in cutting a triangular panel and more mullions in diagonal directions (Glymph, Shelden, Ceccato, Mussel, & Schober, 2004).

DDG was firstly proved as one solution for panelization and structural design of complex curved surfaces in buildings especially fits for the PQ meshes panelization (Bobenko et al., 2008; Sauer, 1970), which works as discrete counterparts of conjugate curve networks. Conical meshes were introduced to

discretise the network of principal curvature lines to analogue the main shape characteristics, and provided an offsetting solutions through normal of discrete surfaces which is suitable for freeform structures (Y. Liu, Pottmann, Wallner, Yang, & Wang, 2006). A general CDF (*conjugate direction field*) design method mixed with quadrangular planarization scheme proves to create PQ mesh robustly and effectively on various architecture models (Y. Liu et al., 2011). Research (Bommes, Zimmer, & Kobbelt, 2009) in put forward a novel method to achieve quadrangulating a triangle mesh through cross field generation and global parametrisation, and subsequently to generate an approximately PR mesh aligned with principle curvature lines by using continuous-discrete optimisation. To achieve evenly distributed vertices of planar quad, conjugate directions could handle the position of singularities, smoothness of meshes, planarity of quads (Zdravec, Schiffner, & Wallner, 2010).

An important part of the realisation process of freeform skins is their decomposition into smaller parts (called *panels*) such that the entire cost of manufacturing and handling is as small as possible, and such that the numerous side-conditions concerning dimensions, overall smoothness, and so on are satisfied. In addition, any resolution of the given design into panels must not visibly deviate from the original architect's design. Further, that we are capable of formulating target functionals for optimisation which - if successful - achieve these properties. It is however important to know that in many cases optimisation without additional geometric knowledge (utilised, for example, by way of initialisation) does not succeed (Wallner & Pottmann, 2011).

2.1.1.3 Computational Geometry

Computational Geometry includes several directions, one of which is to process curves and surfaces based on spline functions, defined as computer representation, analysis, and synthesis of geometric shape information. This field aims to study how to build mathematical models of geometric shapes by means of storing and managing model data through computers flexibly and effectively. It is the mathematical foundation of Computer Aided Geometric Design (CAGD), formed by function approximation theory, differential geometry, algebraic geometry, computational mathematics, especially numerical control (De Berg, Van Kreveld, Overmars, & Schwarzkopf, 1997). Freeform shapes are mostly represented by Bézier, basis spline (B-Spline) and non-uniform rational basis spline (NURBS) (Les Piegl & Tiller, 1996). B-spline models were first mentioned by Schoenberg (De Boor & De Boor, 1978). The curves and surfaces described by B-spline were limited by calculation, and this limit was solved by D. Boor using recursive numerical computation, which is commonly known as D-Boor algorithm (Conte & De Boor, 2017; De Boor, 1972). And NURBS is a mathematical model based on B-splines, it is flexible and precise, and models could be built in both analytical and 3D modelling methods (Foley et al., 1996).

NURBS curves and surfaces are defined by their technical specifications: order, control points of different weights, and knot vectors (Versprille, 1975). NURBS method is now commonly and widely used for freeform surface design in computer-aided design (CAD), computer-aided manufacturing (CAM), and computer-aided engineering (CAE) (G. E. Farin, 1995; Les Piegl & Tiller, 1996). After finishing the model-built process in NURBS software like Rhino, the next step is to adjust the shape of

the curves and surfaces to meet the design functional requirements from both aesthetic and manufacturable perspectives. Based on the specific definition of NURBS, the shape could be modified by only adjusting parameters like changing the knot vectors, moving and changing or weights of the control points separately or simultaneously (Au & Yuen, 1995; Chivate & Jablokow, 1995; Knopf & Kofman, 2001; Sanchez-Reyes, 1997), and this advantage permits the large scale of usage in freeform design and manufacturing (Brujic, Ainsworth, & Ristic, 2011; Knopf & Kofman, 2001). Researchers are trying many other ways to adjust the shape more flexible and rational. One method is to take the geometric features as constraints and to minimise the global energy (Celniker & Welch, 1992), or strain energy (Hu, Li, Ju, & Zhu, 2001) to get the altered control points and weights. Physical-based methods like finite element method and Dynamic NURBS can work as another supporting technique to achieve the complex freeform surface not only by modify the parameters but also by applying physical simulation with geometry constraints (Celniker & Gossard, 1991; Terzopoulos & Qin, 1994).

As the initial model built in software is modified mostly from aesthetic point of view, after the prototype of the freeform surface is manufactured, to analyse and evaluate the error and accuracy of the products is important. Based on the analysis, the error of the machining needs to be compensated, so as to modify the shape of the surface to improve the accuracy to satisfy the manufacturable requirements (X. Zhang, Wang, Yamazaki, & Mori, 2004). This process is named as freeform surface reconstruction, which is widely used in many fields, e.g., reverse engineering design and virtual sculpting etc (Salman, Mansor, & Pinang, 2006). In general, the overall aim of reconstruction is to extract the essential geometry information of a curve or surface and to build a mathematical model based on it to make the geometry analytical (Jiang & Scott, 2020). There are some approaches on surface reconstruction like surface triangulations (Floater, 1997), continuous global optimisation from multiple 3D views (Kolev, Klodt, Brox, & Cremers, 2009) or point cloud (R. Pan & Skala, 2011), and interpolation (G. Farin, 1992). But for freeform surface reconstruction, the mathematical model works as a better approximation method because of the high efficiency and accuracy (Xie, Zou, Yang, & Yang, 2012). Among the mathematical models, B-spline and NURBS are widely used. According to the technical properties of NURBS mentioned above, NURBS shows more flexibility and adaptability than B-spline in a variety of geometry types (Ding et al., 2003). Evolutionary algorithm (EA) worked as an efficient technique for large data set in reconstruction (Sarfranz, Raza, & Baig, 2005). Besides the general ability of EA, when taking the running time of the algorithm performing as another comparing criterion, multi-objective EA method completed successfully in the surface reconstruction process (T. Wagner, Michelitsch, & Sacharow, 2007). But accuracy and the complexity of geometry are still remaining challenges for the EA method (Kodama, Li, Nakahira, & Ito, 2005). For Particle swarm optimisation (PSO) showed robust performance in complicated NURBS surface reconstruction against noise of points (Gálvez & Iglesias, 2012). However, the common disadvantage for particle intelligence is that the random searching is time-consuming. To improve the efficiency, a hybrid algorithm combined with a HOAAI iteration were tested on numerical experiments and showed good performance on accuracy and running time (Xie et al., 2012). For now, most of the freeform surface reconstruction technique focused on many fields, and as

to the detailed application on architecture freeform surface to improve panelization ability needs more discussion.

2.1.1.4 Fractal Geometry

Fractal was first proposed by the mathematician Benoit Mandelbrot in the 1970s. It means irregular and fragmented, used to represent complex graphics and complex processes. This new branch of mathematics dealing with complex fractals is called Fractal geometry (Mandelbrot & Mandelbrot, 1982). Fractal geometry can be used to describe many complex forms in nature with multi-level self-similar structures, for example tree branch. As the fractal-like tree branches had good performance dealing with wind load (James, Haritos, & Ades, 2006), and this inspired the branching structures to be the support for large canopy (Figure 2.1) (Rian & Sassone, 2014). As a main component of nonlinear science, computer technology and computer aided design have become a powerful tool for fractal geometry applied in more complex freeform surface. However, the computer-generated tree branch structure is simplified and is not capable of dealing with complex loads (Rian & Asayama, 2016; Sánchez-Sánchez, Pallarés, & Rodríguez-León, 2014). Under the context of structure behaviour, randomness as another property of fractal geometry, has also been applied on a crinkled canopy imitating the land terrain to test the structural behaviour (Rian & Asayama, 2016). Research of fractal geometry applied on spatial complex structures are few. In (Rian, Sassone, & Asayama, 2018), fractal geometry has been applied in designing and generating a lattice grid shell considering structural rationality.



Source <https://www.bestinteriordesigners.eu/top-interior-designers-santiago-calatrava/>
Figure 2.1 Oriente Station, Lisbon. Santiago Calatrava

2.1.1.5 Topology Geometry

Topology was formed in the 19th century by Poincaré, defined as the properties of geometry in more than ordinary three-dimensional space (Thurston, 1997). Topology geometry gives a new definition to space, and it leaves profound repercussions on architecture, breaking through the limitations of Cartesian geometry (Zavoleas & Taylor, 2019). Computation tools have enabled topology applied in architecture to achieve the compound design aims (Aish, 2013) and concepts like 'folding', 'knots', 'manifolds' has extended architecture (Bonahon, 2002). Also, topology works as a supplement for parametric design to

make it rational using non-manifolds cellular structures (Jabi, Soe, Theobald, Aish, & Lannon, 2017). When taking assembly into consideration, topological interlocking has been tested to create the modular self-supporting units in conceptual stage (Tessmann & Rossi, 2019). The general idea of topology has been widely used in urban or large scale of architecture dimensions. The elastic, lightweight tensile shape derived from minimal surface discovered through the soap film experiment (Figure 2.2) by Frei Otto (Liddell, 2015; Otto, Trostel, & Schleyer, 1973) is an example of topology applied in the freeform surface. This cable-membrane structure utilizes the properties of the membrane material that the force is equal in all directions and finally can be formed to complex shapes such as wave, saddle, and vault etc. (Burkhardt, 2016). Besides the tensile roof structure, the minimal surface is also able to be optimized to modular triply periodic minimal surface units using an iterative algorithm (Tenu, 2009). As for the connection between the minimal surface, T-connections are applied to show the nexus with boundary conditions (Filz, 2013). Considering environmental performance, the optimized minimal surface as a roof structure has better performance in daylight and radiance compared with traditional Euclidean form (Agirbas, 2018). Although there are several research on topology applied in architecture, most of which are mainly focused on urban or building scale. Apart from the tensile structures, the start-of-art review has not found many studies focused on giving more detailed and systematic information of topology geometry used on the freeform surface from generation to optimisation. One of the reasons of this is it is difficult to transform the mathematical formulations of minimal surface into the freeform surface design directly, more guidance of the transformation and detailed application are needed.



Source: <https://www.archdaily.com/623689/ad-classics-german-pavilion-expo-67-frei-otto-and-rolf-gutbrod>

Figure 2.2 German Pavilion by Frei Otto

2.1.2 Computational Design for freeform surface

Computational design has prompted the irregular form of architecture design as an efficient tool, by means of replacing the manual sketches (M Rocker, 2006). There are different concepts or terms describing the computational design, such as digital design (DD), parametric design (PD), generative design (GD) and algorithm design (AD). And the main reason is that there are various knowledges

included in this area, including mathematics, artificial intelligence, performance simulation (Woodbury, 2010). Some think the CD is included in DD because of the design relied on the usage of computer tools like CAD software to develop the digital design (Alfaris, 2009; Knight & Stiny, 2015). However, form-find through experiments could the computational process without using digital tools, for example, the minimal surface experiments by Frei Otto (Rasch & Otto, 1996). As the freeform design is a system considering form, performance, optimisation and fabrication, the computational design offers a hybrid methodology to satisfy the demands of freeform design, (1) using parameters to describe the design, (2) taking algorithms to generate the possible solutions, and (3) using the script to optimize the design to meets the performance requirements (Caetano, Santos, & Leitão, 2020).

2.1.2.1 Definition for the terms

Parametric design (PD) was first defined as designing based on mathematical parameters (Moretti, 1971). Though different researchers defined the PD from a different point of views, some are focused on the process using parameters to define and manipulate the design, (Kolarevic, 2004; Meredith & Sasaki, 2008; Oxman, 2008), whereas some are focused on the optimized results (Eggert, 2005; Schumacher, 2008). After all, the general definition of PD related to the freeform surface is to choose representative parameters of geometry and building performance (R. Yu et al., 2015) to achieve design requirements by using digital tools (Qian, 2009), and taking algorithm into consideration to support later on management and fabrication (Gerber & Pantazis, 2016; Jabi, 2013; Woodbury, 2010).

In 1975, generative design system was divided into three types (analogue, iconic, and symbolic) and design model was stored in data format on which the rational solutions generated based (Mitchell, 1975). Later, GD is regarded as a design methodology being able to handle complex information (McCormack, Dorin, & Innocent, 2004; Van der Zee & De Vries, 2008) through algorithm or evolution methods (Humppi & Österlund, 2016; Krause, 2003) to support design to meet the requirements of aesthetic and building performance (Bernal, Haymaker, & Eastman, 2015; Caldas, 2008). Compared to PD, algorithm has more autonomy in generating solutions in GD process because the black-box nexus between the setting algorithm and target results (Caldas, 2006). Consequently, the results are unpredictable (Chaszar & Joyce, 2016).

For AD definition, the boundaries of it with PD and GD are unclear. AD need parameters to represent the building information, which can be seen as PD (Zboinska, 2015). Also the algorithm taken can be genetic evolution one which is widely used in GD (Terzidis, 2004). Nevertheless, according to the specialized taxonomy for the three terms, AD can be defined as a subset of both PD and GD, with the ability to control the models and generative results through the direct manipulation of the script within the algorithm (Figure 2.3) (Caetano et al., 2020; Queiroz, Dantas, Nome, & Vaz, 2015). For freeform surface form generation and optimisation task, mathematical parameters, algorithms, and generative solutions are all needed (Burry, 2011).

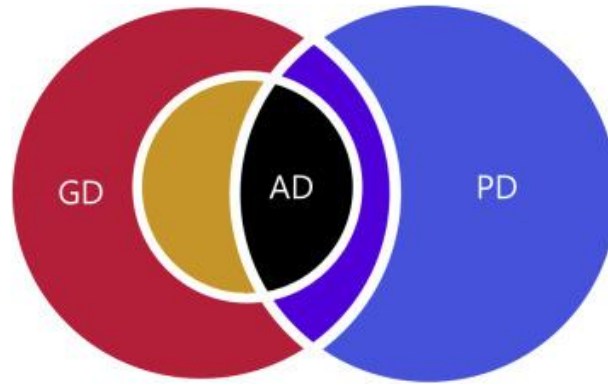


Figure 2.3 Venn diagram for the relations of PD, AD, and GD

2.1.2.2 Applications of CD in decision-making application

The new knowledge from different computational fields has initiated and transferred the paper design process into the digital process taking the performance simulation, structural behaviour, materialisation, and fabrication into consideration (Oxman, 2017; Schumacher, 2016). For complex form, CD can provide decision-making support in conceptual design process, where objectives and constraints of the design are determined (Horváth, 2004; Pahl & Beitz, 2013). Conceptual design is the first phase of the whole design process and the quality of decision in this phase has directly influence of the whole design, especially for product (Chong, Chen, & Leong, 2009; J. Wang, 2001, 2002). The use of CD techniques including PD, GD, and AD has been applied in various architecture conceptual design taxonomies.

Evolutionary algorithm, for example genetic algorithm, is robust to handle complex information and flexible in different optimal objectives from spatial shape to large structure (Adeli & Cheng, 1993; Baron, Fisher, Tuson, Mill, & Sherlock, 1999; Renner & Ekárt, 2003). Thus, when the design objectives and fitness functions are defined, AD can search the global optima in the solution space to give decision-making support (Renner & Ekárt, 2003). PD and AD can be integrated into the collaborative design process searching for the optimum solution in conceptual phase (Saridakis & Dentsoras, 2006).

Structural design is one field that CD is commonly used especially for AD. Ant colony optimisation is taken to achieve structural topology stiffness by minimizing strain energy (Kaveh, Hassani, Shojaee, & Tavakkoli, 2008). Particle swarm optimisation (PSO) together with cellular automata are proposed to optimise truss structure layout with fast convergence rate and less structural analysis compared with standard PSO (Gholizadeh, 2013). Building-performance-oriented design is another focus of CD application. AD is applicable in designing energy-efficient sustainable architecture (Caldas, 2006), and can also be applied to the multi-objectives in object-oriented framework for green building (W. Wang, Zmeureanu, & Rivard, 2005).

Other building performance optimisations objectives include thermal comfort (Chen, Ooka, & Kato, 2008; Magnier & Haghghat, 2010), energy-efficiency (Diakaki et al., 2010), low-cost (Diakaki et al., 2010; Hamdy, Hasan, & Siren, 2011; Ooka & Komamura, 2009). PD together with AD can generate possible solutions for designers to choose from based on performance requirements in conceptual phase (Turrin, Von Buelow, & Stouffs, 2011), for example generating building components (Ercan & Elias-

Ozkan, 2015). However, the detailed research on freeform surface design is not enough. One reason is that the freeform design using CD techniques can use parametric software and plugins like kangaroo, octopus, ladybug directly. These helpful plugins on the one hand can assist designers to achieve better geometry form and performance through the visual code interactively but on the other hand, the software facilitated a mature freeform design process which postponed the innovation at the same time. The insights for more conceptual design methods research are for systematic CD approaches on freeform surface design are distinct (Wortmann & Tunçer, 2017)

This approach contributes to the reduction of limitations of single interface applications as well as the need for multiple software integration.

2.1.3 Machine Learning

Machine learning (ML) is a subfield of Artificial Intelligence. ML mainly focused on building mathematic models to learn the pattern of data from a set of data (Russell & Norvig, 2002). To identify the prediction of ML method used in architectural design process, the applications and potentials of the technique need be reviewed.

2.1.3.1 The concepts of Machine Learning (ML)

Machine learning (ML) is derived from statistics, and the quality of a ML system is determined by the low error rate of prediction or classification (Hastie, Tibshirani, & Friedman, 2009). ML is a new revolution techniques for architecture, which has been used in many other fields like computer vision (Sebe, Cohen, Garg, & Huang, 2005), and image processing (Decenciere et al., 2013). ML system consists of training data set and test data set, using specific algorithms like K-means, and Support Vector Machine (SVM) to operate supervised learning or unsupervised learning on training data (Bishop, 2006). And test data set is utilized to verify the accuracy of the ML system on prediction or classification tasks. Different algorithms have different application, for example, Support Vector Regression is fit for prediction and Support Vector Machines is commonly used in classification (Angra & Ahuja, 2017). Some models like linear or non-linear regression can demonstrate the nexus between the input and outcome, while Neural Networks is a black-box system where the nexus is unexplainable.

2.1.3.2 The application of ML in architecture decision making

According to the contribution of ML dealing with repetitive tasks autonomously in other disciplines, there are exceptions for ML techniques applied in architecture for example design optimisation, design layout etc (Cudzik & Radziszewski, 2018; Das, 2018; Khean, Fabbri, & Haeusler, 2018; Sjoberg, Beorkrem, & Ellinger, 2017). To build a new workflow composed of data, researches have concluded the appropriate applications for ML on architecture design to aid the decision-making in digital fabrication and building performance (Tamke, Nicholas, & Zwierzycki, 2018).

The actual application of ML in architecture is scant, and most of the predictions for ML applied to architecture design process are based on the hypothesis from the succeed practices in other fields. For example, the ability of ML model learning from the training data is similar to the abductive-deductive

reasoning in a design activity, which is a repetitive or iterative cycle of proposing ideas and determining solutions (Johnson-Laird, 2006) based on empirical data (Cramer-Petersen, Christensen, & Ahmed-Kristensen, 2019). Therefore, in (Belém, Santos, & Leitão, 2019) the detailed aspects of ML applications architectural design are concluded.

2.1.3.3 ML in architecture modelling and generation

Besides learning and analysing the data pattern from the provided data, ML can also generate data which can be applied in generative design work using technique like deep neural networks (DNNs) (Larochelle, Bengio, Louradour, & Lamblin, 2009). One of the DNN model that has demonstrated the ability to be applied in geometry generation is the generative adversarial network (GAN) (Goodfellow et al., 2014). The model built through GAN can learn from the existing 2D images and transfer the empirical data into the generative design in 2D form (Oh, Jung, Kim, Lee, & Kang, 2019). A software called “pix2pix” is developed from conditional GANs (cGANs) to solve image-to-image translation (Zhu, Park, Isola, & Efros, 2017) and the software has been applied to generate floor plans (W. Huang & Zheng, 2018).

But the 2D application of GAN is only limited to the 2D plan or façade generations, for architecture generative design, the ability of generating 3D models is required, which is a challenge because of the high dimensionality. In ML area, many attempts have been made to generate 3D objects. One common method is to synthesizing the 3D geometry based on meshes or skeletons (Van Kaick, Zhang, Hamarneh, & Cohen - Or, 2011). Recently, shape synthesis has developed using deep learning through learning from templates to generate new geometry (H. Huang, Kalogerakis, & Marlin, 2015). Based on this, a 3D-GAN was proposed to generate novel and realistic with details 3D models without supervision (J. Wu, Zhang, Xue, Freeman, & Tenenbaum, 2016). But control of the generation and fidelity are still problems for 3D generation. Another way to use GAN is to related to 3D objects is to extract building components to represent the 3D model and to generate the merged ones (As, Pal, & Basu, 2018). One experiment is undertaken using GAN to generate voxel-based represented Manhattan geometry and the results show the 3D generation can be used in conceptual design like urban design (Newton, 2019).

2.1.3.4 The application of ML in structural design

As the ML applications for 3D geometric model is not fully developed, the generative design of freeform surface using ML is much more challenging because of the complicated geometry information. However, the technique of ML has shown the potential in form-finding for structure design (Fuhriemann, Moosavi, Ohlbrock, & D’acunto, 2018). In data-driven design, neural networks (NNs) can predict with the load path 96-100% accuracy (Liew, Avelino, Moosavi, Van Mele, & Block, 2019). ML can solve the time-consuming analysis of shell structure by building near-real-time model in conceptual design (Danhaive & Mueller, 2018). Besides, NNs has also been applied in quantifying the 3D subdividing forms from aesthetic point of views (Zheng, 2019). Apart from quantitative performance, ML can also evaluate neural net qualitatively to come up with solutions to satisfy both engineer and architect (Turlock & Steinfeld, 2019). NNs can simplify the complex space structure into modular segments to optimise structure (Hajela & Berke, 1991), based on this, a trained ANNs model combined with Finite Element

Analysis can solve the long iteration optimisation (Aksöz & Preisinger, 2019). NNs has also been applied in form finding in graphic statics to predict structural performance (Zheng, Moosavi, & Akbarzadeh, 2020). As for the space generation, ML can be used in initial conceptual structural design in a truss type, but still need to be verified in different structures with more detail information like material types (Yetkin & Gönenç Sorğu, 2019).

Related research of ML applications in architectural and structural design show that the applications are still in exploring phase and there are some difficulties to be solved. One of the main difficulties that hinders the development of architectural ML is the data processing (Belém et al., 2019). The procedures include pre-processing, where the features are extracted from 2D or 3D models and translated them into forms that are appropriate for learning process (Kotsiantis, Kanellopoulos, & Pintelas, 2006). Another procedure is post-processing which is converse to pre-processing, converting the learning results into geometry models. Secondly, architectural design focused more on aesthetic and the assessment from this perspective is various and changeable, and ML could not replace the manual work completely, not only because of the lack of experience, but also of the principles of Turing Test (Turing, 2009). Therefore, the appropriate way to apply ML in architectural design task need more validation. For now, ML can be taken as a new design paradigm just like using CD to develop manual draft work. As freeform surface is much more complex than 2D images, so that systematic research is still needed from form generation to optimisation using ML.

2.1.4 Biomimetic Design

2.1.4.1 Basic concepts of biomimicry design

Nature and biology are other disciplines that affect architecture and they have provided mature systematic theoretical guidance to architects (Turner & Soar, 2008). The biological knowledge integrated in architecture is named “*biomimicry*” which provides a systematic theories for the architectural design (Zari, 2007). There are three different layers of biomimetic design concepts in architecture. The first one is called “*biomorphic*” which is only imitating the natural to generate form without biological knowledge (Gruber & Jeronimidis, 2012). The second one exceeds mimicry of form but focuses on the biological or ecological performance and a multi-discipline cooperation between technologies and nature science is required (Benyus, 1997). The performance analogue later on is integrated into architecture, learning the basic organism, behaviour from nature (Mazzoleni, 2013; Pawlyn, 2019). The third one is using new type of material and working on its own which goes beyond the first and the second one and can have close interdisciplinary association with “computer-aided” architectural design (Myers, 2012). Overall, the impact of biology on architecture is categorized into three scales (organism, behaviour, and ecosystem) (Zari, 2007) which can be achieved in two levels: (1) inner logical level: generating geometry forms under the logic of nature and biology; (2) external visual level: imitating and reproducing a natural form (Arslan, 2014). Besides the definition as “*biomimicry*”, there are another term used more widely named “*biomimetic*” which containing more technological theories (Mazzoleni, 2013; Pawlyn, 2019; Zari, 2010) and biomimetic is commonly used in conceptual design to generate solutions (Alexandridis, Tzetzis, & Kyratsis, 2016; Reap, Baumeister, & Bras, 2005).

The main difficulty for biomimicry is the translation of biology related knowledge into design strategies and the uncertainty of the unfamiliar knowledge has hindered the development of this methodology (López, Rubio, Martín, & Croxford, 2017; Yuan et al., 2017). Another difficulty is the scale transformation, which means that most of the mimic origin is in micro scale and architecture scale is much larger than that (Badarnah & Kadri, 2015; Reap et al., 2005).

2.1.4.2 Design concepts generation

To tackle the difficulties, research has been undertaken to explore how and where to enhance biomimetic design. The first important is to understand the “*process*” and how to generate design concepts derived from the biology. TRIZ (Altshuller, 1984) was proved to be adaptive to transfer the analogues from biology to technology using an information-structure regulation model named *Bio-Triz* (Vincent, Bogatyreva, Bogatyrev, Bowyer, & Pahl, 2006). The information-processing model provided a new idea on dealing with biology information which is helpful to develop computational tools (M. E. Helms, Vattam, & Goel, 2008; Vattam, Helms, & Goel, 2008). To better understand how biology inspired engineering and design, an interdisciplinary course was taken in two different processes: problem-driven and solution-driven, and summarized that the problem-defined was insufficient and the analogical transfer was not appropriate (M. Helms, Vattam, & Goel, 2009). Another analogical transformation method is called *Design spiral* which enables designers respond to the constraints taking the innovators from nature and which evaluate the analogical level from three aspects: form, space and ecosystem (Rossin, 2010). There are other translation systems like typological analysis which explained how to analyse the mechanism and scale it to different larger scales (Zari, 2007); while nature studies analysis is more related to architectural design by explaining and analysing the natural principles (A. U. Gamage & Wickramanayake, 2005). Based on the summary of the direct and indirect design approaches and analogical translation systems, biomimicry showed its potential in sustainable design by mimicking the natural form (A. Gamage & Hyde, 2012). In (Badarnah & Kadri, 2015), after analysing some problem-driven and solution-driven strategies for biomimetic design cases, a new generation of design concepts were put forward and a building envelop was chosen to illustrate the process to show the potential for biological inspired design combined with environmental sustainability. The biomimetic design principles could guide different disciplines like construction, material, environment build connections from external morphology and internal mechanism perspectives (Reddi, Jain, Yun, & Reddi, 2012).

2.1.4.3 Biomimetic structure design

Morphology, form, and structure are different biomimicry research topics (El Ahmar, 2011) but a systematic guidance for choosing and applying strategies is lacking (Lepora, Verschure, & Prescott, 2013). The structures from natural has evolved for thousands of years and they are composed of curves and freeform shapes to minimize energy and material consumption in order to fit the natural environment (C. Williams, 2013). The principles for complex geometrical structure using biomimetic design are mostly derived from mechanics, so that the morphologies, forms, and structures are variety (Aldersey-Williams, 2003). These three factors can orient the whole design separately or together. The bio-inspired membrane structures mimic the cell membrane, marine mussel, and lotus showed good performance in

stability and adaptivity as light weight structure (J. Zhao et al., 2014). Learned from the shell of sea urchin with finger-like protrusions, a structured constructed form timber plates with finger-joint was designed to bear high-load (Magna et al., 2013). Apart from the biology inspired structure, cellular structure (L. J. Gibson, Ashby, & Harley, 2010) such as the honeycomb (Q. Zhang et al., 2015) and lattice structure are also widely used even before people realizing the mechanics properties of such structures (Baumeister, Tocke, Dwyer, Ritter, & Benyus, 2014). As for the design process, complex surface from natural morphology was developed using evolutionary computational design method, proving that computational design could be integrated into biomimetic design (Menges, 2012a). Additive manufacturing has guaranteed the customization or optimisation of freeform design and the complexity of biomimetic form design can fully utilize this technique (du Plessis et al., 2019)

2.2 Timber as a construction material for freeform structure

2.2.1 Typologies of Timber products

2.2.1.1 Wood properties and behaviours

Compared with other construction materials like steel, wood and other wood products present strong tensile and compressive mechanic properties as well as elasticity the same as them or even better (Mumford, 2010). Besides, manufacturing wood products from raw material is energy saving while the manufacturing of cement and steel accounts for 94% of global energy consumption (Zapata & Gambatese, 2005). Raw wood materials mean the products from forest or tree without industrial processes like air drying or oven-dry (Ståhl, Granström, Berghel, & Renström, 2004).

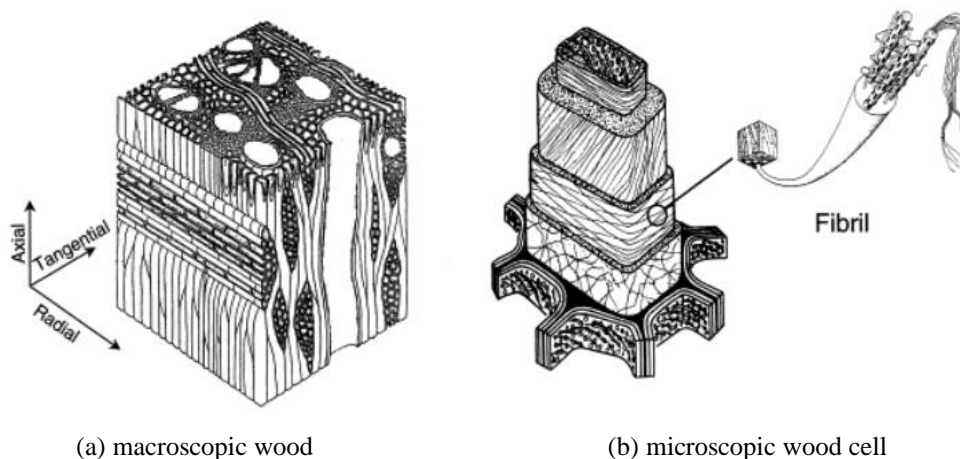


Source: http://www.ltfirewood.com/raw-wood/#tab_0
Figure 2.4 Common Raw wood material forms

The building using wood as the material showed lower carbon dioxide emissions (CO₂), the life cycle of one two-story wooden house showed 20 tons of CO₂ emissions lower than the 72 of one house using bricks (Salazar & Meil, 2009). Timber demonstrates fire resistance predictability of charring rate and residual strength in heavy construction while steel would fail suddenly when heated at about 700-

1000°C (A. H. Buchanan, 2000). Despite of the advantages compared with other building materials, wood still present challenges for industrial construction application.

Wood is composed of different cellulose cells which are arranged in parallel to the growth direction of the trunk or branch and from which the main structure of a tree is made up (Figure 2.5) (Greil, Lifka, & Kaindl, 1998). The hollow cells endow wood the anisotropy, viscous elasticity, and hygroscopicity properties most of which have impact on its application (Dinwoodie, 2000). The grain direction of the tree has deviation according to the growth patterns and this impacts the way to use the material in construction (Denzler & Weidenhiller, 2014). Wood is elastic material but different from steel because of the creep properties, which means the shape of the bending wood is time-changing (L. J. Gibson et al., 2010) and this has required the load demands for the structures that need to be used for long time (Morlier, 1994). Wood can absorb water and the level of moisture content would impact creep deflection (Y. Huang, 2016). So, the control of moisture content under 20% of wood and wood products is essential to keep long time maintenance (Carll & Wiedenhoeft, 2009). There are some other characteristics of natural wood like multi-scalar self-optimizing fibre growth (Matheck & Tesari, 2004) and diversity caused by various reasons such as cellular variation, age of the wood, etc (Zobel & Van Buijtenen, 2012).



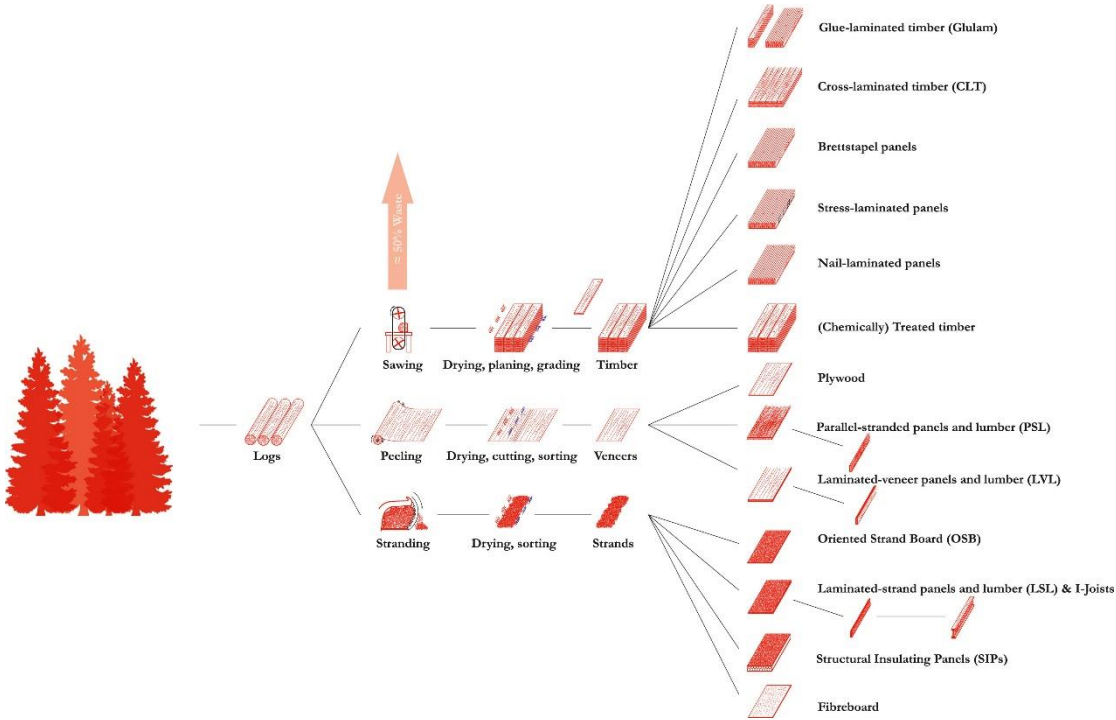
Source (Greil et al., 1998)

Figure 2.5 The macroscopic and microstructure of wood

2.2.1.2 Industrial timber products

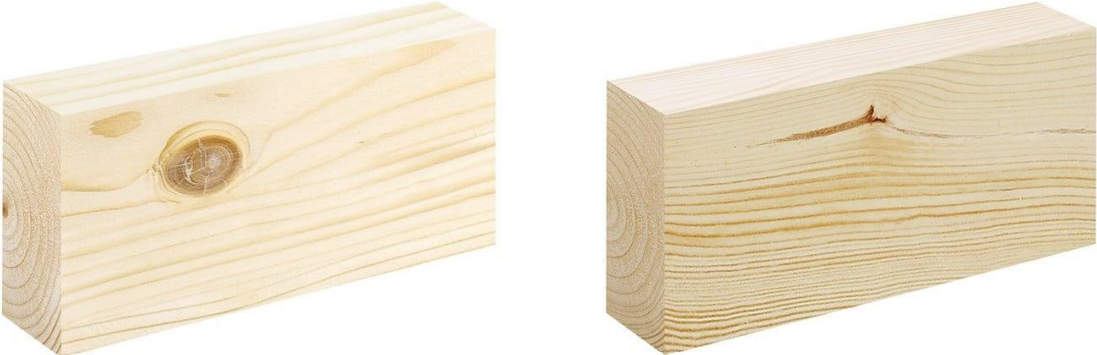
As described above, timber has been used in construction because of its sustainable and renewable properties and development of technology has given impetus for application of timber in irregular geometric form of construction. The precision of the wood products manufacturing has enabled raw material of wood log to produce high quality timber products and has made the structural simulation and results prediction more reliable (Radkau, 2012). The log harvested from forests would undertake different processes to turn the raw material “log” into different types of engineering timber products (Figure 2.6) (Ramage et al., 2017). For construction usage, there are different sets of standards

worldwide like SS-EN 1611-13 and BS EN 14081-14. In BS EN 14081-35, the strength grading includes visual strength grading (VSG) and machine strength grading (MSG). Visual strength is determined by a set of appearance parameters like knots and top rupture which is relevant to the weakness defects, see Figure 2.7.



Source (Ramage et al., 2017)

Figure 2.6 Industrial process turning log into engineering timber products



a) Knots

b) Top rupture

Source: <https://www.swedishwood.com/wood-facts/about-wood/wood-grades/>

Figure 2.7 Defects of timber products

To overcome the uncertainty of these defects when applied as building materials, the raw material can be manufactured into different “engineering timber” products with higher level of stability and more homogenous mechanical properties (Ramage et al., 2017). The manufacturing process is to transform natural wood into standard and stable timber products (Zobel & Van Buijtenen, 2012). Different process

³ Nordic Timber Grading Rules for Pine and Spruce Sawn Timber and the European standard Sawn timber-Appearance grading of softwoods.

⁴ British Standard for Timber Structure- Strength Graded Structural Timber With Rectangular Cross Section, 2005

⁵ BSI. BS EN 14081-3:2012 Timber Structures – Strength Graded Structural Timber with Rectangular Cross Section Part 3: Machine Grading; Additional Requirements for Factory Production Control. 2012

of manufacturing wood would result in different fibre topology and would lead to different engineering wood products and the importance of sawmill is agreed by researchers, which is the first step of transformation (Haygreen & Bowyer, 1996; Walker, 2006). Currently, the predictability of the engineering wood products have been used widely in construction, using the products like glue laminated timber (GLT), cross laminated timber (CLT), plywood, or medium-density fibreboard (Lam, 2001).

To increase the strength and stiffness of the raw wood, one way to reinforce the sawn material is to apply glue or fibre reinforced polymer to stacking single boards to achieve high structural performance (Gilfillan, Gilbert, & Patrick, 2003). One advantage of GLT is that it is easy to be prefabricated the customised shapes and cross sections to be used in large-span or curved geometries (Buell & Saadatmanesh, 2005; Seraphin, 2003). CLT is another construction material technology developed in 1990s, and has been used in tall timber buildings in Europe competing with other materials like steel (Hurmekoski, Jonsson, & Nord, 2015). CLT also shows its capacity in prefabrication and ease to transport to on-site construction (Brandner, 2013). The property of being linear elements, the design for CLT is imperative to take the standardization, joints and the whole structure into consideration (Brandner, Flatscher, Ringhofer, Schickhofer, & Thiel, 2016; Espinoza, Trujillo, Mallo, & Buehlmann, 2016). The quality of raw wood can be increased through development in adhesive techniques to remedy the limits of the original properties (Gardner, 2006). The new type of high-performance materials give more opportunities for large scale or irregular geometric form like freeform structures (Tolszczuk-Leclerc, Bernier-Lavigne, Salenikovich, & Potvin, 2016; Weinand, 2009).

2.2.2 Freeform design concepts for timber structure

Freeform structure using timber as the main materials are driven by the digital technologies on design method and product fabrication for irregular geometries (Monier, Bignon, & Duchanois, 2013). However, the opportunities given by digital techniques to develop freeform design also put forward challenges to consider the material behaviours as well as fabrication process. The workflow needs to be organized under the design and industry with enough flexibility. Multi-scalar modelling is one paradigm to integrate design with structural data in different scales and the design methods (Weinan, 2011) and the methods are specific to different issues (Nicholas, Zwierzycki, Stasiuk, & Thomsen, 2016). And this method is proved to be efficient in data management in GLT freeform design to process discrete types of data from material, fabrication and construction (Poinet, Nicholas, Tamke, & Thomsen, 2016). Multi scalar modelling also shows its potential in dealing with complex information of GLT and giving feedback without high-level requirements for the input (Svilans, Poinet, Tamke, & Thomsen, 2018). Multi-scalar modelling provided a systematic way to design wood digitally and to extend the digital production, however, still, how this method could assist the decision making in conceptual design phase by providing feedback from integration of material properties and fabrication process (Svilans et al., 2019).

Freeform timber construction is a multi-disciplinary research, so the design can be derived for several factors like structure, site constraints, or fabrication (Robeller & Weinand, 2016; Wallner et al., 2010).

How to organize the workflow more efficiently to handle the complexity of manufacturing, geometry and structure needs more systematic guidance. Some research focuses on the digital tools to generate geometry (Scheible & Dimcic, 2011) or toolkit (Mork, Luczkowski, Dyvik, Manum, & Rønquist, 2017). And some research tries to figure out how to organize rational workflow. Grid shell, developed by Frei Otto is defined as a curved shell made of grid (Douthe, Baverel, & Caron, 2006). And with the ability of digital software, the freeform timber using grid shell as a solution has achieved the large-scale buildings (Harris, Haskins, & Roynon, 2008; Naicu, Harris, & Williams, 2014). As for the detailed process, using parametric node design is one approach to design freeform grid shell by simplifying the structure as a combination of nodes and other elements to process the design and analysis (Dyvik, Luczkowski, Mork, Ronnquist, & Manum, 2019).

One important process of the whole design framework is the information exchange between different stage and disciplines. The visual programming ability provided by computer-aided design (CAD) and the geometric and mechanical information included in computer-aided engineering (CAE) model is helpful for spatial timber freeform design (J.-M. Li & Knippers, 2015; Magna et al., 2013). The method called CAD-to-CAE was first developed to optimise the methods for prefabrication, structure design and assembly including identifying the timber plates form, panelising mesh (Robeller, Konakovic, Dedijer, Pauly, & Weinand, 2016). The CAD-to-CAE information exchange algorithm framework is developed for macro model used in a timber plate structure and this method enables the simulation and the analysis of the automation (Rad, Burton, Rogeau, Vestartas, & Weinand, 2021). There are some other approaches for information exchange, including export CAD model to Finite Element numerical analysis (Nguyen, Vestartas, & Weinand, 2019); engineering data management of integrated data from product automation (Hirz, Dietrich, Gferrer, & Lang, 2013). Other than grid shell, there are several structure typologies designed by researchers like the plate shell (J.-M. Li & Knippers, 2015; Magna et al., 2013; Robeller, Gamerro, & Weinand, 2017).

2.2.3 Joints design

The connections of a structure determined the structural behaviour and this principle also works for freeform timber ones (Greicius, Supekar, Menon, & Dougherty, 2009). As freeform timber structure is a complex system including geometry, dimensions of span and boundary conditions, so the design of the connections the structure also needs innovation from traditional to build a stable structure to fit the form and morphology. The new fabrication tools like computer numerical control (CNC) has helped the development of joint design (Robeller, 2015) and different form topologies needs the homologous connections such as: shear resistant connections, moment resistant connections or moment-shear connections (Bitar & Cobucci Paolucci, 2020). And the structural analysis method of the complexity of them are also important.

For timber plate freeform structure, pure wood connection is one connection type. The first pure wood connections in freeform structures are constituted by tab-and-slot joints used in pavilions (Menges, 2006; Scheurer, Schindler, & Braach, 2005). Subsequently, finger joints were developed and applied in single plane (Kaltenbach, 2010), two-plane (Schwinn, Krieg, & Menges, 2013), or segmental plate(J.-

M. Li & Knippers, 2015). A one-degree-of-freedom joints were developed and the angles defining the joints has influence on the mechanical behaviours and the assembly of this type of joints are efficient (Robeller, 2015). Furthermore, three-degree-of-freedom joints are stiffer and have higher resistance to shear forces compared with finger joints. Single or double layered plate structures have utilized these multiple tab-and-slot joints (Robeller et al., 2017; Robeller, Stitic, Mayencourt, & Weinand, 2015) and more improvement are made such as through-tenon joints (Roche, Gamarro, & Weinand, 2016).

Apart from wood-wood connections, there are another type of connections used in freeform timber structure, which is hybrid connections. Literately, the definition of hybrid connections is using two or more types of connections together (Vallée, Tannert, Meena, & Hehl, 2013). Hybrid joints using glue is one large set of adhesive joints including glued-in : (1) steel rods (Bainbridge, Mettem, Harvey, & Ansell, 2002; Tlustochowicz, Serrano, & Steiger, 2011), (2) fibre-reinforced-polymers (FRP) rods (Ansell & Smedley, 2007; Madhoushi & Ansell, 2004, 2008), (3) solid steel plates (Vallée, Tannert, & Hehl, 2011) and (4) perforated steel plates (Bathon, Bletz-Mühldorfer, Schmidt, & Diehl, 2014). The glued-in rods or plates connections shows the capacity of ductility and several design methods are proposed (Schober, Drass, & Becker, 2013). However, the glued-in steel rods connection has not been accepted in engineering design area (Larsen & Munch-Andersen, 2011). One challenge is to describe the transfer process of load on joints because of the stiffness discrepancy between different joints materials like material bolt and adhesive (Kelly, 2005). Subsequently, a procedure to build numerical model was proposed to design hybrid joint system which is made up by fasteners and bonding (Vallée et al., 2013). To better understand the structural behaviour and the capacity of the load-bearing in a freeform timber case, a hybrid T-joint connections with glue were investigated undertaking the algorithm computational methods and found that the load-bearing could be improved by modification (Kohlhammer, Apolinarska, Gramazio, & Kohler, 2017). Besides glued-in rod joints, there is another type of hybrid timber joint named grouted joints, which takes routing technology (I. Gibson, 2005; Hopkinson & Dickens, 2006) using concrete-type as the adhesives (CTA). This type of connections can be widely applied in complex spatial structures like grid-shells (Schober & Tannert, 2016).

2.3 Robotic automation for timber freeform structure

Since 1970s, the scientists, the governments and other organisations started to promote “construction automation” to stimulate the construction industry (Bock, 2015). To improve productivity, economic efficiency, sustainability in construction industry (Linner, 2013), the modification for conventional construction paradigm is necessary (Bock & Linner, 2015). The notion of “Industry 4.0” claims for a new manufacturing system with enough flexibility and autonomy (Zäh et al., 2009). This focused on applying mechanisation concepts into this industry and controlling the process through the computers. It involved large-scale off-site prefabrication of construction components and control of machinery, such as cranes, robots and other positioning system, which largely enhanced the efficiency of the construction sector (Ardiny, Witwicki, & Mondada, 2015a, 2015b).

Automation construction utilizing robotic system can produce real-time feedback and deal with complex information of the fabrication tasks considering sustainability (Bock, 2007). Therefore, the robotic

fabrication method facilitates the manufacturing of the various components and connections of the freeform timber structure (Menges, Schwinn, & Krieg, 2016). This timber automation construction technique covers the above-mentioned contents about the architecture design (geometry generation and optimisation), structural design (material properties of timber), manufacturing (the fabrication of timber products). One important challenge is that how to use digital technology to shift the architecture design integrated with material, structural oriented by the robotic fabrication constraints. And the main objective of this digital fabrication technique is to upgrade it from *craftsmanship* to large-scale industrial application.

2.3.1 Robotic timber fabrication

Digital fabrication technologies have enabled the timber structures becoming more irregular and complex. Compared with Computational Numerical Control (CNC) technique, the mobility, and not high requirements for the working condition of robotic fabrication system are more flexible (Willmann et al., 2016). And this advantage conforms to the development trend - that is to take the design information as the input to produce construction automatically (Bock, 2015). Now, the robotic timber fabrication technique has not only been researched in laboratories but also applied in some large-scale construction applications (Menges et al., 2016; Vercruysse, Mollica, & Devadass, 2018; N. Williams & Cherrey, 2016; Willmann et al., 2016). According to different forms of the components designed by different based-factors, different robotic fabrication types are needed such as cutting, milling, sewing, drilling on different timber products from natural wood to engineering timber products (Menges et al., 2016). According to these practices, it is concluded that this is an interdisciplinary area including the knowledge from material science, mechanics, computational graphics, and robotics. The international conference Robotic Fabrication in Architecture, Art and Design has been held since 2012, and there are more and more cases of using robotic fabrication automation (Brell-Cokcan & Braumann, 2013; Reinhardt, Saunders, & Burry, 2016; Willette, Brell-Cokcan, & Braumann, 2014; Willmann, Block, Hutter, Byrne, & Schork, 2018).

2.3.1.1 Timber fabrication technique typologies

There are different fabrication techniques, and the choice of the technique is based on the components designed for the structure. The research on band saw cutting on speed, different timber conditions, corresponding processes, and dust emission were fully investigated (Nasir & Cool, 2020), however, the ability of band saw on curved surface has not been studied in enough details. The band saw cutting was first implemented on curved strips with a 12-inch band saw mounted on an 6-axis industrial robot arm (Johns & Foley, 2014). While some cutting tasks used linear blade but remained robust technical issues unsolved, one investigation for band saw cutting process was taken to improve the cutting capability (N. Williams & Cherrey, 2016). In “Design + Make” program, the objective of it is to reduce the collision and to balance the size of tooth pitch and smoothness of the rotation (Vercruysse et al., 2018). To handle the complexity rather than using CNC milling technique, the potential of band saw cutting has been explored on curved timber beams (Chai & Yuan, 2018). Subsequently, based on the analysis of the band saw cutting, a design and fabrication framework for large-scale double-curved glulam structure were

organized to show the potential of band saw on dealing with complex geometries (Chai, So, & Yuan, 2021).

Robotic milling is another fabrication technique especially applied in timber plate structures, shown in Figure 2.8. Institute for Computational Design and Construction (ICD) has built several timber structures using robotic milling to fabricate the designed plate (Menges, 2012b). In the lightweight bending-active structure, robotic milling is used to produce 6.5 millimetre thin plywood planar strips (Fleischmann & Menges, 2011). In the project “Landesgartenschau Exhibition Hall”, the finger joints of all the 243 plywood plates in different shapes were fabricated by robotic milling (Oliver David Krieg et al., 2015). Different from other robotic finger joints considering material and tool setup (O. D. Krieg & Menges, 2013; Schwinn et al., 2013), the finger joints in this research is designed taking the constraints of assembly into consideration to take shorter production time. The end-effector set up for the spindle is specific with a tool changer, and the milling process is after the oversized pre-cutting process. The milling workspace is a rotatable so that all the finger joints within one plate could be fabricated. A similar workspace setting for milling is applied in another project named “BUGA”, and is used for milling cassette, which is one modular components of the whole structure (H. J. Wagner, Alvarez, Groenewolt, & Menges, 2020).



(a) Robotic milling on plywood strip



(b) Robotic milling on plywood plate

Source:(Oliver David Krieg et al., 2015)

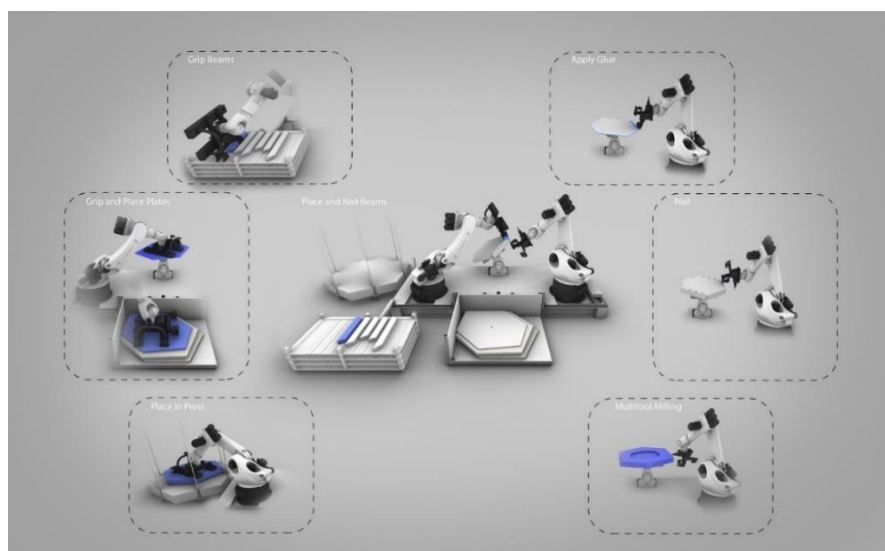
Figure 2.8 Robotic milling

Freeform spatial shell is a new design trend for timber as a substitute for concrete thin shell, however, the main challenge for it is the dimension of the timber products can limit the segments to be fabricated (Schwinn et al., 2013; Schwinn, Krieg, & Menges, 2014). Another challenge is that the complex timber joint in thin shell means the reduce of the material thickness. The aim of protecting the continuity of the cellulose fibre of the wood requires new technique of joint design and textile fabrication technique. There are some textile technique applied on plywood strips of which the edge is connected by thread (Fleischmann, Knippers, Lienhard, Menges, & Schleicher, 2012; Weinand & Hudert, 2010). To expand the application not only restricted to weaving wood strips, but robotic sewing is also chosen for the lightweight timber structure based on the results of few practices. Industrial sewing is applied to connect plywood layers of 4mm on a planar surface by manual work and shows that sewing can produce high quality products (Färg, 2015). And due to the complexity of the sewing process itself, sewing needs

human work together to finish the task. Sewing machine mounted on a robot arm is capable of working in three-dimension working space which is beyond the human ability (Schwinn, Krieg, & Menges, 2016).

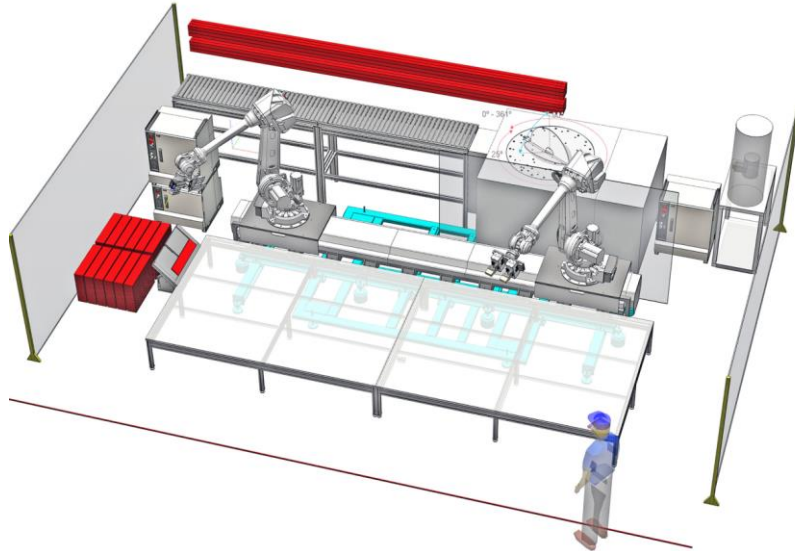
2.3.1.2 Robotic collaboration

Apart from single task operation for robotic, using robot in assembly process together with other technique is another application of robotics (Helm & Knauss, 2015). And usually to achieve the several tasks, cooperation between several robot arms is needed within the workspace which is the main difficulties. In (H. J. Wagner, Alvarez, Groenewolt, et al., 2020), the robotic construction system is constituted by two robotic arm: one is used for gripping and placing, and the other is used for placing adhesive, fixating nails, and milling (Figure 2.9). To investigate the ability of large-scale spatial structure, the fabrication cell is composed of two six-axis industrial robots, which were mounted a conveyor and a three-axis CNC saw (Eversmann, Gramazio, & Kohler, 2017) (Figure 2.10). The robot in the left is used for scanning and gripping the timber slat from the feeding table, and the robot on the right is equipped with a gripper. This robotic cell can also deal with the task like drilling and assembly by lifting the workpiece. To assemble the large-scale structure by discrete timber beams which is reversible and reusable, the collaboration between two robots is employed for tasks like picking and placing by gripping, positioning, screwing (Kunic, Naboni, Kramberger, & Schlette, 2021) (Figure 2.11). In this practice, 14 timber modular blocks are designed to form different aggregation module which is the unit of the whole structure, and the robots are mounted to cover the working desk to operate various tasks. The end-effectors for the robots in this research are customized with a gripper and a screw tip with sensors, which is time saving when changing the tools. This system has also included human assistance when faced with unexpected situations.



Source: (H. J. Wagner, Alvarez, Groenewolt, et al., 2020)

Figure 2.9 Multi-task workspace setting



(a) Robotic workspace setting up with a working table, a linear platform, two robots, a three-axis CNC saw, feeding table with timber slats

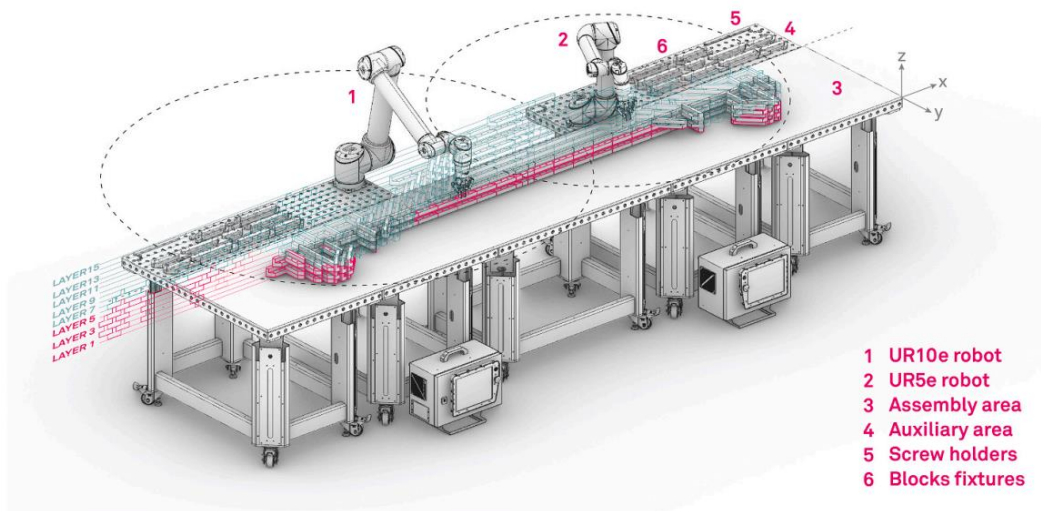


(b) The slat is placed on the table



(c) The timber is gripped to the designated position for cutting

Figure 2.10 a three-axis CNC saw



- 1 UR10e robot
- 2 UR5e robot
- 3 Assembly area
- 4 Auxiliary area
- 5 Screw holders
- 6 Blocks fixtures

Source: (Kunic et al., 2021)

Figure 2.11 Robotic fabrication setup for timber layer assembly

2.3.2 Robotic automation construction design concepts

In automation industry, rapid prototyping is widely used in production development, which is able to produce complex shape (I. Gibson, 2005). Rather than considering the form and performance of a product from objective point of view or external shape pattern, instead the logic from form, manner, function and material perspectives within the product itself is essential (R. Buchanan, 2001). And the products are from many research areas, such as architecture, engineering, etc. Thus, innovations for architectural design concepts require the decision made from internal and external views of the products (Cross, 2011; Oxman, 2017). Under this context of development of fabrication automation technique and the new design concepts, robotic timber automation construction needs its own design concepts oriented by material properties and fabrication methods (Bock & Linner, 2015).

Just as the robotic automation technique in other industry like automotive manufacturing (Nof, 1999), timber robotic automation system, alongside the digital design tools and high quality engineering timber products has shift the design paradigm with higher productivity and flexibility but also puts forward new standard (Bonwetsch, Gramazio, & Kohler, 2012). There are research and practices on building the automation system and process for irregular timber forms from several research institute (Ficca, 2009; Gramazio & Yoon, 2018; Menges & Schwinn, 2012; Pigram & McGee, 2011; Schodek, 2005). These practices show that the robotic timber automation construction needs highly adaptable and specific organized framework for the design driven by different factors (Dunn, 2012). And the workflow to organize knowledge and information from different disciplines is also a challenge for this area.

In the robotic timber automation prototype (Figure 2.12), the whole process commenced in three aspects: (1) assembly-oriented design, (2) material, and (3) robotic construction system (Willmann et al., 2016). In this whole process, the design is driven by the assembly process, and this asks for a new computational design concept, which means that the tolerance during the assembly needs to be considered. If there is a failure during the robotic assembly process, the system would give a real time feedback to ensure the integrity of the whole design. The digital design is finished by Python language, Rhinoceros-3D, and structural analysis software. The structural analysis in this research is about the connections between each component, which is also customized and suitable for the automation system. Every three timber components are connected by one joint, as the response to the constraints from the structure and automation process. For the robotic automation assembly system, the timber components are gripped by the robot arm and are placed in the designated position from the geometric information of the model. The connections of the whole prototype determine the assembly sequence and the path of the robot arm.

In other cases like (Oliver David Krieg et al., 2015), the morphology of the plate structure is inspired by natural biological construction, and the computational approach is based on the principles of biomimetics, which is capable of generation, form-finding, simulating, analysing and optimising automatically but under the constrains from structure performance and robotic fabrication (Figure 2.13).



Source: (Willmann et al., 2016)
 Figure 2.12 Robotic assembly prototype

Following the same biomimetic principles, the project “BUGA” also developed its own computational framework to achieve the seamless prefabrication co-design using two robots (Kunic et al., 2021). In this research, a platform named “TIM” is presented, where the modular timber cassettes are prefabricated to make the largescale timber automation construction is more flexible and adaptable to different working space (H. J. Wagner, Alvarez, Kyjanek, et al., 2020). In these fabrication automation systems, the basic modular units are important parts of the whole structure. This process is consistent with the concepts of prefabrication automation – in an efficient construction, the large proportion of the prefabricated elements can shorten the time in the whole tasks (Weizmann, Amir, & Grobman, 2016). And the modular design provides more opportunities for construction automation when computational design, robotics are integrated together (Wibranek, Wietschorke, Glaetzer, & Tessmann, 2020). But still, the development for the general and applicable robotic automation system, workflow, and framework for freeform timber construction needs more effort and discussion.



(a) Top view of the sand dollar

(b) Plate structure of the Pavilion

Source: (Oliver David Krieg et al., 2015)
 Figure 2.13 Robotic fabricated biometric design

2.3.3 Robotics technical system related to automation construction

From the cases mentioned above, the robotic timber automation construction (RTAC) has developed a relatively mature design workflow within the research areas including architectural geometry generation, structure design and optimisation, development for the end-effector tools. The standardised prefabricated modular units can decrease the uncertainty in the RTAC system, and the standardization has shown the potential for high automaticity (Oliver David Krieg & Lang, 2019; Neelamkavil, 2009; Orłowski, 2019; Popovic, 2018). The RTAC system is especially built for freeform timber structures which are composed of various irregular components, which needs flexible and adaptive systems (H. J. Wagner, Alvarez, Kyjanek, et al., 2020). To apply new types of timber products, minimize tolerance, organize adaptive automation framework, the essential knowledge of robotics is needed to be integrated in this research area to derive the optimum workflow from more technological perspective (Neelamkavil, 2009).

2.3.3.1 Development for robotics related research

From 1952 to 1973, earliest CNC machines has been developed into sophisticated five-axis arms that are now categorize as industrial robots named IRB-6, which was equipped with all-electric motors and an Intel's microcontroller for programming and motion control, introduced by ABB company (Roy, 2013) (Figure 2.14). As for now, industrial robots are extensively being used in mass production lines in different sections of industry, and are especially used for construction industry due to the realization of freeform morphologies (Kohler, Gramazio, & Willmann, 2014; Willmann, Gramazio, Kohler, & Langenberg, 2013). During the last decades robotics research has been aimed at finding solutions to the technical necessities of applied robotics (Garcia, Jimenez, De Santos, & Armada, 2007). The evolution of application fields and their sophistication have influenced research topics in the robotics community. This evolution has been driven by human necessities.

Since 1990s, industrial robots dominated robotics research, and the technical necessities determined areas of investigation for robotics (Garcia et al., 2007). Currently, the research on using robots in construction can be classified into several sub-sections, they are: (1) robot-oriented, which was developed as the design basis for the robot-based construction; (2) robotic industrialization, combining the customized component, module and building prefabrication with automation and robotic technologies; (3) construction robots aiming to develop and deploy the system to be used on the construction site; (4) site automation, which is to integrate single-task construction robot into controlled environment through networked machine system to organize the construction site; (5) ambient robotics focusing on developing service robot systems; according to different context, also including the whole life-cycle assessment of the project (Son, Kim, Kim, Han, & Kim, 2010; Struková & Líška, 2012)

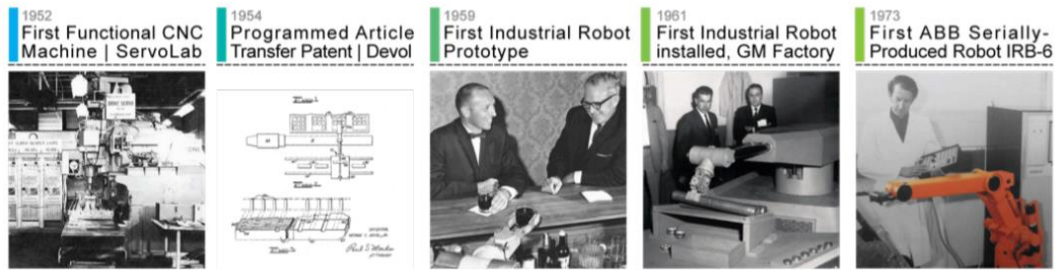


Figure 2.14 Milestones of industrial robots, 1950s-1970s

2.3.3.2 Development of robot applied in construction

The first time of using construction robots was in the early of 1970s, ROCCCO (C. Balaguer, Gambao, Barrientos, Puente, & Aracil, 1996) and BLR (Heintze, Teerhuis, & Weiden, 1996) for brick laying. The robots were more like cranes and were hydraulically driven. The main problem was their limited payload and range. Historically, the construction prototype robots had been used to take single-task in 1980s, the first on-site real-scale robots completed the first building project in Japan (1991) (Bock & Linner, 2016). Later on, in the “FutureHome” project which was part of the Intelligent Manufacturing System global program (Carlos Balaguer et al., 2002), the researchers transformed the tower and gantry cranes into robotic devices (van Gassel, 1993). Then in 1980s, the robots could handle material logistics, components positioning, façade installing and painting and others (Linner, 2013). After surveying the 50 construction robots, Thomas Bock put forward the concept of “ROD” (Robot Oriented Design) in 1988. This concept differentiated robotic construction from human work and redesigned construction process and in consequence boosted the robot application (T. Bock & T. Linner, 2015). Then between 1988 and 2004, this approach had been using in the automated construction sites (Bock, 2007) After that, humanoid robots appeared in construction sites and have been used to undertake simple tasks such as drilling and painting.

Driven by the advanced digital fabrication (Lasi, Fettke, Kemper, Feld, & Hoffmann, 2014), and the Information and Communication Technologies (ICT), the “4th Industrial Revolution”, called “Industry 4.0” call for the highly flexible and adaptable manufacturing system for modular and automated production within the Internet or digital context (Weyer, Schmitt, Ohmer, & Gorecky, 2015). In this context, the built environment has already merged with advanced technology like single-task construction robots (STCRs) approaches, robot system, etc (Bock, 2015). Among these approaches, the robot systems have developed much more advanced that they became ubiquitous to be applied into the many kinds of fields, especially construction. Although the cost of application of robotics into construction is high than human labour, there are some factors, such as sustainability, that can potentially stimulate the robotic automation in construction in real-life (Linner & Bock, 2012).

2.3.3.3 The system of RAC (Robotic Automation Construction) research

Robot can be characterized as programmable automated, flexible and autonomy (Siciliano, Sciavicco, Villani, & Oriolo, 2010):

- 1) Multi-functional: depend on the types of the end-effector.
- 2) Adaptive: depend on the types of sensors to the unknown situation.
- 3) Accurate: depend on the feed-back control technique.
- 4) Repeatable: depend on the programming of the operations.

According to the cases of the robotic timber automation techniques like gripping, milling, to perform these operations better, the following research areas are the key points that needs to be solved.

(a) Kinematic calibration

Kinematic calibration, which is also called geometric calibration, is a key process performed after the operation of the robots or during the recalibration (Santolaria & Ginés, 2013). This is necessary to improve the position and orientation accuracy of the robot, and the error includes geometric and non-geometric (Drouet, Dubowsky, Zeghloul, & Mavroidis, 2002; John M. Hollerbach & Charles W. Wampler, 1996). Through the kinematic calibration the position accuracy could be enhanced through the software rather than modify the robot itself (Abderrahim, Khamis, Garrido, & Moreno, 2006). Normally, the calibration is operated in four steps (Craig, 2005; Messay, Ordóñez, & Marcil, 2016): Denavit-Hartenberg(DH) mathematical modelling, direct measurement, identify the position of end-effector, improve the kinematic model. There were some conventional calibration methods like open-loop, closed-loop and screwed axis methods (John M Hollerbach & Charles W Wampler, 1996). However, there are still new approaches tries to calibrate the robot arm, like measuring joint variable vector and positioning differences compared to the constant position (Abtahi, Pendar, Alasty, & Vossoughi, 2010), using geometric calibration measurement data to optimal measurement configuration options (Y. Wu, Klimchik, Caro, Furet, & Pashkevich, 2015), or using devices like telescoping ballbar to measure the pose of it to calculate the position of the robot (Nubiola & Bonev, 2014), or using the laser tracker to calibrate absolutely (Nubiola & Bonev, 2013). Furthermore, the data can be obtained by the visualization eye-to-hand configuration (Palmieri, Palpacelli, Carbonari, & Callegari, 2018), even, the on-line calibration (C. Yu & Xi, 2018).

(b) Trajectory optimisation planning

Trajectory optimisation planning used in manufacturing, for computing the desired path for robotic arms, which is a process of designing a trajectory that minimizes the time and maximizes the productivity (Chettibi, Lehtihet, Haddad, & Hanchi, 2004). The goal of it is to generate the input for the motion control to make sure the manipulator executing the planned tasks, but also the to control completion of the tasks (Garcia et al., 2007). The present researches combine the motion planning task with the task scheduling problem together to provide a new method for solving the multi-goal in the manufacturing (Paraskevi Th Zacharia, Xidias, & Aspragathos, 2013). The notion of Bump-Surface introduced the above problem to the optimal problem (Azariadis & Aspragathos, 2005), and considering the multiplicity of the Inverse Kinematics, the optimisation could be solved by the Genetic Algorithm (P Th Zacharia & Aspragathos, 2005). Based on the 2 DOF robot, the GA proved to be an effective optimisation method for the trajectory planning even under the complicated environment (Tian & Collins, 2004). When met with the redundant manipulator, it can be solved by constrained nonlinear

programming framework of controlled (Kim & Joo, 2013), or a multi-objective genetic algorithm for the multi-optimisation (da Graça Marcos, Machado, & Azevedo-Perdicoúlis, 2012). The current research shows that the theory of trajectory planning can effectively control the position and posture of the end-effector (Martinec, Mlýnek, & Petrů, 2015).

(c) Motion control

After the planning, the motion control system is required to assure the execution of the tasks. It is worth remarking the end-effector motion and forces are usually carried out in the operational space control and the control actions are usually operated in joint space (Spong, Hutchinson, & Vidyasagar, 2006). The unit dual quaternions is the main published control approaches (Özgür & Mezouar, 2016), and there are already some controller established based on it, e.g., robust (Marinho, Figueredo, & Adorno, 2015), optimal (Figueredo, Adorno, Ishihara, & Borges, 2013), and set-point controller (Pham, Adorno, Perdereau, & Fraisse, 2017). The kinematic equations together with the constraint equations of the unit dual quaternion together can make up the system of kinematic models (X. Yang, Wu, Li, & Chen, 2017). Besides, there are some other methods like robust adaptive control to enhance the tracking accuracy under the parameters acquired from the online adaptation law (Yin & Pan, 2018), the new method called generic method based on factor graphs (Sugiarto & Conradt, 2017), or the flat output to make the open loop control possible (Markus, Agee, & Jimoh, 2017; Markus, Yskander, Agee, & Jimoh, 2016).

(d) Interaction with the environment

The industrial robots are widely used in industry, not only the assembly work to realise the designed motion path, but also the work like grinding, polishing, etc (Lotz, Bruhm, & Czinki, 2014). These operation demands the force control of the interaction between the end-effector and the environment needs to be considered. In the operation like milling or drilling, the force or torque needs to be calculated (Brogårdh, 2009). The force-control in robotics has already been investigated exhaustively (Roveda et al., 2016). Currently, some researcher estimates the forces through the model-based virtual force sensors using the information of motor or estimating it from the motor currents (Linderoth, Stolt, Robertsson, & Johansson, 2013). To try to use the robot force-control algorithms in real-world, one way is to estimate the external forces through the calculation of the thermal state of the manipulator (Villagrossi et al., 2018) combined with the dynamic model equations (Pedrocchi, Villagrossi, Vicentini, & Tosatti, 2014).

From the reviews of the RTAC cases and the technical robotics, it can be concluded that for better efficient RTAC system which is automatic enough to fit for various fabrication tasks and working environment, the design and organisation of the system can be enhanced by taking the above four aspects into consideration and make improvement on: (1) organization and management of the system; (2) design with tolerance; (3) optimisation for the robot.

Digital technologies give more opportunity and possibilities for the shape of architecture through the description of non-Euclidean geometry. New geometric concepts or laws can be simulated by computer programs and appear as a controllable system. Therefore, they are logical in the design generation process, controllable in the analysis and optimisation process, and authentic in the construction process.

2.4 Assessment for freeform structure under RTAC

The research about the robotic automation construction (RAC) have been undertaken in industry and academia, however, the real industrial large-scale implementation of this technique is still in its initial stage. However, the industry attitude towards applying RAC is not very positive and one of the main reasons is the lack of a critical reason for the necessity of applying robotics. Under this context, the sustainability of RAC can activate the industrial fulfilment, which is consistent with the global sustainable development trend (Cf, 2015; Colglazier, 2015). Sustainability has always been especially important but in construction industry (W. Pan & Ning, 2014), and RAC can improve it form reducing construction material waste, improving working conditions, protecting workers' safety, etc (Castro-Lacouture, 2009; Cousineau & Miura, 1998; Linner & Bock, 2012). Recently, some companies have started to employ RAC in the deconstruction task to show the advantages in economic and environmental protection (Lee, Pan, Linner, & Bock, 2015). (de Soto et al., 2018). By analysing the challenges for adoption of robotics qualitative and quantitative methods, robotics can be devised to solve low productivity (Delgado et al., 2019). Besides, 3D printing has shown its potential in economic and environmental perspectives(De Schutter et al., 2018). The detailed research on sustainability of RAC is complex and need thoroughly systematic investigations of all factors and circumstances.

One method to build sustainability assessment framework is to integrate the principles of sustainability to the technology management and to choose the proper criteria for the assessment (Alan C. Brent & Pretorius, 2008). Instead of focusing on evaluating the impact of applying new type of technology, the researches gives full details on management under the macro financial and social context (Alan Colin Brent, Van Erck, & Labuschagne, 2006; Phaal, Farrukh, & Probert, 2004). To build an exhaustive assessment framework, the choice of indicators and evaluation of every process of construction industry under the context of sustainability is important (Labuschagne, Brent, & Van Erck, 2005; Z.-Y. Zhao, Zhao, Davidson, & Zuo, 2012). In (Presley & Meade, 2010), a benchmark framework is built based on strategic and activity, and indicators from LEED and TBL from sustainability can evaluate the construction holistically. However, the gap between large-scale application of RAC due to the sustainability of the technique and the guidance for assessing the sustainability of RAC and still exists. To fill the gap and develop a robust indicator framework for RAC, the domain-based and issue-based combining V-model approaches are adopted and will be translated to assessment method validated in real-practice(M. Pan, Linner, Pan, Cheng, & Bock, 2018a).

As the RAC is one important technique that appertain under innovative building technologies (IBTs), the first conceptual model of co-evolution of IBTs is built which is verified by robotic construction which provides a method of understanding technology theoretically(Y. Yang, Pan, & Pan, 2019). The productivity of digital fabrication of using robotics is verified to be higher than conventional manual work especially in complex structure analysed from time and cost two perspectives(de Soto et al., 2018). A method named weighted Multi Criteria Analysis (MCA) is adopted to assess the prefabricated timber panels. For the products quality of RAC system, techniques like 3D laser have been employed for the post-construction assessment and have been proved as an efficient tool(L. Liu, Chen, Kayacan, Tiong,

& Maruvanchery, 2015). However, the RTAC system, including the geometry form generation and optimisation, timber structural and connections design, robot system setup, need to coordinate every aspect. In (Kumar et al., 2017), the prototype of non-standard concrete fabricated by the RAC has been applied in real project after assessing the structural performance, but the assessment framework is not explicitly built. As the assessment for the RAC is not mature now, the principles of choosing indicators and the method of evaluating the whole system still needs more deeper and detailed research.

2.5 Conclusion

From conventional Euclidean design method to more and more complicated architectural geometry design methods, the research and practises of rationalisation and construction for these non-standard shapes have been constantly updated. The review in 2.1 demonstrated there are variety of methods in generating the morphology for freeform surface and many of them have been applied in real cases. The widespread usage of these methods today is closely linked to the development of computational design tools and digital manufacturing process e.g., generative design using BIM model. Besides, these design methods present a trend towards multidisciplinary integration. Taking advanced geometry for example, the fractal or topology are concepts from the computational graphics or geometry disciplines. The methods to transfer these ideas into architectural geometry generation and to turn the geometric models into real structures are becoming a current research hotspot. The cases from academia and industry indicate the material genre have posed impact on the design methods. For tensile film, with material properties like good tenacity, high tensile strength, not easy to be torn, over 400% ductility, the design methods for membrane structure need to consider morphology characters like long-span and variation in curvature. In this research, timber is selected as the material premise for freeform surface design. As timber is not as concrete or steel can be made into products with any shapes, to ease the complexity in construction including off-site pre-fabrication and on-site assembly tasks, the main structure components would be set as planar panels and linear rods. To finish a freeform structure made with planar or linear engineering timber products, the selection and adaption for appropriate design methods needs identification.

The state-of-the-art review on timber as building materials introduce the development from forest products into industrial products with higher level of strength. The “CE” certificate and more international and national standards on application of timber product as building materials provide guidance on how and where to use timber in a structure. These documents have given impetus to an increasing number of applications and research into free-form timber structures. What are the appropriate methods to design a freeform timber structure? How to pre-fabricate the timber structural components for the structure with high productivity to promote mass production for non-standard timber structure? These questions would need further exploration and would be discussed in the following chapters.

Robotic technique, namely, robot arm with different tools mounted on the end-effector has been gradually applied in academic, especially in architecture field, to test the applicability and feasibility of this technique. The cases and related research discussed in 2.3 illustrate the normal workflow for the

robotic application: multi-discipline design, tool development from automation control, fabrication or construction simulation, path planning and final construction. These cases have pioneered a number of innovation technique from design to tool development and have explored the many and varied possibilities of applying robotic arms in the construction. On the contrary, the hysteresis of adopting the industrial robot into mass production is due to the following reasons:

- (1) **Uniqueness:** The developed tools are specific to each unique design project which is contradictory to mass applicability. The mass production needs high level of standardisation.
- (2) **Efficiency:** The lead time for the cases applying robotic is quite long including collaboration on design, establish the working space, set up the equipment and robotic operation. On the contrary, efficiency matters in mass production.
- (3) **Reusability:** The tools and the workspace are applicable to the corresponding design project. The possibility of reusability of these newly developed tools and working space has not been proven. If the workspace and tools only fit the corresponding design and the flexibility for other similar cases is not enough, then it is not cost-effective, which means it is not easy to promote mass production.
- (4) **Automaticity:** To achieve mass production using robotic technique, the automation production lines with high precision are essential. The whole process needs manual work to operate path planning and quality control. The accuracy and the uncertainty of collision or potential risks have not been testified.

In view of the above shortcoming, the literatures about “Robotics” are discussed in 2.3.3. The research content for “Robotics” provides professional guidance on trajectory planning, motion control and spatial position calculation. These knowledge work as supplement for the present studies on architectural robotic application. For example, the motion control of robotic arm could enhance the stability of the equipment and save time and energy through trajectory planning. By adding professional motion control and trajectory planning to robotic automation in construction, the efficiency and automaticity goals could be achieved gradually. As for the uniqueness and reusability, more optimal designs with standardised structural components can enhance the repeatability of the tools and the workspace.

Currently, the assessment framework for this technique in construction is within the sustainability context, where “technology” is taking less weight and proportion in the whole framework. Whether robotic automation construction technique is an alternative for mass production of freeform structure or MMC, further developed assessment framework e.g., for the product quality is needed. The freeform structure and robotic automation construction are two separate systems. The way to connect them is to take computation design tools and information digitalisation to achieve the information transformation. When a design plan is to be determined including appropriate design method, standard and modular structure components, and material product forms, different stakeholders would have different preferences. It is necessary to investigate how to assist decision-makers in selecting different combination plans to meet their own expectations and preferences.

Following all the discussion and summary for the state-of-the-art review for four main research parts, the hypotheses 1-3 can be tested following the connection between the Robotic Automation

Construction (RAC) System and Freeform Timber Structure (FTS) illustrated in Figure 2.15. RAC could work as a solution to solve the deficiency of current FTS design with low buildability, construction accuracy with deviation from design to final structure and lack of rationality in material and structural performance.

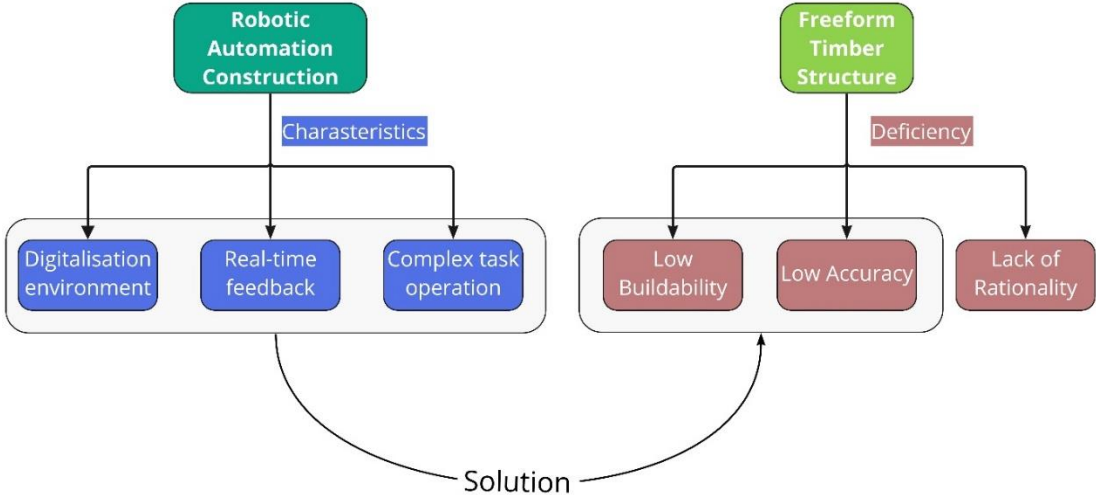


Figure 2.15 Connection between RAC and FTS

In more details, the four main principles of “Robotics” can be applied to the three main parts of freeform timber structure design namely morphology design, mesh generation and mesh optimisation. The requirements for the freeform timber structure are structural stiffness, rationality of structure and morphology as well as the homogenise components to meet the goals of rationality, buildability and construction efficiency. Under the knowledge and guidance of Robotics, the robotic automation technique in construction can meet the requirements of freeform timber structure through end-effector operation, tool path planning and motion control by achieving the industrialisation, automaticity and standardisation requirements.

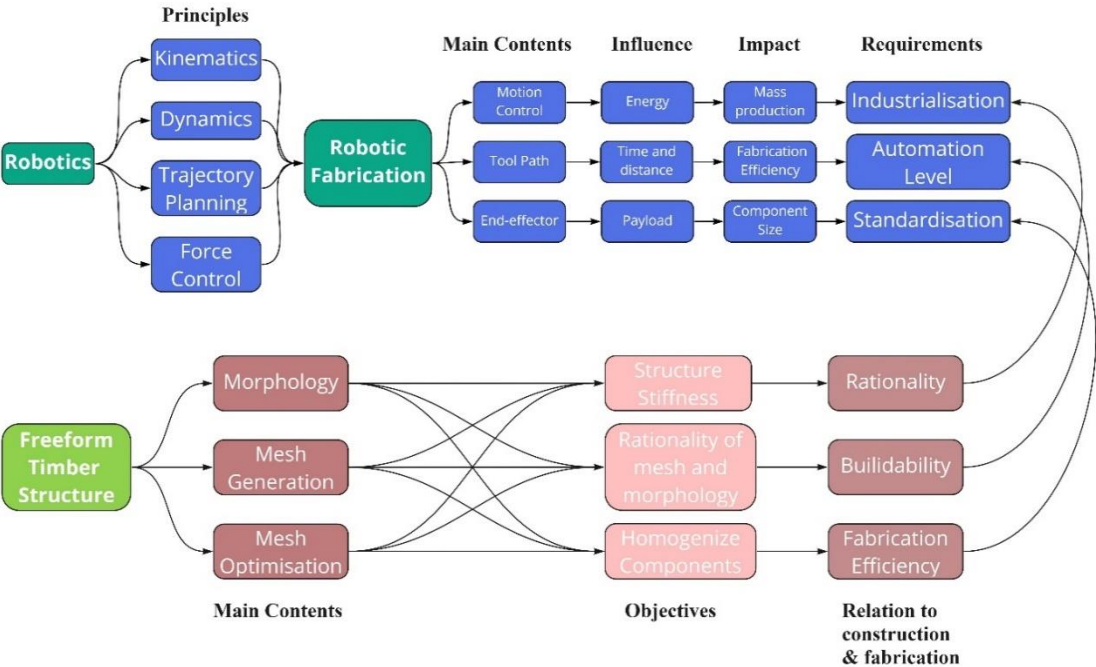


Figure 2.16 Concept map between the principles of robotics and freeform structure

Chapter 3

Framework of the Multi-Objective Optimal Design and Assessment System for Freeform Timber Structure (FTS) Oriented by Robotic Automation Construction (RAC)

According to the most recent research, freeform structure and robotic automation construction are two distinct systems. To organise a workflow to connect the two systems, the RAC-FTS system is proposed in this chapter, with the goal of establishing a framework to couple the RAC technique into FTS application. For robotic automation construction system for freeform timber, the rationality of the geometry generation and optimisation, robust structure design, digitalisation of the timber material, robotic automation system design, and the assessment for every aspect are the essential parts of the theoretical framework of robotic automation construction for freeform timber structure (RAC-FTS). A system model put forward to organise these different parts. The primary objective of this chapter is to examine the interactions between each factor in this multi-discipline system and to propose design and optimization principles for this system. The design strategies and methodologies presented in this chapter serve as the foundation for the subsequent chapters. The RAC-FTS system assessment framework is being built, which includes the method of extracting information, assessing methodology, and standard assessment criteria that will be used for RAC-FTS system decision making. The lack of ability in visualisation and transformation between digital and geometric models is the reason for not adopting CNC in this case.

3.1 Theoretical basis and method of RAC-FTS design based on multi-objective dynamic optimisation system

The system established for this research is known as RAC-FTS. This system is built using a digital model and data transformation platform and is based on robotic automation construction and freeform timber structure. Given the variety of contents, such as morphology design and structure performance, the optimisation problem for all of these included parts is converted into a multi-objective optimisation problem in order to connect the various objectives of different research fields.

3.1.1 multi-objective optimisation problem

Optimisation theory is a discipline developed from mathematics, whose research is concerned with determining the optimal solution among many feasible solutions. In engineering, many problems consist of conflicting and influential multi-objectives. In solving various engineering problems, multiple objectives are needed to reach the optimum as much as possible at the same time, i.e., there exists more than one optimisation objective that needs to be dealt with simultaneously, and such problems are multi-objective optimisation problems. The research topic is a robotic fabricated freeform timber structure, a complex system engineering problem involving multiple disciplines, including material, structure, design, fabrication, and construction. These problems are intertwined, and the disciplines are interrelated,

bringing new difficulties to design and decision making in the conceptual design phase. By introducing multi-objective optimisation techniques, the aim is to effectively assist in the operation of the design and the final decision making. MOO problem consists of the following main components.

(1) Optimisation objectives: The objectives of multi-objective optimisation in the field of architecture are often the building performance indicators, mainly the building environment performance indicators, such as building energy performance indicators, lighting performance indicators, thermal comfort performance indicators, etc. These performance indicators are closely related to the design parameters of the building environment, space, material, and equipment operation.

(2) Design variables: Among all the design parameters that make up the architectural design solution, some are set as constants in the multi-objective optimisation process according to the specific optimisation problem. Other parameters are set to variables that control the direction of the program adjustment, and these variable parameters are called optimisation variables.

(3) Constraints: Architectural multi-objective optimisation must enable program performance and ensure the feasibility of the design parameters and meet the actual design task of design conditions and objective law constraints. The constraints determine the range of values for the architectural design parameters, i.e., the optimal multi-objective design problem domain.

(4) Objective function: The objective function refers to the mapping relationship between the architectural design variables and the optimisation objectives. The MOO algorithm can search for feasible design parameters (feasible solution) with a better performance objective in the design domain based on the evaluation of the objective function.

The mathematical expression of MOO is as follows:

$$\begin{aligned} \text{Variables: } & x = [x_1, x_2, \dots, x_d, \dots, x_D] \\ \text{Objective functions:} & \min/\max \left\{ y = f(x) = \{f_1(x), f_2(x), \dots, f_n(x)\} \right. \\ & \qquad \qquad \qquad \left. n = 1, 2, \dots, N \right. \\ \text{s t } & \left\{ \begin{array}{l} g_i(x) \leq 0, \quad i = 1, 2, \dots, m \\ h_j(x) = 0, \quad j = 1, 2, \dots, k \\ \text{optimisation } d \in \{1, 2, 3, \dots, D\} \end{array} \right. \end{aligned}$$

For the multi-objective optimisation problem MOO (multi-objective optimisation), there is usually no solution $x^* \in D$ to minimise all the objectives $f_i(x), \forall i \in [1, K]$ simultaneously. This is the main difference between MOO problems and single-objective optimisation problems, i.e., the definition of the optimal solution is different. To make multiple objectives as optimal as possible in a given domain at the same time, the solution of multi-objective optimisation is usually a set of equilibrium solutions, i.e., a set of optimal solutions consisting of many optimal solutions, and each element of the set is called a Pareto optimal solution (POS) (D'CRUZ, RADFORD, & GERO, 1983; Tušar & Filipič, 2014).

POS is defined as follows.

Supposing $x^* \in D$, if there is no $x \in D$, satisfies $f(x) \leq f(x^*)$. That is, the following conditions do not hold:

$$f_k(x) \leq f_k(x^*), \text{ and } \exists i, f_i(x) < f_i(x^*), i \in [1, K]$$

Then x^* is the effective solution for the MOO problem. The meaning is if x^* is Pareto optimal solution, then there is no such $x \in D$ that each objective value of $f(x)$ is no worse than the objective value of $f(x^*)$. At least one objective of $f(x)$ is better than the corresponding objective value of $f(x^*)$. That is, x^* is the best and no additional improvement can be made in.

3.1.2 MOO workflow for RAC-FTS

The architectural MOO process generally includes three sub-processes: identifying optimisation problems, constructing performance objective evaluation models, and operating multi-objective optimisation (Figure 3.1). In the optimisation problem identification stage, it is necessary to determine the objectives, design parameters and constraints according to the design requirements and tasks. They establish the reflection relationship between the building design parameters and the optimisation target in the model construction stage. The model can calculate the corresponding optimal solution based on the known values of optimisation parameters. In the search phase, the performance objective evaluation model is coupled with the algorithm. The optimisation algorithm will automatically search for better solutions in the design domain based on the performance evaluation results until the pre-set number of iterations or the termination condition is reached. The solution set will converge generation by generation. Finally, the non-dominated solution set is obtained.

The systematic design process for multi-objective optimisation of the RAC-FTS is developed as follows:

- (1) Identify design requirements and determine the parts to consider in the design system.
- (2) Determine the objectives according to characteristics of different design parts and set suitable quantifiable objective functions.
- (3) Select optimal variables related to the objective function.
- (4) Set reasonable constraint functions based on program requirements and variables.
- (5) Select suitable optimisation methods for optimisation calculations based on optimisation characteristics.
- (6) Calculate practical optimisation results.
- (7) Select appropriate results in the optimisation scheme as the design result of the scheme.

The optimisation objectives of current research on architecture using MOO methods mainly focus on building performance (Hamby, 1994; Radford & Gero, 1980) for sustainability, such as thermal insulation and energy efficiency (D. Liu, Wang, & Liu, 2017), lighting, and ventilation (Arens & Williams, 1977).

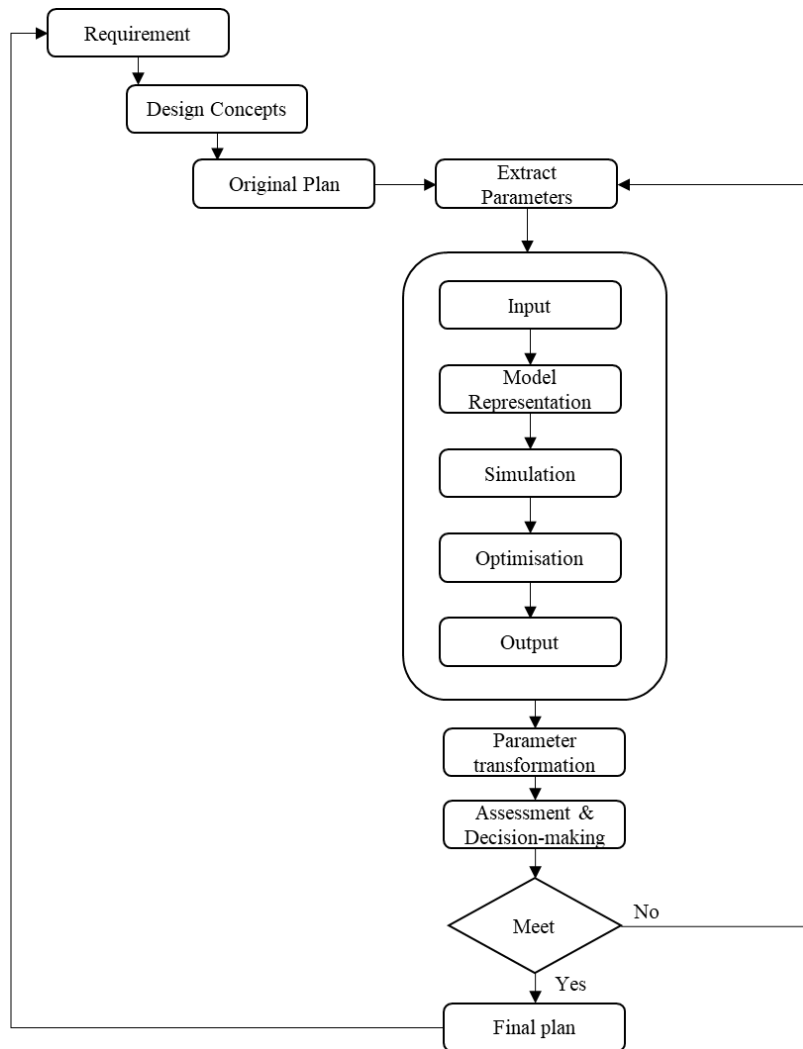


Figure 3.1 Information transformation in MOO for RAC-FTS

In this research aiming at the robotic fabricated freeform timber structure, building performance is not as important as morphology rationality, structural stability, fabrication efficiency and standardisation level of structural components.

3.1.3 Dynamic robotic-oriented workflow

The combination of MOP allows for effective targeted optimisation of the different elements involved in the FTS design. Implementing a dynamic comparative selection process based on the optimized results will be an important part of the process design. As shown in Figure 3.2, the preliminary design is carried out under the combined effect of fabrication and structure. Based on the design and preliminary optimisation results, the structure and fabrication contents are completed, and the information between structure and fabrication is effectively exchanged and optimized. The optimisation results are fed back to the design section which is evaluated to determine whether to operate further optimisation. The information is transferred between design, fabrication, and structure so that the different parts interact dynamically and efficiently.

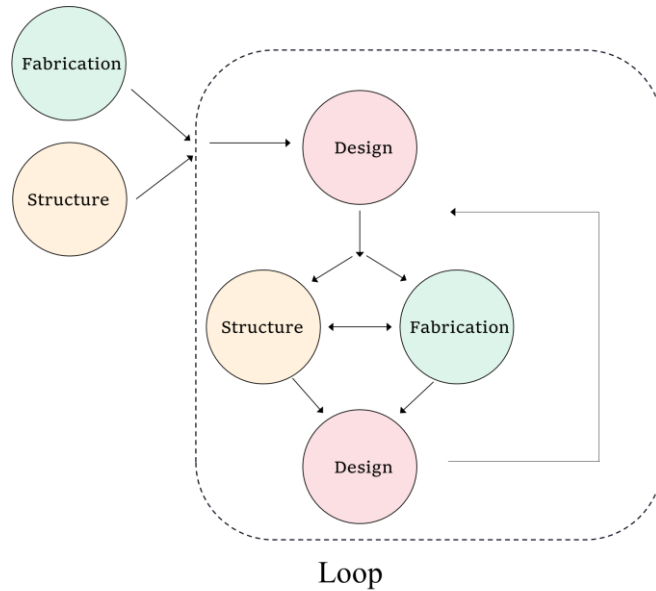


Figure 3.2 Dynamic loop within the workflow

After determining the loop within the workflow to achieve the dynamic information interaction, the robotic-oriented design model is integrated with MOP model, shown as Figure 3.3. The model in figure means the dynamic MOP model under the theories from multi-discipline and taking the constraints of RAC into consideration.

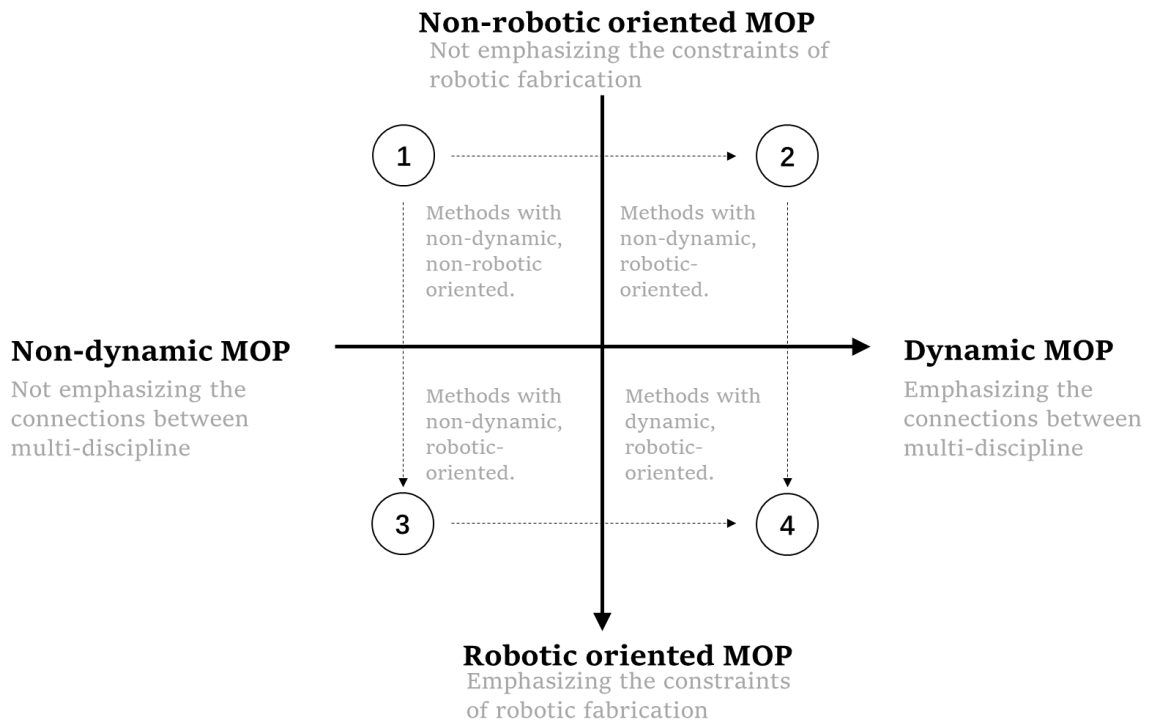


Figure 3.3 Multi-objective robotic oriented model

Together with the dynamic information loop and the robotic-oriented MOP, the comprehensive workflow is shown in Figure 3.4. The workflow has shown three main systems (optimisation, assessment and decision making) and their components separately. The three system compose the dynamic loop to achieve the dynamic data and information interchange.

The RAC-FTS system, which is based on the dynamic multi-objective model, means that the freeform timber structure is oriented by robotic automation construction while taking into account the characteristics (numerical control and visualisation) and limitations (reaching limits, payload). The system's various research contents (morphology design, structure performance, mesh generation and optimisation, and robotic simulation and optimisation) are linked by multi-objective optimisation and evaluation via the digital and numerical model. The system is dynamic, which means that the process of design-optimisation-assessment can continue until the overall performance meets the requirements of the decision-makers.

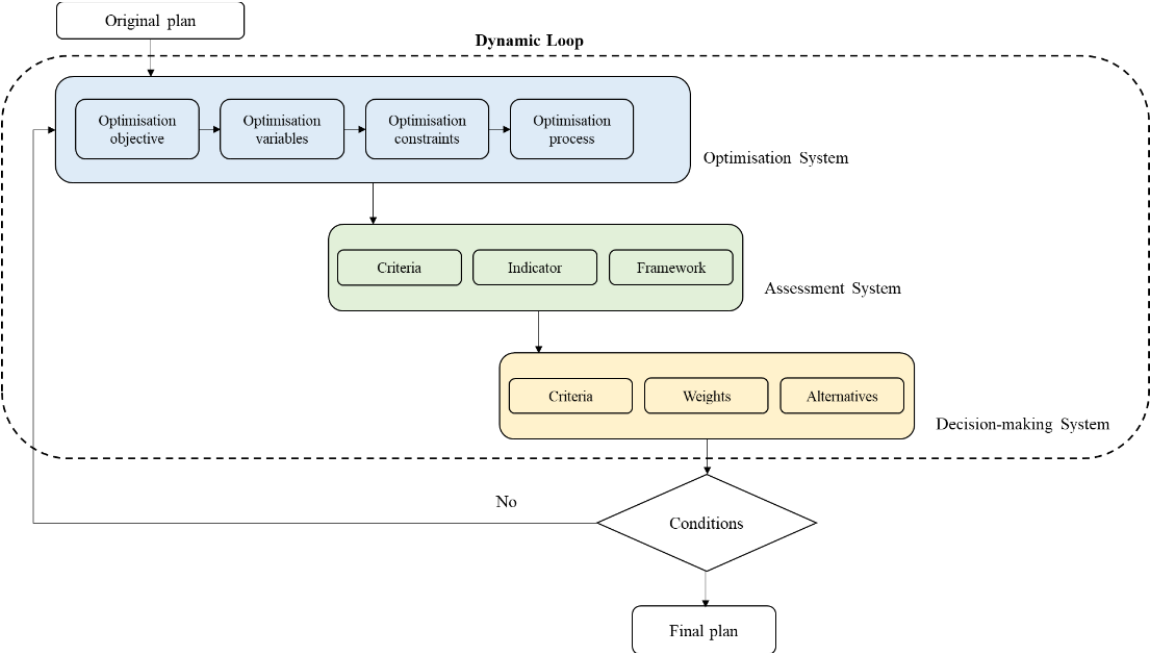


Figure 3.4 Workflow of dynamic MOO for RAC-FTS

3.2 Non-linear interaction between multiple indicators of the RAC-FTS system

The collaborative design of freeform spatial structure and robotic automation construction refers to the collaboration between the robotics system and the various subsystems of the freeform spatial structure, and each subsystem exists as an influencing factor in the design of the freeform timber spatial structure, including the geometric rationality, structure performance, component standardisation level, automation efficiency, etc. The concepts and keywords are summarised in Figure 3.5.

3.2.1 Multiple indicators

FTS is a complex design system, which requires a multidisciplinary and collaborative design. This includes a combination of aesthetic requirements for freeform forms, environmental adaptability, structural stability, and material efficiency. First, the aesthetic evaluation will be one of the essential bases for the overall morphological design of the structure and the layout of the grid (Figure 3.6). Most freeform structures are used for roofing or self-supporting independent structures with ample use space. Therefore, the performance elements such as heat insulation and ventilation, light and shade, ecological

be considered. New lightweight materials will stimulate new structural forms and mesh textures (Figure 3.6). If taken robotic automation technique as another complex system to make up the RAC-FTS, the indicators of this system are classified as follows:

(1) Geometric design: The design in this system refers to the generation of the original geometric form by using different morphological generation methods to generate a geometric surface model with sufficient geometric information, which does not have building information. It is used as the original input for the subsequent morphological optimisation and provides variables for optimisation.

(2) Structure: The freeform surface can be used as a roof structure to bear self-weight and loads such as rain and snow or as a self-supporting independent structure that needs to handle self-weight and other horizontal or vertical loads etc. The inner meaning of the structure includes the stability of the structure.

(3) Material: Materials will be given a more macroscopic connotation in this system, i.e., they will be more actively involved in the overall "design-fabrication-construction" optimal process, based on their physical and material properties, as a significant factor influencing the whole process.

(4) Fabrication: Robotic arm construction includes a range of intelligent construction technologies such as 3D printing, weaving, milling, cutting, etc. Robotic arm machining technology can meet the processing of regular and irregular components and the construction of complex structural forms. Therefore, robotic arm machining technology can be applied to the rapid and accurate production of many standardised or non-standard.

3.2.2 Nexus between design and material, structure

Design and Material

The geometric form of architecture is closely related to structure and material, and the breakthrough of new structural forms is often closely combined with the application of new materials. The interactive development of structures and materials also places new demands on the design of architectural geometry. The architectural firm provides a rational analysis, explanation, and connection between the two elements of material and structure through the language of geometry using mechanical relationships and patterns of the construction organisation. The new materials and structural forms that have emerged expand the possibilities of the architectural form.

Material and Structure

Structural material selection needs to meet the force characteristics. The choice of structural materials should consider the structural loads, force characteristics, and force transfer methods. The selected material type and size can meet the design needs of the structure for material tensile, bending and shear properties. At the same time, under the premise of meeting the force requirements, the building materials are used as effectively as possible to improve the efficiency of the use of materials. The components of the structure are the core of the internal force transmission of the structure, which determines the material force transmission paths and methods. Therefore, the design of structural components and detailing nodes needs to meet mechanics' needs while considering the materials and designing the force transmission paths according to scientific principles.

Design and Structure

The role of freeform surfaces in the structure is divided into support or maintenance two aspects. To avoid focusing on the morphological expression at the expense of the structural rationality and maintenance functions, the morphological expression of the building can be unified with the structural characteristics. In considering the design of structure and form, the excellent performance of the structure proper and respecting the laws of mechanics are the primary principles. The overall design of the structure's form needs to follow the principles of mechanics. Freeform timber structures need to satisfy the architectural expression while achieving the unity of structural form and mechanical codes. First, the overall condition of the structure of various changes in processing should make full use of the laws of mechanics, in line with the transfer of structural forces, which various structural morphology are designed based on. Secondly, the mesh division and texture design of the structure should conform to the transfer logic of the internal force of the structure and follow the transfer path for scientific mesh division and regulation.

3.2.3 Nexus between material, structure, and RAC

Structure and RAC

Construction-aware design strategy coordinates structural properties, material characteristics, unit division, and detailing with geometric form design tools for form generation. This rationalisation process requires geometric calculations to achieve the minimum variation from the original form while meeting panel type control, skin smoothness, cost requirements, etc. Whether the structure is regular or irregular, the design method tools, construction tools, construction process and logic are used throughout architecture development. From CNC machines, rapid prototyping technology to robotic construction, digital construction tools give more possibilities to build non-linear structural forms. On the one hand, digital construction is a tool for the final translation of digital information into physical reality, which is the last stage that non-standardised, non-linear structural forms can achieve. On the other hand, the depth of human-computer interaction and other technologies has prompted architects to be more proactive in delving into innovative applications of traditional structural materials and to develop new structural materials for the realisation of high-performance structural systems. New materials and new construction methods are important driving forces for developing nonlinear structural forms.

Material and RAC

For this research, the concept of "material" in the context of RAC is given a more macro concept based on construction materials. The robotic arm plans the movements of the end-effector in the task of fabrication and construction. The robotic arm platform brings together design, construction, and motion control such as material cutting speed and end-effector operation speed, which are closely related to the material's physical properties and how it is built or processed. The form-finding of the material under the manipulation of the robotic arm is a calculation specific to the material's information about its physical properties. It is reflected in the robotic arm processing during the construction process. In the

traditional design process, the material's physical properties are only reflected in the structural calculations and part of the design process, but not as input in the construction process.

RAC is an essential embodiment of digital construction; the physical properties of materials can be reflected as digital information in the digital construction process. Using the automated platform of the robotic arm, material performance parameters can be collected through simulations and experiments to establish a database, thus reversing the traditional design process in which material is a separate and passive factor and transforming it into active participation in the generation and construction of forms.

The combination of material and RAC expands the logical content of the material. The first is the physical logic of the material, which refers to the study of the material properties, including the inherent properties of the mechanical and physical aspects of the material, such as strength, stiffness, thermoplastic, thermal inertia, and other physical indicators. The study of the processing of the material is used as a basis for the use of the RAC, as it determines how the material is processed, its geometric properties and the way it is connected. The second is the construction logic of the material. With the application of RAC, construction materials from traditional materials to multi-dimensional materials, and new composite materials, digital construction logic is bound to produce new transformations under the development of materials and tools.

3.2.4 Nexus between design and robotic fabrication

To realise the transformation of the design into construction, the plan is placed under the dimension of the building, reflecting the systematic connection between the core elements of architectural design and construction, such as space, form and function. The process of design-build mainly demonstrates the integration of design and construction information. The information related to design and construction is continuously integrated into the building operation project. Both keep influencing each other to improve the design through accurate construction. The most important step from digital design to digital construction is translating and transferring information. With the help of CAD (computer-aided design) related software, the geometry designed does not have architectural details and does not reflect the actual object. For example, in Rhino software, most geometric models' geometric properties are surfaces or polysurfaces and are single-sided, without thickness. Therefore, the corresponding geometric relationships change once the thickness of a single-sided object in the model is given. Therefore, to perform accurate robotic fabrication without changing the original geometry design, architectural information needs to be considered together with the geometry.

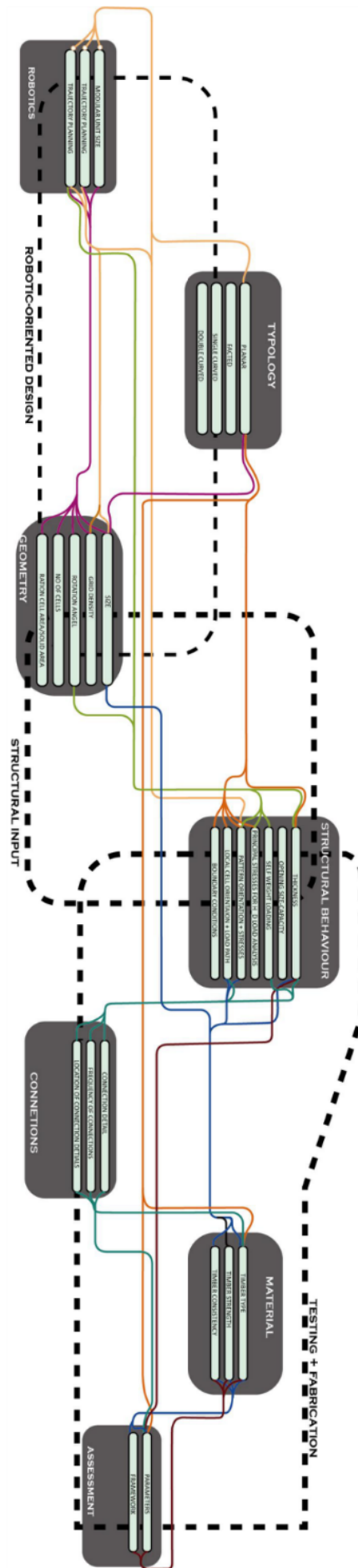


Figure 3.6 Interaction between different indicators

For example, in the BIM software platform, the self-contained BIM information technology tools can translate the structural components into Excel files containing comprehensive information about the features and then pass them to the machining platform for processing and manufacturing. Similarly, the smooth NURBS surface in the Rhino model is not fully realised due to the material properties of the actual building material. Therefore, in solid construction, discrete-continuous planes need to be used instead. Therefore, geometric analysis, geometric reconstruction and geometric optimisation strategies are required in this process. Also, the material properties of the structure and the material will affect the results of the optimisation analysis. In the specific robotic fabrication and construction tasks, complete and accurate geometric information is required in other numerical control machining processes. In this process, the parameters of the geometric elements to be machined and the relationship between each geometric piece are important in converting CAD information to CAM. When facing complex geometric problems such as freeform structures, it is necessary to use the knowledge of complex geometry to reasonably divide and optimise the surface panels. The working conditions in the division process need to be considered in the robot arm's working space range. Thus, the type of panels and the gaps and spacing between panels can be reduced while ensuring the integrity of the surface. These basic panel units need to be numbered, and their composite construction logic and assembly principles are provided.

3.3 Multi-objective design and optimisation principles oriented by robotic automation

In the process of design optimisation, the overall optimisation is in line with the following principles.

3.3.1 Standardisation and Modularisation

The principle of standardisation refers to maximising the homogeneity of components at the construction-oriented level, improving the standardisation and modularity of components, and simplifying the processing process to improve processing efficiency. There are many different sizes and types of components in freeform spatial lattice structures. In sustainable development, diverse parts are not conducive to repetitive machining of robotic arms, which reduces the machining efficiency of robotic arms and leads to energy waste. Therefore, in the optimisation process, a fundamental optimisation principle is to achieve standardisation and modularisation of the components to improve the efficiency of robotic fabrication and more convenient for numbering and management. The concept of modularity is derived from modules and modulus. A module in this section refers to a subsystem with similarity on a structurally consistent basis that contains a multi-level structure of its own, rather than simply referring to a basic timber unit with only material information. Second, the module is semi-autonomous, meaning that the module can be designed independently with full autonomy while following common design principles, i.e., it is a semi-autonomous design element.

By combining architectural design and construction, the scope of application of modules is expanded, either as physical content of structural and functional modules or as virtual content such as technical modules and information modules. According to the definition, modules can be modularised by combining, disassembling, and assembling. Modulus theory focuses on using modules as basic units to create a variety of member combinations through design thinking. The components will be mainly in

bars, panels, and blocks as modules in a freeform timber structure grid. The maximum standardisation and modularisation of component dimensions will be achieved through optimisation in a "design-fabrication-construction" perspective while satisfying the structural variability of freeform surfaces.

3.3.2 Automaticity

The ideal situation for RAC is to realise a workflow from the calibration of the robotic arm to the generation of the toolpath and then to the fabrication and construction process, just like the manufacturing industry, such as vehicle manufacturing. The principle of automaticity refers to the maximum use of automated processing tools for processing and construction, reducing human involvement and intervention in the automated processing and construction process. Automaticity has two primary levels of connotation. The first level refers mainly to the robotic fabrication and construction simulation process. Most of the current robotic arms used in construction often rely on the manual tuning of the tool path to avoid mechanical problems such as kinematic singularities. Such manual involvement reduces the degree of automation of robotic arm processing. Moreover, due to the diversity and variability of the processed components, the processing of components with the same geometry but different sizes require manual involvement for commissioning. Considering robotic arm application to large-scale construction, too much manual intervention will significantly reduce robotic arm processing and construction automation. The second dimension refers to the percentage of the number of robotic fabrication tasks in the whole fabrication process. It is necessary to consider the number of end-effectors needed and robotic arms at this level. For example, a cutting process needs to use a robot arm and a cutting end effector to avoid manual placement or adjustment of the material to be fabricated. Because each time the material is placed manually, the arm needs to be calibrated, which reduces the smoothness and automation of the automated process.

3.3.3 Rationalisation

The principle of rationality refers to the rationality of the geometry's morphology, the design of the components, and the tool path. The rationalisation of the structural morphology of the geometric model requires appropriate form-finding methods which can provide a numerical description of the geometric information. The numerical geometric information extracts important information from the geometric model, thus providing an interactive environment for subsequent morphological adjustments. Morphological rationality requires consideration of both the mechanical performance of the structure and the integrated use of materials. While ensuring the stability and robustness of the structure, the material's mechanical properties are used rationally, and the efficiency of the material is maximised. The rationality of the components means minimising the processing difficulty of the components, i.e., trying to design bars, flat panels, and other ruled surfaces instead of hyperbolic surfaces. Improving the degree of standardisation and modularity of components can effectively reduce the types of components and different sizes of the same type to improve fabrication efficiency. Rationalising the machining path means avoiding kinematic redundancy while avoiding kinematic singularities of the robot arm and improving the manipulating efficiency of the robot arm.

3.3.4 Robustness

The robustness principle includes the robustness of the structure at the micro-level and the robustness of the overall optimised design process at the macro level. The robustness of the structure refers to the stability of the structure and the rationality of the geometry design. The robustness of the optimisation process refers to the smooth exchange and transfer of information between systems, and the optimisation algorithm can effectively carry out the optimisation process within the constraints of the optimisation objective.

3.3.5 Digitalisation

The principle of digitisation is the digitisation of structure and construction information, the realisation of digital processes through digital design software and platforms, and the connotation of digital processes. The complete digital building design process should include three components: design, digital off-site prefabrication and on-site construction. There will be two data interfacing and interaction times in this digital process, and this data transfer is the key part of the digital construction. From a methodological point of view, digital design is a target problem-oriented design approach, most notably by parametrically translating the factors that influence the design of a solution so that the problem can be solved. And the designer generates a design solution that meets the design requirements by establishing functional relationships and iteratively adjusting the parameters.

3.4 Design strategies of the RAC-FTS

3.4.1 Comprehensive geometric form evaluation method

In creating the morphology of a freeform structure, the evaluation method for structural, mechanical rationality will directly impact the outcome of the morphology. The objective of developing freeform structures is to obtain robust and reasonable structures, and how to determine the quantitative evaluation of structural rationality is an important research question. This is because the mechanical performance of the structure involves many aspects, such as static force, dynamic force, stability, and so on; correspondingly, the evaluation indicators for these aspects differ from each other. Most structural designs are currently focused on one factor of the design, after which other factors are tested and adjusted. This idea is also used in this research, which uses static performance to assess the structure's rationality.

As for the optimal methods, there are two types of evaluation methods: multi-objective optimisation and single-objective optimisation. Multi-objective optimisation refers to the simultaneous optimisation for multiple mechanical performance indicators. In contrast, single-objective optimisation optimises the primary objective function while also investigating the variation of other mechanical properties.

To achieve the optimisation for freeform structural morphology, three factors in the whole process need consideration: (1) Geometry design method and numerical description; (2) Evaluation of structural rationality; (3) Morphological optimisation algorithm.

The selection needs to be the scalar for better results comparison in the optimal process. Another problem is the data conversion. The relations between the geometric freeform surface and the optimal objectives need to be described in numerical expressions. The geometry is visual and adjustable in the modelling software for freeform surfaces like Rhino, and information needs conversion for numerical optimisation in software like Matlab.

3.4.2 Fitted design of components

The freeform structure is a multi-component system that relies on tension and pressure between the components. Through the vector mechanism, the decomposition of the force can be performed on a surface or in a three-dimensional orientation. In nonlinear architectural design, the structural grid formed by the structural elements has more freedom, and its infinite form shaping power can be realised. In the process of topology optimisation of freeform mesh structures, the arrangement of the mesh's components (bars, panels, etc.), the arrangement of the nodes, and the mesh's distribution are all elements that can be optimised. After generating and optimising the meshing process for the freeform surface, the mesh is endowed with building information to become structural components. Fitted design methods for components means satisfying the modular design principles and optimising the components into easy and possible to fabricate by robotic arms. Once the meshing strategy has been defined, design the specific subdivision of the components, i.e., the componentisation strategy. The subdivision of components affects the cost of construction to a large extent and directly reflects in the appearance of the building. A good component strategy is the result of both technical and artistic factors. Especially for freeform buildings, the study of componentisation strategy is critical because the manufacturing process of curved surfaces is very complicated. Each part of the freeform surface may be different, making the manufacturing of components very difficult, so component manufacturing should be reduced as much as possible under the premise of fully expressing the design idea.

3.4.3 Highly efficient timber fabrication

The interplay of robotic construction and material calculations can provide new form-finding logic and algorithms for design. This new process-driven design focuses on the relationship between form-generating, construction processes and materials. The material is also considered an influence and driver of the morphogenesis under the new process. The robotic arm effectively links design and fabrication through a digital model, a complete computational model. This continuous model objectively requires that the fabrication and construction process maximise the physical properties of the materials and the laws of construction to reduce manual intervention in the construction process and achieve its construction efficiency. In applying materials from passive to active participation in the raw form process. At the same time, for different materials, it is necessary to develop and design processing tools according to their different material properties. For example, appropriate cutting and milling tools are selected for plate CLT materials, and appropriate force control is performed to avoid damaging the material. For raw wood, the end-effort tool should be used to carry out the task of cutting or cutting.

3.4.4 Smooth Robotic Trajectories

In the fabrication process of the robot arm, the tool path and the robotic motion control method are often not optimal to avoid kinematic singularities, collision, and other situations. This type of fabrication reduces the efficiency of the robot arm, resulting in a waste of energy and even causing some mechanical damage to the arm. Therefore, based on "design-optimisation-machining-build", after completing the design of components of freeform structure, considering the fabrication method (like cutting, drilling), the generated tool path and the control method for the robot arm need to be optimised to shorten the movement time, to avoid collision between the end-effector and the material or other surroundings in the working space, and to reduce energy loss. The material can be protected by reasonable force control of the end-effector.

3.5 Synergetic methodology for RAC-FTS system

3.5.1 Digital design method

Numerical models include geometric models, optimisation models, structural models, fabrication models, etc. The study of the structural morphology of freeform surfaces aims to achieve unity between geometric forms' diversity and structural expression's rationality. To this is added the accuracy of processing and construction of robotic arms. Currently, computer graphics technology is the main means of creating freeform forms. Structural optimisation methods predicated on numerical calculation techniques effectively achieve structural rationalisation for freeform surfaces. Due to the diversity of freeform surface generation methods, a unified mathematical description of freeform surfaces is required to establish morphology creation methods applicable to different surface structures, which provides the entry conditions for freeform structural morphology creation. Geometric modelling is the basis for creating the morphology of freeform structures and provides the optimisation variables for freeform surface morphology. The choice of geometric modelling method needs to express various surface shapes and can be expressed in a unified mathematical form with fewer control variables to improve the computational efficiency of morphology optimisation. Also, considering the commonly used CAD software, the geometric modelling method should be easy to coordinate with its modelling method, thus facilitating the portability and expansion of this geometric modelling method.

3.5.2 Digital design process

Traditional design methods do not balance the design and construction of complex freeform structures that include multiple influencing factors. The digital platform, supported by computer technology, can improve the efficiency and accuracy of design-build collaboration through a multidisciplinary and coordinated digital platform. Digital freeform "design-optimisation-fabrication-build" is different from the traditional design approach: a unidirectional linear relationship between architecture, structure, and processing. The digital design approach is a collaborative consideration and design of all aspects of information through a digital design platform, enabling real-time information interaction.

3.5.3 Building Information Model Platform Environment

The BIM platform realises the data interfacing of different phases and plays the role of integrating data and information flow, which makes multi-system construction possible. The parametric, integrated, standardised, and full lifecycle support features of the BIM platform provide important support for building design and construction integration. Complex buildings, such as freeform structures, require a new production model, so the construction field also wants to learn from the digital manufacturing technology in industrial manufacturing to meet the needs of parametric structure construction.

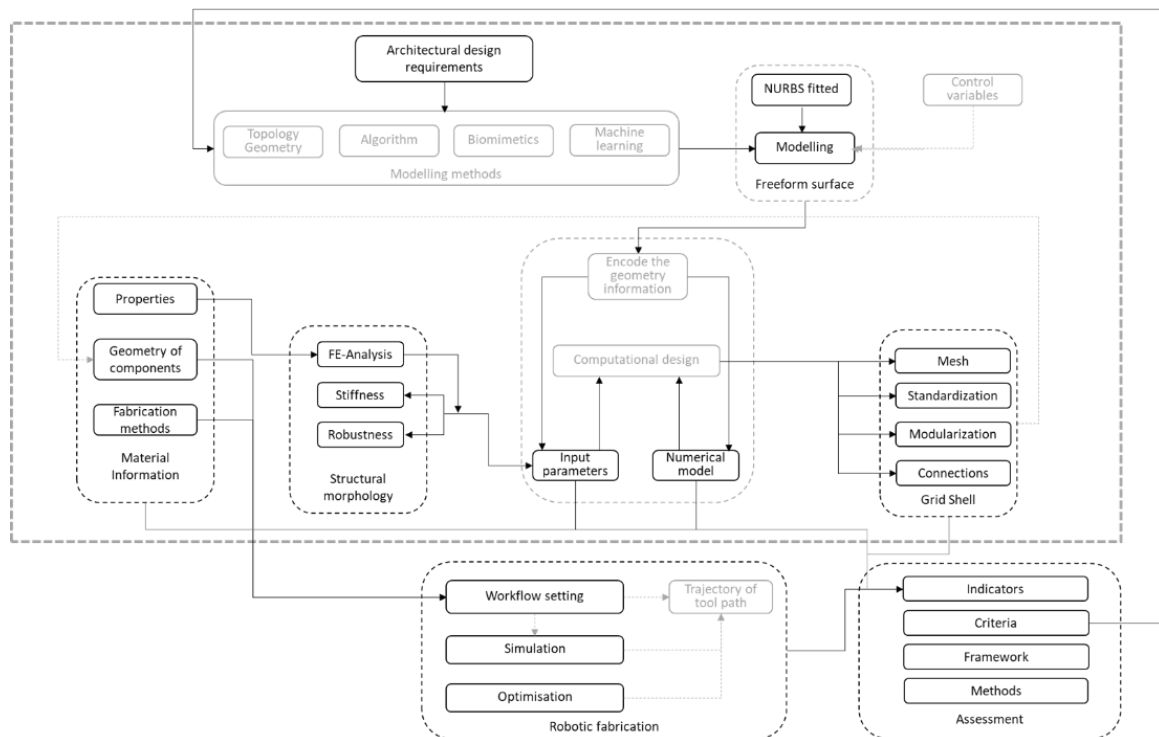


Figure 3.7 Computational digital design system

Digital construction in architecture is also not only for the construction phase but also covers the whole process from the initial conceptual design of a project to the final successful implementation. Among them, the establishment of a building information model is the key. As the building information model integrates all the information in building design and construction, it provides information support for the digital structure later. One of the main problems that need to be solved for RAC and FTS to form a sound system is the problem of data coordination. BIM platforms can effectively solve the problem of data coordination between virtual construction and physical construction. It has a robust information classification management function and can directly interface with the manufacturing side. It can solve the data coordination problem from digital virtual construction to factory prefabrication.

3.5.4 Digital software environment

The architectural high-dimensional multi-objective optimisation platform is based on the architectural high-dimensional multi-objective optimisation process mentioned above, with the architect as the main user. Other professionals can use it, such as materials, structures, robotic arm automation, etc. The RAC-FTS system in this research is designed to provide a platform for building information optimisation in response to the multidisciplinary conceptual design phase and the need to optimise building performance.

The application of the BIM software system allows for efficient and intuitive control of the design process and the results generated in its form while also providing more accurate information for digital construction (Figure 3.8). The BIM platform is a three-dimensional visualisation platform that can meet all aspects of the expression of the building form and can also carry out specific parametric design through its parameterisation function. However, different parametric software or programming environments are needed to achieve overall complex design and construction on the BIM platform.

BIM can be utilised as the base software environment, making full use of the coordination and adaptability of other software with BIM, coordinating, and interfacing the data of RAC and FTS, and effectively taking advantage of each software. The platform takes Building Information Model as a multi-software carrier, integrates various functional types of software including numerical programming, building modelling, building performance simulation, tool path generation, robotic arm optimisation, etc. and suitable interfaces or easy-to-develop APIs to complete the modular design of each program under the platform, making the venue convenient for multidisciplinary crossover, data transfer, and data protection, easy operation, and realisation of a high-dimensional multi-objective optimisation process. The standard approach in architecture is to combine the design and optimisation platform by choosing Rhino + Grasshopper parametric modelling environment, which is a convenient and efficient modelling environment and the existence of many rich optimisation plug-ins based on those applicable to Grasshopper. The parametric modelling approach provides dynamic control over the building geometry and component information in the architectural design phase, allowing designers to quickly change design parameters and evaluate the adjusted solution, resulting in a rich solution design. Revit and Fusion 360 are used to simulate machining and generate preliminary machining methods and paths and visualise the machining process in a robotic arm simulation environment such as KUKA|prc. The arm's pose parameters are imported into Matlab for motion control optimisation, and the optimised machining path information is finally imported into a robot arm language adapted software (e.g., RoboDK).

3.6 Assessment and decision-making system of RAC-FTS

Multi-objective optimisation algorithms produce a series of optimisation results that allow users to make appropriate solution selections according to different project needs. To make better decisions for solution selection, a reasonable evaluation method and system can be designed for the multi-objective optimisation system, and an effective decision system can be developed.

3.6.1 Assessment framework and methodology

A reasonable evaluation of optimisation results is required before the decision-making process is carried out. Optimisation evaluation for high-dimensional multi-objective requires establishing a suitable index framework, selecting indicators, determining indicators, and establishing the index system in combination with the research characteristics of this paper. When establishing the evaluation system, the following principles need to be considered.

- (1) **Comprehensiveness principle:** The evaluation index framework is established to cover the whole process of RAC-FTS from the design to the construction stage as far as possible (operation and maintenance and dismantling in the later use stage are not considered).
- (2) **Hierarchy principle:** The evaluation framework needs to have a clear hierarchy, with apparent subordination between upper and lower levels, to avoid overlapping the same levels as much as possible. Each level of the index system can comprehensively contain the characteristics of its level, and each level should have a corresponding affiliation relationship.

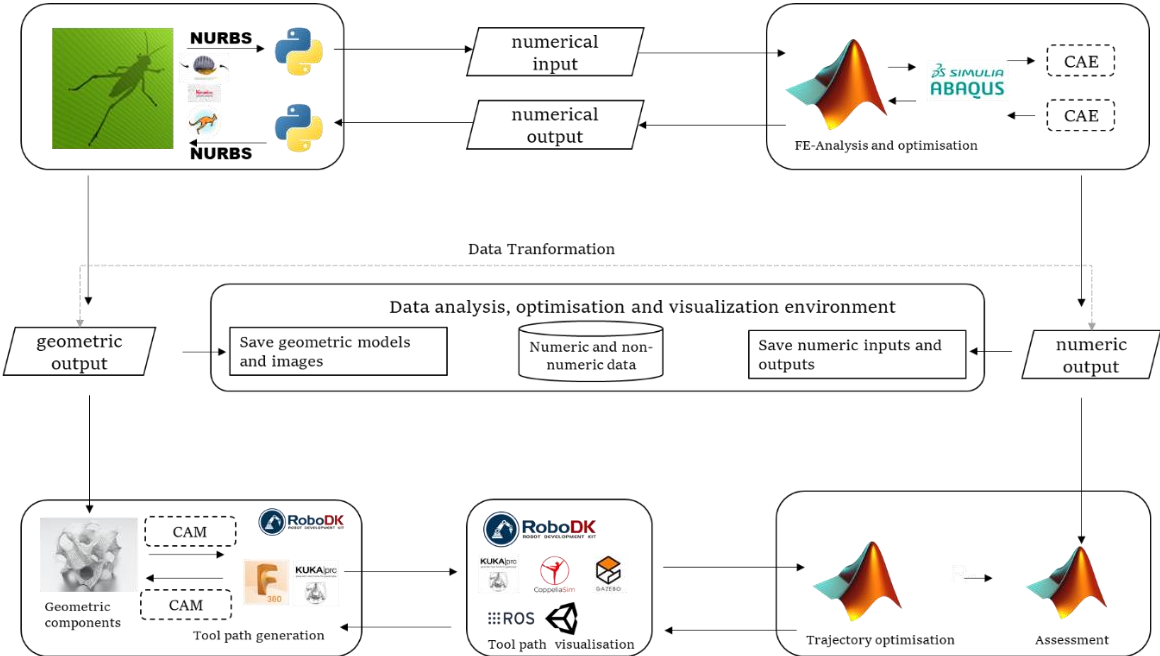


Figure 3.8 Software for data transformation

- (3) **Operability principle:** Considering that the evaluation system needs to be calculated, it is necessary to obtain sufficient data (qualitative or quantitative) for each indicator system to ensure the evaluation system's operability when constructing the indicator system at each level.
- (4) **Practicality principle:** The evaluation system should focus on the current development status of robotic arm processing and construction, linking theory with practice so that the evaluation system can objectively evaluate RAC- FTS from various aspects, thus providing an essential reference for the application of robotic arm in large-scale construction.

In establishing the index framework, it is necessary to select the evaluation target layer (A) and the criterion layer (B) of the evaluation system. The target evaluation layer is the evaluation system of design-optimisation-processing-build for RAC-FTS. Starting from the segmentation of the whole life cycle of the building, the industrialisation process of the building is divided into a criterion layer (B). At the same time, to fit the characteristics of industrialisation and the digital information transfer that should be available in the digital process, the efficiency of information flow transfer needs to be added. Because the system covers many disciplines and the relationship is complex and involves many factors, this evaluation framework mainly hopes to lay the foundation for the subsequent index layer (C) setting through a clear and explicit division. After the evaluation indexes are determined, a suitable evaluation

method is selected for reasonable evaluation by combining international evaluation standards as a reference and basis (Figure 3.9).

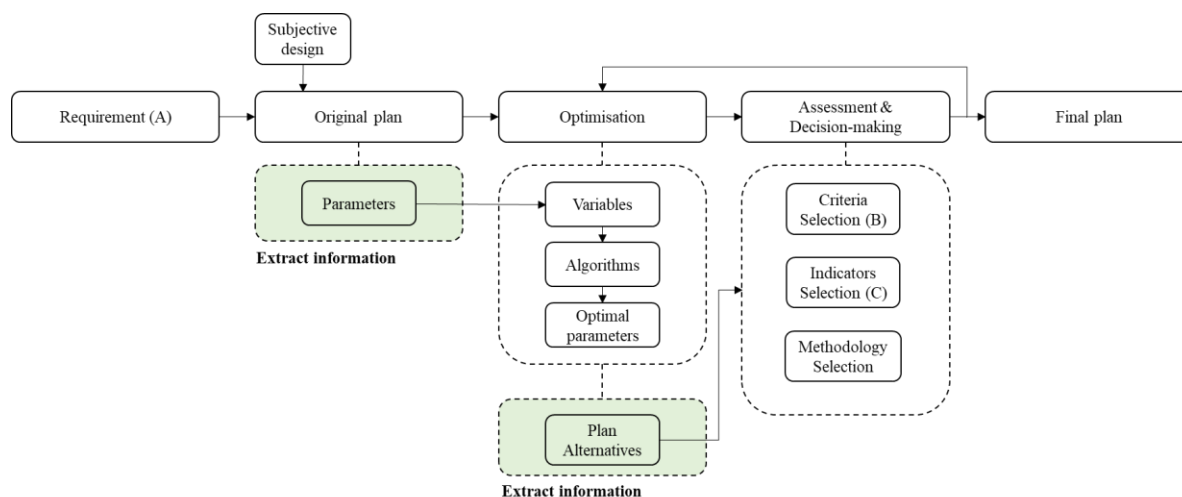


Figure 3.9 Function of Assessment

3.6.2 Decision-making Support System

The non-dominated solution obtained from the high-dimensional multi-objective optimisation of the building is the object of decision analysis in the study, which consists of two parts of data: optimisation objectives and optimal parameters. Most of the existing studies analyse only their building optimisation information objectives and ignore the characteristics of building design parameters when comparing the decision among non-dominated solutions. This is mainly because most building multi-objective studies focus on the degree of improvement of building performance objectives. For this study, the four main components of design, material, structure and processing are covered: multi-attribute decision problems. Two central issues need to be solved for the multi-attribute decision problem in this study: 1) to determine the attribute values of the solution with the optimisation objective in the orientation; 2) to determine the attributes and the corresponding weights and combine them with the attribute values of the solution to obtain the comprehensive value of the solution. And the decision support system needs to have the following functions.

- (1) Collating and making available the various data of the system promptly related to decision-making issues.
- (2) Collect, store, and promptly make a variety of data outside the system relevant to this decision problem.
- (3) Collect, manage, and provide feedback on implementing various decision-making programs.
- (4) Ability to store in some way and manage various mathematical models related to decision making.
- (5) Ability to store and provide common mathematical, optimisation and operations research methods.
- (6) The above data, model, and method management should be easy to modify and add. For example, the change of data schema, the connection or modification of models, the modification of various methods.
- (7) Ability to flexibly apply models and methods to process, aggregate, analyse and forecast data to produce the required comprehensive and predictive information.

(8) Provide good data communication function to collect and process data in real-time as much as possible to send to users.

3.7 Conclusion

This chapter introduces the RAC-FTS system, which is defined as a dynamic and multi-objective optimisation system for fabrication tasks that includes freeform design morphology, structure performance, mesh generation and optimisation, robotic simulation, and motion control optimisation. The RAC-FTS system aims to establish a workflow to improve the structure, material, and fabrication rationality of freeform timber structures constructed using robotic automation techniques.

The emphasis of this chapter is to present the theoretical framework of the full paper, i.e., a robotic arm-oriented design and evaluation system for dynamic multi-objective optimisation. A general introduction to the multi-objective optimisation problem is presented, and a multi-objective optimisation process based on RAC-FTS, which is the focus of this chapter, is proposed. Combined with the dynamic feedback mechanism, a complete workflow including optimisation, evaluation, and decision-making is constructed in this paper. By summarizing the complex indicators of the RAC-FTS system and the complex nonlinear relationships between different indicators, standardisation, automaticity, robustness and digital are proposed as the principles. The design strategy, digitalisation as the core design method and software ecosystem are proposed accordingly. Finally, the role of the assessment system and the general process and framework are introduced. The following chapters working on freeform morphology design, structural performance optimisation, mesh optimisation and robotic optimisation would follow the principles as the optimisation objectives.

Chapter 4

Robotic Timber Fabrication-Case Study

There are already a range of robotic timber fabrication cases by using different tools (cutting, milling, drilling, and sewing, etc.) introduced in Chapter 2. However, in these cases, the robot is used as a tool to process non-standard forms. However, several aspects of robotics, such as dynamics, motion control, and trajectory planning, are not thoroughly discussed, and issues such as low accuracy and singularities can arise. This chapter aims to connect the fundamental principles of robotic arm control to actual robotic arm manipulation through the use of two case studies. A robotic arm's actual machining is to move between planned points to complete a specified job, and this basic point-to-point movement is distinguished between straight lines and curves. This chapter focuses on how to connect a 3D design model with point-to-point control of a robotic arm.

To have a better understanding of the process of Robotic Automation technique applied in construction, the common applications of robot arms need detailed exploration, from the specific operations of the robot arms to macro-level of the Robotic Automation Construction system (RAC). This means to give clear connections between the workflow organization, software platform, management, tool development, numbers of the robots, to the exact orders the end-effectors are given, which is from a macro level to micro one. One four-axis and six-axis robot are assembled to have the first impression of how the robot arm moves, how are they controlled and how are they different from the industrial robot. After that one case of the application of the industrial robot is introduced to give an overall impression for every aspect needs to be considered to finish one robotic fabrication technique. The roadmap for this chapter is shown in Figure 4.1.

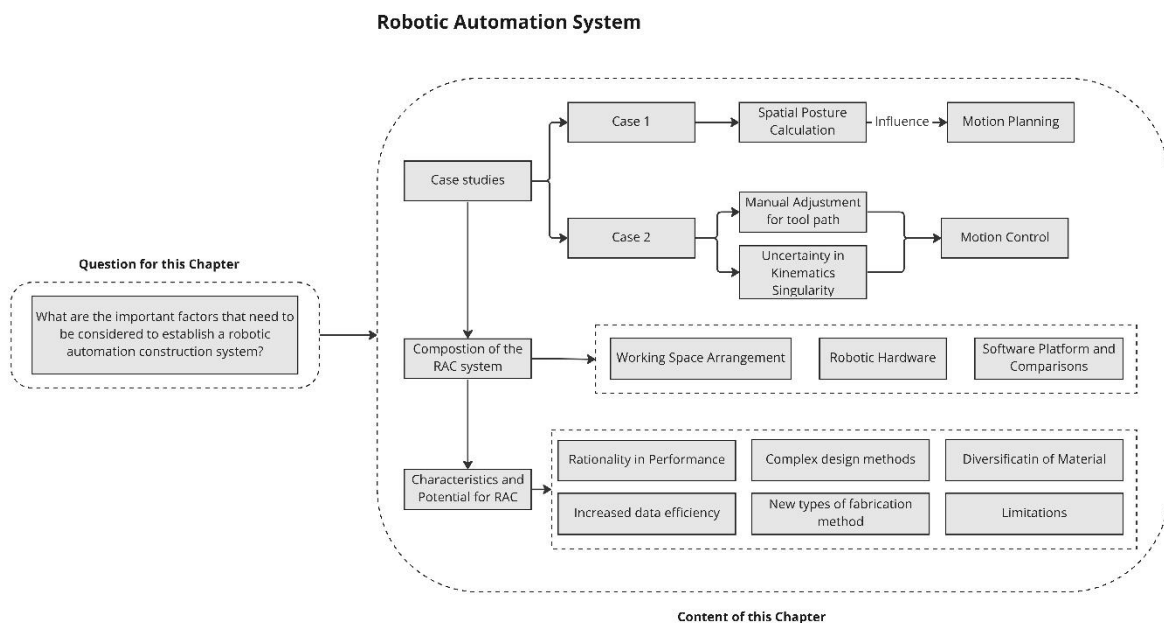


Figure 4.1 Roadmap for Chapter 4

4.1 Robot arm and industrial robot

4.1.1 Self-assembly robot and control system

The 4-axis and 6-axis robot arms are assembled by links and bolts, motivated by the motors shown in Figure 4.2. The most important part is to control the manipulator. Arduino board is widely applied to control the simple robot for its capability of creating device actuators that use sensors to interact with the environment through a different programming language. Arduino also has APIs for different software environments like Matlab, processing for Arduino provides an integrated development environment (IDE) platform written in Java for Windows, macOS, and Linux. The programming language used in Arduino IDE is like C and C++ and provides a software library containing common input/output functions.



Figure 4.2 The layout of Arduino IDE



Figure 4.3 One example of Arduino program

There are several basic components and supplies are needed to operate the robot arm: 1) Arduino board, 2) breadboard, 3) jumper wires, 4) resistor, 5) LED, and 6) servo motors shown in Figure 4.3. Arduino and the robot arm are connected through the wires between the motors on robot arm to the equipped digital and analog input/output (I/O) pins on the Arduino board through the breadboard, shown in Figure 4.4. The Arduino pins are labelled with different numbers to facilitate the identification of input signals for various motors.

- The red wire of the servo is the positive supply, and is connected to the 5V if the Arduino
- The brown wire is the negative supply and should be connected to the ground line.
- The orange wire is the control line and should be connected to a PWM enabled I/O pin on the Arduino board, in this example, pin 9.

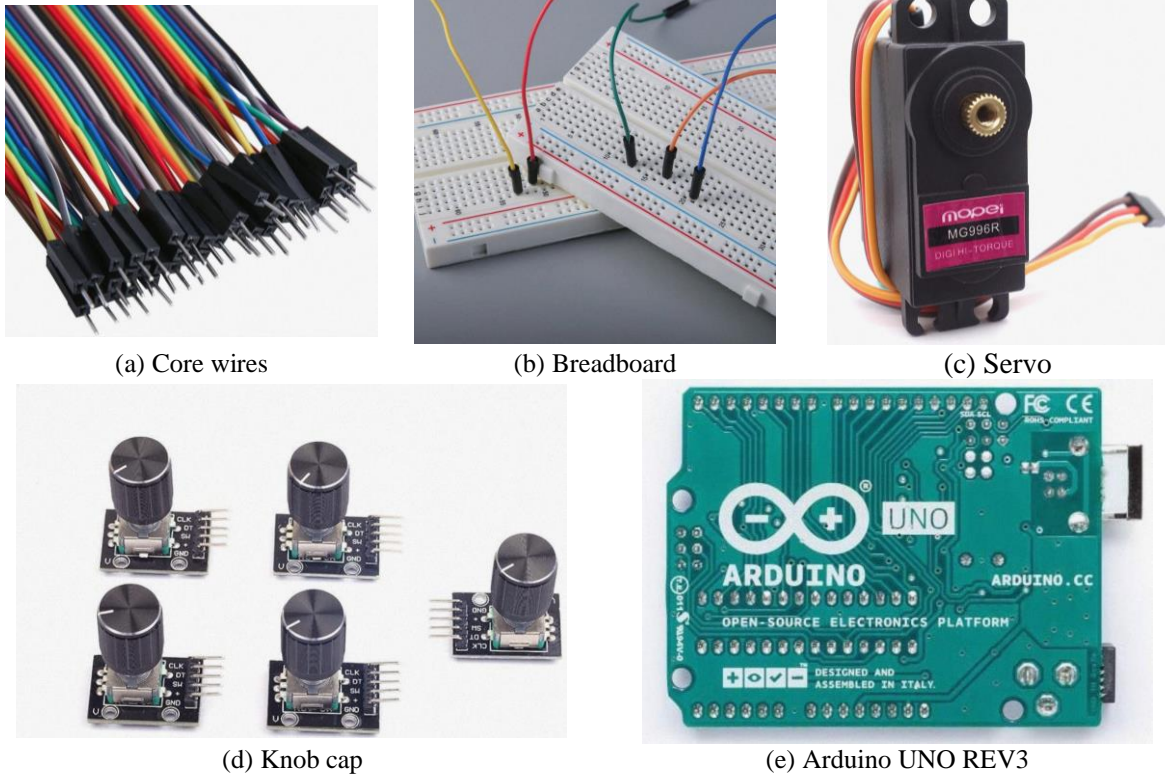


Figure 4.4 Essential kits for operating the robot

Each servo motor has three wires which the red one connects to the positive electrode, the black one to the negative electrode and the yellow one is the signal wire. The yellow signal one is connected to the digital interface on the Arduino board shown in Figure 4.5.

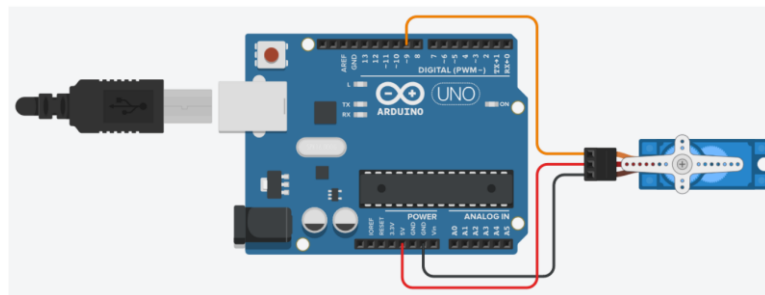


Figure 4.5 Control the servomotor through Arduino

There are two self-assembled robots being used for practical tests to have a better understanding of the mechanism of control and movement of robot arm. The two self-assembled robot are 4-DOF (degree of freedom) and 6-DOF respectively (Figure 4.6-Figure 4.7). The robot arm is controlled manually and automatically taking the led as the operating signal.

Figure 4.8 shows the simple manipulation system of the 4-DOF robot arm. The robot is controlled by the programs in Arduino IDE through the Arduino UNO board through the USB cable connected to the computer. After connecting the servos with the control board through the core wires plugged in the pins of the control board and the breadboard, the robot can rotate through the demands from the program. The LEDs on the breadboard give instructions of the receiving the operating signal. The real connection is shown in Figure 4.9 and the program is the one shown in Figure 4.3.



Figure 4.6 A four-axis robot arm



Figure 4.7 A six-axis robot arm

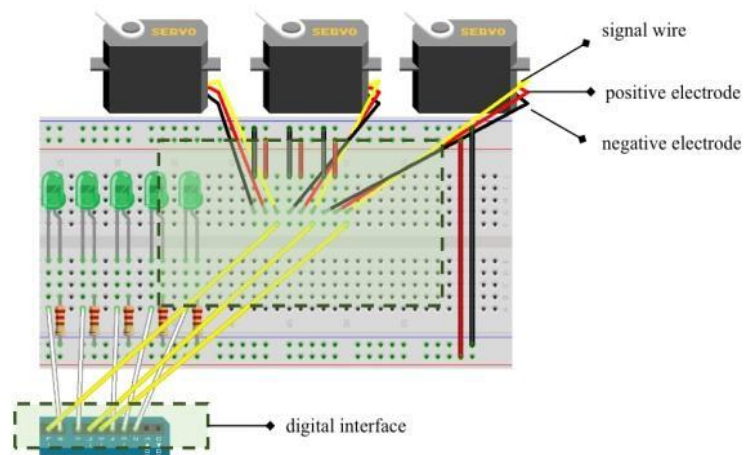


Figure 4.8 Three servo motors connect to the Arduino board

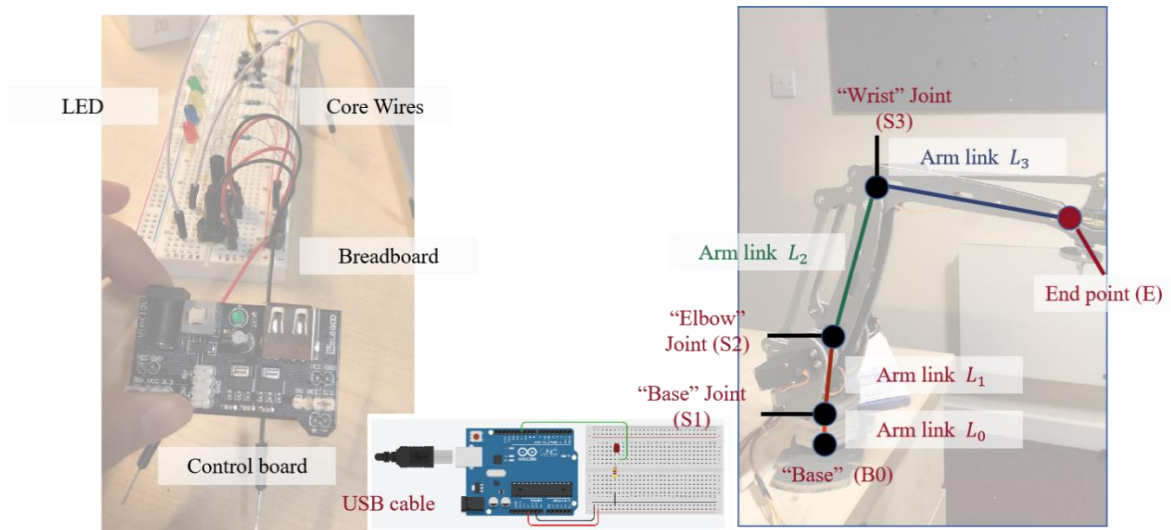


Figure 4.9 Simple connection of the control board and 4-DOF robot arm

4.1.2 Examples and questions

One example of controlling the robot is shown in Figure 4.10. This example is to operate the robot arm moving around by pressing the buttons.

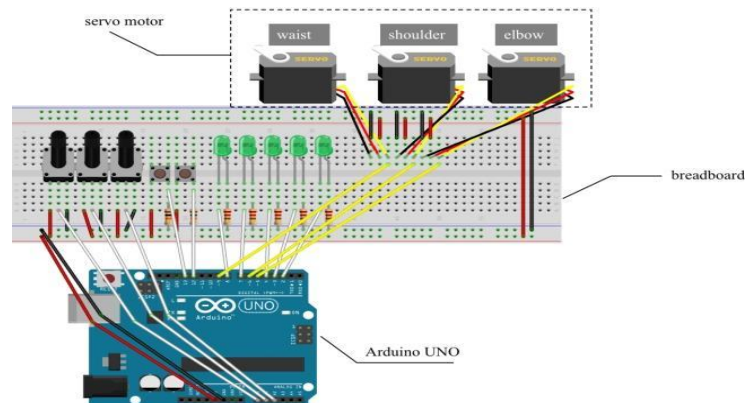


Figure 4.10 Schematic of the Arduino board to control the robot by buttons

In this test, one thing can be observed obviously is that the robot moves one axis by one rather than different axes moving together. This is because the control is one-way control rather than parallel control. So, the axis acts according to the instructions in the programming line by line. This is one main difference from the industrial robot. Industrial robot is much more developed which is a comprehensive technological system that integrates mechanics, electronics, automatic control, computers, artificial intelligence, and other multi-disciplinary fields. Robotics studies how to use machinery, sensors, drives, and computers to achieve certain aspects of human functions which is the supporting technological theory for industrial robot. Obviously, this is a tough task, and it must use research ideas in various "traditional" fields to achieve "non-traditional" objectives. There are many different types of robot arm (cartesian robot, SCARA, delta, etc.,) in different brands in various size, weight, and degree-of-freedom (DOF). The most used industrial robot arms are from KUKA, ABB and Universal.

Another question found when operating the robot is that the end of the robot arm cannot move in straight lines without manual control, instead in circular ways (Figure 4.11). In Figure 4.11, the three lines shows two reference points on the cylinder, and the circle in yellow shows the position of the end-effector. As the distance between the reference points of the end-effector changes, so does the distance between the end-effector and the cylinder. Four movements present the end-effector moves along the cylinder but not in the straight line on the cylinder. One reason for this scenario is that multiple joints cannot move at the same time because the control pad can only control one motor at a time.

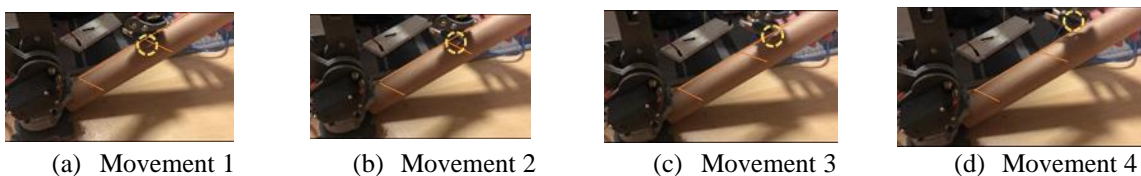


Figure 4.11 Circular movement of single joint movement

Apart from the reason for that the joints of the robot don't move simultaneous; the articulated joint operates circular motions with the point of articulation as the centre of the circle. In more details, the

links of the robot can be simplified as the lines shown in Figure 4.12. Two arms in length L_1 and L_2 are connected by the articulated joint, then the end position of this two-dimensional arm (x, y) is determined by the angles θ_1 and θ_2 , as well as by the length of these two arms. The end of link L_2 moves within the range $|L_1 - L_2| \leq \sqrt{X^2 + Y^2} \leq L_1 + L_2$, shown in Figure 4.13.

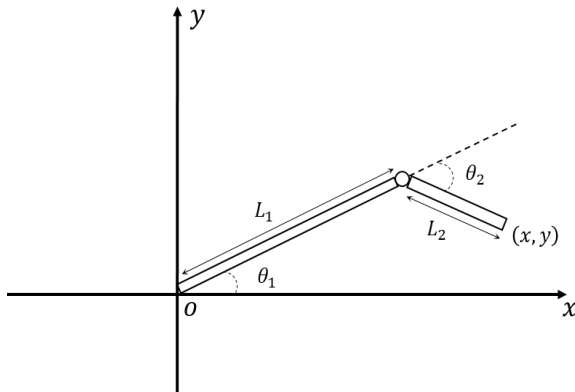


Figure 4.12 Simplified two-link model shown in two-dimension

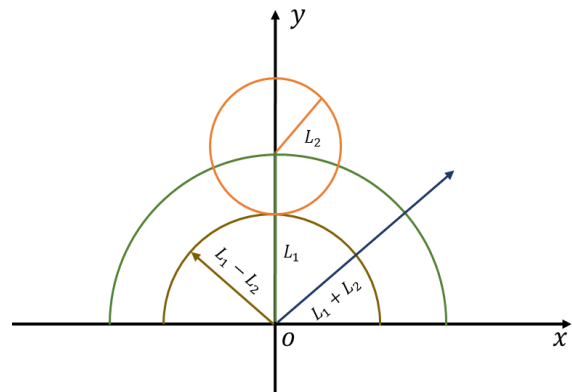


Figure 4.13 Reachable space of the two-link robot

The coordinate of the end point (x, y) can be derived:

$$\theta_3 = 90 - \theta_1 \quad (4.1)$$

$$x = L_1 \cos(\theta_1) + L_2 \sin(\theta_2 + \theta_3) \quad (4.2)$$

$$y = L_1 \sin(\theta_1) + L_2 \cos(\theta_3 + \theta_2) \quad (4.3)$$

Based on the equation 4.1-4.3, the movement of two-link robot arm in two-dimension can be simulated. Figure 4.15 shows one position of the two-link robot arm during the simulation in Processing IDE while the two links can move simultaneously.

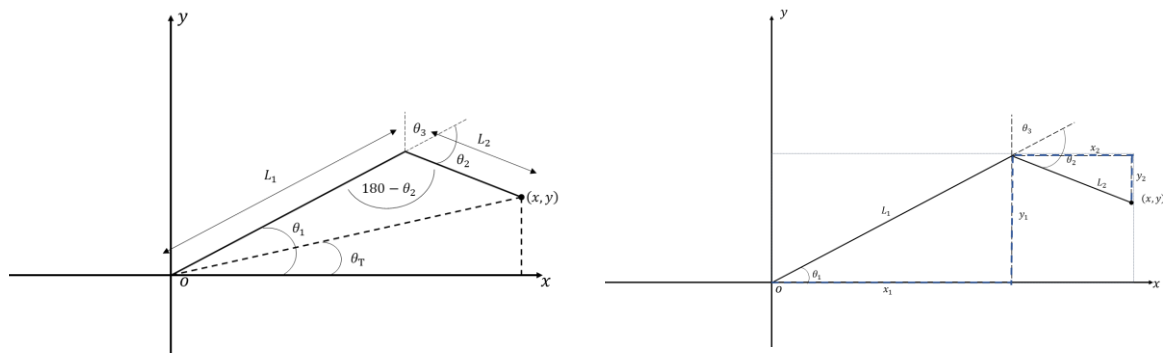


Figure 4.14 o-xy Coordinate for the robot arm

If expand the 2D model into 3D model, the coordinate (x, y) turns into (x, y, z) , shown in Figure 4.16. The same as Eq. (4.1) -(4.3):

Then, based on the value of W , find the values of X and Z .

$$Z = W \sin(\theta_4) \quad (4.6)$$

$$X = W \cos(\theta_4) \quad (4.7)$$



Figure 4.15 Two-link model built in processing

According to the Eq. (4.4) to (4.7), to control the assembled robot to move from one designated point to another point in three-dimension space, precise coordinates of the positions need to be determined by accurate computation. Furthermore, to designate the end of the robot to move in a straight line from a to b , the positions and orientations of the two arms changes all the time. The ideal situation is to rotate the link 1 and link 2 together to move the end point from a to b directly. As the Arduino can only process one direction at a time, the linear movement can only be controlled by rotate link 1 from P_1 to P_2 and then rotate link 2 from a^* to point b .

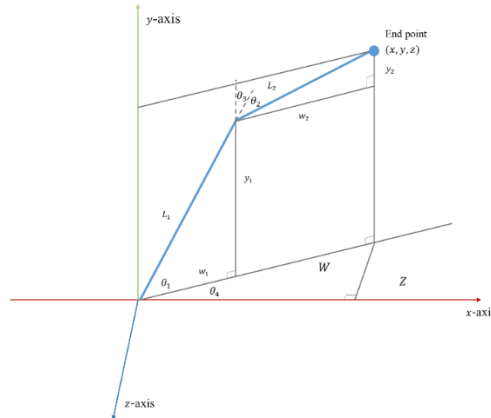
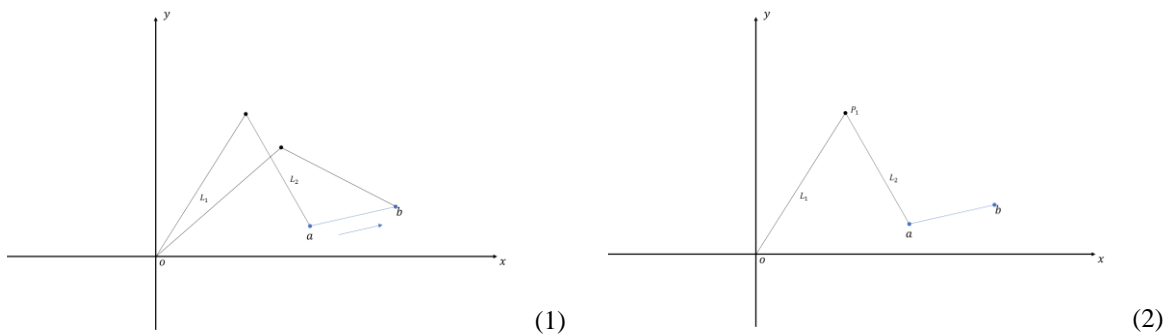
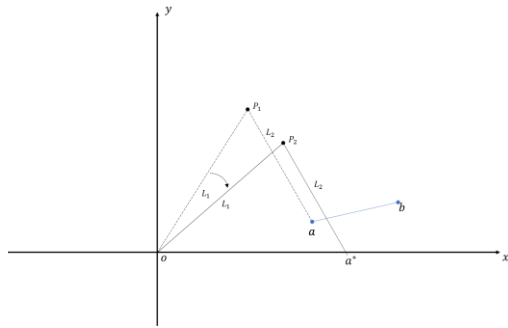
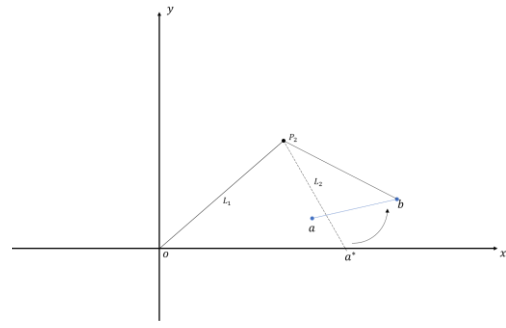


Figure 4.16 Diagram for 3D two-link robot arm





(3)



(4)

Figure 4.17 Steps for controlling the robot to move from a to b

The main difficulty for the task is to determine the position of P_1 and the rotation angle for link 1 and link 2. For industrial robot, as they have parallel automatic control system, the end can move in straight lines by controlling different links and axes at the same time. To fully understand the applications of robot arm in robotic timber fabrication, one practice is introduced in the following part to demonstrate the detailed steps of operations and control.

4.2 Robotic chainsaw cutting

The practice was taken place in a workshop hold in ETH. The aim of the task was to use the chainsaw to cut the raw wood trunk into the designed irregular timber joint. The whole process includes 1) working space setting, 2) scanning of the raw wood, 3) design work, 4) setting and simulating of the robot arm, 5) transfer the simulations into KRC which is a programming language for KUKA robot, 6) fabrication process.



Figure 4.18 Robotic Chainsaw cutting working space

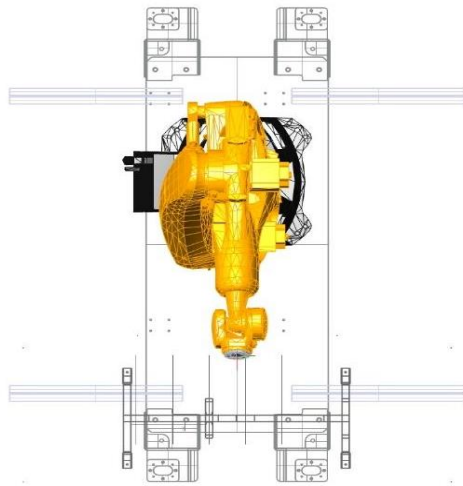


Figure 4.19 Wood joint cutting by the robotic chainsaw from the log

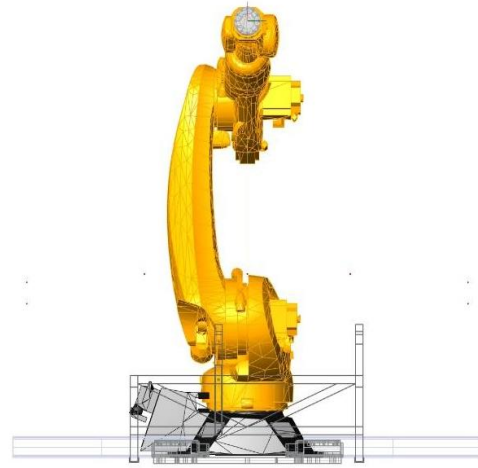
Figure 4.18 and Figure 4.19 presented the robotic chainsaw cutting workspace arrangement and the timber joinery cut results by the robotic chainsaw.

4.2.1 Preparation for the geometry and fabrication

The first step of the robotic fabrication is to organize the working space, shown in Figure 4.20 (a)-(d). The working space includes a stable holding structure for the trunk, which is fixed to the ground, a KUKA KR16 robot arm connected to the robot controller with a cable and is controlled by the teach pendant. The planar chainsaw and a 3D scanner are mounted to the robot. After setting up the robot base and the holding structure, a calibration process is needed. In this working cell, there are five coordinates (shown in Figure 4.21): the world, robot base, robot end, the base, and the tool coordinate. The world coordinate system is permanent in Cartesian system, and it is the base coordinate for the whole working space. The robot coordinate is located at the bottom of the robot, and it is relative to the world coordinate. The base coordinate defines the position of the workpieces which is the centre of trunk in this case. The tool coordinate and the robot end coordinate are closely related as the tool is mounted to the end.



(a) Top view of the working space



(b) Front view of the working space



(c) Right view of the working space



(d) Perspective view of the working space

Figure 4.20 Views for working space organization

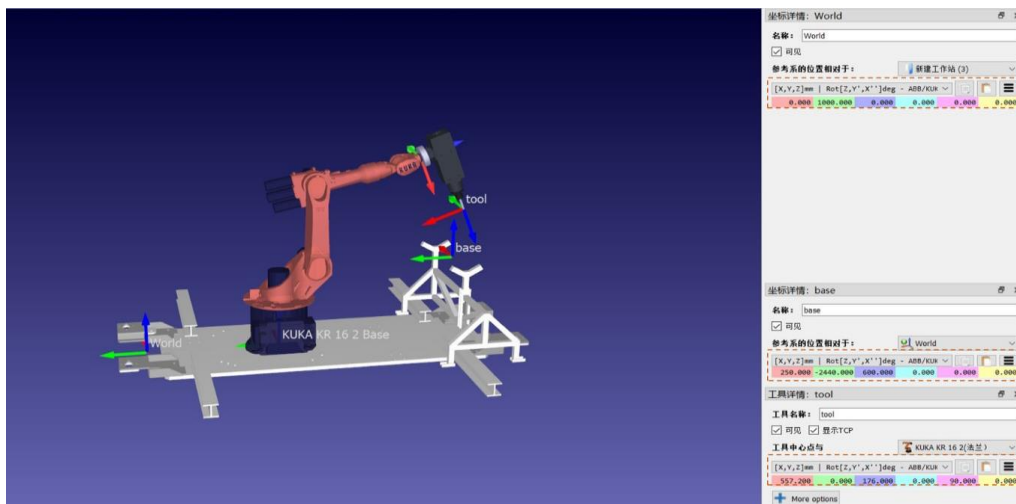


Figure 4.21 Coordinate systems of the working space

The robot tool centre point (TCP) is a point that is used to move the robot to a Cartesian position (e.g., a Cartesian target for a given XYZWPR value.) TCP is defined as a robot flange conversion. TCP definition is critical in any robotics application, whether offline programming is used. The calibration includes the process for tool and base. For tool, the calibration includes the origin of the tool coordinate system and the orientation, shown in figure 4. (a-). There are different ways to calibrate the TCP, one common method is to take three or more configurations in 3D space, shown in figure 4. (b), which can

provide more accurate results and a better estimation of TCP errors. To accurately define TCP, in the simulation environment 8 points are selected to calibrate the TCP minimize the TCP error, shown in Figure 4.22.

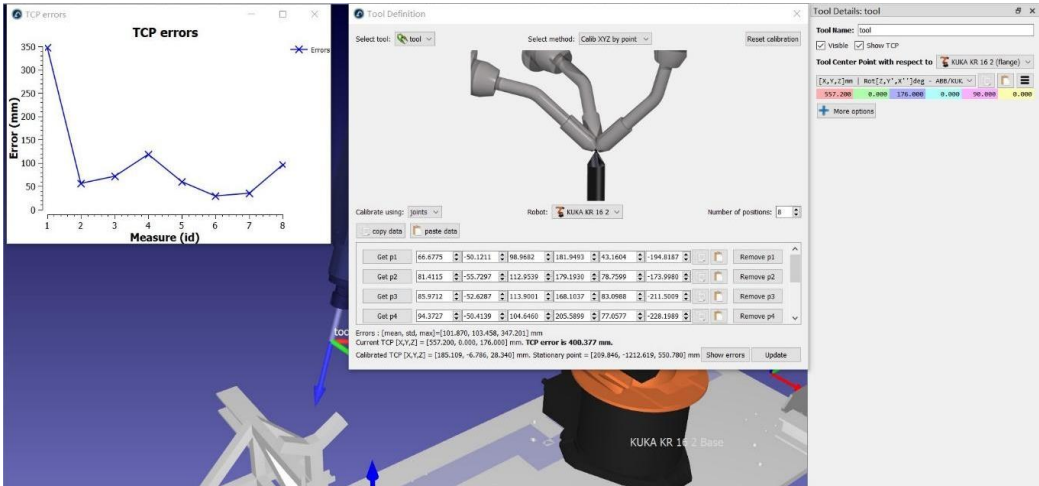


Figure 4.22 8-point calibration

After the origin position of the tool system is calibrated, then it comes to the orientation of the TCP. The tool firstly moves along its tool head direction as the x – axis, and the direction which is vertical to the plane of the tool is set as the z – axis. According to the right-hand rule, the y -axis is deduced. Then the tool moves along y – axis which is known as 2-point calibration. Figure 4.23 shows the 2-point movement, the order of the robot arm end’s movement is target 1 → target 2 → target 4 (the same position as target 1) → target 3, which are the movements in x – axis and y – axis. The calibrated working space with 5 coordinate systems is shown in Figure 4.24.

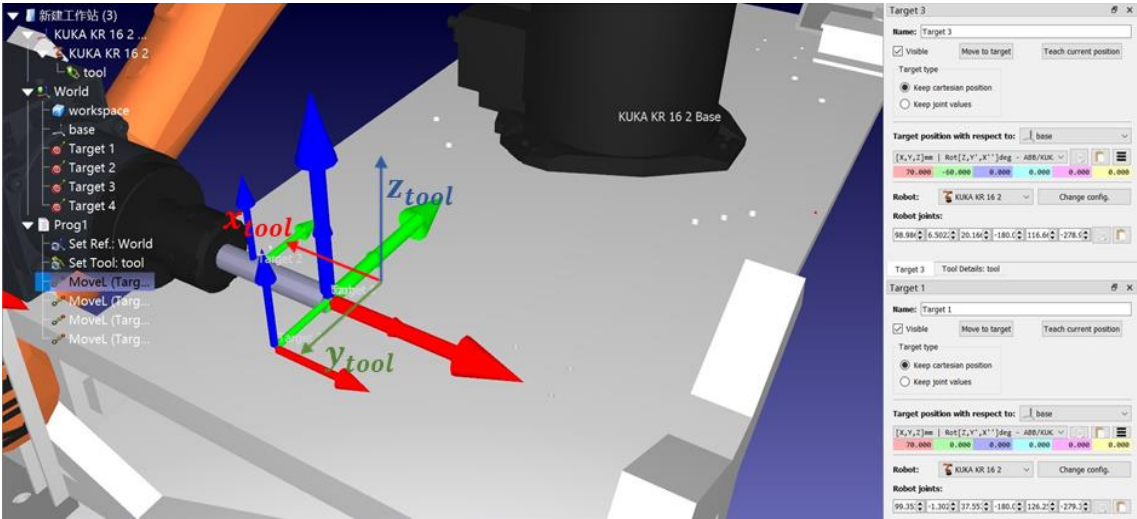


Figure 4.23 Orientation of the tool coordinate system

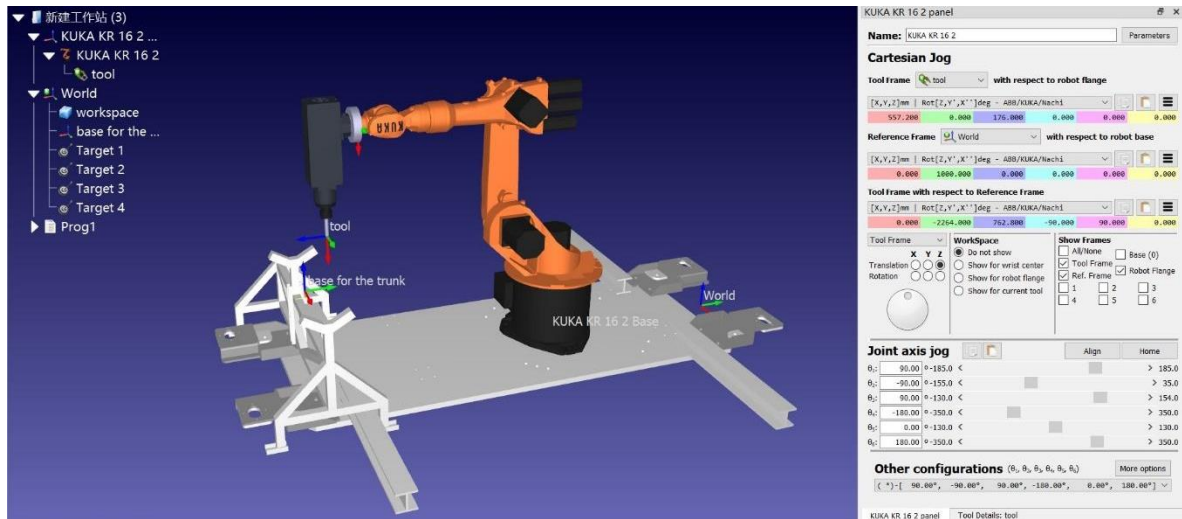


Figure 4.24 Calibrated system for working space

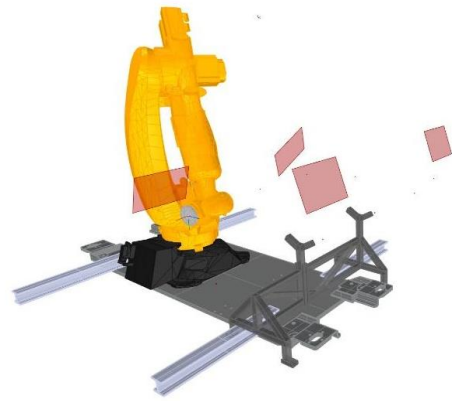
4.2.2 Information transformation

When the calibration for the working cell is finished, the robot arm can scan the information of the item to be fabricated. This step aims to transfer the information of the raw material into the computer software environment. The 3D scanner scanned the details of the trunk like the position, the radius, the length and imported the point cloud into grasshopper. This helps to know the rough radius of different part of the trunk to generate a geometry to stand for the trunk. The usage of 3D scanner on the robot arm can move more flexible to scan as many details of the trunk as possible. Grasshopper of the Rhino is selected as the software platform for the mulch-discipline cooperation. Four planes (shown in Figure 4.25) are set for the robot to switch the positions and the file for scanning is exported to the robot. After scanning, the pint cloud information is stored in CSV files, which are imported to read and to display. Then the boundary beam trunk is built based on the point cloud for further joinery design. The basic setting up for the design and fabrication is finished.

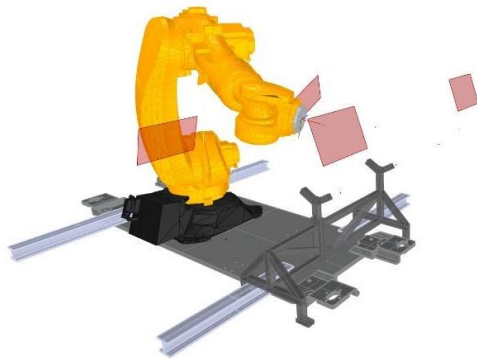
The chainsaw mounted on the robot arm can only cut the regular planar surface, and this is the main constraint for the timber joint design which means the surface with curvature cannot be fabricated by this tool. Accordingly, the part where the joints meet needs to be flat. Figure 4.27 (a) demonstrate the details of the joinery, which is constituted by four parts and is designed to composite the joinery like Figure 4.27 (b) shows. Then the parameters to link the designed timber joinery model with the fabrication orders need to be sorted out. The first thing to consider is how the chainsaw move to cut the planar surface and how these movements are embodied in grasshopper to link them with the geometric information in 3D model.



Position plane 1



Position plane 2



Position plane 3

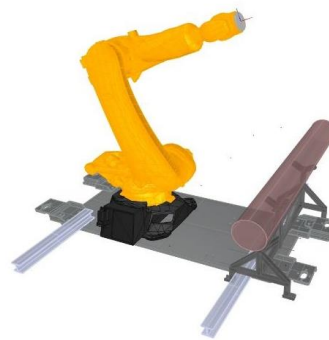


Position plane 4

Figure 4.25 Views for 3D scanning using robot



(a) Point cloud of the scanned trunk



(b) Boundary beam for the trunk

Figure 4.26 3D scan results

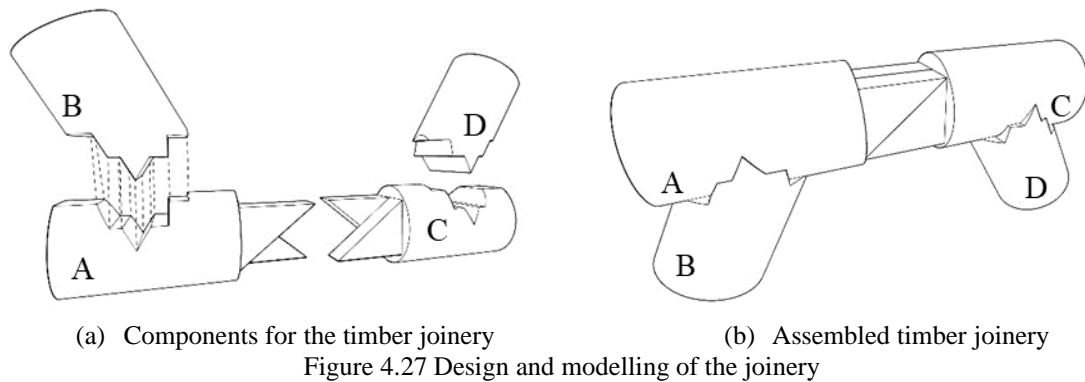
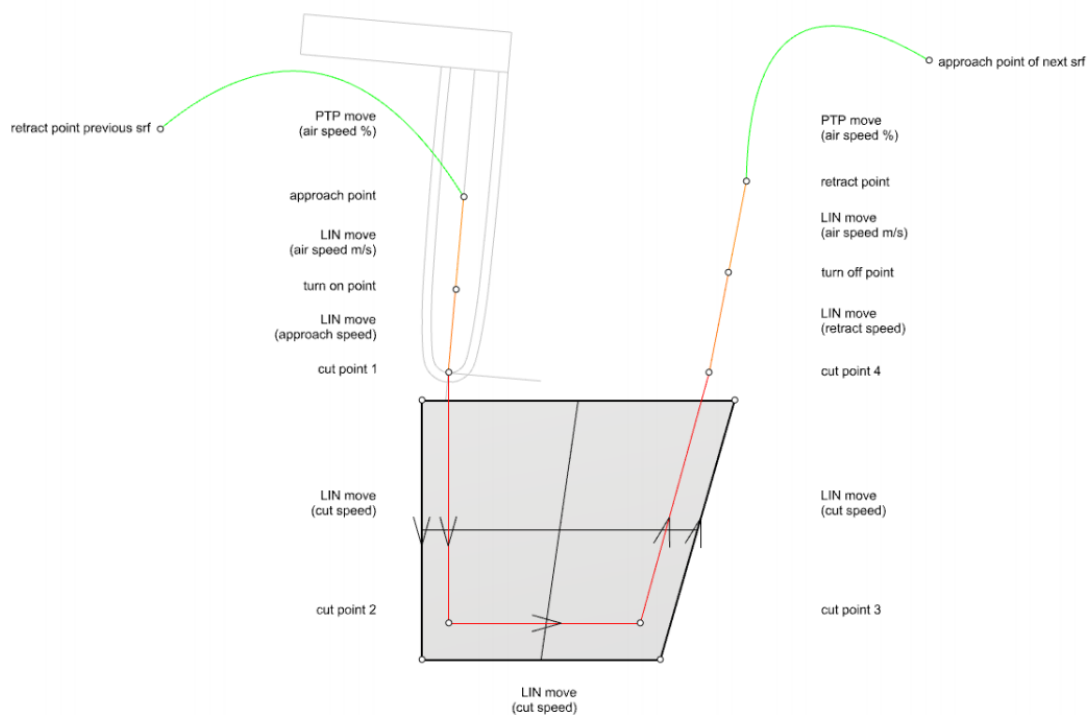


Figure 4.28 shows the tool path within one cutting surface. After finishing the fabrication in one cutting surface, the end-effector moves to the next one from the retract point of the previous surface to the approach point of current cutting surface. In this stage, the tool operates the point-to-point movement. When approaches the cutting surface, there is one approach point which is aimed to change the position and orientation of the chainsaw and after this point, the end-effector takes the linear movement. There are four cut points within one surface, and the tool moves along the boundary of the surface sequentially to generate three linear tool paths in a speed different from the point-to-point movement. After leaving the fourth point of the cutting surface, the chainsaw approaches the retract point of this surface in linear path and again moves to the approach point of next cutting surface in point-to-point movement.



Source: ROB|Arch 2018 workshop
 Figure 4.28 the tool path of the robot arm within one cutting surface

4.2.3 Important input information

From this illustration of the tool path of chainsaw, one important parameter to connect the geometry to the commands for robot arm is the “cutting surface”.

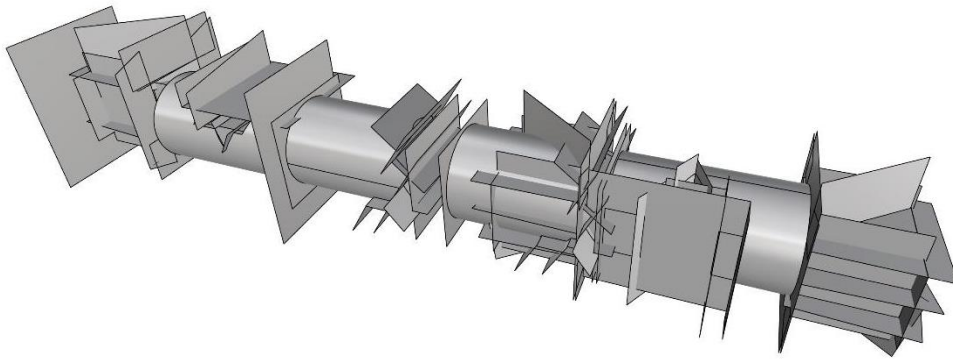


Figure 4.29 Cutting surface set for the timber fabrication

Cutting surface is defined according to the planar surface on the geometry of the joinery. When drawing the surface, the order of drawing the vertices determine the real cutting order, which are the positions of cutting points shown in Figure 4.29. Also, the scale of the cutting surface needs attention in case the boundary of it is out of the reach of the robot arm. After all the surfaces of the joints have been covered by the cutting surfaces, the surfaces are selected as the input to build the link between the geometric model and the robotic fabrication. There are two aspects of information that the input surfaces can convey. First is the order for movement within one surface and the other is the cutting order for the whole process from one surface to another. The second one is especially important for which the movements of the robot arm within one cutting surface following the cutting points and the movements from one cutting surface to another can cause singularities of the robot arm.

In the multiple-cutting task, the surfaces with the same or similar orientation can be classified into one branch to reduce the changes of orientation of the end-effector from one cutting surface to another, Figure 4.30. There could be several different branches in the whole cutting task. After finishing the cutting task in a separate branch, the end-effector moves to the next branch including a series of input surfaces passing by a safety plane to change the orientation without touching or colliding the target object.

Besides the order of setting the cutting surfaces, another factor to consider is about the tool. The offset side of the tool needs to be checked whether it is at the backside of the input surfaces, which can be achieved by flipping the surface. The orientation of the tool needs checking after the calibration before cutting every branch of surfaces. To ensure the robot axes move within its reachable workspace and limited speed, the “hold on” session is needed after certain cuttings. In this practice, “status and turn ” is added after each branch of cutting surfaces to make sure the robot arm moves in the most optimal way and is not the same for every group of input surfaces. And the tool re-oriented automatically after every group of cutting surfaces and before the next group. The height of the end-effector moves from the target object to the safe place in the air to reorient is a clearance distance.

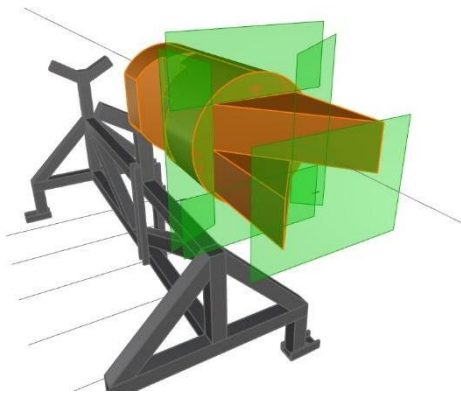


Figure 4.30 positions of cutting points

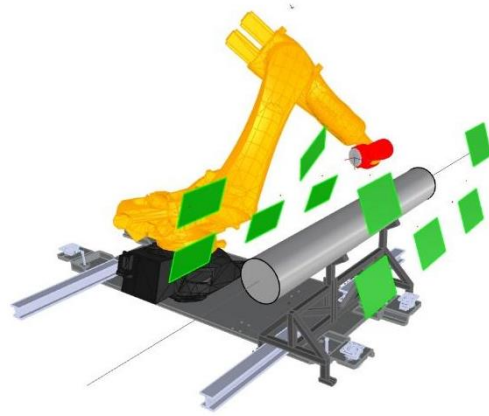


Figure 4.31 Singularity of robot arm when operating

There are some other parameters that need consideration. According to Figure 4.28, after passing the approach point, the chainsaw turns from PTP movement to LIN movement. The speed of point-to-point movement (in %) and linear movement (m/s) is in different settings. To save energy, at which point to turn the chainsaw on matters, which is after the approach point but before the cut point 1, in linear movement in approach speed. From point 1 to point 4, the chainsaw moves in a linear direction at cutting speed. The same as the turn on point and approach point, there are settings for turn off point and retract point to end the cutting from the current cutting surface and move to the next one. The offset length of the end-effector moving in approach speed and retract speed are named approach distance and retract distance respectively.

4.2.4 Practical Questions

After the robotic chainsaw cutting operation, there are some practical questions. In the whole process, some factors can have an impact on the smoothness and stability of operation, even causing the breakout or damage of the tool or the robot. The most important one is the cutting order which would put the robot under the potential risk of singularities. The boundary of the chainsaw is rounded and the boundary of cutting surface is in straight lines. To make sure the chainsaw can cut the raw trunk into the joinery composited by planar surfaces, the cutting surfaces are slightly bigger than the ones on the joinery to make sure the tool can cut off the differential parts. On some occasions like the tool meets the knots of the trunk, the material can become hard or unpredictable to cut or the cutting length is extremely long, it is unnecessary to cut through the material and it is reasonable to cut the remaining part manually.

In the simulation, the singularities can be observed clearly as they are shown in red, Figure 4.31. On the contrary, there is no warning of collision from the simulation. Therefore, the reachability and the collisions need to be checked by manual observation from different perspectives. The collisions mainly come from the reorientations from one branch of cutting surfaces to another. This is because when the chainsaw finishes the cutting task of the clustered cutting branches, the tool needs space to reorient and move to the next branch with different orientations. This means the robot would need large space to move and change position freely to ensure the tool would not collide into the target.

This case poses the question of applying robotic automation techniques to construction.

- (1) What is the appropriate design that can ensure the applicability of the robotic technique in pre-fabrication?
- (2) How to avoid singularities automatically instead of manual adjustment on tool path?

4.3 The initial process for robotic fabrication

From the practice introduction from self-assembled robot to real industrial robot chainsaw cutting, to achieve robotic fabrication in automation construction, it is necessary to sort out the essential elements and main steps for the whole process. Information transformation is the leading part of the whole process, which transforms the geometric model into machine language. The selection of an appropriate form of data transfer as an encoding tool enables the direct transfer of modifiable information between the geometric model and the machine process. Upon the data transformation, to complete the digital design and fabrication platform, three main elements are indispensable: 1) hardware, software, and material. The material is prerequisites for the whole process which determines the fabrication methods and the tools according to the properties and the limitations of the material itself. Hardware refers to the industrial robot and the tools developed for the fabrication process in explicit definition. Software is the environment for building the model and operating the simulation of the fabrication process. After setting the environment, the digital construction requires four dynamic steps to accomplish the process: 1) transform data into the common form to transfer information between different software platforms; 2) filter the valuable data for specific fabrications; 3) transfer the valid data into the tools; 4) generate the dynamic data flow.

The aim of the data transformation is to generate a dynamic data framework so that the information between different software platforms can exchange information in real-time if any data, like a geometric model makes any changes. Compared to the widely used numerical control technique, the main advantage for the robotic fabrication is the ability to establish the connections between the digital model and the fabrication commands, which means the off-line programming and on-line programming for industrial robots. From the case in section 4.2, the connection is turning the surfaces on the joinery into the cutting surfaces which can be read in Grasshopper and turn the vertices of the cutting surface into the cutting direction. Another advantage is the visualisation for the simulation of the whole process. There are several software platforms like RobotStudio, V-rep or plugins for the simulation, like KUKA|prc, HAL, or the open-source operating system like ROS (Robot Operating System) shown in Figure 4.32. This necessitates designers not only overseeing the pre-concept design stage, but also participating in the production and construction processes to improve overall system control. Industrial robots use intelligent dynamic feedback technology to translate information and this materialisation of the information process has become a new focus for the designers.

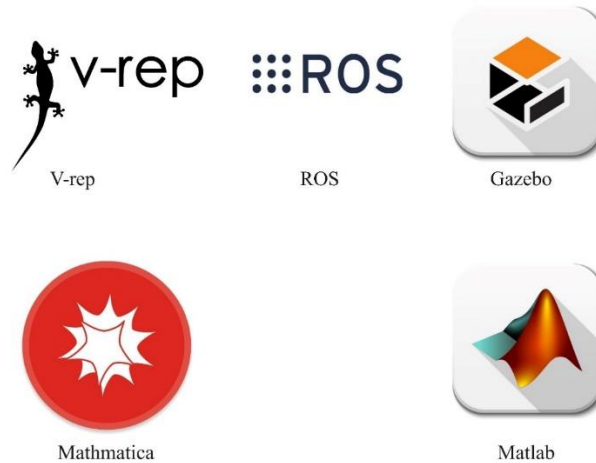


Figure 4.32 Software of robot simulation and visualisation

Robotics applied in construction requires a new design and construction method that is distinct from conventional ones, resulting in a systematic non-linear construction model with integral generation characteristics. Collaborative construction can be realised by reaching a high degree of integration of machinery, computers, and humans. This is a three-dimensional intelligent fabrication and construction approach that uses data to control the whole building process rather than the single-direction linear construction mode of the typical two-dimensional plane drawings to guide the construction in three-dimension. In summary, to make the data flow complete and dynamic, the framework needs consideration from different aspects including the software, the data form. The following sections summarize the basic steps for the robotic fabrication.

4.3.1 Robot system

Each industrial robot is composed of a control system, a robot, and a handheld operator programmer (Figure 4.33). The currently used commercial robot KUKA provides signal commands for the movement of the robot arm and the operation mode of the end-effector via smartPAD remote control. The latest KUKA KRC4 control system reads KUKA ROBOTLANGUAGE (KRL) as well as the general CNC language G-CODE (G-code) and the programming languages of other PLCs (Programmable Logic Controller), such as SPS (Speicher Programmier Steuerung) of Siemens. In worldwide factories, industrial robot systems can perform multiple tasks such as filling materials, handling, welding, painting, and grinding. By installing end-effectors, robotic arm systems can have some of the functionality of CNC machines but are more flexible than CNC machines. The CAM allows the interface between the computer software and the robotic arm system. This allows the robotic arm system to be built digitally.



Source: <https://www.kuka.com/-/media/kuka-corporate/images/products/controllers/smartpad.jpg>

Figure 4.33 industrial robot and controller

Since the complexity of construction is no less than that of the industrial manufacturing industry, however, since construction products cannot be produced and manufactured on the assembly line, coupled with the more restrictive conditions on the site, the robotic arm system for construction needs to be changed in terms of workflow and processing methods, and each processed product needs to be programmed individually within a set of workflows. There are 2 main types of programming methods for robotic arms: (1) teach in: an online programming operated directly on the smart pad; (2) offline programming: divided into graphically assisted computer programming (e.g., Figure 4.) and visual programming with the help of an interface in the smartPAD on a visual programming on a higher-level PC. The offline programming function means that the robot programme is written on a computer, then simulated and debugged before being loaded into the robot controller and ready to run which is the most used method.

The case of 4.2 uses the KRL language exported by KUKA|prc for KUKA robot. When using the robotic arm, the KRL code can be written manually or use soft programming for auxiliary programming, and finally export the SRC file for the robotic arm to read. The programming of robotic arms is usually a modular program, so it can be programmed efficiently according to the structure. Subprograms can be utilized many times over, avoiding repeated writing and adjustment, minimizing possible programming language errors, and reducing time consumption. A global subprogram is developed for one robot but can be called by another robot at the same time. Subprograms save storage space by avoiding code duplication, and each component can be developed separately or replaced at age with a component that has the same performance. The structured program will be broken down into step-by-step tasks, and the subroutine language is shown in Figure 4.34.

RETURN means that the subroutine is terminated. LOOP-END LOOP means that the subroutine is called repeatedly during the operation of the robot arm until the termination condition of the loop is reached. The termination condition can be an external signal input or a judgment statement using IF guidance. The basic format of the C language used by the robot arm is the same operation logic as controlling the simple robot arm with Arduino. The following is the KCL language for the output of the 4.2 case section.

```

DEF MAIN ()
INI
LOOP
    GET_PEN()
    PAINT_PATH()
    PEN_BACK()
    GET_PLATE()
    GLUE_PLATE()

    IF SIN[1] THEN
        EXIT
    ENDIF
ENDLOOP
END

```

```

%%cnc
$PARAM TEMPLATE = C:\KNC\Robotec\Templete\vorgabe
$PARAM EDITNAME = "
DEF RhinoProject ()
EXIT $AS ($AS_COMMAND -IN_REAL -IN)
;FOLD INI
$AS ($INITIOP,0)
--ENCFOOLD (INI)
;FOLD STARTPOS
$MACHINE = FALSE
$ACT_ACT = $DEFAULT
$AS ($STP_001)
$ACT_ACT = ($TOOL_NO 0,$BASE_NO 0,$PO_FRAME $BASE)
$AS ($START)
--ENCFOOLD
;FOLD SET DEFAULT SPEED
$VEL_CR = 1
$AS ($VEL_001)
$AS ($TOOL_0)
$AS ($BASE_0)
--ENCFOOLD
$ADAPTS = 0
PTP $ACT_ACT, skip BCO quickly
; Program generated by RhinoCNC v9.4.5 for KONA KR 210 R2700 on 22/04/2018 12:04:40
; Using nominal kinematics.
$BASE = (FRAME: X 1500.000,Y 1000.000,Z 500.000,A 0.000,B 0.000,C 0.000)
$TOOL = (FRAME: X 997.200,Y 0.000,Z 174.000,A 0.000,B 90.000,C 0.000)
; Show Tool 1
$VEL_CR = 1.00000
PTP $AL -20.00000,$A -77.28429,$B 102.47077,$C -92.40000,$A 0.00000,$B 119.20000)
LIN EX 0.000,Y 20.000,Z 102.500,A -90.000,B -9.207,C -100.000)
LIN EX -0.000,Y 24.000,Z 33.873,A -90.000,B -9.207,C -100.000)
LIN EX -0.000,Y 24.000,Z 33.873,A -90.000,B -9.207,C -100.000)
$VEL_CR = 0.00000
LIN EX -0.624,Y 23.386,Z 33.873,A -90.000,B -9.186,C -178.593)
LIN EX -1.268,Y 23.843,Z 33.873,A -90.000,B -9.170,C -178.179)
LIN EX -1.800,Y 23.871,Z 33.873,A -90.000,B -9.153,C -178.769)
LIN EX -2.347,Y 23.766,Z 33.873,A -90.000,B -9.096,C -178.323)
LIN EX -2.899,Y 23.630,Z 33.873,A -90.000,B -9.067,C -177.909)
LIN EX -3.452,Y 23.460,Z 33.873,A -90.000,B -9.067,C -177.473)

```

Figure 4.34 Example of subroutine language for robot control

4.3.2 Workspace setting

The layout and design of the workspace is one of the key factors in determining the operating efficiency of the robot arm. Under the premise of satisfying the processing safety, the placement of each component and the fixing method need to be considered. The fixing of objects can be done by clamp. The object is fixed to the table and several other surfaces are machined. The disadvantage of this method is that it does not guarantee that every surface can be reached, so an additional adjustment of the fabricated surface is required, which requires a new alignment. It is also possible to set the object in the suspended position and hold it on one end while one fabrication process is completed, and then fix the other end to fabricate the unmachined end. Since the positioning method can be used to position the object in relation to the robot arm at any time, there is less impact in terms of loss of position information. Regardless of the movement of the object itself, the positioning method can be used to find the new position and calculate the relative position of the material to be machined in the simulation environment and adjust the position coordinates in the computer model.

After designing the basic operation space, it is necessary to calibrate the robot arm world coordinate system, basic coordinate system and tool coordinate system. When using the world coordinate system for machining, the origin of the robot arm is at the base of the arm. The coordinates of the table and the position of the object to be machined need to be calculated with reference to the origin. The advantage of the world coordinate system is that the movement of the robot arm can be tracked and predicted, and because the origin and coordinate direction are known, the movement of the robot arm is often fixed. Usually, after the position of the object to be machined is determined, a realistic demonstration is simulated in the visualization interface, allowing the designer to see more clearly the relationship between the object, the manipulator, and the robotic arm to achieve proactive avoidance in the program. The base coordinate system is the coordinate system set up to facilitate the movement of the robot arm along the edge of the object and adjust its attitude. When using the base coordinate system, a reference coordinate plane is defined, and all coordinates are relative to the base coordinate system to facilitate machine positioning and machining according to the machining path. The tool coordinate system is a

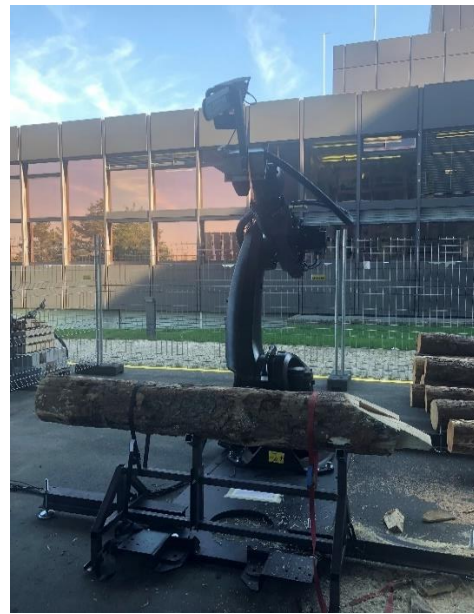
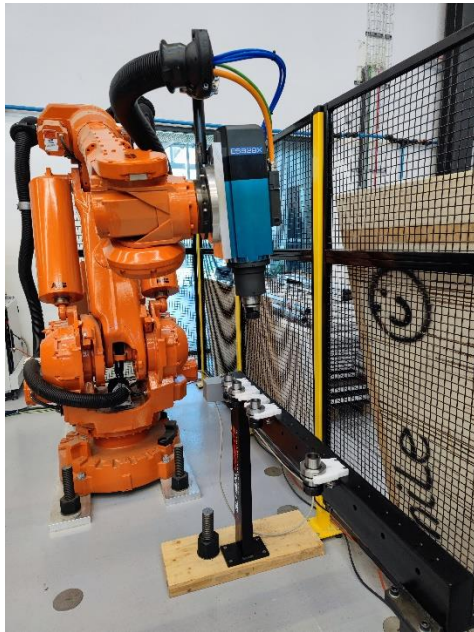
coordinate system in which the tool head of the robot arm is the point of departure, and in which it is possible to move and adjust the attitude along the tooling direction.

It is often easier to use world coordinates for continuous adjustment of the visualization interface because it is possible to visualize the relationship between different objects. This also allows for a more intuitive and realistic simulation when building simulations. The base coordinate system is used to measure whether the material and positioning tools are parallel to the machining table. If a problem occurs during fabrication, the arm needs to be stopped immediately and then switched to the tool coordinate system. The arm is manually controlled to withdraw in the direction of the tool x-coordinate.

For robotic arms that are not equipped with a vision system, it is necessary to ensure that the relative positions of the real object and the robotic arm are the same as in the computer simulation. This is calculated by selecting the global coordinates in smartPAD and entering the distance of the tool head's centre axis from the centre of the flange and the distance of the front end of the tool head from the flange extension into the tool information. Set the head perpendicular to the ground and move the front of the tool head of the robot arm to one of the corner points of the object. Open smartPAD to take a coordinate reading of the actual location and use the *XYZ* point command in Grasshopper to plot the point and enter the coordinates. The point plotted in the computer environment matches the actual position of the robot arm in the computer environment, and the robot arm operation can be simulated by placing the computer model according to the plotted point.

The working cell is composed of several parts, introduced as follows:

1. Mechanism: Known as a work cell which is a set of different parts connected by joints or connections, including robots, positioners, and end-effectors (also known as tools) to composite a kinematic system.
2. Manipulator: the robotic arm is the primary controlled mechanism of a controller. There can be more than one manipulator within an automatic robotic work cell.
3. Tool: Mounted on a robot and refers to end-effector at most of time which means the number of tools is more than one. The end-effector is the part to operate the process like welding, cutting, etc.
4. Positioner: Special part of the mechanism which can move the parts according to the process. Tracks, gantries, and turntable can be seen as positioners. One working cell can have more than one positioner.



(a) Multi-end-effectors workspace

(b) Chainsaw workspace

Figure 4.35 Different workspace setting

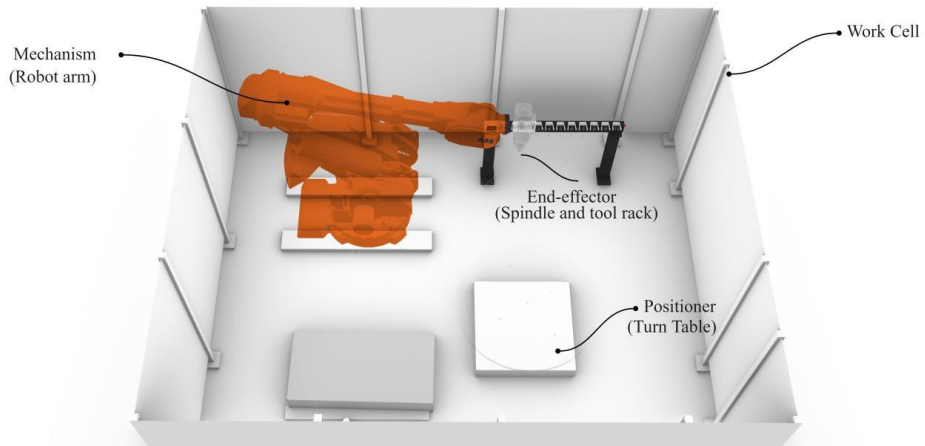


Figure 4.36 Robotic working space setting for welding process

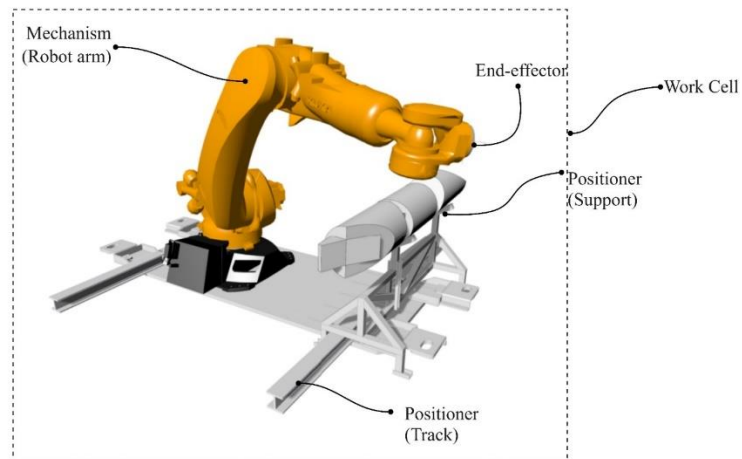


Figure 4.37 Robotic working space setting for cutting process

In a real robotic fabrication process, the following factors are important during the whole workflow and the illustrations are listed in Figure:

- 1.Targets: Targets “teach” the end-effector to go to the designated positions in Cartesian space. The targets are composed of discrete points which can be on a curve or the vertices of surface.
- 2.Endpoint: The centre point of the tool reaches the targets and is referred as TCP. One robotic manipulator can have more than one TCP and during one action, only one TCP is operating.
- 3.The references: The references link the targets to the mechanism. The references provide the frame for different parts of the working space. There are three most basic references including base reference, endpoint, and target reference. And more reference can be added if needed for other parts like turntable, tool rack.

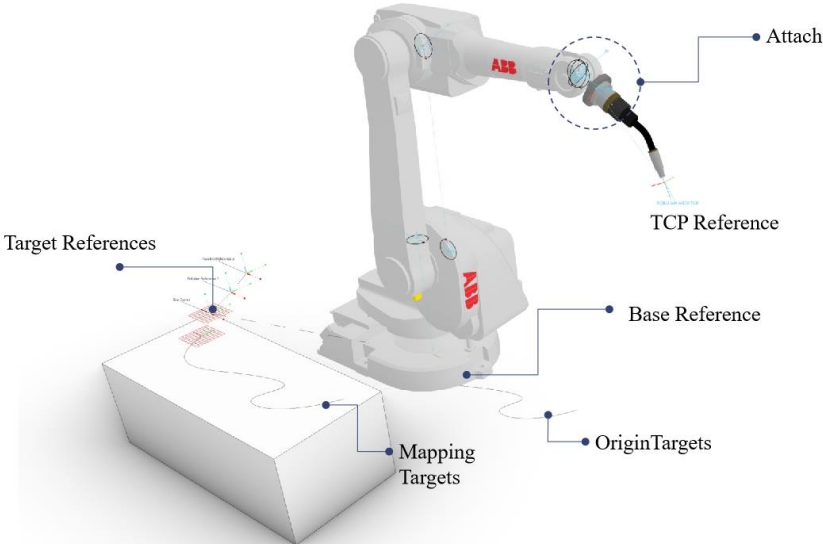


Figure 4.38 References of robotic mechanism

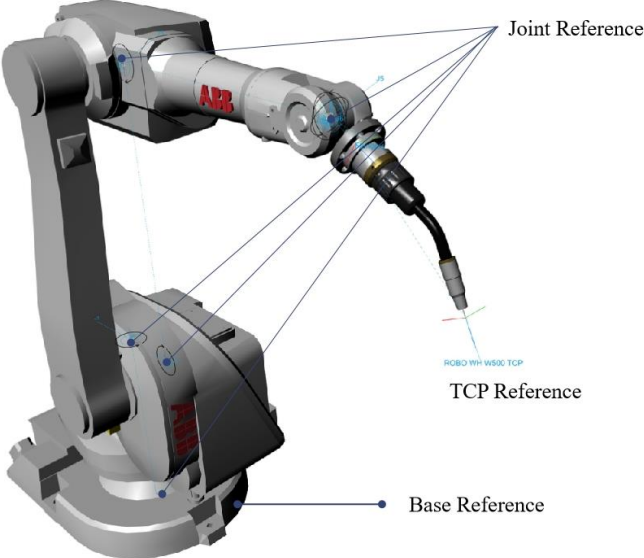


Figure 4.39 References of robotic mechanism

In a welding working cell composed by robotic arm and a rotary plate. The mechanism is to operate the robot arm and the support simultaneously to align the end-effector with the targets, shown in Figure 4.40.

4.3.3 Software platforms and roadmaps

Traditional robotic arm fabrication requires creating a model in modelling software, importing the model into CAM software to process the data and write toolpaths, and then using simulation control software to demonstrate and control the arm. One approach is to convert the Rhino 3DM model to another format, then import the CNC machine programming software Mastercam to write the toolpath and generate the encam file, open the Robotmaster plug-in to set the arm state, use the offline programming method to generate the machining file, and finally import the arm to finish machining.

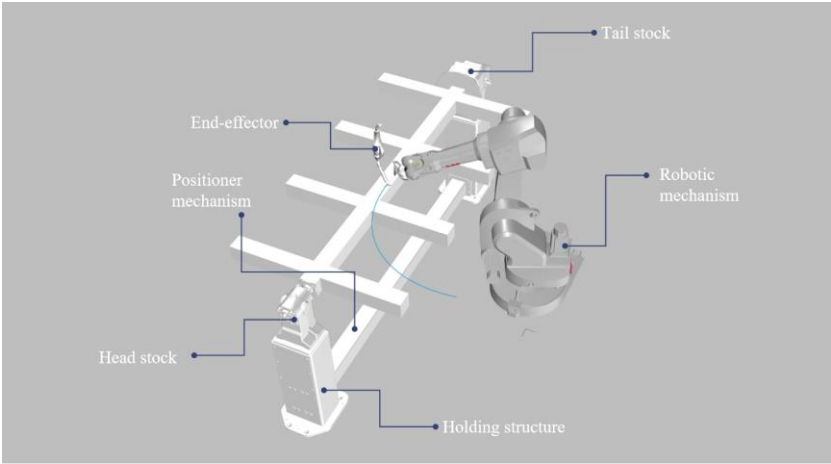


Figure 4.40 The setting for a synchronized process

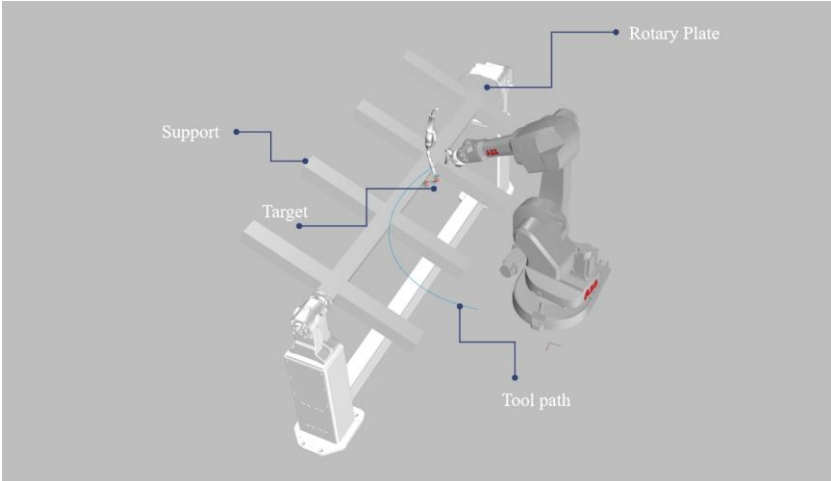


Figure 4.41 A synchronized welding process

However, operating in different software has certain disadvantages, architects not only need to learn different software but also need to master the complex operation methods, and the geometric model conversion in different platforms will also cause data loss. The advantage of the same platform is that the same operation method can be used for design and processing, which enhances the designer's control over the design and construction. With the use of parametric methods, designers can penetrate more processes in the construction project and strengthen their control over the plan.

In the case of 4.2, the digital construction platform was built using Rhino, a common modelling software for architecture, and Grasshopper, a common plug-in for architecture, along with KUKA|prc. Using the digital construction platform for modelling and editing, as well as for manipulating the robotic arm, the architect can control the entire process from parametric modelling to model optimisation to the selection of the construction method to the automatic operation of the machine. It also eliminates the loss of model accuracy and data loss during data conversion between different software and reduces the iterative process of model adjustment. The architect can select the fabrication method through a simple parametric approach and control the robot arm to complete the task. Without the need for lengthy training on the machine, and without the limitations of the machine itself, working with the same platform allows for more flexible fabrication work.

To make it easier to see what is going on when writing a program, modelling software is commonly used to simulate the real environment. In the Rhino interface, the arm is placed at the origin of the axis by default, and the relationship between the arm and its surroundings can be modelled in the software. The entire site is simulated visually, and the position of the model in the simulation environment represents the real object position. The simulation environment can be used to avoid collisions and reduce the construction process. The use of common architectural software for simulation can bridge the gap between the architectural profession and other professions by building and simulating the working environment with common architectural software. This will help architects to understand the working environment and the process, and it will be easier to control the simulation with Grasshopper.

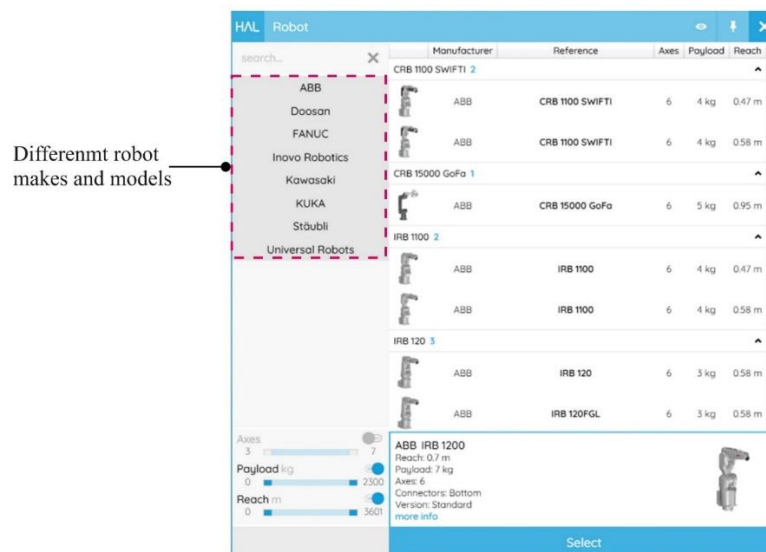
KUKA|prc is built on the accessible visual programming system Grasshopper, which is part of the CAD software Rhinoceros 3D. It provides robotic arm building blocks for integrating KUKA robotic arms directly into the parametric environment. The plug-in operates with simple function blocks that do not need to be coded, but rather interconnected, and the results are immediately visualized. It helps designers to quickly verify the robot arm program and ensure that there are no collisions or unreachable points. The ability to map all axes of motion in the graph allows designers to find and avoid singularities. With instant feedback, designers can visually solve problems by defining the arm motion with the parameterization and observing the results. KUKA|prc simulates all robot arm positions in a short time, giving designers access to all tool positions, all axis values, collision values, IO states, etc. KUKA|prc is fully integrated into the Grasshopper ecosystem, allowing designers to build various algorithms and utilities into their robot arm projects and then optimize tool paths with Grasshopper's built-in evolutionary solver. toolpath optimisation via Grasshopper's built-in evolutionary solver.

KUKA|prc enables architects to program industrial robotic arms directly in a parametric modelling environment, including a complete motion simulation of the arm. The generated files can be executed on the KUKA robotic arm without any additional software. However, the disadvantage of KUKA|prc is that the functions of each cell block are integrated, which is equivalent to integrating and translating subroutines from smartPAD into the grasshopper runtime environment. In the case of some complex operating environment or complex machining paths, the only way to make a reasonable arrangement for the machining path is by hand. This approach will reduce the automaticity of the robot arm, and for

kinematic singularities such as operation problems only human debugging and cannot guarantee the optimal results. Another disadvantage for KUKA|prc is that the plug-in is limited in the types of robots supported. enough support. (A simple illustration showing the robot models supported by the KUKA plug-in).



Figure 4.42 KUKA robot types supported in KUKA|prc



Differenmt robot makes and models

Figure 4.43 Robot models supported by HAL

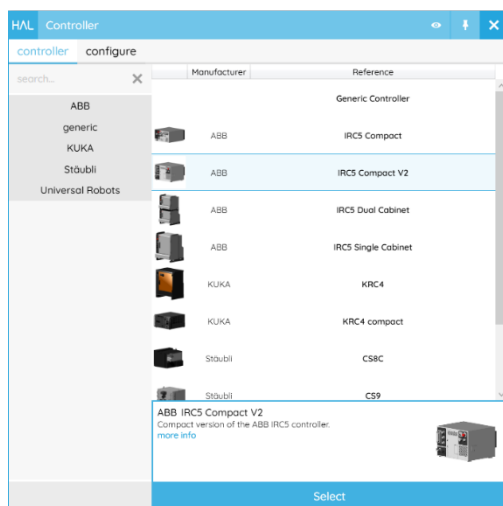


Figure 4.44 Controller options

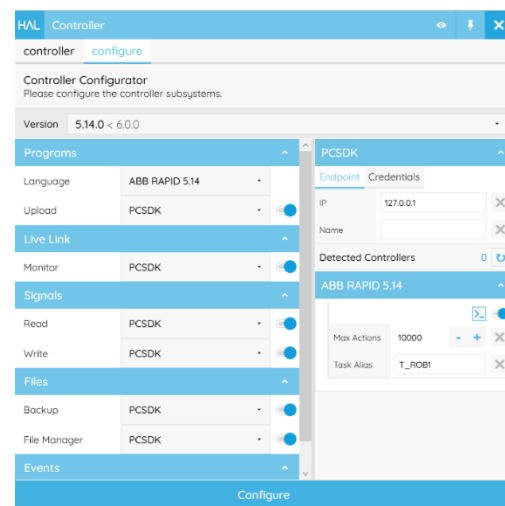


Figure 4.45 Controller configuration

Another widely used plugin within the grasshopper environment is HAL. One specific advantage for HAL is that there are a range of robotic models which are from different makes, shown in Figure 4.43. Another one is that HAL also provides the “controller” options which provide detailed information about mechanism and more precise connection between the simulation and operation environment. If compare these two mainly used robotic plugins, the principles of robotics are the same. The main differences are the “solve” methods, which demands different inputs and generate different options. The “solver” of KUKA|prc needs “commands”, “tool” and “robot”. The output would be generated through the pop-up window which clicks the “setting” button. The “solve” component of HAL needs the “controller” which contains the “mechanism” and the main procedures. The output is “solution” which can be exported in different languages for different robot makes.

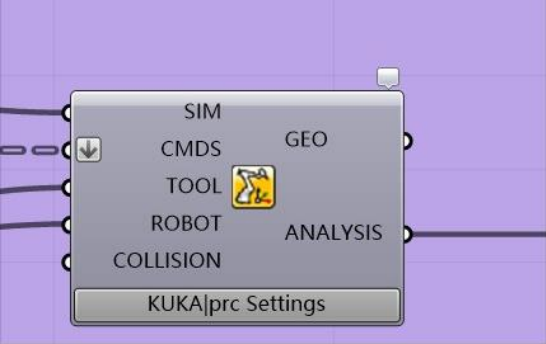


Figure 4.46 Solve component of KUKA|prc

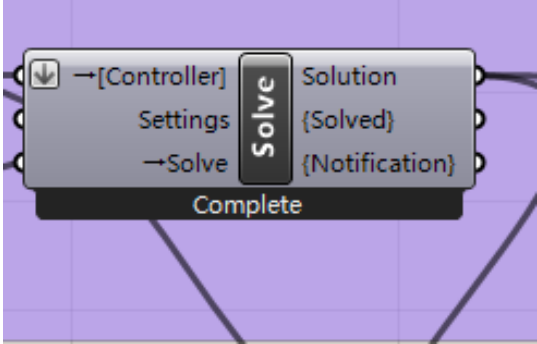
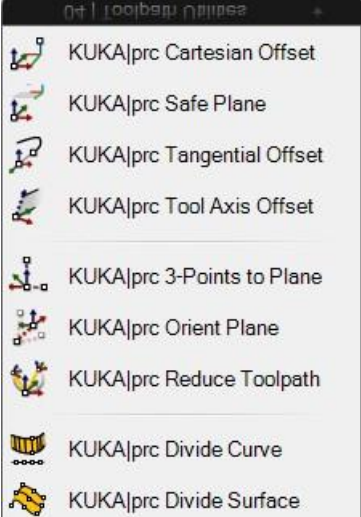


Figure 4.47 Solve component of HAL

The commands for KUKA|prc mainly comes from the “core” and “Toolpath Utilities” two parts, shown in Figure 4.46Figure 4.47. As for HAL, the commands are combined by “motion and “procedure”, and the “solve” component is under the “simulation”. Both of them can export codes to robots and import robotic language to run the simulation. KUKA|prc takes the movement of KUKA robots as the control methods i.g. “LINear Movement” which is a direct method to give commands and is consistent with the robotic motion control methods. HAL has components to define targets compared with KUKA|prc and HAL sovles the procedure mainly throught the sets of “motion” together with “motion settings”.



(a) “Core” component of KUKA|prc



(b) “Toolpath Utilities” of KUKA|prc

Figure 4.48 Main components for KUKA|prc solver

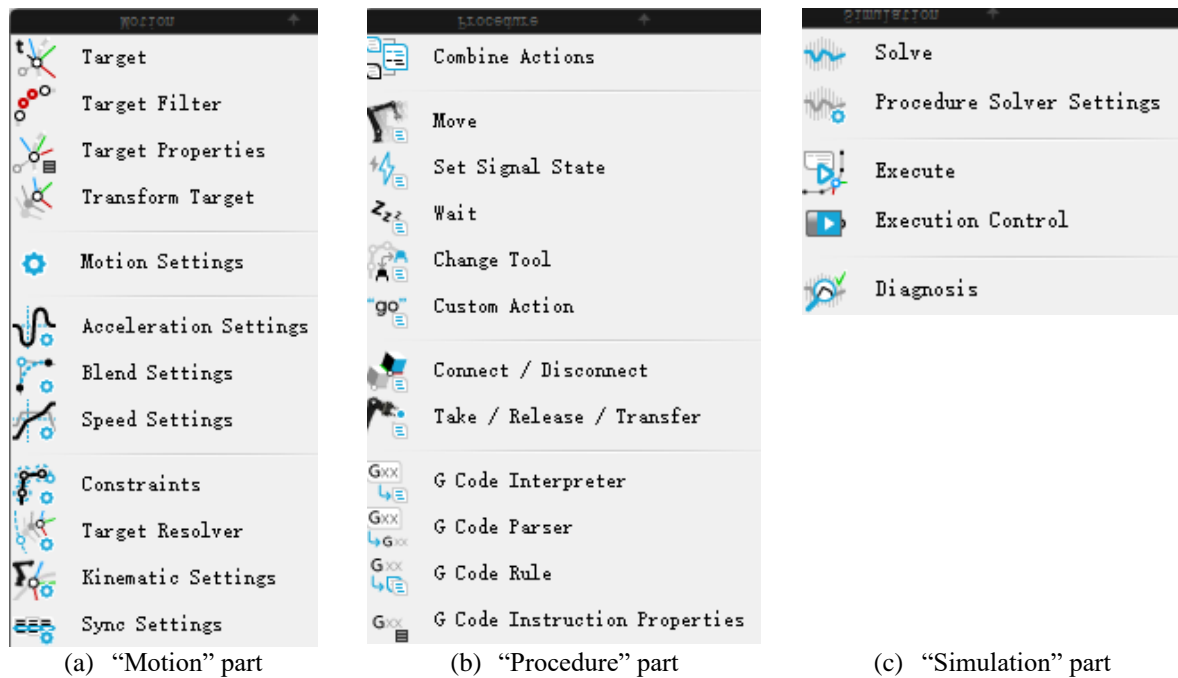


Figure 4.49 Main components for HAL solver

The execution of the process is combined by several parts.

1. Procedure: The main program or task of the overall process, which is a set of actions controlled by the controller.
2. Action: Commands, instructions and operations execute by the controller. The actions can be combined, nested, and synchronized.
3. Single action: This changes the signal during the operation to start a new procedure or makes changes to the mechanism.
4. Thread action: To pass on the signal like waiting, re(start) to the robot from controller.
5. Motion action: Teach the mechanisms to the targets by kinematic or motion settings.

The welding procedure illustrated above is composed by the some of the parts mentioned above and the detailed is shown in Figure 4.50.

There are other simulation software or platforms which can achieve the same goals. ROS is one open-source operating system for robots on Linux systems. The platform provides OS-like services including hardware abstraction description, underlying driver management, execution of common functions, inter-program messaging, program distribution package management, and it also provides tools and libraries for acquiring, building, writing, and executing programs for multi-computer convergence. ROS is a framework for programming robots, a framework that couples otherwise loose parts together and provides them with a communication architecture. although ROS is called an operating system, it is not an operating system in the usual sense of Windows or Mac, it just connects the operating system to the ROS application you develop, so it is also considered a middleware, and ROS-based A bridge of communication is established between applications, so it is also a runtime environment running on Linux, on which the robot's perception, decision making, and control algorithms can be better organized and run.

```

1 Module WeldPrimitivesModule
2 |Declarations
3 |syncident
4 VAR syncident WeldRows:
5
6
7 |tasks
8 FERS tasks T_ROB1_T_ROB2(2):=[["T_ROB1"],["T_ROB2"]];
9
10 |tooldata
11 FERS tooldata AWFSF25:=[True, [[-0.817246, 2.32458, 315.24], [0.939693, 0.0, 34202.0]], [[1, [0, 0, 100], [1, 0, 0, 0], 0, 0, 0]]];
12
13 |wobjdata
14 FERS wobjdata Plate:=[False, False, "STN1", [[0, 0, 0], [1, 0, 0, 0]], [[54.5, -50, 850], [0, 0, 707107, 0, 0, 707107]]];
15
16 |weldPrimitives:
17 EndProc
18
19 Proc WeldPrimitives()
20 Move:
21 Weld:
22 Move:
23 EndProc
24
25 Proc Move()
26 MoveAbsJ [[-82, -2, 26, -50, 52, 70], [9E9, 9E9, 9E9, 9E9, 9E9, 9E9]], [1000, 57295.779513, 5000, 1000], [False, 10, 1, 10, 1, 10, 1], AWFSF25:
27 EndProc
28
29 Proc Weld()
30 PathAccLim TRUE\AccMax:=10, TRUE\DecelMax:=10;
31 SyncMoveOn WeldRows, T_ROB1_T_ROB2;
32 MoveL [[20, 30, 0], [0.183013, -0.683013, -0.183013], [-2, 0, -1, 0], [9E9, 9E9, 9E9, 9E9, 9E9, 9E9]]\ID:=0, [74.3, 572.957795, 5000, 1000], [False, 1, 0, 1, 0, 1, 0], AWFSF25\Wobj:=Plate;
33 MoveL [[24.628772, 38.807434, 0], [0.183013, -0.683013, -0.183013], [-2, 0, -1, 0], [9E9, 9E9, 9E9, 9E9, 9E9, 9E9]]\ID:=1, [74.3, 572.957795, 5000, 1000], [False, 1, 0, 1, 0, 1, 0], AWFSF25\Wobj:=Plate;
34 MoveL [[29.438252, 45.244753, 0], [0.183013, -0.683013, -0.183013], [-2, 0, -1, 0], [9E9, 9E9, 9E9, 9E9, 9E9, 9E9]]\ID:=2, [74.3, 572.957795, 5000, 1000], [False, 1, 0, 1, 0, 1, 0], AWFSF25\Wobj:=Plate;
35 MoveL [[34.356886, 49.532687, 0], [0.183013, -0.683013, -0.183013], [-2, 0, -1, 0], [9E9, 9E9, 9E9, 9E9, 9E9, 9E9]]\ID:=3, [74.3, 572.957795, 5000, 1000], [False, 1, 0, 1, 0, 1, 0], AWFSF25\Wobj:=Plate;
36 MoveL [[39.322323, 51.91967, 0], [0.183013, -0.683013, -0.183013], [-2, 0, -1, 0], [9E9, 9E9, 9E9, 9E9, 9E9, 9E9]]\ID:=4, [74.3, 572.957795, 5000, 1000], [False, 1, 0, 1, 0, 1, 0], AWFSF25\Wobj:=Plate;
37 MoveL [[44.23341, 52.543323, 0], [0.183013, -0.683013, -0.183013], [-2, 0, -1, 0], [9E9, 9E9, 9E9, 9E9, 9E9, 9E9]]\ID:=5, [74.3, 572.957795, 5000, 1000], [False, 1, 0, 1, 0, 1, 0], AWFSF25\Wobj:=Plate;
38 MoveL [[49.048195, 51.707485, 0], [0.183013, -0.683013, -0.183013], [-2, 0, -1, 0], [9E9, 9E9, 9E9, 9E9, 9E9, 9E9]]\ID:=6, [74.3, 572.957795, 5000, 1000], [False, 1, 0, 1, 0, 1, 0], AWFSF25\Wobj:=Plate;
39 MoveL [[53.684925, 46.605182, 0], [0.183013, -0.683013, -0.183013], [-2, 0, -1, 0], [9E9, 9E9, 9E9, 9E9, 9E9, 9E9]]\ID:=7, [74.3, 572.957795, 5000, 1000], [False, 1, 0, 1, 0, 1, 0], AWFSF25\Wobj:=Plate;
40 MoveL [[58.071849, 46.457145, 0], [0.183013, -0.683013, -0.183013], [-2, 0, -1, 0], [9E9, 9E9, 9E9, 9E9, 9E9, 9E9]]\ID:=8, [74.3, 572.957795, 5000, 1000], [False, 1, 0, 1, 0, 1, 0], AWFSF25\Wobj:=Plate;
41 MoveL [[66.06353, 37.900142, 0], [0.183013, -0.683013, -0.183013], [-2, 0, -1, 0], [9E9, 9E9, 9E9, 9E9, 9E9, 9E9]]\ID:=9, [74.3, 572.957795, 5000, 1000], [False, 1, 0, 1, 0, 1, 0], AWFSF25\Wobj:=Plate;
42 MoveL [[81.894466, 17.789926, 0], [0.183013, -0.683013, -0.183013], [-2, 0, -1, 0], [9E9, 9E9, 9E9, 9E9, 9E9, 9E9]]\ID:=10, [74.3, 572.957795, 5000, 1000], [False, 1, 0, 1, 0, 1, 0], AWFSF25\Wobj:=Plate;
43 MoveL [[91.836863, 9.688632, 0], [0.183013, -0.683013, -0.183013], [-2, 0, -1, 0], [9E9, 9E9, 9E9, 9E9, 9E9, 9E9]]\ID:=11, [74.3, 572.957795, 5000, 1000], [False, 1, 0, 1, 0, 1, 0], AWFSF25\Wobj:=Plate;

```

Figure 4.50 Part of execution of the process

ROS supports different programming languages and C++, and python are most widely used. Test libraries for Lisp, C#, Java, and other languages have also been implemented. To support multilingual programming, ROS uses a language-neutral interface definition language to implement messaging between modules. One advantage for ROS is that it has no limits on the robot types, whether it is from KUKA, or ABB does not make an effect, even the developed robot with mobility. As ROS is operated in the terminal of the Linux system, Gazebo and Unity are applied to visualise the simulations and the motions of the robot arm. The cooperation among this different software is strongly connected and are controlled by online or offline programs. And the main difficulty is that the architects need to learn the programming and different software. The advantages and limitations for ROS are summarized in Table 4-1.

Table 4-1 Advantages and Disadvantages of ROS

Advantages	Disadvantages
Provide framework, libraries, and functions	Limited ability in real time communication
Easy to port to other programming environment	System stability does not meet business requirements
Huge user base	No protection on safety
Open source	Only supported on Linux system

There is many other different simulation software for robot arm like RoboDK, Vrep (now has changed to CoppeliaSim), Matlab, Mathematica, etc. RoboDK is a software application for industrial robot simulation and offline programming. In contrast to other vendor-specific machine programming languages, the RoboDK API does its best to help developers emulate and program robots using a variety of unique and open-source programming languages. Any of these programming languages can be used to emulate and program robots by online programming.

CoppeliaSim, a robot simulator with an integrated development environment, is built on a distributed control architecture: each object/model can be controlled individually by an embedded script, a plugin,

a ROS or BlueZero node, a remote API client, or a custom solution. As a result, CoppeliaSim is extremely versatile and ideal for multi-robot applications. C/C++, Python, Java, Lua, Matlab, or Octave can be used to write controllers. CoppeliaSim is used for rapid algorithm development, factory automation simulations, rapid prototyping and verification, robotics education, remote monitoring, safety double-checking, as a digital twin, and many other applications. A feature overview can be found in Figure 4.51.

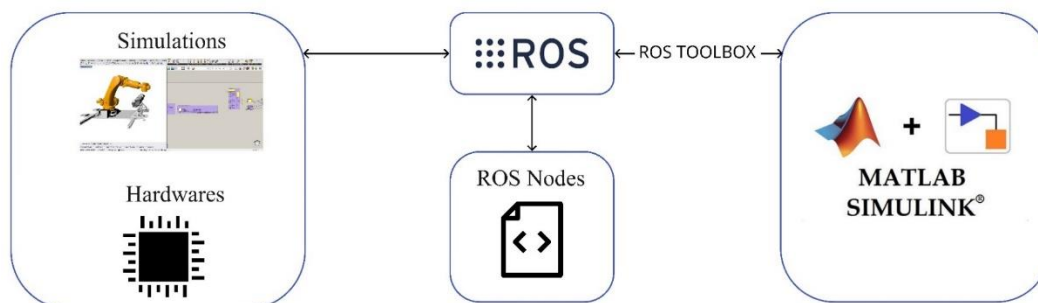


Figure 4.51 ROS Operating System

Matlab and Mathematica work similarly for robotics. Many choose to build their simulation environment on top of Matlab because of the excellent numerical computation and simulation capabilities, it is convenient to use it for development, and Matlab has several development robotic toolboxes that can be called directly with their packaged functions. Mathematica is a scientific computing software that uses Wolfram Language, a rule-based functional programming language. It has manufacturing system modellers for robotic manufacturing and topics for robotics to run the simulation at the same speed as the physical robot and to compare how well the actual path of the robot matches the planned path. The robot model is downloaded from the official website of the robot manufacturer like KUKA, and the model is transformed from STEP into STL, which can be read by Mathematica. The comparison between Matlab and Mathematica is summarized in Table 4-2. These two software focuses more on the algorithm and optimisation for the tool path, rather than exporting the srt files of commands to the robot directly.

Table 4-2 Comparison between Matlab and Mathematica

Features	Matlab	Mathematica
Visualisation	Not very straightforward	Very straightforward
Imported Robotic model	Need to write codes	Built-in functions
Toolbox	Robotic toolbox, SpaceLib, etc	Screws, Robotica
Debug	Easy	Complicated
Length of code	Concise	Cumbersome

The differences of these main software platforms are summarized which is better for choosing the simulation environment based on the specific needs. For plug-ins like KUKA|prc, the environment of them is built in the Grasshopper and Rhino. They can build up a direct connection between the geometric model and the fabrication process. The limitation is that the debug optimisation for the robot is not easy to operate, which under most of the circumstances, is operated by manual adjustment. Software like RoboDK can provide the visualisation for the fabrication process and the tool path and the off-line

programming can be used as the commands for the robot, which provide better cooperation with sensors or scanners. Other software platforms or operating systems like ROS, Matlab, can operate the optimisation easily and develop advanced motion control with other hardware. Software like RobotStudio, are only developed as dedicated software which can only be matched with certain robots. Users can choose the right software according to research needs.

Table 4-3 Comparison of different software of plugin for robotic simulation and visualisation

Selection criteria	Software environment			
	KUKA prc	RoboDK/	ROS	Matlab/Mathematica
Connection with geometric models	Very directly connected to the grasshopper files.	Need to import the .stl files to the software.	Need URDF files of robot or build the robot model by codes.	STL files of robots imported from Solidworks or build the robot model by codes.
Optimisation	Not easy to optimise the robotic parameters.	Not easy to optimise the robotic parameters.	Not easy to optimise the robotic parameters.	Easy to optimise the robotic parameters.
Direct programming	Can program in python or C# in grasshopper.	Can use many programming languages through API.	Easy to program in Linux system.	Easy to program within the software.
Connection with other hardware	Not direct connection.	Can connect to robot to achieve real-time programming and control.	Can connect to Arduino.	Can connect to hardware through Simulink.
Supported robot model	Only support KUKA robots.	Support many kinds of robots from different brands.	Support almost all kinds of robots even the self-built one.	Support almost all kinds of robots even the self-built one.
Debug function	Can visualise through the simulation for singularities.	Give warning of singularities, collisions or out of range.	Debug in the programs.	Easy to debug directly in the software.
Export command files	Can export the command files to robot.	Can export the command files to robot.	Can export the command files to robot.	Cannot export the command files.

4.4 The characteristics and Potential of RAC

There are many cases of applying RAC technique in fabrication, assembly and construction tasks using different kinds of materials. To summarize, there are some common characters of the robotic fabrication in different aspects.

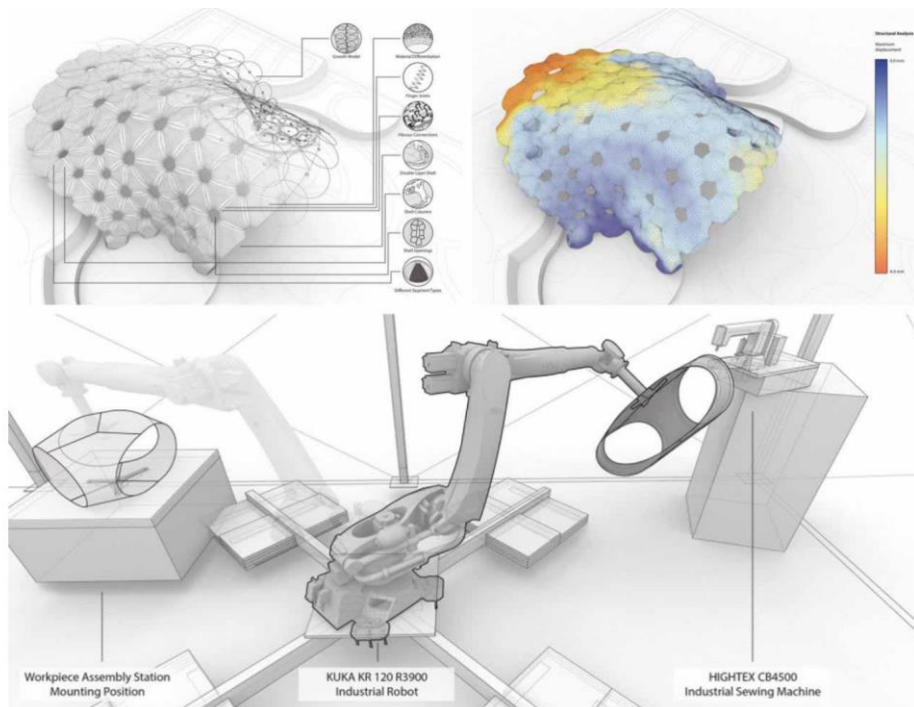
4.4.1 Rationality in performance

The design for complex architecture is combined with performance according to the robotic factor because the design aims for accuracy and efficiency. The evolution of the natural world has shown that highly rationalised performance frequently takes on aesthetically pleasing forms, such as the formally beautiful and functional forms of marine crustaceans. Therefore, bionics is becoming more popular in digital design. This return to nature's iterative laws is a biomorphic strategy that connects performance and form. The design forms oriented by digital construction utilising robotic arms are distinguished by an inherent logic involving performance data, such as structural stability, wind resistance, and seismic resistance, as well as building performance e.g., light and ventilation, and the rationalisation process of these properties results in changes in form. Construction can be carried out in a way that minimises the use of materials and the weight of the structure while maintaining a stable and spanning range, with the introduction of structural performance, finite element simulation and robotic arm technology.

With digital design and numerically controlled machinery, the optimum calculation of performance is incorporated into the design and the aesthetic characteristics inherent in performance are expressed through the logical and highly rational presentation of performance. The design and construction approach based on robotic arm technology provides a suitable entry point for the materialisation of performance biomorphology. The results of performance biomorphic as an information model often require high precision machining technology to put the design into practice, and the robotic arm manufacturing process intervenes to meet the needs of performance design. The information data obtained from performance biomorphic can be translated directly into specific movement commands for the robot arm, demonstrating the formal aesthetics of a highly rationalised performance.

The building design paradigm has shifted from a post-rationalization approach to design and build derived performance to a dynamic integrated system from performance to design and build design. Based on this shift in design thinking, robotic arm technology becomes an important medium for correlating information models with materialised entities, where performance is no longer an uncontrollable influence, whether it is structural performance, material performance, all can be homogenised into parametric information. Parametric information can be calculated and optimised for specific objectives, and the performance parameters can be geometrically translated to generate geometric data. The geometric data is further translated into human materialised operational behaviour at the operation level and culminates in a digital construction workflow.

The Institute of for Building Structures and Structural Design of The University of Stuttgart conducted the first experiment in wood sewing construction in 2016. The experiment combined sewing technology with robotic arm technology for the robotic sewing construction of wooden panels. The shape of the project was inspired by shell animals, and structural physical simulations and bionic methods were used in the biomorphic process (Figure 4.52). In addition to the simulation of the overall structural form, each module also simulates the bending of the wooden panel elements, calculating the bending deformation pattern and the bending amplitude.



Source: <https://www.icd.uni-stuttgart.de/projects/icditke-research-pavilion-2015-16/>

Figure 4.52 Structural form find and translation

4.4.2 Complexity in design methodology and of the theory

As modernist architecture continued to be challenged by its homogeneity in the 1960s, postmodern architecture came to the fore. The aesthetics of complex forms became the dominant aesthetic trend in contemporary design. The uncertainty of architecture: The uncertainty of architecture, the design vision of playful complexity came to dominate, and the definition of 'architecture' became more inclusive. The definition of 'architecture' has become more inclusive. The traditional boundaries between construction and industrial production are becoming increasingly blurred, and the development of industrial technology is slowly seeping into the construction sector. The development of industrial technology is slowly penetrating the building construction sector, largely influencing the mode of construction, which is becoming prefabricated and customisable. In the 1980s, the post-modernist design concept was born. In the 1980s, post-modernist design concepts gave birth to deconstructionism, and the need for formal complexity and chaos grew stronger. The need for formal complexity and chaos grew stronger. Figure 4.53 shows the MOCAPE Museum in Shenzhen, completed in 2016, made clever use of robotic arm welding technology to process and weld the hyperbolic surfaces of the building's metal skin which is achieved by robotic on-site welding.



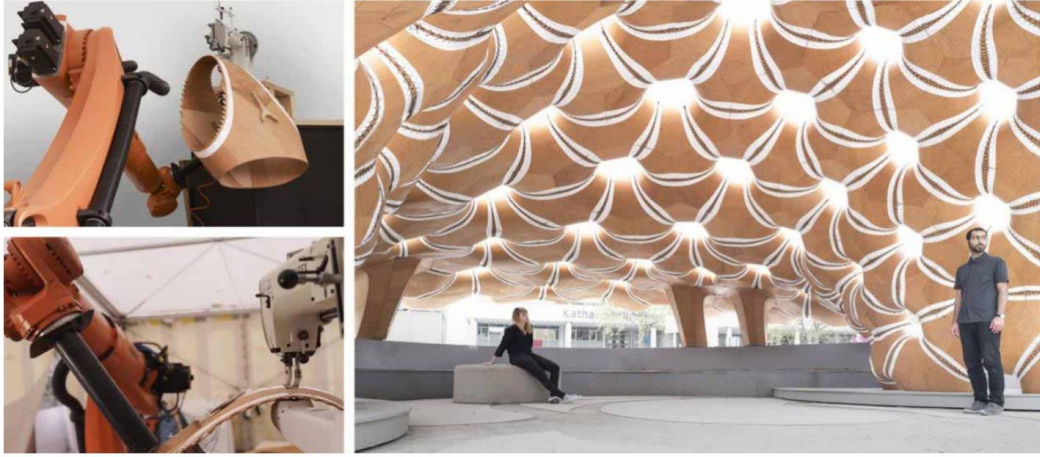
Source: <https://www.dezeen.com/2016/11/28/coop-himmelblau-flat-curving-form-contemporary-art-complex-shenzhen-robots/>

Figure 4.53 MOCAP Museum

4.4.3 Diversification of design materials

Materials are the material basis of construction. The traditional design is limited by materials because of the lack of simulation of materials. Because materials cannot be processed too intricately or precisely by hand or by traditional data processing, traditional buildings are composed of flat geometric forms through standardised components. Robotic arms offer more scope for construction materials as an efficient and viable new digital processing technology. Take timber, for example, which is often found in timber-framed buildings in the form of rods or panels. Through digital design and digital construction with robotic arms, simulation techniques such as finite element analysis can be used to show the properties of timber more fully and to make the most of them in the design and construction process. By modelling the specific parameters of timber rods and timber nodes, digital robotic fabrication technology can make full use of the material properties of timber and avoid the disadvantages of using timber in more curved forms. This data can be converted into machining data for the robotic arm, which can be used for precise machining by bending and cutting. The 3D sewing tool in the Figure 4.54, for example, allows complex timber nodes to be machined, not just interspersed nodes in a particular plane. The sewing of timber panels by robotic arm sewing demonstrates the possibility of lightweight construction by removing the metal nodes from the construction. 151 prefabricated units are made up of jagged joints, which are fixed by robotic arm sewing.

This shows that when the properties of a material are transferred to data in a more comprehensive way, the material has more scope and potential to be used. This shows that even raw materials that have not been machined have more scope to play with the digital machining intervention of the robot arm. The emergence of new materials also shows that there are more possibilities for construction methods. Examples include the 3D printing of robotic arms using composite materials, and the robotic arm weaving process using composite fibres. Whether it is for traditional or new materials, the robotic arm intervention allows the properties of the material to be fully exploited and expands the construction process as well as the geometry.



Source: <https://www.icd.uni-stuttgart.de/projects/icditke-research-pavilion-2015-16/>
 Figure 4.54 Sewing the connections between components

4.4.4 Increased efficiency of data exchange

The technology of the robot arm establishes a direct connection between digital design and digital construction. Traditional architectural design is a one-way output process. The designer makes a design plan, draws construction drawings, and then builds according to the drawings and procedures. However, with the participation of digital technology, this linear construction is replaced by a systematic construction method. Designers need to have a macro-control of the entire workflow, including the analysis of the transmission of the information and the software design platform they rely on, to design the entire system. Therefore, the emergence of CNC machinery such as robotic arms has made the information interaction between computer models and the actual construction more flexible and diverse.

On one hand, the CNC machinery can receive various types of data, including not only mechanical behaviour data translated from computer information models but also environmental information, on-site construction conditions, and human behaviour. This information can be homogenized into computer data parameters. Different types of parameters are calculated by strict logic defined by the designer, and the motion model of the CNC machinery is obtained by means of multi-agent algorithms. For example, the “Light Object” project conducted by the Robotics Laboratory of the California School of Architecture studied the data interaction between human behaviour and the motion of a robotic arm. Another example is the robot construction experiment of Tsinghua University in 2014, which studied the possibility of human behaviour data guiding the operation of the robot arm. Through these innovations in interactive methods, the application of CNC machinery such as robotic arms enable more data types to be introduced into the input of digital construction. On the other hand, the application of the robotic arm also makes the interaction between external parameters and construction data a dual-way process rather than a one-way procedure. Meanwhile, besides the computer data as one of the inputs, the on-site construction condition generated by the robotic arm itself can also be fed back to the robotic arm, which will in turn participate in the computer data calculation process. Thus, the data exchange achieves an information loop of the positive and negative interaction and feedback.

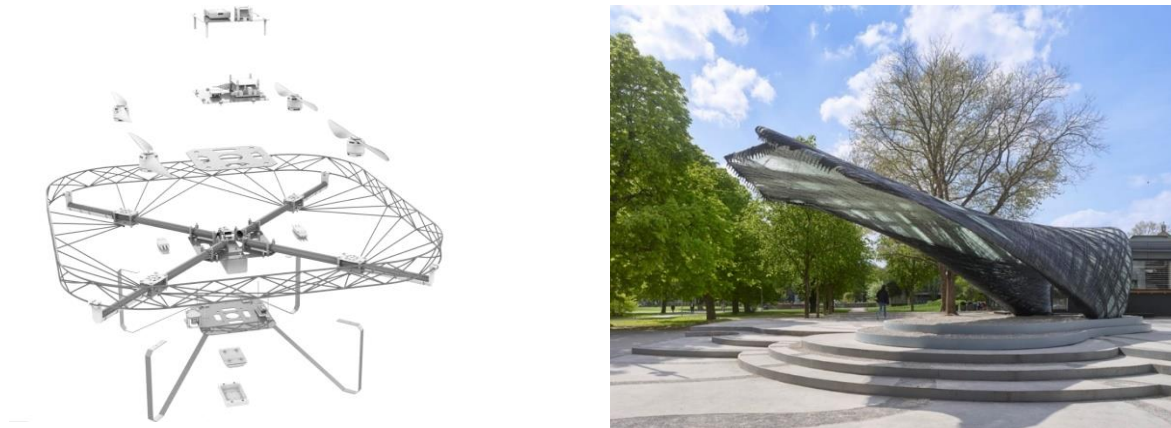
4.4.5 New types of fabrication

The complex design of the building's structural form requires a greater variety of fabrication methods to meet the needs from design to construction. The use of robotic arms in digital construction has led to a revolutionary improvement in construction process technology, which is manifested in two main ways: an increase in the dimensionality of the manufacturing process and an expansion of the manufacturing process categories. In terms of the construction dimension, traditional construction processes can basically be grouped into two categories, one that relies primarily on the subjective judgement of the human brain and basic measuring tools, such as traditional brickwork. However, humans are unable to process overly complex information on their own and can only cope with simple geometric forms. The other is desktop machining processes, which operate with a higher degree of precision than human operations but are still mostly restricted to a two-dimensional machining environment. The limitations of the process therefore limit the variety of design forms. Taking cutting technology as an example, conventional cutting technology such as laser cutting, CNC milling cutting, chainsaw cutting, waterjet cutting, the common feature is that these methods can only be processed in two-dimensional plane to cut perpendicular to the table cut. With the development of technology, five-axis CNC and other multi-dimensional CNC machinery has now also appeared, but still, they are subject to certain dimensional constraints. If the dimension of processing is limited, the most immediate effect is that the form or articulation of the material is also limited in dimension.

And by combining traditional cutting tools with robotic arms as ports for technical integration, then the process will make a dimensional leap. If the milling process is combined with the robotic arm to obtain the robotic arm milling cutting process, it can be three-dimensional bevelled surface cutting of materials, similarly the combination of chainsaw and robotic arm to obtain the robotic arm chainsaw cutting process can be cut on the curved surface of the stone. The expansion of the dimensionality of the process not only frees up material shapes and articulation, but also allows for the direct processing of materials in three dimensions to achieve material savings and optimum performance. The involvement of robotic arm technology is not only in the two-dimensional to three-dimensional conversion, but also as a dynamic processing process linked to the time dimension, and its construction results are closely related to the construction process, for example, the robotic arm can make information feedback and data update adjustment according to the construction situation in the field, which makes the design and construction with the robotic arm autonomous decision making ability and shows the randomness of the results. In terms of manufacturing process categories, robotic arm technology serves as a vehicle for the integration of more and more cross-disciplinary technologies into digital construction. For example, robotic arm sewing technology has emerged from the combination of robotic arms and sewing machines, which would have been difficult to imagine in the past in the construction sector.

In Figure 4.55, two robotic arms were used in the project as well as a drone, which passed the ends of the fibres back and forth between the two robotic arms to achieve a larger span of composite fibre tension. The most significant feature of the pavilion is its 12-meter-long overhang, covering a much larger area than the grounded base section, which is almost impossible to achieve with conventional

construction techniques. The complex form is achieved by the fibre tensioning based on high progress structural simulation calculations and thorough material lightweight properties to achieve pre-stress equilibrium.



Source: <https://www.itke.uni-stuttgart.de/research/icd-itke-research-pavilions/icd-itke-research-pavilion-2016-17/>

Figure 4.55 Lightweight, Long Span Fibrous Construction

4.4.6 Limitations

According to the cases of various fabrication methods, there are different road maps for this new technique, from the proportion of the components fabricated by the robotic arm in the whole structure to the scale of the structure to which the robotic technique is applied from component scale to construction scale. In summary, there are limitations for this technique when

(1) Flexibility and adaptivity

Due to the limitation of the reachable workspace of the robot arm, most of the size of the particles fabricated by the industrial robot are constrained, especially the robot without mobility. This means that the industrial robot is more applicable in fabricating the components. In this application, the components can be classified into connections, bars, panels, load-bearing ones, and enclosure ones, varying in detail, size, and total number. Most of the cases introduced of robotic fabrication are in irregular shapes, leading to the design of the nonlinear components. The diversity of these components means the adjustment of the parameters, modules, and operation commands in every fabrication process. These constraints from the design of the components reduce the flexibility of the robotic fabrication. The specific tool path developed for one component with a certain size and shape is not adaptable to another component in the same shape but of different size because of the singularities or out of the reach of the workspace. Besides, if the component needs more than one fabrication method like cutting and drilling together, this requires the development of a specific tool-changer or different end-effectors, even more than one robot. These limitations mean to finish one whole structure composed of many components in various sizes and shapes, different tool paths and tools are needed if fabricated and constructed all by robotic technique. This limitation puts forward the need for the modularity and standardization of the components or to develop a workflow constituted by several robots with flexibility and adaptivity.

(2) Accuracy and Reliability

The industrial robot itself is a fully developed technique with high accuracy to operate precise fabrication tasks in the manufacturing industry. However, the accuracy of the robotic fabrication differs depending on the working conditions, material properties, tools, and control methods. For working conditions, robotic fabrication is applied on-site and off-site both. Most of the on-site construction demands the mobility of the robots and this brings the needs for accuracy of the position of the robots, besides the complex terrain or weather condition of the construction site. The materials like wood have complex material properties because of the knots, moisture content, direction of the grains, which impact the accuracy when fabricated. The tools mounted on the robot arm have a direct impact on the accuracy. The force control, the speed of approaching, the position of the tools all affects the results. The demands for the accuracy also vary in different scales, from 0.1mm in component scale to 1 mm in construction scale. If robotic fabrication is applied to manufacture the small size components like milling or cutting panels in complex shape, then the demand for accuracy is high, whereas in large scale like the 3D printing applied in the whole structure with not much details. This limitation can be reduced by off-site prefabrication. Prefabrication means the mass production of certain types of small-scale components and the deviation can be eliminated by adjusting the proper tool parameters, moderate force interaction, and swift tool paths.

(3) Economic Efficiency

From an economic point of view, robotic automation fabrication is a new technique in manufacturing and the cost is high in this beginning stage. For now, robotic fabrication also puts high demands on the properties of material, which needs the development of new types of material suitable for the technique including fluidity, strength, or tenacity requirements. Correspondingly, the usage of these newly developed materials also requires the alternation for the end-effector tool to be adaptive to the specific materials like glue when fabricating engineering timber. Most of the cases applying the industrial robots are mostly in irregular and non-linear shapes. Because of the complexity of the geometry shape, every component in the whole structure is not the same. When fabricating these non-standard components, it would cause low material efficiency. To overcome this limitation, the homogenization of the structure to generate components with uniformity to reduce the standard errors and variance errors of the size of components to enhance the material efficiency.

(4) Evaluation of building performance

Robotic fabrication is strongly connected to digital design. The design takes inputs to generate plentiful geometric shapes which cannot be controlled. The final decision for robotic fabrication would be selected according to some standard among the unpredicted results. Whether the standard of selecting the geometry suits the fabrication has no conclusions. The evaluation for the materials developed for the robotic fabrication, building performance of the digital structure, automaticity of the robotic technique, accuracy of the fabrication, and the efficiency of the operation of the digital workflow from design to fabrication. As for now, there are not enough evaluations from these aspects, the robotic fabrication can

be only applied on an academic scale for research aims. For further development in the construction industry, these evaluation results matter.

4.5 Conclusion

Based on the introduction of two real robotic arm cases, this chapter demonstrates the workflow to generate the tool path for different scenarios (off-site prefabrication and on-site construction) after the robotic working environment, which includes both hardware and software, is set.

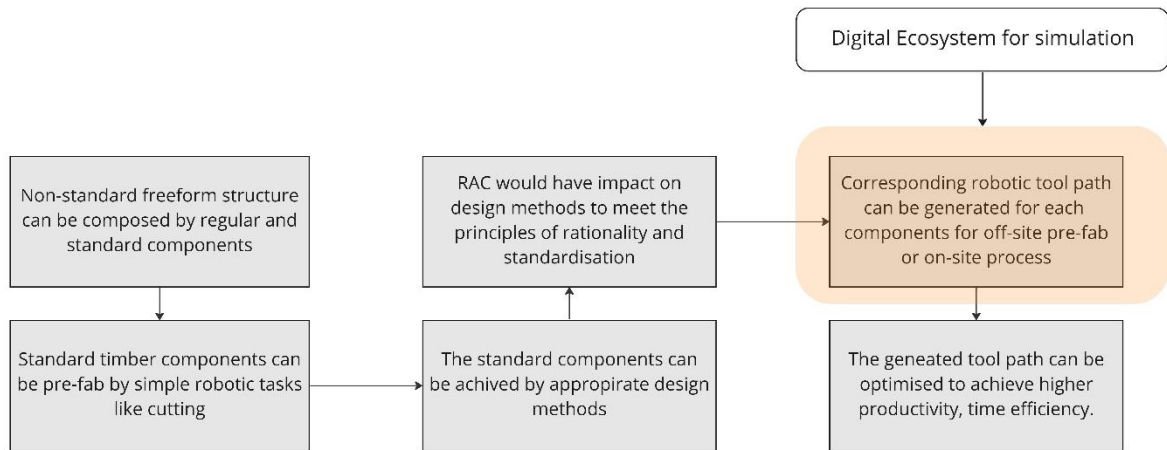


Figure 4.56 Connection to Hypothesis

In details, a preliminary understanding of robot motion control principles is achieved through the motion control of a self-assembled simple robot arm. By presenting a specific robot arm fabricated timber joinery example using robotic chainsaw, a comprehensive introduction to working space, workflow, import parameters, data import and export is presented. Based on the two cases, the RAC system is more comprehensively explained from working space setting, robot system and different software for simulation and visualisation aspects. Through the analysis of many different types of robotic fabrication and construction cases in recent years, the characteristics (rationality in performance, complex geometric design, using diverse material and needs for new fabrication techniques) and some shortcomings is be summarized, which aims to provide a more adequate theoretical basis for future research trends and development directions.

The first case put forward the needs for connecting the spatial position of robotic arm to the motion control and the second case poses the questions of low productivity and uncertainty in path planning. These two questions would be solved in Chapter 8. Besides, the second case also demonstrated one problem that when adjusting the cutting order still could not avoid the singularities, then the geometry design needs to be changed. This raise another question that how to determine the design can be achieved through robotic automation construction technique and how to select the appropriate design methods for freeform structure, which would be discussed in Chapter 6 and 8 respectively, shown in Figure 4.57.

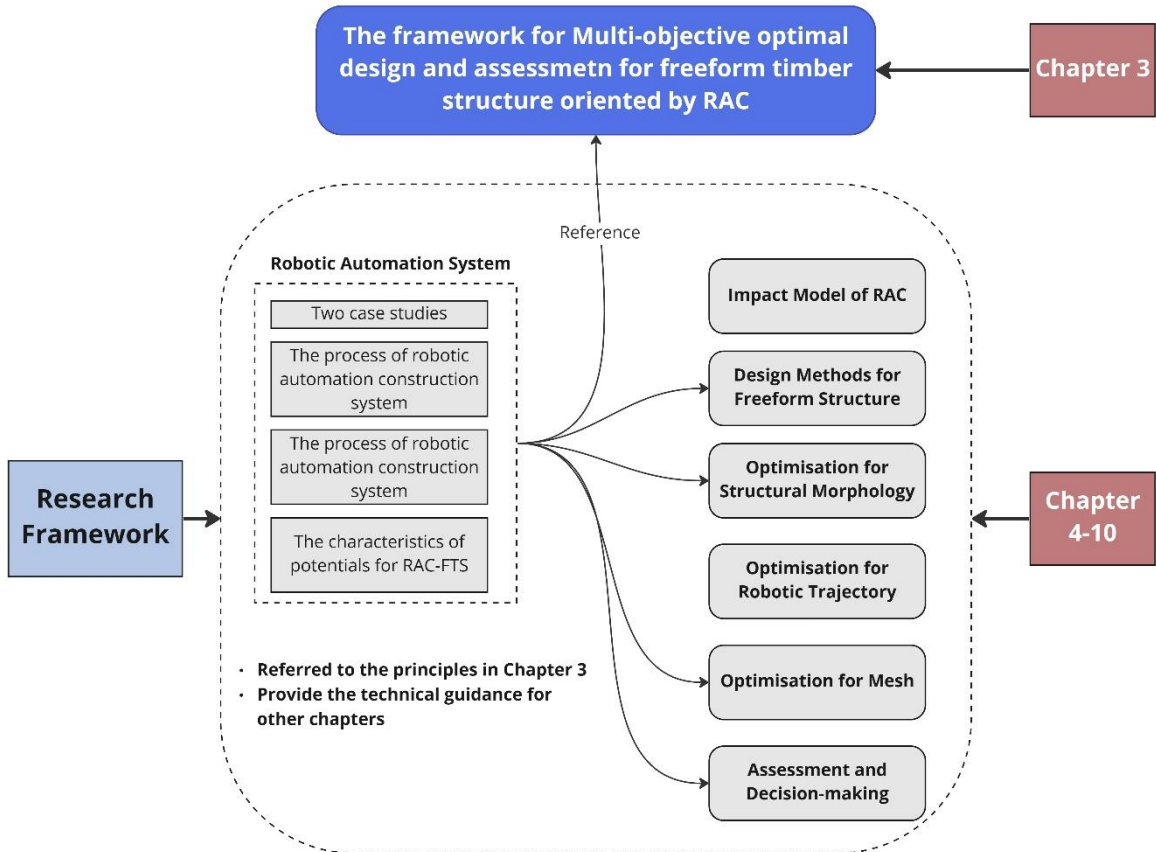


Figure 4.57 Connection with other chapters

Chapter 5

Hierarchy impact model of Robotic-automation Oriented Design System (RAOD)

Case 2- robotic chainsaw cutting depicts one scenario in which the design needs modification in order to generate a tool path free of singularities and within the reach of the robotic arm. Then whether the technical factor – “Robotic Automation” would have an influence on the design is put forward. Faced with the gap between the design model and current fabrication (or construction) technique performance on accuracy and flexibility, the specific impact factors and impact level of the robotic construction technique, as one main factor for freeform morphology needs to be identified and quantified. The influences on the challenges mentioned above on the freeform morphology design need further discussion from a quantitative perspective to support the determination for the appropriate freeform morphology design methods.

The factors that have an impact on the design outcome of robotic automation (RA) are analysed in this chapter. As the evaluation for impact level is subjective and qualitative, certain quantitative analysis methods need be adopted to quantify the impact of RA on the design, establishing a numerical relationship between design and RA from impact level analysis aspect. The overall roadmap for this chapter is shown in Figure 5.1. For the research question, text clustering is selected to provide reference for the impact factor determination. The Freeform Timber Structure system would be defined to different parts to evaluate the impact separately. Fuzzy-AHP is selected to operate the assessment based on a Multi-input and Multi-output (MIMO) system model for freeform timber structure.

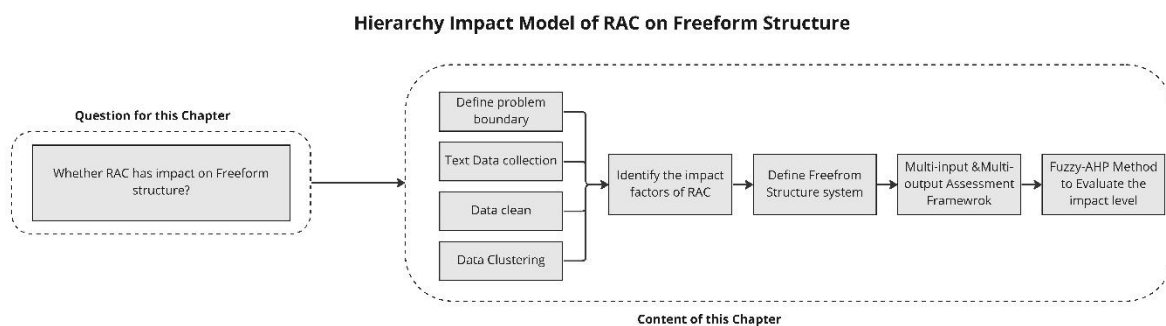


Figure 5.1 Roadmap for Chapter 5

5.1 Impact factor identification for RAC Impact Model on FTS through Text Clustering

Robotic-automation Oriented Design (RAOD) is to achieve rational and fabrication-oriented design from the start to the end throughout the whole process. More specifically, the fabrication-awareness permeates pre, during and post the design. How to apply this awareness to the design process and how the fabrication-oriented design differs from normal design are the main focuses in the RAOD. Figure 5.2 shows that in RAOD system, to get the design output based on the design requirements as input, the impact from robotic fabrication needs to be analysed first. As robotic automation (RA) is a new trend in construction industry, the production types, specific techniques and aims varied throughout the entire

process from design to results. Correspondingly, the conditions of evaluating the impact of this new fabrication method on designs differed as well.

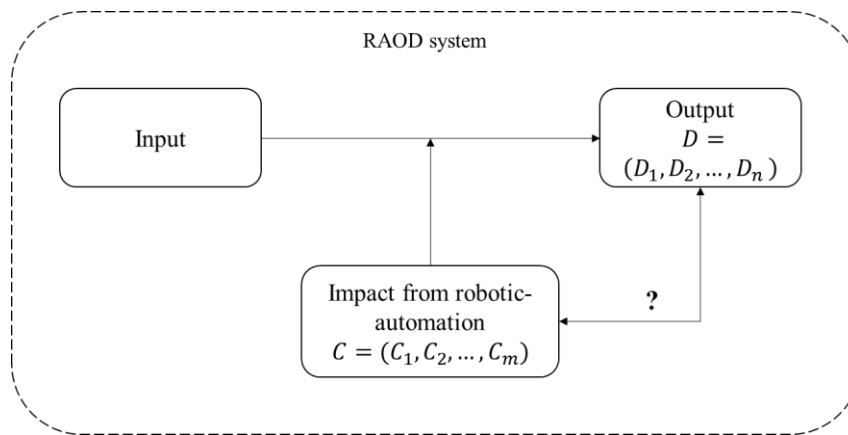


Figure 5.2 RAOD system composed by Input, output, and impact

Different from general impact analysis research with one evaluation criterion, the freeform timber structure design (FTS-D) includes several criteria for the whole design. In the complex RAC-FTS system, the contributing elements that can influence the final design results are numerous. Every factor that has an effect can be utilised as an indicator to evaluate the impact level on different criteria.

However, selecting too many evaluation indicators throughout the process is not recommended to avoid duplication. As a result, establishing a complete, objective, and reasonable impact level evaluation indicator system is critical to acquire valid, quantitative and accurate results. It is necessary to conduct an accurate and comprehensive analysis of the impact factors to ensure that the indicator selection for evaluation objectively reflect their impact on the entire system, to the greatest extent possible. Considering RA practices operated in academia and industry are in full swing, the indicators would be summarized by the following case studies including different kinds of material and robotic end-effector tools.

5.1.1 Text dataset for Robotic Automation Construction and Freeform Structure

The analysis includes papers, research, and case studies with the aim of summarising the main key words of robotic technology and the effect they have on the comprehensive freeform structure design system (design, fabrication, construction and management) in order to provide the references for the impact factor determination for the impact model.

The process for the text clustering is shown in Figure 5.3. The first step is to identify the research scope to determine the search area for the text including the questions, key words for searching, the replacement words and the needed information e.g., title. Then the data could be collected in different way e.g., crawling data⁶⁶ from the webpage in the original format. The collect would go through the cleaning process to only keep the useful text data. The text would be counted to turn into numerical data to operate the clustering. Then the final results would be visualised.

⁶⁶ Crawling data means that the program is used to obtain information about the content of a website or any file that is needed, such as text, video, images and other data

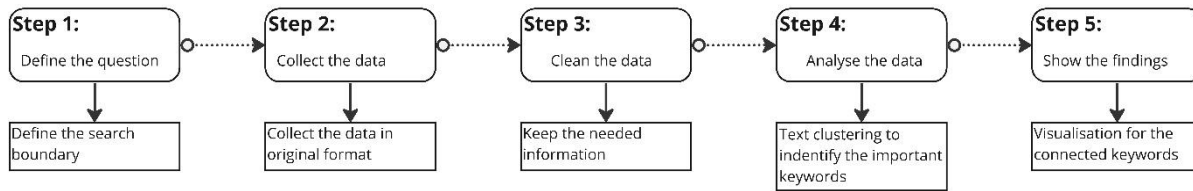


Figure 5.3 Text Clustering Process

The detailed text clustering process is operated as follows:

Step 1: Define the search boundary

The level of search progresses from general concept “Robotic Automation” (RA) to detailed technique “Robotic Automation Construction in Freeform Timber Structure” shown in Figure 5.4. The literature is gathered to sort out the different levels of topics contained within RA to sort out the logical relationships between RAC and FTS to conclude the indicators for RAOD.

The boundary for the data is a collection of literature in the field of robotics, digital fabrication, and computational design. The text clustering includes the abstract review to filter the needed literatures and full-text review to extract the important information without reading every word of the full-text (Aggarwal & Zhai, 2012). The findings of its analysis, which resulted in the identification of impact factors, can be used to quantify the factors, and reduce the bias or deficiencies inherent in subjectivity.

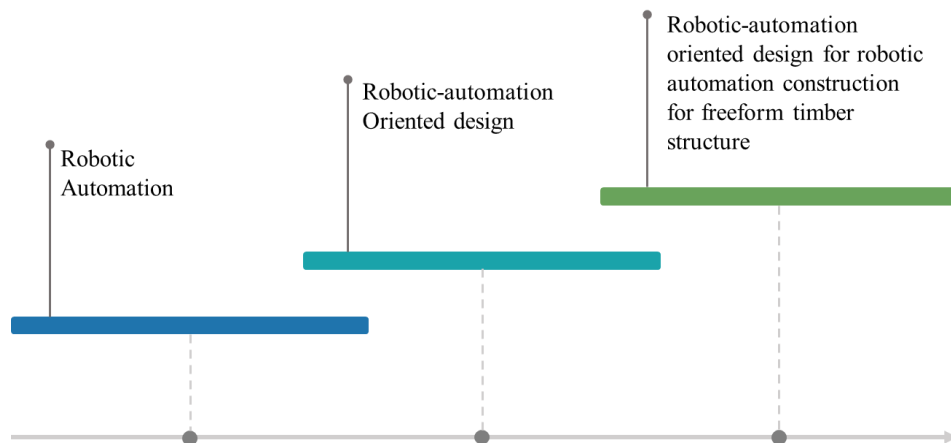


Figure 5.4 Level of literature research

The preliminary step of text data collection is to construct the dataset of the literatures including conference papers, journal papers, which is to filter the papers related to RAOD manually. The searching takes the Scopus as the main database and includes three main categories:

- (1) Search keyword “robotic fabrication” to search the research that link ‘robotics’ to ‘architecture’.
- (2) Search keyword like “robotics” to find the specific and related research about robot.
- (3) Search keyword like “complex design” to identify the connection between the new type of design methods and the demands for fabrication techniques.

Step 2: Collect the Data

The search takes two steps: 1) rough search; 2) detailed search. Web of science (WOS) is selected as the dataset for searching and the time is limited to publication date from 01.01.2010 to 31.12.2020 using the core collection of WOS. In searching for the related research, there are some variations for the keywords. For example, some papers would use “digital fabrication”, “robotic automation construction” to substitute “robotic fabrication”. The same for “complex design”, in some circumstances, the researchers use “digital design” or “computational design” to replace “complex design”. More detailed information for the search details can be found in Appendices – 2 Table A2 1.

Table 5-1 Summary of rough search details

Source list	Description
Source website	Web of science
Years	2010-2020 (11 years)
Text type	Articles; Reviews; Conference paper; Book chapter
Collection size	13775
Reference size	113691

The rough search is taken at first to figure out the levels of categories of each search word and then research areas within the search keywords are selected accordingly. More detailed information about the searched literatures e.g., different research categories can be found in Appendices -1 from Figure A1 1- Figure A1 5. More details for searching results along the timeline can be found in Appendices – 2 Table A2 2-Table A2 3 Table .

Step 3: Clean the data

After step 2 including the rough search and detailed search, a file containing different types of information would be formulated shown in Figure 5.4. The figure shows irrelevant information is also included in the file. After data cleaning, only the important information would be kept. In this case, the selected information includes “Title”, “Abstract” and “Keywords”. The benefit of data cleaning is not limited to retaining useful information, but it can also verify the efficiency of the data source, which in this case is the literature. Normally, in meta-analysis for systematic review, the “Prisma” is needed to validate the source of the literatures. Text from the literature is converted into "data" in text clustering, which is then analysed using counts for the number of occurrences. For the situation like not qualified literatures or not relevant search results, as the text dataset is “big data”, and because clustering only selects factors with higher weights, the effect of the error generated will gradually decrease over several iterations and will have no effect on the final results’ validity. After data cleaning process, the text dataset would be like Figure 5.5 with only the information relevant to the text clustering for important impact factors.

Publication Type	Authors	Book Authors	Group Authors	Book Group Author/Researcher ORCID	Book Editor/Author - AI Article Title
J	Wagner, Hans Jakob; Alvarez, Martin; Kyjank, Ondrej; Bhiri, Zied; Buck, Matthias; Mer				Flexible and transportable robotic timber construction platform - TIM
P	APLIN R H, JENNER V M				Method for processing timber by control system for in-feed assembly of timber processing system, involves receiving feedback from alignment system, and actuating marshalling system to enable progression of piece of notched timber
C	Leder, Samuel; Weber, Ramon; Wood, Dylan; Bucklin, Oliver; Menges, Achim			IEEE	Design and prototyping of a single axis, building material integrated, distributed robotic assembly system
C	Reinhardt, Dagmar				Sousa, JP Design Robotics Towards human-robot timber module assembly

Figure 5.5 Example of Original Text Dataset

Article Title	Abstract	Keywords
Flexible and transportable robotic timber construction platform - TIM	This paper presents a new approach to robotic fabrication in the building industry through the conceptualization, development and evaluation of a largescale, transportable and flexible robotic timber construction platform - named TIM. Novel solutions are necessary to make robotic fabrication technologies more accessible for timber construction companies. The developed robotic system is location independent and reconfigurable. It can be rapidly integrated into existing fabrication environments of typical carpentries on a per-project basis. This allows the exploitation of emerging synergies between conventional craft and specialized automation technologies and benefits both quality and productivity of the trade. We portrait how the platform enabled the effective robotic prefabrication of a complex segmented wood shell structure and discuss the fabrication system based on critical performance parameters. Further research is needed to disentangle the mutual dependencies of building-systems and respective automation technologies.	Robotic, Timber, Flexible, Fabrication, Automation Technolog
Method for processing timber by control system for in-feed assembly of timber processing system, involves receiving feedback from alignment system, and actuating marshalling system to enable progression of piece of notched timber	NOVELTY - The method involves receiving spatial dimensions of a progressed notched timber piece sensed by a measurement system from the measurement system. An alignment system (159) is actuated to engage notches of the progressed notched timber piece and position based on the sensed spatial dimensions. A feedback is received from the alignment system that the progressed notched timber piece is collected by a robotic stacking tool. A marshalling system (161) is actuated to enable progression of another piece of notched timber in response to the feedback. USE - Method for processing a timber by a control system for an in-feed assembly of a timber processing system (all claimed). ADVANTAGE - The method enables indexing individual timber pieces past the marshalling system, while the remainder of the timber pieces is prevented from progressing past extended stopper units. DETAILED DESCRIPTION - INDEPENDENT CLAIMS are also included for the following: (1) an in-feed assembly (2) a control system (3) a computer readable medium comprising a set of instructions for processing a timber (4) a robotic tool for engaging and disengaging timber from an in-feed assembly (5) a timber processing system (6) a transporting robot for collecting and transferring timber from an in-feed assembly of a timber processing system (7) a method for controlling a timber processing system. DESCRIPTION OF DRAWING(S) - The drawing shows a perspective view of an in-feed assembly. in-feed assembly (100) Conveyor system (120) Driven roller (122) Alignment system (159) Marshalling system (161)	Control system, Timber processing, Robotic tool, Alignment system
Design and prototyping of a single axis, building material integrated, distributed robotic assembly system	The creation of a new generation of small, modular, simplified robots for the assembly of custom-built structures is highly relevant in the fields of architectural design and construction. The aim of the research is to present a new feasible robotic system that could be implemented for the assembly of strut structures. The research showcases the development of bespoke single axis, double gripper robots that as a distributed robotic system assembles structures from standardized timber struts. We present a control scheme for collective assembly, only enabled by the collaboration of multiple robots and timber struts, shifting away from prefabrication towards autonomous, robotic, on-site construction in architectural scale.	Robotic system, Assembly, Collaboration
Design Robotics Towards human-robot timber module assembly	This paper presents research into an ecosystem of human-robot collaborative manufacturing of timber modules that can respond to diverse environmental conditions through construction tolerances. It discusses the design and robotic workflow for two case studies with unskilled participants in an academic context, for the production of non-standard spatial and structural scaled prototypes that develop new systems for thinking and making architecture.	Collaboration, Design, Human-robot, Timber

Figure 5.6 Example of Cleaned Text Dataset

Figure 5.7 shows the count and ratio of each research area within the categories in the left line and the proportion of different research areas covered by each research category in the right line. In the automation construction category, “management” and “technology” takes important parts in the field, while the research progress on “on-site” and “off-site” is relatively consistent.

In this chart, “complex design” and “robotic fabrication” research categories have a crossover of research area “material”, where “complex design” constitutes 85 percent of the total. The visible intersecting relationship shown in the right line helps to identify the impact factors to avoid duplicating or missing information. This proves the assumption that “material” is a very suitable entry point for integrating design and processing. In searching for “freeform timber”, there are 22 results for it, which implies that design rationalisation and fabrication techniques are inextricably linked to complex design.

The technical support for the complex architecture is provided by automation construction technology. In this context, the combination of the two, from the macro-automation plan to the fabrication and construction of specific complex projects, necessitates the use of relevant robotics elements to realise micro-level design and optimisation.

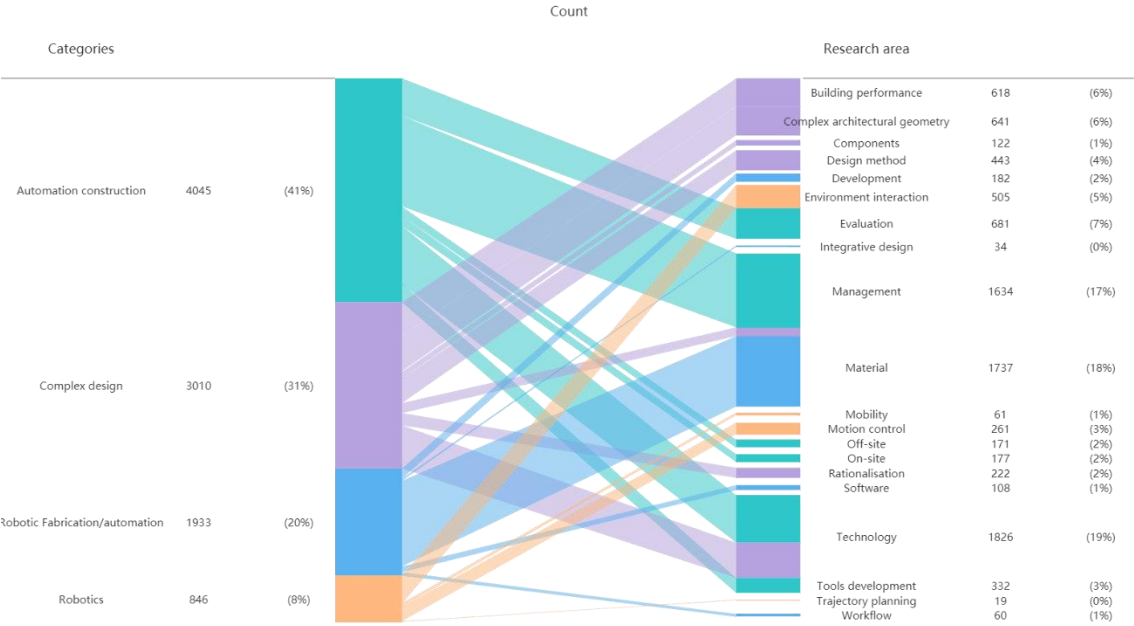


Figure 5.7 Bilinear chart for the count of the research areas and categories

Step 4 would be operated in the following section.

5.1.2 Impact factor identification method (Impact factor and output factor analysis) for RAOD

The scientific validity of the study depends to a large extent on the adequacy of the identification of the relevant impact factors. Figure 5.8 illustrates the objective, which is to identify the impact factors $C = \{c_1, c_2, \dots, c_m\}$ and design result $D = \{d_1, d_2, \dots, d_n\}$, so that to evaluate the impact level quantitatively based on the overall input of the RAOD system setting as the premise. The factors identification is general which includes different material (i.e., timber, concrete, carbon fibre) and different fabrication methods (i.e., 3D printing, welding, sewing) in different scale and various working conditions. The general impact factors determination is to specialise the specific factors restricted to the RAC-FTS, which is one special case under the RAOD. As RAC-FTS is determined, so the input can be set as freeform and timber structure. The following part is to figure out the C in *Impact* and D in *Output*.

There are no specific methods of identifying the potential impacts. Risk management has formed a relatively well-developed method and process for identification, which can be applied to determining the impact factors. Table 5-2 shows the most common methods which are derived from risk identification.

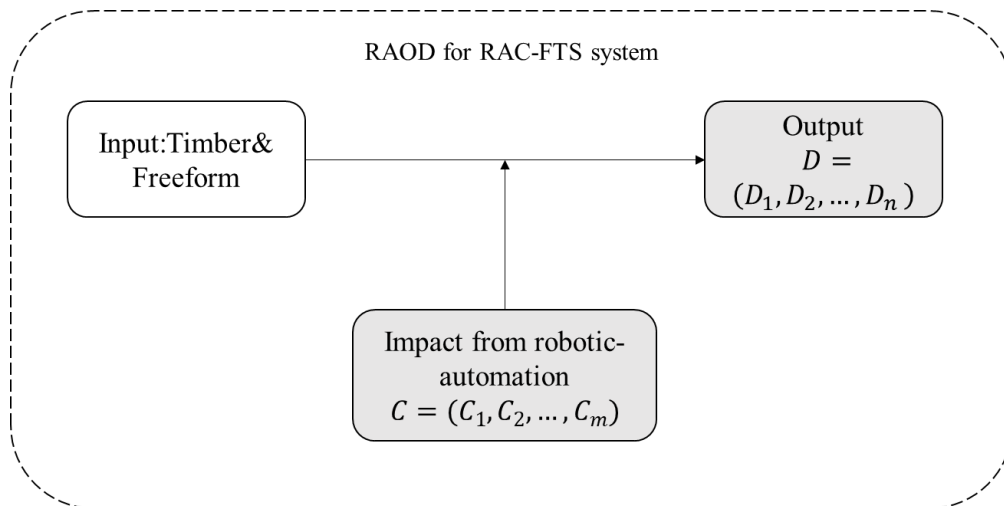


Figure 5.8 RAOD for RAC-FTS design system

Table 5-2 Risk identification method

Classification	Specific method	Definition
Analytical method	Fault Tree Analysis (FTA)	Beginning with a specific incident, use logical reasoning to break it down layer by layer to identify the various potential risk factors.
	Check list	According to the checklist, professional risk identifiers assess which risks are there in the project based on previous experience with similar projects that were created and prepared in advance.
	Work Breakdown Structure (WBS)	The system is decomposed systematically (project overall, unit work and sub-component work), risks are discovered by analysing project components, relationships between components, and links with external environment.
Expert investigation	Delphi	In accordance with specified protocols, a questionnaire is produced by the surveyor and experts contacted by letter. After numerous rounds of feedback, experts connect with each other anonymously through the surveyor's feedback to acquire more consistent risk identification
	Brainstorming	Invite experts to participate in a brainstorming session where they can come up with ideas and approaches to identify hazards as fully as feasible
	Self-judgement	To create individual judgments on project hazards based on the micro-intelligence structure of specialists, which are subsequently summarised and compiled to obtain broad conclusions.

Different analysis methods differ in advantages and disadvantages, for example, the FTA method has the advantages of clear cause-effect relationships, rigorous logic, which can be used for both qualitative and quantitative analysis, with the disadvantages of being difficult to construct and prone to errors and omissions. A clear hierarchy, structure and logic are advantages of the WBS approach and on the other hand, it suffers from the huge decomposition of the work structure. As a quick and easy way to discover hazards, checklists have the advantage of being quick and easy. However, they also have the disadvantage of demanding a high level of skill from the tabulator. As architectural robotic automation is still in its development stage, only a few studies on impact factor analysis of this system have been conducted. For expert investigation, it is hard to reach a consensus about the detailed and specific impact factors of robotic automation on architecture design.

To make the identification for impact factor subjective, text mining is applied to ascertain the intrinsic and extrinsic non-linear relationships between various topics and keywords. Text clustering is a common

text mining method that looks for similarities between texts in text data and classifies the data, accordingly, ensuring that different classes of data are as distinct as possible while similar data are as similar as possible. Clustering, as opposed to classification, is a type of unsupervised learning in which categories are not humanly specified but are the result of data analysis and are carried out entirely automatically by the computer without human intervention. Text analysis encompasses information retrieval, lexical analysis to investigate the frequency distribution of words, pattern recognition, tagging annotation, information extraction, and data mining techniques such as link and association analysis, visualisation, and predictive analysis. There are numerous clustering methods available, each with its own set of characteristics, such as hierarchical methods, partitioning methods, density-based methods, and so on. Text clustering is a high-dimensional⁷ clustering problem for this paper, which necessitates strong clustering ability, high execution efficiency, simple parameter setting, and visual representation of high-dimensional data in low-dimensional space to fully identify the impact factors.

One of the more representative neural network-based clustering methods is SOM (self-organizing maps), which can handle non-linear relationships in high-dimensional data (Vesanto & Alhoniemi, 2000). SOM was firstly proposed in 1981 by neural network expert Professor Kohonen (Kohonen et al., 2000) and is structurally like the now popular multi-layer perception (MLP) like artificial neural networks (ANNs) model in that both are made up of very simple neuronal structures. SOM is a clustering algorithm that uses unsupervised learning to learn about data. Its goal is to detect sample similarity for category imputation. SOM has proved its efficiency in text clustering (S.-H. Huang, Ke, & Yang, 2008; Isa, Kallimani, & Lee, 2009; Y.-c. Liu, Wu, & Liu, 2011; Paukkeri, García-Plaza, Fresno, Unanue, & Honkela, 2012).

SOM is, in essence, a neural network with only one input layer and one output layer which is called competitive layer as well. A competitive layer node represents a class that needs to be clustered. Unlike general neural networks, which are trained by backward transfer of loss functions, it employs a competitive learning strategy, with neurons competing with one another to gradually optimise the network. SOM can find complex non-linear relationships hidden in high-dimensional data and present them as simple geometric relationships in low-dimensional space. One of the SOM's characteristics is that the nodes in the competitive layer are topologically related. This topology is determined by the dimension of the model. If a one-dimensional model is needed, the hidden nodes are connected sequentially in a line, similarly, a plane for a two-dimensional model, shown in Figure 5.9. The dimension of the input vector determines the number of neurons in the input layer, and one neuron corresponds to one feature. Because the competitive layer is topologically related, it is also possible to state that the SOM can discretize any dimension input onto a discrete space of one or two dimensions (higher dimensions are not common). The Computation layer nodes are fully connected to the Input layer nodes.

⁷ Words in text are transferred to vectors and the number of the text determines the dimensions of the data. Data dimensionality is typically high (>100) in areas such as text clustering, web mining, and so on.

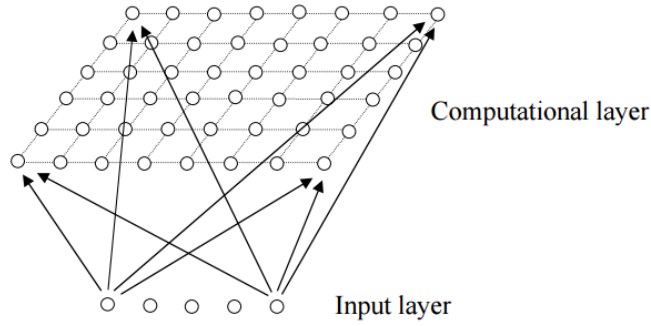


Figure 5.9 A two-dimensional model

The framework of SOM system for the text clustering in this section is shown in Figure 5.10. The abstracts and conclusions of collected literatures are selected as the raw data. Before the training, the text documents need pre-processing to reduce the dimensions greatly to reduce encoding time. The text data is broken down into small units which are also known as tokens. Less important words which is not helpful in illustrating or explaining information like definite articles, prepositions can be classified to stop words and can be removed, the same to punctuations. After the pre-processing, the frequencies of the words in each document are counted using the Term Frequency - Inverse Document Frequency (tf-idf) method.

$$tf \times Idf(T) = tf(T) \times \log\left(\frac{N}{df(T) + 1}\right) \quad (5.1)$$

N : number of documents in the entire document set.

$tf(T)$: total number of frequencies of word T in the entire text set.

$df(T)$: number of texts containing the word T.

Each document is represented as a collection of word frequencies after pre-processing. In this part, after the computation of tf-idf, top 8 keywords are selected to represent the document. A document library can be represented as a $m \times n$ word document matrix D , with different words corresponding to different rows of matrix D and each document corresponding to a different column of the matrix, where:

$$D = [d_1, \dots, d_i, \dots, d_n]_{m \times n} \quad i = 1, 2, \dots, n \quad (5.2)$$

$$d_i = [t_{i1}, t_{i2}, \dots, t_{ij}, \dots, t_{im}]^T, \quad j = 1, 2, \dots, m \quad (5.3)$$

Then the new form of representation of each document needs to be transferred into structured data using vector space model (VSM) (Aas & Eikvil, 1999). The document space is viewed as a vector space made up of orthogonal feature vectors. Words in a document are considered feature terms, and the document is represented as a feature vector in a vector space made up of feature terms. It is written as $V(d) = (w_{t_1}(d), \dots, w_{t_i}(d), \dots, w_{t_n}(d))$. t_i is the feature term, and $w_{t_i}(d)$ is the weight of t_i in document d_i . The weight is also calculated by tf-idf method:

$$w_{ij} = tf_{ij} \times idf_j = tf_{ij} \times \log\left(\frac{N}{df(t_i) + 1}\right) \quad (5.4)$$

w_{ij} : the weight of feature word t_{ij} in document d_i ;

tf_{ij} : the frequency of t_{ij} in document d_i ;

idf_j : the inverse document frequency of t_{ij} ;

N : the number of documents

$df(t_i)$: number of documents containing the t_{ij} ;

To cluster the featured keywords, the feature space of neurons and the topology of SOM needs to be constructed. The feature space of SOM is built upon the extracted featured keywords. The process of clustering is shown in Figure 5.10.

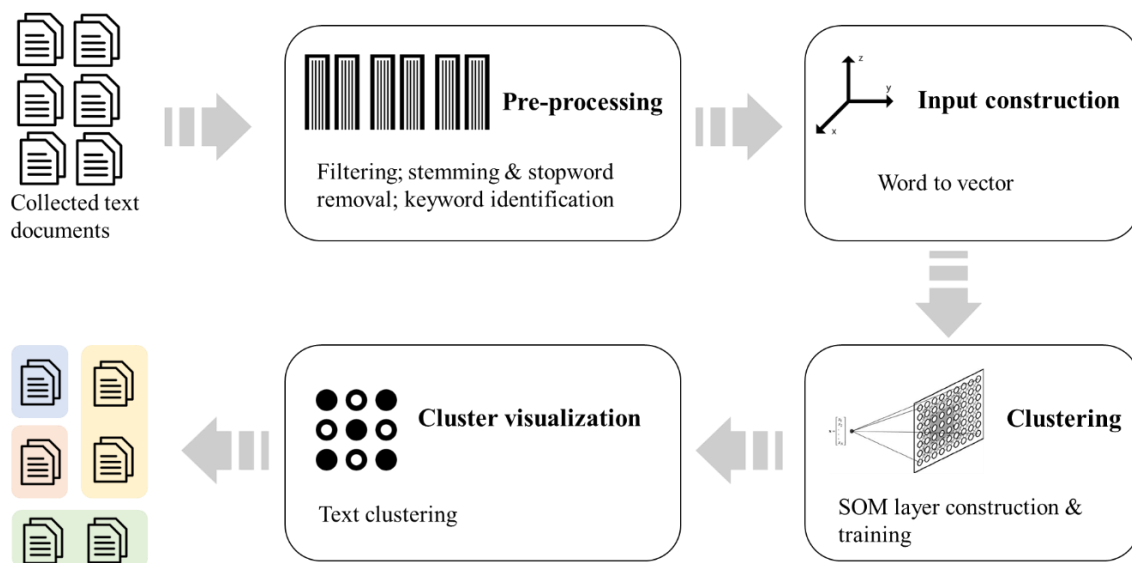


Figure 5.10 The process of SOM cluster

Once the topological relationships have been determined, the calculation process begins. During training, each input sample finds a node in the hidden layer that best matches it, which is referred to as its activation node, also known as a "winning neuron." The activation node's parameters are then updated using stochastic gradient descent. Simultaneously, the points near the activation node are updated appropriately based on their proximity to the activation node. In more detail, the process is divided into several steps:

- (1) Each node initialises its own parameters at random. The number of parameters per node is the same as the Input dimension.
- (2) Take a random sample of input X_i ;
- (3) Iterate through all the nodes in the competitive layer to compute the degree of similarity between X_i and the discriminant function can be the Euclidean distance:

$$d_j(\mathbf{x}) = \sum_{i=1}^D (x_i - w_{ji})^2 \quad (5.5)$$

The node with the shortest distance is chosen as the winner node, also known as BMU (best matching unit).

(4) Determine the nodes that will be in the superior neighbourhood based on the neighbourhood radius (σ), and then use the neighbourhood function to calculate the magnitude of their respective updates (the basic idea is the closer to the superior node, the greater the update magnitude; the further away from the superior node, the smaller the update magnitude).

(5) The gradient descent is applied to update the node parameters.

$$\Delta w_{ji} = \eta(t) \cdot T_{j,I(\mathbf{x})}(t) \cdot (x_i - w_{ji}) \quad (5.6)$$

$$W_v(s+1) = W_v(s) + \theta(u, v, s) \cdot \alpha(s) \cdot (D(t) - W_v(s)) \quad (5.7)$$

(6) Complete one iteration i (then $i = i + 1$), then return to the second step until the specified number of iterations is reached.

5.1.3 Character of impact factor and impact factor analysis system

Subjectivity: The ease of manufacturing process and tool development, as well as the designer's satisfaction with the final design outcome, are used to judge the impact factors involved in RAOD. The evaluation of quantitative design results is usually objective, whereas the evaluation of qualitative aspects such as the ease of development process is subjective. This is related to the professional experience and knowledge of the researchers and experts involved, as well as the scale of the project, the degree of innovation and difficulty.

Complexity: According to the cluster diagram of connections between factors showed above, RAOD has a complex hierarchy of contents and multiple intersecting levels which is a non-linear nexus, which implies that the influence of the impact factor varies across different sizes and types of studies or actual practices.

Dynamic: The machine condition is not constant and is in a dynamic state of change due to the processing conditions of the robotic arm. At the same time, changes in design and materials can have a time-series effect on machine processing. The dynamic nature of the influencing factors necessitates constant attention to the impact of the influencing factors.

each other, so that the indicator system comprehensively reflects the system's integrity and characteristics, and the overall evaluation ability of the constructed evaluation system is greater than the sum of individual evaluation indicators.

- **Consistency:** To fully reflect the purpose of the evaluation of the impact of robotic fabrication on the design, the indicator system should be set up in a way that is consistent with the evaluation's direction. The evaluation indicators chosen should reflect both the direct and indirect effects.
- **Scientific:** Use a combination of scientific qualitative and quantitative methods, the intrinsic elements of the RA of the RAOD system are interrelated with the essential content contained in the design, objectively reflecting the quantitative relationship between the different influencing factors and the design results through the degree of influence.
- **Independence:** In the evaluation system of the impact of RA on RAOD, the evaluation indicators at the same evaluation level should not contain each other, to ensure that the evaluation indicators reflect the actual situation of the degree of impact of RA on design from various perspectives.
- **Measurability:** The evaluation indicators of the degree of RA impact should be chosen in a measurable and quantifiable manner; choosing too complex indicators will frequently result in errors in the evaluation results.
- **Comparability:** The evaluation index system should be highly comparable in order to improve the credibility of the assessment results. To put it another way, the evaluation indicators and criteria must be comparable and objective.

5.2 AHP method to determine the hierarchies and factor weights

After establishing the impact evaluation index system for RA processing, a suitable method for determining the weight of the evaluation index need to be chosen. For now, there are many methods for calculating the weights of evaluation indicators, such as the expert scoring method, principal component analysis (PCA) and the mean square difference method, each of which has its own advantages and disadvantages. For example, the expert scoring method assigns weights to evaluation indicators based on experts' experience, which is subjective and difficult to evaluate if faced with too many evaluation indicators; the PCA method requires a large amount of accurate information in determining the weights of indicators and cannot make good judgment on evaluation systems that lack certain data information. Analytic Hierarchy Process (AHP) is a widely used method for determining indicator weights that excels at analysing complex decision problems with multiple objectives and criteria.

RAC-FTS is a complex system, and the RA impact level evaluation system is a multi-layer objective decision problem with fuzziness and uncertainty. This section chooses the AHP method to determine the weights of impact level evaluation indicators. The principles and characteristics of the AHP, and the

specific operation steps of the AHP method in constructing the evaluation index system are introduced as follows.

5.2.1 The principles and characters of AHP

AHP is a systematic analysis method that combines the qualitative and quantitative analysis put forward by an expert of operation theory named T.L.Saaty in 1970s. The main premise of AHP is to regard the complex problem under investigation as a huge system, and by analysing different factors within the system, sort out the orderly hierarchy of interactions between the various factors inside the system. A bottom-up cascade hierarchy is created based on the research objectives and attributes of the system. As each level's impacting factors are more objectively assessed, a quantitative representation is provided to illustrate their relative importance. The relative relevance of all factors at each level is then calculated and ranked using a mathematical model. Weightings based on ranking outcomes are used for planning and selecting specific solutions. The AHP has the following characteristics:

(1) Simple and easy to understand: Using AHP to make decision, the input information involves a lot of choices and judgments on behalf of the decision maker. The outcome reflects the decision maker's comprehensive understanding. As a result of its straightforward and unambiguous approach to decision making, AHP facilitates good communication between the decision-maker and the decision analyst. AHP method can be used directly by in many circumstances, which boosts the scientific validity of their conclusions.

(2) Flexibility and practicality: There are both quantitative and qualitative analyses that may be carried out using AHP. As a result, the experience of making decisions can be made the best use of by employing relative scales to quantify non-quantitative and quantitative, as well as intangible and tangible aspects in a unified approach. It has also overturned the traditional belief that optimisation techniques are frequently limited to quantitative problems, and is now widely employed in resource allocation, system analysis and solution evaluation difficulties as well as planning challenges.

(3) Systematic: There are three broad approaches to categorising decisions: one is to treat the problem as a whole system, so that decisions are made based on studying the environment in which the system is located and the components of the system in relation to their interrelationships; another is the causal inference approach, which is essentially convenient and simple in most simple decisions, and which form the basis of the causal inference approach. Another effective way of thinking about systems for complex problems is decisional thinking, which is due to a broad class of systems with recursive hierarchical relationships. AHP reflects the decision-making characteristics of such systems and can be extended to study more complex systems.

The characteristics of AHP demonstrate that the method can resolve the complex RAC-FTS systemic problem with multiple levels and objectives. The method of decision making is based on the objective quantification of subjective human judgements using certain scales by analysing the interrelationship of the influencing factors and internal components of the problem, establishing a framework with a

hierarchy, and converting the problem-solving process into a mathematical process by virtue of a small amount of quantitative information.

5.2.2 The steps for AHP

The steps of hierarchical analysis modelling primarily include: (1) establishing the structural model of hierarchical order; (2) constructing the judgement matrices of indicators at all levels; (3) single indicator ranking; (4) consistency test; (5) overall indicator ranking and consistency test. The detailed steps are described as follows:

(1) Establish the structural model of hierarchical order

To develop a hierarchical structural model, the research item is hierarchized when using hierarchical analysis to analyse a decision problem. Consequently, the complex problem is broken down into a collection of hierarchical elements that may be reached via characteristics and links. The elements of the preceding levels are taken for granted as guidelines that regulate the relevant elements of the later levels, but they are not taken for granted as guidelines. They can be categorised into three categories: top, middle, and bottom tiers of a pyramid. A hierarchical model (Figure 5.12) has a certain number of layers, which is decided by complexity and the level of the required detailed. Number of levels can be unlimited, but there should only be one element each level that dominates the rest of the elements. In the case of a two-by-two comparison, too many strong components can make it impossible to create a judgement matrix.

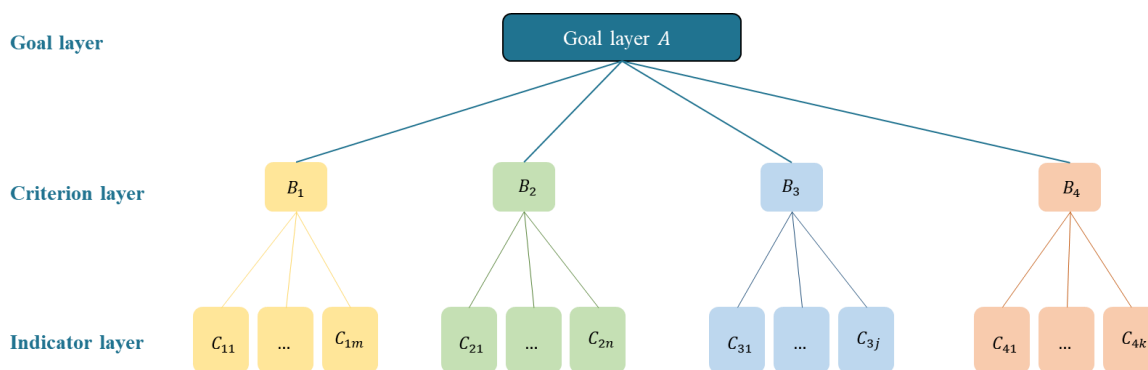


Figure 5.12 Hierarchy Chart

(2) Construct the judgement matrix

To provide more credible data, a method of creating a comparing matrix composed by two-by-two comparison of the factors is adopted to compare the level of impact of several n impact factors $X = \{x_1, x_2, \dots, x_n\}$ on a certain research object Z . The relative importance of the elements in each layer is judged, and the 1-9 scale is typically used to assign values to these importance judgments, thus quantifying the qualitative problem and forming a judgement matrix. The matrix shows the link between sub-indicators in terms of their importance. On the basis of impact factor from a higher-level. The judgement matrix is expressed as:

$$\mathbf{A} = ((a_{ij}))_{n \times n} = \begin{bmatrix} a_{11} & \dots & a_{1n} \\ \vdots & \ddots & \vdots \\ a_{n1} & \dots & a_{nn} \end{bmatrix} \quad (5.8)$$

That is, two different factors x_i and x_j are taken at a time and the ratio of the degree of influence of x_i and x_j on the target Z is expressed in terms of a_{ij} , where the results of the comparison can all be expressed in matrix $A = (a_{ij})_{n \times n}$, which is said to be the judgment matrix between $Z - X$. And the ratio of the degree of influence of x_j and x_i on the target Z is $a_{ji} = 1/a_{ij}$. While solving issues using the AHP method, the number of indications at each level shouldn't exceed nine, as too many signs at one level can make it difficult to determine their value. The standard 1 to 9 scale method is shown in Table 5-3.

There are $n(n - 1)/2$ times of mutual judgement to take. Thus, an appropriate ranking can be derived through iterative comparison of the numerous indicators based on the derived information.

Table 5-3 Assignment standard of Elements in the Judgement Matrix

Impact level	Definition
1	factor i and j are equally important
3	factor i is slightly more important than j
5	factor i is significantly more important than j
7	factor i is strongly more important than j
9	factor i is extremely more important than j
1/3	factor i is slightly less important than j
1/5	factor i is significantly less important than j
1/7	factor i is strongly less important than j
1/9	factor i is extremely less important than j
2, 4, 6, 8	at the middle of the above two adjacent comparison scales
1/2, 1/4, 1/6, 1/8	

Table 5-4 Assignment standard of Elements in the Judgement Matrix

C	c_{11}	c_{12}	...	c_{1i}	...	c_{1n}
c_{11}	1	$\frac{c_{11}}{c_{11}}$...	$\frac{c_{11}}{c_{11}}$...	$\frac{c_{11}}{c_{11}}$
c_{12}	$\frac{c_{12}}{c_{11}}$	1	...	$\frac{c_{12}}{c_{11}}$...	$\frac{c_{12}}{c_{11}}$
...
c_{1i}	$\frac{c_{1i}}{c_{11}}$	$\frac{c_{1i}}{c_{12}}$...	1	...	$\frac{c_{1i}}{c_{1n}}$
...
c_{1n}	$\frac{c_{1n}}{c_{11}}$	$\frac{c_{1n}}{c_{12}}$...	$\frac{c_{1n}}{c_{1i}}$...	1

(3) Consistency test

According to matrix theory, if $\lambda_1, \lambda_2, \dots, \lambda_n$ satisfies the following equation, then λ is the eigenvalue of matrix A .

$$A\lambda = \lambda x \quad (5.9)$$

For all $a_{ii} = 1$, there is:

$$\sum_{i=1}^n \lambda_i = n \quad (5.10)$$

When the matrix has full consistency, $\lambda_1 = \lambda_{max} = n$, and other eigenvalues equals zero. And when the matrix **A** is not perfectly consistent, $\lambda_1 = \lambda_{max} > n$, and other eigenvalues has the following relationship:

$$\sum_{i=2}^n \lambda_i = n - \lambda_{max} \quad (5.11)$$

The steps of the consistency test for the judgment matrix are as follows:

Because the judgement matrix serves as the foundation for the final weight calculation, it is critical that it be broadly consistent. This is to avoid making judgments that contradict common sense, such as ‘A is significantly more important than B, B is significantly more important than C, and C is significantly more important than A,’ which would violate the principle of authenticity in evaluation. As a result, the judgement matrix's error and compatibility must be investigated. Setting the consistency index as:

$$C.I = \frac{\lambda_{max} - n}{n - 1} \quad (5.12)$$

When the consistency index (C.I) is larger, the judgement matrix is deviating from full consistency; when the value of CI is smaller (tends to zero), the matrix is closer to full consistency. When the judgement matrix has different orders, the C.I requirements differ as well. And the average random consistency RI can be used to determine whether the consistency of the judgement matrix is satisfactory. Table 5-5 displays the values of random index (R.I) for judgement matrices of order 1 to 9.

Table 5-5 Value of R.I with different matrix order

Matrix order (n)	1	2	3	4	5	6	7	8	9
R. I	0	0	0.58	0.9	1.12	1.24	1.32	1.41	1.45

After a series of amendments, consistency ratio (C.R) becomes:

$$C.R = \frac{C.I}{R.I} \quad (5.13)$$

In general, if $C.R < 0.1$, we consider the judgement matrix to be a consistency matrix, and the consistency values calculated accordingly are acceptable, the judgement matrix must be reworked; otherwise, the judgement matrix must be reworked.

(4) Single indicator ranking

To express the level of importance between indicators at the same level, a hierarchical single ranking is used. In most cases, an iterative algorithm is used to find the maximum eigenvalue and the eigenvector corresponding to the maximum eigenvalue. In hierarchical single ranking process, the judgement matrix's eigenvectors corresponding to its maximum eigenvalues λ_{max} are normalised to provide a ranking weight of the relative importance of the corresponding factor at the same level to a factor at the higher level. The maximum eigenvalue and the eigenvector corresponding to the maximum eigenvalue are calculated as follows:

a) Calculate the product of the elements of each row of the judgment matrix M_i :

$$M_i = \prod_{j=1}^n u_{ij} \quad i = 1, 2, \dots, n \quad (5.14)$$

b) Calculate the n^{th} root of M_i :

$$\bar{W}_i = \sqrt[n]{M_i} \quad (5.15)$$

c) Normalise the vector $\bar{W} = [\bar{W}_1, \bar{W}_2, \dots, \bar{W}_n]^T$:

$$W_i = \frac{\bar{W}_i}{\sum_{j=1}^n \bar{W}_j} \quad (5.16)$$

$\mathbf{W} = [W_1, W_2, \dots, W_n]^T$ is the eigenvector needed.

d) Calculate the maximum eigenvalue λ_{max} of the judgment matrix:

$$\lambda_{max} = \sum_{i=1}^n \frac{(AW)_i}{nW_i} \quad (5.17)$$

Where $(AW)_i$ denotes the i^{th} element of the vector \mathbf{AW} .

(5) Overall indicator ranking and consistency test

The total hierarchical ranking is used to calculate the relative importance of the elements in the indicator layer to those in the target layer. Supposing there are m factors A_1, A_2, \dots, A_m in the first layer A , and the weight values for their final hierarchical total ranking are listed in the following order a_1, a_2, \dots, a_m . Similarly, supposing there are n factors B_1, B_2, \dots, B_n in the second layer B and their final sorted single hierarchical weight value respective A_j is $b_{1j}, b_{2j}, \dots, b_{nj}$ ⁸. The next is to calculate the weight of each element in layer B relative to the total target layer A , which means to find the weight values for the total ranking of each element level b_1, b_2, \dots, b_n through the following equation:

$$b_i = \sum_{j=1}^m b_{ij}a_j, i = 1, \dots, n \quad (5.18)$$

At last, the same consistency test is required for total hierarchical ordering, which is still done in the same manner as the previous hierarchical single ordering, step by step for all levels from top to bottom. The judgement matrix of each relative comparison of the elements related to A_j in criterion layer B is tested for consistency in the final single ranking test, resulting in a single ranking consistency hierarchy indicator $C.I(j), (j = 1, 2, \dots, m)$.

⁸ When B_i is irrelevant to A_j , $b_{ij} = 0$.

Table 5-6 Weight synthesise method

	A_1	A_2	...	A_m	Overall ranking of weights of layer B
	a_1	a_2	...	a_m	
B_1	b_{11}	b_{12}	...	b_{1m}	$\sum_{j=1}^m b_{1j}a_j$
B_2	b_{21}	b_{22}	...	b_{2m}	$\sum_{j=1}^m b_{2j}a_j$
...
B_n	b_{n1}	b_{n2}	...	b_{nm}	$\sum_{j=1}^m b_{nj}a_j$

Their corresponding average randomly selected consistency indicators are $R.I(j)$. The final total sorted random consistency ratio of layer B is:

$$C.R = \frac{\sum_{j=1}^m C.I(j)a_j}{\sum_{i=1}^m R.I(j)a_j} \quad (5.19)$$

When $C.R < 0.1$, the result of the hierarchical total ranking is considered to be of a more satisfactory consistency and results of this analysis can be accepted.

5.3 Multi-level fuzzy comprehensive evaluation model

It's important to note that every evaluation method has different application background and focuses, which means while it has certain advantages, it also has certain limits. RAC-FTS is a complicated system, including many impact factors which have overlap effects on the multiple criteria with fuzziness nexus between each other without clear boundary which means no absolute, which means there is no absolute, precise affirmation, or negation. To evaluation the impact level of these factors and to develop the general and specific ROAD strategy, a quantified and synthesise evaluation for the non-linear connections among these factors is needed to provide comparable quantitative results. In this research, fuzzy comprehensive evaluation (FCE) is selected to build the evaluation model.

5.3.1 Characteries of Fuzzy comprehensive evaluation

FCE is a type of evaluation method that implements the theory of fuzzy mathematics to assess a specific object system. This method transforms a research object subject to as a specific fuzzy set characterized by multiple factors, creates a level of membership function to match it, and performs quantitative analysis using fuzzy mathematics operations and transformations. FCE employs mathematical methods to study and deal with objective fuzzy phenomena by performing a general evaluation of objects or phenomena that are affected by multiple factors. The model is simple and easy to understand, and it deals with complex problems with multiple factors and levels efficiently, for which is widely used by the majority of scientific and technical research groups dealing with risk management and decision making.

The characters of FCE methods can be summarized as:

(1) **Multi-level evaluation:** this evaluation process of this method can be looped repeatedly. The comprehensive evaluation result of the last level can be used as input data for the next level. That is, a single-level FCE or a multi-level one can be applied on a complex research object. The progressive relationship avoids the singularity of a specific criteria evaluation in traditional evaluation methods and generate yield more realistic weighting data.

(2) **Weighting factor:** in regard to the fact that the weights of the influencing factors of each level are quantitative data obtained through comprehensive scoring, the obtained weights reduce the probability of inconsistency. Even if the weights aren't completely accurate, they're still more reasonable. The outcome of the evaluation will not have a large impact and can be used as a basis for decision-making.

(3) **Uniqueness:** the evaluation result is a set of fuzzy vectors, not a specific value, and it is unique to the evaluated object.

(4) **Quantization:** reciprocal affiliations among different impact factors are established to help to develop an evaluation system which can scientifically reflect the overall impact, development trends, and response measures to be taken by quantifying these indicators and criteria.

The impact factors and evaluation criteria in RAC-FTS system concluded in last section are discrete, complex qualitative variables without explicit boundaries. The features of FCE indicate that it could perform accurate quantitative analysis and evaluation for RAC-FTS system.

5.3.2 Principles of the fuzzy comprehensive evaluation method

Fuzziness is a universal state manifested by objective things that embodies the phenomenon that boundaries cannot be distinguished, quantified, or clearly described and controlled. And fuzzy mathematics aims to solve objects whose attributes, boundaries, and states are unable to be determined. FCE is a highly effective multi-factor decision-making method for performing a comprehensive evaluation of the complex system that are affected by multiple factors. Its distinguishing feature is that the evaluation result is not categorically positive or negative, but rather expressed by a fuzzy set.

The basic principle of this method is to determine the set of evaluation index of the evaluation object $U = (U_1, U_2, \dots, U_m)$ and the set of fuzzy evaluation set $C = (C_1, C_2, \dots, C_n)$. U_i is the i^{th} single index, and C_i is the evaluation level result for U_i . After determining the set of C , then the weight W of each index needed to be defined, which means the importance level of each factor among all the others. After constructing the degree of membership function, the degree of membership vector r is obtained to constitute the fuzzy evaluation matrix R by fuzzy transformation using fuzzy mathematics. Finally, the fuzzy evaluation matrix R and the weight vector set of the indicators W are synthesised using mathematical methods, and the results are normalised to obtain a fuzzy comprehensive evaluation result vector set S . As a result, set (U, C, R, W) is the comprehensive evaluation model for the evaluation object.

5.3.3 Steps for the fuzzy comprehensive evaluation method

To perform FCE, the basic steps are introduced as following:

(1) Impact indicator and evaluation level

I. Determine the impact indicator sets of each level

First-level indicator: Setting $U = \{U_1, U_2, \dots, U_i, \dots, U_m\}$, $i = 1, 2, \dots, m$. m is the number of indicators of first level and i means the i^{th} indicator of this level.

Second-level indicator: This means the index corresponding to each first-level one. Setting $U_i = \{u_{i1}, u_{i2}, \dots, u_{ij}, \dots, u_{ik}\}$, $j = 1, 2, \dots, k$. u_{ij} is the j^{th} second-level indicator of first-level indicator U_i . k is the number of indicators of related to U_i .

Third-level indicator: Continue the same method's arrangement and calculation based on the upper-level indicator sets if a third level is needed.

II. Set the evaluation level set

The fuzzy evaluation set is $C = (C_1, C_2, \dots, C_n)$. The impact evaluation is usually divided into five levels: lowest, general low, intermediate, relatively high, highest. It can be presented in percentile score like 100 or value range like $[0, 1/5)$.

(2) Level of membership function and weight vector

I. Determine the fuzzy level of membership matrix

After setting the evaluation level set, the fuzzy level of membership matrix can be constituted by the quantified impact factors. r_{ij} indicates the degree of membership of the i^{th} indicator U_i relative to the j^{th} evaluation level of C_j . The evaluation level vector of i^{th} indicator U_i is $r_i = (r_{i1}, r_{i2}, \dots, r_{ij}, \dots, r_{ik})$, $j = 1, 2, \dots, k$. After quantifying all the impact factors, a number of m evaluation vectors are obtained to compose the overall evaluation matrix R . Fuzzy level of membership matrix R represents the performance of the evaluated object in terms of the factor u_i , and determining R necessitates additional mathematical transformations like the level of membership function⁹. R is expressed as:

$$R = (r_{ij})_{m \times n} = \begin{bmatrix} r_{11} & r_{12} & \cdots & r_{1n} \\ r_{21} & r_{22} & \cdots & r_{2n} \\ \vdots & \vdots & \ddots & \vdots \\ r_{m1} & r_{m2} & \cdots & r_{mn} \end{bmatrix} \quad (5.20)$$

The level of membership function is the foundation for the use of FCE, and whether or not the function is correctly formulated is one of the keys to an evaluation model. The process of determining the function

⁹ If there is a number $A(x) \in [0,1]$, corresponding to any element x in the domain of U , then A is called a fuzzy set on U , and $A(x)$ is called the level of membership of x versus A . When x changes in U , $A(x)$ is a function, called the membership function of A .

should be objective, but as everyone's understanding of the same fuzzy concept differs, determining the affiliation function is subjective. There is no mature or general method for establishing the level of membership function, and most systems are built rely on subjective experience and experimentation. Different people will establish different functions for the same fuzzy concept.

II. Determine the weighting factor

To complete the evaluation procedure, it is necessary to determine the impact level of each factor among all, which is known as weight W , as each has a different magnitude of influence on the object in the comprehensive evaluation. W corresponds to different level of impact factors, e.g., the weight set of first-level indicators is $W = \{w_1, w_2, \dots, w_i, \dots, w_m\}$; and the weight set of second-level indicators appertain to U_i can be expressed as $w_i = \{w_{i1}, w_{i2}, \dots, w_{ij}, \dots, w_{ik}\}$. In this chapter, the weight vector W of every impact indicator is calculated using hierarchical analysis in the previous subsection, so that the corresponding weight vectors could be derived. The weights need to be normalised before synthesis, which means:

$$\sum_{i=1}^m w_i = 1 \quad (5.21)$$

(3) Model of impact level

In R , each row represents one factor's level of membership with each evaluation level. By synthesising the weight vectors W of the different rows, the level of membership of the evaluated object to each level fuzzy subset is obtained. B , as a fuzzy subset on C , is also known as the decision set.

I. Primary fuzzy transformation

For each factor in $U_i = \{u_{i1}, u_{i2}, \dots, u_{ij}, \dots, u_{ik}\}$, the evaluation is carried out according to the original model. By setting the fuzzy subset of the factor's importance degree of U_i as W_i and the overall level of membership matrix of the elements of U_i as R_i , the primary fuzzy evaluation matrix can be obtained, shown as:

$$B_i = W_i * R_i \quad (i = 1, 2 \dots m) \quad (5.22)$$

B_i is the single evaluation for U_i . Accordingly, the fuzzy vector for u_{ij} is:

$$B_{ij} = W_{ij} \cdot R_{ij} = (b_{ij1}, b_{ij2}, \dots, b_{ijt}, \dots, b_{ijm}) \quad (5.23)$$

II. Secondary fuzzy transformation

Setting the fuzzy subset W stands for the level of importance between each element in $U = \{U_1, U_2, \dots, U_i, \dots, U_m\}$ and $W = \{W_1, W_2, \dots, W_i, \dots, W_m\}$. The overall evaluation matrix B for U is:

$$\mathbf{B} = \begin{bmatrix} \mathbf{B}_1 \\ \mathbf{B}_2 \\ \vdots \\ \mathbf{B}_m \end{bmatrix} = \begin{bmatrix} W_1 * R_1 \\ W_2 * R_2 \\ \vdots \\ W_m * R_m \end{bmatrix} \quad (5.24)$$

The comprehensive secondary evaluation result, which is also the result for $U = \{U_1, U_2, \dots, U_i, \dots, U_m\}$ is:

$$\mathbf{B} = W * R \quad (5.25)$$

In general condition, $*$ is the operator symbol and different selection of operator leads to different evaluation model. Furthermore, if the result is $\sum B_i \neq 1$ in the fuzzy subset $\mathbf{B} = (B_1, B_2, \dots, B_m)$, then it should be normalised to make sure $0 \ll b_j < 1$, which is:

$$\mathbf{B}^* = \begin{bmatrix} \frac{B_1}{\sum_{i=1}^m B_i}, B_2 \\ \frac{B_1, \dots, B_i}{\sum_{i=1}^m B_i}, \dots, B_i \\ \frac{B_m}{\sum_{i=1}^m B_i}, \dots, \frac{B_m}{\sum_{i=1}^m B_i} \end{bmatrix} \quad (5.26)$$

(4) Model of impact level result analysis

The maximum level of membership rule enables the evaluation's result to be calculated. To make the evaluation results more accurate, the actual results from each factor are reflected in matrix \mathbf{B} to present the information in a comprehensive way. At this point, the evaluation levels can be assigned to reflect the results visually, expressed in:

$$\mathbf{C} = (C_1, C_2, \dots, C_n)^T \quad (5.27)$$

The evaluation level parameters are evaluated as:

$$\mathbf{B}^* * \mathbf{C} = \mathbf{p} \quad (5.28)$$

\mathbf{p} is a real number that converts a qualitative assessment into a quantitative result.

5.4 Fuzzy-AHP evaluation method for impact factor from RAC on FTS design

5.4.1 Establishment of Fuzzy-AHP Assessment System

Based on the identification of the impact factors in 5.1, it was determined that the RAC-FTS system is a complex, multifactorial system that needs to be assessed from different perspectives. Therefore, the corresponding model evaluation index system contains both quantitative and qualitative indicators, and the quantitative indicators are of different scales, making it difficult to obtain correct results from objective evaluation methods. Considering the above factors, the thesis is based on hierarchical analysis and fuzzy mathematical theory to establish a model for evaluating the impact of RAC on FTS. The model has the following advantages: the mathematical model is simple and intuitive, easy to grasp, better for multi-level and multi-factor evaluation, and can give a more comprehensive and objective

evaluation result, more credible and reliable. In this study, the model is used to evaluate the impact of RAC on the FTS system. The first step is to construct a system of indicators for evaluating the impact of RAC, then use hierarchical analysis to determine the impact weights of each indicator, and finally use fuzzy synthesis to evaluate the impact score. Details of the specific workflow are shown in Figure 5.13.

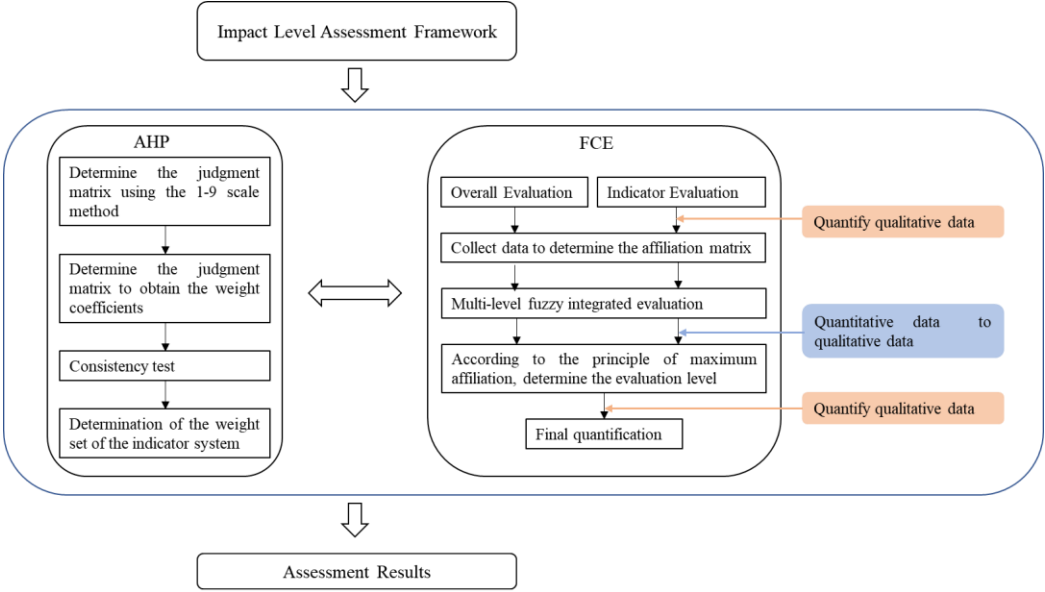


Figure 5.13 Fuzzy-AHP Assessment Process

According to the initial model in Figure 5.2, multiple impact factors and multiple evaluation criteria in the RA impact assessment model for RAOD is transformed into the multiple input multiple output (MIMO) shown in Figure 5.14. Based on the introduction for AHP and FCE. One manifest discrimination of MIMO assessment model from general AHP is that the objectives in output layer has cross relationship with the elements in criteria layer and alternative layer. General hierarchy model has one objective in the target layer with the relationship of belonging, progression, and non-intersection that exists between different levels. This means the general hierarchy model with one objective is not applicable for RA impact level analysis, for which the impact assessment model built into the MIMO one. MIMO as a concept widely used in new technologies like radio communication, has also been applied for prediction(J. Li, Hua, Qian, & Guan, 2021) (Kumbhakar & Lai, 2021).

For common robotic arms used for fabrication and construction purposes, it is a forward process where after the completion of the design, the end-effectors, workspace layout are modified to meet the fabrication and construction needs. In this study, a reverse process is used to analyse the impact of RAC based on the cases of robotic fabrication and construction, by analysing the impacts of different aspects of RAC system on the overall design system. The overall design system includes not just the design part, but an integrated design system for the FTS covering processing, construction, and management. There is currently no unified system for evaluating the impact of RAC on design. Therefore, there are no uniform criteria for the selection of evaluation indicators.

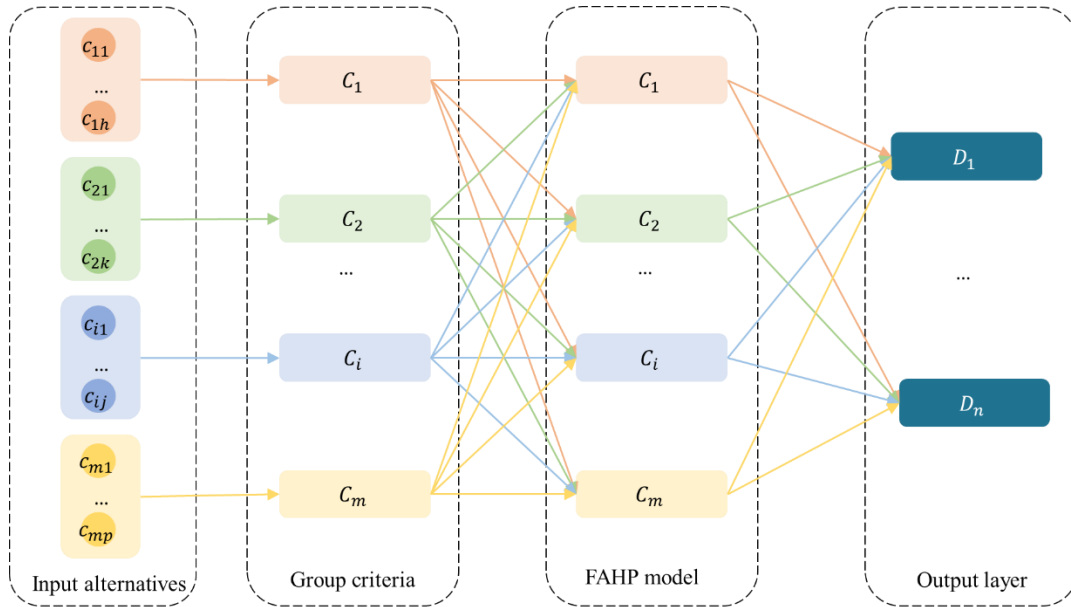


Figure 5.14 Multiple input multiple output assessment model

In this section, based on the risk assessment methodology, many research papers are analysed using mathematical and statistical methods. Based on the proposed principles for the selection of impact factors, aspects that can reasonably and comprehensively describe the RAC are selected as the criteria for assessment, which the extraction of indicators are selected from. The filtered impact factors are organised in different hierarchies. The assessment process of Figure 5.14 was used to evaluate the extent of the impact of RAC on FTS based on the MIMO system constructed in this study. The indicator hierarchy has been selected as shown below:

- (1) Technology aspects of robotic arms: robotic arm motion control, robotic arm calibration, robotic arm force control, robotic arm interactivity.
- (2) Work environment aspect: number of robotic arms, robotic arm collaboration, number of tool heads; ability to move; real-time feedback.
- (3) Material aspect: material type, material properties, material dimensions, number of material types.
- (4) Application aspect: standard element prefabrication, non-standard element fabrication, assembly on site, construction on site.

The indicator hierarchy is constructed shown in Figure 5.15 and Table 5-7.

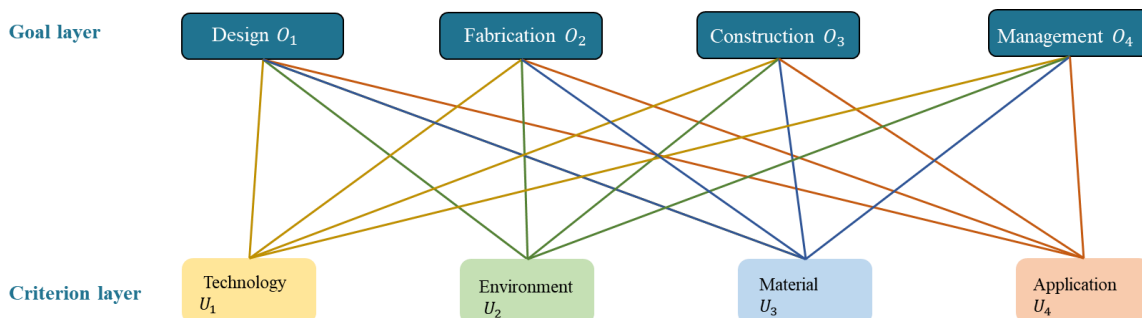


Figure 5.15 Hierarchy Structure between the goal layer and criterion layer of MIMO

Table 5-7 Hierarchy Structure between the criterion layer and indicator layer

Criterion U_i	Indicator u_{ij}
Technology U_1	Robotic Motion control u_{11}
	Robotic calibration u_{12}
	Robotic force control u_{13}
	Interactivity u_{14}
Environment U_2	Number of equipment u_{21}
	Cooperation between robots u_{22}
	Number of end-effectors u_{23}
	Mobility u_{24}
	Real-time feedback u_{25}
Material U_3	Material types u_{31}
	Material properties u_{32}
	Material dimensions u_{33}
	Number of material types u_{34}
Application U_4	Standard element prefabrication u_{41}
	Non-standard element fabrication u_{42}
	Assembly on site u_{43}
	Construction on site u_{44}

5.4.2 Determination of indicator weights

Once the impact factors have been identified and the hierarchy established, the difficulty remains that the factors are difficult to assess quantitatively and consistently. The Monte Carlo simulation method (MCS) is used to reduce the chance and subjectivity of the judgement matrix. The MCS is a numerical calculation method based on the statistical theory of probability and is a traditional method of simulating experiments. The time series are first generated iteratively through a random process, statistics and parameter estimates are calculated and then the characteristics of the data are studied and analysed, essentially a statistical experiment and a random sampling method. As RAC and FTS have the uncertainty of construction engineering and architecture, probabilistic models are used to model the possible outcomes for the uncertainty of impacts. The greater the number of experiments, the greater the accuracy. Therefore, the operational steps are as follows.

- (1) Create an initial judgement matrix and perform consistency tests until it meets $C.R < 0.1$.
- (2) Random numbers are generated at positions of the judgement matrix; experiments are operated for many times until the number are in norm distribution.
- (3) Combine the data and select a consistent judgment matrix to obtain data results.

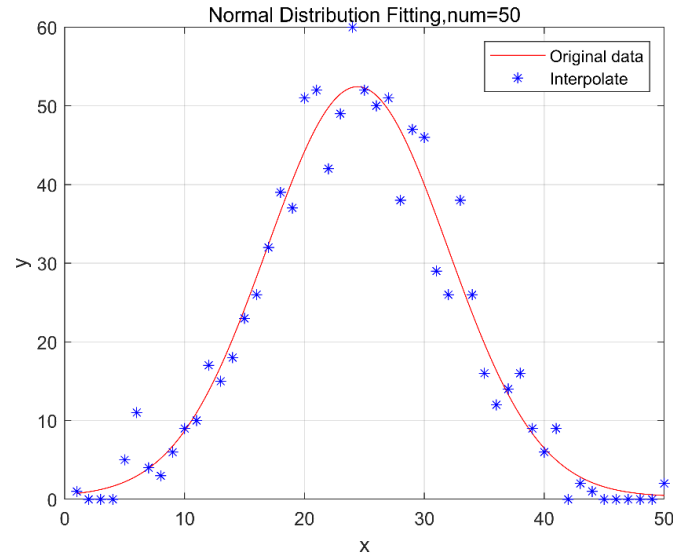


Figure 5.16 Distribution of manipulated data

The simulated data fits the norm distribution in Figure 5.16. By applying the simulated data, Table 5-8 to Table 5-12 are the values of the criterion listed in Table. Other weights of $U_i - U_{ij}$ of RAC on fabrication O_2 , construction O_3 , and management O_4 are listed in table in Appendices-2 Table A2 4 - A2 24.

Table 5-8 Judgement Matrix of Criterion $U-U_i$ for Design O_1 (CR=0.0530)

	Technology U_1	Environment U_2	Material U_3	Application U_4	W
Technology U_1	1	1/3	1/3	1/2	0.1034
Environment U_2	3	1	1/3	2	0.2507
Material U_3	3	3	1	3	0.4884
Application U_4	2	1/2	1/3	1	0.1575

Table 5-9 Judgement Matrix of Criterion U_1-U_{1i} for Design O_1 (CR=0.0797)

	Robotic Motion control u_{11}	Robotic calibration u_{12}	Robotic force control u_{13}	Interactivity u_{14}	W
Robotic Motion control u_{11}	1	3	1/3	2	0.247248
Robotic calibration u_{12}	1/3	1	1/3	1/3	0.093934
Robotic force control u_{13}	3	3	1	3	0.482683
Interactivity u_{14}	1/2	3	1/3	1	0.176135

Table 5-10 Judgement Matrix of Criterion U_2-U_{2i} for Design O_1 (CR=0.0768)

	Number of equipment u_{21}	Cooperation between robots u_{22}	Number of end-effectors u_{23}	Mobility u_{24}	Real-time feedback u_{25}	W
Number of equipment u_{21}	1	1/2	1/3	1/3	2	0.135614
Cooperation between robots u_{22}	2	1	2	2	2	0.315263

Continue Table 5-10 Judgement Matrix of Criterion U_2-U_{2i} for Design O_1 (CR=0.0768)

	Number of equipment u_{21}	Cooperation between robots u_{22}	Number of end-effectors u_{23}	Mobility u_{24}	Real-time feedback u_{25}	W
Number of end-effectors u_{23}	3	1/2	1	1/2	1/2	0.173214
Mobility u_{24}	3	1/2	2	1	1/2	0.226853
Real-time feedback u_{25}	1/2	1/2	2	2	1	0.149056

Table 5-11 Judgement Matrix of Criterion U_3-U_{3i} for Design O_1 (CR=0.0611)

	Material types u_{31}	Material properties u_{32}	Material dimensions u_{33}	Number of material types u_{34}	W
Material types u_{31}	1	2	3	2	0.419719
Material properties u_{32}	1/2	1	2	3	0.289203
Material dimensions u_{33}	1/3	1/2	1	2	0.167799
Number of material types u_{34}	1/2	1/3	1/2	1	0.123278

Table 5-12 Judgement Matrix of Criterion U_4-U_{4i} for Design O_1 (CR=0.0038)

	Standard element prefabrication u_{41}	Non-standard element fabrication u_{42}	Assembly on site u_{43}	Construction on site u_{44}	W
Standard element prefabrication u_{41}	1	2	3	4	0.477831
Non-standard element fabrication u_{42}	1/2	1	2	2	0.25612
Assembly on site u_{43}	1/3	1/2	1	1	0.137989
Construction on site u_{44}	1/4	1/2	1	1	0.12806

The weights of the indicators are summarized in Table 5-13.

Table 5-13 Weights of the Impact Level Evaluation Indicators

Criterion U_i	W	Indicator u_{ij}	W
Technology U_1	0.1034	Robotic Motion control u_{11}	0.2472
		Robotic calibration u_{12}	0.0939
		Robotic force control u_{13}	0.4827
		Interactivity u_{14}	0.1761
Environment U_2	0.2507	Number of equipment u_{21}	0.1356
		Cooperation between robots u_{22}	0.3153
		Number of end-effectors u_{23}	0.1732
		Mobility u_{24}	0.2269
		Real-time feedback u_{25}	0.1491
Material U_3	0.4884	Material types u_{31}	0.4197
		Material properties u_{32}	0.2892
		Material dimensions u_{33}	0.1678
		Number of material types u_{34}	0.1233
Application U_4	0.1575	Standard element prefabrication u_{41}	0.4778

Continue Table 5-13 Weights of the Impact Level Evaluation Indicators

Criterion U_i	W	Indicator u_{ij}	W
		Non-standard element fabrication u_{42}	0.2561
		Assembly on site u_{43}	0.1380
		Construction on site u_{44}	0.1281

5.4.3 Impact level of RAC on FTS

The five levels of satisfaction were used to determine the quality level of each evaluation indicator by using the five levels of "very high, high, average, low and very low" as described in 5.2 for the general evaluation level classification method, so that the level of impact is:

$$V = \{Very\ High, High, Average, Low, Very\ Low\} \quad (5.29)$$

To facilitate a direct comparison between the various impact indicators of RAC on FTS, the quantitative evaluation levels can be further quantified by assigning values to the evaluation levels, as shown in Table 5-14 to achieve the transformation between the qualitative and quantitative data.

Table 5-14 Evaluation level assignment

Level V	Very High	High	Average	Low	Very Low
Value	95	85	75	65	55

After operating MCS random number generation experiments, the values of impact level of indicators of RAC on u_{11} to u_{44} are shown in Table 5-15.

Table 5-15 Comprehensive values of impact levels

Indicators		Very High	High	Average	Low	Very Low
Technology U_1	u_{11}	3	19	71	28	29
	u_{12}	12	10	63	39	26
	u_{13}	60	21	8	58	4
	u_{14}	7	10	8	32	93
	u_{21}	10	20	20	69	31
Environment U_2	u_{22}	25	59	34	9	22
	u_{23}	46	44	13	25	22
	u_{24}	9	38	40	10	53
	u_{25}	50	3	52	24	21
	u_{31}	55	12	43	20	20
Material U_3	u_{32}	18	2	77	26	28
	u_{33}	28	14	12	76	19
	u_{34}	38	61	18	11	21
Application U_4	u_{41}	12	37	70	16	15
	u_{42}	10	29	30	9	72
	u_{43}	3	27	59	52	10
	u_{44}	13	26	15	40	57

Based on the plurality of Table 5-15, constructing the affiliation function C

$$C = \begin{cases} 0, & u_{ij} \leq 10 \\ \frac{u_{ij} - 10}{150 - 10} & 10 < u_{ij} < 90 \\ 1, & u_{ij} \geq 90 \end{cases} \quad (5.30)$$

The affiliation matrixes of $U_1 - U_4$ are shown:

$$R_1 = \begin{bmatrix} 0.064 & 0.436 & 0.000 & 0.129 & 0.136 \\ 0.014 & 0.000 & 0.207 & 0.379 & 0.114 \\ 0.357 & 0.079 & 0.000 & 0.343 & 0.000 \\ 0.000 & 0.000 & 0.000 & 0.157 & 1.000 \end{bmatrix} \quad (5.31)$$

$$R_2 = \begin{bmatrix} 0.000 & 0.071 & 0.071 & 0.421 & 0.150 \\ 0.107 & 0.350 & 0.171 & 0.000 & 0.086 \\ 0.257 & 0.243 & 0.021 & 0.107 & 0.086 \\ 0.000 & 0.200 & 0.214 & 0.000 & 0.307 \\ 0.286 & 0.000 & 0.300 & 0.100 & 0.079 \end{bmatrix} \quad (5.32)$$

$$R_3 = \begin{bmatrix} 0.321 & 0.014 & 0.236 & 0.071 & 0.071 \\ 0.057 & 0.000 & 0.479 & 0.114 & 0.129 \\ 0.129 & 0.029 & 0.014 & 0.471 & 0.064 \\ 0.200 & 0.364 & 0.057 & 0.007 & 0.079 \end{bmatrix} \quad (5.33)$$

$$R_4 = \begin{bmatrix} 0.429 & 0.193 & 0.014 & 0.043 & 0.036 \\ 0.000 & 0.136 & 0.143 & 0.000 & 0.443 \\ 0.350 & 0.121 & 0.000 & 0.300 & 0.000 \\ 0.021 & 0.114 & 0.036 & 0.214 & 0.336 \end{bmatrix} \quad (5.34)$$

(1) Primary fuzzy evaluation:

The degree of impact of Technology U_1 on Design O_1 is assessed as:

$$B_1 = A_1 \cdot R_1 \quad (5.35)$$

$$P_{U_1} = B_1 \cdot V = A_1 \cdot R_1 \cdot V \quad (5.36)$$

$$= [0.2472 \quad 0.0939 \quad 0.4827 \quad 0.1761] \cdot R_1 \cdot [95 \quad 85 \quad 75 \quad 65 \quad 55]^T = 60.9113 \quad (5.37)$$

The same for $U_2 - U_4$:

The degree of impact of Environment U_2 on Design O_1 is assessed as:

$$P_{U_2} = B_2 \cdot V = A_2 \cdot R_2 \cdot V \quad (5.38)$$

$$= 54.9665$$

The degree of impact of Material U_3 on Design O_1 is assessed as:

$$P_{U_3} = B_3 \cdot V = A_3 \cdot R_3 \cdot V \quad (5.39)$$

$$= 56.1373$$

The degree of impact of Application U_4 on Design O_1 is assessed as:

$$P_{U_4} = B_4 \cdot V = A_4 \cdot R_4 \cdot V \quad (5.40)$$

$$= 56.7054$$

(2) Second level fuzzy evaluation

On the basis of the primary fuzzy evaluation, using the weights of the primary indicators, the overall level of impact on the design level can be calculated as follows:

$$B = A \cdot R \quad (5.41)$$

$$= [0.2559 \quad 0.2056 \quad 0.2302 \quad 0.1336 \quad 0.1747]$$

$$P_U = B \cdot V = 77.5575 \quad (5.42)$$

77.5575 is between the average and high level according to Table 5-14, which means the impact of RAC factor on freeform design process and results cannot be neglected. The calculation for the influence of the 17 impact factors on the four criteria layers for fabrication O_2 , construction O_3 and management O_4 follows the same route and the detailed number can be found in Appendices -2 .

5.5 Conclusion

In connection to the hypothesis put forward in Chapter 1, through the Fuzzy-AHP impact model, the impact of RAC on freeform timber structure complex design system has been evaluated quantitatively

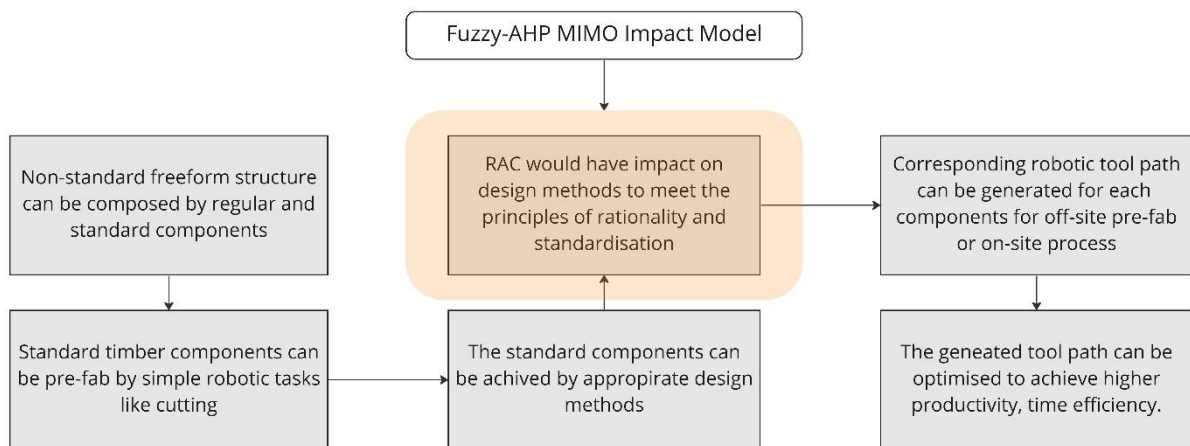


Figure 5.17 Connection to the Hypothesis

For the entire RAC-FTS system, the comprehensive design for freeform timber structure will be influenced by a variety of parameters throughout the whole process, including material specificity, machine restrictions, and diverse design needs. The text cluster analysed by SOM provides reference to determine the impact factors for RAC on FTS, which are categorised into four criteria, namely: Technological U_1 , Environment U_2 , Material U_3 , and Application U_4 . Based on the impact factors, a Multi-Input and Multi-Output (MIMO) model including four criteria and 17 indicators for four parts (Design O_1 , Fabrication O_2 , Construction O_3 and Management O_4) is built for the RAC-FTS system.

Fuzzy-AHP is adopted to determine the weights based on the MCE experiments results to evaluate the impact level of RAC on design, fabrication, construction and management separately. The result of RAC on freeform design sector is 77.5575, which is above the average level. This means the assessment for the impact of RAC on freeform design ahead of the overall stage (design, equipment setup, and material selection) is critical.

As a result of Chapter 5, in response to the challenges posed by robotic automation technical sector, the strategies for freeform morphology design need to be established to identify the characteristic of appropriate design methods. To meet the constraints of the Environment (e.g., number of robots), Material (e.g., product forms) and Application (e.g., off-site), the way to identify the working space limitations, enhance the efficiency of the limited fabrication tools, optimise the structural components to reduce the complexity of fabrication and improve the productivities would be discussed in the following chapters. The following Chapter 6 would take the evidence of this chapter to develop the appropriate design methods considering the impact of RAC see Figure 5.18.

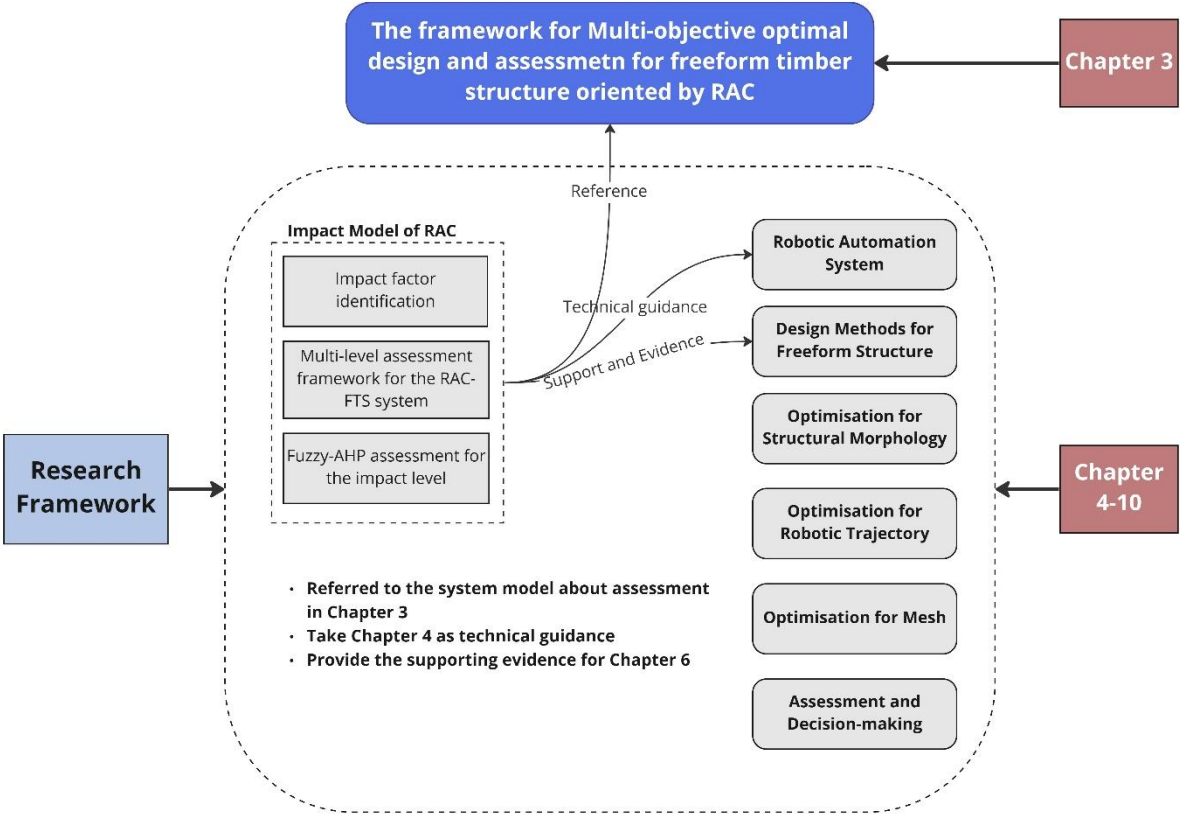


Figure 5.18 Connection to other chapters

Chapter 6

Robotic-automation Oriented Design (RAOD) for Initial Freeform Timber Structure Morphology

Section 6.4 is a published conference paper. The content is extracted from part of the paper to reduce the length of the chapter. More details can be found in Appendices 4.

In Chapter 3, the framework for Robotic Automation Construction - Freeform Timber Structure (RAC-FTS) is proposed as a way to combine the RAC and FTS two systems through design, optimisation, and assessment using a digital model. The results of impact level assessment in Chapter 5 show that several factors of RAC, e.g., technical constraints, has a greater than average impact on morphology design for Freeform Timber Structures throughout the whole process. As "rationalisation" is one important principle for the FTS design to achieve rationality in structure, material, and construction mentioned in Chapter 1, the research focus for this chapter is on appropriate design methods and strategies considering the impact of RAC to fulfil rationality requirement.

Robotic Automation Oriented Design (RAOD) is the design technique considering the impact of characteristics (6 Degree-of-freedom) and constraints (the type of fabrication, the dimensions of working space) of robotics as a technique on architectural geometry design. The RAOD design strategies would be proposed in response to the impact and constraints. To generate the initial geometry of Freeform Timber Morphology (FF-TM), this chapter would discuss the detailed design methods using the geometric model method to fulfil the RAOD principles.

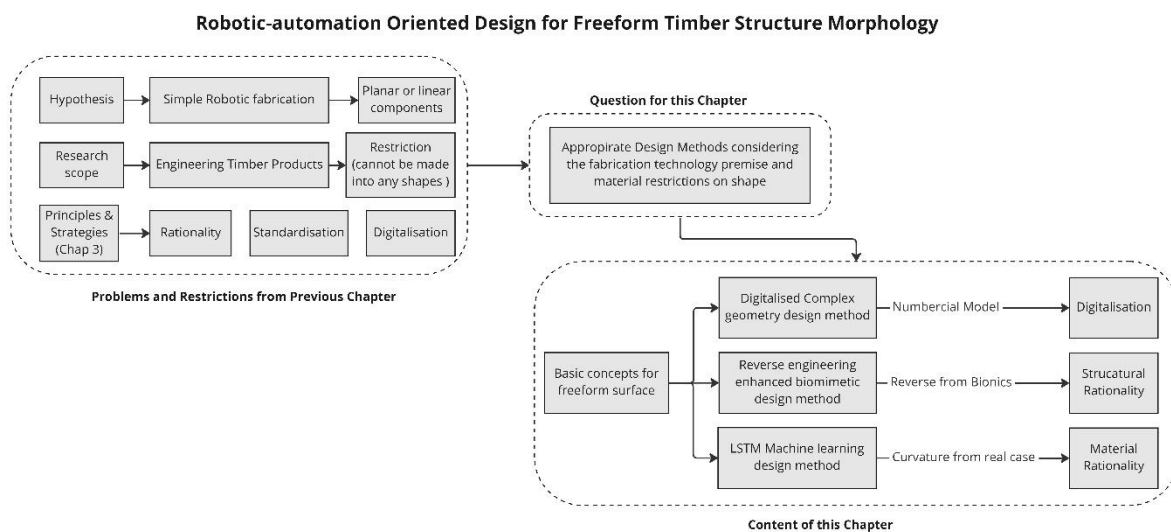


Figure 6.1 Roadmap for Chapter 6

6.1 Basic concepts for RAOD for Freeform Timber Morphology (FF-TM)

RAOD design is put forward in this section based on the analysis of RAC on overall design system including design, fabrication, construction, and management for freeform timber structure project. To fully reflect robotic fabrication as the orientation for design and to imply the dynamic MOO model into

the morphology design for freeform timber, different workflows where the ‘fabrication’ process is involved in different stage of the overall project are listed below. The normal development of the project is that the fabrication follows the structural design, shown in Figure 6.2 (a). To achieve the robotic-oriented design, the concepts of design could be formulated before the two orientations or after them, as Figure 6.2 (b), (c) show. When adding the dynamic interaction and optimisations, the workflow can work as a two-layer loop, shown in Figure 6.2 (d). This means the basic concepts of structure and fabrication lead the conceptual design, which could have direct impact on structure design and fabrication process. While factors like the machining error could have impact on the structural performance, the first loop starts between the structure and fabrication to achieve the optimisation objectives. Based on the results of the first loop, the overall design is assessment to compared it with the requirement to determine whether to operate the second-layer loop or not. This two-layer optimisation loop is the basic idea for RAOD.

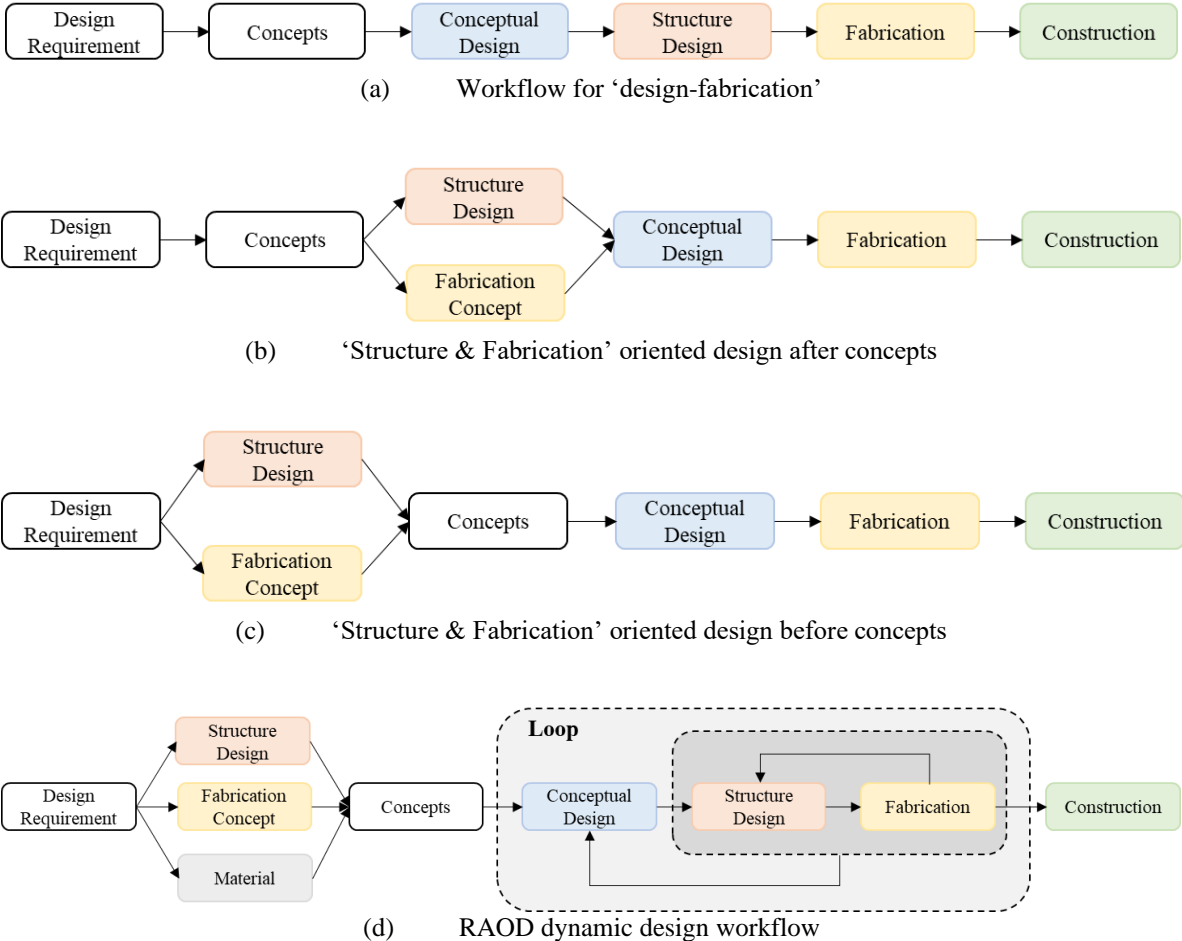


Figure 6.2 Structure and fabrication involved in different stage of design

Morphology has evolved into a multi-discipline that encompasses many research fields such as biology, mathematics, and so on. According to the critical points of morphology, the definition of the concepts would be explained. Freeform modelling has been an important topic in the fields of computer graphics, computer geometry-aided design and computer-aided design, and computational geometry and differential geometry are important geometric foundations of this theoretical system. This technology has been extended from the aerospace, marine, automotive and mechanical sectors to the construction sector. Unlike freeform surfaces, conventional surfaces are often used as basic surfaces to fit complex

freeform surfaces due to their simplicity of generating and ease of analysing and optimisation. This section will introduce the classification of common surfaces, introduce the process of finding the form of freeform surface morphology, suggest the morphological features that should be present in RAC-FTS and suggest the principles of form-finding methods.

6.1.1 Surface classification

In this sub-section, freeform surfaces are distinguished from traditional conic surfaces, hyperboloid surfaces and other surfaces that can be generated by traditional geometric methods. These include the following types.

Rotational Surface: A rotational surface is a geometric shape formed by rotating a curve around a straight line. The curve is called the Generating Line, the line is called the axis of rotation, and the circle resulting from the rotation is called the woof. There are two modes of generating rotational surfaces, one is the rotation of a plane curve that is coplanar with the axis of rotation, and the other is the rotation of two sets of curves in opposite directions that are not coplanar with the axis of rotation. For example, a hyperbola can be formed by the rotation of a parabola or by the rotation of two lines whose axes of rotation are not co-linear (Figure 6.3).



Source: <https://specials-images.forbesimg.com/imageserve/5fbbc8466f2c8474693ed250/960x0.jpg?fit=scale>
Figure 6.3 Swiss Insurance Headquarters Building with the prototype of the revolving surface

Translational Surface: A translation surface is a surface formed by translating a curve along another line or curve. On the one hand, translational surfaces allow for more complex surface forms than rotational surfaces, and on the other hand, the presence of two sets of parallel curves in a translational surface facilitates discretization and construction. For example, the Japanese pavilion at the Hanover Expo in Germany (Figure 6.4), designed by Shigeru Ban, created a large span of exhibition space without columns, and the shape of this pavilion was presented as a hyperbolic, translational surface.

Ruled Surface: Ruled surfaces are obtained by sweeping or rotating a straight-line segment along a curve, known as a directrix curve. If the direction of the straight line is constant with respect to the curve, the surface is like that of a paper tape, while the line is continuously varied, the resulting surface can take on a more free and complex form (Figure 6.5).



Source; <https://www.architectmagazine.com/project-gallery/japan-pavilion-hannover-expo-2000>
 Figure 6.4 The Japan Pavilion at the Hannover Expo

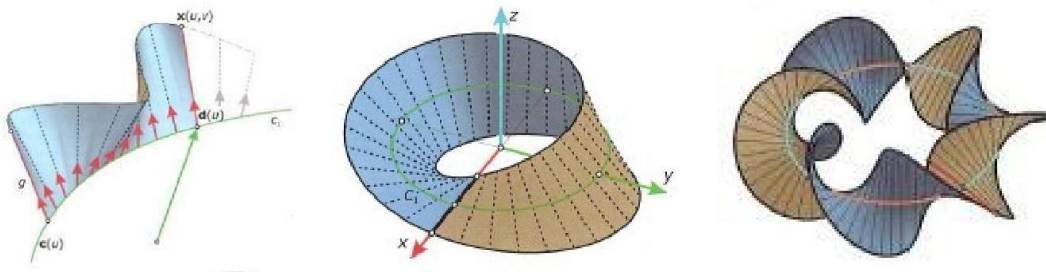


Figure 6.5 Generation of ruled surfaces

A Doubly Ruled Surface is a type of ruled surface in which two different curved straight lines exist at each point on the surface. Hyperbolic Paraboloids are a typical example of a doubly ruled surface, and this geometric property allows the surface to be constructed entirely from straight bars. In addition, the hyperbolic paraboloid, known as torsional shell in the civil and hydraulic fields, allows for thin, large-span shell structures due to its positive static properties. For example, the Pengrowth Saddledome in Calgary, Canada (Figure 6.6) is currently the largest concrete shell stadium with a hyperbolic paraboloid form.



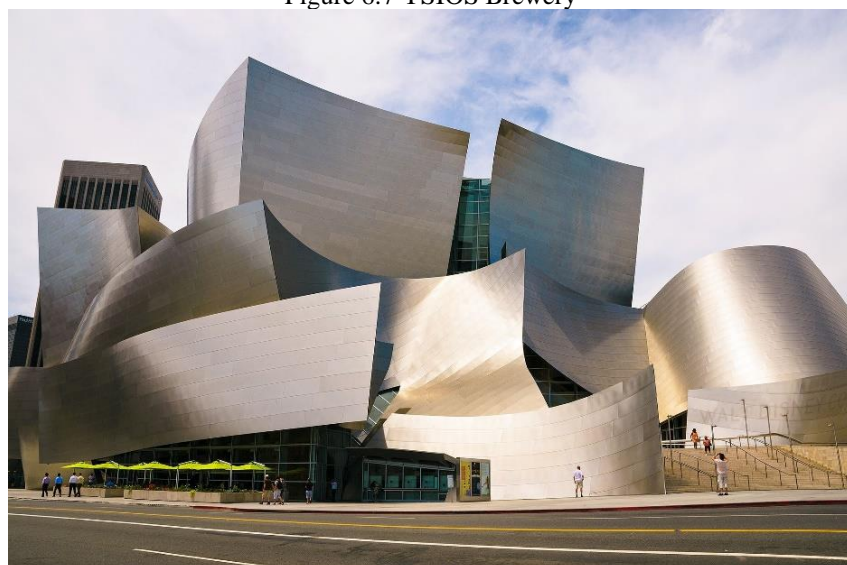
Source: <https://www.metalconstruction.org/index.php/case-studies/St-Aloysius-Church-Jackson-NJ?case%5Bproduct%5D=1993>
 Figure 6.6 Hyperbolic paraboloid construction

Because straight surfaces consist of a series of straight lines, they are very easy to construct, especially in solid concrete and timber frame buildings. From a geometrical point of view, the straight surface is an infinite surface due to the linear extension of the lines of variation Figure 6.7.

Developable Surface: A developable surface is a special ruled surface, while a straight surface with a unique tangent surface along the generating line is a developable surface. The greatest advantage of a developable surface is that it can be covered evenly with small pieces of sheet metal to achieve a smooth surface. Developable surfaces and planes are isometric Mappings, i.e., they have the same gaussian Curvature. An important feature of these surfaces is zero Gaussian curvature. The greatest advantage of developable surfaces is that they can be uniformly covered by small pieces of sheet metal to achieve a smooth surface. These surfaces contain a set of straight lines, thus facilitating the design and construction of the supporting structural framework. For example, the Guggenheim Museum in Bilbao, the Walt Disney Concert Hall in Los Angeles, and the Stata Centre at MIT have all been optimised with curved surfaces that can be developed and finished with titanium panels.



Source: <http://nisowinetours.com/project/ysios/>
Figure 6.7 YSIOS Brewery



Source: <https://www.pinterest.com/pin/372813675380189274/>
Figure 6.8 Walt Disney Concert Hall in Los Angeles

Definition of freeform Structure

The spatial grid structure is one used widely structure form, which is composed of various components connected by joints and is organised in regular geometric patterns. The patterns are flexible and

adaptable to different geometric shapes to present multiple forms. To define the freeform structure (FFS) in this chapter, the first need to know is the concept of the freeform surface. The freeform surface is one surface that cannot be denoted in analytic functions or expressed in descriptive geometry. Therefore, the freeform structure in this chapter is defined as the spatial structure composed of freeform surface in two-dimension or three-dimension. For now, in the freeform research area, there are no rigorous conceptual classification methods. In this chapter, the form of FFS is sorted by three ways: number of dimensions, component form, and structure form. The freeform structure can be classified according to different criteria.

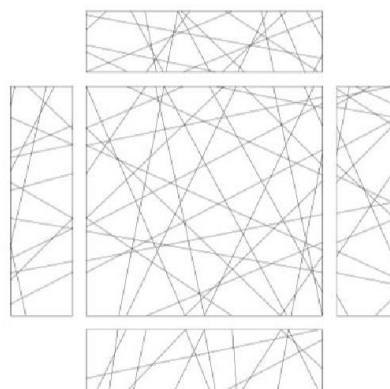
Classified by dimensions

(a) Freeform surface in facade dimension

This refers to free grid space structures where the grid structure extends in two dimensions and the morphological interface of the structure is flat (Figure 6.9-Figure 6.10). Planar free-grid spatial structures are generally easy to construct, simple interface, limited span, single morphology, etc.



Source: <https://www.gettyimages.co.uk/detail/news-photo/serpentine-gallery-summer-pavilion-2002-london-united-news-photo/157875768>
Figure 6.9 Serpentine Gallery in London



Source: <http://chasemitchelljordan.com/structural-analysis-toyo-itos-serpentine-pavilion/>
Figure 6.10 Planar free grid spatial structure

(b) Freeform surface in roof dimension

This refers to the extension of the grid structure on a three-dimensional surface and the formation of a freeform grid structure with a three-dimensional surface as the interface. Curved freeform lattice structures are generally characterised by a smooth and rich interface form, high spatial fit and flexible spatial span (Figure 6.11- Figure 6.12)

(c) Freeform surface in Construction dimension

Instead of taking a definite surface as the reference plane, the grid structure extends or grows in all directions in three-dimensional space according to a certain logic, and the structural interface presented is not a definite single surface or plane, but a free grid space structure with the characteristics of three-dimensional space volume (Figure 6.13).



Source: <https://www.flickr.com/photos/cybertect/1170583711>
Figure 6.11 The roof of British Museum



Source: <https://visitabudhabi.ae/en/where-to-go/islands/yas-island>
Figure 6.12 The roof of Yas Island of Abu Dhabi

The three-dimensional free-grid spatial structure is generally characterised by a strong sense of volume and space, flexible span changes, strong load resistance and a high degree of spatial fit. Freeform structures can be composed of panels, bar elements. There can also be integral shells, which can also be used as integral support structures (Figure 6.14).



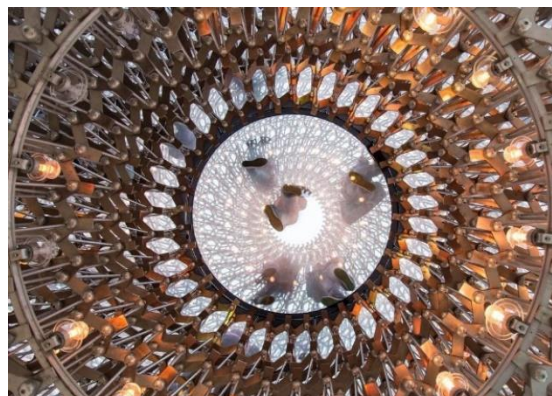
Source: <https://www.arup.com/projects/chinese-national-aquatics-center>
Figure 6.13 The spatial structure of Water Cube



Source: <https://fineartamerica.com/featured/exoskeleton-douglas-barnard.html>
Figure 6.14 The spatial structure of Federation Square

If classified the freeform structures in components, the classifications are shown as followings:

(1) **Unitary bar pattern:** This bar system evolved from the traditional spatial lattice structure and consists of linear elements of a certain length, connected in a corresponding way to form basic cells, each of which is independent of the other, and which are formed by the accumulation and grouping of the basic cells to form the corresponding structural form Figure 6.15.



Source: <https://archello.com/project/uk-pavilion-milan-expo-2015>
Figure 6.15 British Pavilion at Milan Expo

(2) **Weaving pattern:** Weaving refers to the intersection of linear elements in two or three dimensions, forming a grid system with different density. This linear organisation is like the weaving of a bamboo basket, where the linear elements are interwoven in space to form a virtual interface, and the structure has a sense of rhythm, and the rods are mostly long linear elements, so the structure is more integral.



Source: <https://www.arup.com/offices/Germany>
Figure 6.16 Centre Pompidou Metz



Source: <https://www.area-arch.it/en/haesley-nine-bridges-golf-clubhouse/>
Figure 6.17 Nine Bridges Golf Club

6.1.2 Form-find of Morphology of Freeform surface

In conjunction with the above analysis of the characteristics of free grid space structures, it can be seen from numerous examples that freeform structures are suitable for buildings with the following characteristics:

- (1) Dynamic and smooth architectural form.
- (2) A rich variation of spaces.
- (3) Light structure.
- (4) The pursuit of permeability in the expression of architectural interfaces.
- (5) An emphasis on integrated design of the building structure and skin.
- (6) The pursuit of a gridded or woven formal language for the architectural skin.
- (7) A high level of natural ventilation and natural light requirements within the structure, etc.

For freeform architecture, the first step is morphological design, finding a suitable geometric shape for it, i.e., finding the form. Determining the overall geometry of the freeform mesh structure is the first problem to be faced. In the case of conventional regular surfaces, architects can model them quickly by means of explicit analytical functional equations, but to design irregular, freeform forms, other methods must be used. Research has mainly included experimental and theoretical analyses based on physical models and biomorphic designs based on biological forms. Computer-aided geometric design is now increasingly being used in the morphological design of freeform mesh structures due to improvements in the level of computer-aided design. There are three main form finding commonly used methods:

- (1) Physical experiments: Physical shaping of surfaces is a method of constructing complex surfaces based on physical constraints, using mechanical principles or experiments. Physical shape-finding originated with Gaudi's model of suspended chains, which was followed by methods of shape-finding that combined computational models with inflatable films, soap bubbles and draped fabrics to create

conical surface forms. The most famous of these methods are the inverse hanging experiment and the surface construction method for cable and membrane structures. Physical shaping ensures that the morphology of complex curved surfaces is structurally sound, making full use of the structural properties of this form of building.

(2) Curved geometric transformations: Geometric transformation is a method of transforming and combining basic planar geometry to produce complex surfaces such as straight, rotated, and expandable surfaces. The geometrical transformations allow complex surfaces to be constructed based on basic geometrical elements, making it easier to create models for processing and to discretize and reconstruct surfaces.

(3) Irregular forms: For complex surfaces that are not expressed analytically and cannot be obtained by combining simple surfaces, surface fitting techniques are used to approximate a given discrete point or curve. This method allows more freedom in the construction of complex surfaces and more accurate representation of the design intent. However, it is not easy to find a balance between form and structure, and the design is likely to deviate from the original design aim. This method is highly dependent on the architect's knowledge of the design concept and control of the structure form, which need the application of computer-aided optimisation method.

Three design approaches can be distinguished according to the sequence of morphogenetic operations, as follows:

(1) Up-bottom: Up-bottom means design from the whole to the parts. The overall form is formed first in the design, the form is subdivided based on the established final form with certain rules and the basic units are fitted into the final form. Tessellation is a top-down design process in which smaller scale subdivisions are made because of the already formed building form.

(2) Bottom-up: Bottom-up means design from parts to the whole. The final form cannot be predicted until the result is reached, but only the basic form of the unit and its constitutive laws can be predicted.

(3) Hybrid method: Starting from both ends (the whole and part) at the same time, the interaction of the overall form and the local units is considered simultaneously.

6.1.3 RAC-FTS form-finding methods

To realise the logical design-build relationship and the technical route, it is important to find the appropriate start point. The main consideration is the form finding of the initial freeform surface, based on the previous analysis of the impact of RAC on the FTS design and the "modularity" principle of design optimisation in Chapter 4. Modular design starts with a clear understanding of how the module intervenes in the design. Bars, panels, and units are the basic component elements that operate on 4 different levels: point, line, surface, and structure. Bar, panel, and unit modules reduce relatively abstract elemental concepts to make them more architecturally meaningful and fit in with modular decomposition operations, reflecting the multi-layered structural connotations of modular decomposition resulting in modules. Bars, panels, and units can be transformed into each other to a

certain extent by decomposition and concentration. The "design-structure-fabrication" operation is characterised almost exclusively by the organisation of space by three basic elements: the bars do not represent components in the traditional sense, but also contain a system of bars associated with space and form, which have a significant impact on the design of the building through their lap, arrangement, and combination. The panels define the boundaries of the space, and their own internal information is concealed during the design operation phase, creating a sense of flow and uncertainty in the space by shifting, arrays and folding between panels, thus creating a spatial experience with rich tension. The volume outlines the form of the space, shifting the spatial design perspective to the spatial manipulation between units. The RAC-FTS design is therefore modular in character, with rods, panels, and blocks as the design dimension, and reflects an integrated approach to materials, processing, and construction.

There are many methods for generating freeform surfaces, so a suitable RAC-FTS form-finding method is required. Based on the above translation of modularity as a 'design-structure' approach, the choice of freeform surface generation method needs to be made in conjunction with the modular concept and its characteristics. Different methods have their own advantages and characteristics, and different logics are needed to constrain the construction of complex surfaces according to different design requirements, such as the accuracy of the surface fit, so that the structural and aesthetic requirements are better integrated, the collaboration between architects and structural engineers is better achieved, and the design intentions are more accurately expressed to achieve the complex form of the surface. A freeform surface finding approach requires the following characteristics, easy gridding, easy numerical and easy to prototype.

In current modular operations, the meaning and design connotations of the modules themselves are relatively absent. The importance of prototypes in modularisation is that they provide a guide to the division of modules and give them their original concept, giving them a certain design connotation, while the modules materialise the concept of the prototype. The interface between modularity and prototype adds a method of operation for the architect when setting up top-down modules, not only by directly intervening with bar, panel and unit modules, but also by using the prototype as a guide, which is often presented as a combination of three systems, or as a higher-level system, giving the module itself a certain design information; there are three main relationships between modularity and geometric prototypes:

- a) Geometric prototyping as a module applied to design operations.
- b) The geometric prototype itself has a certain modular character that forms a guide to the modular division of intrinsic.
- c) Some of the geometric prototypes realise their prototypical features with the help of modular operations.

The appropriate form-finding methods for RAC-FTS needs to have at least one of the following characteristics:

- (1) Easy to prototype and modularise. As the premise for this research is the main building materials are planar panels or linear rod, the morphology would be turned into structure components in the materialisation process. If the morphology can be turned into standard mesh without deviation, then it would also ease the pre-fabrication process.
- (2) Easy to turn to digital information. According to the definition and research scope for freeform surface in this research, it means no mathematical expression for the 3D model. Considering the connection between 3D information of geometric model and numerical information of robotic technique, if the 3D model can generate numerical information, it would improve the data efficiency.
- (3) Rationality. The rationality means the rationality in structure performance, material buildability, and fabrication applicability.

6.2 Complex geometry in RAC-FTS morphogenesis

6.2.1 Complex geometry together with mathematics

In *Digital Morphogenesis*, Brabko Kolarevic argues that in contemporary architectural design, digital media is no longer a tool for visual communication but a source of form and transformation - that is, digital morphogenesis. Based on digital generation technology, the design process is moving from making of form to finding of form. An important source of digital morphogenesis is the idea of topological geometry, and the platform for experimentation is the current powerful digital modelling software. A second source of digital morphogenesis is the design of parametric processes or computer scripts. Complex geometry and freeform morphogenesis are divided into the following main methods:

(1) Polygonal geometry

Polygonal geometries or polyhedral are geometric entities formed by the enclosure of planar polygons, including not only symmetrically balanced classical geometries such as the Platonic and Archimedean polyhedral, but also more complex variants of polyhedral. This complex geometry began with Deconstruction and Constructionism, a break from *Modernism* and *Postmodernism*, whose formal essence was the destruction and deconstruction of Structuralism. By translating, cutting, and superimposing the original geometry the final state is broken, messy, blurred and uncentered. Non-linear or non-Euclidean geometry has been incorporated into the deformation and displacement of the architectural elements of *Deconstructionism*. Radiolarian, for example, takes as its starting point the beautiful and delicate skeletal system of the radiolarian. The pentagonal and hexagonal frames are organised algorithmically in a complex surface form.

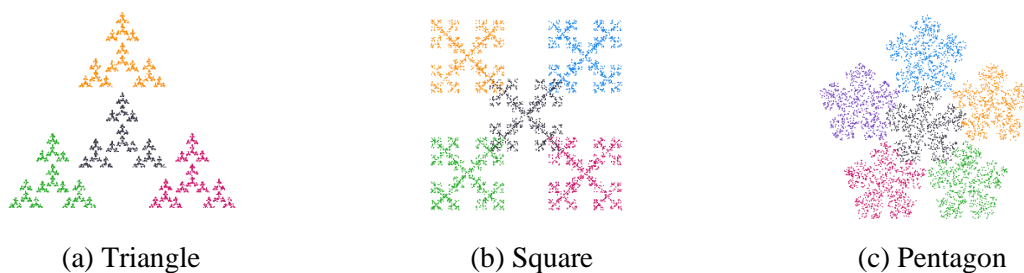
(2) Fractal geometry

Fractals were introduced by Mandelbrot in the 1970s and were originally introduced into the natural sciences for the purpose of characterising complex shapes and complex processes, meaning irregular, fragmented objects.



Source: <https://scriptedbypurpose.wordpress.com/participants/christan-troche/>
 Figure 6.18 Radiolarian project of Christian Troche

A broader definition was given by Mandelbrot in 1986: "A fractal is a shape in which the parts and the whole are in some way similar". This definition emphasises the self-similarity of geometric figures and of spatial trajectory figures, which have multiple levels and span different scales. The graphs of fractal geometry are characterised by three features, namely self-similarity, self-affine and fine structure. The characteristics of fractal geometry are quite different from those of Euclidean geometry. Fractal geometry is irregular and not smooth in any interval, whereas Euclidean geometry is regular and smooth segment by segment. As an important part of non-linear science, fractal geometry has been used in non-linear architectural design thinking, particularly in algorithmically generated design methods, and its study as a computer graphics object has become a direct digital illustration of architectural generation. Many fractal patterns are used in façade design or spatial division of buildings because they not only have the abstraction of Euclidean geometry, but also present a multi-layered and multi-scale complexity.



(a) Triangle

(b) Square

(c) Pentagon

<https://mathigon.org/course/fractals/sierpinski>

Figure 6.19 5000 steps of Chaos Game of different shapes

(3) Topology Geometry

Topology is a discipline that studies geometries that change continuously. Topology began as a study of geometric problems based on the needs of mathematical analysis and has evolved into a discipline that studies the invariant properties and invariants of topological spaces under topological transformations.



Source: https://www.hparc.com/images/works/wGEM01_Render-Translucent_Stone_Wall_Night.png

Figure 6.20 Egypt Museum

The Möbius ring is undoubtedly the most famous topological figure, having been discovered by the German mathematician Möbius in 1858. It is a paper strip twisted by 180 degrees and bonded at both ends, a model that enables the infinite interweaving and continuity of the front and back sides of the strip, transforming a two-dimensional object into a three-dimensional one.

(4) Folding

Sophia Vyzoviti in *Folding as a Morphogenetic Process in Architectural Design* refers to folding as a generative process in the architectural process as experimental, indeterminate, non-linear, and bottom-up. Under this concept, surface is introduced and has a richer connotation than the façade and skin of a building. It completely breaks down the dimensions of walls, roofs, and floors, blurring the boundaries between inside and outside space. The boundary between inside and outside space is blurred. The renowned origami scientist and artist P. Engel emphasises the close connection between origami, mathematics, and nature as analogous to the minimal value problem, fractals, and chaos theory. There is a profound knowledge of geometry and mathematics in origami and the axioms and algorithms behind it and the construction of computer models are still a work in progress.



Source: https://www.archdaily.cn/cn/760447/dan-mai-guan-2010nian-shang-hai-shi-bo-hui-big/5008f42b28ba0d27a7000ec7-denmark-pavilion-shanghai-expo-2010-big-photo?next_project=no

Figure 6.21 Denmark Pavilion Shanghai Expo

More current creations are based on a process that combines manual manipulation and computerisation. Folding forms include Origami, Origami Tessellations, Kirigami, Ruling, Curved Crease Origami.



Source: <https://parametric-architecture.com/foldfinding-origami-pavilion-tal-freidman/>
Figure 6.22 Origami Pavilion

Based on the methods of morphogenesis using complex geometry described above, the design of the RAC-FTS requires a method that is easy to numerise and reflects the optimal principle of 'modularity' to produce a homogeneous mesh structure, based on the fabrication characteristics of the RAC as well as the timber material properties and common timber fabrication methods. When considering the 'design-build' factor, an important process is the extraction of geometric information into digital information and its transformation into valid information on the morphological surfaces of the geometric model.

6.2.2 Minimal surface in RAC-FTS

If a copper wire is formed into a closed spatial curve like a kink, and then placed into a soap solution and gently removed, the soap solution will form a film in equilibrium on the copper wire framework. This film is the minimal surface, which is the smallest surface area that satisfies the surrounding air conditions and the morphology of the film-forming framework, and where the surface pressure is equal everywhere. This soap film experiment is the famous Prato experiment, and the process of solving for this very small surface is called the Prato problem. The minimal surface experiment is a typical example of the general model of the universe, the principle of minimum action, proposed by the French scientist Pierre Louis Moreau de Maupertuis in 1744. In mathematical concepts, a minimal surface is a surface with zero mean curvature. Minimal surfaces are defined in terms of curvature and are surfaces with zero mean curvature. In addition, a minimal surface is a surface with the smallest area that satisfies certain constraints. Minimal surfaces are used extensively in architectural design. On the one hand, because of their rich and varied spatial topological properties, minimal surface algorithms can be used to generate flow spaces, where the continuous flipping of spatial variations brought about by minimal surfaces breaks down traditional spatial boundaries. In addition, the minimum surface area of very small, curved surfaces allows for an effective reduction in the shape coefficient of building¹⁰. The concept of minimal

¹⁰ The ratio of the exterior area of a building in contact with the outdoor atmosphere to the volume it encloses.

surfaces was introduced into the design of tent-like spatial structures by Frei Otto as early as the 1950s. This type of membrane structure makes use of the equal force characteristics of the membrane material in all directions, resulting in complex forms such as sail spire, arch, wave, and other complex forms.

As timber structures are different from membrane structures, monolithic structures cannot be generated. Therefore, after generating a freeform surface with minimal surface characteristics using mathematical formulas, it needs to be converted into surface information that fits the timber and the workable range of the robotic arm. Figure 6.23 shows a minimal surface that can be subdivided into small segments. The segments can combine multiple prototypes with modular properties. These prototypes can be used as a single freeform morphology or in combination to create a more diverse morphology.

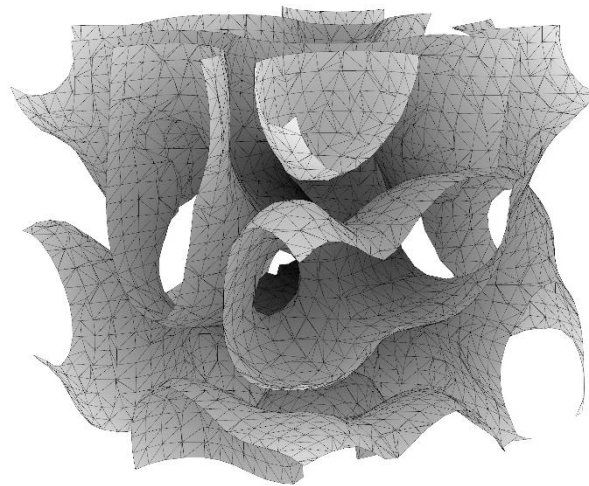


Figure 6.23 Minimal surface example

6.2.3 Construction feasibility analysis

In the case of complex freeform timber structure, the practical construction problems arise from the material properties of the timber and the extent to which it can be fabricated. Currently, most complex surfaces are built using a sub-panel approach, whereby the surface is simulated, a suitable subdivision strategy is selected, and the optimum sub-panel approach is determined, then the individual component information is modelled and delivered to the downstream fabricator to complete the component. Surfaces, due to their difficult construction characteristics, need to be analysed and optimised in preparation for later sub-panel construction. A proper analysis will identify the defects in the surface shape and adjust it to the next step in the construction process.

(1) Curvature analysis

The term used to describes the degree of curve of a geometry, such as the deviation of a surface from a plane or the deviation of a curve from a straight line is called curvature (Koenderink & Van Doorn, 1992) and is defined as:

$$K = \frac{1}{r} \quad 6.1$$

where r is the radius of a sphere or circle, such that the smaller the radius the greater the curvature of the circle, and a straight line can be seen as a circle of infinite radius. Curvature is mainly used to analyse the flatness of a surface. The greater the curvature the greater the curvature of the surface. In addition, minimal surfaces and expandable surfaces, especially expandable surfaces, are widely used due to their ease of processing. Thus, when a curve is a straight line, its curvature is zero everywhere. There are two types of curvature for surfaces in three dimensions: Gaussian curvature and Mean curvature. By definition, a minimal surface is a surface with zero mean curvature everywhere, while an expandable surface is a surface with zero Gaussian curvature everywhere. For curves, the curvature of a curve can be defined in terms of the curvature of a close circle. Where the curve is flat, the radius of the close circle is large, where it is curved, the radius of the close circle is smaller

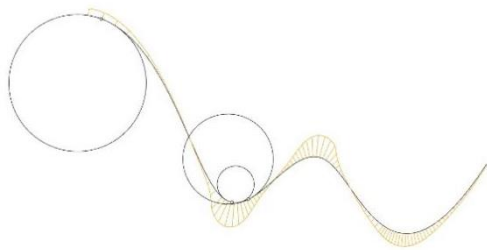


Figure 6.24 Radius of Osculating circle and curvature of curve

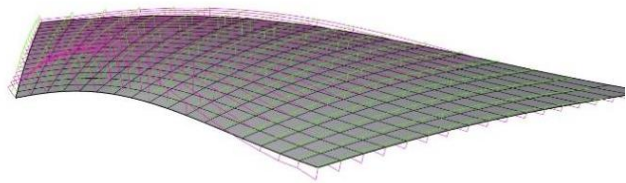


Figure 6.25 Curvature of surface

(2) Continuity analysis

Continuity of surfaces is a concept that addresses the stitching of surfaces. As most complex surface geometries cannot be represented by a single complete surface, but require multiple surfaces to be stitched together, the quality of the intersection of these surfaces becomes an important issue. In terms of both material construction and the human visual experience, the continuity of curved surfaces in architecture is not very high and is less important than in the case of industrial products such as cars, for example. However, good continuity of curved surfaces is necessary to ensure fine construction results. Firstly - G_0 , G_1 , G_2 , G_3 and G_4 are levels that describe the way in which surfaces, and curves are continuous and how smooth they are. The higher the level, the better the continuity and smoothness.

G_0 positional continuity: curved surfaces or curves are continuous at points. Curves do not break apart but have sharp corners. There are no holes or cracks on surfaces, but with sharp flutes. The mathematical interpretation is that the intersection line (or surface) of the curve(s) is continuous everywhere.

G_1 tangential continuity: surfaces or curves are continuous, and all connected line segments and surface pieces are tangential to each other. Curves have no sharp corners and surfaces have no fluting. The mathematical interpretation is that the intersection lines (surfaces) of the curves (surfaces) are continuous everywhere and the first order derivatives are continuous.

G_2 curvature continuity: surfaces or curves are continuous and have their curvature curves continuous without breaks and with sharp angles. The mathematical interpretation is that the intersection lines (surfaces) of the curves (surfaces) are continuous everywhere and that the second order derivatives are continuous.

G3 - curvature rate of change continuous surface or curve continuous, curvature analysis done on curves, curvature curve continuous, no break points, no sharp corners. The mathematical interpretation is that the intersection lines (surfaces) of the curves (surfaces) are continuous everywhere and that the third order derivatives are continuous.

G4 - The further continuity of G4 is difficult to observe. G4 continuity level provides a smoother continuity effect (G3 is generally sufficient). The mathematical interpretation is that the intersection lines (faces) of the curves (surfaces) are continuous everywhere and that the fourth order derivatives are continuous.

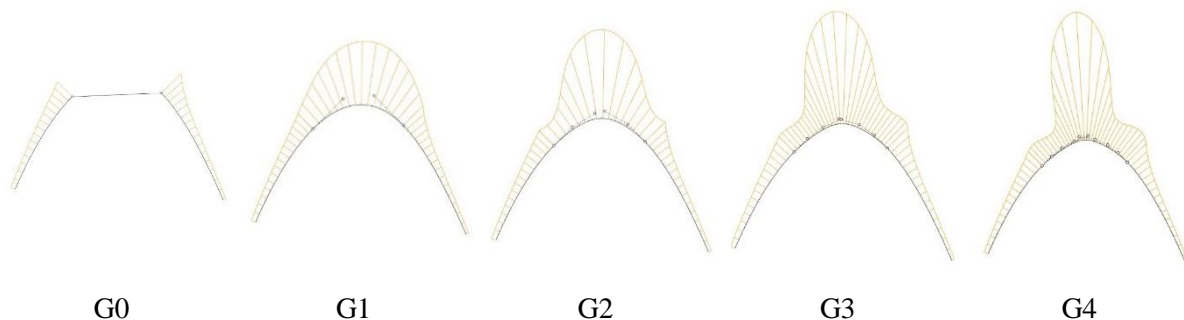


Figure 6.26 continuity of curved surfaces

6.3 Biomimetic and construction feasibility analysis

6.3.1 The relationship between bionics and freeform biomorphism

Structural biomimicry introduces new perspectives on design through the simplicity, efficiency, aesthetic diversity, and systematic integration of the natural world. Bionics is the study of nature's structures and forms to meet the morphological design of architectural structures. By using natural structural forms such as micro-organisms, plants and animals, and humans as prototypes, and by drawing on a variety of material combinations and cross-sectional variations, structural bionics can be used to optimise the design of structural supports for building construction, which can improve the efficiency and reduce the cost of building construction. The design of freeform timber structures is of great importance. The bionic structure is characterised by its good structural properties, form versatility, and aesthetic appeal. Therefore, the bionic approach is one of the most important tools in the design of freeform timber structures, allowing for a reasonable and diverse range of structural forms. Emerging biomimetic structural forms are an effective combination of architectural artistry and structural economy by using new materials and technologies to reveal the laws of nature.

In general, morphological innovation in architecture is achieved through three main approaches: morphological similarity, geometric laws consistency, and mechanical logic rationalisation. In terms of morphological similarity, bionic structural systems are essentially a distillation and processing of natural structural prototypes so that the morphological simulation directly reflects the mechanical logic. This approach is simple, practical and accounts for a significant proportion of the forms of bionic structure in use today. In terms of consistency in geometrical laws, the resulting bionic structures are sometimes not directly apparent. Still, they are entirely consistent when viewed about the numbers since the rules

are sometimes clearly visible as forms and sometimes the mathematical logic behind the forms is not readily apparent. The bionic structure is based on rigorous analysis of the mechanical system in terms of the rationality of mechanical logic.

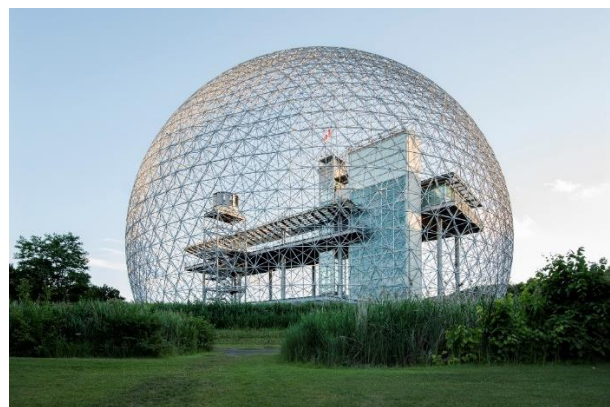
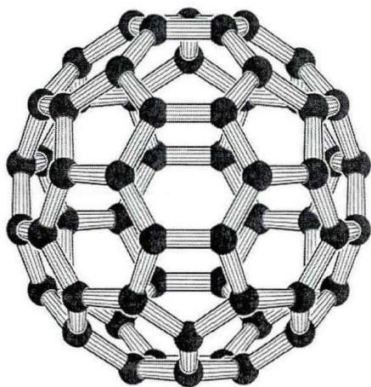
The method of creating biomimetic building forms broadly encompasses four dimensions, and its specific content in relation to the generation of freeform timber forms is summarised below.

(1) Morphomimetic

Morphological mimicry of plants and creatures in nature is most directly related to freeform morphogenesis. It is an effective method of innovation that explores the possibilities of application in architecture by studying the patterns of living things in their many forms, not only by integrating function, structure, and new forms but also by moving beyond imitation to a mature design process.

(2) Mechanical bionics

Buildings that correctly mimic the structure of living organisms are often characterised by material-efficient, strong, rigid, stable, and aesthetically pleasing structures. Many of the most material-efficient, durable, and aesthetically pleasing forms of spatial structure are conscious or subconscious simulations of natural structural forms, including parts of the organism, the main structure, its nest, or some feature of its surroundings. Simulation refers to the use of mathematics, physics, and other research tools to study and analyse the structural forms of certain materials in the natural world, to extract factors that are useful for the design of architectural structures from the complex and varied lifelike prototypes, and to create new structural patterns through these methods, thus enriching the creative approach to architectural design. For example, in the microscopic world, atoms are arranged in a regular pattern, and the different arrangements lead to other substances being formed. It can be used as a solid lubricant. Structural experts have studied the crystalline form of atoms and molecules and applied it to buildings, inventing grids that can withstand high pressures and have certain regularity. The presence of rods increases the strength of the material and helps to save building materials.



Source: https://www.architectmagazine.com/design/buckminster-fullers-biosphere-celebrates-50_o
Figure 6.27 Fuller Molecular Structure and American Pavilion

(3) Material bionics

Material bionics is more mainly concerned with analysing the structure, properties, and growth mechanisms of natural biological materials and their replication. The natural honeycomb form has always been of interest to scientists and engineers as an efficient structure resulting from natural selection. In the fourth century AD, the ancient Greek mathematician Papos proposed the 'honeycomb conjecture' that a honeycomb with a hexagonal cross-section was built with a small amount of beeswax Figure 6.28. This conjecture has been confirmed, and the honeycomb structure uses the least amount of material and has the most significant structural stability and creates the greatest amount of space. This form has been widely used in industrial design, architectural design, materials science, and aeronautics. The geometric logic behind this structured pattern is the space-filling of polygons. And indeed, the honeycomb is one of the simplest and most regular filling methods. Crystals, amorphous and quasi-crystals in nature all imply a great variety of filling rules and forms, which can be used to inspire architectural forms and structural design.



Source: <https://www.flickr.com/photos/justaslice/24000433744/>
Figure 6.28 Honeycomb Speculation

(4) Functional bionics

Biomimicry also has a 'functional' dimension, mimicking the 'skills' of living things in nature; for example, the leaves of each plant are attached to the stem in a certain way, in an order called leaf order. Leaf order can usually be divided into three types: alternate, opposite, and whorled. Regardless of the leaf order, they all follow a pattern that means that the leaves maintain the maximum light exposure surface, forming a mosaic arrangement of leaves. This characteristic results from the green leaves ensuring the production of more photosynthetic products adapted to long-term sun exposure. Similarly, the asymmetrical character of the canopy indicates its spontaneous adaptation to orientation, living space, light, and wind direction. But with the generation of free-surface morphology overlaps with all three of these dimensions.

6.3.2 Reconfiguration Bionics: A bionic design approach combined with reverse engineering

The traditional design method is mainly forward design, and the conventional forward design and manufacturing process is a well-established and widely used development model. The flow chart of the complex surface design and manufacturing process is shown in Figure 6.29, where the process from detailed design to evaluation and validation takes the longest time. Without a reference prototype or design experience, it is often challenging to complete the design if modelled using traditional forward design methods. Reverse design can be achieved by reconstructing the surface from point cloud data measured in kind to obtain the same CAD model as the prototype. After rebuilding the complex surface and creating the CAD model, the CAD model of the workpiece can be quickly constructed with improvements or innovations. The rapid design process is illustrated in the flow chart in Figure 6.30 and allows for part redesign, CNC machining or additive manufacturing.

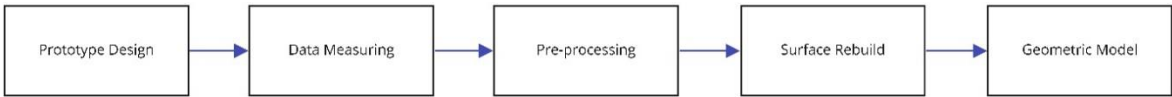


Figure 6.29 Process of reverse engineering

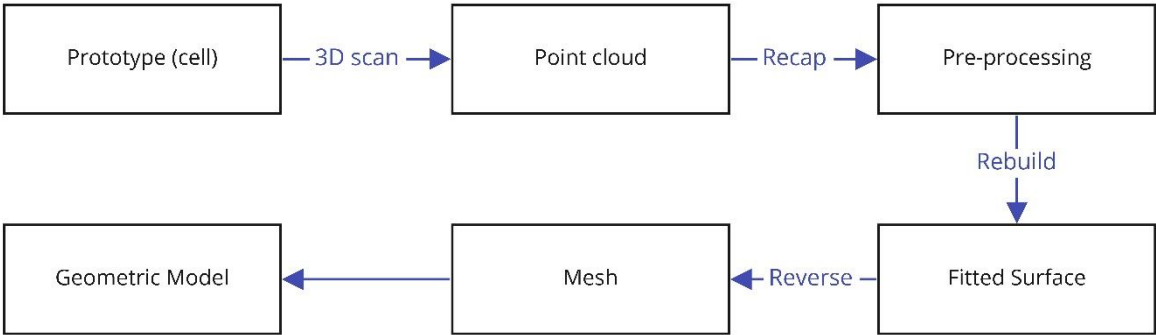
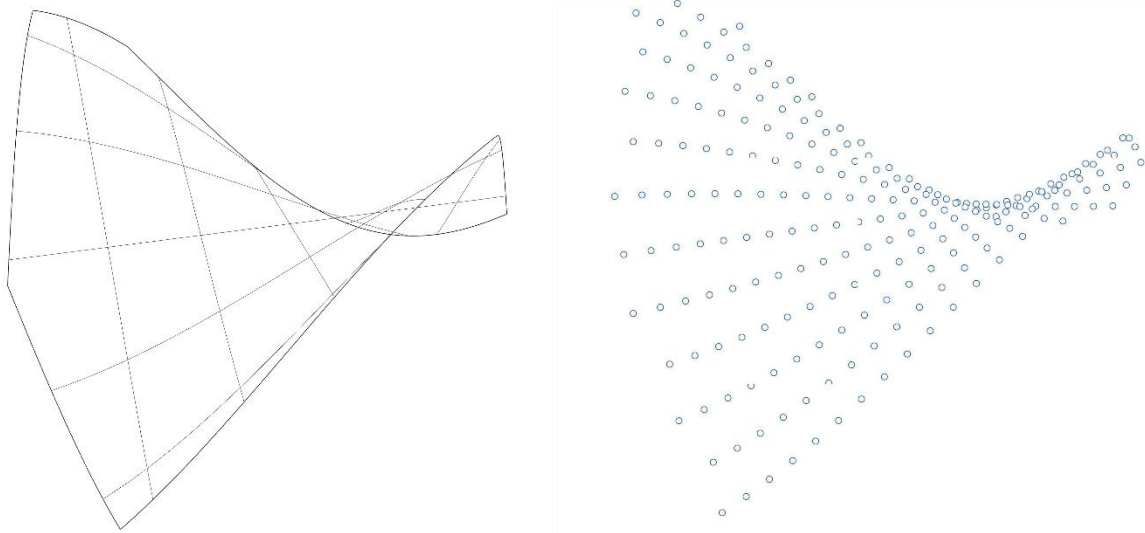


Figure 6.30 Biometrics with reverse engineering

Reverse design technology was proposed in 1982 by 3M and others in the USA. Due to its characteristics of rapid design and relatively strong ability to deal with complex surfaces, it has entered a boom in related research worldwide. Since the 21st century, reverse design has played an important role in significantly reducing the development cycle and enhancing the competitiveness of enterprises. In the past three decades, reverse design has made many achievements in theory and application, especially the emergence of several commercial computer-aided reverse design software, which provides a wealth of reverse design functions. The reverse design of complex surfaces is not simply replicating the existing part shape and structure. Still, it is based on the CAD prototype, with the help of computer-aided technology CAT (Computer Aided Technology), Virtual Product Development (VPD) and computer-aided engineering CAE (Computer Aided Engineering). Computer Aided Engineering (CAE) and other technologies complete the part form and structure. The reverse design process of complex surfaces is usually sample data measurement, pre-processing, surface reconstruction, and CAD model creation. The reverse design process is shown in Figures 1-7. In this process, the measurement and pre-processing of the data can be done by using machine learning for image recognition, using many images of freeform

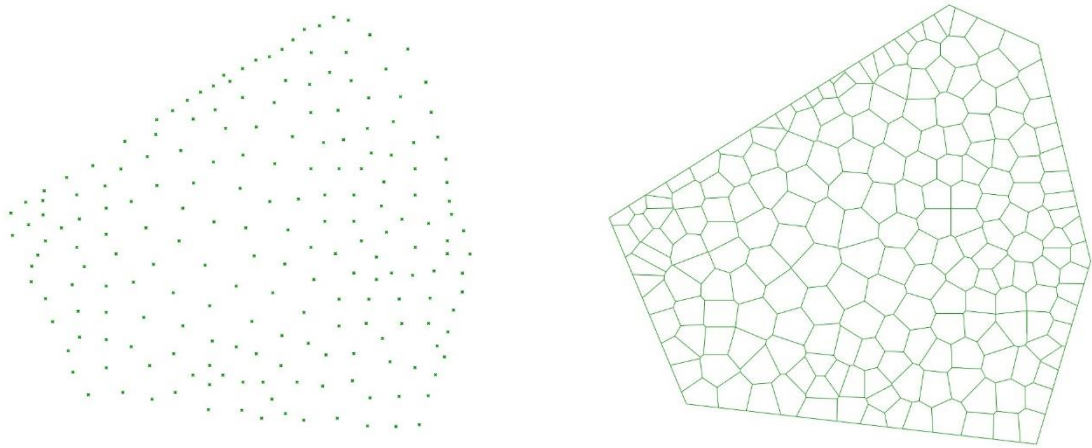
timber structures to extract digital information that can be used as a training data set for machine learning. This workflow is a "soft" application of machine learning to freeform construction.

The workflow can work as follows. When there is a bionic case, the geometry can be scanned to generate a 3D point cloud. The initial surface in 3D geometry Figure 6.31 (a) is recapped to the point cloud with 3D coordinate information Figure 6.31(b). The point cloud is mapping in two-dimensional uv domain, shown in Figure 6.32 (a). The points can be processed in different methods, in this case, Voronoi pattern is selected to connect these mapped points, shown in Figure 6.32 (b).



(a) Original surface (b) Point cloud
Figure 6.31 Original surface and point cloud

After the mapping process, the points are remapped from uv domain to the three-dimension Cartesian coordinate system. After the generative design process shown in Figure 6.33, the new surface is generated by the new point cloud. The process of extract the point cloud from the bionic case into and the surface is fitted by the meshing methods (Figure 6.34).



(a) Original point cloud mapping (b) Clustering point cloud
Figure 6.32 Point cloud mapping

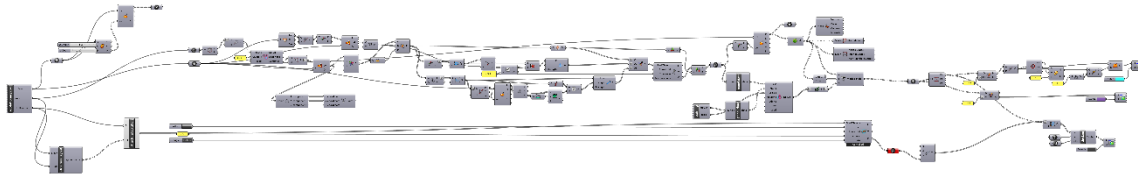
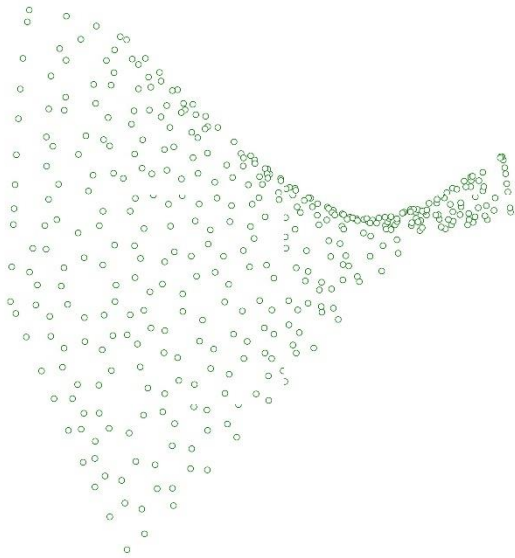
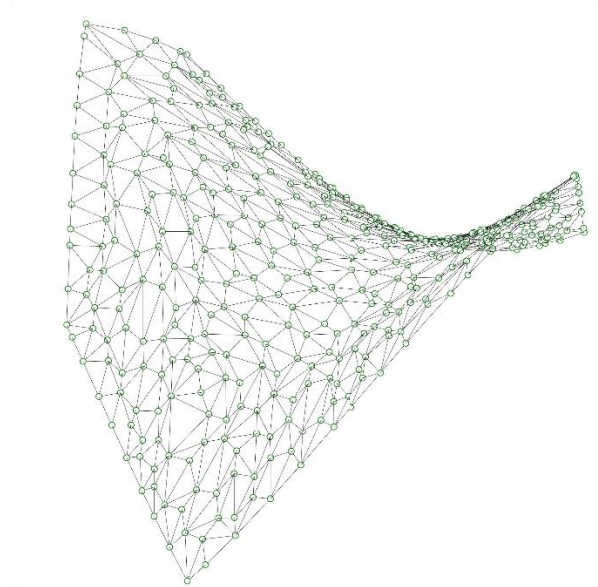


Figure 6.33 Generative Design Process



(a) Remap clustered points



(b) Fitted new surface

Figure 6.34 Fitted new surface

6.4 Machine learning form finding and construction feasibility analysis

Machine Learning (ML) has always been a comprehensive concept, and its definition and performance have been understood in different ways at different times. According to Arthur Samuel, machine learning is the ability of a computer to learn without explicit programming instructions. Machine learning is not a new term; it was introduced in 1959 by Samuel, an American engineer working on computer games and artificial intelligence. The concept of machine learning was refined in the subsequent development of computational learning theories for pattern recognition and artificial intelligence. Machine learning is the process of learning algorithms from known data to learn the data's knowledge and perform related tasks. Such algorithms can build models to overcome problems that completely static programs cannot solve. We can think of this as a machine with a specific learning capability within an artificially defined learning framework. The machine is given a large amount of data and, through a series of algorithmic choices, is trained to produce a set of input-to-output mapping logics capable of producing a relatively reliable output for a sample of data that has never been seen before. Machine learning is mainly divided into supervised learning¹¹ and unsupervised learning¹². Its uses are mainly divided into prediction and classification. Currently, machine learning is available in

¹¹ Supervised learning is trained using already labelled classification or regression samples as training data. The machine is given a set of samples with both features (input) and labels (output).

¹² In contrast to supervised learning, artificially specified training outputs are not required at the outset of training.

architectural design using GAN networks for planar structure, but more research is needed to design freeform surfaces.

Based on the morphological design requirements of freeform timber structures for RAOD presented in this paper, the ability of machine learning to process and analyse data is used to explore suitable applications of machine learning.

The pathway to machine learning raw forms

- (1) choose the appropriate input and output.
- (2) transform the input and output into training set (in numbers or figures).
- (3) select the training method.
- (4) test the training accuracy.

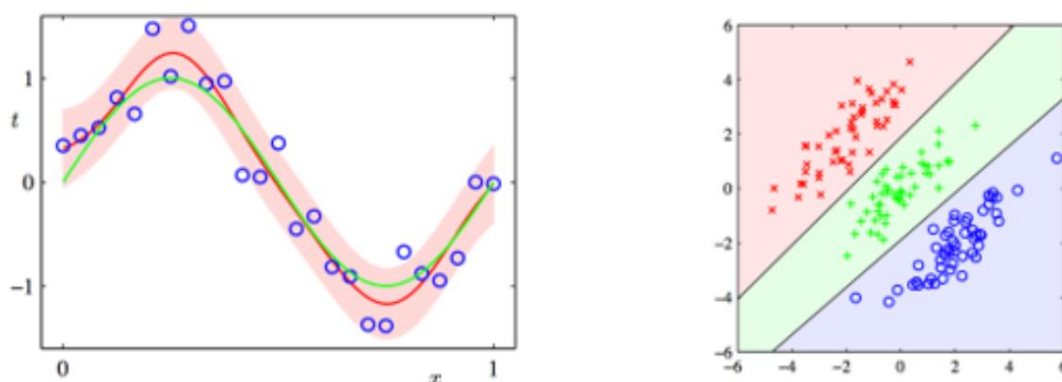


Figure 6.35 Classification and Regression of ML

In this process, the main idea of using machine learning to “learn” to “generate” curves is choosing the curved timber beams as the learning input in real practice. This input means how could be timber products could be shaped into. After the training, a new curve can be generated, which is learned from the current freeform timber cases, considering timber as the specific construction material. One advantage of this method is to combine the design with the material factor. Though the interpretability of the method or the particular property of timber is not linked to the design process clearly, it still provides a way of applying machine learning in freeform design or “generation”.

6.4.1 LSTM workflow for curve prediction

Long short-term memory (LSTM) is one machine learning method that can deal with the classification and the regression task. Based on the morphological design requirements of free-form timber structures for RAOD presented in this chapter, the ability of machine learning to process and analyse data is used to explore suitable applications of machine learning.

The pathway of LSTM machine learning for predicting the curve:

- (1) Choose the appropriate input and output.
- (2) Transform the input and output into training set (in numbers or figures).
- (3) Select the training method.

(4) Test the training accuracy.

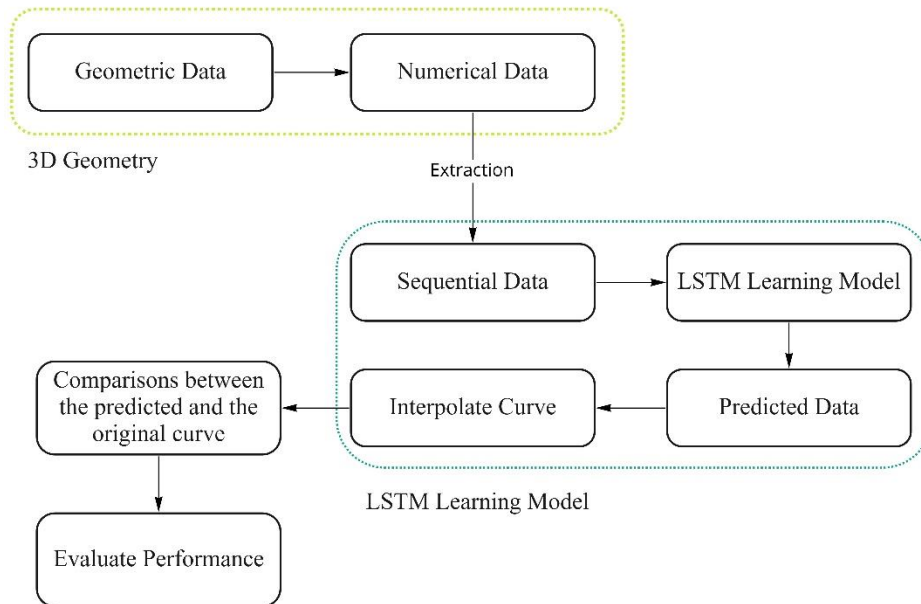
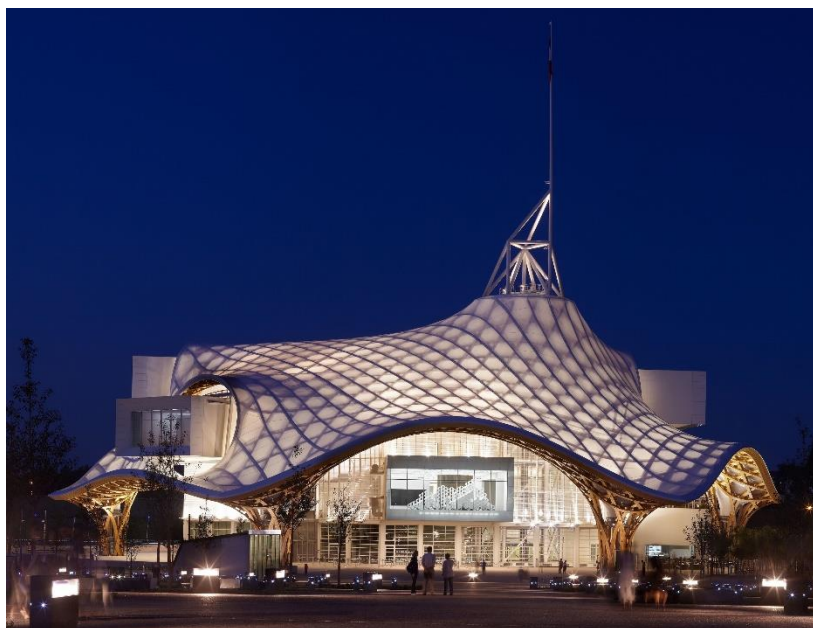


Figure 6.36 Workflow of the LSTM prediction for Curve of Freeform Surface

The main difficulty for freeform geometry design using the machine learning method is the geometric design is stored in three-dimension form (like 3dm, obj) while machine learning deals with numbers. Even in image processing, the image would be transformed into the matrix of the RGB values of the pixel. The geometric model is in three-dimension; if the model is presented in the figures from the top, front and right views, there would be a loss of geometric information. Then the machine learning training model could lead to poor learning results. The idea of data transformation is to find the proper way to store geometric information of the geometric model (Figure 6.38).



Source: "L'aventure de la couleur" au Centre Pompidou-Metz - Michel D

<https://www.micheldestot.fr/echos/laventure-de-la-couleur-au-centre-pompidou-metz/ESTOT>

Figure 6.37 Centre Pompidou-Metz

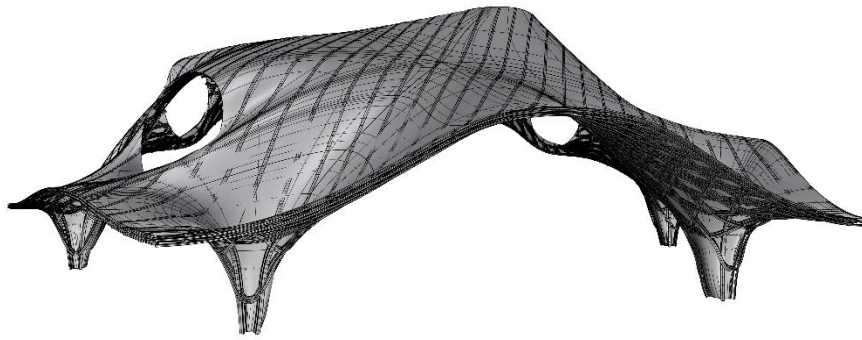


Figure 6.38 Geometric Model

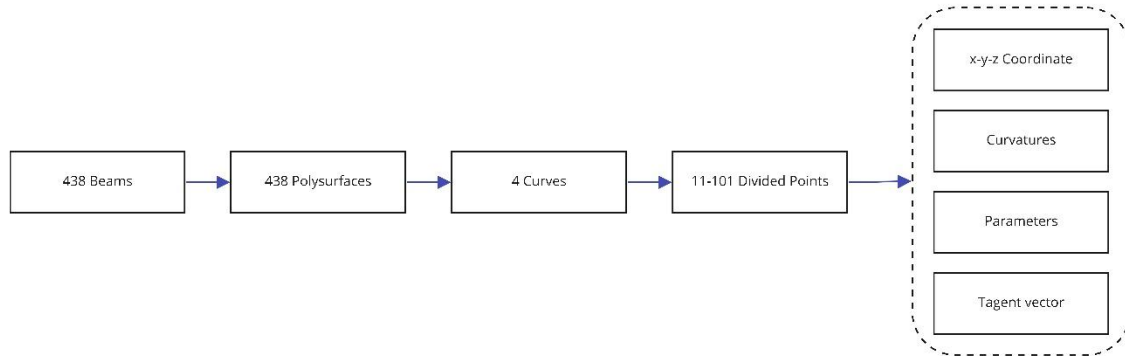


Figure 6.39 Geometric information for the model

6.4.2 Data Transformation

To complete the prediction learning task, the appropriate free-form model matters in the learning task. This research takes the Centre Pompidou-Metz Model (Figure 6.38) as a case to extract the data for LSTM. In the Centre Pompidou-Metz model, the structure is in a weave pattern and is built from Glue-laminated timber. The point is a good learning input for which all the timber beams and columns are curved to form a freeform shape. After modelling this model in Rhino and grasshopper, the next step is to extract the geometric information and transform it into discrete numbers. Every beam or column has six faces and 12 boundary lines in which there are four curves. These curves are the important geometry element to generate this curved geometry. The training model needs the input to be in sequences for the input. Then in this research case, one important step is to transform the information of the points into sequential data. In Figure 6.40, the data transformation workflow for the geometric model transformed into sequential data for training is demonstrated, and the predicted sequential data is interpolated to generate the geometric model.

6.4.3 Train and test

There are six variables to describe one curve: the output for training in this case. According to the features of the discrete numbers extracted from the curves of the timber columns and beams, the LSTM training model is selected to predict the six variables of every curve for the best result. For the data transformation in this condition, assuming the number of curves to be analysed in N , every curve has been divided into $(M - 1)$ parts evenly. There are six parameters to describe this curve, the position of

the division-point $P(x, y, z)$, curvature K , the position of the point on the curve t_1 , the tangent of the points t_2 . Every curve can be described by a matrix, which is $Q_{m \times 6}$.

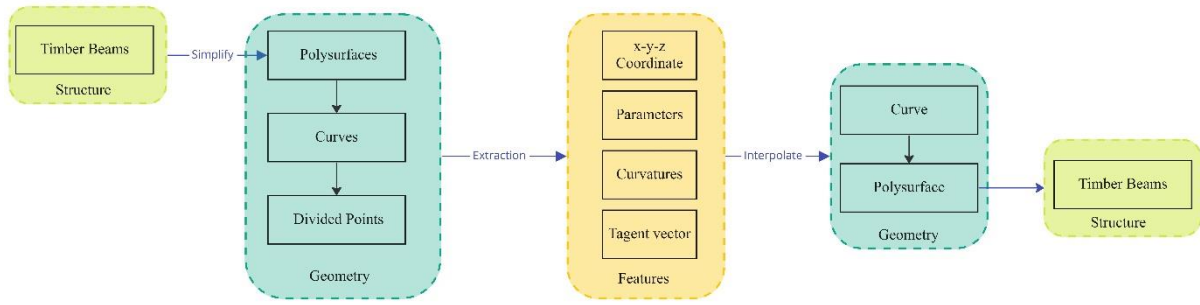


Figure 6.40 Process to transfer geometric data into sequential data

The detailed of matrix Q is shown as

$$Q_{M \times 6} = \begin{bmatrix} x_1 & y_1 & z_1 & a_1 & b_1 & c_1 \\ x_2 & y_2 & z_2 & a_2 & b_2 & c_2 \\ \dots & \dots & \dots & \dots & \dots & \dots \\ x_M & y_M & z_M & a_M & b_M & c_M \end{bmatrix} \quad 6.2$$

when combining all the curves together an overall matrix is obtained, which is $U_{NM \times 6}$, shown as

$$U_{NM \times 6} = \begin{bmatrix} x_1 & y_1 & z_1 & a_1 & b_1 & c_1 \\ x_2 & y_2 & z_2 & a_2 & b_2 & c_2 \\ \dots & \dots & \dots & \dots & \dots & \dots \\ x_{NM} & y_{NM} & z_{NM} & a_{NM} & b_{NM} & c_{NM} \end{bmatrix} \quad 6.3$$

Matrix U can be seen as the combination of column vectors, which is:

$$U_{NM \times 6} = [\mathbf{x}, \mathbf{y}, \mathbf{z}, \mathbf{a}, \mathbf{b}, \mathbf{c}] \quad 6.4$$

where $\mathbf{x} = [x_1, x_2, \dots, x_{NM}]^T$, other elements are in the same pattern.

The workflow is shown in Figure 6.41. To generate geometric information for the prediction task, the geometry form is set as the input. The sequential data is then transformed from the initial geometric information using the curve parameters. The transformed dataset is divided into input and output features for learning. The LSTM method then uses the dataset to learn how to generate output from the input data, after which it is tested for accuracy and feasibility in the prediction tasks.

In this prediction, the input is set as $\{x - coordinate, y - coordinate, z - coordinate, parameter\}$ and the output is set as $\{curvature, vector_x, vector_y, vector_z\}$. In the prediction for 21 divided-points, the geometric information of 15 curves are selected and one curve is set as the test data and the training process in shown in Figure 6.42. The learning curve presents the convey tendency which means the LSTM can predict the $\{curvature, vector_x, vector_y, vector_z\}$ for the curve with a good learning rate.

Figure 6.43 and Figure 6.44 show the prediction error compared to the test data, where the MSE for all four outputs is close to zero. The minimum MSE is the prediction for curvature. To further test the prediction accuracy, the predicted tangent vector and the corresponding curvatures of the divided points are applied to interpolate the curve to compare with the original ones.

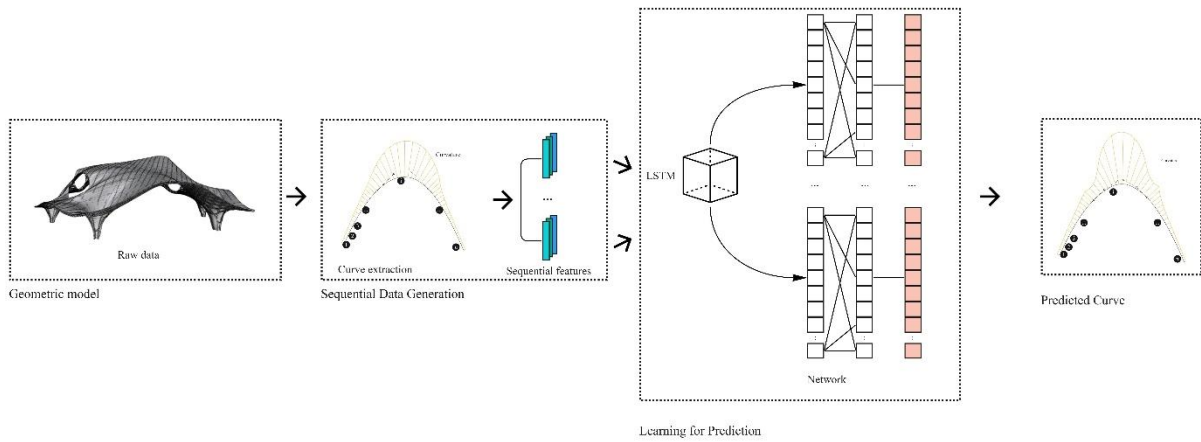


Figure 6.41 Learning and Prediction Process for LSTM

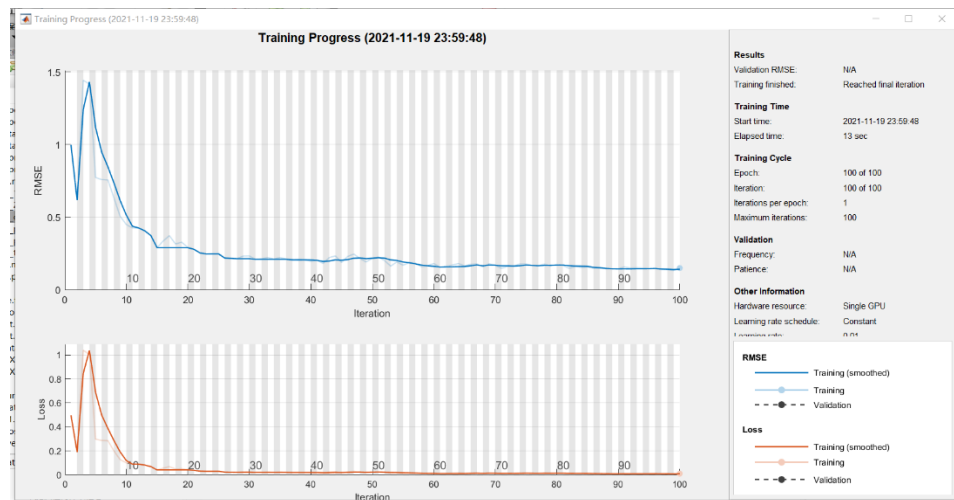


Figure 6.42 Training results with 21 points

In Figure 6.45 (a)-(d), the generated curve is compared with the tested curve which is the original one. The blue one is the curve interpolated with the predicted curvatures and vectors, the red one is the original one. In perspective view for the curve shown in Figure 6.45 (a), the predicted vectors (colour green) and the original vectors (colour blue) are presented on the two curves. The image shows that the predicted curves almost exactly match the original curves and the vectors are in the same direction.

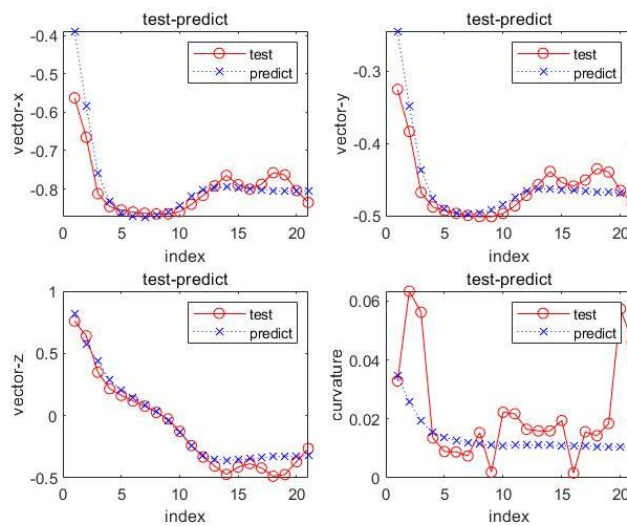


Figure 6.43 Test results with 21 points

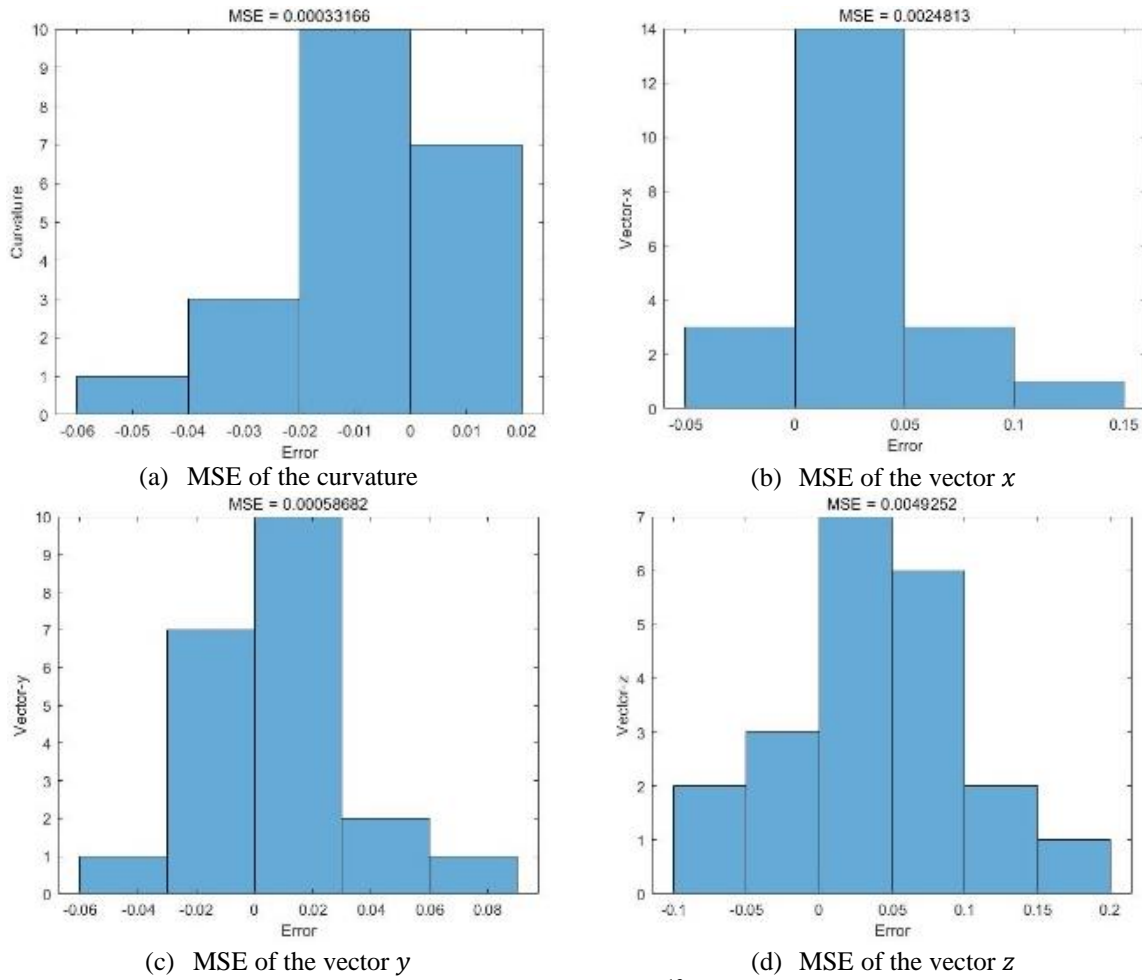


Figure 6.44 Histogram of the MSE¹³ of the prediction

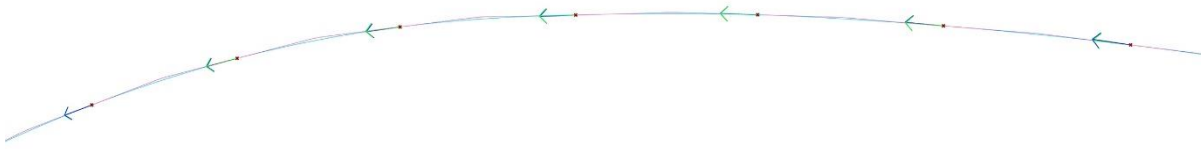
Figure 6.45 (b)-(d) are the projections of the two curves in xoy , $yozy$, and $xoyz$ planes to show the deviations between the predicted one and the original one. Again, the two curves show an exact match.

6.5 Conclusion

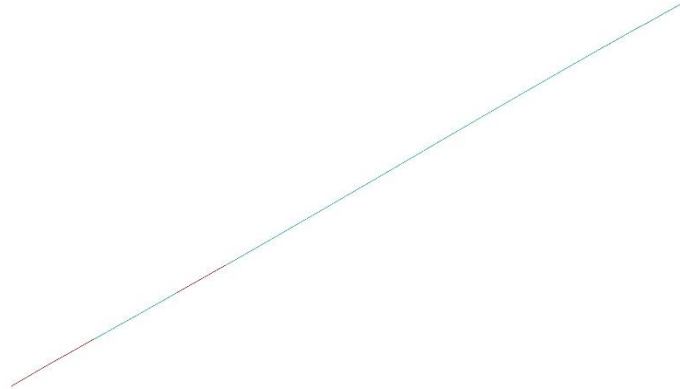
Within the whole research, this chapter solves the appropriate design methods problem. Modifications and adaptations are made to the current freeform surface morphology design methodologies to fit the RAOD principles and characterise considering the impact of RAC on design.

Based on the results of the comprehensive design impact assessment of RAC on FTS in the Chapter 5, this chapter focuses on proposing specific morphology design methods of RAOD for FTS. This chapter first provides a specific introduction to freeform surface and introduces the concept of form finding and the classification of methods. According to the RAC characteristics, suitable form finding methods for RAC-FTS are proposed to have the characteristics as easy to mesh, easy to prototype and rationality in material.

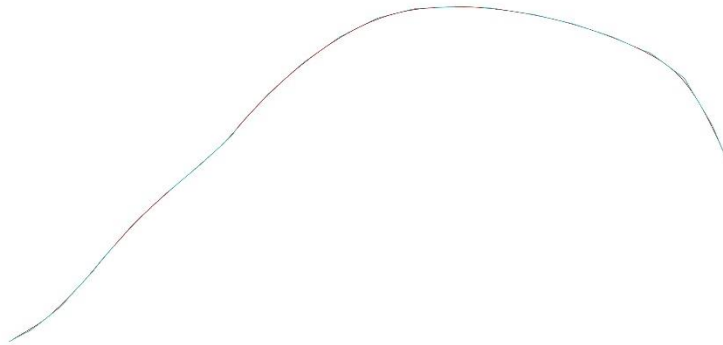
¹³ MSE is the mean of the sum of squares of the errors at the corresponding points of the predicted and original data



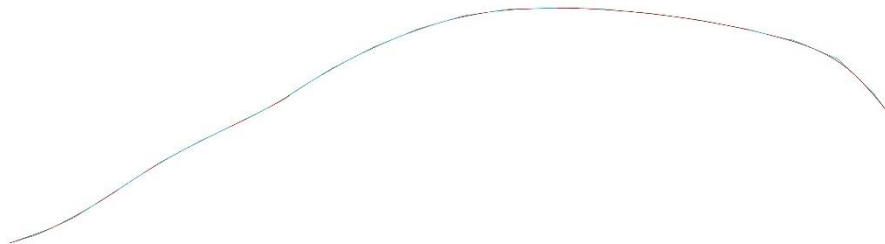
(a) Generated curve vs tested curve



(b) Generated and tested curve in xoy projection



(c) Generated and tested curve in yoZ projection



(d) Generated and tested curve in xoy projection

Figure 6.45 Comparison of the generated curve and the tested curve

Three types of methods are proposed, and specific examples are presented based on digitalisation, modularity, and prototype features. Minimal surface is chosen as the application of complex geometry in RAC-FTS, which reflects the features of easy prototype and easy digitalisation. The bionic method is combined with the combined reverse engineering method, and the pre-processing of meshing is carried out by the point cloud information of mapping, which facilitates the subsequent meshing process while satisfying the structural rationality. By using LSTM in the machine learning method, curves that

conform to the reasonable curvature interval of the material are generated, and thus generate surfaces that conform to the material mechanical properties.

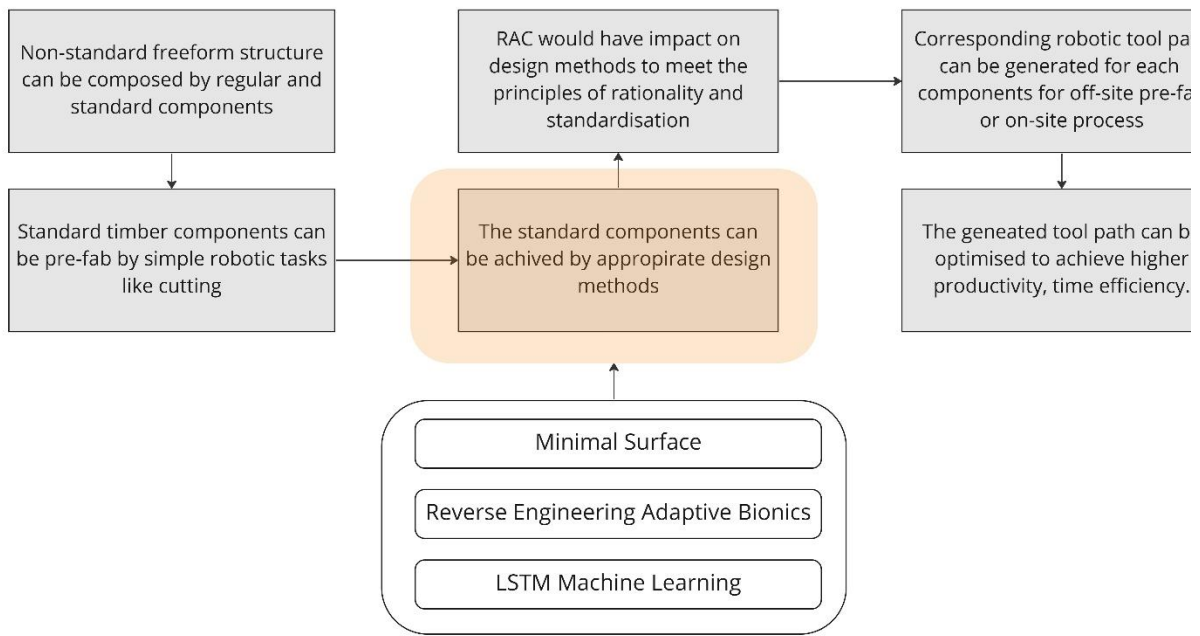


Figure 6.46 Connection to hypothesis

The rationality discussed in this chapter focuses on the form-finding which referred to the principles put forward in Chapter 3. As for the principle of “rationality in structure” and “structure stability” would be discussed in Chapter 7 about morphology optimisation to achieve higher level of structural reliability, see Figure 6.47.

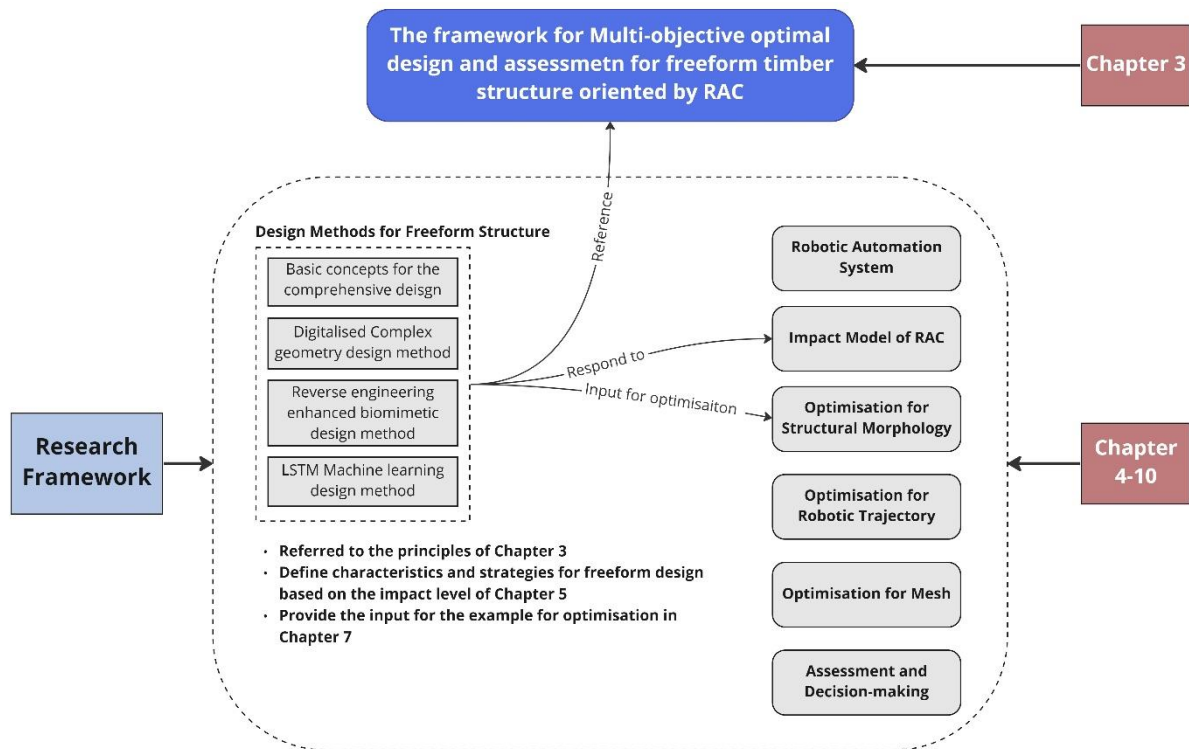


Figure 6.47 Connection to other chapters

Chapter 7

Multi-objectives Optimisation for Morphology of Freeform Timber Structure based on NURBS

The geometric freeform models generated by the adaptive morphology design methods meet the principles of form-finding rationality with the characteristics as easy to mesh and easy to modularise. To make the freeform geometric model more buildable and reliable, more performance index like structural behaviour is needed. As morphology has derived many cross-discipline, structural morphology is to study the relationship between architectural geometry and structural performance from the whole perspective to achieve coordination and unity of the two factors. *Structural morphogenesis* is an important subset of structural morphology which can be achieved through different methods, including experimental, bionic, and numerical methods. This chapter presents the idea of creating complex freeform structures through numerical optimisation as follows: adjusting the 'geometry' to achieve the structural form by taking the rationalisation of the 'structure' as the optimisation target. After determining the optimisation objectives, the numerical analysis model would be built according to the finite element analysis method. After the optimisation, the optimal parameters would change the morphology and the comparisons between the original and the optimal one would be presented.

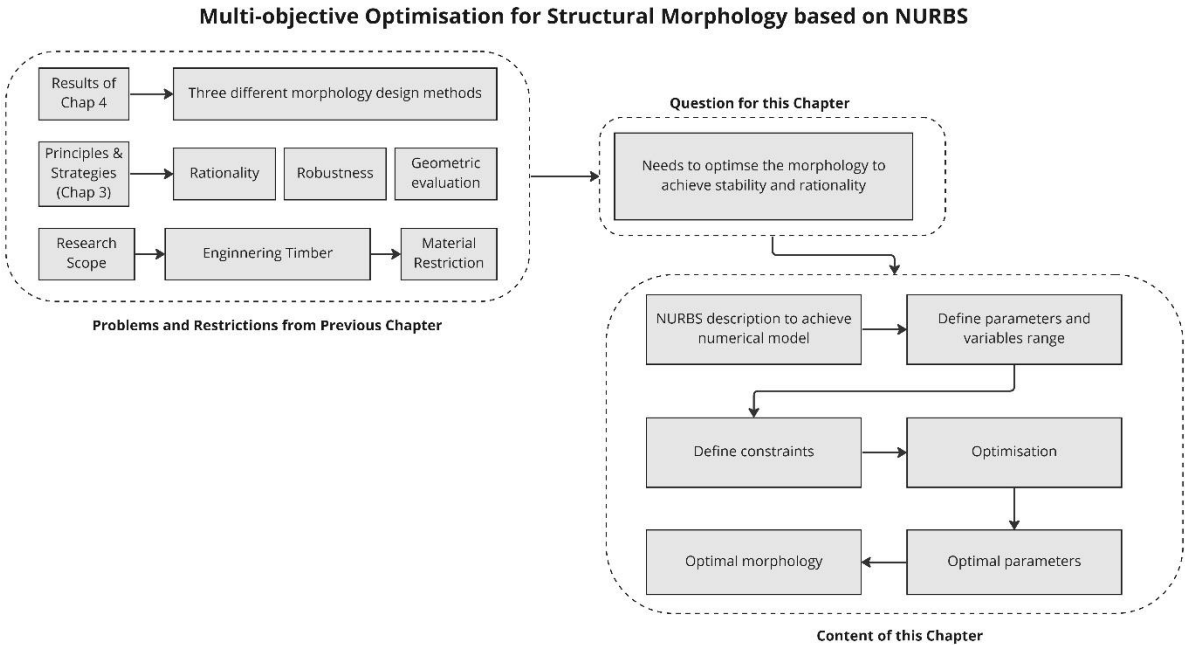


Figure 7.1 Roadmap for Chapter 7

7.1 Numerical method for structural morphogenesis

The research aim of structural morphogenesis is to achieve the unity of the diversity of 'structure and the rationality of 'geometry'. The basic idea is to combine the freeform geometric modelling method (fitted by NURBS) with structural rationality evaluation methods (strain energy and robustness) and to

use optimal algorithms (e.g., gradient descent) for optimal objectives to create rational freeform structural morphology.

In this research, to generate rational structural morphology for different types of complex timber freeform surface structure, three questions need to be solved through numerical analysis:

(1) Geometry design method and numerical description

Due to the varicosity of complex freeform surface design methods, a unified mathematical model is required to describe the freeform geometric model to provide the initial conditions for creating freeform structures. Geometric modelling is the basis for creating freeform structures to provide optimisation variables and make the results visible. Based on these considerations, the choice of geometric modelling method needs to satisfy the following constraints:

- 1) it can represent a variety of surface shapes with high applicability.
- 2) it can be expressed in mathematical formulations with control variables to improve the computational efficiency of morphological optimisation.
- 3) it can describe the properties of timber material.
- 4) it is compatible with the existing mainstream CAD software to make this method easily transposed and extended in other software platforms.

(2) Evaluation of structural rationality

In the process of designing freeform surfaces through optimisation, different evaluation methods of the structure will lead to different optimisation results, which is highly related to the selection of optimisation objectives and the determination of the optimisation methods. Firstly, the optimisation objectives need to: 1) reflect mechanical performance of the structure comprehensively, making as many indicators as possible optimal simultaneously; 2) express the relationship between the objective function and the control variables in mathematical formulation easily to facilitate programming. In structure evaluation, it is common to set multiple indicators as the optimisation objectives. The prerequisite for multi-objectives optimisation is that the indicators are contradictory or less correlated.

(3) Morphological optimisation algorithm

To create a rational structural morphology with novel shape and robust mechanical properties, freeform geometry design methods need to be combined with optimisation algorithm to adjust the shape by changing the determining parameters through optimisation. In the optimal process, firstly, the optimisation variables need to be identified. Secondly, an appropriate optimisation method needs to be selected, and the magnitude and direction of adjustment of the variables need to be determined. As freeform geometry is influenced by various parameters, the relationship between geometry and mechanical behaviours are complex, a fit optimisation method needs to satisfy the requirements for

simplicity of the optimisation variables, feasibility of the process, diversity of the optimal results, as well as speed in numerical computation.

7.2 Numerical description of the geometry and optimisation

In the next chapter, different methods in designing and generating complex freeform surface would be combined with the structural morphology optimisation. To establish a unified approach to rationalise the mechanical properties of the structures designed by the different types of freeform modelling techniques, a standardised mathematical description for the geometries is first required. Numerical methods based on computer graphics can describe the process of creating the geometry accurately. There are several numerical methods for freeform surfaces commonly used: Non-Uniform Rational B-Spline (NURBS) (Ohmori & Hamada, 2006), B-spline (X. Li, Wu, & Cao, 2011), Pascalian shapes (Bagn eris, Marty, Maurin, Motro, & Pauli, 2010) etc. NURBS is chosen to be the unified mathematical description method for freeform surface in this research due to the following characters (Les Piegel & Tiller, 1996):

- (1) Provides a unified mathematical description of analytic geometry and freeform surfaces.
- (2) The shape of the surface can be manipulated by various parameters (control points and weights).
- (3) Highly efficiency in algorithm computing, and stability in results.
- (4) Invariance in geometric transformation which means the shape is determined and influenced by the relative position of the control points rather than the absolute position in xyz coordinate.

7.2.1 Basic knowledge of B-spline

The theory of NURBS is developed based on B-spline. The definition of B-spline is firstly presented by Gordon and Riesenfeld (Gordon & Riesenfeld, 1974). The definition for a p times B-spline curve is:

$$C(u) = \sum_{i=0}^n N_{i,p}(u)P_i, a \leq u \leq b \quad (7.1)$$

$C(u)$ means the coordinate of a random point on B-spline curve in x - y - z space, $\{P_i\}$ is the control point, $N_{i,p}(u)$, $i = 0, 1, \dots, n$ is the i^{th} p times B-spline base function, which is called B-spline. They are p times segmented polynomials, namely p times polynomial spline, determined by sequence U combined of non-decreasing parameter u which is called knot vectors: $u_0 \leq u_1 \leq \dots \leq u_{i+p+1}$. U is defined as:

$$U = \left\{ \underbrace{a, \dots, a}_{p+1}, u_{p+1}, \dots, u_{m-p-1}, \underbrace{b, \dots, b}_{p+1} \right\}, m = n + p + 1 \quad (7.2)$$

Commonly, $a = 0, b = 1$.

$N_{i,p}(u)$ is defined as:

$$\begin{cases} N_{i,0}(u) = \begin{cases} 1, & \text{when } u_i \leq u \leq u_{i+1} \\ 0, & \text{others} \end{cases} \\ N_{i,p}(u) = \frac{u-u_i}{u_{i+p}-u_i} N_{i,p-1}(u) + \frac{u_{i+p+1}-u}{u_{i+p+1}-u_{i+1}} N_{i+1,p-1}(u) \quad p \geq 1 \end{cases} \quad (7.3)$$

In equation (4.3), u is the parameter, u_i is the knot, the i in $N_{i,p}(u)$ means the number of B-spline, which indicates the position of this B-spline on the axis of u and p is the number of orders of B-spline. According to (4.3), p times B-spline $N_{i,p}(u)$ can be recurred by two $p - 1$ times B-splines $N_{i,p-1}(u)$ and $N_{i+1,p-1}(u)$. To determine B-spline $N_{i,p}(u)$, $p + 2$ nodes altogether are needed, which are $u_i, u_{i+1}, \dots, u_{i+p+1}$. The interval $[u_i, u_{i+p+1}]$ is the supporting interval for $N_{i,p}(u)$. Denominators of two coefficients $\frac{u-u_i}{u_{i+p}-u_i}$ and $\frac{u_{i+p+1}-u}{u_{i+p+1}-u_{i+1}}$ is the length of supporting intervals of two $p - 1$ times B-splines. And numerators of the coefficients are the lengths of two parts of the interval $[u_i, u_{i+p+1}]$ divided by parameter u . Similarly, one quadratic B-spline can be recurred by two primary B-splines. Figure 7.2 described the formation process of one cubic B-spline, which is consisted of two quadratic, three primary and four zero-time B-splines in order.

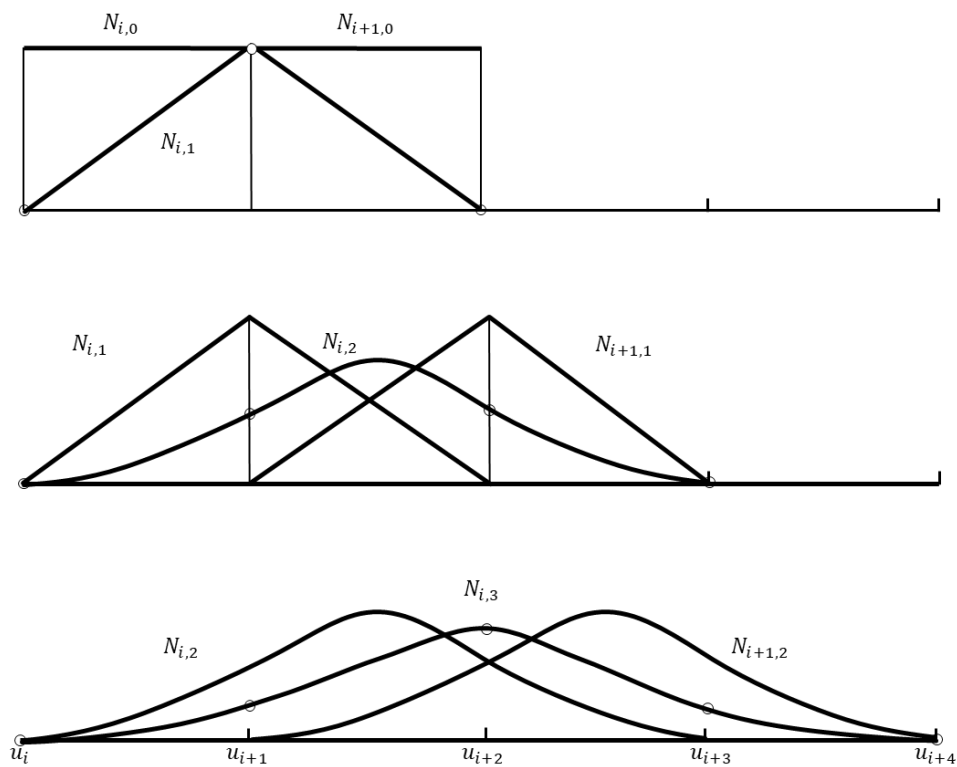


Figure 7.2 Formation of cubic B-spline

B-spline has good mathematical properties, which are briefly summarised as:

- (1) Recursiveness: the defining Eq (7.3) illustrates this property well.
- (2) Normality: for any parameter in the domain of definition, the sum of all p -time B-spline base functions is constant to 1, that is $\sum_{i=0}^n N_{i,p}(u) = 1$.
- (3) Local support: for the parameter in half-open interval which is known as i -th knot span $u \in [u_i, u_{i+1})$, there are at most $p + 1$ non-zero p -time B-splines $N_{j,p}(u)$, $j = i - p, i - p - 1, \dots, i$, where the other p -time B-splines are zero in this domain.

(4) Differentiability: the B-spline is infinitely differentiable inside the knot interval, and at the knots it can be differentiated for $p - k$ times, where r is the knot multiplicity ¹⁴.

For a $p \times q$ times B-spline surface, it is defined by a two-dimension grid composed of control points, two knot vectors, and single-variable B-spline base functions, and the function is expressed as:

$$S(u, v) = \sum_{i=0}^n \sum_{j=0}^m N_{i,p}(u) N_{j,q}(v) P_{i,j} \quad (7.5)$$

$$U = \left\{ \underbrace{a, \dots, a}_{p+1}, u_{p+1}, \dots, u_{r-p-1}, \underbrace{b, \dots, b}_{p+1} \right\}, r = n + p + 1 \quad (7.6)$$

$$V = \left\{ \underbrace{a, \dots, a}_{q+1}, v_{q+1}, \dots, v_{s-q-1}, \underbrace{b, \dots, b}_{q+1} \right\}, s = m + q + 1 \quad (7.7)$$

$S(u, v)$ is the three-dimension coordinate of a random point on the surface. $S(u, v) = \{\mathbf{x}(u, v), \mathbf{y}(u, v), \mathbf{z}(u, v)\}^T$. $\{P_{i,j}\}$ is a $(p + 1) \times (q + 1)$ matrix combined by control points, and $N_{i,p}(u)$, $N_{j,q}(v)$ are B-spline base functions defined on knot vectors U and V respectively and are the same as Eqs (7.3-7.4).

7.2.2 NURBS curve and surface

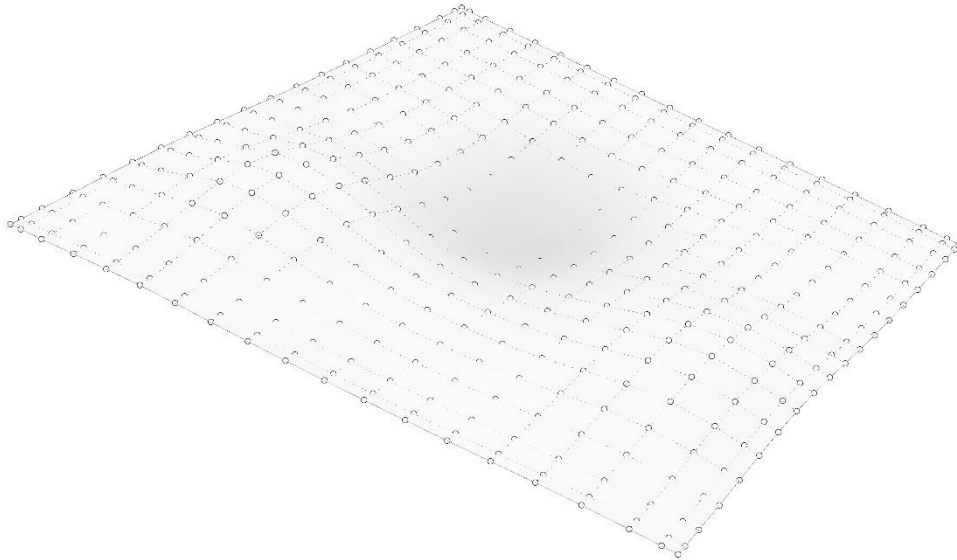


Figure 7.3 Example of NURBS Surface

Though B-spline a mature method in designing curves and surfaces (L. Piegl, 1989a, 1989b), other complex geometry could not be described explicitly except parabola or paraboloid. Based on rational B-spline, Non-rational B-spline (NURBS) is developed by adding an extra parameter called weights (Au & Yuen, 1995) . A p times NURBS curve is defined as:

¹⁴ A knot u_i appears k times (i.e., $u_i = u_{i+1} = \dots = u_{i+k-1}$), where $k > 1$, u_i is a multiple knot of multiplicity k , written as $u_i(k)$.

$$C(u) = \frac{\sum_{i=0}^n N_{i,p}(u)\omega_i P_i}{\sum_{i=0}^n N_{i,p}(u)\omega_i}, a \leq u \leq b \quad (7.8)$$

The meaning of $C(u)$, $\{P_i\}$, $N_{i,p}(u)$ is the same as equation (4.1). $\{\omega_i\}$ is the weight factor. As the knot vector U of $N_{i,p}(u)$ is non-uniform and equation (4.8) is in rational form, the curve is named Non-Uniform Rational B-spline (NURBS). The coordinate of a random point on NURBS surface can be expressed in the below formulation:

$$S(u, v) = \frac{\sum_{i=0}^m \sum_{j=0}^n N_{i,p}(u)N_{j,q}(v)\omega_{i,j}P_{i,j}}{\sum_{i=0}^m \sum_{j=0}^n N_{i,p}(u)N_{j,q}(v)\omega_{i,j}}, a \leq u \leq b; c \leq v \leq d \quad (7.9)$$

Where: u, v are the parameters of the surface; p, q are the number of powers of the surface; surface is the segmentation functions about u, v ; knot vectors U, V are combined by knots u, v . For curved surface, $\{P_{i,j}\}$ forms a control grid in two directions and the number of control points are $(n+1) \times (m+1)$; $\{N_{i,p}(u)\}$ and $\{N_{j,q}(v)\}$ are base functions of u and v directions; $\{\omega_{i,j}\}$ is weight factor. Knot vectors U, V are defined as:

$$U = \left\{ \underbrace{a, \dots, a}_{p+1}, u_{p+1}, \dots, u_{r-p-1}, \underbrace{b, \dots, b}_{p+1} \right\}, r = n + p + 1 \quad (7.10)$$

$$V = \left\{ \underbrace{c, \dots, c}_{q+1}, u_{q+1}, \dots, u_{s-q-1}, \underbrace{d, \dots, d}_{q+1} \right\}, s = m + q + 1 \quad (7.11)$$

Assuming the set of control points is $\mathbf{P} = \{P_{i,j} \in \mathbb{R}^3; i = 1, \dots, m; j = 1, \dots, n\}^T$, where $P_{i,j} = (P_{i,j}(x), P_{i,j}(y), P_{i,j}(z))$ represents the components in Cartesian coordinate of one random control point. Corresponding to control points, weight vectors are defined as $W = \{\omega_{i,j} \in \mathbb{R}; i = 1, \dots, m; j = 1, \dots, n\}^T$. The relative sizes of the numbers in the vector indicate the proximity of the surface to the corresponding control points. For example, if $\omega_{i,j} = 1$, according to the properties of B-spline function, the denominator in equation (7.9) is equal to 1, and the NURBS surface is transformed to B-spline surface. Thus, the NURBS function maps several discrete points in Cartesian coordinate system to a freeform surface by means of a weighting.

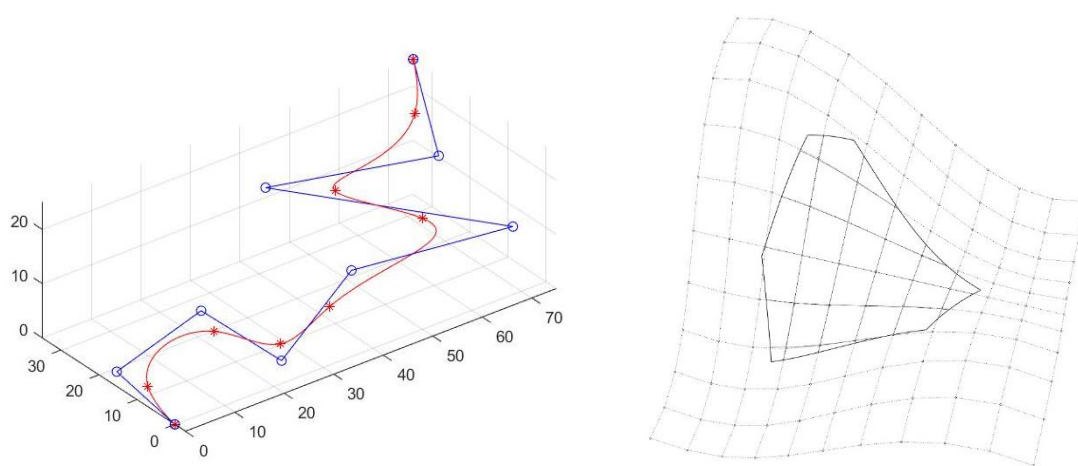
There are some geometric properties of NURBS that would be important in complex freeform surface modelling.

- (1) Interpolability: NURBS surfaces control the four corner points via the point grid $\{P_{i,j}\}$.
- (2) Strong convexity: Assuming $i, j, \omega_{i,j} \geq 0$, parameter (u, v) belongs to interval $[u_{i_0}, u_{i_0+1}) \times (v_{j_0}, v_{j_0+1}]$, $S(u, v)$ locates in the convex hull composed by control points $P_{i,j} (i = i_0-p, \dots, i_0, j = j_0-q, \dots, j_0)$.
- (3) Local modifiability: Moving control point $P_{i,j}$ or changing the numerical value $\omega_{i,j}$ would only affect the surface in $[u_{i_0}, u_{i_0+1}) \times (v_{j_0}, v_{j_0+1}]$ field.

7.2.3 Determine parameters of NURBS

The shape of the surface or curve needs to be constantly adjusted during the creation of the morphology to obtain a freeform structure with sound mechanical properties. Therefore, it is necessary to first identify the parameters that determine the shape of the freeform surface. According to the definition of NURBS, the main factors that control the shape of NURBS surface (or curve) are: (1) the location of the control points, the number; (2) the weight factor, generally the larger the weight factor, the closer the surface (or curve) is to the control points; (3) the knot distribution of parameters u, v and the order of the surface.

A third time NURBS is taken as an example to illustrate the influences of control points, weight factor and knot vector on the shape of the curve. The NURBS curve with control points is shown in Figure 7.4 (a) and (b) shows the relationship between NURBS surface and control points.



(a) NURBS curve

(b) NURBS surface

Figure 7.4 NURBS curve and surface with control points

After comparing three figures, it can be inferred that the influences of three parameters on NURBS curve are different and the patterns of changing are various. Detailed description is as follows:

(1) Control points, which are most effective in controlling the shape of curve (or surface), determine the undulation of the line. Control points are suitable for constructing the overall shape of curve or surface.

(2) Weight factor: The numerical value of the weight factor can be interpreted as the adsorption capacity of a control point to curves and surfaces. The larger the weight factor, the closer the curve (or the surface) to the control point according to the local modification property, whereas the rest of the nearby control points will have less adsorption to the curve (or surface). On the contrary, the lower the value, the effect is reversed. Therefore, the weight factor is suitable for fine-tuning the shape of curve (or surface).

(3) Knot vector: non-uniform is for knot vectors. The knot vectors of curve L1 is uniform, while the rest of the curves are non-uniform splines. The adjustment of knot vectors on curve (or surface) is complex and its pattern is hard to summarize.

It can be analysed that modifying the shape of the surface by altering the control points as well as the weight factors can reduce the number of unknowns and thus improve the efficiency of the calculation. It is appropriate to use both as optimisation variables to adjust the shape of the surface.

7.3 Strain energy evaluation methods for structural rationality

With the advancement of computer technology, numerical analysis has been used widely and commonly, resulting in the concept of *Computational Morphogenesis*, i.e., the creation of rational structural morphology through computer graphics and structural optimisation methods. Complex freeform structure is one important research topic in morphology creation, with the aim of designing and optimising complex surface geometry to fulfil both aesthetic and mechanical requirements with certain constraints. As mentioned in 3.3.1, the optimisation method and objectives for structural mechanical rationality have a direct impact on the outcome of the morphology. Optimal objective is commonly set as displacement, stress, strain energy and others, and displacement and stress are vectors that reflect the structure's local characteristics, whereas strain energy is scalar.

The determination of the interrelationships between mechanical properties is a critical issue to address during the morphology creation process. The structural balance equation is:

$$F = K \cdot \delta \quad 7.12$$

F – Force vector of structure nodes

K – Structural stiffness matrix

δ – Displacement vector of the structure

When the structure is subjected to small elastic deformation, the strain energy is expressed as:

$$U = \frac{1}{2} F^T \delta \quad 7.13$$

The Eq. 7.13 deduces the relationship between strain energy and structure internal force. Research has demonstrated that when strain energy is selected as the objective function, as the strain energy of the structure decreases, not only does the stiffness of the structure increase, but the bending moments is greatly reduced, increasing the ultimate load capacity. Assuming that the load is constant, the structure's strain energy is proportional to the displacement of the structural nodes; that is, decreasing the displacement results in decreasing the strain energy. The smallest strain energy, smallest structural displacement, and largest structural rigidity are all mutually unified.

The strain energy is a scalar, and its value can be thought of as the sum of the strain energies of all the elements in the structure. Besides, the strain energy is unrelated to the selected coordinate system. In the global coordinate system, the strain energy equals to the strain energy in the local coordinate system. In complex structure system, the finite element method is commonly used to divide the structure into several elements when calculating them.

$$U = \sum_{i=1}^N \bar{u}_i \quad 7.14$$

Where:

\bar{u}_i – Strain energy of every element

N – Total number of the elements in the structure

7.3.1 Strain Energy formulation for grid shell

The following is the formula derivation for structural strain energy with element stress and strain as variables. Under the external forces, stress $\{\sigma\}$ and strain $\{\epsilon\}$ are generated gradually inside the structure. In the process of increasing the load, the work done per unit of the volume is called strain energy density, named as \bar{U} . To simplify, initial stress and initial strain are not considered. In a common spatial analysis, \bar{U} can be calculated as:

$$\bar{U} = \int_0^{\epsilon_x} \sigma_x d\epsilon_x + \int_0^{\epsilon_y} \sigma_y d\epsilon_y + \int_0^{\epsilon_z} \sigma_z d\epsilon_z + \int_0^{\gamma_{xy}} \tau_{xy} d\gamma_{xy} + \int_0^{\gamma_{zx}} \tau_{zx} d\gamma_{zx} = \int \{\sigma\}^T d\{\epsilon\} \quad 7.15$$

According to the relation between $\sigma - \epsilon$: $\{\sigma\} = [D]\{\epsilon\}$, the equation (7.15) is transferred to:

$$\bar{U} = \int \{\epsilon\}^T [D] d\{\epsilon\} = \frac{1}{2} \{\epsilon\}^T [D] \{\epsilon\} = \frac{1}{2} \{\sigma\}^T [D]^{-1} \{\sigma\} \quad 7.16$$

$[D]$ is elastic matrix of which is related to *Elastic Modulus E* and *Poisson's ratio v*.

The strain energy is the integration inside the whole volume:

$$U = \frac{1}{2} \int \int \int \{\epsilon\}^T [D] \{\epsilon\} dx dy dz \quad 7.17$$

To combine strain $\{\epsilon\}$ with displacement $\{\delta\}$, substitute $\{\epsilon\} = [B]\{\delta\}$ into the equation:

$$U = \frac{1}{2} \{\delta\}^T \left(\int \int \int [B]^T [D] [B] dx dy dz \right) \{\delta\} \quad 7.18$$

$[B]$ is strain matrix of which the elements are the functions of coordinates.

According to the strategies of minimising the strain energy for structural robustness design in 3.3.1, to achieve the optimisation objective, combining the theory of Finite Element Analysis for thin shell, the analysis for spatial thin shell structure can be substituted by the thin sheet. The stress of the structure can be divided into two parts: plate stress and bending stress (Bofang, 2018):

$$U_i = U_i^p + U_i^b \quad 7.19$$

where:

U_i^p - plate stress.

U_i^b - bending stress.

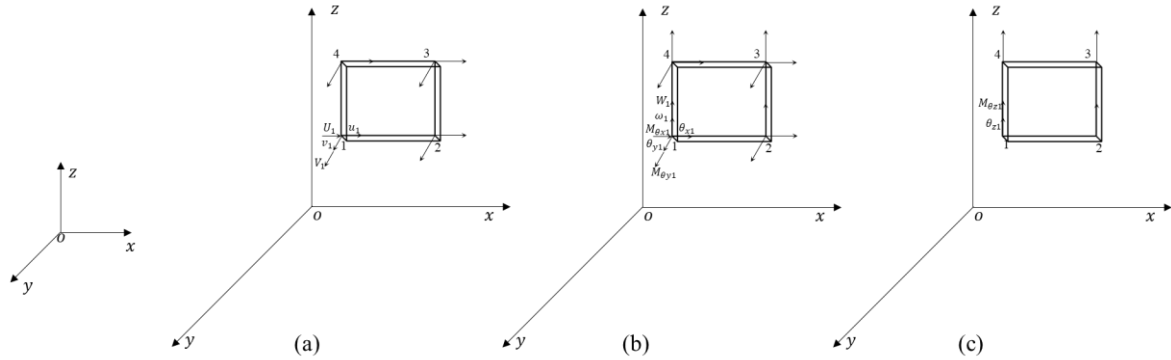
According to equation (7.16-7.18),

$$U_i^p = \frac{1}{2} \int_{V_i} \{\sigma^p\}^T \{\varepsilon\}^p dV_i = \frac{1}{2} \int_{V_i} \{\sigma^p\}^T [D]^{-1} \{\sigma\}^p dV_i = \frac{1}{2} \quad 7.20$$

$$U_i^p = \frac{1}{2} \{F_i^p\}^T \{\delta^p\} = \frac{1}{2} \{\delta^p\}^T \left(\iiint [B]^T [D] [B] dx dy dz \right) \{\delta^p\} \quad 7.21$$

$$U_i^b = \frac{1}{2} \{F_i^b\}^T \{\delta^b\} = \frac{1}{2} \{\delta^b\}^T \left(\iiint [B]^T [D] [B] dx dy dz \right) \{\delta^b\} \quad 7.22$$

In finite element analysis for shell, shells are frequently replaced by combinations of triangular or rectangular sheet units. In this research, the plate rectangular shell element is used as the object in this paper to systematically study the relationship between strain energy and other mechanical performance evaluation indexes. A planar shell element is a type of commonly used finite element that can be thought of as a hybrid of a plate stress element and a flat plate bending element. Figure 7.5 depicts the specific element information. These two statuses have no effect on each other, they can be added directly.



(a) plate stress element; (b) bending stress; (c) plate torsion;

Figure 7.5 plate shell element

The analysis element is discretised to rectangle element. For plate stress, the element stiffness matrix function is:

$$k_e^p \delta_e^p = F_e^p + F_{Ee}^p \quad 7.23$$

F^p is used to represent all the element node force for short:

$$F_e^p + F_{Ee}^p = F^p \quad 7.24$$

Where $k_e^p = (k_{ij}^e)^p$ is the stiffness of plate stress, the subscript p means the plate stress status. δ_e^p , F_e^p , F_{Ee}^p means displacement of the nodes of the element, element node force of, and element equivalent nodal load. F_e^p , F_{Ee}^p are corresponding to δ_e^p .

$$\begin{Bmatrix} F_1^p \\ F_2^p \\ F_3^p \\ F_4^p \end{Bmatrix} = [k^p] \begin{Bmatrix} \delta_1^p \\ \delta_2^p \\ \delta_3^p \\ \delta_4^p \end{Bmatrix} \quad 7.25$$

$$\delta_e^p = (\delta_1^{pT}, \delta_2^{pT}, \delta_3^{pT}, \delta_4^{pT})^T, \delta_i^p = (u_i, v_i)^T \quad (i = 1,2,3,4) \quad 7.26$$

$$F^p = (F_1^{pT}, F_2^{pT}, F_3^{pT}, F_4^{pT})^T, F_i^p = (U_i V_i)^T \quad (i = 1,2,3,4) \quad 7.27$$

For thin shell bending, the element stiffness equation is:

$$k_e^b \delta_e^b = F_e^b + F_{Ee}^b \quad 7.28$$

$$F^b = F_e^b + F_{Ee}^b \quad 7.29$$

The subscript b means the bending status, other meanings of the symbol are like plate stress status.

$$\begin{Bmatrix} F_1^b \\ F_2^b \\ F_3^b \end{Bmatrix} = [k^p] \begin{Bmatrix} \delta_1^b \\ \delta_2^b \\ \delta_3^b \end{Bmatrix} \quad 7.30$$

$$\delta_i^b = (\omega_i, \theta_{xi}, \theta_{yi})^T \quad (i = 1,2,3) \quad 7.31$$

$$F_i^b = (W_i M_{\theta xi} M_{\theta yi})^T \quad (i = 1,2,3) \quad 7.32$$

In order to transfer the element stiffness matrix under the local coordinate into global one and to assemble stiffness matrix of the structure, θ_{zi} is added to the node displacement matrix, and correspondingly virtual bending moment $M_{\theta zi}$ is added to the node force matrix. Therefore, one node displacement of planar shell element matrix can be combined as:

$$\begin{aligned} \{\delta_i\} &= (u_i^p \ v_i^p \ \omega_i^b \ \theta_{xi}^b \ \theta_{yi}^b \ \theta_{zi})^T \\ &= (\delta_i^{pT} \ \delta_i^{bT} \ \theta_{zi})^T \end{aligned} \quad 7.33$$

And the corresponding node force is:

$$\begin{aligned} \{F_i\} &= (U_i \ V_i \ W_i \ M_{\theta xi} \ M_{\theta yi} \ M_{\theta zi})^T \\ &= (F_i^{pT}, F_i^{bT}, 0)^T \end{aligned} \quad 7.34$$

The equation of node force, node displacement, and node stiffness matrix within one rectangular element can be summarised as:

$$\{\delta\}^e = (\delta_1^T, \delta_2^T, \delta_3^T, \delta_4^T)^T \quad 7.35$$

$$\{F\}^e = (F_1^T, F_2^T, F_3^T, F_4^T)^T \quad 7.36$$

$$\{F\}^e = [k]^e \{\delta\}^e \quad 7.37$$

$$k^e = (k_{ij}^e)_{4 \times 4} \quad 7.38$$

7.3.2 Stiffness matrix for grid thin shell element

The node force $\{F_i^p\}$ under plate stress and the node displacement of bending $\{\delta_i^b\}$ do not affect each other, and this principle is applicable to node force $\{F_i^b\}$ and node displacement $\{\delta_i^p\}$. According to this theorem, the node stiffness matrix k_{ij}^e can be combined as:

$$k_{ij}^e = \begin{pmatrix} k_{ij}^p & 0 & 0 \\ 0 & k_{ij}^b & 0 \\ 0 & 0 & k_{ij}^t \end{pmatrix}_{6 \times 6} \quad (i, j = 1, 2, 3) \quad 7.39$$

where $[k_{ij}^p]_{2 \times 2}$, and $[k_{ij}^b]_{3 \times 3}$ are the corresponding stiffness matrix for plate stress element and plate bending one, and $[k_{ij}^t]_{1 \times 1}$ is the torsion stiffness matrix.

The detailed composition of k^e is shown in Figure 7.6.

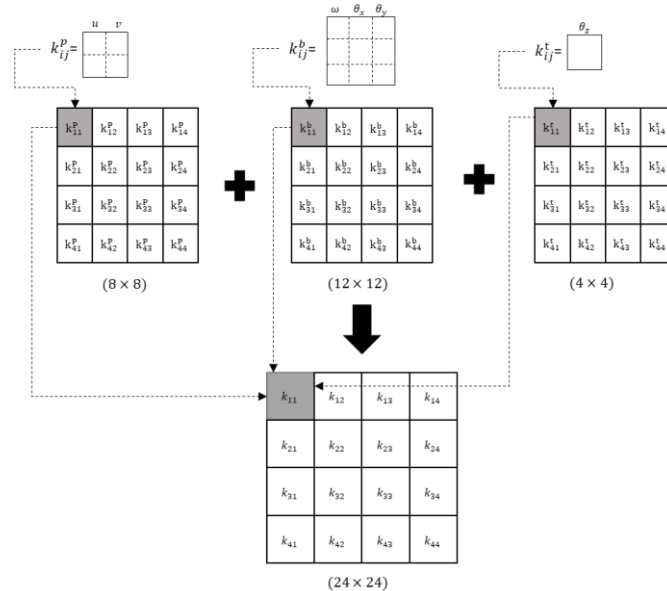


Figure 7.6 Element stiff matrix for thin shell element

7.3.3 The morphogenesis optimisation method for freeform surface

Based on the optimal model put forward in 3. and combined with the equation (4.9) of NURBS, the optimal model can be expressed as a nonlinear function on multidimensional space formed by vector P :

$$\begin{cases} \min U(P) \\ s. t. \end{cases} \quad 7.40$$

Finding the minimum of $U(P)$ can be seen as solving the extreme value problem for nonlinear multivariate functions. The solution to the extreme value problem can be achieved by a one-dimensional

search, which means the direction of descent of the objective function $U(P)$, which is used to adjust the optimisation variables P to gradually converge to the optimal solution. Assuming the strain energy function U is differentiable around the initial value of $P^0 = \{p_{i,j}^0\}$, a Taylor expansion of the strain energy function at P^0 can be expressed as follows:

$$U(P^0 + \Delta P) = U(P^0) + \sum_{i=1}^M \sum_{j=1}^N \left(\frac{\partial U}{\partial p_{i,j}^0} \cdot \Delta p_{i,j} \right) + o\|\Delta P\| \quad 7.41$$

where:

$\frac{\partial U}{\partial p_{i,j}^0}$ – the derivative of the strain energy with respect to each component of the vector P^0 .

ΔP – increment of vector P^0 .

$\Delta p_{i,j}$ – increment of vector ΔP .

$o\|\Delta P\|$ – infinitesimal quantities related to the increment ΔP .

$U(P^0)$ and $U(P^0 + \Delta P)$ indicates the structural strain energy before and after surface shape are adjustment, respectively. Neglecting higher order infinitesimals, to make the adjusted structural strain energy lower, the value of $\sum_{i=1}^M \sum_{j=1}^N \left(\frac{\partial U}{\partial p_{i,j}^0} \cdot \Delta p_{i,j} \right)$ can be set as negative to decrease $U(P)$ by iteratively calculation, which means:

$$U(P^{(k+1)}) = U(P^{(k)} + \Delta P^{(k)}) = U(P^{(k)}) + \sum_{i=1}^M \sum_{j=1}^N \left(\frac{\partial U(p_{i,j}^{(k)})}{\partial p_{i,j}^{(k)}} \cdot \Delta p_{i,j}^{(k)} \right) \quad 7.42$$

k – calculating the number of iterations steps.

$U(P^{(k)})$, $U(P^{(k+1)})$ – the strain energy of k^{th} , $(k+1)^{th}$ iteration step.

$\frac{\partial U(p_{i,j}^{(k)})}{\partial p_{i,j}^{(k)}}$ – derivatives of strain energy of k^{th} step with respect to each component.

$\Delta p_{i,j}^{(k)}$ – increment of k^{th} step of variable $p_{i,j}$.

According to the principles of gradient method, if the direction of increment vector $\Delta P^{(k)} = \{\Delta p_{i,j}^{(k)}\}$ is consistent with negative gradient direction of strain energy $P^{(k)}$ and the value is rational, then the structure strain energy will decrease gradually, which is:

$$U(P^{(k)} + \Delta P^{(k)}) \leq U(P^{(k)}) \quad 7.43$$

Generally, $\Delta U(P^{(l)})$ can be expressed as a function about the gradient:

$$\Delta P^{(k)} = \lambda^{(k)} \cdot (-\nabla U(P^{(k)}))$$

where:

$$\nabla U(P^{(k)}) = \left\{ \frac{\partial U^{(k)}}{\partial p_{i,j}^{(k)}} \right\} - \text{gradient for strain energy.}$$

$\lambda^{(l)}$ – the step increment for k^{th} $P^{(l)}$;

The incremental equation for the variable $p_{i,j}^{(k)}$ is thus established as follows,

$$p_{i,j}^{(k+1)} = p_{i,j}^{(k)} - \lambda^{(k)} \cdot \frac{\partial U(p_{i,j}^{(k)})}{\partial p_{i,j}^{(k)}} \quad 7.44$$

In Eq. 7.44, step increment $\lambda^{(k)}$ has the most optimised value $\lambda_{opt}^{(k)}$, which would improve the strain energy reduced speed effectively.

Assuming that the load does not change with the shape of the surface, which means: $\frac{\partial F^{(l)}}{\partial q_{i,j}^{(l)}} = 0$. Then, the process of deriving the gradient expression for the derivative of the strain energy with respect to the control point or weight factor is as follows:

Taking the freeform surface structure got in the k^{th} step as the object, the derivative of each side of the Eq. 7.44 with respect to each element of the equation is:

$$\frac{\partial K^{(k)}}{\partial p_{i,j}^{(k)}} \cdot \delta^{(k)} + K^{(k)} \cdot \frac{\partial \delta^{(k)}}{\partial p_{i,j}^{(k)}} = \frac{\partial F^{(k)}}{\partial p_{i,j}^{(k)}} = 0 \quad 7.45$$

Therefore:

$$\frac{\partial \delta^{(k)}}{\partial p_{i,j}^{(k)}} = -(K^{(k)})^{-1} \cdot \frac{\partial K^{(k)}}{\partial p_{i,j}^{(k)}} \cdot \delta^{(k)} \quad 7.46$$

The derivation of Eq. 7.46 with respect to $p_{i,j}^{(k)}$ is:

$$\frac{\partial U(p_{i,j}^{(k)})}{\partial p_{i,j}^{(k)}} = \frac{1}{2} \left(\frac{\partial F^{(k)T}}{\partial p_{i,j}^{(k)}} \cdot \delta^{(k)} + F^{(k)T} \cdot \frac{\partial \delta^{(k)}}{\partial p_{i,j}^{(k)}} \right) = \frac{1}{2} F^{(l)T} \cdot \frac{\partial \delta^{(k)}}{\partial p_{i,j}^{(k)}} \quad 7.47$$

Combine Eq. 7.45 and Eq. 7.47, the gradient for strain energy could be derived:

$$\frac{\partial U(p_{i,j}^{(k)})}{\partial p_{i,j}^{(k)}} = -\frac{1}{2} \delta^{(l)T} \cdot \frac{\partial K^{(k)}}{\partial p_{i,j}^{(k)}} \cdot \delta^{(k)} \quad 7.48$$

According to principles of NURBS, the change in the position or weight factor of a control point only affects the area of the surface controlled by of a number of points adjacent to that one.

Based on the derivation of the expressions for the control points and weight factors for the strain-energy fit to the NURBS surface, the diagram depicts the basic flow of the gradient method and specifies the basic implementation steps for the creation of the freeform surface morphology. On this basis, when calculating the internal forces of a structure using the finite unit method and solving for the strain energy gradient, only the unit stiffness matrix corresponding to the knots associated with $p_{i,j}^{(k)}$ is needed, which is:

$$\frac{\partial K^{(k)}}{\partial p_{i,j}^{(k)}} \rightarrow \sum_e \frac{\partial K_e^{(k)}}{\partial p_{i,j}^{(k)}} \quad 7.49$$

where:

$K_e^{(k)}$ – stiffness matrix related to $p_{i,j}^{(k)}$

The relation between the stiffness matrix under the global coordinate and local coordinate is as follows:

$$K_e^{(k)} = T^{(k)T} \cdot \bar{K}_e^{(k)} \cdot T^{(k)} \quad 7.50$$

where:

$\bar{K}_e^{(k)}$ – stiffness matrix under the local matrix.

$T^{(k)T}$ – transformation matrix.

Transformation matrix is combined by the directional cosine matrix of unitary local coordinates and the expression L . When taking knot i as the origin of the element coordinate system, and the direction of knot $i \rightarrow j$ as the x-axis, y-axis is in the plane of the element and perpendicular to the axis and z-axis is determined according to the right-handed coordinate system. Transform matrix T and directional cosine matrix L is shown as:

$$L^{(l)} = \begin{bmatrix} l_{xx}^{(l)} & l_{xy}^{(l)} & l_{xz}^{(l)} \\ l_{yx}^{(l)} & l_{yy}^{(l)} & l_{yz}^{(l)} \\ l_{zx}^{(l)} & l_{zy}^{(l)} & l_{zz}^{(l)} \end{bmatrix} = \begin{bmatrix} l_x^{(l)T} \\ l_y^{(l)T} \\ l_z^{(l)T} \end{bmatrix} = \begin{bmatrix} \cos(x, x') & \cos(x, y') & \cos(x, z') \\ \cos(y, x') & \cos(y, y') & \cos(y, z') \\ \cos(z, x') & \cos(z, y') & \cos(z, z') \end{bmatrix} \quad 7.51$$

$$T = \begin{bmatrix} L & & & & \\ & L & & & 0 \\ & & L & & \\ & & & L & \\ 0 & & & & L \\ & & & & & L \end{bmatrix} \quad 7.52$$

$$\frac{\partial K_e^{(k)}}{\partial p_{i,j}^{(k)}} = \frac{\partial T^{(k)T}}{\partial p_{i,j}^{(k)}} \cdot \bar{K}_e^{(k)} \cdot T^{(k)} + T^{(k)T} \cdot \frac{\partial \bar{K}_e^{(k)}}{\partial p_{i,j}^{(k)}} \cdot T^{(k)} + T^{(k)T} \cdot \bar{K}_e^{(k)} \cdot \frac{\partial T^{(k)}}{\partial p_{i,j}^{(k)}} \quad 7.53$$

To determine the expression for the derivative expression of the element stiffness matrix to the control points and weight factors in the global coordinate, derivative of element stiffness matrix in local coordinate system $\frac{\partial \bar{K}_e^{(k)}}{\partial p_{i,j}^{(k)}}$ and of the coordinate transformation matrix $\frac{\partial T^k}{\partial p_{i,j}^{(k)}}$.

According to Eq. 7.11 and freedom of the triangle plate shell, for plate shell element, the element stiffness matrix is expresses as:

$$\bar{K}_e^{(k)} = \bar{K}_{e(P)}^{(k)} + \bar{K}_{e(B)}^{(k)} + \bar{K}_{e(\theta z)}^{(k)} \quad 7.54$$

Where $\bar{K}_{e(P)}^{(k)}$, $\bar{K}_{e(B)}^{(k)}$, $\bar{K}_{e(\theta z)}^{(k)}$ stand for plate stiffness, bending stiffness and hypothetical stiffness matrix, which is added to avoid the odd structure of the stiffness matrix when calculating.

Therefore,

$$\frac{\partial \bar{K}_e^{(k)}}{\partial p_{i,j}^{(k)}} = \frac{\partial \bar{K}_{e(P)}^{(k)}}{\partial p_{i,j}^{(k)}} + \frac{\partial \bar{K}_{e(B)}^{(k)}}{\partial p_{i,j}^{(k)}} + \frac{\partial \bar{K}_{e(\theta z)}^{(k)}}{\partial p_{i,j}^{(k)}} \quad 7.55$$

From the derivation of the above equations, in the process of establishing the derivative of the stiffness matrix to the control points or the weight factor, the stiffness matrix can be expressed as a function of the coordinates of the knots of the structure, and the spatial point coordinates on the NURBS surface can be expressed as a function of the weight factor and the control points. Therefore, the derivative of the stiffness matrix can be expressed as a function of derivate of the point of NURBS surface $S^{(k)} = (S_x^{(k)}, S_y^{(k)}, S_z^{(k)})$ to control points or weight factors, which is,

$$\frac{\partial K_e^{(k)}}{\partial p_{i,j}^{(k)}} = f \left(\frac{\partial S^{(k)}}{\partial p_{i,j}^{(k)}} \right) \quad 7.56$$

Therefore, it is necessary to establish the derivative of coordinate of the nodes of the surface to control point and weighting factor. The coordinate of one control point of NURBS after the k^{th} optimisation is $P_{I,J}^{(k)} = (P_{I,J(x)}^{(k)}, P_{I,J(y)}^{(k)}, P_{I,J(z)}^{(k)})$, and the corresponding weight factor is $w_{I,J}^{(k)}$, and the derivate of the nodes is shown as follows:

$$\frac{\partial S_x^{(k)}}{\partial P_{I,J(x)}^{(k)}} = \frac{\partial S_y^{(k)}}{\partial P_{I,J(y)}^{(k)}} = \frac{\partial S_z^{(k)}}{\partial P_{I,J(z)}^{(k)}} = \frac{w_{I,J}^{(k)} \cdot B_{I,k}(u) \cdot B_{J,l}(v)}{\sum_{i=1}^M \sum_{j=1}^N w_{i,j}^{(k)} \cdot B_{i,k}(u) \cdot B_{j,l}(v)} \quad 7.57$$

$$\frac{\partial S_x^{(k)}}{\partial w_{I,J}^{(k)}} = B_{I,k}(u) \cdot B_{J,l}(v) \cdot \frac{\sum_{i=1}^M \sum_{j=1}^N (P_{(x)I,J}^{(k)} - P_{(x)i,j}^{(k)}) \cdot w_{i,j}^{(k)} \cdot B_{i,k}(u) \cdot B_{j,l}(v)}{\left(\sum_{i=1}^M \sum_{j=1}^N w_{i,j}^{(k)} \cdot B_{i,k}(u) \cdot B_{j,l}(v) \right)^2} \quad 7.58$$

To compute $\frac{\partial S_y^{(k)}}{\partial w_{i,j}^{(k)}}$ and $\frac{\partial S_z^{(k)}}{\partial w_{i,j}^{(k)}}$, the variable $P_{(x)I,J}^{(k)}$ and $P_{(x)i,j}^{(k)}$ could be substituted following $P_{(x)I,J}^{(k)} \rightarrow P_{(y)I,J}^{(k)} \rightarrow P_{(z)I,J}^{(k)}$ and $P_{(x)i,j}^{(k)} \rightarrow P_{(y)i,j}^{(k)} \rightarrow P_{(z)i,j}^{(k)}$. On the basis of expressions for derivate of strain energy to control points and weight factors of NURBS, and combined the gradient decent, the steps for morphology generation and optimisation are shown in Figure 7.7.

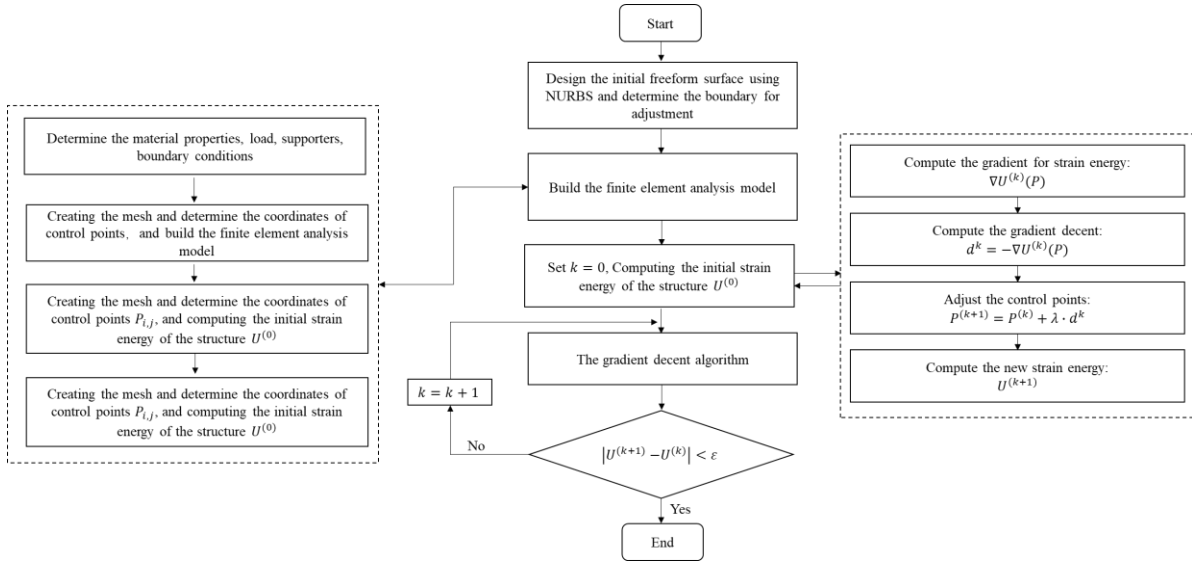


Figure 7.7 Flow chart of structural morphology using gradient decent for strain energy

The detailed description for the flow is listed below:

- (1) According to architectural design conditions, modelling the initial freeform surface shape by selecting a suitable design method and determining the coordinates of spatial points (control points or a number of known points on the surface).
- (2) Determining the adjustment of surface according to the constraints and space requirements of the building design by modifying the parameters of control points (z-coordinate, weighting factors).
- (3) Defining the information of material properties, supports, loads, and setting the ε , converting the surface into mesh and building the finite element analysis model.
- (4) Setting the number of iterative steps $k = 0$.
- (5) Computing the initial strain energy $U^{(0)}$ and the gradient $\nabla U^{(k)}(P)$ of strain energy on control parameters of NURBS surface.
- (6) Determining negative gradient direction $d^{(k)} = \nabla U^{(k)}(P)$ and the increment $\Delta P^{(k)} = \lambda \cdot d^{(k)}$ of control-point coordinate and weighting factors.
- (7) Adjusting the control parameters of NURBS surface $P^{(k+1)} = P^{(k)} + \Delta P^{(k)}$.
- (8) Modifying the NURBS according to the adjusted parameters of control points and computing the corresponding strain energy $U^{(k+1)}$.

(9) Determining whether the convergence condition $|U^{(k+1)} - U^{(k)}| < \varepsilon$ is satisfied, if so, the surface is the optimal one; if not, setting $k = k + 1$ and going back to setp (4) to continue the computing.

In summary, according to the principles of gradient decent, to achieve the above-mentioned algorithm, the focus is to establish the derivative relationships between strain energy and control variables (coordinate of control points/weighing factors) of the NURBS surface. And then, based on the numerical relationship, the direction and amplitude of the increments are determined to obtain the surface shape with the minimum strain energy by adjusting the control variables.

7.4 Robustness evaluation for structure rationality

Strain energy, as one structural evaluation indicator for stability and rationality, can represent the comprehensive structural behaviour. Another evaluation criteria for structure rationality is robustness. The mechanical behaviours of freeform structure are closely connected to its geometric form, and due to the complexity and variety of freeform surface, it is difficult to consider the structural behaviour and geometry form simultaneously when designing and modelling. Current structural robustness research focus on the evaluation and analysis for existing structures, which means the simulation for damage by removing components after the structure design. If the robustness index is not satisfied, measures such as improving the structure's ductility, energy consumption, and redundancy are implemented to improve the structure's robustness. The research of structure design directly oriented by robustness is still needed.

7.4.1 Robustness system based on H_∞ theory

After the concept of robustness was proposed in the 1960s, it was first applied in the fields like system control, computer networks, etc. Some building collapse accidents make structural robustness a priority for engineers. Make engineers aware of the significance of structural robustness. Many scholars have elucidated the concept of structure robustness. In the field of structural vibration control, for example, the goal of robust control is for the control system is to meet the predetermined requirements when the controlled structure is uncertain. For the robustness of the structure itself, different researchers have put forward various definitions based on their own experience. Lee refers to the quality control theory of Taguchi Method and believes that robustness means insensitivity of the performance of a product to changes in materials, geometry, production process, and operating environment ; starting with the probability characteristics of structural performance, Doltsinis believes that the standard deviation σ of structural performance is as important as its mean value μ , and that the standard deviation can be used to evaluate the structure's robustness ; Agarwal, Starossek keeps the point that disproportionate consequences not commensurate with the original cause should be produced in robust structure .

Quantitatively assessing the structural robustness has long been a problem in engineering fields. H_∞ control theory is a relatively successful and complete theoretical system in the field of system control. Many robust performance criteria can be described by H_∞ norm constraints. The H_∞ robust control index reflects the system's sensitivity to external interference, or its ability to resist external interference. Quantitative structural robustness assessment can effectively reflect the influence of external

interference, structural uncertainty, redundancy, and other factors on structural robustness, and this index can be applied to spatial structures such as spatial grid shells. H_∞ theory is one index for evaluating the structure robustness which has been successfully applied to the parameter analysis of space structures such as grid shells and the search for critical path of the structure. This indicator believes that if the initial cause is viewed as a set of input signals to the structural system, and the damage consequences are viewed as the structure's output response signal. The structure's robustness expresses whether the output signal is commensurate with the input signal, which can effectively reflect factors like external interference, uncertainty of the structure, redundancy on the structure's robustness.

The state equation of a linear time-invariant system is shown as follows [53]:

$$\begin{cases} \dot{\eta}(t) = A_0\eta(t) + B_0u(t) \\ y(t) = C_0\eta(t) + D_0u(t) \end{cases} \quad 7.59$$

where:

$\eta(t)$, $u(t)$, $y(t)$ represent state vector of structural system, input vector and output vector; A_0 , B_0 , C_0 , and D_0 are constant system matrix with appropriate dimensions. After Laplace transform, the transfer function matrix of the system can be expressed as:

$$T(s) = C_0(sI - A_0)^{-1}B_0 + D_0 \quad 7.60$$

s is the complex frequency, and according to superposition principle, there is $Y(s) = T(s)U(s)$, where $U(s)$, $Y(s)$ are transformed from $u(t)$, $y(t)$ through Laplace transform. Therefore, input function $U(s)$ is a mapping of the output function $Y(s)$.

Eq. 7.59 depicts the structural system of normal design, however, there are frequently uncertainties in the geometry, material parameters, and loads of the actual structure. And the structure is under the disturbance from external uncertain loads, which creates uncertainty for the structural system and may result in disproportionate damage to the structure. The basic idea of H_∞ theory is to consider the structural system as a structural family with uncertainties, and to design all objects in the structural family (including the actual structure) to meet the expected performance requirements. Assuming the transfer function from interference $w(t)$ to output $y(t)$ is $G_w\Delta y$. Then the optimal problem of H_∞ is to minimize the norm of H_∞ for $G_w\Delta y$, which means $\min\|G_w\Delta y\|_\infty$, to ensure that the worst performance index in the structure family is optimal, with the robust performance of the system meeting the requirements. The definition of H_∞ is:

$$\|G(s)\|_\infty = \sup_{\omega \in [0, \infty)} \sigma_{max}[G(j\omega)] \quad 7.61$$

where \sup denotes supremum; σ_{max} is the maximum singular value of matrix; j is imaginary unit and ω is real variable.

Robustness can be regarded as the ability of structure to withstand disproportionate damage as a result of external interference. When "interference" is regarded as the structural system's input signal, and

"damage" is regarded as the output signal, if the ration of "damage consequence" and "cause" can be calculated, it is possible to characterise the structure's anti-interference ability and obtain the robustness index expression. If the resulting input signal is small and the output signal is large, this structure is more susceptible to initial interference and its robustness is poor.

For a general structure, under the assumption of ideal elastic material and small deformation, the equation of structural motion with n-degree of freedom is:

$$M\ddot{x}(t) + C\dot{x}(t) + Kx(t) = u(t) \quad 7.62$$

Where M , C , K are the mass, damping and tangent stiffness matrices of the structure respectively; $u(t)$ is the load vector of the node. $x(t)$, $\dot{x}(t)$, $\ddot{x}(t)$ represent the displacement, velocity, and acceleration vectors of the node. And damping matrix generally uses Raleigh damping, which is:

$$C = \alpha M + \beta K \quad 7.63$$

The damping proportional coefficient α and β are calculated using the damping ratio corresponding to the two modal frequencies:

$$\begin{cases} \alpha = \frac{2\xi\omega_i\omega_j}{\omega_i + \omega_j} \\ \beta = \frac{2\xi}{\omega_i + \omega_j} \end{cases} \quad 7.64$$

Setting state vector $\eta(t) = [x(t) \quad \dot{x}(t)]^T$, input vector is $u = u(t)$, output vector is $y = x(t)$, and the system state equation is:

$$\dot{\eta}(t) = A_0\eta(t) + B_0u(t) \quad 7.65$$

where:

$$A_0 = \begin{bmatrix} 0 & I \\ -M^{-1}K & -M^{-1}C \end{bmatrix} \text{ and } B_0 = \begin{bmatrix} 0 \\ M^{-1} \end{bmatrix}.$$

Considering the interference caused by external load uncertainty $\omega(t)$, and the transfer function for input $u(t)$ to output $y(t)$ is G_{uy} , and transfer function for interference $\omega(t)$ to interfered output $\Delta y(t)$ is $G_{\omega\Delta y}$, which is $\begin{bmatrix} y(t) \\ \Delta y(t) \end{bmatrix} = \begin{bmatrix} G_{uy} & 0 \\ 0 & G_{\omega\Delta y} \end{bmatrix} \begin{bmatrix} u(t) \\ \omega(t) \end{bmatrix}$. For linear system, G_{uy} and $G_{\omega\Delta y}$ is equivalent.

Therefore, the structural robustness can be expressed as:

$$I_R = \|G_{\omega\Delta y}\|_{\infty} = \|G_{uy}\|_{\infty} \quad 7.66$$

The transfer function matrix of the nonlinear structure system is related to the input, to compute robustness index, L_2 performance criteria is introduced, then the nonlinear robustness of the structure can be expressed by the induced norm L_2 of the structure system.

$$I_R = \|G_{w\Delta y}\|_{\infty} = \sup_{\|w\|_2 \neq 0} \frac{\|\Delta y(t)\|_2}{\|w(t)\|_2} \quad 7.67$$

I_R represents the response value of the system to external interference, the lower of the value, the better of the structural robustness.

7.4.2 The morphology optimisation based on robustness

The H_{∞} robustness is selected as the optimisation objective to realize the robustness design directly connected to structure design. This indicator can represent the deformation of the structure in marco level by constructing an intrinsic link between freeform surface variables and structural robustness. The same as the optimisation for strain energy, the coordinates of control points, weighting factors are selected as the variables to adjust the structural morphology. Different from the relationship between the strain energy and control variables of NURBS, it is hard to build the function between the robustness indicator and geometric control variables. Intelligent algorithm is needed to perform as the optimal tool.

Evolution rate (ER): The ration between the column V_k and V_{k+1} of the optimized structure into two consecutive steps:

$$ER = \frac{V_k}{V_{k+1}} \quad 7.68$$

$$V_{k+1} = V_k(1 \pm ER)(k + 1, 2, 3, \dots) \quad 7.69$$

Volumn Addition Ratio (AR_{max}): The ratio between maximum number of elemetns to be added per step and all shell elements:

$$AR_{max} = \frac{n_{add}}{N} \quad 7.70$$

While in Karamba plugin, $ER = \frac{1-TargetRatio}{MaxIter} + \frac{AR_{max}}{2}$

Element mean compliance or elemental strain energy. When a solid element is removed from a structure, the change of the mean compliance or total strain energy is equal to the elemental strain energy (CHU 1996.) This change is defined as the elemental sensitivity number:

$$\alpha_i^e = \Delta C_i = \frac{1}{2} \mathbf{u}_i^T \mathbf{K}_i \mathbf{u}_i \quad 7.71$$

\mathbf{u}_i is the nodal displacement vector of the ith element

\mathbf{K}_i is the elemental stiffness matrix

Sensitivity number:

$$\alpha_i = \frac{\sum_{j=1}^K w(r_{ij}) \alpha_j^n}{\sum_{j=1}^K w(r_{ij})} \quad 7.72$$

K is the total number of nodes

$w(r_{ij})$ is the linear weight factor

Linear weight factor:

$$w(r_{ij}) = r_{min} - r_{ij} (j = 1, 2, \dots, K) \quad 7.73$$

Solid element would be removed if:

$$\alpha_i \leq \alpha_{del}^{th} \quad 7.74$$

Void element would be added if:

$$\alpha_i > \alpha_{add}^{th} \quad 7.75$$

7.5 Example of multi-optimisation

The multi-objective optimisation is operated by taking one freeform surface as an example, shown in Figure 7.8.

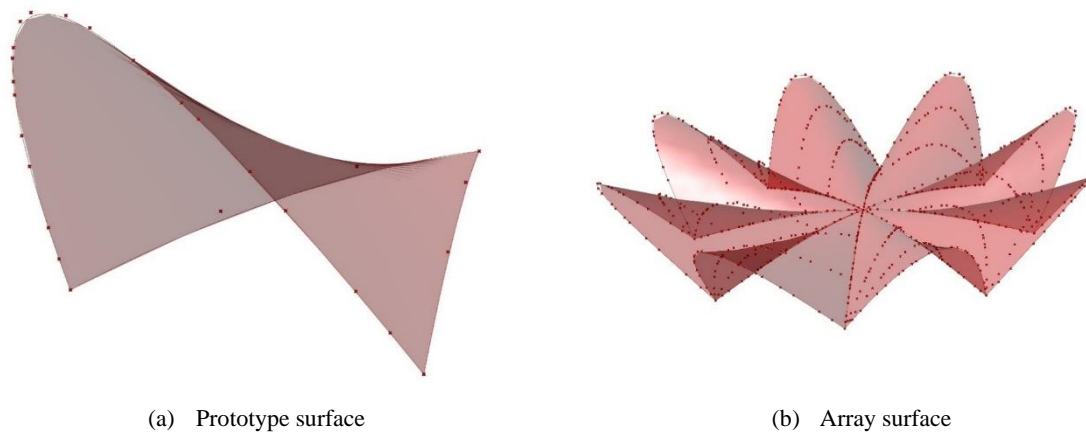


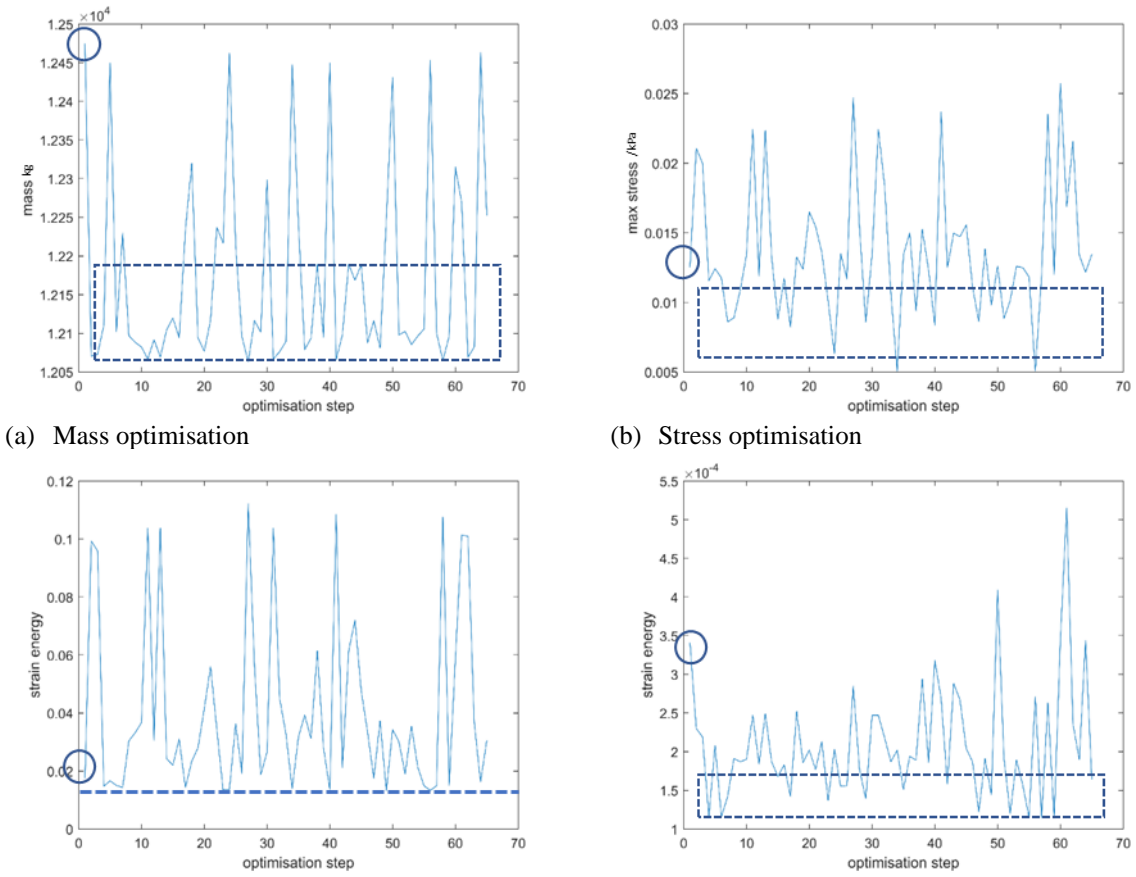
Figure 7.8 Example surface

As freeform morphology refers to complicated forms that cannot be represented mathematically, simple examples such as random surfaces adjusted through control points in Rhino or arched surfaces may not be appropriate. Furthermore, this chapter follows Chapter 6 on the proper design methods for freeform surfaces with robotic automation construction as the primary fabrication technique. The example in this Chapter uses the predicted curve from Chapter 6's LSTM method for freeform morphology. The advantage of using this example is that, in addition to being able to optimise the morphology, it is also possible to demonstrate the efficacy of this morphology generation method.

The surface is fitted by the curved predicted using the method (LSTM prediction) proposed in section 6.4, which is to generate curve with fitted the curvature of GLT engineering timber. The prototype surface (Figure 7.8 (a)) is created through patch method using three curves, namely two ridge curves and one arch curve. Four control points can be extracted from each ridge curve and twenty-two control

points from the arch curve, which are used as the variables for the optimisation tasks in the following section based on the NURBS properties of these points. The example surface (Figure 7.8 (b)) is generated using polar array methods from the prototype surface shown in Figure 7.8 (a), yielding a combination of 8 prototype surfaces.

The optimisation variables are chosen as the z-coordinate of the two control points of the two side curves and the weights of the 11th and 12th control points. The optimised objectives are set as the strain energy of gravity load and 0.02 mesh load, the mass, the max stress in z-direction, and the optimal results are shown in Figure 7.9 Optimisation results compared with the original values. Figure 7.9 Optimisation results compared with the original values. (a) presented the optimal mass throughout the whole optimisation. As the figure shows, the optimal value for the mass keeps in the range of $1.205 \times 10^4 - 1.22 \times 10^4 \text{ kg}$ as the original value is $1.245 \times 10^4 \text{ kg}$ with 3.6% decrease. The curve shows a trend of convergence in oscillation which means the optimal is effective in multi-optimisation process to get the optimal value. The stability of the algorithms needs to be enhanced. For the stress optimisation Figure 7.9 (b), the best optimal value is 0.005 compared with the original one as 0.013. The optimal results fluctuating in a range of 0.005-0.011 with at least 15% reduction. The optimisation for the strain energy under gravity load and mesh load are shown in Figure 7.9 (c)-(d). The optimisation for strain energy under gravity load is not significant reducing from 0.02 to 0.018. And the optimal results for strain energy under mesh load reduces from nearly 3.5 to 1.1 with 68% decrease.



(a) Mass optimisation

(b) Stress optimisation

(c) Strain energy of gravity load optimisation

(d) Strain energy of mesh load optimisation

Figure 7.9 Optimisation results compared with the original values

The visualised optimised results and comparisons of 15th, 30th, 45th and 60th step are listed in Figure 7.10 to Figure 7.18. Figure 7.10 shows the morphology change throughout the whole optimisation. Figure 7.10 (1), (2), (4) and (7) presents the morphology change after 15th, 30th, 45th and 60th step optimisation as the z-coordinate of the control points would change during the optimisation to change the overall morphology. Figure 7.10 (5) (6) compares the morphology achieved from 45th step and the one from 30th step. Similarly, Figure 7.10 (8) (9) compares the difference between 45th step and 60 step in whole morphology and details.

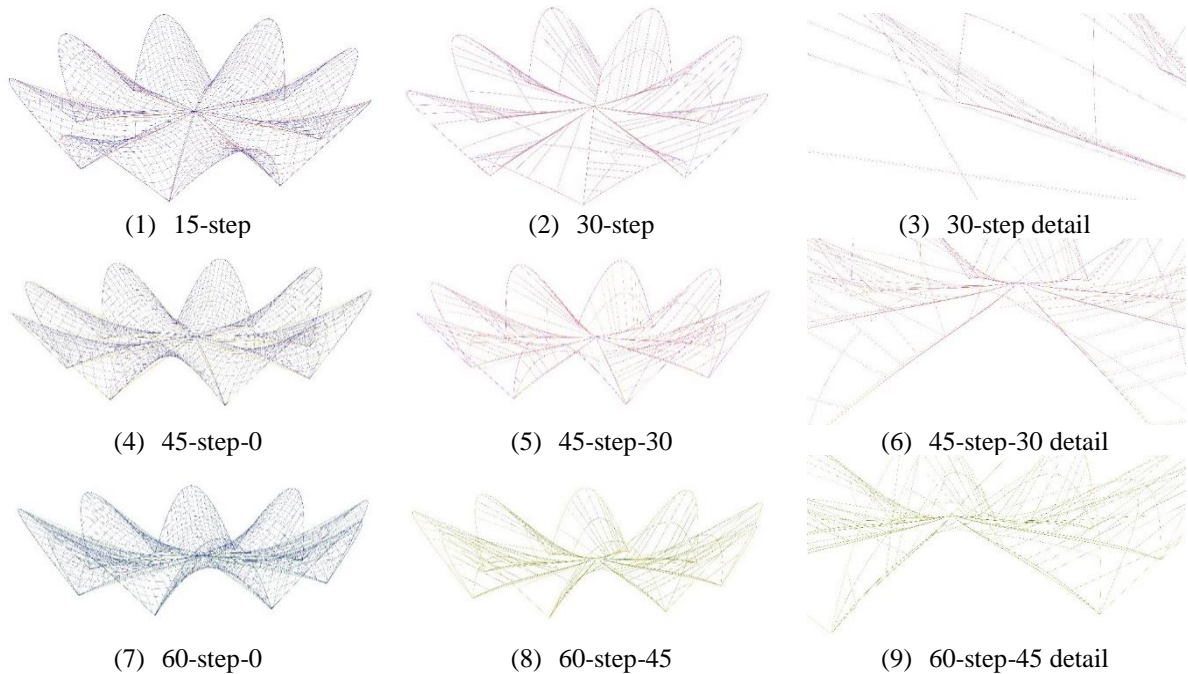


Figure 7.10 Geometry comparison of evolution steps

Figure 7.11 demonstrate the displacement of the whole structure under gravity and mesh load in three different views: Front, Right and Top. The lighter the colour is, the less of the value for the displacement. The figures show that the biggest displacement happen in the edge of the structure.

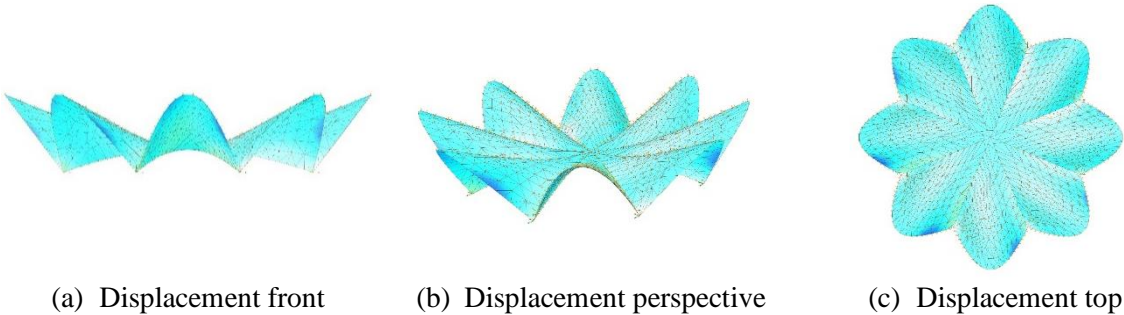


Figure 7.11 Displacement of original morphology

Figure 7.12 compares the displacement after 15th, 30th, 45th and 60th step of the optimisation in three views. Throughout the whole optimisation, the displacement in the edge reduces until 30th step. And the displacement value goes back as the optimisation goes on¹⁵. There are some reasons for this situation.

¹⁵ In this case, the best value does not emerge at the end of the optimization process.

One could be the optimisation is trapped in the local optimisation rather than the global optimisation. The solution could be run the algorithm again or change the range of variables.

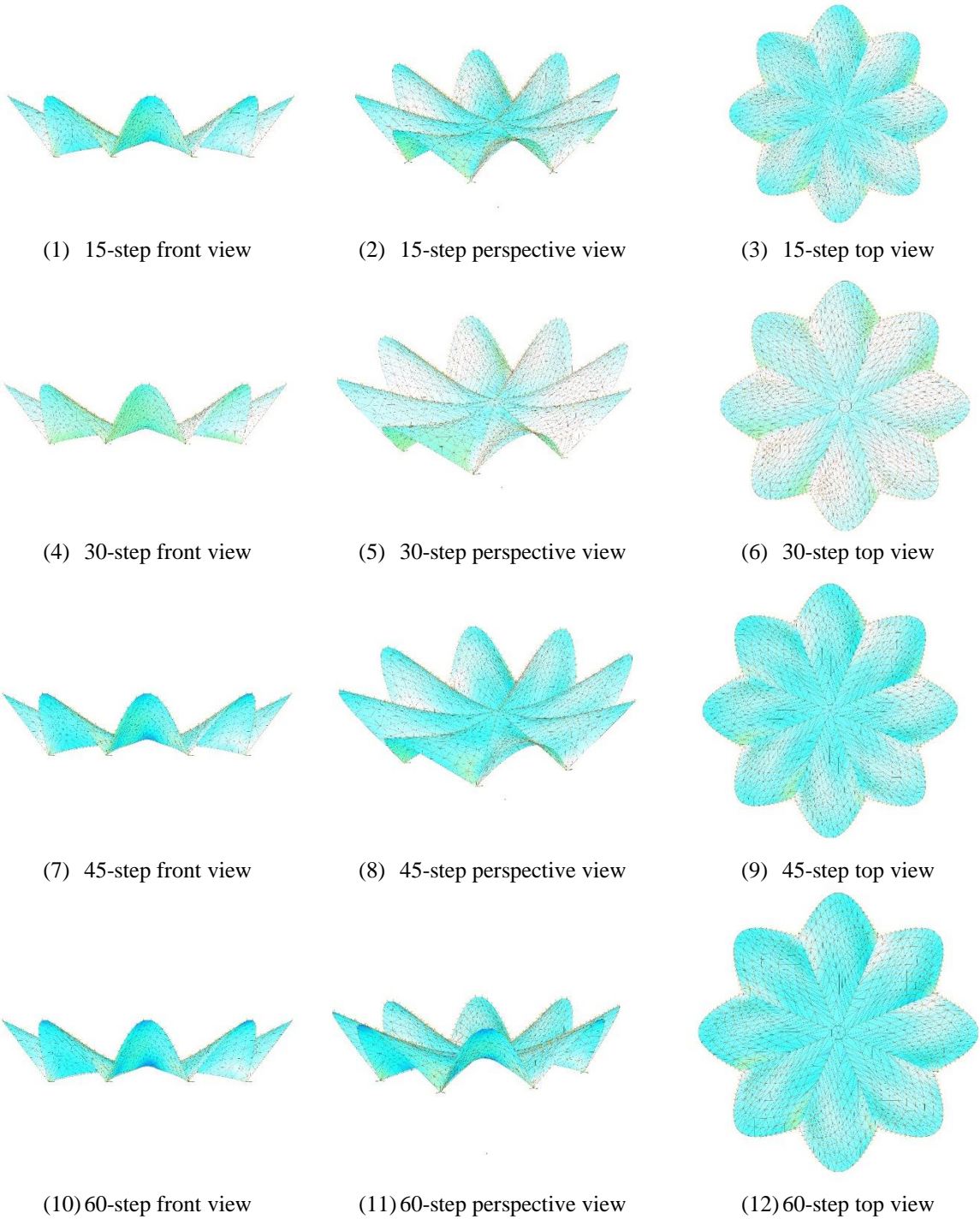
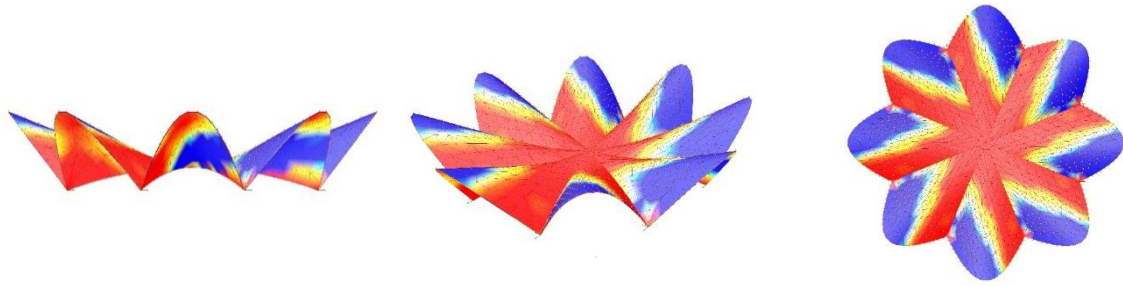


Figure 7.12 Displacement of 60-step evolution

Figure 7.13 demonstrate the structure utilisation rate of the whole structure under gravity and mesh load in three different views: Front, Right and Top. Colours range from yellow blue to red.

Same as the visualisation for displacement, Step 30 shows the best results with more homogeneous structure utilisation through the whole 60 step optimisation shown in Figure 7.14.

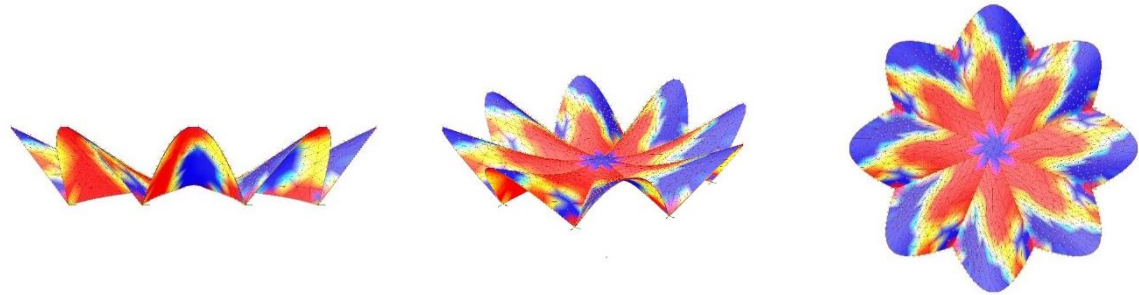


(a) Front view

(b) Perspective view

(c) Top view

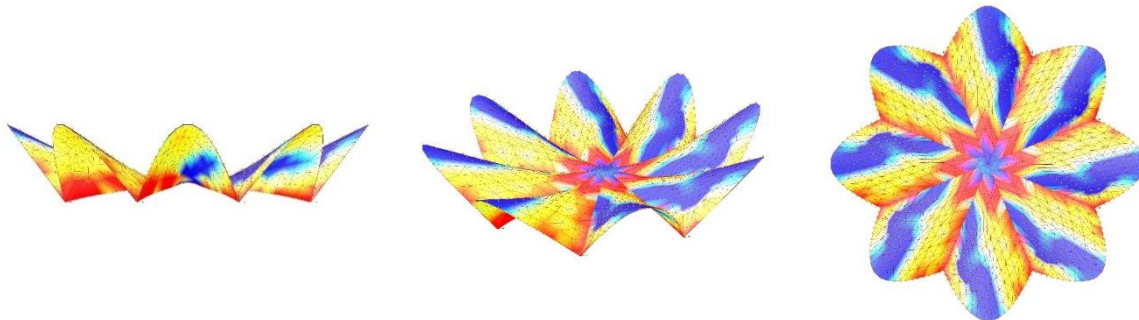
Figure 7.13 The utilisation of original morphology



(1) 15-step front view

(2) 15-step perspective view

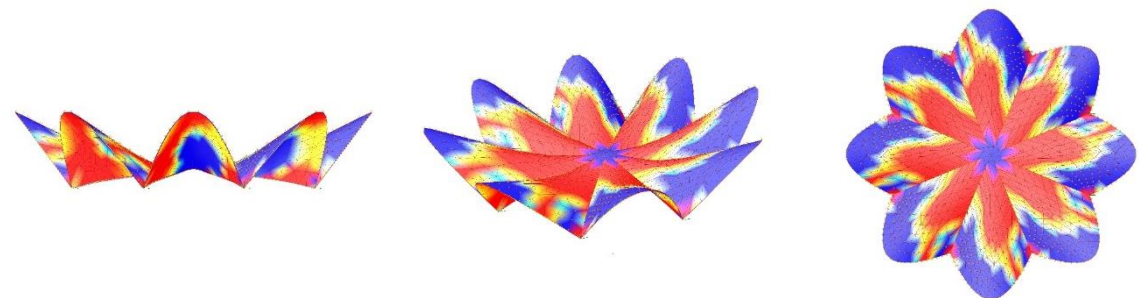
(3) 15-step top view



(4) 30-step front view

(5) 30-step perspective view

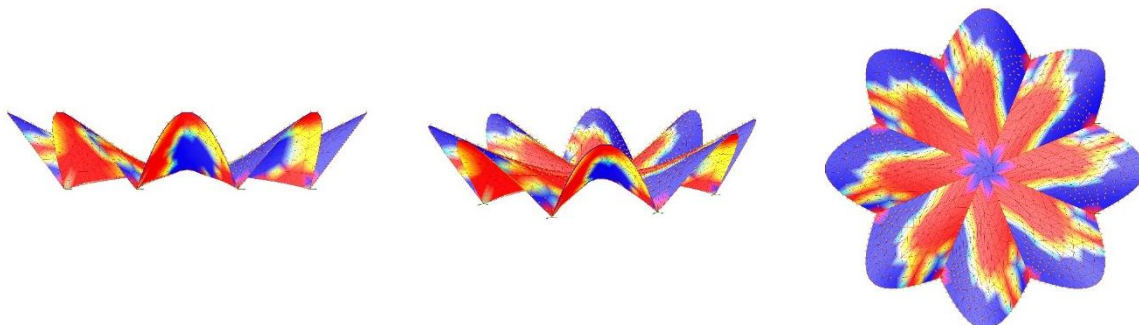
(6) 30-step top view



(7) 45-step front view

(8) 45-step perspective view

(9) 45-step top view



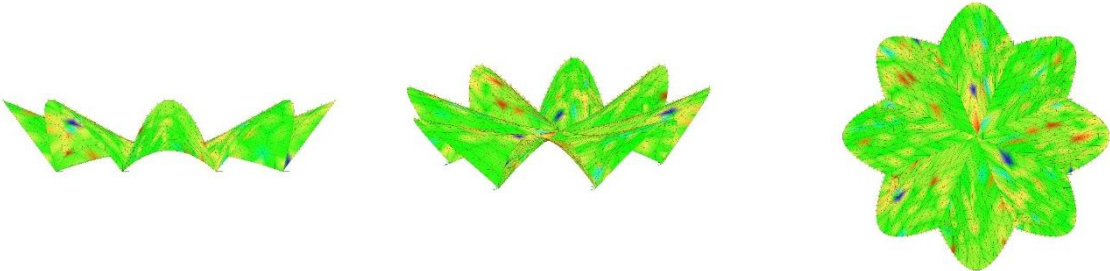
(10) 60-step front view

(11) 60-step perspective view

(12) 60-step top view

Figure 7.14 The utilisation of 60-step evolution

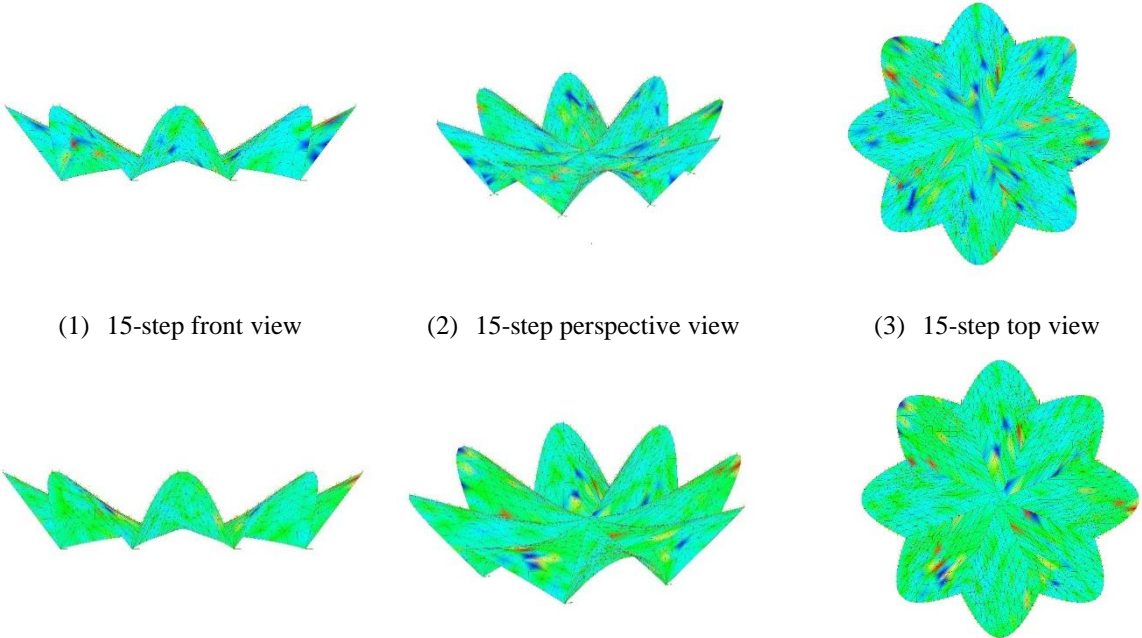
Figure 7.15 demonstrate the principal stress of the whole structure under gravity and mesh load in three different views: Front, Right and Top. Colours range from yellow, green to blue. The Figure 7.15 shows that most of the part of the structure is in green with small proportion in yellow or red which means the structure has a good stress distribution.



(a) Front view (b) Perspective view (c) Top view

Figure 7.15 the principal stress of the original morphology

From Figure 7.16 (4), the best result in this 60-step optimisation happens in the 45th step with more uniform stress distribution. The difference between 45th step and 60th is not great. Compared to the original results in Figure 7.15, the value for the stress reduces significantly, with the very few locations where stress distribution is not concentrated generally exist at ridges or connection between different parts.



(1) 15-step front view (2) 15-step perspective view (3) 15-step top view

(4) 30-step front view (5) 30-step perspective view (6) 30-step top view

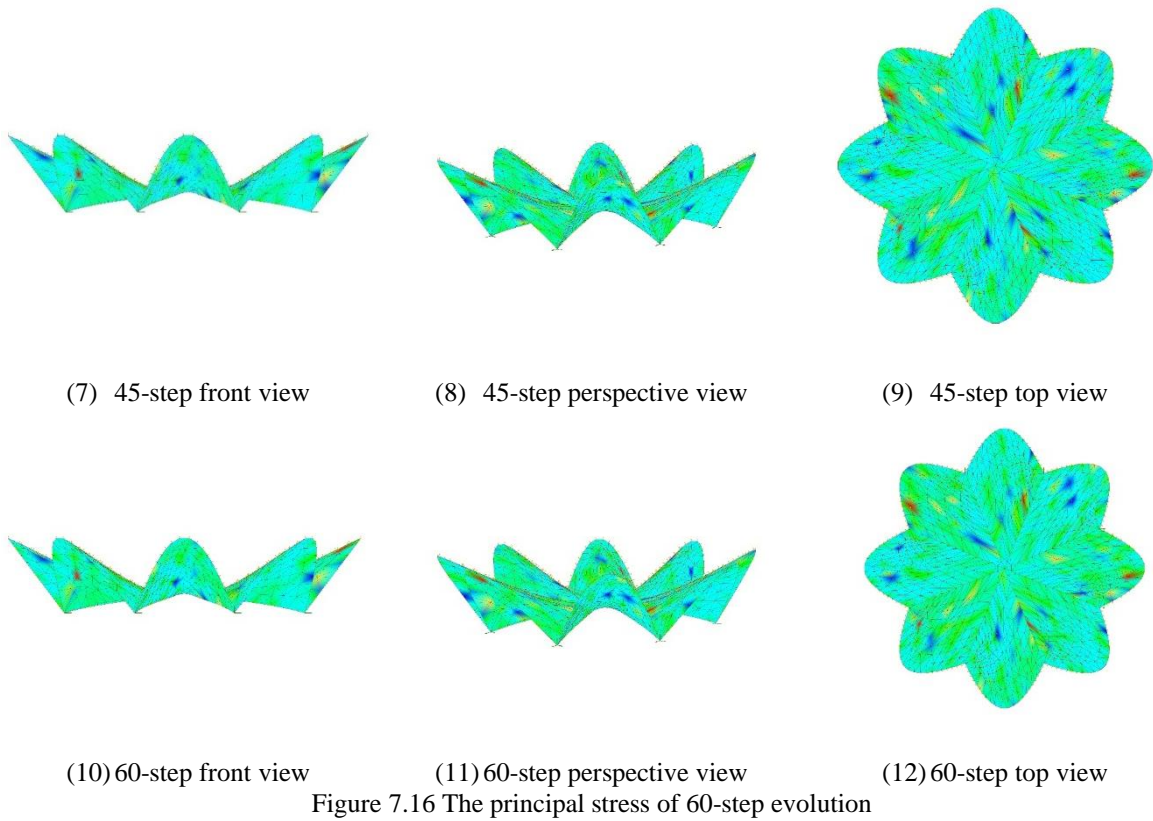


Figure 7.17 demonstrate the second principal stress of the whole structure under gravity and mesh load in three different views: Front, Right and Top. Colours range from green, blue to red. The stress distribution is normal and the ridges parts and the connections parts are areas of high stress variation.

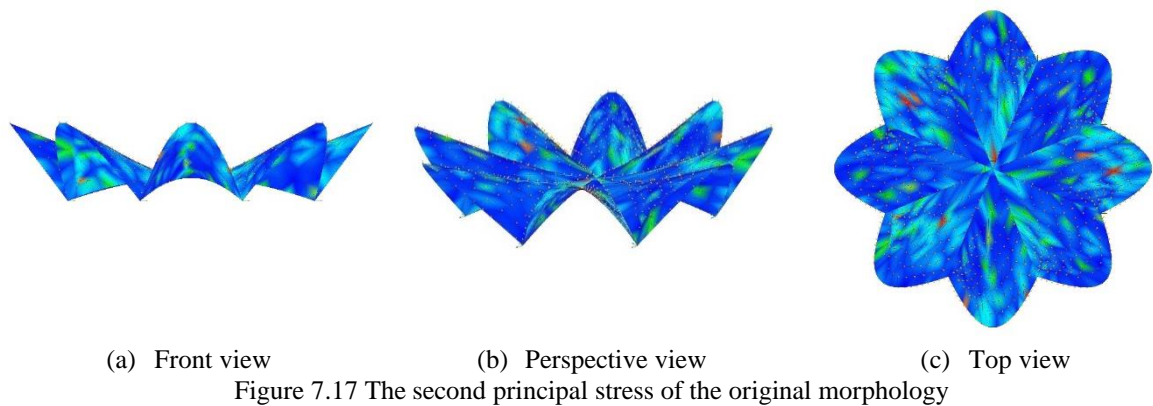


Figure 7.18 presents the optimal results for second principal stress distribution and compared the results between different step of optimisation. Step 15 and step 30 have the similar results better than the results achieved from step 45 and step 60.

The optimal results show that the through multi-objective optimisation, the stiffness and stability can be enhanced through more even stress distribution, less displacement and more even structural utilisation. The results of the 60-step optimisation shows that the optimal value for different structural performance index cannot be achieved at the same time. This is the common question for multi-objective optimisation which needs the determination for the weights for different indicators to select the most suitable plan according to different situations.

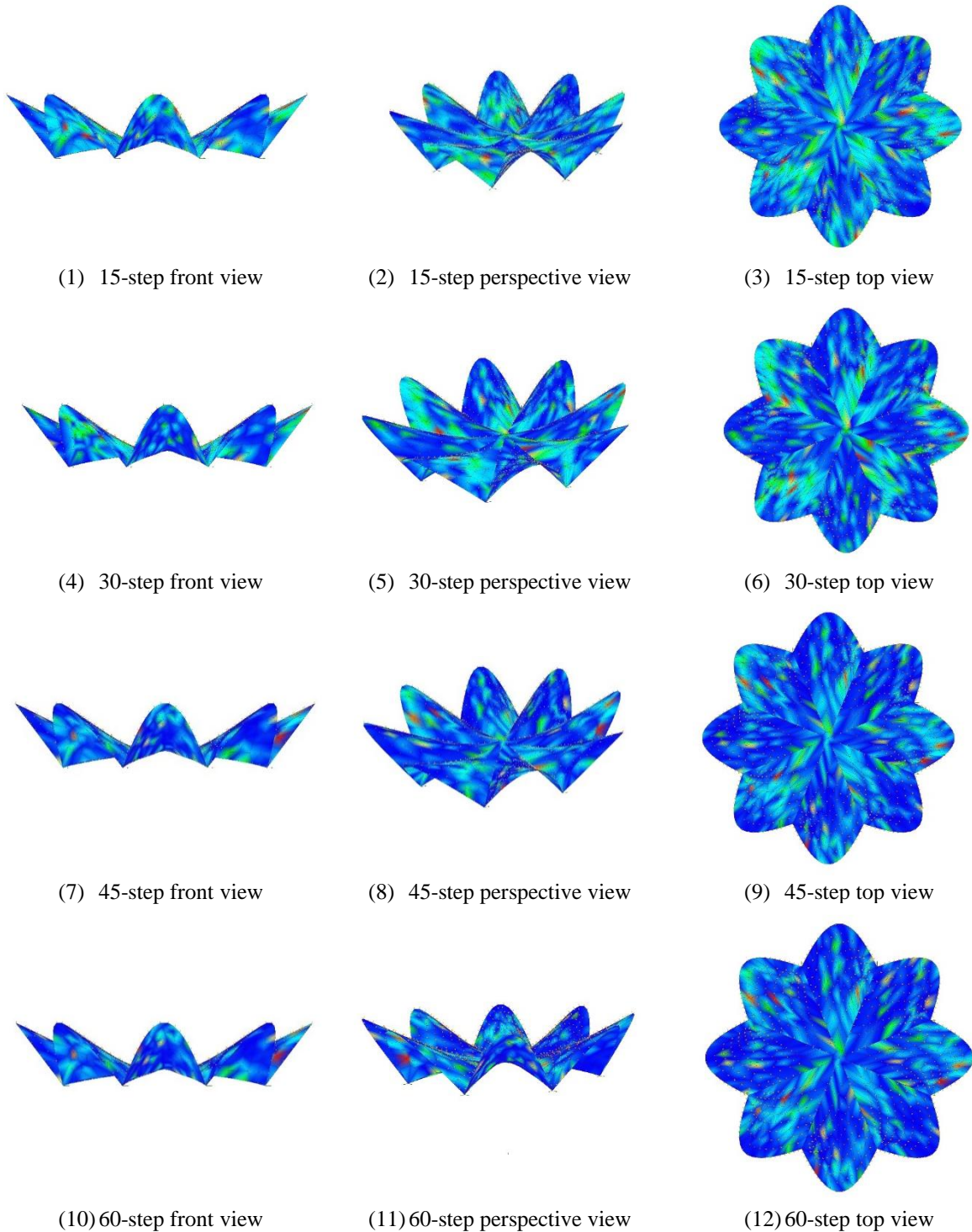


Figure 7.18 The second principal stress of 60-step evolution

7.6 Conclusion

This chapter works as a following part for Chapter 6 on morphology. Chapter 6 deals with the rationality in form-finding and this chapter optimise the morphology generated from one method developed in Chapter 6 to achieve higher level of rationality including structural performance.

Based on the results of morphology creation in Chapter 6, this chapter simulates the structural properties of the freeform surface and optimizes them. By introducing NURBS, this chapter uses NURBS-based techniques to describe the geometric information of the freeform surface. Control points and weight

factors are used as optimisation variables. And the overall strain energy of the structure and the mass of the structure are used as optimisation objectives to achieve the common minimization optimisation goal.

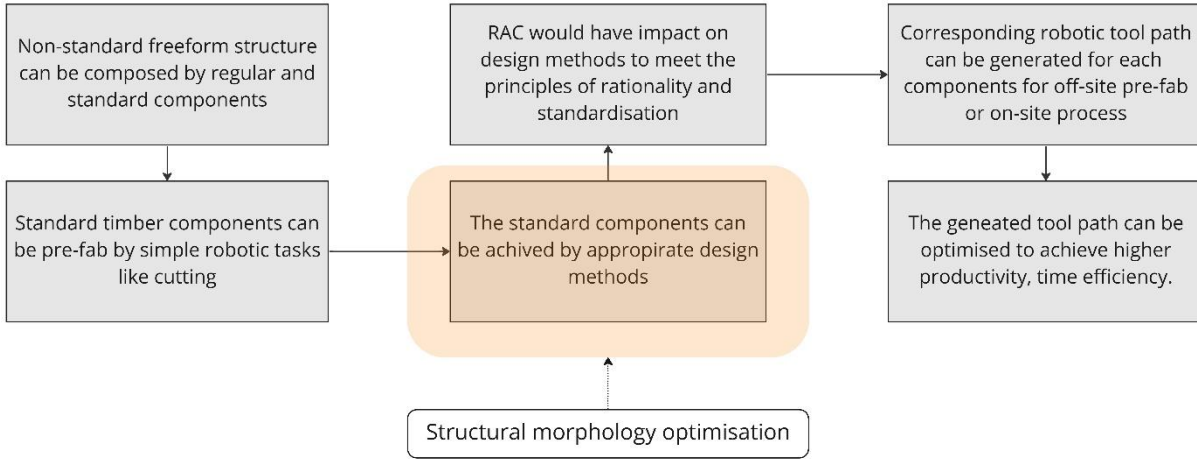


Figure 7.19 Connection to the hypothesis

The freeform surface is formed by a simple geometric transformation using the curve conforming to the GLT curvature fitted in Chapter 6. The z-coordinates of the control points of this curve and the corresponding weights are used as optimisation variables, and the optimisation objectives are optimized by combining gradient optimisation and the evolution algorithm, while the trends of the mechanical performance evaluation indexes such as the maximum displacement in the z-direction and the internal force of the structure are observed. The optimisation results show that the maximum displacement in z-direction and the internal force show a decreasing trend in the optimisation process without buckling.

The example generated from the predicted curve in Chapter 6 is used in the optimisation. The optimisation process not only demonstrates the structural rationality of the geometry model design using the LSTM method, but it also presents a workflow for optimising structural rationality in order to have better structure performance such as stiffness and robustness. NURBS provides a method for converting a geometric model into numerical information, which is required in the optimisation process.

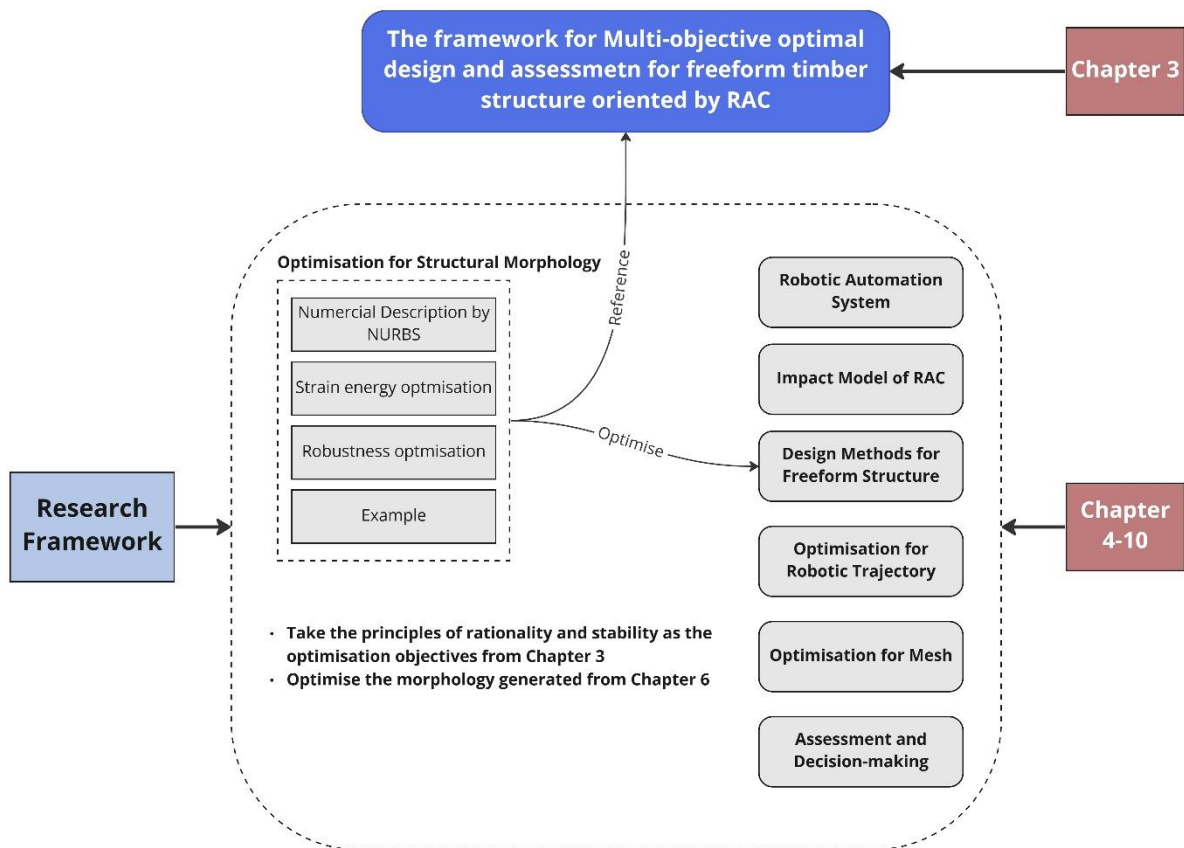


Figure 7.20 Connection to other chapters

Chapter 8

Optimisation for Trajectory and Motion Control to Minimize Travel Length and Operation Time

Section 8.5-8.7 is a published journal paper. The content is extracted from part of the paper to reduce the length of the chapter. More details can be found in Appendices 4.

In the case introduced in section 4.1 about the robotic timber joinery fabrication, the debug process mainly focuses on the robot's singularities. The program can be used in another type of timber joint; however, more adjustments will be needed to avoid the singularities or collisions. This manual work could not assure the final tool path exported to the robot has the shortest travel distance or travel time. Furthermore, the manual process reduces the automaticity of the robotic process. In this chapter, the research zooms in more about robotics, from its system composition to the principles of automatic control. First, the original process of the simulation for the robotic arm in Grasshopper using KUKA | PRC is illustrated by introducing the components within this plugin. After, the principles of robotics are introduced. The optimisation method is introduced afterwards to give the theory support for optimisation for the case. Finally, the optimisation for the robotic cutting is operated and tested on other components generated in chapter 6.

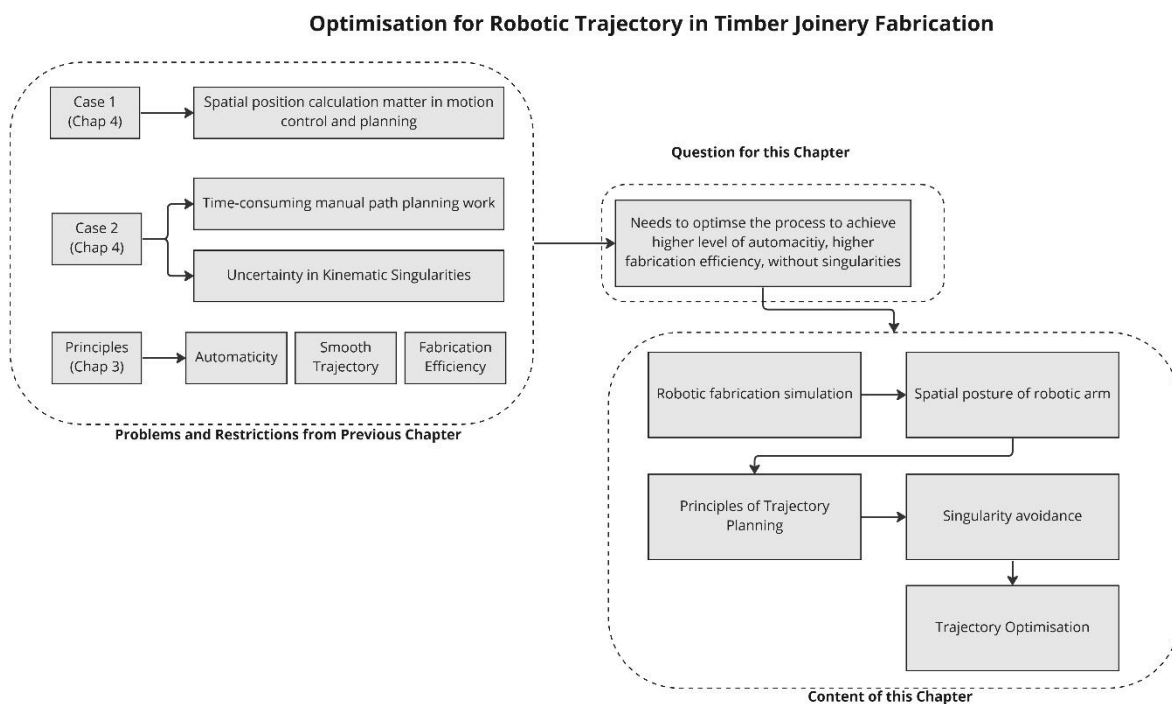


Figure 8.1 Roadmap for Chapter 8

8.1 Process of robotic simulation in Grasshopper

In technical terms, the mechanical system of an industrial robot consists of a manipulator, a control system, a handheld operator programmer. All other devices not included in the mechanical system are called peripheral devices: tool ends (effectors/tools), protection devices, belt conveyors, sensors, etc.

The manipulator is made up of many movable, interconnected joints. We call this the kinematic chain, which we see in everyday life. The kinematic chains are the axes of motion of the robot arm Figure 8.2

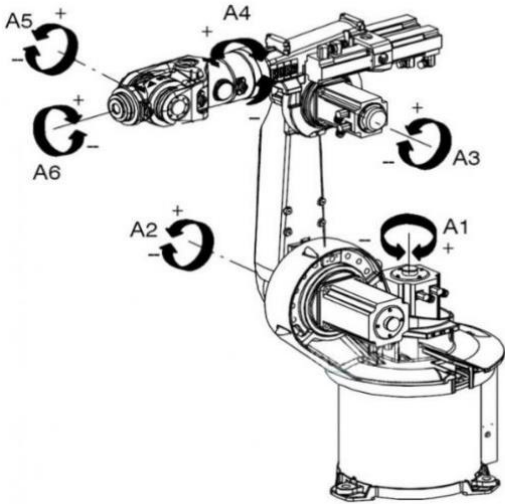


Figure 8.2 The motion of the robot arm

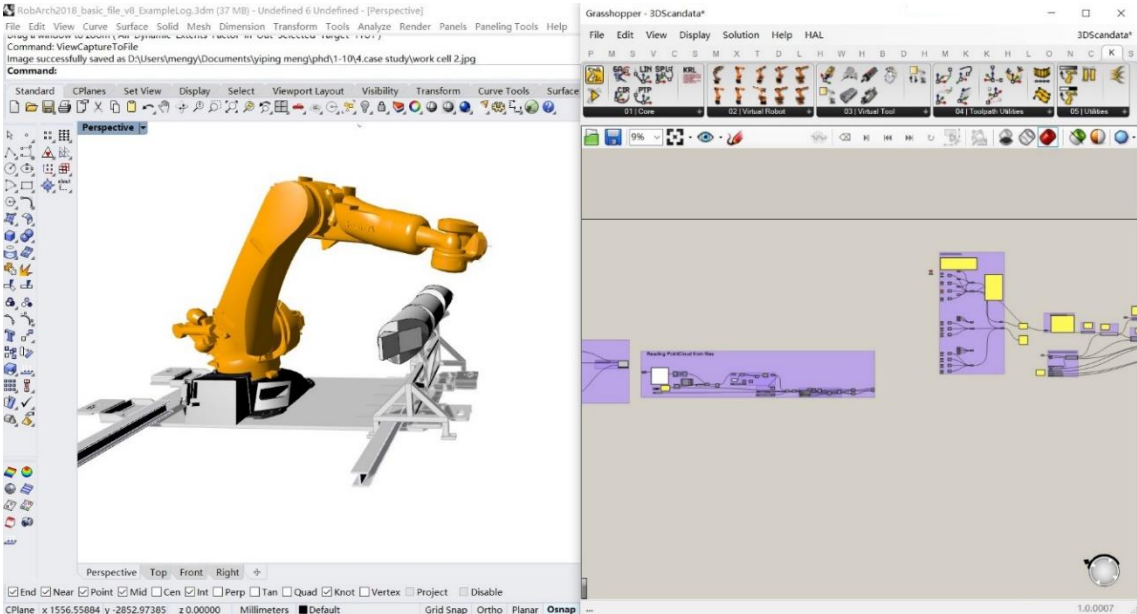
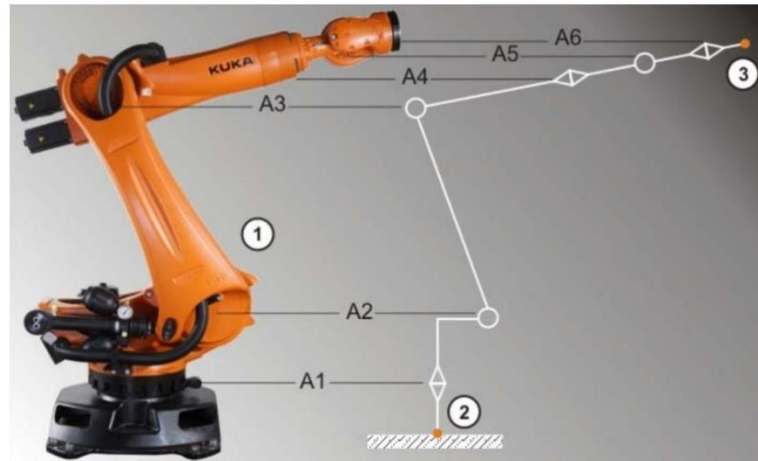


Figure 8.3 The visualisation of the simulation process

8.1.1 The working principle of industrial robotic arms

The construction of a KUKA robot, for example, consists of the robot hand (the mechanical system of the robot), the starting point of the kinematic chain (the robot foot Robroot) and the open end of the kinematic chain (the flange Flange) (Figure 8.4). The servo motors control the movement of the axes in a targeted manner. The servomotors are connected to the robot components via reducers for precise positioning. The robot arm is represented by a six-axis arm consisting of six servo motors and encoders. By adding a horizontal linear slide to the six-axis arm, the arm's working range can be extended to achieve a seventh axis and more complex operations.



Modified from <https://www.kuka.com/en-gb/products/robotics-systems/industrial-robots/kr-cybertech>:
Figure 8.4 The kinematic chain of a robot arm

8.1.2 Movement mechanisms of industrial robotic arms

The main mechanical system of the robot is the arm. A servo motor achieves the mechanical movement of the arm, and the control system that controls this motor is called the control cabinet. The control system is the pivotal part of the arm's movement and can control the arm's six axes and up to two additional external axes.

Robotic arm path planning is where the robot arm locks onto the start and end points in an obstructed scene and selects a suitable path, ensuring safety and no collisions in the process. The shortest route can be selected for execution when it is confirmed that there is no collision. Principles of path selection: The robot can choose a path with the designer's design or with the addition of equipment and software. Three principles need to be considered in the selection process: 1 clear starting and ending point, two avoidance of obstacles, and three path optimisations.

8.2 Spatial posture of the robot

8.2.1 Spatial description and coordinate system

Spatial positions and rotations are required to represent robots, workpieces, and paths. Vectorised vectors can represent positions in space. A Cartesian coordinate system based on the origin and orthogonal axes must define vectorised vectors that express positions. It is generally assumed that the components are rigid so that the relative positions of a set of position points corresponding to the components are fixed. For the description of a single positional point, the position and rotation of the corresponding member are represented by the position and rotation of the coordinate system in which it is located.

Regarding controlling the robot arm for linear motion, the spatial position relationship between the two bars is represented by trigonometric functions by establishing two bars' two-dimensional and three-dimensional coordinate systems. However, when the number of bars exceeds two, the representation of the spatial position relationship by trigonometric functions can be cumbersome and cause computational difficulties due to the different angular relationships between the individual bars. A concise

mathematical expression is proposed in robotics to solve the robotic arm bars' spatial position and angle relationship.

The Pose Position and Orientation of a robot is generally the spatial position and attitude of the robot's end-effector, and sometimes also the spatial position and attitude of each of the other articulated arms. Once a coordinate system has been established, any position in space can be described by a 3×1 position matrix as shown below.

$$P = \begin{bmatrix} x_p \\ y_p \\ z_p \end{bmatrix} \quad (8.1)$$

where x_p, y_p, z_p represent the three coordinate components of the point P in the coordinate system $\{A\}$, respectively. The attitude of the end-effector can be expressed as a third-order attitude matrix consisting of the cosines of the directions of the three axes in the spatial coordinate system, i.e., the cosines of their two angles, as shown in Eq. 8.2.

$$R = \begin{bmatrix} \cos(x, x_p) & \cos(x, y_p) & \cos(x, z_p) \\ \cos(y, x_p) & \cos(y, y_p) & \cos(y, z_p) \\ \cos(z, x_p) & \cos(z, y_p) & \cos(z, z_p) \end{bmatrix} \quad (8.2)$$

Coordinate transformations usually include translational, rotational, and combinations of the first two. A coordinate transformation operation is required when the two objects in question are in different coordinate systems.

(1) Translation Transformation

Let two coordinate systems $\{i\}$ and $\{j\}$ have the same pose, but their coordinate origins do not overlap. If P_{ij} is used to represent the vector from the origin of the former to the origin of the latter, then the former can be transformed into the latter by translational transformation along the vector P_{ij} , and so the vector P_{ij} is called the translational transformation matrix, as shown in Figure 8.5.

If a point in space is represented in the coordinate system $\{i\}$ as r_i and in the coordinate system $\{j\}$ as r_j , then the two are related as follows

$$\vec{r}_i = \vec{P}_{ij} + \vec{r}_j \quad 8.3$$

(2) Rotation Transformation

Suppose there are two coordinate systems $\{i\}$ and $\{j\}$ whose origins coincide, but whose poses are different. Then the coordinate system $\{i\}$ can be transformed into the coordinate system $\{j\}$ by a certain rotation transformation operation. The process of rotational transformation is generally complex, so the following is the simplest case of rotating an angle of θ about the z-axis to illustrate the rotational transformation matrix, as shown in Figure 8.6.

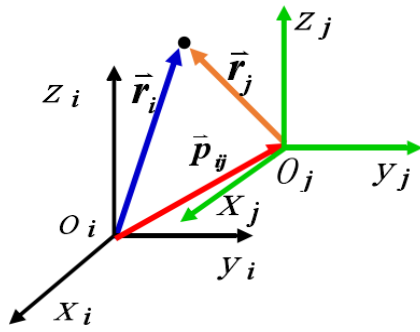


Figure 8.5 the translational transformation

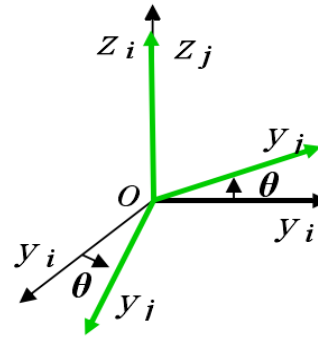


Figure 8.6 the rotation transformation

The origin of the two coordinate systems $\{i\}$ and $\{j\}$ coincide and the direction of each axis in the coordinate system $\{j\}$ is rotated by an angle of θ with respect to $\{i\}$. The positive and negative θ angles are usually determined by the right-hand rule, i.e., counterclockwise is positive if viewed from the sagittal end of the z -axis. The rotation transformation matrix for the three ways of rotating the θ angle about the x -axis, y -axis and z -axis are in turn as follows:

$$R(x, \theta) = \begin{bmatrix} 1 & 0 & 0 \\ 0 & \cos \theta & -\sin \theta \\ 0 & \sin \theta & \cos \theta \end{bmatrix} \quad 8.4$$

$$R(y, \theta) = \begin{bmatrix} \cos \theta & 0 & \sin \theta \\ 0 & 1 & 0 \\ -\sin \theta & 0 & \cos \theta \end{bmatrix} \quad 8.5$$

$$R(z, \theta) = \begin{bmatrix} \cos \theta & -\sin \theta & 0 \\ \sin \theta & \cos \theta & 0 \\ 0 & 0 & 1 \end{bmatrix} \quad 8.6$$

(3) Composite Transformation

Given two coordinate systems $\{i\}$ and $\{j\}$, where the former needs to be transformed not only by translation but also by a rotational transformation operation to become the latter, i.e., it needs to be done by a composite transformation, the representation of any point in space in the two coordinate systems $\{i\}$ and $\{j\}$ is then related as follows,

$$\vec{r}_i = \vec{P}_{ij} + R_{ij} \cdot \vec{r}_j \quad 8.7$$

A set of axes represents the poses of a coordinate system, and the relative positions of two coordinate systems are represented by the vector ξ .

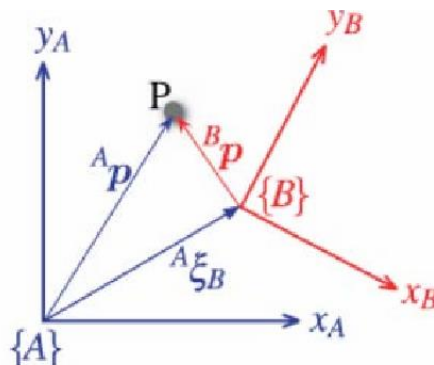


Figure 8.7 The position of Point P and two coordinate system

As shown in Figure 8.7, the point P can be expressed in the coordinate system {A} or in the coordinate system {B} by different vectors, and the locus pose of the coordinate system {B} with respect to the coordinate system {A} can be expressed by conforming to ${}^A\xi_B$. By means of the relative poses ${}^A\xi_B$, the different representations of the same poses in the coordinate system {A} and the coordinate system {B} can be transformed into each other [12]. The mathematical relationship between the expression A_p of the location point P in the coordinate system A and its expression B_p in the coordinate system B is given in Eq. 8.8.

$${}^A p = {}^A \xi_B \cdot {}^B p \quad 8.8$$

This transformation between vectors is ultimately expressed as a different description of the same coordinate point in different coordinate systems. If one coordinate system can be represented by another coordinate system through relative poses, as shown in the diagram, then the individual coordinates can be multiplied in turn to represent the new mathematical relationship between each other, as shown in Eq. 8.9.

$${}^A \xi_C = {}^A \xi_B \cdot {}^B \xi_C \quad 8.9$$

The equation means that the positional relationship of the coordinate system {C} with respect to the coordinate system {A} can be generated by the relative poses of the coordinate system {B} to the coordinate system {A} and the relative poses of the coordinate system {C} to the coordinate system {B}.

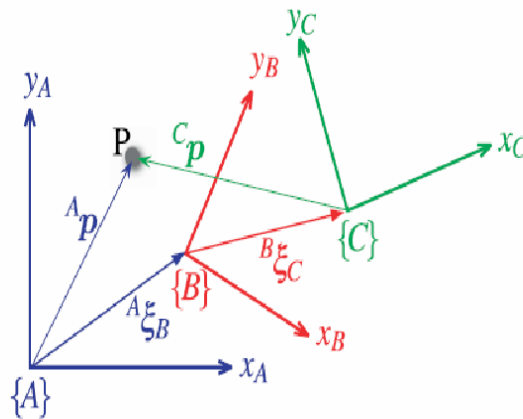


Figure 8.8 The position of point P, three coordinate systems

If the relative positions of the two coordinate systems and the position of a point in one of them are known, then the position of the point in the other coordinate system can be obtained. As can be seen from Figure 8.8, the reference coordinate system {A} can express the coordinate system {B}. Specifically, the position of the origin of the coordinate system {B} in the coordinate system {A} is represented by the vector $t = (x, y, z)$ and the coordinate system {B} is subjected to some complex rotation operations with respect to {A}.

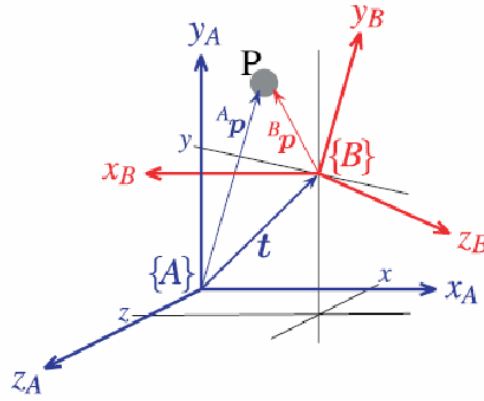


Figure 8.9 Rotation transformation for two coordinate systems

As shown in Figure 8.9, the two right-handed coordinate systems have different rotational poses, and reference can be made to one of them to describe the other. It is conceivable that the properly rotated coordinate system $\{A\}$ could coincide with its rotational attitude and the coordinate system $\{B\}$. Euler's rotation theorem shows that any rotation relation can be obtained or expressed by rotating about different axes of rotation. It is important to note that the final rotation relation is closely related to the order of rotation about the different rotation axes, and the final attitude obtained by different rotation orders is generally different. The rotation coordinate system $\{A\}$ and the rotation attitude coordinate system $\{B\}$ can be converted by the following equation,

$$\begin{bmatrix} A_x \\ A_y \\ A_z \end{bmatrix} = {}^A R_B \cdot \begin{bmatrix} B_x \\ B_y \\ B_z \end{bmatrix} \quad 8.10$$

$$R_x(\theta) = \begin{bmatrix} 1 & 0 & 0 \\ 0 & \cos \theta & \sin \theta \\ 0 & \sin \theta & \cos \theta \end{bmatrix} \quad 8.11$$

$$R_y(\theta) = \begin{bmatrix} \cos \theta & 0 & \sin \theta \\ 0 & 1 & 0 \\ -\sin \theta & 0 & \cos \theta \end{bmatrix} \quad 8.12$$

$$R_z(\theta) = \begin{bmatrix} \cos \theta & -\sin \theta & 0 \\ \sin \theta & \cos \theta & 0 \\ 0 & 0 & 1 \end{bmatrix} \quad 8.13$$

8.2.2 Posture analysis of jointed robots

The motion of a multi-axis robot is essentially the control of the joint angles under the control of the controller to achieve the goal of reaching the target point at the end of the robot. The choice of motion strategy is divided into the positive and inverse kinematics, where positive kinematics refers to motion control under known joint angles, and inverse kinematics refers to finding the joint angles under known target point conditions.

In this section, we will focus on the theoretical analysis of the positive solutions of robots. From a structural point of view, industrial robots are open-loop linkage systems consisting of several arms and rotating joints connected in series with each other. Therefore, to describe the interrelationships between these links, a reference coordinate system needs to be set up at each joint, which in robotics is known as

the D-H parametric model. Also, to be able to describe the relative positional transformations between coordinate systems more efficiently, a chi-square transformation matrix representation is usually utilised.

Let the relative relationship between the robot from one linkage to the next to be denoted A . Matrix A represents the flush transformation of the close translations and rotations between the linkage coordinate systems. Thus, the flush transformation matrix T from the end of the robot to the base system $\{0\}$ is

$$T_6 = A_1 \cdot A_2 \cdot A_3 \cdot A_4 \cdot A_5 \cdot A_6 \quad 8.14$$

where A_1 represents the attitude transformation of linkage one regarding the base system $\{0\}$, A_2 , etc., there are many uncertainties in the linkage of a multi-joint robot, such as material properties, rod strength and stiffness. Therefore, to simplify the calculation process, the kinematic equations of the mechanism are often created by treating the linkage as a rigid body and using straight lines in space to represent the joint axis position. A simplified diagram of a spatial linkage is shown in Figure 8.10 [31].

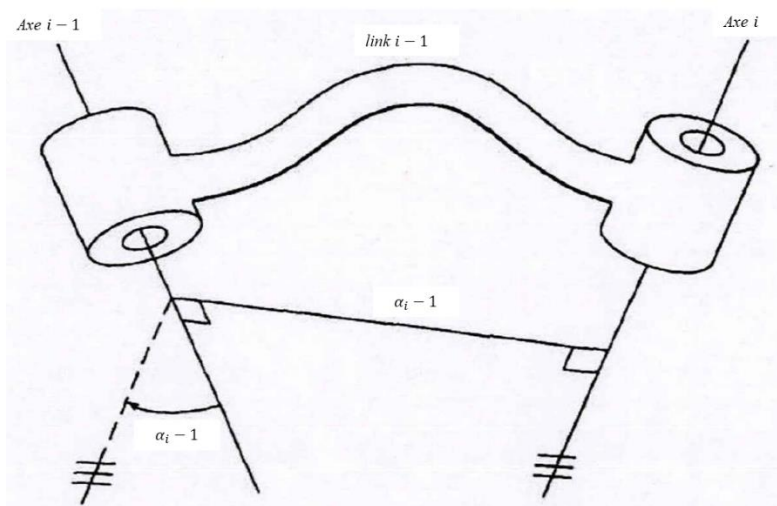


Figure 8.10 Schematic diagram of space link (Craig, 2009)

In the space illustrated in Figure 8.11, the length of the connecting rod α_{i-1} is defined as the standard vertical line between the two axes ($i-1$) and (i). By projecting the joint axes ($i-1$) and (i) onto the normal plane of the standard plumb line and turning around the joint axis ($i-1$) to the axis (i) according to the right-hand rule, the angle of rotation of the two joint axis links is obtained, i.e., the angle of rotation around the X_i axis, from Z_i to Z_{i-1} . The distance along the common axis of the two neighbouring links is therefore defined as the link deflection distance. Figure 8.11 shows that the distance along the Z_i axis, moving from X_{i-1} to X_i , is the linkage bias d_i . The figure shows that the joint linkage's rotation angle around the axis is defined as the joint rotation angle, noted as θ_i . Therefore, based on the above settings, the D-H parameter model that any multi-axis robot has can be determined, and These parameters can describe any multi-joint robot.

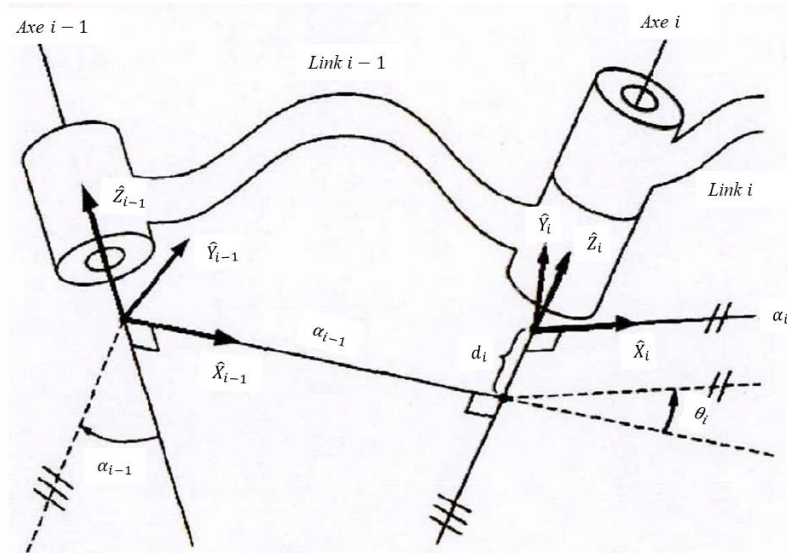


Figure 8.11 Joint linkage of two axes (Craig, 2009)

8.2.3 Establishment of the robot coordinate system

In robotics, the positional relationship between adjacent links is the basis for constructing a robot motion model. Therefore, to accurately represent this relationship, the base coordinate system is set up as shown in Figure 8.11 above, starting from the base, and then defining the corresponding linkage coordinate system according to the number of each linkage location, so that $\{i\}$ represents the solid linkage on linkage i . The coordinate system is defined according to the location of each link in turn. The general procedure for establishing the linkage coordinate system is

- (1) Identify the individual joint axes on the articulated robot and mark the extensions of these axes.
- (2) Extend the joint axis to determine the standard vertical line between the joint axis i and $i + 1$. The origin of the linkage coordinate system i is determined by the intersection of the joint axis i and $i + 1$ or the corner of the standard vertical line with the joint axis.
- (3) Specify the pointing of axis Z_i along joint axis i
- (4) Specify the pointing of the axis X_i along the standard vertical line and, if the joint axis i intersects $i + 1$, specify that the X_i axis is perpendicular to the plane in which the joint axis i and $i + 1$ lie.
- (5) The y-axis is determined according to the right-hand rule, based on the determination of the z- and x-axes. As the sequence of coordinate systems is not clearly defined, the default coordinate system $\{0\}$ coincides with (Technologies & Terminology) in the base, and for the coordinate system $\{i\}$, the x-direction can be chosen arbitrarily. However, in the selection process, the rod parameters should be as close as possible to 0.

8.2.4 Establishment of the robot coordinate system

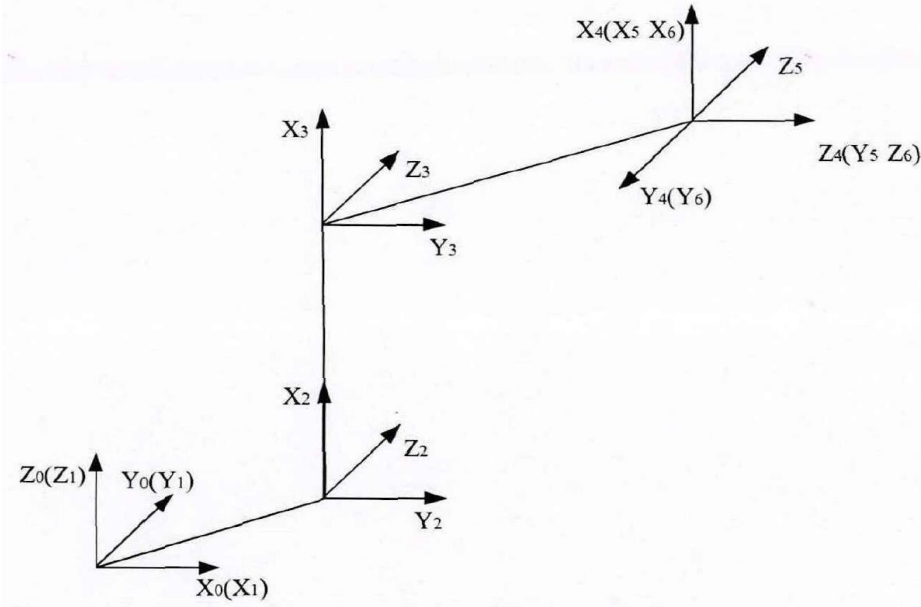


Figure 8.12 The D-H coordinate system of the linkage (Craig, 2009)

The results of the transformation matrix for the joint linkages 1-6 in Figure 8.12 are as follows.

$$\begin{aligned}
 {}^0T_1 &= [c\theta_1 \quad -s\theta_1 \quad 0 \quad 0 \quad s\theta_1 \quad c\theta_1 \quad 0 \quad 0 \quad 0 \quad 0 \quad 1 \quad 0 \quad 0 \quad 0 \quad 0 \quad 1] \\
 {}^1T_2 &= [c\theta_2 \quad -s\theta_2 \quad 0 \quad a_1 \quad 0 \quad 0 \quad -1 \quad -d_2 \quad s\theta_2 \quad c\theta_2 \quad 0 \quad 0 \quad 0 \quad 0 \quad 0 \quad 1] \\
 {}^2T_3 &= [c\theta_3 \quad -s\theta_3 \quad 0 \quad a_2 \quad s\theta_3 \quad c\theta_3 \quad 0 \quad 0 \quad 0 \quad 0 \quad 1 \quad d_3 \quad 0 \quad 0 \quad 0 \quad 1] \\
 {}^3T_4 &= [c\theta_4 \quad -s\theta_4 \quad 0 \quad a_3 \quad 0 \quad 0 \quad -1 \quad -d_4 \quad s\theta_4 \quad c\theta_4 \quad 0 \quad 0 \quad 0 \quad 0 \quad 0 \quad 1] \\
 {}^4T_5 &= [c\theta_5 \quad -s\theta_5 \quad 0 \quad a_4 \quad 0 \quad 0 \quad -1 \quad d_5 \quad s\theta_5 \quad c\theta_5 \quad 0 \quad 0 \quad 0 \quad 0 \quad 0 \quad 1] \\
 {}^5T_6 &= [c\theta_6 \quad -s\theta_6 \quad 0 \quad a_5 \quad 0 \quad 0 \quad -1 \quad -d_6 \quad s\theta_6 \quad c\theta_6 \quad 0 \quad 0 \quad 0 \quad 0 \quad 0 \quad 1]
 \end{aligned} \tag{8.15}$$

where the position of d_2 is the position of the vector element at position (Technologies & Terminology) of the coordinate system.

According to the previous equation, the total transformation matrix of the six-axis robot, and using the transformation matrix concatenation method, the transformation matrix determinant is calculated from A_1 to A_6 as follows,

$${}^4T_6 = [c_5c_6 \quad -c_5c_6 \quad -s_5 \quad 0 \quad s_6 \quad c_6 \quad 0 \quad 0 \quad s_5s_6 \quad -s_5s_6 \quad c_5 \quad 0 \quad 0 \quad 0 \quad 0 \quad 1] \tag{8.16}$$

$$\begin{aligned}
 {}^3T_6 = {}^3T_4 \cdot {}^4T_6 &= [c_4c_5c_6 - s_4s_6 \quad -c_4c_5c_6 - s_4s_6 \quad -c_4s_5 \quad 0 \quad s_5s_6 - s_5s_6 \quad c_5 \quad d_4 \\
 &\quad -s_4s_5s_6 - c_4s_6 \quad s_4c_5s_6 - c_4c_6 \quad s_4s_5 \quad 0 \quad 0 \quad 0 \quad 0 \quad 1]
 \end{aligned} \tag{8.17}$$

where s_6 in the above equation represents $\sin\theta_6$ and s_5 in the same way. As in the above equation, multiplying 1T_2 with 2T_3 yields,

$${}^1T_3 = {}^1T_2 \cdot {}^2T_3 = [c_{23} \quad -s_{23} \quad 0 \quad a_2c_2 \quad 0 \quad 0 \quad 1 \quad d_2 \quad -s_{23} \quad -c_{23} \quad 0 \quad -a_2s_2 \quad 0 \quad 0 \quad 0 \quad 1] \tag{8.18}$$

where c_{23} denotes $\cos(\theta_2 + \theta_3)$.

Multiplying Eq. 8.18 above with Eq. 8.17 again gives,

$${}^1T_6 = {}^1T_3 \cdot {}^3T_6 = \begin{bmatrix} {}^1n_x & {}^1o_x & {}^1a_x & {}^1p_x & {}^1n_y & {}^1o_y & {}^1a_y & {}^1p_y & {}^1n_z & {}^1o_z & {}^1a_z & {}^1p_z & 0 & 0 & 0 & 1 \end{bmatrix} \quad 8.19$$

Expanding the parameters 1n_x in Eq. 8.19 yields,

$$\begin{aligned} {}^1n_x &= c_{23}(c_4c_5c_6 - s_4s_6) - s_{23}s_5c_6 {}^1n_y = -s_4c_5c_6 - c_4s_6 {}^1n_z \\ &= s_{23}(c_4c_5c_6 - s_4s_6) - c_{23}s_5c_6 {}^1o_x \\ &= -c_{23}(c_4c_5c_6 + s_4s_6) + s_{23}s_5s_6 {}^1o_y = s_4c_5c_6 - c_4s_6 {}^1o_z \\ &= s_{23}(c_4c_5c_6 + s_4s_6) + c_{23}s_5c_6 {}^1a_x = -c_{23}c_4c_5 - s_{23}c_5 {}^1a_y \\ &= s_4s_5 {}^1a_z = s_{23}c_4s_5 - c_{23}c_5 {}^1p_x \\ &= a_2c_2 + a_3c_{23} + a_1 - d_4s_{23} {}^1p_y = d_2 {}^1p_z \\ &= -a_3s_{23} - a_2s_2 - d_4c_{23} \end{aligned} \quad 8.20$$

Thus, the total chi-square transformation matrix of the robot can be found as follows,

$${}^0T_6 = {}^0T_1 \cdot {}^1T_6 = \begin{bmatrix} n_x & o_x & a_x & p_x & n_y & o_y & a_y & p_y & n_z & o_z & a_z & p_z & 0 & 0 & 0 & 1 \end{bmatrix} \quad 8.21$$

Where:

$$\begin{aligned} n_x &= c_1[c_{23}(c_4c_5c_6 - s_4s_6) - s_{23}s_5c_6] + s_1(s_4c_5c_6 + c_4s_6) n_y \\ &= s_1[c_{23}(c_4c_5c_6 - s_4s_6) - s_{23}s_5c_6] - c_1(s_4c_5c_6 + c_4s_6) n_z \\ &= -s_{23}(c_4c_5c_6 - s_4s_6) - c_{23}s_5c_6 o_x \\ &= c_1[c_{23}(-c_4c_5c_6 - s_4c_6) + s_{23}s_5s_6] + s_1(c_4c_6 - s_4c_5s_6) o_y \\ &= s_1[c_{23}(-c_4c_5c_6 - s_4c_6) + s_{23}s_5s_6] - c_1(c_4c_6 - s_4c_5s_6) o_z \\ &= -s_{23}(-c_4c_5c_6 - s_4c_6) + c_{23}s_5s_6 a_x \\ &= -c_1(c_{23}c_4c_5 + s_{23}c_5) - c_1s_4s_5 a_y \\ &= -s_1(c_{23}c_4c_5 + s_{23}c_5) + c_1s_4s_5 a_z = s_{23}c_4c_5 - c_{23}c_5 p_x \\ &= c_1(c_{23}a_3 - s_{23}d_4 + a_1 + c_2a_3) - s_1d_2 p_y \\ &= s_1(c_{23}a_3 - s_{23}d_4 + a_1 + c_2a_3) + d_1 p_z \\ &= -c_{23}d_4 - s_{23}a_3 - s_2a_3 \end{aligned} \quad 8.22$$

where $[p_x \ p_y \ p_z]$ represents the position of the end-effector relative to the base coordinate system $\{0\}$, and the third-order sub-matrix $[n_x \ o_x \ a_x \ n_y \ o_y \ a_y \ n_z \ o_z \ a_z]$ represents the pose relative to the base coordinate system $\{0\}$. The pose of the end linkage coordinate system $\{6\}$ relative to the base coordinate system $\{0\}$ is obtained using the pose transformation by specifying the relevant parameters of the robot and establishing a D-H parametric coordinate system based on the model for the research demonstration.

8.2.5 Inverse kinematic solutions

Although the positive solution of the robot enables the motion control of the arm, in engineering applications, it is more often the case that the robot is required to be able to move from a starting point to a target point, given a target point. Given the position and pose of the robot's end-effector, finding the angle of rotation of each joint is called the inverse kinematics of the robot and is an essential part of kinematic analysis.

At the same time, in the inverse solution process, because there is no general solution to the nonlinear equations, the solution method is broadly divided into two categories: closed solutions and numerical solutions, but the numerical solution method has an iterative nature resulting in too slow solving efficiency, so the closed solution method is commonly used to solve the equations. For this reason, Dr Piper has developed an inverse solution process for most multi-axis robots.

For the six-axis robot shown in Figure 8.11 above, the n, o, a, p in the transformation matrix 1T_6 are fixed values since the end poses are known, and the variable θ_1 is obtained by multiplying the corresponding inverse transformation matrix left by Eq. 8.19 above, independently of ${}^{0T_1} \cdot {}^0T_6 = {}^1T_6 - s_1p_x + c_1p_y = d_2$. Then,

$$\theta_1 = \arctan\left(\frac{p_y}{p_x}\right) - \arctan\left[\frac{d_2}{\pm\sqrt{p_x^2 + p_y^2 - d_2^2}}\right] \quad 8.23$$

After obtaining the turning angle of joint 1, the corresponding joint turning angle can be obtained by multiplying the inverse matrix of T by θ_1 ,

$$\begin{aligned} [{}^1T_2]^{-1} \cdot [{}^0T_1]^{-1} \cdot {}^0T_6 &= {}^2T_6 [{}^2T_3]^{-1} \cdot [{}^1T_2]^{-1} \cdot [{}^0T_1]^{-1} \cdot {}^0T_6 \\ &= {}^3T_6 [{}^3T_4]^{-1} \cdot [{}^2T_3]^{-1} \cdot [{}^1T_2]^{-1} \cdot [{}^0T_1]^{-1} \cdot {}^0T_6 \\ &= {}^4T_6 [{}^4T_5]^{-1} \cdot [{}^3T_4]^{-1} \cdot [{}^2T_3]^{-1} \cdot [{}^1T_2]^{-1} \cdot [{}^0T_1]^{-1} \cdot {}^0T_6 = {}^5T_6 \end{aligned} \quad 8.24$$

To solve for θ_1 as an example, by $\sin(\phi - \theta_1) = \frac{d_2}{\rho}$, it follows that

$$\cos(\phi - \theta_1) = \pm\sqrt{1 - \left(\frac{d_2}{\rho}\right)^2} \quad 8.25$$

Followed by,

$$\phi - \theta_1 = \text{atan2}\left[\frac{d_2}{\rho}, \pm\sqrt{1 - \left(\frac{d_2}{\rho}\right)^2}\right] \quad 8.26$$

Therefore,

$$\theta_1 = \text{atan2}(p_y, p_x) - \text{atan2}\left(d_2, \pm\sqrt{p_x^2 + p_y^2 - d_2^2}\right) \quad 8.27$$

where $\rho = \sqrt{p_x^2 + p_y^2}$; $\phi = \text{atan2}(p_y, p_x)$. The plus and minus signs correspond to the two solutions obtained for θ_1 , respectively.

In the inverse solution solving process, $\theta_1, \theta_2, \theta_3$ due to the \pm sign, there are eight possible joint angle choices for the same wrist part stance for this six-axis robot. Also, because the first three joint angle equations exist for p_x, p_y, p_z , the second three joint angles $\theta_4, \theta_5, \theta_6$ exist for the stance angles n_x, n_y, n_z . Therefore, when the second three axes of the six-axis robot intersect at a point, the wrist mainly determines the robot stance, and the first three joints mainly determine the robot end position.

For the incremental roots that appear during the calculation process, a reasonable conclusion to the calculation must be chosen based on the feasibility of the robot kinematics.

8.3 Principle of trajectory planning

The trajectory planning of the robot mainly includes trajectory planning in joint space and trajectory planning at the end Cartesian space. When trajectory planning of the robot in joint space, only the beginning and end positions of the end motion of the robot need to be determined, and the position, velocity and acceleration of the end are not concerned. Then the angle change amount of each joint is obtained through the inverse kinematic solution. Then some interpolation algorithms are used to interpolate the angle change values of each joint. The angle change value of each joint is then interpolated using some interpolation algorithms to obtain a smooth and continuous joint angle change curve to achieve the desired angle, angular velocity, and angular acceleration. The end Cartesian space trajectory planning is mainly the description and definition of the end trajectory, which requires the use of mathematical expressions and is more concerned with the position, velocity, and acceleration of the end of the robot, and the optimal end trajectory satisfying the constraints is solved by some optimisation algorithms, and then the inverse solution is solved to obtain the angle change values of each joint. This chapter introduces joint space trajectory planning and end Cartesian space trajectory planning and presents forward and inverse kinematic simulations for a six-axis robot.

8.3.1 Trajectory planning in joint space

The joint space trajectory planning only focuses on the beginning and end positions of the robot's end, thus deriving the amount of joint value change for each joint.

When planning the trajectory in joint space, it is only necessary to know the beginning and end posture states of the robot's end motion, to obtain the joint angle variation by inverse kinematic solution, and then to interpolate the joint angle variation, and finally to find the joint angle value at each moment. The joint angle value, i.e., the joint trajectory, should satisfy the following conditions.

- (1) The joint angle change curve $\tilde{\theta}(t)$ should be smooth and monotonically increasing or decreasing from the start point θ_0 to the endpoint θ_1 within a set planning time α .
- (2) The joint angle, angular velocity and angular acceleration curves should satisfy two boundary conditions at the starting point ($t = 0$) and the end point ($t = t_f$), as follows,

$$\left\{ \begin{array}{l} \tilde{\theta}(t=0) = \theta_0 \\ \dot{\tilde{\theta}}(t=0) = 0 \\ \ddot{\tilde{\theta}}(t=0) = 0 \\ \tilde{\theta}(t=t_f) = \theta_f \\ \dot{\tilde{\theta}}(t=t_f) = 0 \\ \ddot{\tilde{\theta}}(t=t_f) = 0 \end{array} \right. \quad 8.28$$

(3) The angular velocity of the joint should be less than or equal to the maximum velocity $\dot{\tilde{\theta}}_{max}$, and the angular acceleration of the joint should be less than or equal to the maximum acceleration $\ddot{\tilde{\theta}}_{max}$.

8.3.2 Joint space trajectory interpolation

In joint space trajectory planning, interpolation functions are mainly used to interpolate joint angles, with polynomial interpolation functions being the most widely used. Cubic and quintuple polynomials are the most used among the polynomial interpolation functions. There are advantages and disadvantages to each, with the cubic polynomial interpolation function satisfying the constraints on an angle and angular velocity, but not on angular acceleration; the quintuple polynomial interpolation function meets the constraints on an angle, angular velocity, and angular acceleration, but as it is a higher-order function, it may cause the robot to jitter.

(1) Three-valued polynomial interpolation functions

If the joint angle values and the angular velocity at the beginning and end positions are known, the joint angle can be interpolated using a cubic polynomial function,

$$\tilde{\theta}(t) = a_3 t^3 + a_2 t^2 + a_1 t + a_0 \quad 8.29$$

when the constraints are,

$$\begin{cases} \tilde{\theta}(0) = \theta_0 \\ \dot{\tilde{\theta}}(0) = 0 \\ \tilde{\theta}(t_f) = \theta_f \\ \dot{\tilde{\theta}}(t_f) = 0 \end{cases} \quad 8.30$$

The polynomial coefficients can be obtained by combining the above equations to give the angle, angular velocity, and angular acceleration

$$\begin{cases} \tilde{\theta}(t) = (\theta_f - \theta_0) \left[-2 \left(\frac{t}{t_f} \right)^3 + 3 \left(\frac{t}{t_f} \right)^2 \right] + \theta_0 \\ \dot{\tilde{\theta}}(t) = \frac{(\theta_f - \theta_0)}{t_f} \left[-6 \left(\frac{t}{t_f} \right)^2 + 6 \left(\frac{t}{t_f} \right) \right] \\ \ddot{\tilde{\theta}}(t) = \frac{(\theta_f - \theta_0)}{t_f^2} \left[-12 \left(\frac{t}{t_f} \right) + 6 \right] \end{cases} \quad 8.31$$

When $t = \frac{t_f}{2}$, the angular velocity value lies at the maximum position $\dot{\tilde{\theta}}_{max} = \frac{3}{2} \left(\frac{\theta_f - \theta_0}{t_f} \right)$; when $t = 0$ or

$t = t_f$, the absolute value of the angular acceleration is maximum at this point, $|\ddot{\tilde{\theta}}_{max}| = 6 \frac{(\theta_f - \theta_0)}{t_f^2}$. Let

the $\bar{\theta} = -2 \left(\frac{t}{t_f} \right)^3 + 3 \left(\frac{t}{t_f} \right)^2$ and $\bar{\theta}$ be the normalized form of $\tilde{\theta}$ and $\bar{\theta} \in [0, 1]$.

(2) Quintuple polynomial interpolation

If the values of the joint angle, angular velocity and angular acceleration at the beginning and end positions are known, the joint angle can be interpolated using a fifth-order polynomial function as follows,

$$\tilde{\theta}(t) = a_5t^5 + a_4t^4 + a_3t^3 + a_2t^2 + a_1t + a_0 \quad 8.32$$

when the constraints are,

$$\begin{cases} \tilde{\theta}(0) = \theta_0 \\ \dot{\tilde{\theta}}(0) = 0 \\ \ddot{\tilde{\theta}}(0) = 0 \\ \tilde{\theta}(t_f) = \theta_f \\ \dot{\tilde{\theta}}(t_f) = 0 \\ \ddot{\tilde{\theta}}(t_f) = 0 \end{cases} \quad 8.33$$

The polynomial coefficients can be obtained by combining the above equations to get the angle, angular velocity, and angular acceleration,

$$\begin{cases} \tilde{\theta}(t) = (\theta_f - \theta_0) \left[6 \left(\frac{t}{t_f} \right)^5 - 15 \left(\frac{t}{t_f} \right)^4 + 10 \left(\frac{t}{t_f} \right)^3 \right] + \theta_0 \\ \dot{\tilde{\theta}} = \frac{(\theta_f - \theta_0)}{t_f} \left[30 \left(\frac{t}{t_f} \right)^4 - 60 \left(\frac{t}{t_f} \right)^3 + 30 \left(\frac{t}{t_f} \right)^2 \right] \\ \ddot{\tilde{\theta}} = \frac{(\theta_f - \theta_0)}{t_f^2} \left[120 \left(\frac{t}{t_f} \right)^3 - 180 \left(\frac{t}{t_f} \right)^2 + 60 \left(\frac{t}{t_f} \right) \right] \end{cases} \quad 8.34$$

When $t = \frac{t_f}{2}$, the angular velocity value lies at the maximum position $\dot{\tilde{\theta}}_{max} = \frac{15}{8} \left(\frac{\theta_f - \theta_0}{t_f} \right)$; when $t = \frac{3-\sqrt{3}}{6}$ or $t = \frac{3+\sqrt{3}}{6}$, the absolute value of the angular acceleration is maximum at this point, $|\ddot{\tilde{\theta}}_{max}| = \frac{10}{\sqrt{3}} \left(\frac{\theta_f - \theta_0}{t_f^2} \right)$. Let the $\bar{\theta} = 6 \left(\frac{t}{t_f} \right)^5 - 15 \left(\frac{t}{t_f} \right)^4 + 10 \left(\frac{t}{t_f} \right)^3$ and $\bar{\theta}$ be the normalized form of $\tilde{\theta}$ and $\bar{\theta} \in [0, 1]$.

8.3.3 End-to-end Cartesian spatial trajectory planning

Compared to the trajectory planning in joint space, the trajectory planning, in the end, Cartesian space is more universally applicable and is the most used. The end Cartesian trajectory planning mainly describes and defines the end trajectory, which requires mathematical expressions. It is more concerned with the position, velocity, and acceleration of the robot's end. However, once the planning is complete and the corresponding trajectory is followed, each joint must be solved in real-time.

However, after planning, the inverse kinematic solution of each joint must be solved in real-time to calculate the corresponding joint angle, which is computationally intensive and difficult to implement in real-time. The basic interpolation algorithms in robot motion control systems are linear and circular interpolation.

(1) Linear interpolation

Spatial linear interpolation is the process of finding the poses of each trajectory point by knowing the poses, i.e., position and pose, of the initial and termination points of a line. The following is a simple introduction to the principles of positional interpolation. The coordinate $P_0(X_0, Y_0, Z_0)$, $P_1(X_1, Y_1, Z_1)$ and their poses of the initial and termination points of the line are known, as shown in Figure 8.13. Let v be the required velocity; t_s be the interpolation time interval.

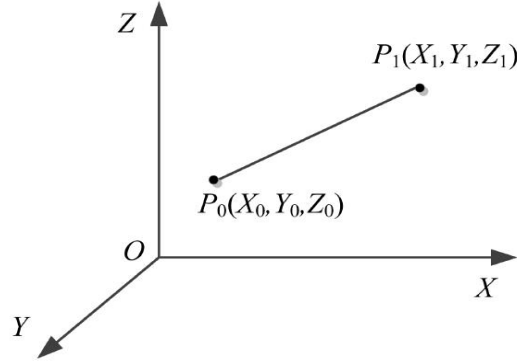


Figure 8.13 Space linear interpolation

The length of the straight line is

$$L = \sqrt{(X_1 - X_0)^2 + (Y_1 - Y_0)^2 + (Z_1 - Z_0)^2} \quad 8.35$$

The travel in time t_s is

$$d = vt_s \quad 8.36$$

The total number of interpolation steps is

$$N = INT \left(\frac{L}{d} \right) + 1 \quad 8.37$$

The increments for each axis are

$$\begin{cases} \Delta x = \frac{(x_1 - x_0)}{N} \\ \Delta y = \frac{(y_1 - y_0)}{N} \\ \Delta z = \frac{(z_1 - z_0)}{N} \end{cases} \quad 8.38$$

This gives the coordinates of each interpolation point as

$$\begin{cases} x_{i+1} = x_i + i\Delta x \\ y_{i+1} = y_i + i\Delta y \\ z_{i+1} = z_i + i\Delta z \end{cases} \quad 8.39$$

(2) Circular interpolation

A planar arc is a circular arc in a plane in the reference coordinate system, as opposed to a circular arc in space, and the interpolation of angles in the XOY plane is described below. Three points P_1, P_2 and

P_3 , are known to be non-coincident in space, and the attitude of the robot end-effector corresponding to these three points is known in Figure 8.14 and Figure 8.15

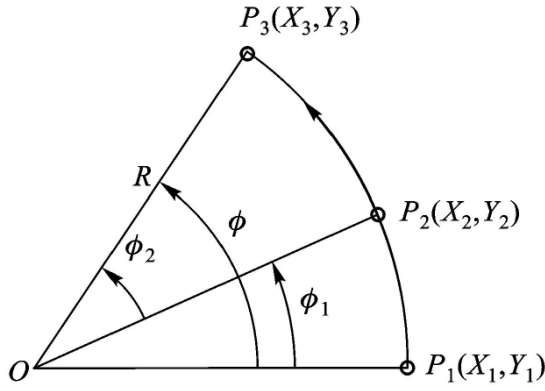


Figure 8.14 Three-point arc

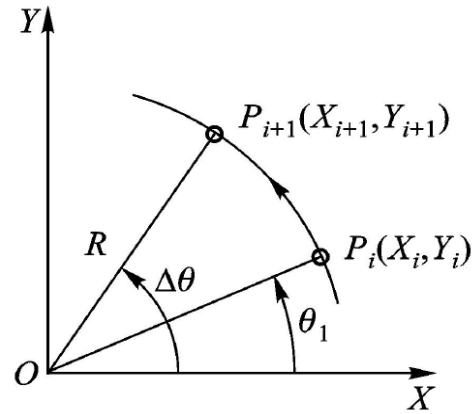


Figure 8.15 Circular interpolation

Let v be the velocity along the circular arc; t_s is the interpolation time interval. The solution process is like linear interpolation and proceeds as follows.

- (1) The radius R of the arc determined by P_1 , P_2 and P_3 is given by the radius formula $R = \frac{abc}{4S}$, where a , b and c are the side lengths of the three points, i.e.,

$$\begin{cases} a = \sqrt{(X_1 - X_2)^2 + (Y_1 - Y_2)^2} \\ b = \sqrt{(X_1 - X_3)^2 + (Y_1 - Y_3)^2} \\ c = \sqrt{(X_2 - X_3)^2 + (Y_2 - Y_3)^2} \end{cases} \quad 8.40$$

and the Heron formula,

$$S = \sqrt{p(p-a)(p-b)(p-c)} \quad 8.41$$

$$p = \frac{a+b+c}{2} \quad 8.42$$

This gives the radius of the arc as

$$R = \frac{abc}{\sqrt{(a+b+c)(a+b-c)(a+c-b)(b+c-a)}} \quad 8.43$$

- (2) The total circular angle $\phi = \phi_1 + \phi_2$, and

$$\phi_1 = \arccos \frac{(X_2 - X_1)^2 + (Y_2 - Y_1)^2 - 2R^2}{2R^2} \quad 8.44$$

$$\phi_2 = \arccos \frac{(X_3 - X_2)^2 + (Y_3 - Y_2)^2 - 2R^2}{2R^2} \quad 8.45$$

- (3) The angular displacement in time t_s is

$$\Delta\theta = \frac{vt_s}{R} \quad 8.46$$

- (4) Total number of interpolation steps are

$$N = INT \left(\frac{\phi}{\Delta\theta} \right) + 1 \quad 8.47$$

Therefore, for the coordinates of P_{i+1} , there are

$$X_{i+1} = R \cos(\theta_i + \Delta\theta) = R \cos \theta_i \cos \Delta - R \sin \theta_i \sin \Delta = X_i \cos \Delta - Y_i \sin \Delta \quad 8.48$$

where $X_i = R \cos \theta_i$; $Y_i = R \sin \theta_i$.

Similarly, it follows that

$$Y_{i+1} = R \sin(\theta_i + \Delta\theta) = R \sin \theta_i \cos \Delta + R \cos \theta_i \sin \Delta = Y_i \cos \Delta + X_i \sin \Delta \quad 8.49$$

The equation $\theta_{i+1} = \theta_i + \Delta\theta$ determines whether interpolation is complete. If $\theta_{i+1} \leq \phi$, interpolation continues; if $\theta_{i+1} > \phi$, the step size $\Delta\theta$ of the last step is corrected by $\Delta\theta' = \phi - \theta_i$. The position interpolation of the plane arc is therefore

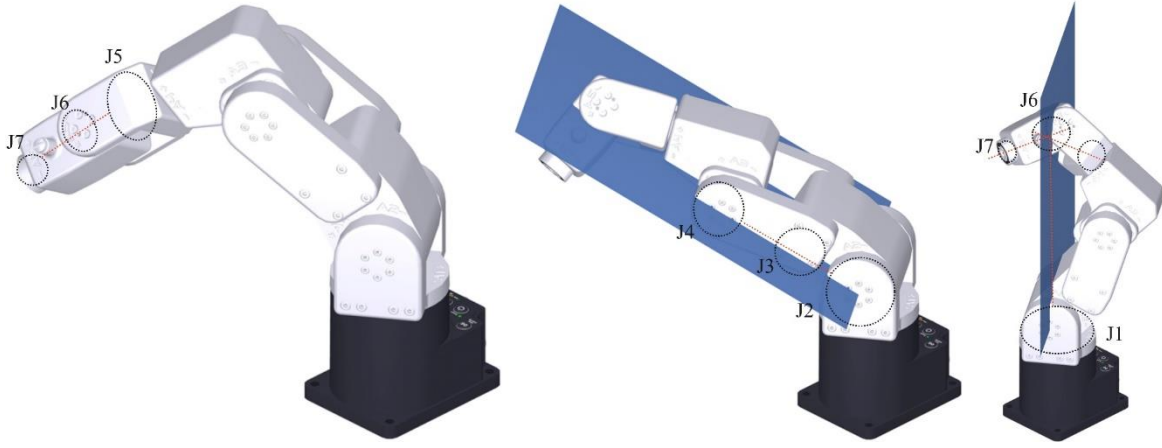
$$\begin{cases} X_{i+1} = X_i \cos \Delta\theta - Y_i \sin \Delta\theta \\ Y_{i+1} = Y_i \cos \Delta\theta + X_i \sin \Delta\theta \\ \theta_{i+1} = \theta_i + \Delta\theta \end{cases} \quad 8.50$$

8.4 Singularity avoidance and optimisation algorithms

When operating and controlling a robot, it is often necessary to set its end tools quantitatively. For example, there are specific requirements for the robot's positional attitude to reach the required workstation in manufacturing processes. At the same time, the basic mechanical structure of a tandem robot is now a relatively well-developed robot model. However, there are still some problems with tandem robots, such as singularity problems. This impacts the position control of the robot in production and can even be a cause of industrial accidents. This chapter, therefore, focuses on how to avoid 'stalling' at the singularity when the robot is close to the singularity and to achieve smooth robot operation in the singularity region.

8.4.1 Six-axis robot singularity analysis

The singularity problem is mainly due to a particular state where the Jacobi inverse solution matrix of the velocity equation cannot be solved precisely, resulting in a stall. There are specifically three central singularity locations, as shown in Figure 8.16. The singularity at a is also known as the wrist singularity, mainly because the 4 and 6 axes are parallel; the singularity at b is morphologically similar to the root node of the wrist due to the extension line of $A2 - A3$ going directly through The human shoulder joint, hence also known as the shoulder singularity; the singularity at c lies at the intersection of the $A4, A5$ and $A6$ axes where the root node of the wrist lies just above the $A1$ axis, referred to as the elbow singularity.



Modified from <https://www.mecademic.com/en/what-are-singularities-in-a-six-axis-robot-arm>
 Figure 8.16 Singularity locations of the robot arm

8.4.2 Jacobi matrix solutions

In robot motion control, there is a corresponding matrix mapping between the joint velocity and the corresponding end-effector velocity and angular velocity as in the correspondence of the previous section, and this mapping reflecting the interrelationship between joint velocity and end velocity is known in robotics as the "Jacobi matrix ". It is expressed as follows,

$$V_e = J[q] \cdot \dot{q} \quad 8.51$$

where V_e is the robot end velocity, $J[q]$ denotes the Jacobi matrix equation for the mapping from joint velocity to end velocity, and \dot{q} is the robot joint velocity. Specifically, V_e contains the terminal linear velocity and the angular velocity, which is

$$V_e = [p_e \ w_e] \quad 8.52$$

where p_e is the linear velocity of the wrist joint at the end of the robot and w_e is the angular velocity.

The Jacobi matrix $J[q]$ is therefore also divided into different Jacobi matrices depending on the type of terminal velocity, as shown in Eq.8.53 below,

$$J[q] = [J_p[q] \ J_o[q]] \quad 8.53$$

Thus, the relationship between the end velocity of the robot and the joint velocity can be expressed as

$$V_e = [p_e \ w_e] = [J_p[q] \ J_o[q]] \cdot \dot{q} \quad 8.54$$

For a six-axis robot, where $J_p[q]$ is the $3 \times n$ action matrix of the joint velocity on the terminal linear velocity, $J_o[q]$ is the $3 \times n$ action matrix of the joint velocity on the terminal angular velocity. In the Jacobi matrix, the number of rows and columns of the matrix is clearly defined, the number of rows of the matrix is the number of degrees of freedom of the robot in the Cartesian spatial coordinate system, and the number of columns of the matrix is equal to the number of joints of the robot so that the Jacobi matrix can be chunked as

$$[p_e \ w_e] = [J_{P1} \ J_{P2} \ J_{P3} \ J_{P4} \ J_{P5} \ J_{P6} \ J_{W1} \ J_{W2} \ J_{W3} \ J_{W4} \ J_{W5} \ J_{W6}] \cdot [\dot{q}_1 \ \dot{q}_2 \ \dot{q}_3 \ \dot{q}_4 \ \dot{q}_5 \ \dot{q}_6]^T \quad 8.55$$

The linear velocity p_e of the above equation is therefore expressed about the angular velocity w_e for each joint velocity \dot{q} as

$$p_e = J_{P1} \cdot \dot{q}_1 + J_{P2} \cdot \dot{q}_2 + \dots + J_{P6} \cdot \dot{q}_6 \quad W_e = J_{W1} \cdot \dot{q}_1 + J_{W2} \cdot \dot{q}_2 + \dots + J_{W6} \cdot \dot{q}_6 \quad 8.56$$

where the equations J_{pi} , J_{wi} represent the terminal linear and angular velocities caused by the unit angular velocity of joint i , respectively.

The vector product method and the differential transformation method are usually used in calculating the Jacobi matrix. The Jacobi matrix of the robot's rotating joint i concerning the z-axis of the coordinate system i is given by the differential rotation d_θ of joint i concerning $i - 1$,

$${}^T J_i(\theta) = [{}^T dx \ {}^T dy \ {}^T dz \ {}^T \delta x \ {}^T \delta y \ {}^T \delta z] = [(p \times n)_z \ (p \times 0)_z \ (p \times a)_z \ n_z \ o_z \ a_z] d\theta_i \quad 8.57$$

where n, o, a, p is the coordinate axis vectors and posture vectors under joint i , respectively. In Eq. 8.57, $(p \times n)_z, (p \times 0)_z, (p \times a)_z$ are denoted as

$$(p \times n)_z = -p_y n_x + p_x n_y \quad (p \times o)_z = -p_y o_x + p_x o_y \quad (p \times a)_z = -p_y a_x + p_x a_y \quad 8.58$$

Combined with the tandem six-axis robot model used in this thesis, the Jacobi matrix should be six columns, and ${}^T J_i(\theta)$ is calculated from the rotation matrix ${}^i T_n$.

8.4.3 Singularity generation mechanism

In robot path planning, the joint velocity is obtained by multiplying both sides of the equation left by $J[q]^{-1}$ via Eq. 8.51 and converting $J[q]^{-1}$ to a component equation, as shown in Eq. 8.59.

$$q = J[q]^{-1} \cdot V_e = \frac{(J[q])^*}{|J[q]|} \cdot V_e \quad 8.59$$

In Eq. 8.59, if $|J[q]|$ is not of full rank, i.e., there is unsolvability in the inverse solution of the robot velocity when the robot is at the singularity position. Therefore, according to $|J[q]|$ non-full rank when the θ position is different into wrist axis singularity, wrist root singularity. The wrist axis singularity is shown in Modified from <https://www.mecademic.com/en/what-are-singularities-in-a-six-axis-robot-arm>

Figure 8.16 above when 05 is 0° , axis 4 is co-linear with axis 6, resulting in s_5 being 0 in the Jacobi matrix, $\det \det (J(\theta)) = 0$. As known from Eq. 8.59, the denominator tends to 0, and the fraction tends to infinity, eventually making the robot stall near this singularity, causing some industrial hazard.

8.5 Optimisation of robotic arms

A six-axis robot is a highly non-linear, spatially linked mechanism. Its structure is subject to many constraints and technical requirements, making optimal robot control difficult. In addition, when the robot is in an environment with obstacles, it must follow a planned geometric path during operation and avoid all obstacles. Therefore, the robot's trajectory can be pre-planned and then the robot can be controlled to follow this optimised trajectory. That is, the optimal trajectory is planned in offline mode and then tracked online in real-time.

Both the joint and Cartesian spaces constrain the robot trajectory optimisation problem. It is necessary to translate the quintic polynomial function that interpolates the robot's joints from Cartesian space into joint space and then control the robot's joint operation in joint space. It is, of course, possible to translate the constraints in joint space into Cartesian space and then control the robot for trajectory finding. However, due to the highly coupled and non-linear nature of the robot dynamics equations, the latter approach is complicated via analytic equations. In contrast, it is much more convenient and easier to handle in joint space. And operating in joint space has the advantage that the control system acts as an operational joint rather than an end-effector. Therefore, it is easier to adapt the trajectory to the design requirements in an articulated space. Moreover, planning the robot's trajectory in joint space also avoids the problems of kinematic singularities and operator redundancy.

Therefore, the predetermined trajectory of the robot arm in Cartesian space is translated into the trajectory of each joint in joint space, with each joint having a corresponding joint trajectory. A curve fitting method can take some appropriate points on the predetermined trajectory of the robot arm in Cartesian space and convert them into joint coordinates by inverse kinematic methods. Each joint uses a fifth-order polynomial function to smoothly connect the points to form the intended trajectory of that joint. In this way, each trajectory in Cartesian space has a corresponding joint trajectory in joint space. Finally, each joint follows the corresponding trajectory during the motion of the robot's articulated arms. The result of all the articulated arms moving simultaneously is that the end of the robot's arm approximately follows the trajectory predetermined in Cartesian space. For the robot's state of motion, the mechanical characteristics of the robot require that the velocity and acceleration at each joint are limited to the maximum value that their structure can provide so that the drive does not exceed the full load. Therefore, given the geometrical path of the robot, it is also necessary to optimise the parameters such as speed and acceleration for the operation of each joint. To not cause mechanical resonance in the robot, the trajectory of the joints needs to be smooth and continuous. The acceleration profile is also desirable to be straight and smooth, so the acceleration is bounded. It is essential to limit the acceleration because higher acceleration values increase the wear and tear on the mechanical structure, stimulate mechanical resonance and reduce the life of the mechanical components. In contrast, lower joint acceleration makes the robot more accurate and efficient in performing tasks.

General trajectory planning studies perform optimisation in the following areas: shortest time, lowest energy consumption, most minor impact, or a combination of several metrics together in multi-objective optimisation. Optimising the shortest time trajectory requires finding an optimal time sequence that allows the robot to complete a given task in the shortest time, provided that the constraints of the problem and the specified performance metrics are satisfied. On the other hand, energy minimisation trajectory optimisation requires that the robot consumes the least amount of energy to complete a given task while satisfying the constraints of the problem and the specified performance metrics. Impact minimisation trajectory optimisation, on the other hand, involves optimising parameters such as the robot's speed and acceleration to reduce robot vibration and impact while satisfying the requirements of the problem.

When the robot is working on a task, the time between interpolation points can be adjusted by calling the optimised control program for the set trajectory. The problem constraints are met, thereby reducing the movement time of the joints throughout the process much as possible. At the same time, the time interval is optimised, and the time at each interpolation point is calculated. Then a real-time online calculation is performed based on the time series of each joint to achieve real-time control of the robot. However, as optimisation of robot trajectories is a non-linear dynamic optimisation problem, it is complex to solve. Many researchers have applied artificial intelligence optimisation methods to optimise robot trajectories in recent years, with good results.

8.6 Algorithm simulation and analysis

The example of using robotic arm to fabricate timber joint introduced in Chapter 4 shows one problem in tool path planning. The non-standard geometric model needs cutting surface to teach the end-effector to follow the tool path. The vertices of the cutting surfaces and different order of the cutting surface can lead to singularities. The designating process is operated manually and needs to be checked with kinematic singularities, shown in Figure 8.17. Whether the adjusted tool path is the best one with the shortest distance and minimum energy is not determined and this needs further validation.



Figure 8.17 Kinematic singularities

During the robot's motion, the joints should run smoothly, as jerky movements increase the wear and tear of the machine components and can cause vibrations in the robot arm, resulting in a poor quality of work that does not meet the desired work requirements well. For this reason, the selected expression for the motion trajectory description function must be continuous, and the degree of smoothness of the expression must be determined according to the work requirements. The trajectory planning operation can be carried out either in joint or Cartesian spaces. Trajectory planning in joint space involves

expressing the rotation angle of each joint of the robot as a function of time and analysing the robot's motion at each moment using these function expressions; In contrast, trajectory planning in Cartesian space involves expressing the position, velocity, and acceleration of the end of the robot arm as a function of time. The corresponding motion state of each joint information is derived through the state information of the end-effector.

To optimise the whole robotic fabrication process including travel distance and travel time, the optimal model is set as follows:

Minimize distance D :

$$D = \sum_{i=1}^N L_i + \sum_{i=1}^{N-3} \sum_{j=1}^M L_{i,j}$$

Subject to:

$$\left\{ \begin{array}{l} p_k(t) \in U_j, k = 1, 2, \dots, n \\ x_e(t) \in U_x \\ y_e(t) \in U_y \\ z(t) \in U_z \\ |J|q| \neq 0 \end{array} \right.$$

Minimize travel time T :

$$T = \sum_{i=1}^{n-1} h_i = \sum_{i=1}^{n-1} (t_{i+1} - t_i)$$

Subject to:

$$\left\{ \begin{array}{l} |\dot{p}_i(t)| \leq VC_i, i = 1, 2, \dots, N \\ |\ddot{p}_i(t)| \leq WC_i, i = 1, 2, \dots, N \\ |\ddot{p}_i(t)| \leq JC_i, i = 1, 2, \dots, N \end{array} \right.$$

The overall optimisation step is:

- (1) Build the robotic arm model in Matlab using DH method, shown in Figure 8.18;
- (2) Transform geometric model of tool path in Rhino (Figure 8.19) into the numerical data in Matlab (Figure 8.20).
- (3) Compute the working space limits for robotic arm, shown in Figure 8.21;
- (4) Compute the optimisation model using Particle Swarm Optimisation (PSO) and Adaptive Genetic Algorithm (AGA) optimisation algorithm, shown in Figure 8.22;

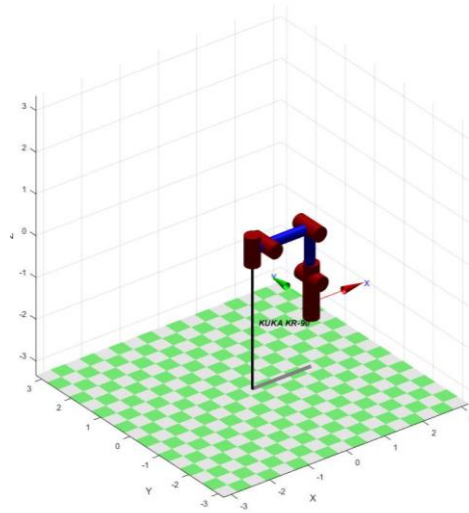


Figure 8.18 KUKA KR-90 Robotic arm model

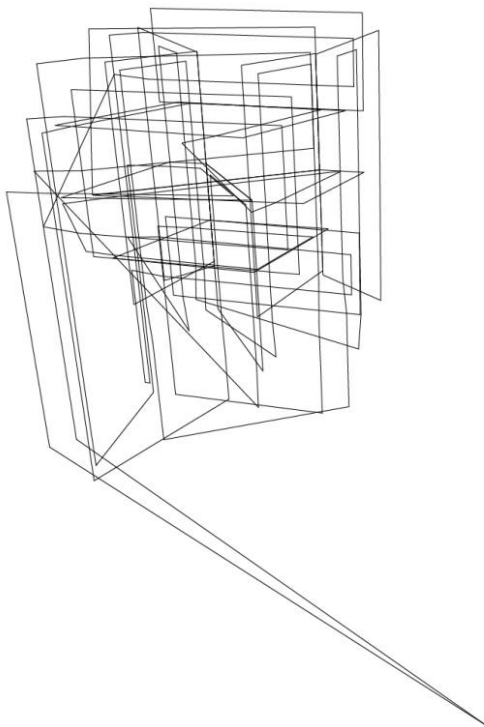


Figure 8.19 Tool path from Rhino

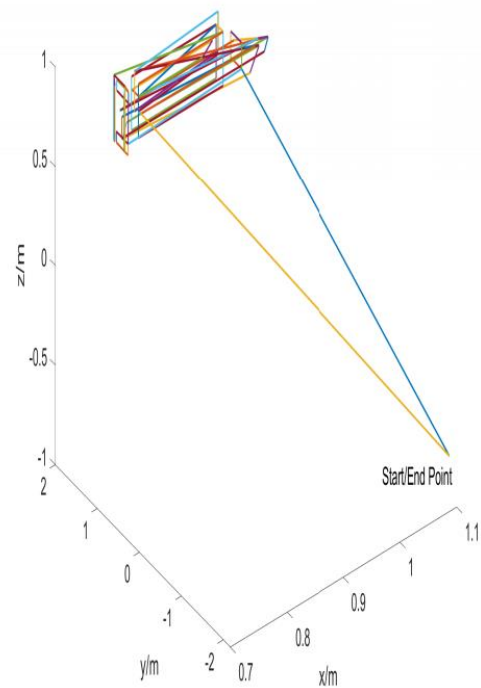
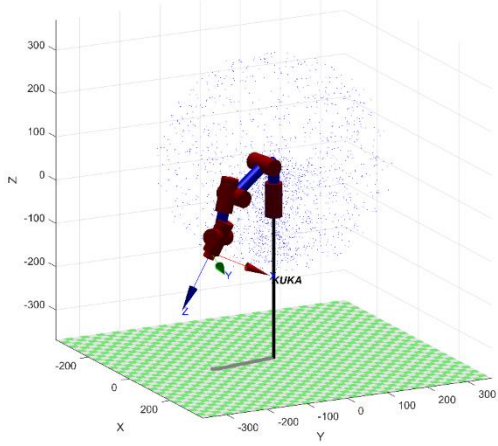
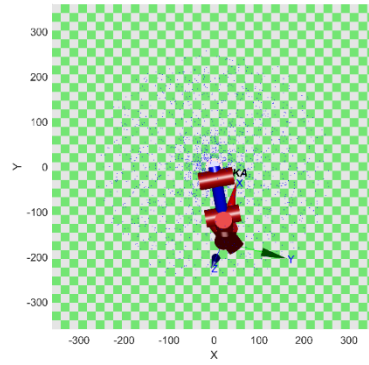


Figure 8.20 Tool path in Matlab

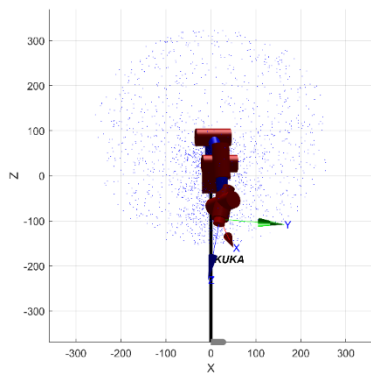
The example selected 13 cutting surfaces which has 66 tool paths. The initial trajectories of the 66 paths of six joints are shown in Figure 8.23. Figure 8.24 presents the initial and optimised tool path between each cutting surface as the travel within every cutting surface is the same. The travel distance has shortened after 350 iterations.



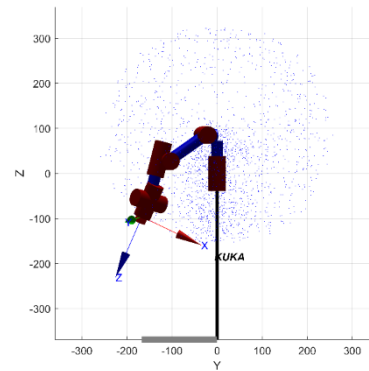
(a) Working space limits in three-dimension



(b) Working space limits in xoy coordinate



(c) Working space limits in xoz coordinate



(d) Working space limits in yoz coordinate

Figure 8.21 Working space limits

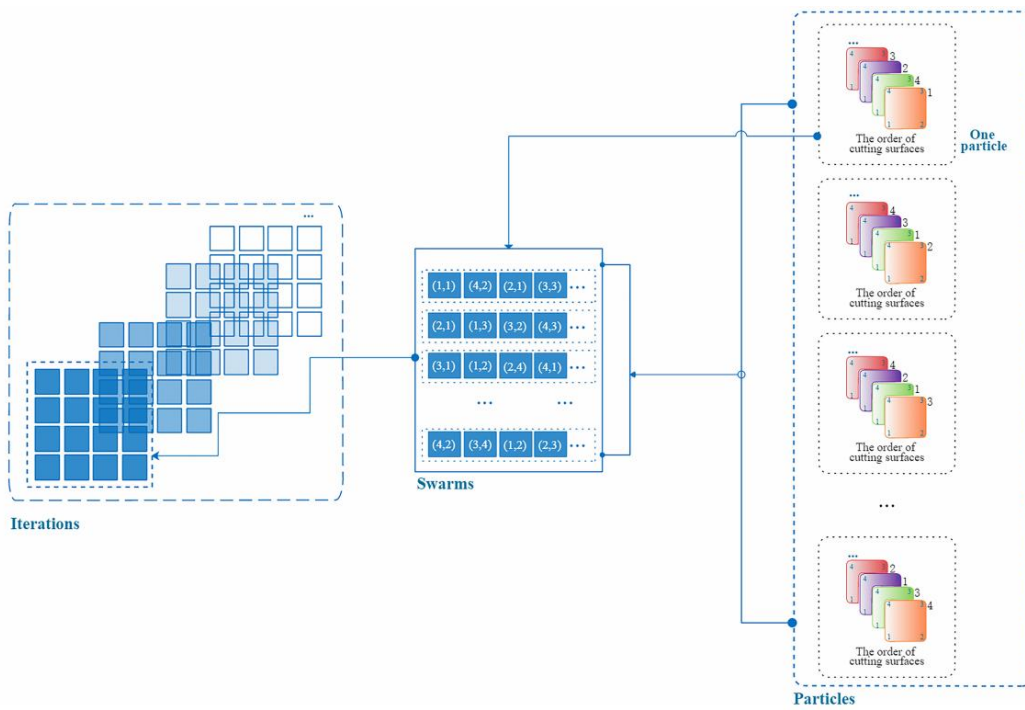


Figure 8.22 Modified PSO model for path planning

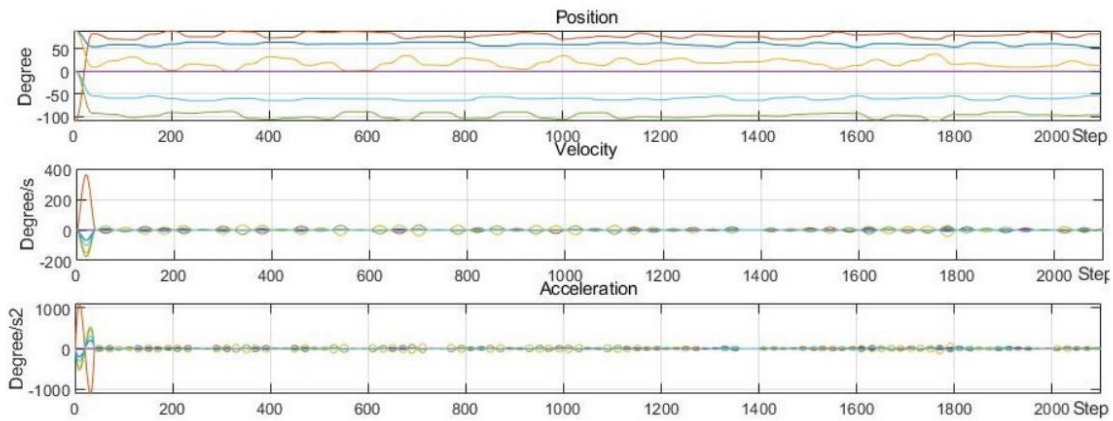


Figure 8.23 Trajectories of 66 tool paths

Because the robotic end-effector moves in a linear way within each cutting surface, the distance between them is the one to optimise. Figure 8.24 depicts a comparison of the original tool path and the optimal one. For clarity, the travel within each cutting surface is omitted. The optimisation performance is shown in Figure 8.25. This shows the value for the travel distance decreases as the number of iterations increases which demonstrates the effectiveness of PSO algorithm in optimising the travel distance with sharp decrease rate. Furthermore, the reduced travel distance is a new cutting order for the new tool path that is free of singularities. PSO can automatically generate the path with the shortest distance and no singularities.

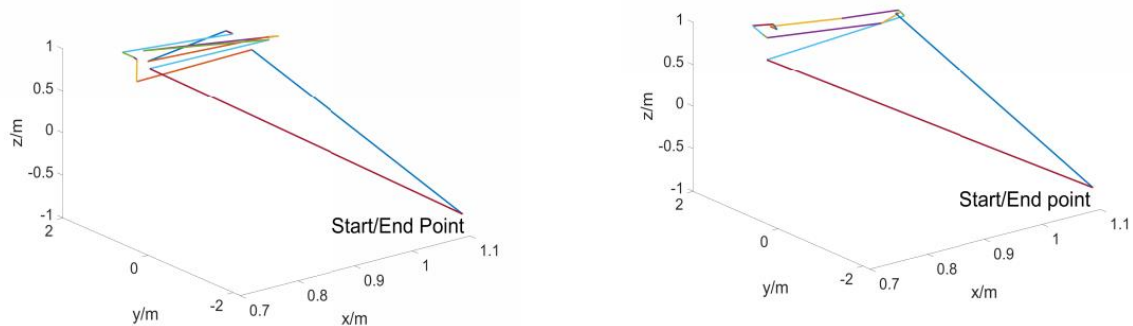


Figure 8.24 The initial tool path and the optimised tool path

The AGA optimisation selected the first cutting surface as the optimisation objective which has four tool paths. The initial trajectories of the joints in position, velocity and acceleration are shown in Figure 8.26 (a), (c), (e) and the optimised ones are shown in Figure 8.26 (b), (d), (f). The evolution of 100 generations of six joints are shown in Figure 8.27-Figure 8.29 which validates the convergence of the optimisation with increased fitness value and decreased travel time. The smooth trajectories of the six joints of four tool paths also means the smooth operations of the robotic arm which can reduce the vibration of the machine. More detailed description can be found in Appendix 3.

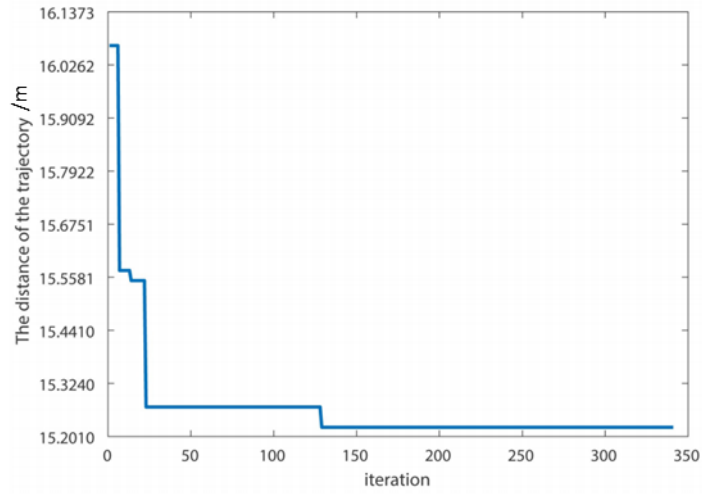
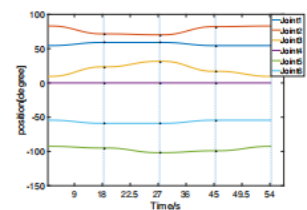
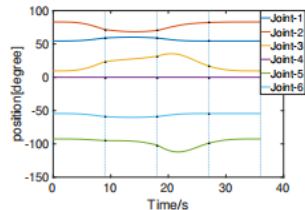


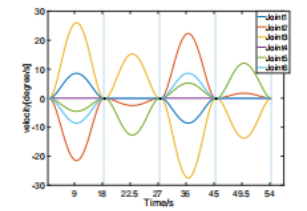
Figure 8.25 The optimised travel distance



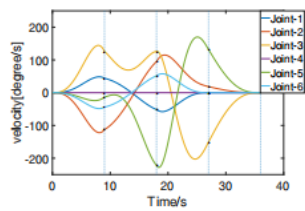
(a) Position of 6 Joints for the Initial Trajectory



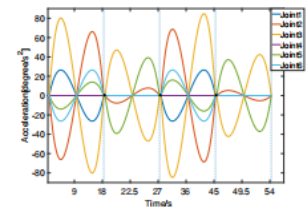
(b) Position of 6 Joints for the AGA Time-Optimal Trajectory



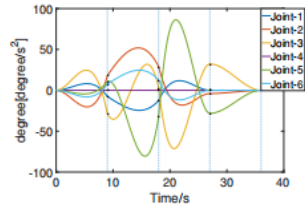
(c) Velocity of 6 Joints for the Initial Trajectory



(d) Velocity of 6 Joints for the AGA Time-Optimal Trajectory



(e) Acceleration of 6 Joints for the Initial Trajectory



(f) Acceleration of 6 Joints for the AGA Time-Optimal Trajectory

Figure 8.26 Initial trajectories and optimised trajectories of six-joints

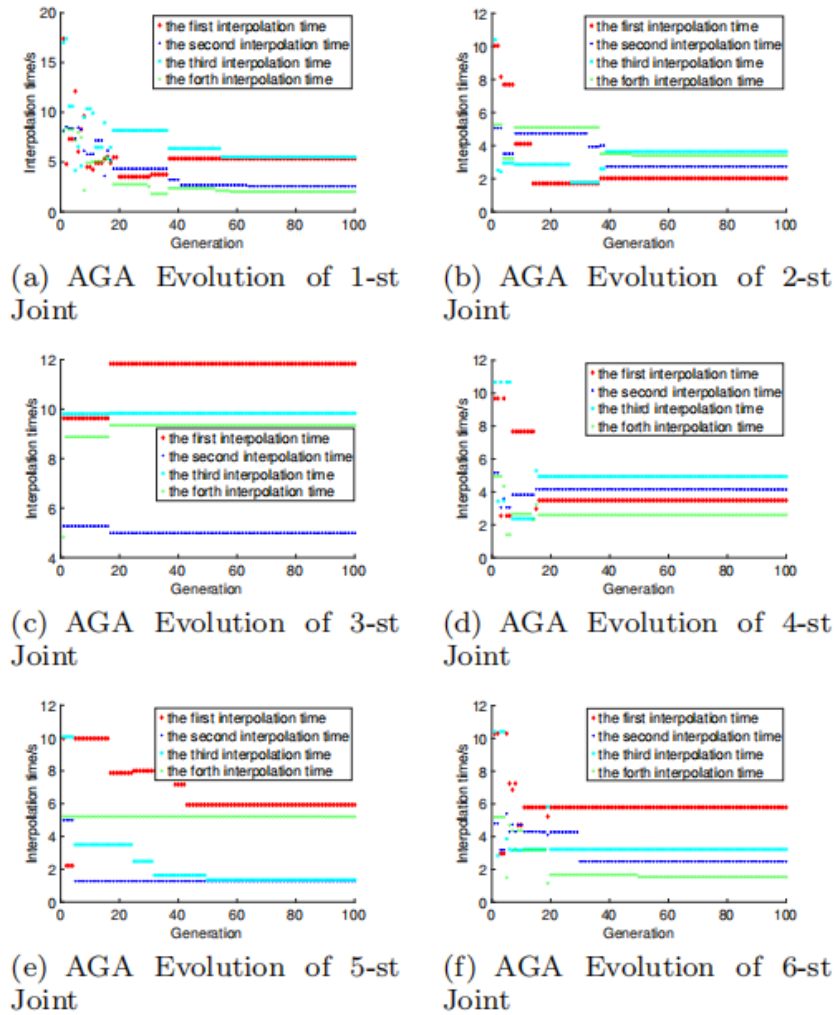


Figure 8.27 The evolution results of AGA of six joints of four tool paths

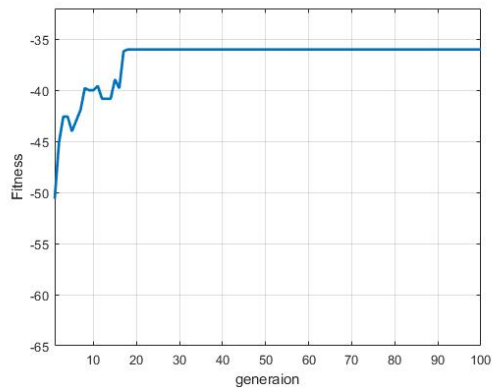


Figure 8.28 Fitness value after 100 generation

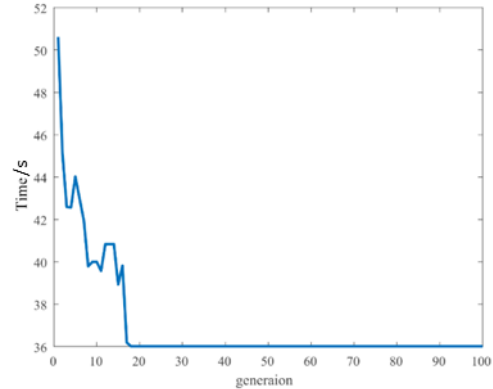


Figure 8.29 Time value after 100 generation

The comparisons between the optimal values and the original values on time and travel distance are shown in Figure 8.30. The travel distance has shortened from 16.1m to 15.2m with a 5.6% reduction. The reason for the lower decrease is that the travel distance includes the distance within each cutting surface as well as the distance between surfaces. Because the distance between each cutting surface remains constant, 5.6% is insignificant. The travel time reduces from 55s to 35s within each one cutting surface with a 36.3% reduction.

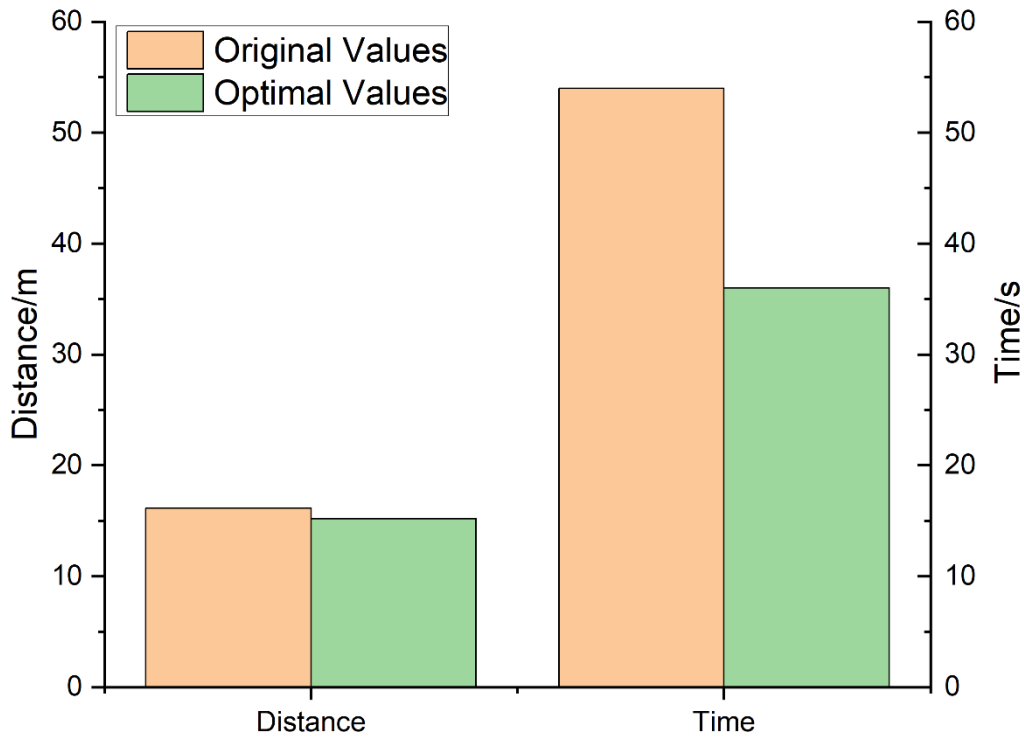


Figure 8.30 Comparisons between the original and the optimal value for time and distance

The optimisation results mean that in this robotic chainsaw cutting case, the reduced operation time means higher productivity in a same period of time. Besides, the comparisons of the curve in Figure 8.26 shows the optimal curve is smoother than the original one which means energy saving in dynamics context. Though the robotic arm is heavy, it is not a rigid body, and smooth motion control can bring stability to the equipment, which means it is more cost effective in the long run.

8.7 Conclusion

Based on the question put forward in Chapter 4 about how to adapt robotic automation technique into larger scale production by saving time and manual work in adjustment, this chapter establish a workflow to solve the questions. Furthermore, this chapter tests the hypothesis in Chapter 8 that either standard or non-standard objects can be fabricated by common robotic fabrication tasks such as cutting as long as the working limitation of the robotic arm is calculated in advance.

This chapter provides a more comprehensive introduction to the robotic arm from a robotics perspective. Chapter 4 mentions the two-link robotic arm in two and three dimensions using trigonometric functions for its spatial position. This chapter uses robotics to express the multi-degree-of-freedom robot through mathematical models using quaternions as well as spatial transformation matrices. In Chapter 4, the actual robotic chainsaw cutting case is presented, which deals with the theory of robot forward and inverse kinematics, robot arm trajectories, and motion control. Through a comprehensive and systematic introduction of the DH method, the interpolation simulation method of forward and inverse kinematics, the optimisation of the motion distance and time of the trajectory of the six-axis robot arm in the actual cutting process is proposed. By extracting the geometric information from Rhino and modelling the robot arm in Matlab using the DH method and simulating the original machining path, PSO and AGA

are used to optimize the motion distance and motion time, respectively. The effectiveness and rationality of the two algorithms for the specific machining process of robotic arm cutting are obtained.

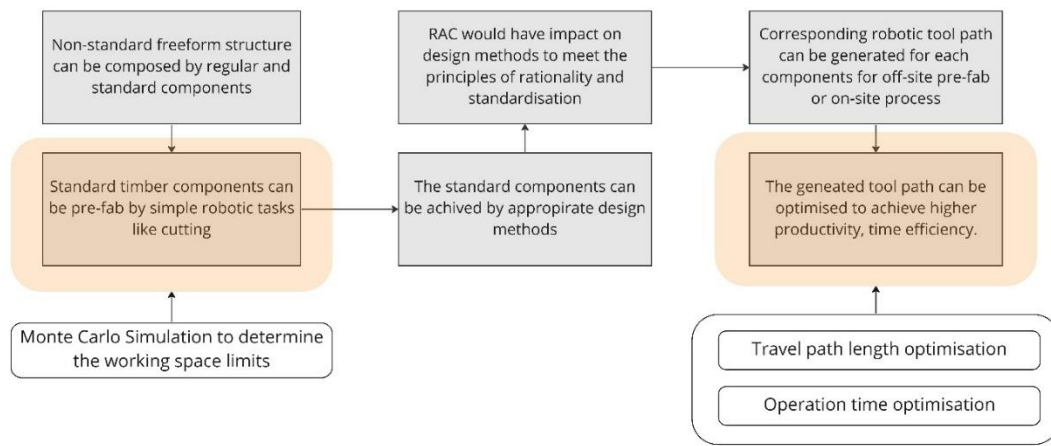


Figure 8.31 Connection to Hypothesis

The workflow and algorithms are applied in the robotic chainsaw cutting case. However, this workflow is general and can be applied in other scenarios. For example, in a milling case, the travel distance and the operation time can still be optimised by following the steps: transform the geometric information into spatial position for robotic arm, define the parameters for optimisation, interpolate the trajectories, define the constraints and operate the optimisation. The results of the optimisation show that after certain optimisations, robotic automation construction can achieve a higher level of automaticity, time efficiency, energy efficiency, and flexibility to be used in mass production for non-standard structures. As referring to the optimal principles in Chapter 3, this whole chapter shows the complexity of optimizing the tool path for different structure components. How to reduce the complexity of fabrication by optimising the freeform surface design is put forward which would be solved in Chapter 9 see Figure 8.32.

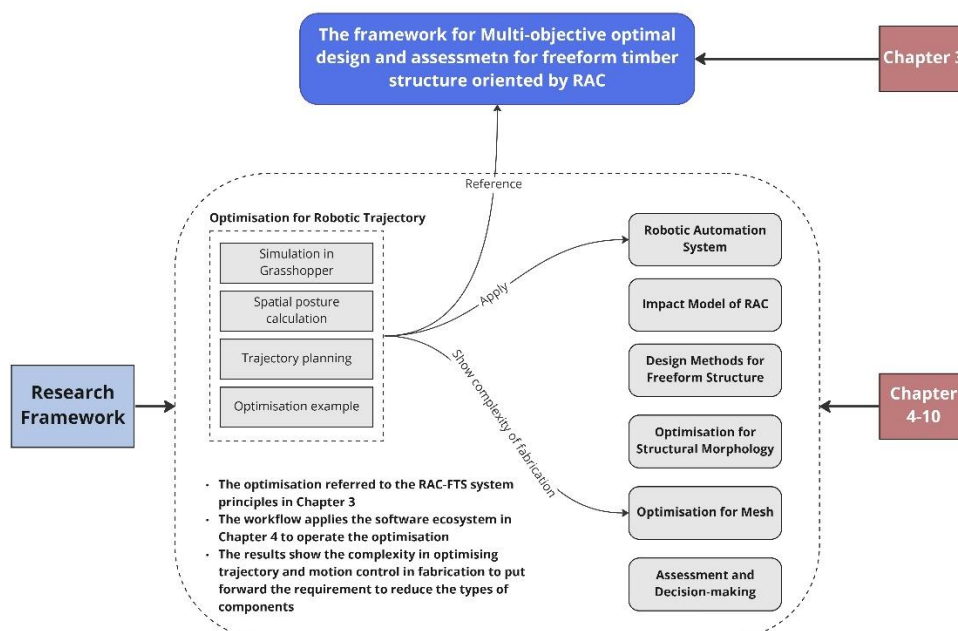


Figure 8.32 Connection to other chapters

Chapter 9

Rationalisation and Modularisation of Freeform Timber Structure Components

Based on the simulation of the robotic trajectory in Chapter 8, the optimised algorithm can be applied to different geometries. The components to be manufactured are part of a FTS, which is a non-linear structural system with a wide range of components that require individual trajectory optimisation for different sizes and geometries in order to produce a trajectory with no kinematic singularities and time or energy optimisation. This means that in mass production, a separate optimisation is required for each component fabrication, and the number of tool paths almost equal to the number of components which means low repeatability of the equipment. Such extensive optimisation and path generation reduces fabrication efficiency and is not in line with the characteristics and principles put forward in Chapter 3.

Based on the optimised geometry, it is necessary to move from geometric design to component scale design, with the aim of standardisation to reduce the variability of many components. Therefore, to realise this process, this chapter introduces the theory of modular design for assembled buildings and composes its main theories. Its architectural characteristics and advantages are systematically analysed, and the discussion is developed in terms of the classification of the modular design system for assembled buildings, the constituent elements, and the architectural advantages, and the concept is introduced to non-standard freeform structures. The standardisation of the components is achieved through the process of freeform mesh homogenisation, which improves the quality of the mesh cells and increases the geometric accuracy of the components because of satisfying the processing efficiency of large-scale automated manufacturing. This provides a sufficient basis for the robotic arm to be used in mass production.

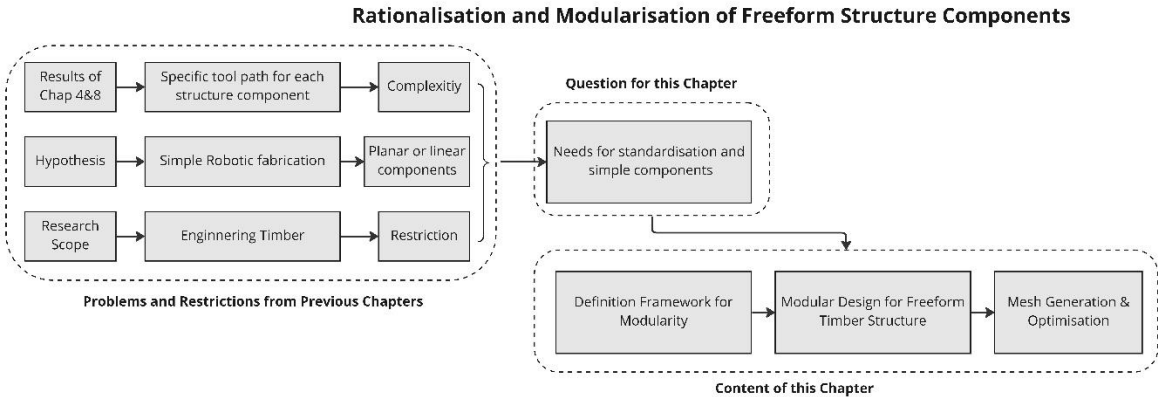


Figure 9.1 Roadmap for Chapter 9

9.1 Overview of modularity

Modularity has its own theoretical basis and its own history of development. By studying the development of modularity theory and the use of modularity in other professional fields, modularity from the point of view of design thinking is more borrowed from the idea of industrial design, i.e., a

high degree of unity between design and construction. In the current era of information technology, the professional division of labour in the construction industry has put forward higher requirements for inter-professional cooperation and synergy. The modular design of assembled buildings differs from that of traditional buildings in its use of modular design thinking. On the one hand, it is necessary to consider the characteristics of assembled buildings, and on the other hand, it is necessary to satisfy the need to combine modular design ideas into the design of assembled buildings.

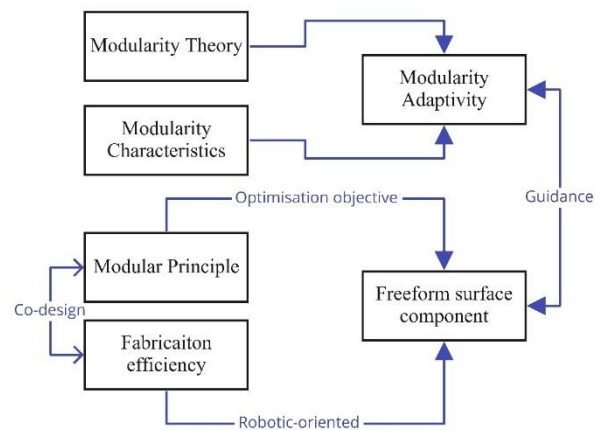


Figure 9.2 Research concept of chapter 9

9.1.1 The Theory and Aim of Modularity

Modularity theory started out in the field of industrial organisation and evolved into a methodology for solving complex problems as modularity was applied from production to design. Modularity theory is based on the relationship between 'decomposition' and 'combination', in which complex systems are decomposed into modules, which are then efficiently configured to form systems by combining different functional modules. It addresses the question of how a system is decomposed into modules and how the modules are brought together to form a system. Because modular theory is an interdisciplinary approach to research, it often incorporates the researcher's own field of study. The characteristics of modular operation (modular independent design, modular extensibility and flexibility, modular adaptability) have all contributed to the use of modular theory in various fields. This has also created the conditions for the introduction of modularity theory into the construction industry as a tool and strategy for solving architectural design problems.

Another important concept in modularity is that of modulus. Modern modulus theory in architecture proposes two concepts, modulus, and modulus series. Modulus refers to the repeated use of a reference dimension for the sake of uniformity in design and calculation, the modulus can be seen as a reference for other dimensions, which are used as multiples of the reference dimension. If M is the basic modulus, then M is the minimum size base, which can form $1M$, $2M$, $3M$, etc. Similarly, M can be divided into $1/2$, $1/3$ and $1/4$ moduli as partition moduli. The fixed ratio of the moulded parts allows for maximum interchangeability and compatibility. The modal system of construction has been implemented in architecture to specify the smallest building components, elements, and products such as bricks, blocks, windows, doors, and sanitary equipment, as well as the span, column spacing, floor height and layout

axis of a building. The use of the modal theory of architecture can increase the generality of building components and improve the industrialisation of buildings.

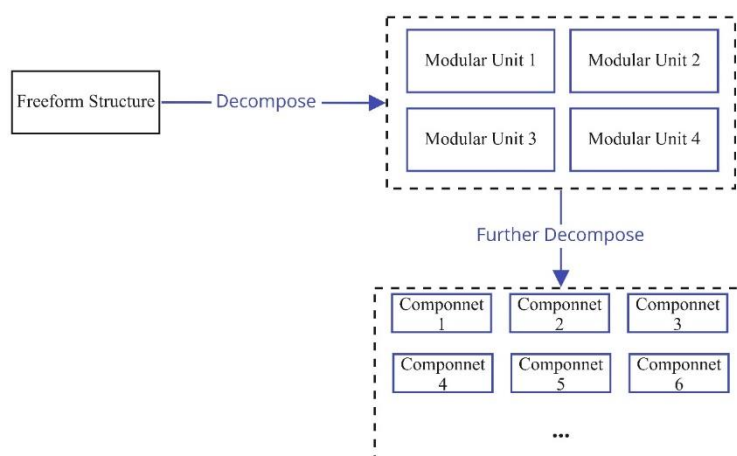


Figure 9.3 Modularisation of freeform structure

The modular thinking of modular construction makes extensive use of modular units and components, shown in Figure 9.3, all of which are prefabricated in the factory and transported to the site for lifting and installation. The modular elements have their own structure and function and can exist independently of the outside world. At the beginning of the twentieth century, when social production began to shift from handicrafts to large industries, the traditional efficiency of construction in the field of architecture was no longer sufficient to meet the demands of modern industrialised production. To adapt architecture in terms of function, structure, and form to the development of industrialised society, the modernist movement began to emerge. As a representative figure in this movement, Le Corbusier proposed the "Domino" system¹⁶. The system expresses the concept of modular design and construction in a more purely structural prototype and reproducible product. Since then, a series of architects have used simple and basic modular forms to create a wide variety of architectural forms.

Modularity as a tool for thinking, it makes the structural system of the object of study more inviting through modularity, makes its composition orderly and standardised, and improves the overall operational efficiency of the object of study. Specifically, it simplifies the structure of complex systems through the modularisation of the system, to improve design efficiency and increase the flexibility of the product. Modularity has several purposes at the RAC-FTS:

(1) Optimising the structure of components : Conventional components are generally composed directly according to the project requirements and the components are almost always completely new designs. Components are therefore High production costs and difficulty in production. They are slow to iterate and cannot be adapted to complex market changes. The modular component approach therefore enables the most varied products to be produced with a minimum of components.

¹⁶ The "domino", which translates from Latin as "dwelling domus" and also means domino, is a system of six columns with a floor slab that forms the base plane and can be replicated in an infinite number of vertical superimpositions.

(2) Optimisation of the production structure model: The traditional production model for a construction project often invests huge amounts of money in construction and production cycles, which is determined by the way it is built. The significance of modular production, on the other hand, greatly solves the problem of production efficiency. The modular, prefabricated production allows most of the work to be carried out within the modular unit. Installation of the modules work can be carried out quickly and efficiently on the production site, and production and construction begin to shift towards semi-automation.

(3) Optimisation of management systems: In life cycle construction, management involves the collaboration and division of labour between different parts of the work. With the development of information technology in recent years, construction projects are becoming more and more complex and diverse. The coordination of the different parts of the project requires rapid co-ordination and decision making, which is why the traditional management system lags behind to a greater or lesser extent. By applying the idea of modularity to the management system, the functions of each department are regarded as different functional modules, and these modules are combined into various subsystems. These modules are combined into sub-systems, which in turn form the larger system. In this process, a clear organisational structure for engineering can be established and management efficiency can be improved.

(4) Optimising the information structure: Current construction industry is gradually taking on the characteristics of information technology. Faced with a large amount of information, it is necessary to be able to classify and process all types of information according to their properties by establishing a modular information management approach, to access optimised information access channels and to process all types of information more efficiently.

9.1.2 Features of Modularity

Modularity as a form of standardisation as well as being widely used in all aspects of life, but the meaning of modularity varies in different areas. This section reviews and analyses the concept of modularity by analysing its use in life and summarises its characteristics.

The development of modular design is a new idea developed on traditional design thinking and has now become a new idea that is widely used. Especially in the information age, the use of modular thinking in the field of architecture is also increasing. The main trend in the development of modular design methods is to study the system composition of building modules rather than to study the solution of specific problems, secondly, the main design method of modularity is to use the decomposition and combination of systems to analyse module design, and finally, modular design has a strong flexibility, and the design process is a sustainable, dynamic Thinking process. The functions and spaces of buildings change over time, and modular design can solve these problems through flexible design strategies. The idea of modularity is now widely used in a number of fields, and it is meeting the needs of industrial mass production while also expanding its use through customisation and diverse design approaches. The development of combined machine tools has made modularity a step forward. Machine tools are made

up of components such as power heads, columns, slides and spindle boxes, and machine tools can be made up of components for specialised machines with different functions. Some of these components are universal, some are specialised, and when a new product is required, it is only necessary to design the combined relationship of the components in accordance with the product process, which can constitute a new product machine tool. In the case of machine tools, the basic feature of modularity is that a system can be broken down into a number of individual components, which can then be combined to form new system. In the 1950s, experts introduced the concept of 'modular design'. Since then, experts from various industries have supplemented and improved modular design and its theory, and modular design has become a common design thinking used in many fields. The basic idea is to select the smallest unit that can represent the basic function as the basic module, and through different organisation and deployment methods, to build a whole system that can be adapted to different uses. The designer only needs to control the functional relationships of the different modules, avoiding a lot of duplication of work. For modular building design, the core of modular architecture is simply the use of uniform building units to solve complex design problems.

9.1.3 Analysis of the Applicability of Modularity to FTS

Modularity can be applied to the FTS through two main methods: 1) digital holistic design approach and 2) Standardised unit combination design.

Digital holistic design approach: There are many ways of designing architectural forms, for example, the religious architecture of the medieval period in Western Europe took a non-Euclidean approach to geometric design, using a series of mathematical formulas to extrapolate and study the proportions and geometry of architectural space. In Descartes' analytic geometry, coordinate algebra replaced the visual intuition of spatial entities, while the advent of fractal geometry allowed for a vastly expanded range of perceptions of shape. Modern digital technology uses computerised parametric algorithms to shape architectural forms. The most difficult part of traditional architectural form design is the drawing and creation of forms. The use of digital technology not only allows complex relationships to be constructed in the computer, but also expands the designer's spatial imagination.

Standardised unit combination design: The design of a building unit is a method of designing the space and form of a building from a combination of units. A building unit is an independent spatial form with the same shape, volume, or structure, which emphasises the independence of the space, structure, and form of the unit. The combination of architectural units is a way of designing the space and form of a building according to a certain organisation, using the units as the basic elements. The design of the building unit combination is suitable for FTS with repeated patterns.

Modular design is a method and idea that increases design efficiency as well as solving complex problems. It is achieved by analysing a complex system and dividing it into several sub-levels, interchangeable, independent modules. Depending on the requirements, suitable modules are selected for the design of combinations, and different modules can be combined to create different systems. The modular design of assembled buildings needs to be based on traditional design methods and steps, but

compared to it the modular design concept, the use of modularly designed FTS structural elements offers the following advantages:

(1) Advantages in construction technology

- a. The technical advantages of modularity: modular assembly buildings can be flexibly relocated, in line with the modern concept of sustainable development. Compared to traditional buildings there is a more refined construction process and quality control is guaranteed. In the beginning, the modular product was relatively homogeneous, and the building style was not simple enough to meet the requirements of the owner. With the development of technology, modular units have been able to meet most of the requirements of people by being built in conjunction with other building forms.
- b. The advantages of modular construction and design: modular construction has a shorter construction cycle, generally between one-half and one-third shorter than traditional construction processes. Due to this feature this type of building is also suitable for areas with severe housing shortages and for those waiting for a solution to their housing problems. The modular design thinking dictates a close relationship with industrial manufacturing and a more precise and clear coordination between design and construction. The high degree of integration of the construction factor into the design at the early stages of the design process allows for a better adaptation of this type of building.
- c. The comparative advantages of modular and traditional buildings: modular products are processed and prefabricated in factories, with the advantage of advanced construction technology, which is better than traditional buildings in terms of construction speed. The choice of materials, mostly composite materials, takes into account the efficiency and speed of building construction while solving the technical problems of construction. In terms of building expandability, modular products can be adjusted according to changes in functional form, and the main body of the building can be flexibly expanded or reduced in area.

(2) Advantages of the design approach:

- a. The use of modular units can save time in design and construction, and modular units can be combined to meet the needs of many building types and shorten the building construction cycle.
- b. The modular unit, although generic and standardised, can be combined in a variety of ways and can be used in mixed structural forms. The modular units, although generic and standardised, can be combined in a variety of ways and can be used in a mix of structural forms. The resulting structure is also diverse.
- c. Large-scale application is possible. When mass production is required, as long as the basic module units are summarised and the design rules are thought through, designers can still rely on rapid module design to complete design projects of a certain scale under very tight time constraints. The modular units are built in an industrial way, making many large and detailed

elements more uniform. Not only does it improve the efficiency of construction drawing and save labour costs, but it also allows for mass production according to the modules during construction and reduces production costs.

- d. Good scalability. The modular design system is an open system formed by the combination of individual modules, which allows the richness of the system to continue to develop while ensuring the stable integrity of the current phase.
- e. Sustainability. Designed to meet the needs of sustainable development. Modularity in modular construction is at the forefront of the application of sustainability theory as a highly industrialised approach. Building materials can be disassembled and replaced, quick installation and construction, etc. gives the building more flexibility and change.

9.2 Modular FTS Design

The most important element of architectural modularity is the building module unit with its own function and space. From the modular concept, a module is an individual unit that can be combined into a whole system with a defined function, which from the modular design point of view contains the following points.

Structure: defines the role and composition of the different modules in the system.

Interface: defines the interconnection between modules and their role.

Criteria: checks whether the modules comply with the design conditions and rules.

When applied to architecture, this refers to the structural system of the modular units, the standardised design of the modular units. The form of connection between the modular units.

9.2.1 Characteristics of Modular FTS

Clarifying the characteristics of modular building units helps to identify the main design approaches in the modular design of freeform timber structures and to exploit the advantages of modular design. The characteristics of modular FTS units can be divided into the following points:

(1) Independent design of modular units: Each modular unit needs to be designed in compliance with the standards, while the functionality of the modules can differ from each other. Module The independent design of the modules allows for a certain independence, which enables innovations to be realised on a single module.

(2) Variability of module units: The modular unit itself can be transformed from a single module by splitting, combining, and adding, for example If a module needs to be replaced in terms of space and functionality, it can be quickly updated to form a new module.

(3) Ductility of modular units: The most common way in which modular design of assembled buildings is organised is through the combination of modular building units. The building can be extended

functionally and spatially through the combination of modules. In terms of function, the modular units can be organised and combined to meet different functional requirements. In terms of spatial design, the modular units can be superimposed on each other and mixed with other structures to create a rich spatial relationship.

(4) Adaptability of the modular units; The adaptability of the modular units is brought about by their prefabricated factory production, i.e., the ease of relocation and renewal. This is reflected in the fact that the building can be quickly updated according to the changing functional requirements of the building and that the dismantling of individual modular units has relatively little impact on the building. This facilitates the renewal of the building. In addition, the modular units can be adapted to a wide range of environmental requirements and can be organised and arranged more freely in sites with complex topography, with minimal impact on the environment.

(5) Repetition of modular units: Repetition is one of the main ways in which modular units are used to form a whole building. Repetition is one of the main ways in which modular units are used to form buildings. The repetition is not an exact replication, but rather a partial variation of the repetition to expand the different uses of the building.

(6) Diversity of module units: The traditional approach to industrial standardisation does not take much account of the diversity of buildings but is more about economic rationality. To solve this problem, an in-depth study is needed on how standardisation can be applied to modular design strategies, so that they can address the issue of architectural diversity while meeting the economics of building construction.

9.2.2 Standardisation of components

In the design process, the structural form of the building and the functional space are determined by the project conditions. When modular design is applied, the modularity of the assembled building and factory prefabrication are considered.

(1) Simultaneous design and construction

As the modular units are prefabricated directly in the factory, they are designed and built at the same time and the designer needs to consider the design and construction of the modular units in their entirety. The modular unit is treated as a basic building unit and its implement ability is considered from the outset. Essentially, this is the idea of 'design-construction'. The design is seen from the point of view of construction and how the building is designed in relation to industrial manufacturing. The process of processing and producing the modules in the factory requires a great deal of interdisciplinary technology and information technology and requires the solution of a wide range of specialist problems in architecture, structure, and equipment, including design, processing, transport, and construction. Designers are required to have a high level of comprehensive quality and to be able to integrate various disciplines for integrated design. At the same time the range of machining of the robotic arm is a limiting factor for its development, as its dimensions are prefabricated and shaped in the factory, the impact of the dimensions needs to be fully considered.

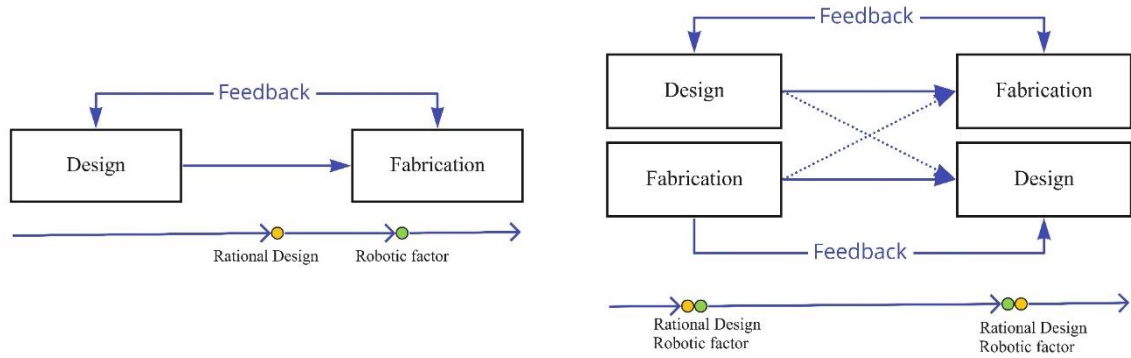


Figure 9.4 Comparison between modular design and conventional forward design

(2) Prioritise modular unit design

In terms of design thinking, it is more about the integrity of the building's modular units themselves. The modular design of assembled buildings is based on the idea of designing modular units with independent functions and spaces, and then solving large architectural problems through the combination of modular units. Therefore, the first thing needed to consider in the design is the architectural aspects of the modular units and how they can meet the needs of the assembled building design.

9.2.3 Modular Mesh Design for FTS

Freeform mesh configurations are spatial mesh structures where the overall geometry of the structure cannot be accurately expressed or fitted with an analytical function and can be freely varied in any way. In practice, freeform spatial meshes can be further subdivided into triangular meshes and quadrilateral meshes depending on the shape of the mesh, and single-layer meshes, and double-layer meshes depending on the number of layers. For freeform architectural surfaces, the grid cells need to be divided in order to facilitate construction, and the surface form of the divided cells may not be the same, so the surface cells also need to be optimised, and the more common grid cells are currently flat panel cells, single curved panel cells, ruled panel cells and hyperbolic panel cells, of which the use of flat panels to cover or use polyhedral surfaces to form freeform. This paper focuses on the planar panel cell. There are many ways to divide a planar polygon mesh, but triangular, quadrilateral and hexagonal meshes are the most widely used in architectural surface design.

The freeform single-layer mesh shell is often used in practice with glass panels as a structural element and as an architectural decoration due to the small number of components, the regular flow of the grid in terms of visual effect and the good permeability, as shown in the figure. Single-layer mesh shells can be used either in the form of a triangular grid (Fig.) or in the form of a quadrilateral grid (Fig.) But when using a quadrilateral grid, due to the irregularity of the geometric shape, it is difficult to ensure that all four corner points of the quadrilateral are in the same plane, and the heterogeneous quadrilateral will bring difficulties to the installation of the roof, especially the installation of the glass panels, therefore, it can generally only be used in a geometrically gentler and simpler shape, so that In contrast, triangular meshes can describe arbitrary geometric shapes, and the three corner points of the triangle are

necessarily in the same plane, providing a high degree of flexibility in roof installation, and therefore triangular meshes are used extensively in freeform single skin structures.

The freeform double-layered grid structure is more stable than the single-layered mesh shell, and the computational analysis process is simpler. However, due to the large number of grid components, it is easy to look cluttered and poorly permeable from a visual point of view, so in practice, glass panels are generally not used, but rather opaque roofing, and the grid structure is only used as structural support. The double-layered grid structure can also take the form of a triangular grid or a quadrilateral grid, as shown in the diagram.

The mesh layout of a freeform structure should meet both the aesthetic and structural requirements of the building. To achieve such an ideal grid arrangement, a continuous process of generation, modification and optimisation is usually required, which is the task of grid design. Grid design consists of two main aspects: grid generation and grid optimisation, which can be further subdivided into the following basic aspects:

(1) Determine the shape of the mesh. The shape of the grid should be selected according to the characteristics and complexity of the overall geometry of the shape, commonly used are mainly triangular and quadrilateral. When the shape changes more gently, the quadrilateral grid can be chosen, otherwise the triangular grid, especially when using timber panels.

(2) Selecting a suitable method for mesh generation. There are many methods of mesh generation, but not all of them are applicable to freeform spatial mesh structures. Many of them are proposed in the fields of computer graphics, finite elements, etc. And different mesh generation methods have different concerns, so it is necessary to choose the method that can meet both the aesthetic and structural requirements of the building.

(3) Optimise the mesh as required. Most of the time, the directly generated mesh is not optimal and can be optimised in terms of homogeneity, smoothness, topological regularity, etc.

(4) Mesh adjustment. In practical engineering, mesh design is usually carried out under certain constraints, such as fixed support positions. When the generated mesh cannot meet these constraints, mesh adjustment is required.

Many methods have emerged during the research process of mesh generation technology, and after decades of superiority and inferiority, some methods have stagnated in research and application, while others have become highly adaptable and widely used general methods after continuous in-depth, improvement and development. Currently, some of the more common mesh generation methods include the Mapping Method, the Advancing Front Technique (AFT), and the Delaunay Method, etc.

(a) Mapping Method

The basic step is to first map the problem domain defined in physical space to a regular shape in the parametric domain, then generate a parametric domain mesh, and finally reflect the parametric domain

mesh back into physical space to form a mesh of the original problem domain. It is generally used to generate structured meshes, but unstructured meshes can also be generated. The mapping method is simple and the idea behind its mesh generation is to establish a mapping relationship between the surface to be profiled and the parametric domain, then divide the mesh in the parametric domain, then map the parametric domain mesh back into physical space to generate the mesh on the surface, as shown in Figure 9.5.

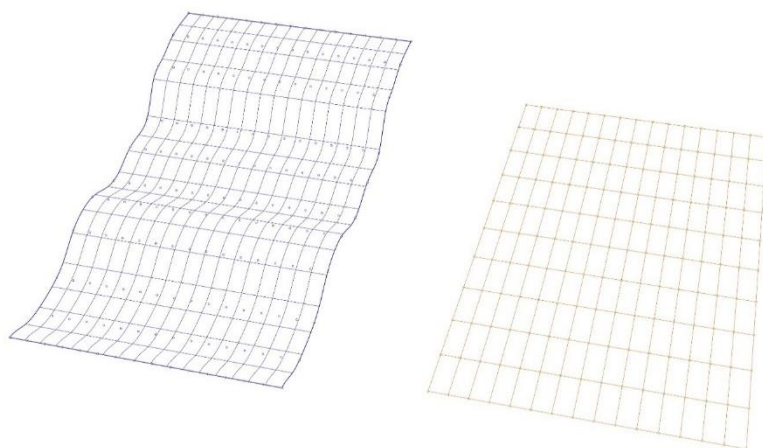


Figure 9.5 Mapping

The mapping method has the advantages of simple algorithms, fast generation, controllable cell quality, and is the optimal method for generating structured meshes, which can be easily combined with other algorithms. However, the mapping method also has its drawbacks, the most common of which is the mesh distortion problem. This is since the mapping relationship between the physical space and the parametric domain is not linear, so often the high-quality mesh generated in the parametric domain will be greatly distorted in the physical space to which it is mapped.

(b) Advancing Front Technique

The AFT method can be used to generate both triangular and quadrilateral meshes. The basic principle of the AFT method is to first discretize the boundary of the domain to be dissected into cells, which for a surface is a line segment called the initial frontier; then, starting from the initial frontier, each frontier is the known base of a triangle, and nodes are inserted into the interior of the domain to be dissected to form a triangle with the frontier, and a new frontier is generated; thus, the frontier is continuously advanced until the entire domain to be dissected is divided, as shown in the figure. as shown in the diagram.

There are many studies on wavefront methods, for example, literature attempts to generate quadrilateral meshes by wavefront method by merging triangles; literature solves the problem of sick meshes when applying wavefront method to folded surfaces; literature investigates the method of wavefront mesh generation and intersection judgement in the parametric domain of parametric surfaces and then mapping back to the surface.

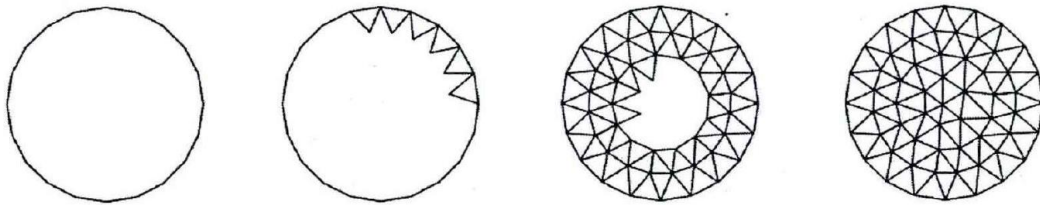


Figure 9.6 Process of AFT

The basic process of the AFT method is:

- (1) Discrete the boundary of the problem domain to obtain the initial frontier.
- (2) Starting from the current frontier, insert a new node or connect an existing node inside the problem domain to form a new cell.
- (3) Update the frontier so that the frontier advances towards the interior of the problem domain.

The disadvantages of the frontier advancement method are the convergence problem of the 3D AFT algorithm due to the many difficulties in triangulating the "remaining polyhedral"; the large number of geometric intersection judgements, inclusion judgements and distance calculations when generating new cells, which are difficult to implement and less efficient to execute.

(c) Delaunay Method

The Delaunay method is also one of the popular and versatile fully automatic unstructured mesh generation methods, which utilises the Delaunay Triangulation DT principle for the mesh generation of the problem domain. The Delaunay method has the advantages of being mathematically sound, fast and efficient and producing good quality grid cells. To introduce the Delaunay method, it is necessary to introduce the Voronoi diagram, which is the dual of the two. Given scattered data points in the plane (or in space), a domain is constructed for each data point such that any point in the domain is closer to that scattered point than to any other scattered point, and the resulting graph is called a Voronoi diagram. The triangulation of pairs of scattered data points in a Voronoi diagram that share a common domain boundary is called Delaunay triangulation. For a given set of scattered data points, triangulation is optimal.

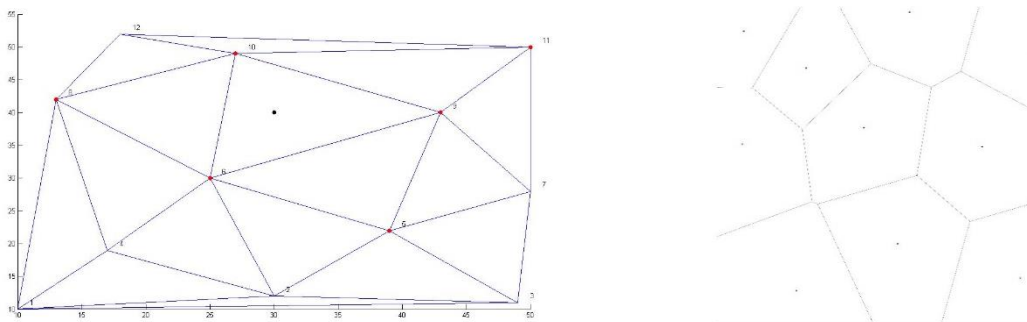


Figure 9.7 Delaunay triangle and Voronoi

9.3 Mesh optimisation methods

9.3.1 Geometry optimisation

Geometric optimisation, which is carried out to improve the geometric properties of a mesh, can be divided into the following categories, depending on the purpose of the optimisation.

(1) Size optimisation

In a spatial mesh structure, the length of the rods must be as uniform as possible and when the resulting mesh is unevenly distributed, it needs to be optimised. A common method used in dimensional optimisation is the merging and splitting of cells, i.e., when the mesh size is too small, the small cells can be eliminated by merging the mesh, and when the mesh size is too large, the mesh can be split to reduce the size, as shown in the figure. In the case of spherical shells in a spatial grid structure, the "grid reduction" process commonly used when using ring-assisted grids is also based on the merging principle.

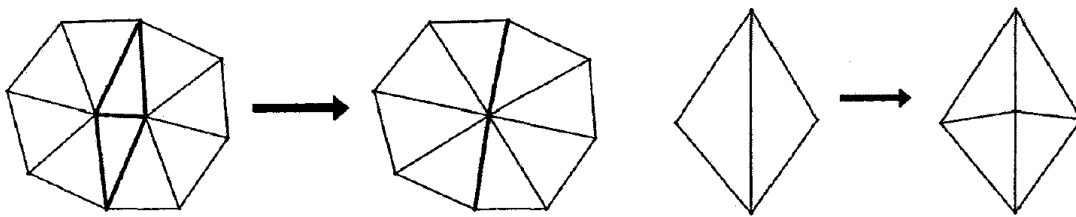


Figure 9.8 The merging and splitting of mesh

(2) Angle optimisation

The spatial two-grid structure also requires that the angle between the bars should be as large as possible to prevent the members from touching each other. Therefore, when there are narrow cells in the mesh, angle optimisation is required. A common method is diagonal edge swapping, as shown in the figure. This method is only applicable to triangular meshes and the swapped mesh will satisfy the minimum internal angle maximisation criterion of the method.

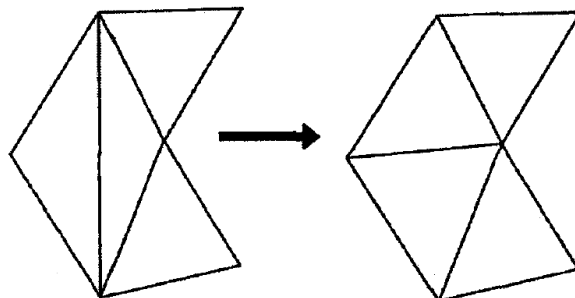


Figure 9.9 Interchange of edges

9.3.2 Mesh smoothness optimisation

To make the mesh better meet the requirements of the spatial mesh structure, both dimensional and angular optimisation should be considered in the optimisation. The Laplacian smoothing algorithm is

one of the most classical integrated optimisation algorithms, in which each internal non-fixed node is moved to the centre of a polygon formed by its surrounding nodes and can be iterated several times to make the mesh appear more homogeneous and smoother by continuously moving the internal nodes. The literature introduces a surface energy method smoothness criterion for the overall optimisation of freeform meshes by adjusting the smoothness factor; the literature proposes a multi-objective method for optimising the geometry of freeform meshes, setting the objective function with the same length of the bars and the same angle of the bars, and optimising the mesh without changing the mesh topology.

9.3.3 Structure Optimisation

For freeform structures, where the mesh cells are the structural elements, the arrangement of the mesh not only affects the geometrical appearance but also the mechanical properties of the configurations. Therefore, mesh optimisation methods based on the properties of the configurations have been proposed, although these methods are generally accompanied by mesh generation as they involve a change of topology.

For freeform mesh structures, P Winslow proposes a multi-objective genetic algorithm for mesh generation based on structural properties, which can set multiple structural responses as the objective function and can be under one or more loads. Topology optimisation of mesh configurations is based on genetic algorithms and satisfying stress criteria, where the objective function is the total weight of the bars. Stress traces are introduced into the mesh generation for freeform structures, and the stress traces are used as guidelines for mesh generation to optimise the mechanical properties of the mesh structure. In practical structural design, the optimisation of meshes based on mechanical properties places greater demands on the engineer, as freeform spatial meshes are aesthetically pleasing and the optimisation of mechanical properties must consider aesthetics, which in many cases is even contradictory, requiring the structural engineer to have sufficient design experience and knowledge of mechanics. Single-glass grid structure of the Milan Exhibition Centre is presented. The grid design strategy is to divide the planar and near planar areas of the form into a quadrilateral grid, transform the quadrilateral grid into a triangular grid by adding diagonals, and extend the two directional lines of the surrounding planar grid spirally at an angle to the interior of the surface so that the direction of the grid is consistent with the direction of the 'force flow'. This is shown in the Figure 9.10.

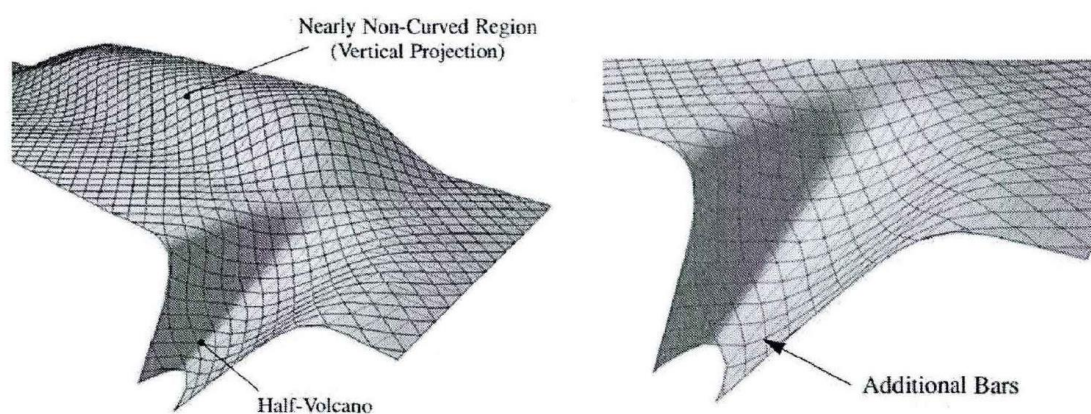
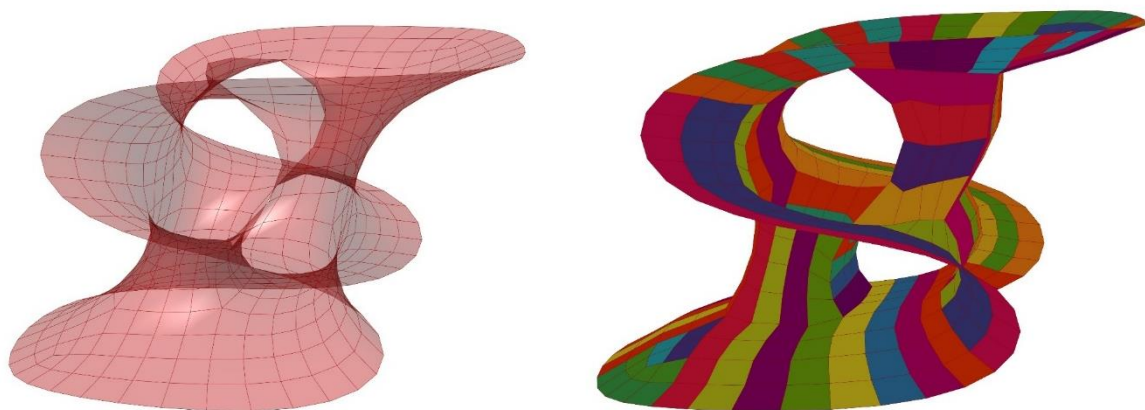


Figure 9.10 The mesh optimisation at half-volcano position

9.3.4 Example

There are several reasons why simple cases are not used to demonstrate the procedure. First, there are simpler methods (such as the Delaunay triangle algorithm) for generating mesh for simple surfaces because there are no complicated issues such as trim edges. Second, the methods chosen are appropriate for the complicated freeform morphology generated by the three methods established in Chapter 6, which would link morphology generation with mesh generation and optimization. On the other hand, if simple or random cases which are not mentioned in the previous chapter, the morphology of the simple surface may not follow the principles proposed in Chapter 4 as rational and structurally reliable, and in Chapter 6 as easy to digitalize and modularize.

This example shows the optimisation for the triangular mesh and quads mesh in geometry and smoothness. The freeform surface is the one applying the minimal surface morphology form-finding method. The first step is to generate the mesh for the surface and the original one, shown in Figure 9.11 (a). The mesh is optimised in Laplacian smoothness and geometry including the length and panel areas. The length means to the average length, length, and the variance of length of edges, and the same to the areas. After the first optimisation, one problem is that the deviation between each mesh unit and the plane of the four vertices, which means the planarity of the panels. The planarity of the panels has the direct relationship to fabrication, that is the higher planarity of the panel, the easier to fabricate and the easier to achieve construction. Figure 9.11 (b) shows the planarity optimisation for the quad mesh. The optimisation results show every panel is planar surface, with zero planarity, however, the planarity means the loss for smoothness. The loss of smoothness is obvious where the curvature of the surface varies considerably.



(a) First optimisation of quad mesh

(b) Laplacian smoothness of quads mesh

Figure 9.11 Quad mesh for minimal surface

To make the deviation between the quad mesh and the planar surface clearer, the results shown in Figure 9.12-Figure 9.13 show the measuring points between the mesh and the polysurface composed by planar surfaces fitted by the vertices of the mesh. Different colour of the points indicates the quality of the points which means that the blue points are on surface while the cyan points are good points with distance less than 0.001. The points in Figure 9.12 indicate that the points are mainly distributed in areas of high curvature variation where the points with distance larger than 0.01 are located in. The mean

distance of 187 measuring points is 0.0049. The results of the planarity optimisation indicate the optimised mesh is consistent with the fitted quads with 0 distance of 2354 points.

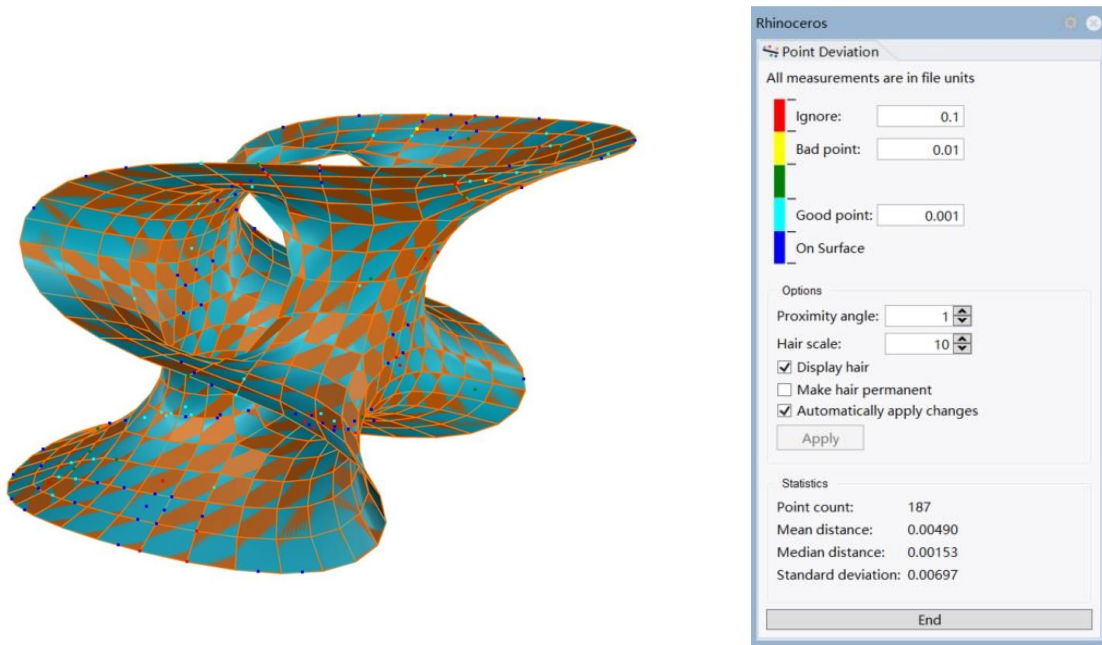


Figure 9.12 Point deviation between the mesh and the fitted surface of first optimisation

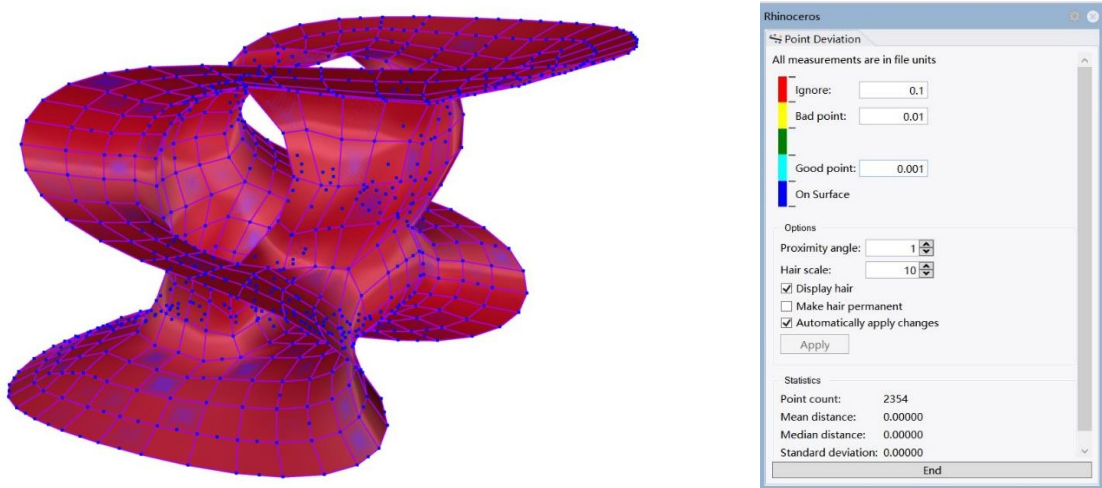


Figure 9.13 Point deviation between the mesh and fitted surface of second optimisation

The differences between the two optimisations are compared in Figure 9.14. The blue wireframe is the results of first optimisation and the red one is the results of second optimisation. The blue wireframe has better smoothness compared with the second optimisation results, which means the optimisation objectives of smoothness and planarity cannot be achieved at the same time. The balance between the two objectives is needed to have good smoothness and enough planarity of panels.

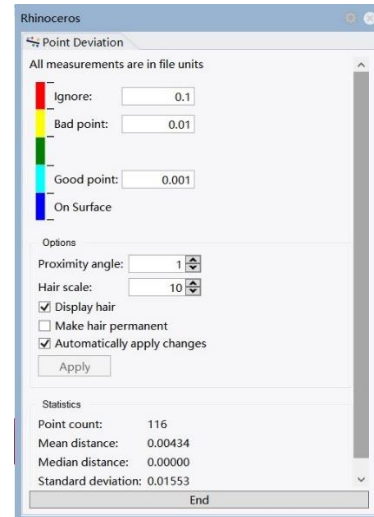
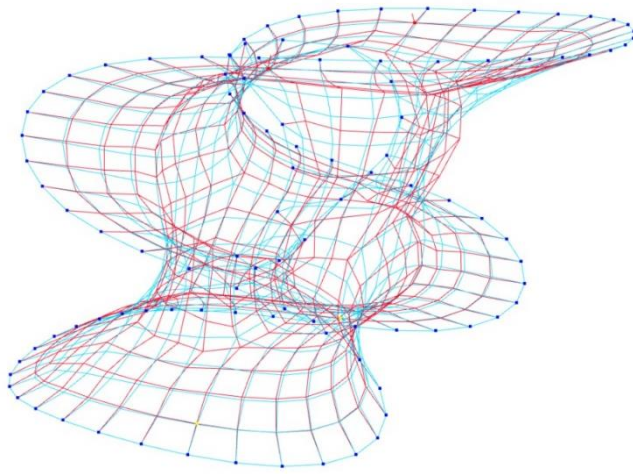


Figure 9.14 The comparison between two optimisations

In the planarity optimisation process, there are 512 quads altogether. In Figure 9.15, the results of planarity of different panels are presented. The optimisation process has 179 steps and after 40 steps, the planarity of all the quads is nearly zero, which means all the quads are in planar surface. The results list the 1st, 2nd, 200th, and 512th panels to summarize all the quads.

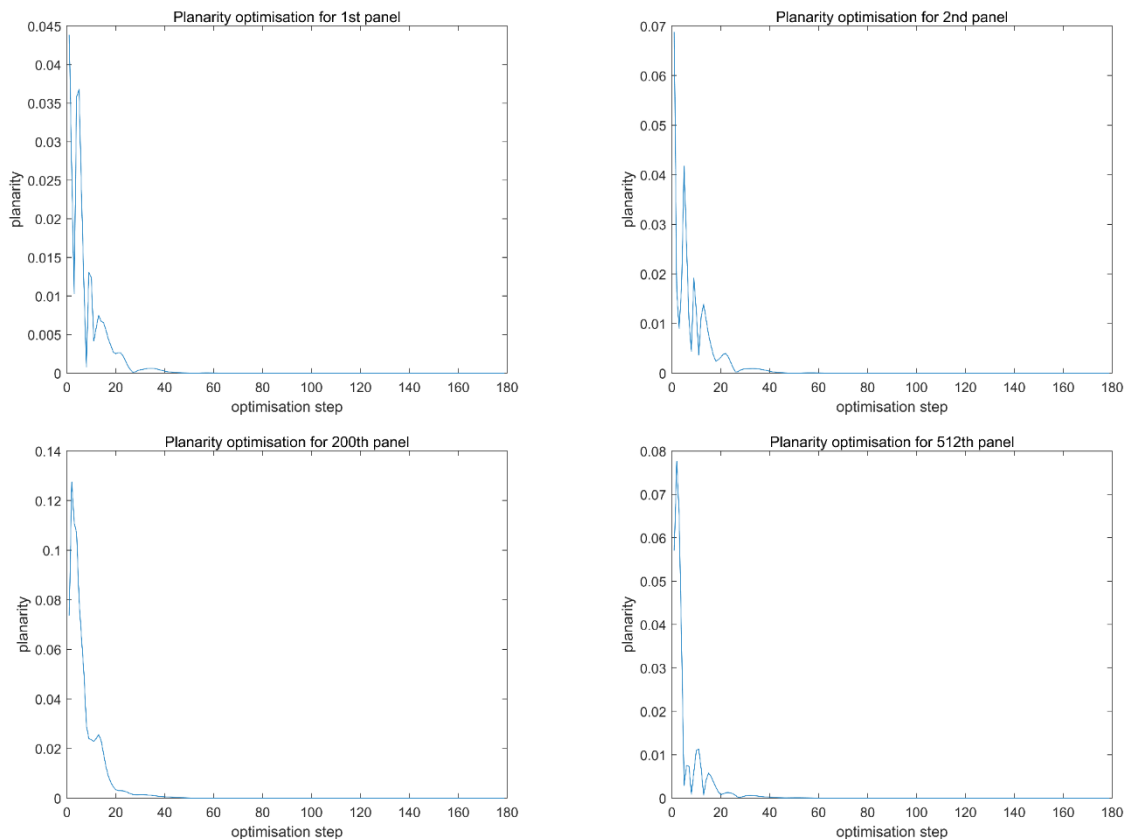


Figure 9.15 Planarity of different panels

The optimal results tested the hypothesis that standard planar panels and linear rods can compose the non-standard structure by transforming the freeform surface into standardised mesh. In this example, the form of the mesh is in triangular and quad shape. The quad mesh has one more planar optimisation to achieve all the mesh are planar surface which means can be fabricated by robotic cutting rather than

more complicated processes. The triangular and the quad mesh can be composed by both panels or rods.

9.4 Evaluation of the quality of modular mesh

In the traditional architectural design process for freeform mesh structures, the architect or engineer evaluates the mesh based on subjective judgement. This is reasonable from an aesthetic point of view. However, it is important to consider the needs of the architectural design process not only on an aesthetic level, but also on a mechanical level. Smoothness indicators, shape quality indicators and rod length indicators can quantitatively describe the smoothness, shape, and rod length of the grid, where shape and rod length have a direct influence on the mechanical properties of the structure and the level of difficulty in manufacturing. These quantitative evaluation indicators can be used as a reference for the architectural design process.

9.4.1 Criteria for evaluation

In this section, mesh system evaluation indicators are proposed in relation to the requirements of the mesh-shell structure in terms of both rod length and mesh shape. Based on these indicators, the mesh generation results can be better evaluated.

(1) Component length indicator

Bars are the basic building blocks of a mesh structure. On the one hand, the length of the rods should be as uniform and close to the given desired rod length as possible; on the other hand, there should be as few types of bars as possible to facilitate processing. Based on the above principles, this section proposes length evaluation indicators, including total bar length S_L , average length \bar{L} , standard deviation of bar lengths δ_L , length uniformity factor U_L for an overall evaluation of the length of the bars of the mesh system.

$$S_L = \sum_{i=1}^N L_i \quad 9.1$$

$$\bar{L} = \frac{1}{N} \sum_{i=1}^N L_i \quad 9.2$$

$$\delta_L = \sqrt{\frac{1}{N} \sum_{i=1}^N (L_i - \bar{L})^2} \quad 9.3$$

$$U_L = \frac{N - C}{N - 1} \quad 9.4$$

Where N is the sum of the bars (edges), C is the number of bar (edge) length categories, L_i is the length of the i th bar (edge). The closer \bar{L} is to the desired length, the more desirable the bar length is; the smaller δ_L is, the more uniform the bar length is, which also reflects the more uniform size of the mesh.

U_L is between 0 and 1, the larger the value the more uniform the length of the bars, when U_L is equal to 1 all bars are the same length, when it is equal to 0 all bars are different from each other.

(2) Quality of shape

The appearance of deformed and narrow meshes in mesh-shell structures not only affects the structural force performance, but also causes the angle between the bars to be too small, which is not conducive to node construction, etc. Therefore, this section proposes shape quality evaluation indexes for triangular and quadrilateral meshes, which are common in mesh-shell structures, with reference to the guidelines for judging the shape quality of meshes in finite elements.

For triangle Δ_{ABC} , the area is $A\Delta_{ABC}$, the three edges of the triangle are $|AB|$, $|BC|$, and $|AC|$, then the shape quality factor of the triangle φ is:

$$\varphi = 4\sqrt{3} \frac{A\Delta_{ABC}}{|AB|^2 + |BC|^2 + |AC|^2} \quad 9.5$$

The value of φ for a triangle range from 0 to 1, with $\varphi = 1$ when the triangle is equilateral and 0 when the triangle degenerates to a line; the larger the value of φ , the better the quality of the triangle shape. Like triangles, for quadrilaterals \square_{ABCD} , the lengths of the four sides $|AB|$, $|BC|$ and $|CD|$, and $|AD|$, respectively. Then the shape quality factor of the quadrilateral ψ is:

$$\psi = 4^4 \sqrt{\frac{A\Delta_{ABC} \cdot A\Delta_{ADC} \cdot A\Delta_{ADB} \cdot A\Delta_{CBD}}{(|AB|^2 + |BC|^2)(|AD|^2 + |CD|^2)(|AB|^2 + |AD|^2)(|BC|^2 + |CD|^2)}} \quad 9.6$$

The value of ψ for a quadrilateral is between 0 and 1, with $\psi = 1$ when the quadrilateral is a square, and $\psi = 0$ when the quadrilateral degenerates into a triangle, the higher the value of ψ , the better the quality of the quadrilateral shape.

To measure the shape quality of the overall grid, the mean \bar{G} and standard deviation δ_G of the shape quality coefficients of all grid cells are used as the shape quality evaluation index of the grid system.

$$\bar{G} = \frac{1}{M} \left(\sum_{i=1}^{m_p} \varphi_i + \sum_{j=1}^{m_q} \psi_j \right) \quad 9.7$$

$$\delta_G = \sqrt{\frac{\sum_{i=1}^{m_p} (\varphi_i - \bar{G})^2 + \sum_{j=1}^{m_q} (\psi_j - \bar{G})^2}{M - 1}} \quad 9.8$$

Where: m_p , m_q are the number of triangles and quadrilaterals in the mesh system, respectively. M is the total number of grids. The larger the \bar{G} the better the overall shape quality of the mesh and the smaller the δ_G indicates that the smaller the difference in shape quality of the mesh.

Example:

Following the equation 9.1-9.8, the parameters are taken to compare different mesh methods. Figure 9.16 - Figure 9.17 show two meshes where one is in triangular polygon and the other is in quadrilateral polygon. The two optimisations are operated on the two meshes with 179 steps.

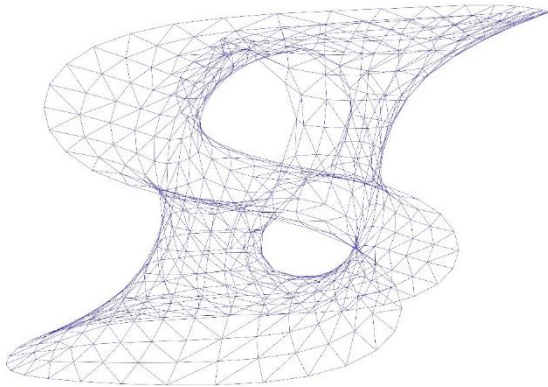


Figure 9.16 Triangular mesh

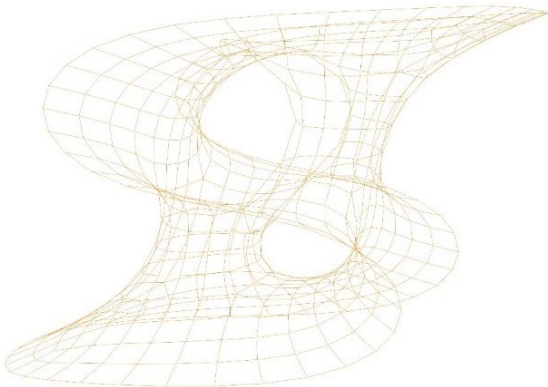
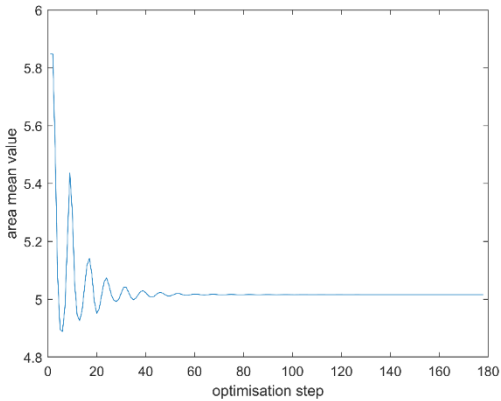


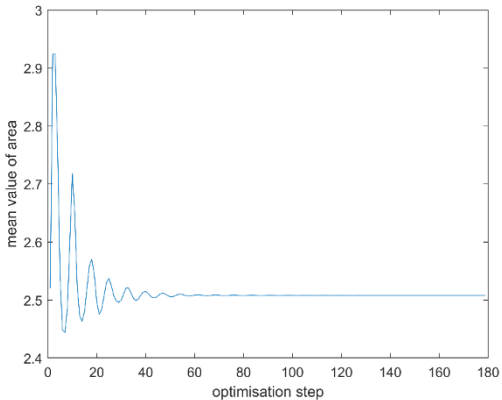
Figure 9.17 Quadrilateral mesh

The results of optimisation of geometry for mesh in different polygons are presented in Figure 9.18. The optimisation process has 179 steps and the mean of the panel area and the edge length and the variance of them converged after 60 steps which proves the effectiveness of the optimisation process. The comparisons between the quad mesh (512 panels) and triangular mesh (1024 panels) shows the same convergence trends and the mean value of quad mesh is two times of the triangular one. The tri-mesh has lower variance compared the quad one.

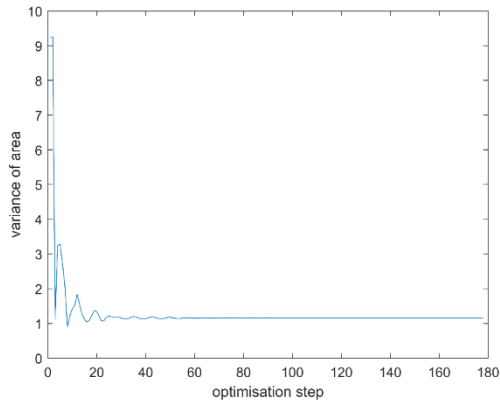
The mean values of two different mesh are almost equal, and the value of the quad mesh is slightly lower than the triangular one. In contrast to the panel area, the variance of edge length of quad mesh is lower than the tri-mesh. In summary, the quad mesh has less components compared with the triangular one. In terms of panel area, the triangular mesh is more homogeneous than the quadrilateral one, while in the perspective of edge length, the result is the opposite. Furthermore, there is no need to optimise the planarity of tri-mesh since the triangular panels are all planar surfaces and the quad-mesh needs two optimal steps if consider the effectiveness and simplicity of fabrication.



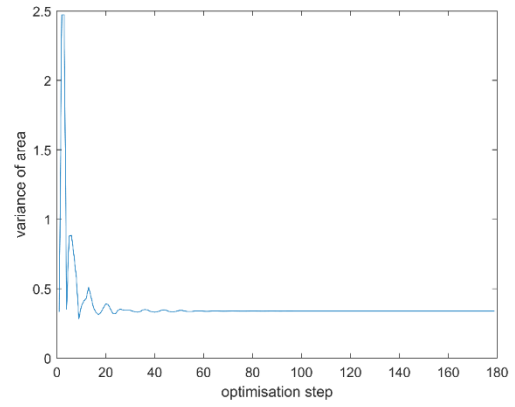
(a) Mean of quad panel area



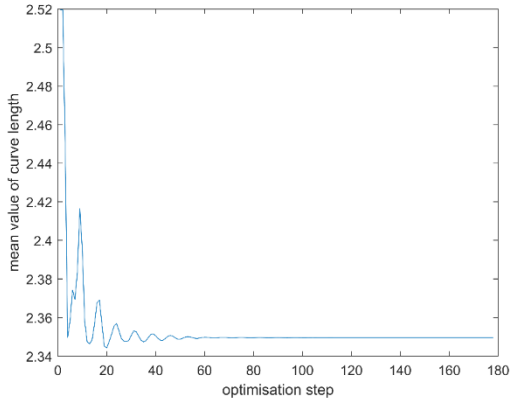
(b) Mean of triangular panel area



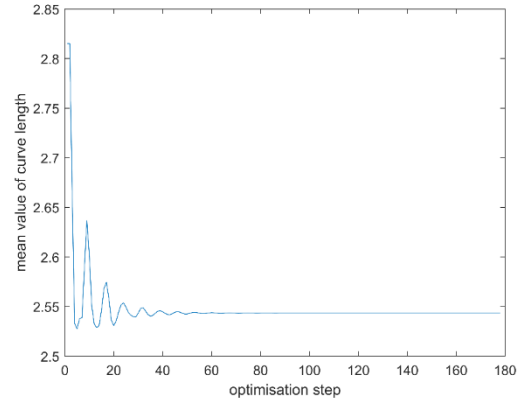
(c) Variance of quad panel area



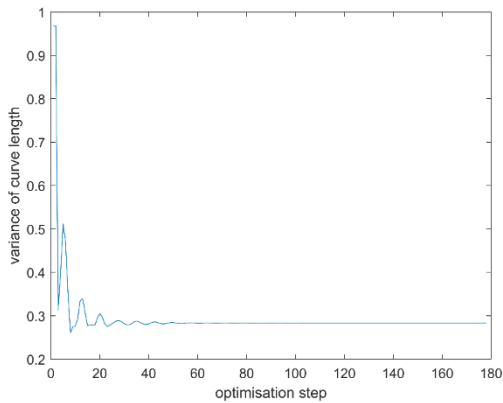
(d) Variance of triangular panel area



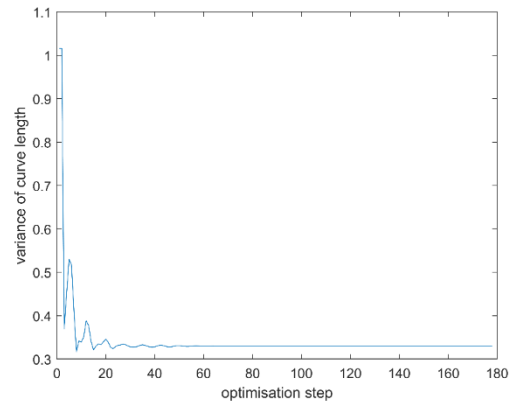
(e) Mean of edge length of quad mesh



(f) Mean of edge length of triangular mesh



(g) Variance of edge length of quad mesh



(h) Variance of edge length of triangular mesh

Figure 9.18 Optimisation for quad and triangular mesh

9.4.2 Determination of fabrication errors

After the modular meshing of the freeform surface has been completed and the component fabricated in the "design-fabrication" process, further machining errors need to be determined to achieve a more comprehensive evaluation. The fabrication error (FE) of a surface is the spatial deviation of the actual surface of a part from the theoretical surface after machining. The FE of a surface describes the machining accuracy of a freeform part and is a key element in improving the machining accuracy of a part. The error of a surface can be measured by the distance between a point p on its theoretical surface and the intersection of point p along its normal vector direction n or vertical direction v to the actual surface, as shown in the diagram.

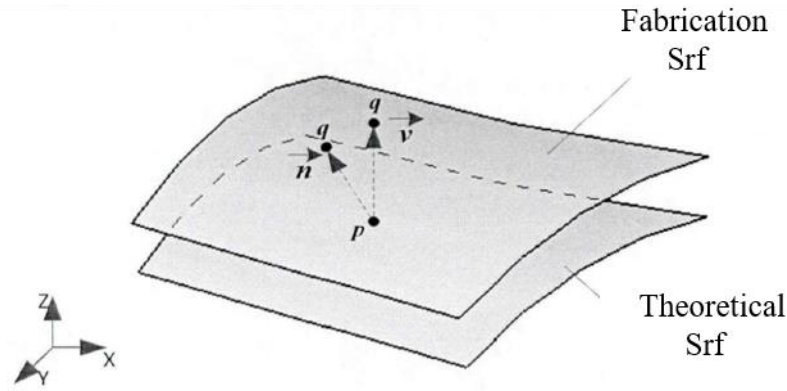


Figure 9.19 The fabrication error of the fabricated surface

Based on the above description of the surface machining error, the magnitude of the surface machining error ε can be expressed as the distance between the point $p(x_p, y_p, z_p)$ on the theoretical surface and the intersection point $q(x_q, y_q, z_q)$ along its normal vector direction n or vertical direction v to the actual surface, and the distance between them can be calculated using the formula:

$$\varepsilon = \|q - p\| = \sqrt{(x_q - x_p)^2 + (y_q - y_p)^2 + (z_q - z_p)^2} \quad 9.9$$

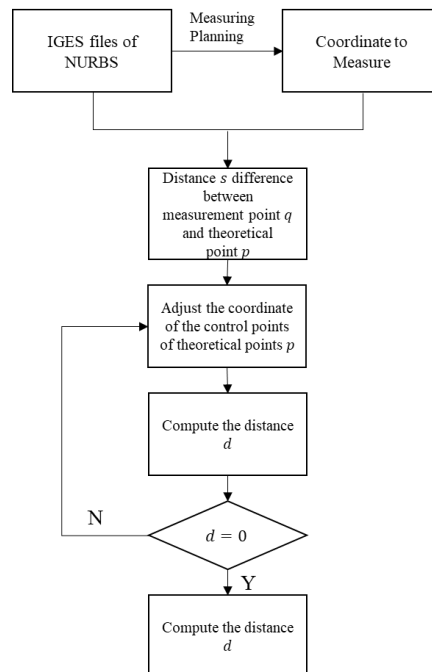


Figure 9.20 Process of Rebuild of the NURBS surface

For a point $q(x_q, y_q, z_q)$ in space and a given parametric surface $p(u, v)$, there always exists a point $p(u_p, v_p)$ on the surface such that there is a minimum distance d_{min} between the point q and the surface:

$$d_{min} = \|q - p\| \quad 9.10$$

where point p is called the nearest point of point q on the parametric surface $p(u, v)$. Similarly, if point q is in the direction of the exterior normal to the point, then the distance between point p and point q is known to be the minimum distance from point q to the surface.

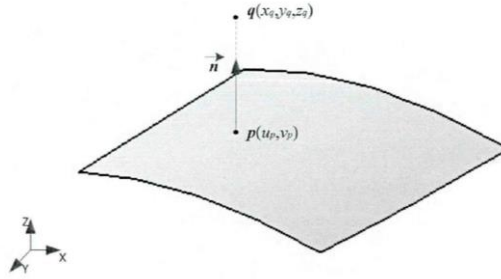


Figure 9.21 The shortest distance between point and surface

The minimum distance from a point to a surface is in the direction normal to the corresponding point on the surface, so this paper calculates the minimum distance from a point to a surface to represent the magnitude of the normal error of the surface and therefore the magnitude of the FE error of the surface. When calculating the minimum distance from a point to a surface to calculate the machining error for the whole surface, this can be done in two ways:

- 1) Calculate the minimum distance from a point on a theoretical surface to the actual surface;
- 2) Calculate the minimum distance from a point on the actual surface to the theoretical surface;

The FE of a surface is calculated by calculating the minimum distance between the point on the actual machined surface and the theoretical surface, which gives a better description of the amount of variation of the actual surface relative to the theoretical surface. Firstly, the fabrication surface is reconstructed according to the introduced theoretical method based on NURBS control point reconstruction and the coordinate data of the measurement points obtained from the on-machine measurements. Then the fabrication surface is discretized according to the parameter values u, v to obtain the coordinates of a series of discrete points, and the FE of the surface is described by calculating the minimum distance between these points and the theoretical surface. Suppose there is a point $p(u, v)$ on the theoretical NURBS surface, and a point $q(x, y, z)$ on the actual machined surface, $p(u, v) = (p_x(u, v), p_y(u, v), p_z(u, v))$, where $p_x(u, v), p_y(u, v), p_z(u, v)$ are the x, y, z coordinates of the point $p(u, v)$. To simplify the calculation, the square of the minimum distance from a point q on the fabricated surface to the theoretical surface can be expressed by the formula:

$$\min F(x) = \min f^2(u, v) = (x - p_x(u, v))^2 + (y - p_y(u, v))^2 + (z - p_z(u, v))^2 \quad 9.11$$

where $X = [u \ v]^T$.

For the machined part, it not only has the dimensional error, the point, line, and surface of the component may also have the shape and position error, which can be described by the **Geometric Dimensioning and Tolerancing** to describe the error of the part in shape and position. Geometric Dimensioning and Tolerancing includes both shape and position errors and describes the amount of variation between the actual elements being measured and the ideal elements. The machined surface of a freeform part can be described by the surface profile controls of the form and position errors. In accordance with BS ISO 6707 for shape and position errors, the surface profile controls of machined surfaces are assessed with reference to their theoretical surface profile, using the variation of the actual measured profile in relation

to the ideal profile to describe the machining accuracy of the freeform surface. Surface profile errors are classified as either datum or non-datum requirements¹⁷.

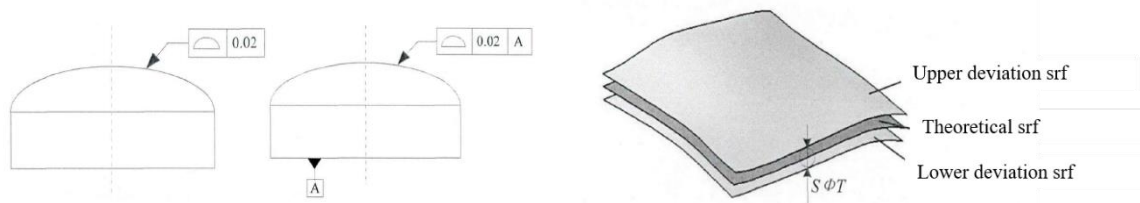
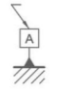



Figure 9.22 Error measurement

The description of symbols of GTS is listed in Figure 9.23.

The tolerance zone for the surface wheel temple error is the area between the upper and lower deviation surfaces that envelop a series of balls of diameter T , where the centre of the ball of diameter T is on the theoretical surface, as shown in the figure. The minimum inclusive area method can be used to assess the surface profile error of a surface. To assess the surface profile error using the minimum inclusive area method, the normal distance to the surface, i.e., the normal error, needs to be calculated first. The minimum distance from the actual surface to the theoretical surface is calculated as described in the section, and then the minimum inclusive area of the surface is determined by the maximum of the minimum distances, which allows the surface profile error to be obtained and the surface machining error to be assessed.

APPLICATION	TYPE	CHARACTERISTIC	SYMBOL
Individual Features	Form	Straightness	—
		Flatness	▭
		Circularity	○
		Cylindricity	∅
Individual or Related Features	Profile	Line Profile	⤿
		Surface Profile	⤿
Related Features	Orientation	Angularity	∠
		Perpendicularity	⊥
		Parallelism	∥
	Location	Position	⊕
		Concentricity	◎
		Symmetry	≡
	Runout	Circular Runout	↗*
		Total Runout	↗↘*
 			
		Datum	Feature Control Frame

Source: <https://formlabs.com/blog/gdt-geometric-dimensioning-and-tolerancing/>
Figure 9.23 Symbols for tolerance control

¹⁷ The surface profile is controlled as a shape tolerance when there is no datum, and as a shape and orientation and position tolerance when there is a datum.

9.5 Conclusion

In response to the hypothesis, the modular concept is introduced into the mesh workflow in this chapter which is one solution to compose the non-standard structure with simple and standard structural components. The use of planar panels and linear rods eliminates the need to develop new types of tools to pre-fab the complicated components such as double curved timber beams, providing support for the hypothesis of using simple robotic fabrication to complete the complicated structure.

Based on the example of robotic trajectory optimisation in Chapter 8 and the optimisation principle of modularity proposed in Chapter 3, this chapter proposes the design of meshing and mesh homogenization of freeform surfaces to realize freeform components with standardisation characteristics.

This chapter provides a brief overview of the concept of modularity and proposes a mesh generation and optimisation method to achieve the modularity of FTS components.

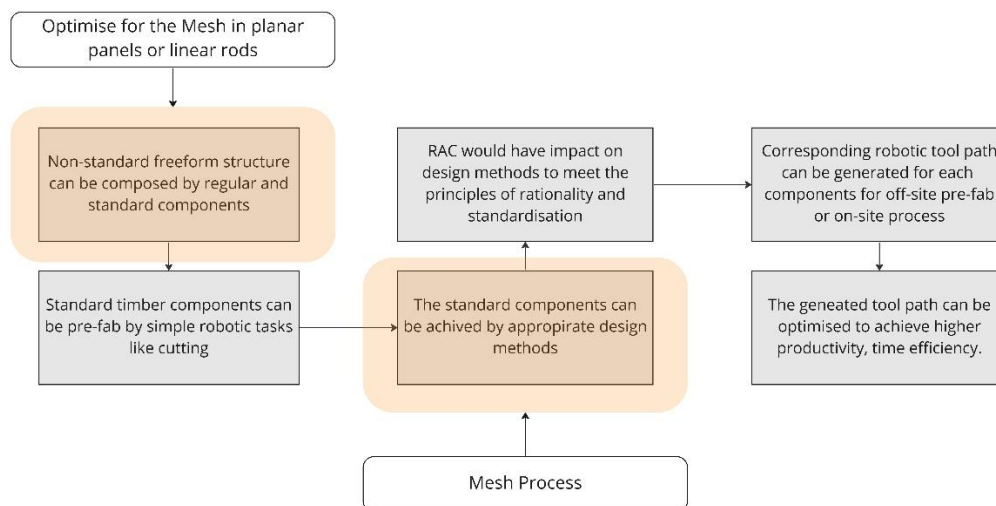


Figure 9.24 Connection to Hypothesis

The mesh method is introduced by means of an example, which optimizes geometry and smoothness to achieve a homogeneous flat component. At the end of the chapter, the machining error of the surface is introduced and a spatial expression for the magnitude of the freeform surface error is given. The magnitude of the normal machining error of the surface is expressed by calculating the minimum distance between the point on the actual machined surface and the theoretical surface. The amount of variation of the actual machined surface with respect to the theoretical surface is described by using the surface wheel temple error in the form error, which in turn indicates the accuracy of the fabrication of the component by the robotic arm as a criterion of the quality of the mesh. By combining modular principles, the number of mesh component types in size and shape can be reduced, potentially easing the pre-fabrication process by improving tool path repeatability related to Chapter 8.

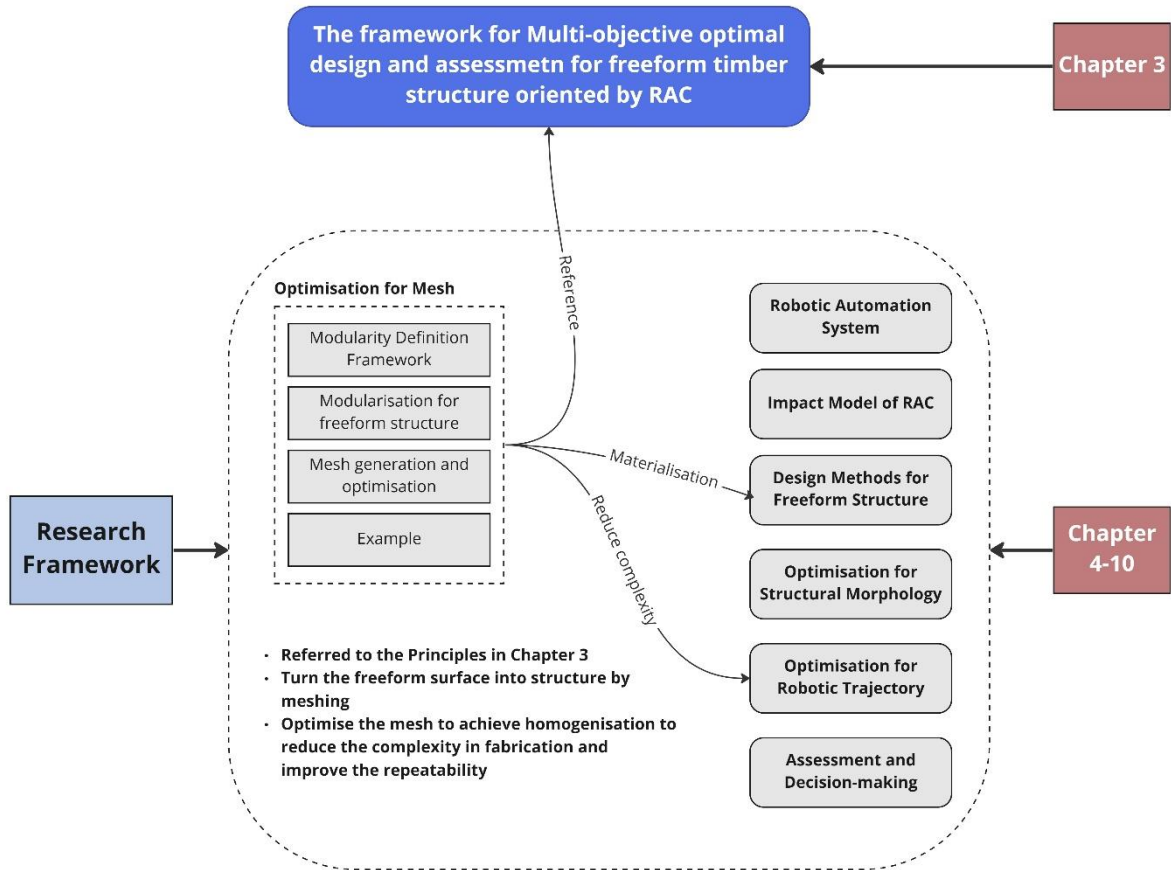


Figure 9.25 Connection to other chapters

Chapter 10

Multi-criteria Assessment and Decision-making Support System for Robotic Automation Construction-Freeform Timber Structure (RAC-FTS)

Chapters 6 through 9 describe various components of the RAC-FTS system, including the four main aspects of the system: geometric form design, structural optimisation, mesh optimisation, and tool path optimisation. Three methods are developed in Chapter 6 to generate freeform morphology that is adaptive to the characteristics of RAC. In Chapter 9, various types of mesh are generated in order to materialise the geometric model into a building information model. There are numerous combinations plans available when constructing a new freeform structure with RAC. Different stakeholders, such as clients or contractors, will have different preferences when making decisions. To support the decision making for FTS, this chapter aims to establish a multi-criteria assessment framework to assess the overall performance for RAC-FTS as a whole consider different criteria e.g., technology, sustainability, design quality and so on. Based on the assessment framework, a decision-making support system would be developed to support different stakeholders make decisions. For the establishment of the evaluation system, the criteria that can comprehensively describe the RAC-FTS are selected, and the system is described by a targeted selection of non-intersecting and representative indicators, thus creating a simplified and rational evaluation system. Given the non-uniqueness of the multi-objective optimisation results, a decision support system is built on top of the evaluation results to assist the designer or other relevant personnel in making a reasonable solution according to the project needs.

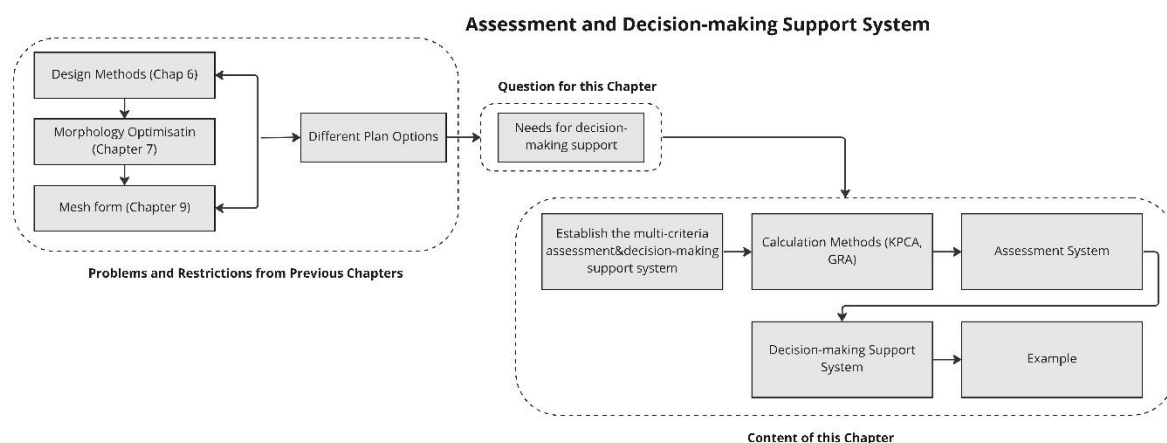


Figure 10.1 Roadmap of Chapter 10

10.1 Establishment of evaluation systems and decision-making systems

Based on the characteristics of multi-objective optimisation to generate non-analytic solutions, the optimisation results including modelling method, meshing method, and processing method are combined to generate multiple RAC-FTS solutions that satisfy the optimisation objectives. In the final solution selection process, an evaluation-decision system is proposed in order to achieve scientific and objective decision making. At the same time, this system can provide sufficient information feedback

to the design system and the optimisation system, so that the RAC-FTS has a dynamic feedback mechanism.

10.1.1 Purpose and process of evaluation

This chapter establishes the evaluation and decision system design for RAC-FTS optimisation design based on the theoretical model proposed in Chapter 3. Firstly, the evaluation purpose, evaluation process and evaluation index selection principles are defined, and then an all-round flexible evaluation index system is established to select the indicators reasonably and comprehensively and to qualify and quantify the indicators of each criterion. RAC-FTS is a complex and comprehensive system as an evaluation object, and the establishment of its evaluation index system and the construction of comprehensive evaluation methods need to be based on clear evaluation purposes and scientific evaluation principles. The evaluation and decision-making system are constructed as shown in Figure 10.2.

The process shown in the picture is consistent with the Dynamic MOO function proposed in Chapter 3. Guided by the optimisation objective, the multi-objective problem is reasonably optimized in the selected variable range interval, and the optimized parameters are fitted to a model. The fitted model and the corresponding parameters are input into the evaluation system for a systematic and comprehensive evaluation. Since different projects have different design requirements, for example, some projects emphasize the efficiency of material usage, and some emphasize the automation efficiency of robotic arm processing. Therefore, after obtaining the comprehensive evaluation results, the different solutions and the corresponding evaluation results are input into the assisted decision system, and the criteria are selected according to the different project requirements in a targeted manner and the designed decision system is used to provide support to assist the decision making.

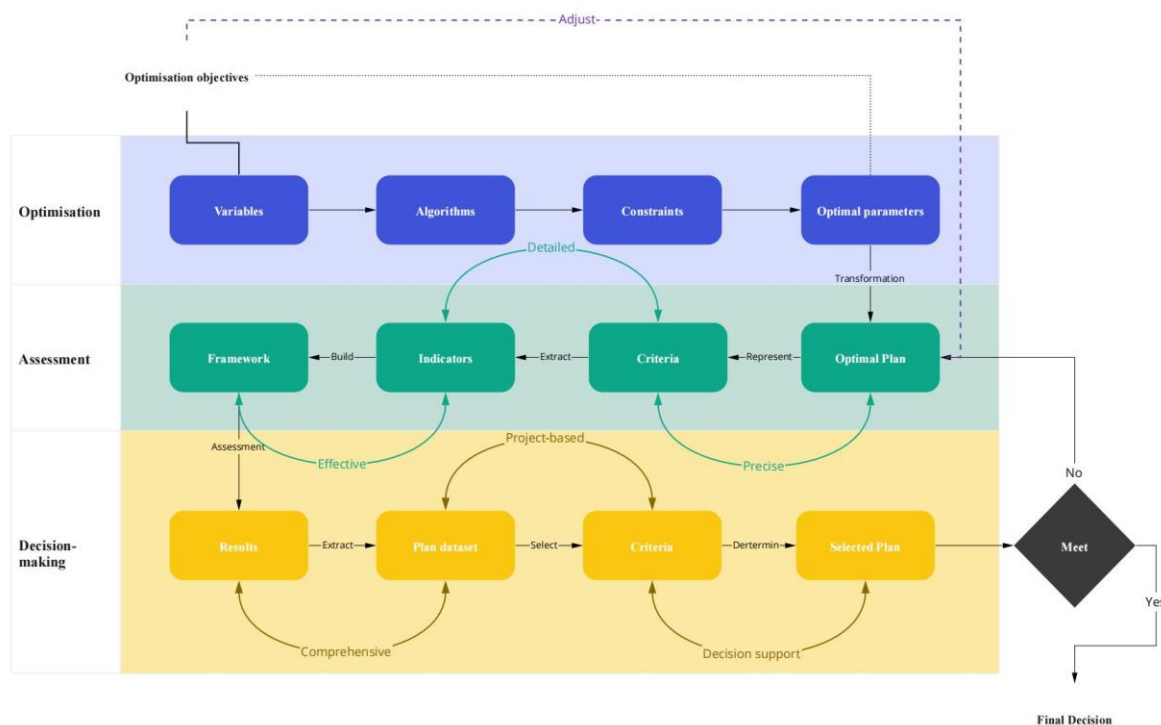


Figure 10.2 The evaluation and decision-making system

10.1.2 Choice of evaluation indicators

Traditional construction projects are complex, long-term, and multifactorial, covering policy, resources, materials, environment, economy, and the public from project conception, planning and design, construction to operation and maintenance. The RAC-FTS, therefore, requires a comprehensive and multi-faceted analysis of the factors influencing the whole process of design-optimisation-processing-build-maintenance and thorough consideration and definition. Referring to the complete index selection principles, the evaluation index selection principles for multi-objective optimisation of robotic arm processing wood constructions are as follows.

Scientific principles:

The selection of evaluation indicators and the establishment of the evaluation indicator system should have a scientific and theoretical basis, the indicators themselves should be clear in purpose, well defined and quantifiable, and the evaluation indicator system should reflect all aspects of the characteristics of the multi-objective RAC-FTS system in a comprehensive, objective, and adequate manner.

Systemic principles:

The systemic principle means that the evaluation indicators should be selected from the overall perspective of the system, reflecting as comprehensively as possible the numerous qualities of the development of the RAC-FTS system from different angles and achieving structural optimisation of the evaluation system.

Simplicity principles:

The selection of evaluation indicators should be as simple as possible, selecting the indicators that have a more significant impact on evaluating the RAC-FTS system. Each indicator has a certain degree of representativeness and can clearly and accurately reflect a particular aspect of the problem.

Independence principles:

The RAC-FTS system is complex. The selection of evaluation indicators should comply with the principle of non-linearity. Each indicator should have relative independence; the correlation should be minimised, not to contain each other, to optimise the structure of the indicator system and facilitate analysis.

Operability principles:

The purpose of the evaluation system for the RAC-FTS is to analyse the system, identify problems in its development so that it can effectively guide the operation of the system and improve the efficiency of information transfer between the different modules of the system, so simple, practical, and easily accessible indicators should be selected to be able to illustrate the problem more concisely and intuitively.

10.1.3 Choice of evaluation method

As can be understood from Chapter 5, FTT is a multi-input, multi-output non-linear dynamic complex system. However, in common with Chapter 5, the evaluation is also a multi-indicator complex evaluation. Still, several differences require a different dynamic evaluation system and methodology from AHP and FCE, as follows.

(1) The difference in the directionality of data

The impact factor analysis is based on the impact of the design and structure on the fabrication of the robot arm and is an inverse analysis process. The comprehensive solution evaluation analysis is a holistic evaluation of the design, structure, components, and fabrication, based on the methods and data mentioned above, and is a forward analysis process.

(2) The difference in criteria

Chapter 5 deals with analysing the degree of influence of the robotic arm on the design system, using a combination of AHP and FCE methods to analyse the degree of impact of robotic automation on design, processing, construction, and management. The robotic arm is the object of analysis. The four criteria of robotic arm technology, robotic arm processing conditions, materials used for robotic arm processing and robotic arm use are selected from the four criteria. The aim is to establish a hierarchical and quantitative relationship between the influence factors and the different target layers. The objective of the research in this section is to synthesise the morphological and structural design approach for freeform timber structures based on the premise of robotic arm fabrication, the grid modularity and the control optimisation approach for robotic arms presented in the previous section to establish a dynamic evaluation and analysis model and to assist in the decision analysis for the selection of combinations of solutions between different systems. Therefore, in the comprehensive evaluation system in this section, the robotic arm will be used as one of the criteria to be evaluated. If the same methodology is used, the repetition of data will make the evaluation system unstable.

(3) The difference in data sources and forms

The data analysed in Chapter 5 were generated by collating the literature and going through simulated experiments, with data formats including text and numbers. The data is therefore crudely classified using AHP for the stereotypes. The data in this section are based on simulations generated by the previous method. The data format includes textual, numerical, and geometrical parameter information, which is multidimensional and requires data processing methods to synthesise it to avoid the loss of important information.

The evaluation system will be weight calculation, impact factor correlation analysis, evaluation result, and evaluation level correlation calculation. In this paper, a combination of principal component analysis and entropy weighting method is used to determine the total weights of the indicators, and the grey correlation model and the cloud meta-model are applied to model the comprehensive evaluation, respectively.

10.1.4 Decision Support Systems

Decision support system is an information management and processing system based on mathematical theory that uses computer technology to assist management. The RAC-FTS system proposed in this study is a multidimensional nonlinear complex system, and the multidimensional information can be processed effectively using the decision system. Data on design, meshing, processing, material, and structural properties are collected and organized to establish a complete data framework from modular design, optimisation, processing, and construction. Therefore, in this chapter, we select a suitable method to build a distributed multi-object RAC-FTS decision making system.

10.2 Integrated evaluation method modelling

10.2.1 Calculation of weights

As there are different decision-making priorities in different solutions. For example, some design goals tend to increase the fabrication efficiency of the robot arm for use in large-scale construction; others tend to focus on the design of complex geometries, while others focus on the stability of the structure. Therefore, each system will have a different weight of influence for the various design objectives, which will affect the weight coefficients of the parameters of each technique. Depending on the focus of the solution, a reasonable and efficient method of assigning weights is required.

Principal component analysis (PCA) eliminates the influence of different scales and overlapping information between indicators, thus ensuring the objectivity and reasonableness of the indicator weights. The entropy weighting method determines the weight of each indicator according to its degree of variation (i.e., entropy value), which can reduce the influence of subjective factors on the weighting bias. This paper applies the principal component analysis and entropy weighting methods to calculate the index weights and obtain the total weights by combining the weights.

PCA is a dimensionality reduction algorithm based on correlation analysis to find a new set of variables to replace the original variables and retain as much information as possible about the actual variables.

The original matrix R is normalised according to the formula $r_{ij}^* = \frac{r_{ij} + r_i}{S_j}$ to obtain the new matrix R^* , where r_j is the mean value of the j -th indicator, S_j is the standard deviation of the j -th indicator.

Accordingly, the correlation coefficient matrix Z can be calculated by $Z = (z_{ij})_{p \times p} = \frac{(R^*)^T R^*}{n-1}$. Then eigenvalues of the matrix Z , $\lambda_1 \geq \lambda_2 \geq \dots \geq \lambda_p \geq 0$, are solved by $|Z - \lambda I_p| = 0$. Let the number of principal components is m and makes it possible to retain more than 80% of the original information,

i.e., $\frac{\sum_{j=1}^m \lambda_j}{\sum_{j=1}^p \lambda_j} \geq 0.8$. For each eigenvalue λ_j , the unit vector $b_j^a = \frac{b_j}{\|b_j\|}$ is obtained by $Zb = \lambda_j b$. Suppose

that there are m principal components for the matrix $R^* = (r_{i1}^*, r_{i2}^*, \dots, r_{ip}^*)^T$, the decision factor matrix

$L = (l_{ij})_{p \times m}$ for the principal components is calculated by $l_{ij} = R_i^{*T} \cdot b_j^a$. Once the contribution of

each principal component $\varphi_j = \frac{\lambda_j}{\sum_{j=1}^m \lambda_j}$ is acquired, the weight of each indicator ω_i can be obtained by

$\omega_i = \frac{\sum_{j=1}^m \varphi_j l_{ij}}{\sum_{j=1}^m \varphi_j}$ through weighted average of the principal component decision coefficients and normalisation.

Kernel Principal Components Analysis (KPCA) is a non-linear generalised principal components analysis based on PCA and takes advantage of the kernel function's weak generalisation ability and strong learning ability. It has better results in non-linear statistics and higher-order statistical feature extraction. It has better evaluation ability than the traditional features of the observed data of principal components analysis. The original space is transformed to the high-dimensional space by transformation so that the non-linear relationship becomes linear in the high-dimensional space. Then the data in the high-dimensional space is transformed by PCA. By applying the kernel principal component analysis method to coordinate projection transformation, the process of linear and non-linear correlations between indicators can be broken down more efficiently, and the dimensionality reduction effect is more pronounced. In addition, the kernel principal component analysis algorithm allows multiple types of indicators to participate in the calculation, and the evaluation results obtained are more comprehensive, realistic, and reliable. The kernel principal component analysis method can highly concentrate the contribution of comprehensive indicators and use a small number of comprehensive indicators to evaluate different design solutions comprehensively.

By applying the kernel principal component analysis method to coordinate projection transformation, the process of linear correlation and non-linear correlation between indicators can be broken through, and dimensionality reduction is more prominent. In addition, the kernel principal component analysis algorithm allows multiple types of indicators to participate in the calculation, and the evaluation results obtained are more comprehensive, realistic, and reliable.

Therefore, the process of calculating the weights is shown below:

- (1) Calculate the basis kernel function, where the basis kernel function $k(x, y) = \exp\left(-\frac{\|x-y\|^2}{2\sigma^2}\right)$.
- (2) The following process is the same as those shown above.

The detailed equations for KPCA could be found in Appendices-2.

10.2.2 Comprehensive evaluation model

The grey correlation model is an evaluation model that uses the grey correlation to measure the degree of strength and weakness between objects. It measures the degree of correlation between factors in two systems that change from one thing to another. Two factors are considered highly correlated if there is a consistent trend in their change during the development of the system; otherwise, they are less correlated. The grey correlation model provides a quantitative measure of the changing dynamics of a system and is well suited to dynamic process analysis. The basic process is as follows.

- (1) Determine the optimal set of indicators. With n indicators, the optimal set of each indicator is $x^* = [x_1^*, x_2^*, x_3^*, \dots]$.

- (2) Transformation and normalisation of the original data matrix into a standard matrix.
- (3) Calculate the grey correlation coefficients of each indicator and the corresponding optimal set of indicators to obtain the grey correlation coefficient matrix E.
- (4) Obtain the overall grey correlation matrix.
- (5) Analysis of evaluation results.

Define the grey ecoefficiency is

$$\zeta_i(k) = \frac{\min_i \min_k |x_0(k) - x_i(k)| + \rho \cdot \max_i \max_k |x_0(k) - x_i(k)|}{|x_0(k) - x_i(k)| + \rho \cdot \max_i \max_k |x_0(k) - x_i(k)|} \quad 10.9$$

where $\rho \in (0, \infty)$ are adjustable coefficients that generally take values in the range $[0,1]$. '0' means no correlation and '1' indicates the strongest correlation. That is the smaller the ρ , the greater the discrimination. When $\rho \leq 0.5463$, there exists the best discriminatory, which makes ρ equal to 0.5.

The grey clustering analysis can be carried out because of the calculated correlations. We can see from the values of the correlations that there is a specific "clustering" of the data; for example, scenario 0.528, scenario 0.513 and scenario 0.51 are closer, while scenario 0.474 is behind. However, as this is not a precise quantitative calculation, it lacks precision, and the analysis of the results is not intuitive enough. This paper uses a grey clustering method and the detailed process can be found in Appendices-2.

10.3 Establishment of the evaluation system

10.3.1 Establishment of the framework

According to the literature part on assessment, there is no certain saying in the assessment framework for robotic automation construction or freeform structure. To establish a multi-criteria assessment framework, the determination for the indicators would follow the current assessment framework for sustainability and BIM, e.g. the indicators listed in (Cavalliere, Dell'Osso, Favia, & Lovicario, 2019; M. Pan et al., 2018a) shown in Figure 10.3 and Figure 10.4. The current commonly used sustainability assessment focused on three main areas: environment, economic and social and some research would add technology (Pons & Aguado, 2012). Considering the robotic automation construction and freeform timber structure as two complicated system, these indicators about sustainability can only take a small amount for the framework. The guideline level which is the main criteria for the assessment. The main research fields are selected together with sustainability and information transformation performance. Freeform design methods are assessed from the rationality perspective and mesh for the freeform surface is measured in mesh quality. Robotic as one technique of MMC which values productivity, accuracy, repeatability and flexibility, the requirements from Industry 4.0 can be selected as the indicators to evaluate the technical performance, construction performance and fabrication performance. The assessment for BIM as a computation tool and platform would value more on the efficiency on data exchange.

Indicators of the technological performance of CAR.

Categories	Performance issues	Key Indicators	References
Robustness	Technology validity	Technology popularity and reputation	(Dunmade, 2002; Mahbub, 2008)
	Technology reliability	Technology readiness level Mean time to repair Mean time between failures	(Dunmade, 2002) (Dunmade, 2002) (Dunmade, 2002)
Adaptability	Ease of use	Friendliness of interface with manual workers Interoperability with other technologies	(Bock and Linner, 2016a; Warszawski and Navon, 1998) (Bock and Linner, 2016a; Warszawski and Navon, 1998)
	Flexibility of technology	Size, weight, power and mobility Reusability in different scenarios Flexibility of function	(Bock and Linner, 2016a; Warszawski and Navon, 1998) (Bock and Linner, 2015, 2016a; 2016b; Dunmade, 2002) (Bock and Linner, 2015, 2016a; 2016b; Dunmade, 2002)
Accessibility	Technology availability	The ability to future upgrades	(Bock and Linner, 2015, 2016a; 2016b; Dunmade, 2002)
		Technology suppliers	(Dunmade, 2002; Mahbub, 2008)
	Technology acceptability	Local availability of servicing resources Local availability of machine components Public awareness level Availability of supportive policies	(Dunmade, 2002; Mahbub, 2008) (Dunmade, 2002; Mahbub, 2008) (Assefa and Frostell, 2007; Dunmade, 2002; Mahbub, 2008) (Abbott, L.F., 2013; Dunmade, 2002; Mahbub, 2008)

Source: (Cavalliere et al., 2019)

Figure 10.3 Indicators of technology within sustainability

Factors and strategies of building flexibility.

Reference	Principles/factors	Definition/strategies
Slaughter [25]	Inter-system interactions	Reduce the interdependency with other system to facilitate the maintenance
	Intra-system interactions	Reducing the connections/interactions between the components
	Interchangeable components	Provide economies in ordering materials and facilitate their replacement
	Layout predictability	The regularity of the physical layout can provide critical signals to reduce the duration and extent of demolition to find the required components
	Improve physical access	Provide easy access for maintenance activities
	Specific system zone	Keeping specific areas or volumes free from other components and systems
Till and Schneider [26]	System access proximity	Increasing the physical proximity of the access points of specific systems to reduce the need for significant renovations
	Improve flow	Improving the flow of people or things throughout a space can accommodate change through the strategic location of specific system components
	Phase system installation	Using components that are designed to accommodate either growth in a specific system the removal of all or a portion of a system
	Simplify partial demolition	Less specified use of the space
	Space	Structures allowing easy future intervention
	Construction	Predicting future scenarios and adaptations onto the plan
Israelsson and Hansson [20]	Design for adaptation	Clear identification of layers of construction from structure, skin, services, internal partitions to finishes
	Layers	Generic and indeterminate space
	Typical plan	Locating services to allow future change and upgrading
	Services	Materials with a life suitable for both existing and future activities
	Material standards	Prefabrication leads to more flexible techniques of manufacturing
	Production	A very high degree of planning is required because of difficulty in changing installations
Živković and Jovanović [19]	Installations	Future planning determines the possible future functions to which a building can be adapted
	Planning for future changes and service life	Flexible solutions increase the initial cost by an average of about 2%, which can be saved directly during the first renovation
	Financial aspects	Property-owners and builders have to be aware that the building is subject to change
	Awareness	One-sided, two-sided or three-sided orientation
	Orientation of housing unit	Dispersed or compact form of housing units
	Geometry of plan	Relationship between structure and size of the flat and family structure
Cellucci and Di Sivo [7]	Structure and size of the flat	Central or peripheral
	Number and disposition of the entrance	Grouped or individually placed, with the central or peripheral position
	Position of technical services	Massive or skeleton structure
	Building structure	The organization of interior space is conditioned by the position of fixed elements
	Achieved degree of freedom of interior space	Ability of changing the function of rooms without changing their spatial dimensions
	Potential for multifunctional use of space	The space division is changeable by using flexible partitions
Cellucci and Di Sivo [7]	Changes in number and size of the rooms	Redundancy access; customizing privacy and social needs; undefined units; using mobile equipment
	Spatial flexibility in a fixed surface area	Increase the surface area within the existing support; increasing the dwelling's surface area in a new structure and the increasing of the initial volume; increasing the internal surface area by the addition of living units
	Evolutionary spatial flexibility	Adjustment and adaptability of the building envelope; using closures dried stratified; structural regularity and adaptable floors
	Technological flexibility related to construction techniques	Integrating home automation systems; redundancy and inspection of the equipment
	Technological flexibility related to the easy maintenance of installations	

Source: (M. Pan et al., 2018a)

Figure 10.4 Indicators for flexibility for BIM

The assessment system is established as Table 10-1 showed with target level, guideline level and indicator level.

Table 10-1 Index framework of an assessment system for RAC-FTS

Target level	Guideline level	Indicator layer
Evaluation of multi-objective optimisation for automated construction of	Design performance (B_1)	Rationalisation of geometric form design (C_{11})
		Design Method Synergy (discipline) (C_{12})

Continue Table 10-1 Index framework of an assessment system for RAC-FTS

Target level	Guideline level	Indicator layer
freeform timber structures machined by robotic arms (A)		Ease of design method (type of software) (C_{13})
		Reasonableness of the combination of materials (C_{14})
		Difficulty of meshing (C_{15})
	Materialisation information performance (B_2)	Degree of geometric information matching (C_{21})
		Mesh quality (C_{22})
		Degree of modularity (C_{23})
	Technical performance (B_3)	Automaticity (C_{31})
		Robustness (C_{32})
		Adaptability (C_{33})
		Accessibility (C_{34})
	Fabrication performance (B_4)	Fabrication planning optimisation level (C_{41})
		Fabrication quality management level (C_{42})
		Industrial fabrication efficiency (time) (C_{43})
		Degree of fabrication error (design and fabrication error) (C_{44})
	Construction performance (B_5)	Assembly of construction efficiency (C_{51})
Optimising the efficiency of construction organisation plans (C_{52})		
Construction quality level (C_{53})		
Sustainability performance (B_6)	Material efficiency (C_{61})	
	Energy (C_{62})	
	Standardisation of components (C_{63})	
Information transmission (B_7)	Information Sharing (C_{71})	
	Information Management (C_{72})	
	Information transfer efficiency (C_{73})	

10.3.2 Extraction of evaluation support information

The evaluation indicators are mostly dimensionless and are mostly non-directly derived data, which require digitisation of the indicators to be carried out, with the information being qualitative and quantitative indicators. The extraction method is shown in the table. The indicators are quantified in assembly design, multidisciplinary collaboration, and technical performance to evaluate objectively and comprehensively. The important impact factors for each indicator are explained in Table 10-2-Table 10-8.

Table 10-2 Extraction methods for qualitative and quantitative indicators - design performance (B1)

Indicator layer	Practical information	Measurement and assessment methods
Rationalisation of geometric form design (C_{11})	Stability of structural form (D_{111})	Structural strain energy (scalar)
	Degree of design integration with material properties (D_{112})	(1) Whether the form is unique to the material properties (2) Consideration of material properties in the design process (3) Structural morphology of curvature in line with the workability of building materials

Continue Table 10-2 Extraction methods for qualitative and quantitative indicators - design performance (B1)

Indicator layer	Practical information	Measurement and assessment methods
	The extent of consideration of robotic arm processing methods (D_{113})	(1) The design process is completed by considering the materials used and the processing methods (2) Consideration of the space limitations of the working space of the robot arm (3) Consideration of the basic modulus of the basic module of the geometric form
	Professional-wide BIM model application (D_{121})	(1) Application of BIM eco-software to complete the whole process (2) No need to repeat modelling (3) Enables distributed parallel work on a model with a reasonable collaborative environ
Design Method Synergy (discipline) (C_{12})	The extent of digital information in design (D_{122})	(1) Transformation of 3D models into digital information for easy information transfer (2) Transformation of key parameter variables into digital information
	Degree of linkage to other disciplines (D_{123})	(1) Use of content from other disciplines to support the birth form (2) Use of content from other disciplines for optimisation
	Number of software (D_{131})	Type of software and number of the software used in the whole process
Ease of design method (type of software) (C_{13})	Model storage efficiency (D_{132})	Average access time per unit of information (M/s)
	Optimisation rate of design time (D_{133})	Design time reduction/traditional design time (%)
	Design optimisation time (D_{134})	Time spent in the design optimisation phase (h)
	Degree of mechanical properties of the material (D_{141})	The use of wood with better compression than tension properties
Reasonableness of the combination of materials (C_{14})	Designed to utilise the proportion of wood (D_{142})	Wood and other materials supporting the structure
	The material meets design needs Degree of processing innovation (D_{143})	Need to develop new fabrication tools, fabrication space
	Ease of using processing methods for processed materials (D_{144})	Type of processing required
Difficulty of meshing (C_{15})	Degree of meshing (D_{151})	Deviation of the freeform surface from the original character by meshing, the variance of surface points

Table 10-3 Extraction Methods for Qualitative and Quantitative Indicators - Building Information Performance (B₂)

Indicator layer	Practical information	Measurement and assessment methods
Degree of geometric information matching (C_{21})	Giving architectural information to geometric forms (D_{211})	The similarity of the model to the original geometric model after the geometric information has been given architectural information, evaluated with discrete and key point information

Continue Table 10-3 Extraction Methods for Qualitative and Quantitative Indicators - Building Information Performance (B_2)

Indicator layer	Practical information	Measurement and assessment methods
	Intelligent splitting (D_{212})	Building intelligent split designs based on prefabricated component databases
Mesh quality (C_{22})	Mesh homogenisation (D_{221})	Types of basic components $N = \{N_1, N_2, \dots, N_m\} (i = 1, 2, \dots, m)$ Type of component $m = \frac{\max N_i}{n}$, Total number of components n .
	Degree of mesh flattening (D_{222})	Similarity to the original grid information after the grid has been flattened and conformalised
Degree of modularity (C_{23})	Degree of refinement in design (D_{231})	(1) standardised, modular approach to complex structures (2) design to meet the requirements of production, assembly, and construction by the processing process, accurate, clear, and reasonable design of nodes, support, etc.
	Information richness of assembled components (D_{232})	(1) Types and numbers of essential component families based on BIM and prefabrication databases (2) Visualisation of standardised builds

Table 10-4 Extraction Methods for Qualitative and Quantitative Indicators - Technical performance (B_3)

Indicator layer	Practical information	Measurement and assessment methods
Automaticity (C_{31})	Degree of automation in generating fabrication paths (D_{311})	Automatic generation of fabrication paths according to the size and type of component to be machined
Robustness (C_{32})	Degree of robustness for different fabrication categories (D_{321})	Robotic arm optimisation with sufficient reliability for different components and fabrication methods
Adaptability (C_{33})	Degree of adaptability to different fabrication tasks (D_{331})	Robotic arm optimisation for different working environments, different components, and different fabrication methods with a high degree of adaptability and flexibility
Accessibility (C_{34})	Degree of ease of use (D_{341})	Availability of robotic arm under different fabrication contexts.

Table 10-5 Extraction Methods for Qualitative and Quantitative Indicators - Fabrication performance (B_4)

Indicator layer	Practical information	Measurement and assessment methods
Fabrication planning optimisation level (C_{41})	Fabrication time optimisation rate (D_{411})	(Estimated production time - actual production time) / Estimated Fabrication elapsed time (%)
	Degree of refinement in Fabrication planning (D_{412})	Fabrication planning is based on an integrated analysis of design data (component types, quantities, basic information, and detailed drawings) and process management information (raw materials, moulds, machinery) for completeness and optimisation
	Fabrication quality control (D_{421})	Establishing a component information base based on information sharing and collaboration throughout the BIM

Continue Table 10-5 Extraction Methods for Qualitative and Quantitative Indicators - Fabrication performance (*B4*)

Indicator layer	Practical information	Measurement and assessment methods
Fabrication quality management level (<i>C</i> ₄₂)	Technical share (<i>D</i> ₄₂₂)	design, fabrication, and construction process
		(1) A finished component information base is established by sharing information on the BIM design, fabrication, and construction process. (2) Fabrication quality control using RFID technology.
Industrial fabrication efficiency (time) (<i>C</i> ₄₃)	Degree of standardisation of prefabricated components (<i>D</i> ₄₃₁)	Three components of the same size as a proportion of the total (%)
Degree of fabrication error (<i>C</i> ₄₄)	Design and fabrication errors (<i>D</i> ₄₄₁)	Error determination for robotic arm fabrication components Variance of deviation distance of key point information

Table 10-6 Extraction Methods for Qualitative and Quantitative Indicators - Construction performance (*B*₅)

Indicator layer	Practical information	Measurement and assessment methods
Assembly of construction efficiency (<i>C</i> ₅₁)	Percentage of prefabricated assembly components (<i>D</i> ₅₁₁)	Prefabricated component processing time / non-prefabricated processing time (%)
		Number of components to be prepared for rework due to broken rings / Total number of members (%)
		(Estimated duration - actual duration) / Estimated duration (%)
Optimising the efficiency of construction organisation plans (<i>C</i> ₅₂)	Degree of refinement in construction planning (<i>D</i> ₅₂₂)	(1) The designation of the construction organisation plan is based on the coded deepening design model synchronised with the IoT information (progress, quality, errors) data, synergy and optimisation with the construction management information (workspace, machinery, and equipment). (2) Total control of progress can be broken down to the accuracy at key nodes, statistics on the use of materials and robotic tools, the optimisation of resources and the number of workspaces and equipment used.
		Real-time interaction between site construction progress, quality levels and BIM models for information-based supervision
Construction quality level (<i>C</i> ₅₃)	Construction information management (<i>D</i> ₅₃₁)	Deviation analysis with original geometry information, component information
	Construction Integrity (<i>D</i> ₅₃₂)	Time taken to carry out a complete volume of work (h)
	Quantity statistics (<i>D</i> ₅₃₃)	

Table 10-7 Extraction Methods for Qualitative and Quantitative Indicators - Sustainability performance (B6)

Indicator layer	Practical information	Measurement and assessment methods
Material efficiency (C_{61})	Material utilisation of standardised modular components (D_{611})	Traditional design methods for the use of materials - standardised use of materials/traditional design methods for the use of materials (%)
Energy (C_{62})	Energy savings from automated machining with robotic arms (D_{621})	Energy savings during use
The proportion	Proportion of standardised parts applied (D_{631})	Number of complements to the application database in the design/number of HQ items (%)

Table 10-8 Extraction Methods for Qualitative and Quantitative Indicators - Information transmission (B7)

Indicator layer	Practical information	Measurement and assessment methods
Level of information sharing (C_{71})	Application of full process BIM data (D_{711})	(1) Ensure the uniqueness and data transferability of BIM data (2) Unify the data form of the whole process, realise the sharing of data and establish the application mechanism of data in different stages
	Right to limit co-working mechanisms (D_{712})	Collaborative working mechanisms between the various parties involved (design, optimisation, fabrication, construction, maintenance, materials) for the entire project life cycle;
Information Management (C_{72})	Data integration by segment (D_{721})	(1) All BIM platform software has an API for the secondary development of application software. (2) Secondary development language is as consistent as possible
	Multiform visualisation of models (D_{722})	(1) Dynamic visualisation of the model (2) Virtual browsing of the model on mobile
Information data transfer efficiency (C_{73})	Real-time synchronisation of production and construction plans for efficiency (D_{731})	Real-time feedback on construction information efficiency
	Information interaction between the design model and the production management system (D_{732})	(1) Conversion of BIM design data to robotic arm processing data. (2) Coding of prefabricated components, correlation of BIM models and component databases to achieve quality management with full life-cycle traceability of components.
	Information interaction between the design model and the construction management system (D_{733})	(1) The coded and deepened BIM model and IoT synchronised data can be used directly by the project management platform. (2) The mobile terminal carries out on-site information collection and processing, returns the information to the IoT system, and synchronises the data to the BIM model and the project management platform to achieve real-time transmission of construction information.

10.3.3 Determination of weights based on KPCA

Based on the different morphogenetic, meshing and contractorisation methods, the following design plans were devised for the RAC-FTS. Two examples for the following plan 7 and plan 8 are demonstrated in Figure 10.5 and Figure 10.6. The two examples are generated by the bionics enhanced by reverse engineering. The advantages for this method is the rationality of the morphology in structure and the geometric model can be turned into numerical information easily with a reasonable mesh. Then the mesh in Plan 7 is generated by homogenised hexagonal methods and Voronoi patterns in Plan 8. The timber products are selected as planar panels and linear rods respectively.

Plan 1: Complex geometry method + homogenised triangular mesh + planar plates

Plan 2: Complex geometry method + homogenised quadrilateral mesh + planar plates

Plan 3: Complex geometry method + homogeneous hexagonal mesh + planar plates

Plan 4: Complex geometry + Voronoi mesh + planar triangular plates + linear rods

Plan 5: Reconfiguration bionics + homogenised triangular meshes + planar plates

Plan 6: Reconfiguration bionics + homogenised quadrilateral meshes + planar plates

Plan 7: Reconfiguration bionics + homogenised hexagonal mesh + flat panels

Plan 8: Reconfiguration bionics + Voronoi meshes + planar triangular plates + linear rods

Plan 9: Machine learning to generate guidelines + homogenised triangular meshes + planar plates

Plan 10: Machine learning to generate guidelines + homogenised hexagonal meshes + linear rods

Plan 11: Machine Learning Guided Line Method + Voronoi Mesh + Flat Triangular Plates + Linear Rods

Plan 12: Machine learning guided line method + homogenised hexagonal method + linear rods

Two cases are chosen to demonstrate the meaning of various combinations of morphology design method, mesh generation method, and timber product used to build the entire structure. And the multi-criteria assessment is based on the performance of different combination plans.

Figure 10.5 depicts one example of Plan 7, which combines the use of reconfiguration bionics (see section 6.3.2) to generate the initial morphology and the homogenised hexagonal method to develop the mesh. The geometric mesh would materialise using planar plates.

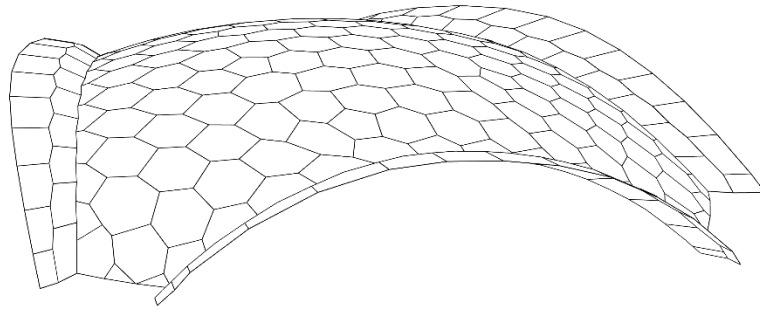


Figure 10.5 Example for Plan 7

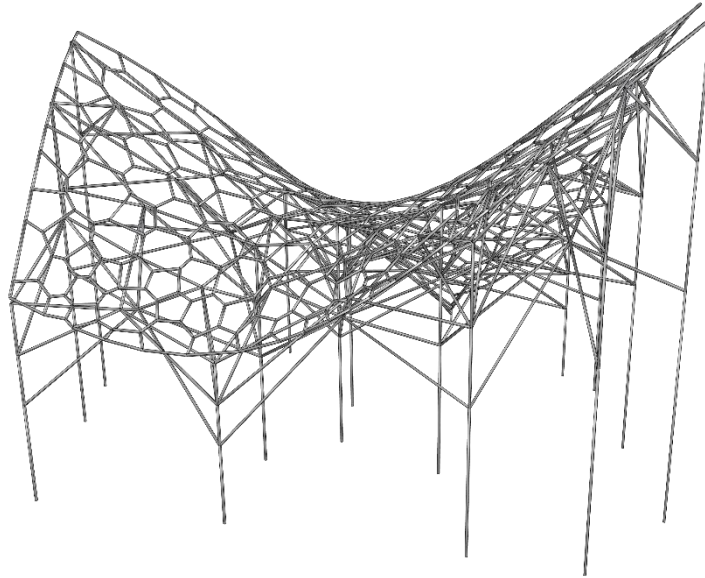


Figure 10.6 Example for Plan 8

One example of Plan 8 is presented in Figure 10.6. This example uses the same initial morphology generation method as the previous one - reconfiguration bionics. The mesh is generated using Voronoi patterns (see Figure 9.7) and then optimised to achieve the smallest variance in the length of the components. The mesh is made up of linear rods that are used to build the entire structure.

The values of each evaluation indicator for each design method are shown in the table below. The score fits for the normal distribution (Figure 10.7).

Table 10-9 Values of each evaluation indicator for each design method ($\sigma = 25$)

Indicators	Design plan											
	P1	P2	P3	P4	P5	P6	P7	P8	P9	P10	P11	P12
C_{11}	45	45	45	45	72	72	72	72	85	85	85	85
C_{12}	3	5	7	7	5	7	7	7	7	7	8	9
C_{13}	7	7	7	6	3	3	3	4	3	3	2	2
C_{14}	32	26	24	28	32	35	36	32	45	42	42	40
C_{15}	4	6	6	6	3	5	6	4	5	7	8	7
C_{21}	36	44	56	39	29	33	38	30	38	49	55	32
C_{22}	78	65	54	72	82	77	65	78	80	64	63	68
C_{23}	9	6	6	7	8	8	8	9	5	4	4	5
C_{31}	8	7	6	4	8	6	5	5	6	5	5	3
C_{32}	9	7	6	6	9	5	5	3	7	5	5	3

Continue Table 10-9 Values of each evaluation indicator for each design method ($\sigma = 25$)

Indicators	Design plan											
	P1	P2	P3	P4	P5	P6	P7	P8	P9	P10	P11	P12
C_{33}	8	6	6	4	7	6	5	4	6	4	5	2
C_{34}	8	6	5	6	7	5	5	6	8	6	5	3
C_{41}	7	6	6	7	6	5	5	4	6	6	5	3
C_{42}	85	80	70	65	76	72	70	68	78	64	60	55
C_{43}	74	76	77	78	85	84	76	88	87	88	85	88
C_{44}	2	3	2	4	3	3	3	4	3	5	5	7
C_{51}	87	85	78	76	74	72	78	70	78	72	76	77
C_{52}	87	78	76	72	82	75	77	76	78	80	82	89
C_{53}	78	79	76	80	82	80	78	76	86	82	85	88
$C_{61}/\%$	75	72	68	75	77	74	73	78	82	80	82	80
C_{62}	82	78	74	72	77	72	70	68	76	72	70	65
C_{63}	8	8	7	6	7	6	6	4	7	7	6	4
C_{71}	3	3	3	4	6	6	6	6	7	7	8	8
C_{72}	5	5	5	6	7	7	7	8	6	6	6	7
C_{73}	80	80	82	84	82	80	84	88	88	88	90	90

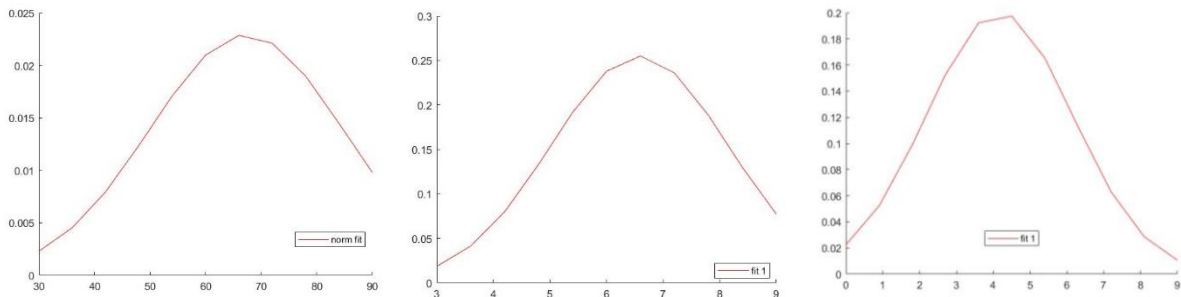


Figure 10.7 Norm fit of first three rows

Based on the values of indicators summarised in Table 10-9 and KPCA shown above, the principal indicators and the related weights are shown in Table 10-10.

Table 10-10 Kernel principal component data processing

Indicators	Eigenvalue sorting	Eigenvalue	Contribution rate	Cumulative contribution rate
C_{11}	1	9.2938	0.5915	0.5915
C_{12}	2	2.1741	0.1383	0.7299
C_{13}	3	1.4449	0.0919	0.8219
C_{14}	4	1.0508	0.0668	0.8888
C_{15}	5	0.4952	0.0315	0.9203
C_{21}	6	0.4220	0.0268	0.9471
C_{22}	7	0.2452	0.0156	0.9628
C_{31}	8	0.1270	0.0080	0.9708
C_{23}	9	0.1232	0.0078	0.9787
C_{32}	10	0.0796	0.0050	0.9838
C_{33}	11	0.0745	0.0047	0.9885
C_{34}	12	0.0410	0.0026	0.9911
C_{41}	13	0.0358	0.0022	0.9934
C_{43}	14	0.0297	0.0018	0.9953
C_{44}	15	0.0279	0.0017	0.9971

Continue Table 10-10 Kernel principal component data processing

Indicators	Eigenvalue sorting	Eigenvalue	Contribution rate	Cumulative contribution rate
C_{42}	16	0.0264	0.0016	0.9987
C_{51}	17	0.0074	0.0004	0.9992
C_{52}	18	0.0048	0.0003	0.9995
C_{53}	19	0.0027	0.0002	0.9997
C_{61}	20	0.0022	0.0001	0.9998
C_{63}	21	0.0010	6.3775e-05	0.9999
C_{73}	22	0.0007	5.0745e-05	1.0000
C_{72}	23	0.0004	2.9465e-05	1.0000
C_{71}	24	0.0002	1.5496e-05	1.0000
C_{62}	25	-4.588e-16	-2.9202e-17	1.0000

According to the contribution rate of the eigenvalues, 97.87% of the information can be obtained by selecting the first eight non-linear principal components, which can represent the original 25 evaluation index system. The corresponding contribution rates are normalized to the corresponding composite index weights, and the eigenvalue numbers and index weights ω_m are 1: 0.614416, 2: 0.142537, 3: 0.09397, 4: 0.067986, 5: 0.031889, 6: 0.027102, 7: 0.015715, 8: 0.008123.

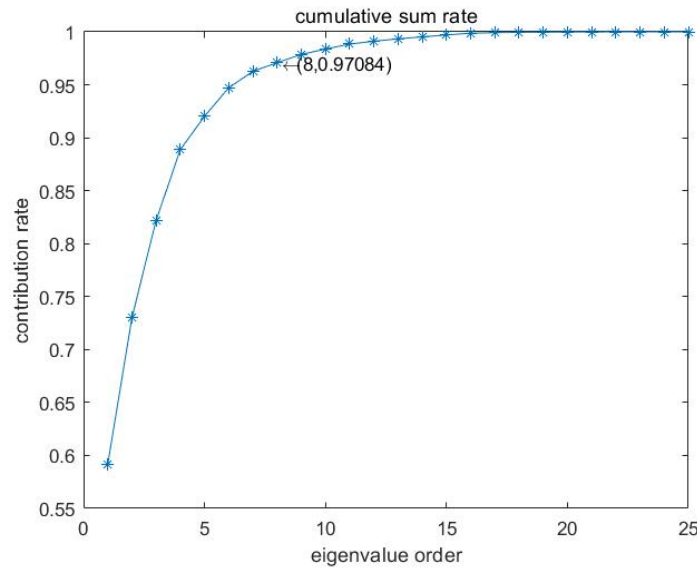


Figure 10.8 The contribution rate of the eigenvalues

10.3.4 Comprehensive evaluation of indicators using grey correlation

Based on the grey correlation analysis discussed above, the grey relational coefficients of the selected principal indicators, the grey correlation degree and the grey clustering of the indicators are shown below. Table 10-11 shows the coefficients of the eight factors for the 12 plans. The grey correlation degree is calculated based on the coefficients according to Eq. 10.9. The numerical relationships of the grey correlation degree are shown in the Figure 10.9.

Table 10-11 Matrix of grey relational coefficients

I	Plans											
	P1	P2	P3	P4	P5	P6	P7	P8	P9	P10	P11	P12
C_{11}	0.50 24	0.50 24	0.50 24	0.50 24	0.75 65	0.75 65	0.75 65	0.75 65	1	1	1	1

Continue Table 10-11 Matrix of grey relational coefficients

I	Plans											
	P1	P2	P3	P4	P5	P6	P7	P8	P9	P10	P11	P12
C_{12}	0.39	0.49	0.66	0.66	0.49	0.66	0.66	0.66	0.66	0.66	0.79	
	69	68	38	38	68	38	38	38	38	38	79	1
C_{13}				0.71	0.38	0.38	0.38	0.45	0.38	0.38	0.33	0.33
	1	1	1	42	46	46	46	45	46	46	33	33
C_{14}	0.61	0.52	0.49	0.54	0.61	0.67	0.69	0.61		0.87	0.87	0.80
	42	14	64	90	42	42	69	42	1	34	34	54
C_{15}	0.77	0.52	0.52	0.52		0.62	0.52	0.77	0.62	0.45	0.40	0.45
	01	75	75	75	1	61	75	01	61	57	11	57
C_{21}	0.54	0.66		0.58	0.47	0.51	0.57	0.47	0.57	0.77	0.95	0.49
	49	62	1	48	00	01	09	94	09	38	99	94
C_{22}	0.91	0.71	0.60	0.80		0.89	0.71	0.91	0.95	0.70	0.69	0.75
	36	33	170	8795	1	42	33	360	48	14	00	13
C_{31}		0.77	0.62	0.45		0.62	0.53	0.53	0.62	0.53	0.53	0.40
	1	27	96	94	1	96	12	12	96	12	12	47

Table 10-12 Grey correlation degree

Indicator	C_{11}	C_{12}	C_{13}	C_{14}	C_{15}	C_{21}	C_{22}	C_{31}
GCR ¹⁸	0.7530	0.6529	0.5632	0.6944	0.6012	0.6358	0.8046	0.6375

The elements of the clusters are first drawn on a row in order of increasing to decreasing relatedness. The elements are connected in order from largest to smallest grey similarity relationship values on the maximum tree. It is important to note that whether two or several elements are linked, and whether they pass through one or sever levels, if they are already linked at some λ value, these elements are equivalent at the λ level. Another element is connected to one of them, which is the same as linking to all of them. Following such a principle, the genealogical diagram for this example can be drawn in Figure 10.10. The results means that C14 (Reasonableness of the combination of materials) and C12 (Design Method Synergy) have similar impact on the overall performance of the whole system as 0.9928. The third one would be C31 (Automaticity) with the value 0.9345. If the threshold for the clustering is set as 0.9, then these three factors can be selected as the most important ones in making decisions or taking into consideration in design process.

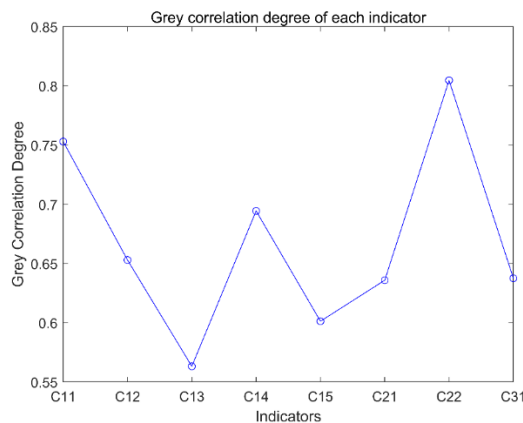


Figure 10.9 Grey correlation degree

¹⁸ GCR: grey correlation degree

Table 10-13 Grey Clustering

Index	1	2	3	4	5	6	7
Clustering	0.8203	0.8464	0.9928	0.9345	0.8310	0.7775	0.8177

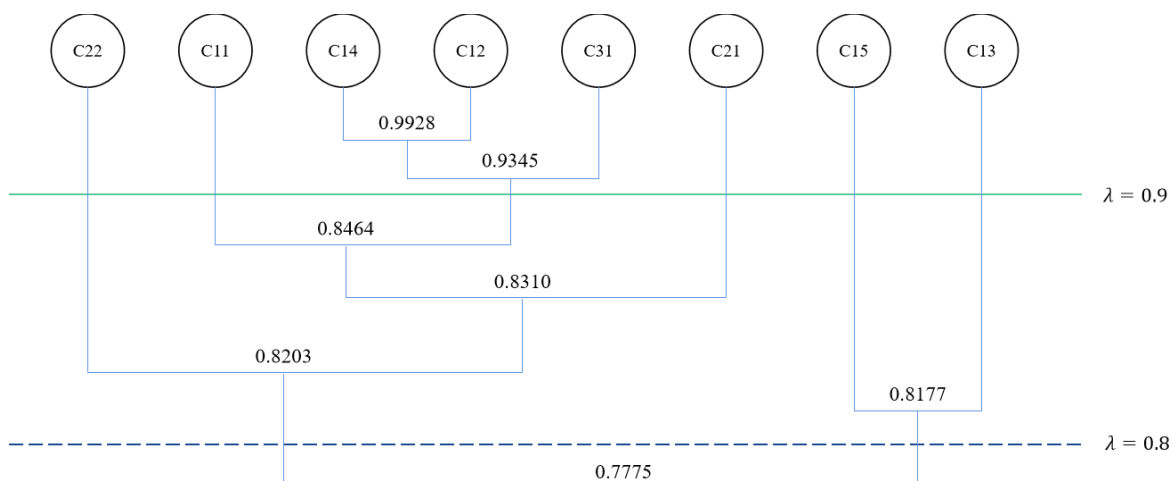


Figure 10.10 Pedigree chart of grey clustering

10.4 Decision-making and forecasting systems

For the FTT system presented in this paper, after the evaluation method described above has been carried out to evaluate the different combinations of scenarios hierarchically, the evaluation results will generate richer data for the FTT system presented. Another objective of the system is to train a prediction system based on the parameters and evaluation results of the different combinations of solutions. This intelligent prediction system is prepared by introducing machine learning clustering methods to assist in solution decision making. Decision-making problems can be classified as deterministic and stochastic based on the data type¹⁹. The intersection of multiple disciplines and systems designed in FTT scenario decision making is a multi-attribute decision making problem based on the definition of the attributes of the decision objectives²⁰. This section investigates intelligent prediction systems and Agent-based decision support systems. A framework and process for intelligent prediction and decision systems are established to provide technical support for later applications in conjunction with this FTT system.

10.4.1 Prediction systems

Clustering analysis is an important area of research in data mining and is a crucial tool and method for data segmentation or grouping processing. It has been widely researched and successfully applied in many fields, such as pattern recognition, data analysis, image, processing, market research, customer segmentation, Web document classification, etc. Clustering partitions a data set into different classes or clusters according to a particular criterion (e.g., distance criterion). The similarity of data objects within the same cluster is as significant as possible. In contrast, the differences of data objects not in the same

¹⁹ Deterministic decision problems are for decisions with exact information values, using data to build a model and get the optimal solution as the solution, stochastic decision problems have no exact quantitative values in the decision-making process, but use mathematical tools to assist in the process of getting the optimal solution.

²⁰ The evaluation of solutions in decision making is made up of multiple attributes, called multi-attribute decision problems, and multi-attribute decision making has scientific and practical characteristics.

cluster are as substantial as possible. In other words, after clustering, data from the same class are clustered together as much as possible, and different data are separated as much as possible. Various clustering methods have also been proposed and improved, and different approaches are suitable for different data types. Currently, there are many clustering algorithms (Xu & Wunsch, 2005). As for specific applications, the choice of clustering algorithm depends on the type of data, the purpose of the clustering. In the practical system application of this FTT, the final prediction of the evaluation classification also has a particular uncertainty due to the uncertainty of the objective development of things. A fuzzy clustering algorithm is chosen for the clustering analysis to combine this uncertainty into the evaluation results.

Since the famous scholar Zadeh proposed fuzzy sets, fuzzy numbers have been used to deal with the uncertainty that arises in real-life information and have been well used. Gradually, fuzzy set theory has been applied to various practical applications. Clustering analysis based on fuzzy set theory has emerged to overcome the disadvantages of either/or classification. FCM is an algorithm that determines the degree to which each data point belongs to a particular cluster by its degree of affiliation. E. Ruspini first proposed FCM, and later, J. C. Dunn and J. C. Bezdek generalised the E. Ruspini algorithm from a complex clustering algorithm to a fuzzy clustering algorithm. The FCM algorithm is a data clustering method based on optimising an objective function. The clustering result is the degree of affiliation of each data point to the cluster's centre, which is expressed as a numerical value. The FCM algorithm is an unsupervised fuzzy clustering method that does not require human intervention in implementing the algorithm. The clustering algorithm is an improvement from the traditional complex clustering algorithm.

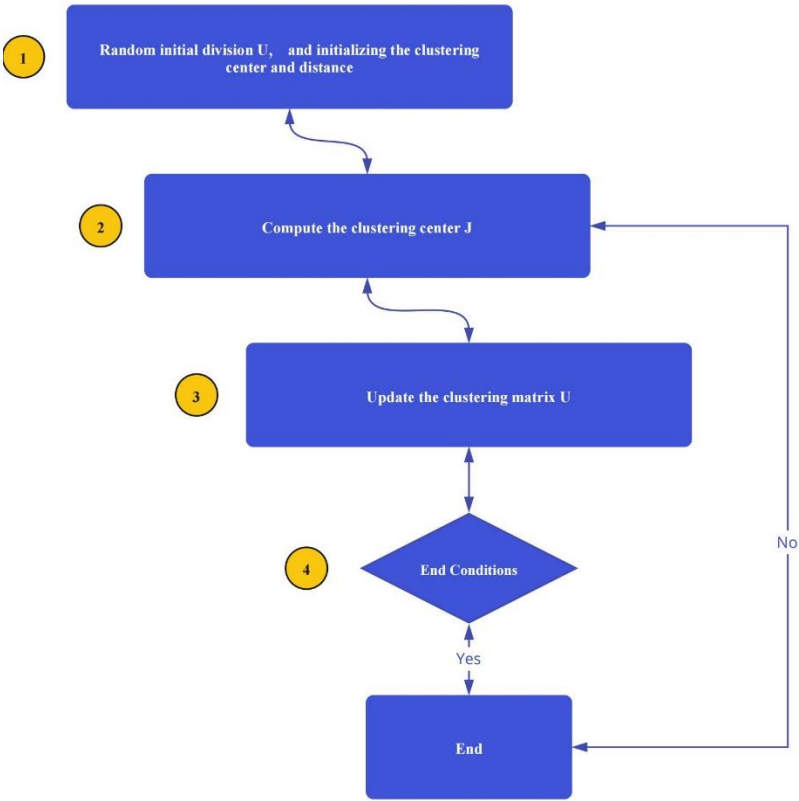


Figure 10.11 Workflow of FCM

Let the data set $X = \{x_1, x_2, \dots, x_n\}$, its fuzzy c division can be represented by the fuzzy matrix $U = [u_{ij}]$, and the element u_{ij} of the matrix U denotes the subordination of the $j(j = 1, 2, \dots, n)$ data point belonging to the $i(i = 1, 2, \dots, c)$ class degree. u_{ij} satisfies the following condition,

$$\forall j, \sum_{i=1}^c u_{ij} = 1 \quad 10.15$$

$$\forall i, j, u_{ij} \in [0, 1] \quad 10.16$$

$$\forall i, \sum_{j=1}^n u_{ij} > 0 \quad 10.17$$

The widely used clustering criterion is to take the very smallest value of the sum of squared intra-class weighted errors, i.e.

$$(\min)J_m(U, V) = \sum_{j=1}^n \sum_{i=1}^c u_{ij}^m d_{ij}^2(x_j, v_i) \quad 10.18$$

where V is the cluster centre, $m > 1$ is the weighting index, and d_{ij} is the distance norm. Then,

$$d_{ij}^2 = \|v_i - x_j\|_A = (x_j - v_i)^T A(x_j - v_i) \quad 10.19$$

$$d_{ij}(x_j, v_i) = \|v_i - x_j\| \quad 10.20$$

where A is the weight.

To obtain the optimal solution of the objective function for fuzzy clustering, subject to the constraint of extreme values: $\sum_{i=1}^c u_{ij} = 1$, such that, $(\min)J_m(U, V)$, i.e.,

$$\min\{J_m(U, V)\} = \min \left\{ \sum_{j=1}^n \sum_{i=1}^c (u_{ij})^m (d_{ij})^2 \right\} = \sum_{j=1}^n \min \left\{ \sum_{i=1}^c (\mu_{ij})^m (d_{ij})^2 \right\} \quad 10.21$$

The problem can be understood as follows: subject to the constraint of affiliation $\sum_{i=1}^c u_{ij} = 1$, such that,

$$\min \left\{ \sum_{i=1}^c (\mu_{ij})^m (d_{ij})^2 \right\} \quad 10.21$$

Its solution process is applied to the Lagrange method of solving, and the procedure is as follows.

Let the Lagrange function be: $F = \sum_{i=1}^c (u_{ij})^m (d_{ij})^2 + \lambda(\sum_{i=1}^c u_{ik} - 1)$, with λ being a parameter.

From $\frac{\partial F}{\partial \lambda} = 0$, we get: $\frac{\partial F}{\partial \lambda} = (\sum_{i=1}^c u_{ij} - 1) = 0$; From $\frac{\partial F}{\partial u_{ij}} = 0$, we get $\frac{\partial F}{\partial u_{ij}} = [m(u_{ij})^{m-1}(d_{ij})^2 - \lambda] = 0$. Then,

$$u_{ij} = \left[\frac{\lambda}{m(d_{ij})^2} \right]^{\frac{1}{m-1}} = \left(\frac{\lambda}{m} \right)^{\frac{1}{m-1}} \left(\frac{1}{(d_{ij})^2} \right)^{\frac{1}{m-1}} \quad 10.22$$

Bringing in the constraints on affiliation yields,

$$\sum_{i=1}^c u_{it} = 1 \quad 10.23$$

$$\sum_{i=1}^c u_{it} = \sum_{i=1}^c \left(\frac{\lambda}{m}\right)^{\frac{1}{m}} \left[\frac{1}{(d_{it})^2}\right]^{\frac{1}{m-1}} = \left(\frac{\lambda}{m}\right)^{\frac{1}{m-1}} \left\{ \sum_{i=1}^c \left[\frac{1}{(d_{it})^2}\right]^{\frac{1}{m}} \right\} = 1 \quad 10.24$$

$$\left(\frac{\lambda}{m}\right)^{\frac{1}{m-1}} = \frac{1}{\sum_{i=1}^c [(d_{it})^2]^{\frac{1}{m-1}}} \quad 10.25$$

After combine u_{ij} , Eq. 10.25 is

$$u_{ij} = \frac{1}{\sum_{i=1}^c \left[\frac{d_{ij}}{d_{it}}\right]^{\frac{2}{m-1}}} \quad 10.26$$

Solve for clustering centres shown as,

From $\frac{\partial J_m(U,V)}{\partial P_1} = 0$, we obtain

$$\begin{aligned} \frac{\partial J_m(U,V)}{\partial P_i} &= \sum_{i=1}^n (u_{ij})^m \frac{\partial \left[(x_j - V_i)^T A(x_j - V_i) \right]}{\partial V_i} = \sum_{i=1}^n (u_{ik})^m [-2A(x_j - V_i)] \\ &= -2A \left[\sum_{j=1}^n (u_{ij})^m (x_j - P_i) \right] = -2A \left[\sum_{j=1}^n (u_{ij})^m x_j - \sum_{j=1}^n (u_{ij})^m V_i \right] \\ &= 0 \end{aligned} \quad 10.27$$

From Eq. 10.27, the clustering centres are obtained.

$$v_i = \frac{\sum_{j=1}^n (u_{ij})^m x_k}{\sum_{j=1}^n (u_{ij})^m} \quad 10.28$$

The algorithm flow is as follows.

- (1) Standardise the data matrix
- (2) Create a fuzzy similarity matrix and initialise the affiliation matrix.
- (3) The algorithm starts iterating until the objective function converges to a minimal value.
- (4) Based on the results of the iterations, the final subordination matrix determines the classes to which the data belong and displays the final clustering results.

10.4.2 Rank clustering by FCM

The evaluation indicators were graded according to the composite scores in Table 10-9 and divided into five levels. The intervals for each level and the corresponding section domains for each evaluation indicator are summarised in Table 10-14.

Table 10-14 Grading of evaluation indicators

Indicators	Level 1	Level 2	Level 3	Level 4	Level5	Domain
C_{11}	[0,20)	[20,40)	[40,60)	[60,80)	[80,100]	[0,100]
C_{12}	[0,2)	[2,4)	[4,6)	[6,8)	[8,10)	[0,10]
C_{13}	[0,2)	[2,4)	[4,6)	[6,8)	[8,10)	[0,10]
C_{14}	[0,10)	[10,20)	[20,30)	[30,40)	[40,50)	[0,50]
C_{15}	[8,10)	[6,8)	[4,6)	[6,8)	[0,2)	[0,10]
C_{21}	[0,20)	[20,40)	[40,60)	[60,80)	[80,100]	[0,100]
C_{22}	[0,20)	[20,40)	[40,60)	[60,80)	[80,100]	[0,100]
C_{23}	[0,2)	[2,4)	[4,6)	[6,8)	[8,10)	[0,10]
C_{31}	[0,2)	[2,4)	[4,6)	[6,8)	[8,10)	[0,10]
C_{32}	[0,2)	[2,4)	[4,6)	[6,8)	[8,10)	[0,10]
C_{33}	[0,2)	[2,4)	[4,6)	[6,8)	[8,10)	[0,10]
C_{34}	[0,2)	[2,4)	[4,6)	[6,8)	[8,10)	[0,10]
C_{41}	[0,10)	[0,10)	[0,10)	[0,10)	[0,10)	[0,10]
C_{42}	[0,20)	[20,40)	[40,60)	[60,80)	[80,100]	[0,100]
C_{43}	[0,20)	[20,40)	[40,60)	[60,80)	[80,100]	[0,100]
C_{44}	[0,2)	[2,4)	[4,6)	[6,8)	[8,10)	[0,10]
C_{51}	[0,20)	[20,40)	[40,60)	[60,80)	[80,100]	[0,100]
C_{52}	[0,20)	[20,40)	[40,60)	[60,80)	[80,100]	[0,100]
C_{53}	[0,20)	[20,40)	[40,60)	[60,80)	[80,100]	[0,100]
$C_{61}/\%$	[0,20)	[20,40)	[40,60)	[60,80)	[80,100]	[0,100]
C_{62}	[0,20)	[20,40)	[40,60)	[60,80)	[80,100]	[0,100]
C_{63}	[0,2)	[2,4)	[4,6)	[6,8)	[8,10)	[0,10]
C_{71}	[0,2)	[2,4)	[4,6)	[6,8)	[8,10)	[0,10]
C_{72}	[0,2)	[2,4)	[4,6)	[6,8)	[8,10)	[0,10]
C_{73}	[0,20)	[20,40)	[40,60)	[60,80)	[80,100]	[0,100]

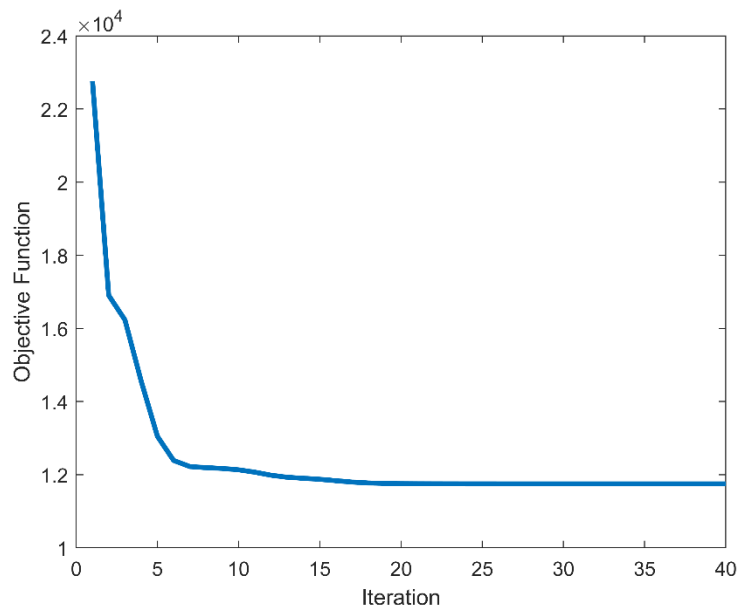


Figure 10.12 Iterations of the objective function

Table 10-15 FCM Affiliation Matrix

Cluster	Design Plans											
	P1	P2	P3	P4	P5	P6	P7	P8	P9	P10	P11	P12
C1	0.06	0.01	0.08	0.01	0.06	0.03	0.18	0.07	0.06	0.85	0.87	0.41
C2	0.12	0.01	0.10	0.02	0.63	0.87	0.39	0.71	0.07	0.04	0.04	0.20
C3	0.54	0.93	0.39	0.03	0.06	0.02	0.12	0.04	0.02	0.02	0.02	0.06
C4	0.08	0.01	0.06	0.01	0.19	0.05	0.16	0.11	0.83	0.07	0.05	0.24
C5	0.19	0.04	0.38	0.94	0.06	0.03	0.15	0.06	0.02	0.02	0.02	0.08

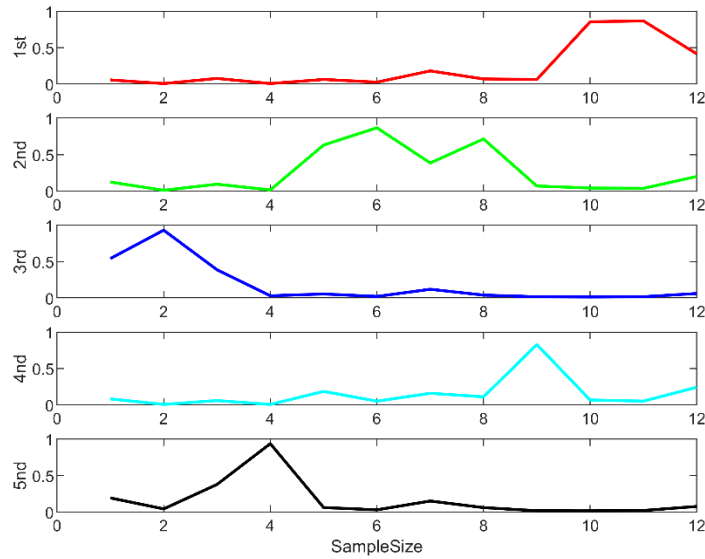


Figure 10.13 Affiliation of FCM

Table 10-16 Design plans affiliation

	Design Plans											
	P1	P2	P3	P4	P5	P6	P7	P8	P9	P10	P11	P12
Cluster	C3	C3	C3	C5	C2	C2	C2	C2	C4	C1	C1	C1

10.4.3 Decision-making systems

A decision support system is a system that uses all kinds of data and information available, organically combines many models (mathematical models and data processing models, etc.), and assists decision-makers at all levels to achieve scientific decisions through human-computer interaction. An intelligent decision support system is a new type of decision support system based on decision support systems combined with artificial intelligence technology. It is characterised by the ability to solve problems qualitatively in the form of knowledge-based reasoning through artificial intelligence techniques and quantitatively through integrated statistics and operations research, improving the scope of application and decision-making of the whole decision support system through the organic combination of qualitative analysis and quantitative calculation.

The term "decision support systems" (DS) was first introduced by Kehne and Seth Moorton in the 1970s, marking a new stage in researching and applying computers and information to support decision-making and forming a new discipline of decision support systems. The new field of decision support systems. A decision support system is a computerised management system with fundamental connotations.

(1) Support for problem-solving. Problem-solving support is not intended to replace decision-makers and automatically solve decision problems, but rather to help decision-makers by providing data, information, models, and methods related to decision problems to improve their problem-solving ability and decision-making level.

(2) The DSS can make up for the lack of information storage in the human brain by not only providing information passively as required by the decision-maker but also by inducing the decision-maker, to a

certain extent, to actively provide the decision-maker with non-self-seeking information so that the decision-maker can focus on important information.

(3) Support for decision makers' knowledge management DSS can compensate for the deficiencies in decision makers' knowledge management due to various factors, as the knowledge held by DSS and the relationships between its knowledge pieces extend the cognitive map of decision-makers and relax the limitations in knowledge representation for decision-makers. The fast and large capacity of DSS in knowledge processing also significantly overcomes the deficiencies in knowledge processing speed and power for decision-makers.

In the light of the above, it can be argued that a decision support system is an intelligent human-computer system based on management science, operations research, cybernetics, and behavioural science, and using computer technology, simulation and information technology as a means to support decision-making activities. The system provides decision-makers with the data, information and background materials needed for decision making, helps to define decision objectives and problem identification, builds, or modifies decision models, provides various alternatives, and evaluates and optimises them, analyses, compares and judges them through human-computer interaction and provides the necessary support for correct decision making.

Since the emergence of DSS, the main system structures of DSS have been two-bank, three-bank, and four-bank structures. Based on the decision-making requirements of this FTT system, a three-bank design was chosen. The three-bank system consists of a database, a method library, and a model library. It is characterised by separating the decision methods from the model library and the storage of standard techniques used in the decision-making process, such as optimisation methods, forecasting methods, Monte Carlo methods and matrix equation rooting methods, as subroutines in the method library. The operation of the three-base DS logic can be described as follows (Figure 10.14): the user inputs the decision problem to be solved through the session system, the session system passes the input problem information to the problem processing system, and then the problem processing system starts to collect data information and to judge and identify the problem based on the knowledge available in the knowledge machine. The problem-solving model is searched for, and the solution and feasibility analyses are computationally inferred, and the decision information is provided to the user.

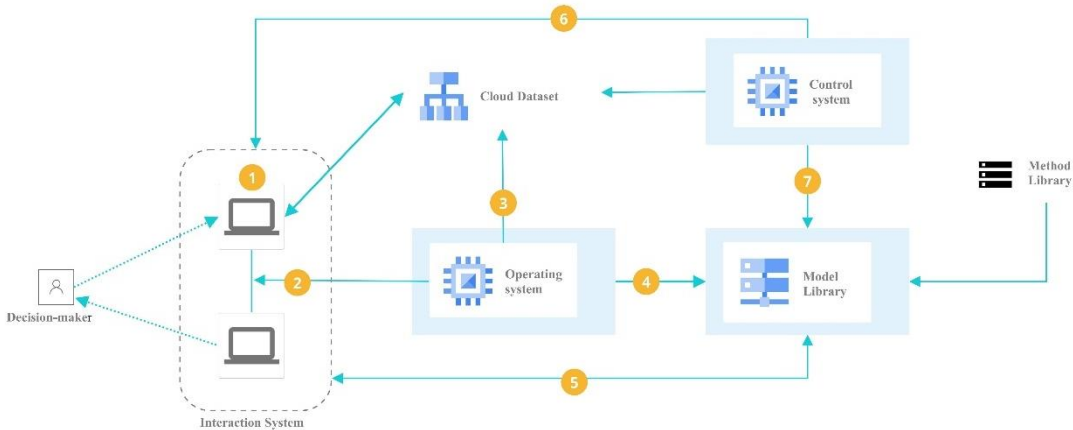


Figure 10.14 Three-layer DSS system

The concept of Agent was introduced in the book "The Self-Intelligent Society" by Professor McKay in 1986, who used it to describe hardware, software or any other natural artefact with self-adaptive and self-manufacturing capabilities and considered Agent as a skilled individual with social interactivity and intelligence. In the 1990s, with the development of computer networks and computer communication technologies, the study of agents became a hot topic in distributed artificial intelligence and information technology, licensing technology, and other related technical fields. Distributed, autonomous and cooperative agents have become the primary object of artificial intelligence research. Multi-Agent Systems (MAS for short)" have also become a more challenging object of study in AI. There is no unified standard for the definition and classification of Agent.

Agent technology has been used as an essential method for developing distributed intelligent systems. Still, the complexity of real-world application problems dictates that a single Agent cannot solve them. Furthermore, even if a single Agent can solve a particular problem, the complexity of the problem may cause problems in terms of processing speed, reliability, flexibility, and modularity. MAS offers a more optimal solution to such issues. Several independent and primarily funded agents interact to form the MAS framework. These Agents interact to solve problems beyond the capabilities or knowledge of individual Agents. In MAS, each Agent either performs their role, communicates with other Agents to obtain information, or collaborates to solve the entire problem. MAS theory is based on single-agent theory, and its main features are: (1) distributed storage and control; (2) parallel processing; (3) robustness; and (4) ease of expansion and modification. Communication between agents is the basis for inter-agent interaction, and the main methods of communication between agents are blackboard systems and message communication systems.

A multi-agent system (Figure 10.15) is a group of problem solvers formed by imitating the organisational form of human society, so it also has a specific internal organisational structure, which determines the relationship between control and communication between agents in a multi-agent system. Current multi-agent-based systems can be divided into hierarchical, federated and distributed autonomous structures. Decision-making is a typical multi-member collaborative behaviour. The Agent is an entity with communication, perception, and problem-solving capabilities, which can replace each functional unit in a decision support system and solve complex problems through the coordinated cooperation of all Agents in the system to achieve intelligent decision support. (1) task sharing and (2) result sharing.

A multi-Agent-based intelligent decision support system is a hierarchical and dynamic structure, which integrates two types of problem-solving: task sharing and result sharing.

Based on the above analysis, we decompose the problem-solving process of the MAS intelligent decision support system into the stages of problem reception, problem decomposition, sub-problem assignment, sub-problem solving, result in a synthesis, problem completion and validation, etc, shown in Figure 10.16

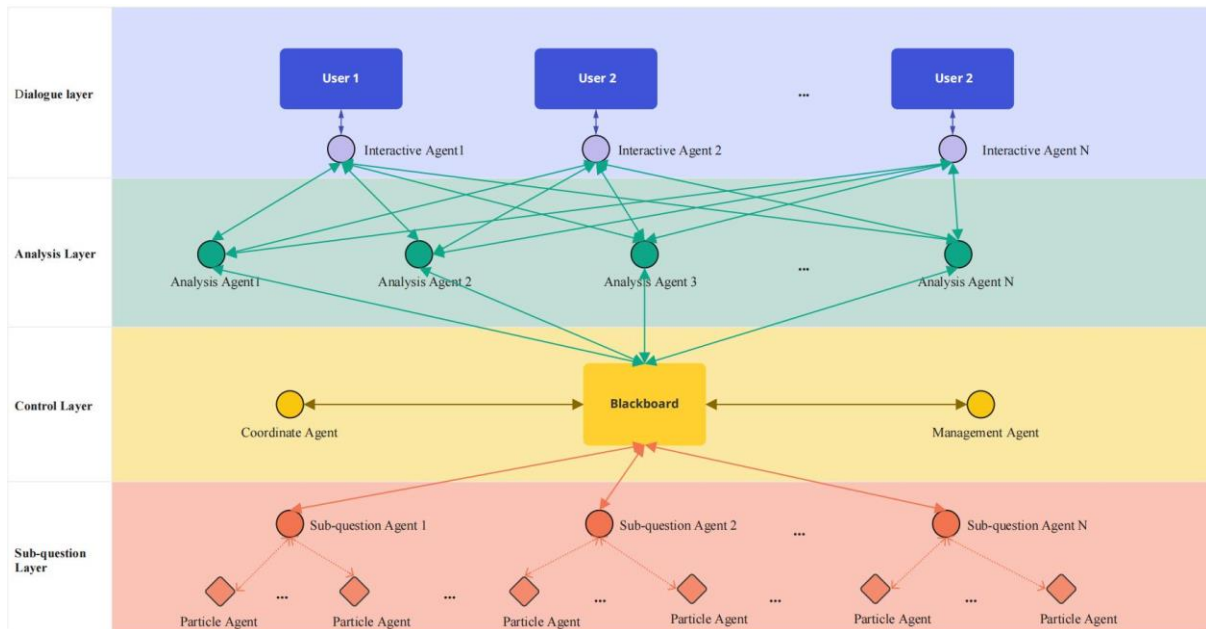


Figure 10.15 Multi-agent Decision Support System

The corresponding agentive completes each stage. The problem-solving process is as follows:

- (1) The problem is accepted by the Interface Agent.
- (2) The problem decomposition agents work together to decompose the problem using an instance-based approach.
- (3) The coordinating Agent assigns the sub-problems from the problem decomposition to the corresponding sub-problem Agent for a solution.
- (4) Each sub-problem Agent cooperates with its atomic problem Agent to solve each sub-problem.
- (5) If a sub-problem cannot be solved efficiently, the sub-problem Agent.

10.5 Conclusion

This chapter aims to assess all of the research results obtained in the previous chapters. To establish the multi-criteria assessment and decision-making support system, this chapter first identifies the ideas and principles for the establishment of the indicator framework in accordance with the workflow in Chapter 3, as a prerequisite for ensuring the standardization and consistency of the entire evaluation process. Next, the selection process of evaluation indicators is elaborated to try to summarize all aspects of the RAC-FTS system in a comprehensive and systematic manner. Then specific indicators including qualitative and quantitative ones are explained, and their definitions and scope are clarified.

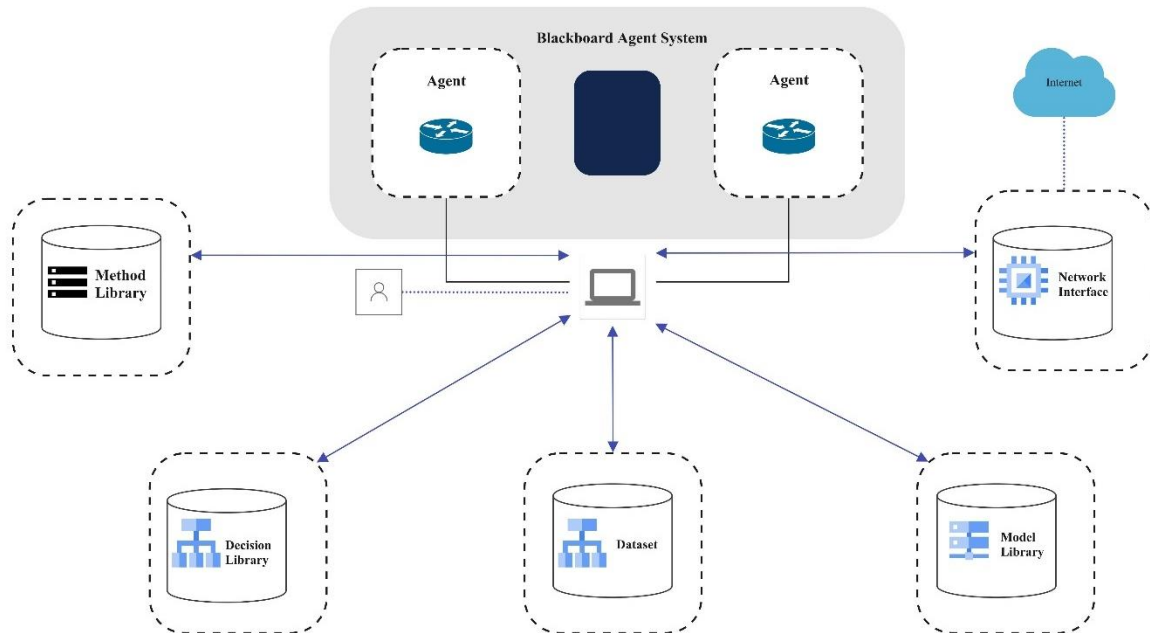


Figure 10.16 Agent-based Collaborative Design Decision-making Workflow

The MCS method was used to generate assessment data that conformed to a normal distribution, and the KPCA method was used to reduce the dimensionality of 25 indicators and select 8 features with a total contribution value of more than 97%. Using these 8 features, the association degree of different indicators to different programs is calculated using GRA, and the association degree of different indicators is clustered by GC.

Based on the evaluation, the FCM method is used to predict the 12 solutions in five categories, and the affiliation of each solution to different clusters is derived, which in turn leads to the rank of each solution's affiliation, thus aiding decision making. This multi-criteria assessment has considered several the hot topics in construction industry like digital transition, sustainability development goals to have a comprehensive assessment for the overall performance of RAC-FTS system. Different stakeholders will have different preferences when making decisions. This assessment and decision-making system would assist decision-makers in having a better overview of all performance from various sectors.

By referring to the principles and strategies in Chapter 3, this chapter wraps all of the results of Chapters 6-9 into the multi-criteria assessment and decision-making support system in the overall research framework, the connection is shown in Figure 10.17.

Chapter 11

Conclusion

11.1 Discussion and conclusion for the results

In this research, a comprehensive and multi-discipline research of Robotic Automation Construction - Freeform Timber Structure (RAC-FTS) is conducted. The research investigates the six hypotheses advanced in Chapter 1 that a non-standard freeform surface can be composed of standard planar panels or linear rods with strong rationality and sufficient creativity using an appropriate morphology design and optimisation process, as well as an efficient software ecosystem for data transformation. The simple structure components can reduce pre-fabrication complexity without the need to develop new types of tools to fit the design. The non-standard freeform structure can be completed by simple robotic fabrication operation like cutting. Productivity, energy efficiency, and cost efficiency can be improved by optimising robotic motion control and trajectory planning to meet the requirements of mass production in the context of Industry 4.0. The detailed main findings and research results are summarised as follows.

1. Chapter 3: A framework for RAC-FTS is established with four different types of system model with the characteristics of either dynamic or multi-objective optimisation (MOO). The whole system includes design, structure performance, optimisation, robotic control, data processing, assessment and decision-making support. To complete the establishment of the comprehensive and interdisciplinary system, design, optimisation, structure behaviour, robotics, assessment, and decision-making are connected through digitalization of geometric information and fabrication information. On the basis of the overall system design, the optimisation principles are put forward as standardisation and modularisation of structure components, automaticity of robotic automation construction, freeform morphology rationalisation, robustness of structure and automation process, digitalisation of the whole process to meet the development goals of Industry 4.0, MMC and Green Book of UK.

2. Chapter 4: Through one simple motion control case of a self-assembled 4-axis and a 6-axis robot arm, one research question is summarised as the relationship between joint angle and spatial position are needed to plan the motion planning for the 4-axis robot arm through the Arduino IDE. The simple spatial relationships are derived in 2-dimension and 3-dimension Cartesian coordinate system using trigonometric functions. A specific case of robotic chainsaw cutting as a result from the ETH ROB|Arch Workshop is introduced in details, including workspace design, basic information about the offset of the chainsaw, design process and tool path export. This case raised some practical questions. In this whole process, to avoid singularities, the cutting order needs to be adjusted by manual work. Sometimes, the design even needs to be adjusted if only adjusting the order could not solve the problems. This case put forward questions to appropriate design methods with applicability of robotic as the main construction technique and to motion control of robot to avoid singularities automatically. The results of the two cases put forward questions for the following chapters and the design methods and motion control would have been discussed in Chapter 6 and 8 respectively.

According to a real robotic chainsaw cutting case, the essential parts of this automation system have been demonstrated. The arrange of working space, hardware set up and software environment selection are three main steps to prepare for the robotic automation construction tasks. The characteristics of robotic automation construction in freeform structure are summarised with complex design methods, new types of tools, and diverse material selection. Still, there are some limitations for this technique with not enough accuracy and efficiency.

3. Chapter 5: To analyse whether RAC as a new technique to architecture field has impact on design method determination, an impact level assessment framework is built. To determine the indicators of the assessment framework, Text clustering is selected to select the important keywords to identify the important impact factors. The text database is established by organising the titles, keywords, abstracts, and conclusions of over 10,000 relevant documents. Using the SOM text clustering method, the keywords were clustered to identify impact factors. The RAC-FTS system is transformed into a MIMO system problem, and the impact factor is evaluated by using Fuzzy-AHP methods to determine the degree of impact of RAC on the different components of design, fabrication, construction, and management of the FTS system. The result of the impact on design is 77.5575, which means design methods needs to be adaptive to RAC technique.

4. Chapter 6: Based on the impact level assessment, the characteristics for appropriate design method of RAOD are put forward as easy to prototype and modularize, easy to digitalise, and rationality in material, structural performance and fabrication. Three methods are selected and developed based on the current cutting-edge widely used methods. The minimal surface is selected from the advanced complex geometry method as it can turned into prototype and modular units. The biomimetic method is developed with reverse engineering for RAC-FTS morphology design. The reverse engineering takes the points cloud from bionics, which assures the rationality of structure. The points cloud with enough numerical information makes these adaptive biomimetic methods connected with robotic fabrication information. LSTM is selected from Machine learning methods. For training set, a real case is transformed into a series dataset. As the curvature is learned from a real Glulam timber case, the training guarantee the range of the curvature which can be achieved in engineering timber products. These three methods satisfy the characteristic of the appropriate design methods following the principles discussed in Chapter 3.

5. Chapter 7: The RAC-FTS morphology optimisation method is by using NURBS to describe the morphology of freeform surfaces. Two important parameters are selected as optimisation variables-the control point coordinates and the weight factor. The strain energy of the surface, the mass of the structure and the maximum displacement of the nodes in the vertical direction are chosen as the optimisation objectives. The optimisation results show the effectiveness of the optimisation process and the tendency of minimizing the mechanical properties such as structural displacements and structural internal forces. As the morphology optimisation takes the results from Chapter 6, the optimisation process demonstrate that the design methods have material rationality together with structural stability.

6. Chapter 8: After the completion of the morphological design and structural optimisation, the process of building informatization needs to be carried out. Before that, further analysis of robotic orientation needs to be performed. Based on the robot arm practice in Chapter 4, the content involving robotics is expressed using a more in-depth mathematical approach. And the trajectory in the robotic chainsaw case is optimized using PSO and AGA algorithms for the travel distance and time of the cutting task. The results show the effectiveness and rationality of the algorithms, which can better improve the processing efficiency and stability of the robotic arm. The whole workflow is not limited to the robotic chainsaw cutting case, but can be applied to different type of fabrication process like milling as long as following the step: transform 3D model into numerical information, define the constraints, determine the optimisation objectives and appropriate algorithms. The optimal results mean that the productivity of robotic automation construction can be improved through motion control and trajectory planning. The time efficiency and energy efficiency of the robotic automation construction means more sustainability in construction.

7. Chapter 9: Based on the optimisation of the robot arm path, the process of standardization of the components of the FTS is carried out. To transform the freeform geometric model into building information model, mesh is the important step to materialization. Different forms of meshes are generated and optimized in terms of geometry and smoothness to standardise and homogenize the components and to satisfy the proposed optimisation principle of modularity. To measure the quality of design and fabrication, the concept of surface processing error is used as an indicator of mesh quality.

Chapter 10: RAC-FTS is a complex system including different disciplines and contents. To assess the quality or data efficiency of the whole process, a multi-criteria assessment and decision-making support system is established to support different stakeholders to choose the plan according to their own preferences. The evaluation and decision-making system for RAC-FTS is constructed by selecting reasonable criteria and screening qualitative and quantitative indicators, calculating weights by KPCA method, and calculating correlations between indicators and cluster analysis by GRA and GC methods. In the decision-making system, FCM can effectively predict the clusters to which different proposals belong. The prediction results can support the final decision making for different combinations of solutions.

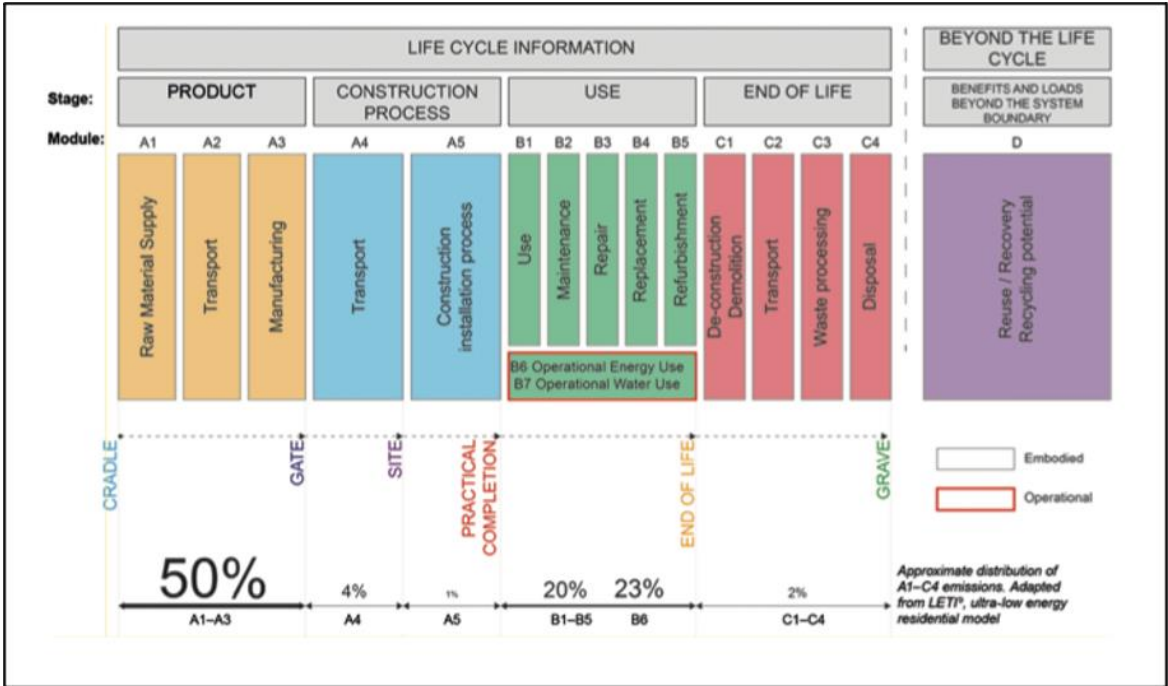
The results achieved from Chapter 3-10 testified the hypothesis put forward in Chapter 1 by following the research premise and research scope. RAC technique has impact on freeform morphology design based on the impact model. Appropriate adaptive freeform morphology design methods can generate the morphology that can be composed by planar panels or linear lattice to approximate the geometric model. The working space limitation can be simulated by Monte Carlo Methods means the size for the components can be determined ahead of the whole process. By selecting the appropriate design methods and operating the optimisation, engineering timber could be the main building material for freeform structure after robotic automation construction process like cutting. The tool path for the robotic fabrication can be generated automatically with high efficiency through motion control and trajectory planning optimisation.

11.2 Main Contribution

According to the overall background introduction about Industry 4.0, digital trend, material development and optimal design in Chapter 1, the results achieved from the whole research can provide knowledge to the current research hotspots and development goals on digitalisation, sustainability, standardisation and productivity.

11.2.1 Non-linear design system model

Embedding the concepts of rationality, sustainability and optimisation into design strategies can be one solution to enhance the level of reliability of these non-common structure types (Rohden & Garcez, 2018). If taking product life cycle into consideration, the design strategies have become non-linear which means the design can receive feedback from all the different stages of product life cycle. Then how to develop a design system with optimisation following the principles of Industry 4.0 and the digital are discussed in Chapter 3, 6-9.



Source: EN 15978 on Sustainability of construction works
 Figure 11.1 Product life cycle stages

In Chapter 3, a dynamic multi-objective optimisation system oriented by robotic arm technique is proposed shown as Figure 3.3. There are four types of models that can be applied to the RAC-FTS system including:

- Non-dynamic and non-multi-optimal model: This system means the whole system is a linear system. Every procedure from design, optimisation, to construction is progressive with single optimisation for single objective of each process.
- Non-dynamic and multi-optimal model: This system means the results of each procedure of RAC-FTS is in linear relationship and the results from different procedures would be optimised simultaneously.

- Dynamic and non-multi-optimal model: This means every part of the system would have non-linear interaction, e.g., the fabrication would send feedback to design rather than linear “design-structure-fabrication” relationship. The results of each stage would be optimised separately.
- Dynamic and multi-optimal model: This is the most complicated system for RAC-FTS which means every part and procedures would have non-linear interactions and the results achieved from different parts would be optimised separately or simultaneously, shown as Figure 3.9.

The whole system establishment has considered different factors design, structure performance, optimisation, robotic control, data processing, assessment and decision-making support and turns the traditional linear “design-construction” process into an interactive loop by receiving the information from different factors. The system starts from the conceptual design, after several optimisation on morphology, robotic motion control and mesh typologies, the loop would end until the final decision is made by the decision-makers (Figure 10.2). As non-standard design becomes more prevalent, rational design with high structure stability and longer lifespan can provide big opportunities for the large-scale promotion and application in infrastructures and public buildings. The non-linear design system can make the freeform structure design meet the above-mentioned goals through receiving and analysing the feedback from other parts.

11.2.2 Software ecosystem for digitalisation of RAC-FTSS

Industry 4.0 calls for higher efficiency and digitalisation to achieve upgrading and transformation of the conventional construction industry to meet the sustainability development goals (SDG). To meet the principles, the overall strategies and synergetic methodology are put forward aiming at transforming information from different disciplines smoothly and efficiently. In this case, a digital software environment combining different software to dealing with different types of information (geometry, fabrication, structure and material) is built through Matlab and Rhino (Figure 3.7-3.8). Rhino can export geometry information that can be turned into matrix which is the most common data type Matlab deals with. The design modelling is finished in Rhino in Chapter 6 and the geometry information can be turned into matrix to be processed in Matlab to operate numerical infinite element analysis. The timber joint model introduced in Chapter 4 is built in Rhino, and the geometry information is transformed into the spatial position of robotic arms processed in Matlab. The software ecosystem can combine geometric modelling, structure analysis and robotic fabrication information can be processed synergistically with high data efficiency. This ecosystem works aside with the non-linear design system for RAC-FTS to deal with the information effectively to support the non-linear system exchange information between different parts to achieve the optimisation objectives corresponding to each part of RAC-FTS system.

11.2.3 Architectural Artificial Intelligence for freeform morphology design

Architecture, as a creative discipline, is hard to apply artificial intelligence which is the training results relied on large amount of similar dataset. In this research, the machine learning method is applied on the prediction for the curve of freeform surface. The normal way of applying ML in architecture is taking GAN(W. Huang & Zheng, 2018) to generate the 2D drawing rather than a 3D model which is full of

difficulties. In this research, the application of LSTM presents one possibility of using machine learning in freeform morphology design by transforming the 3D geometry model into numerical information to operate classification or prediction machine learning tasks. The results from Chapter 6 about LSTM proves the feasibility of transforming the geometry information into series data and the effectiveness in predicting the curvature and vector of the divided points on the curve. Machine learning applied to freeform surface morphology design gives more scope for freeform design method development. Besides, the data collected for the machine learning training and the data received from the training results can provide more data source for further digital twin development.

11.2.4 Standardisation for RAC-FTS

A multi-criteria assessment and decision-making system for RAC-FTS is established in this research. As sustainability, productivity, and circularity have become the requirements for construction industry, a certain way to evaluate the performance of RAC-FTS is needed to help the standardisation for application of robotic automation technique in MMC or construction industry. Built on the assessment framework from (M. Pan et al., 2018a), the assessment framework add more factors about technology, data, design and structure perspectives aiming at develop a multi-criteria assessment framework to evaluate the RAC-FTS performance more comprehensively considering the design quality, structural behaviour, and fabrication productivity. The productivity, data efficiency, and sustainability of the RAC-FTS can be evaluated according to construction regulations. When there is enough data collected, the corresponding standardisation for applying robotic automation construction technique and data management would be established to fulfil the requirement of Industry 4.0.

11.3 Limitations

1. **Only conceptual design:** The current design is mainly for conceptual design. The design needs to be further deepened, such as the design of joints, the design of the connection method between components, and the optimisation of the cooperation between multiple robotic arms and multiple fabrication types. Thus, the system of RAC-FTS can have higher application value in construction industry.
2. **Only simulation:** The structural behaviour is demonstrated by simulation rather than mechanical experiments. The consideration for not taking mechanical experiments is that there are more than one example using different design methods or mesh formats, one experiment could not cover all the different performances.
3. **Only complete and continues freeform surface:** The freeform surfaces in this study are mainly complete and continuous surfaces, so the trim surface needs to be explored and compared with the complete surface. In addition, the boundary characteristics, span, and anchor points of the freeform surface are not used as a design and optimisation variable, so they can be discussed in more depth.
4. **No fabrication error analysis in structure failure:** Structural failures are not discussed in this research. A more systematic, in-depth study of structural stability is needed to discuss the mechanism

of freeform surface failure. Machining errors are collected and their effects on structural stability are calculated to further improve the design methods of freeform structures.

5. **Not enough data for LCA analysis:** Data collection of the whole life cycle is not realized. Data from the beginning of the supply chain, as well as data on site construction, use, maintenance, dismantling and even recycling can be collected for a more complete evaluation system.

6. **Not enough engineering timber products:** The data concerning timber are mainly utilized from GLT's material mechanical property data. More actual processing data of engineered wood can be collected, and mechanical performance data can be compared with simulation results to further improve the design optimisation method of RAC-FTS.

11.4 Further development

11.4.1 Dynamic system modelling through digital twin

This research puts digitalisation as one important principle for the whole RAC-FTS system. Currently, the interaction between different software or parts are off-line. For example, when the details of the design change, the corresponding optimal tool path cannot be generated simultaneously as they are operated in different software. Further step would develop API to connect Rhino and Matlab to achieve the real-time interaction. Real-time interaction can turn the whole system into a digital twin model to monitor different process more preciously and timely.

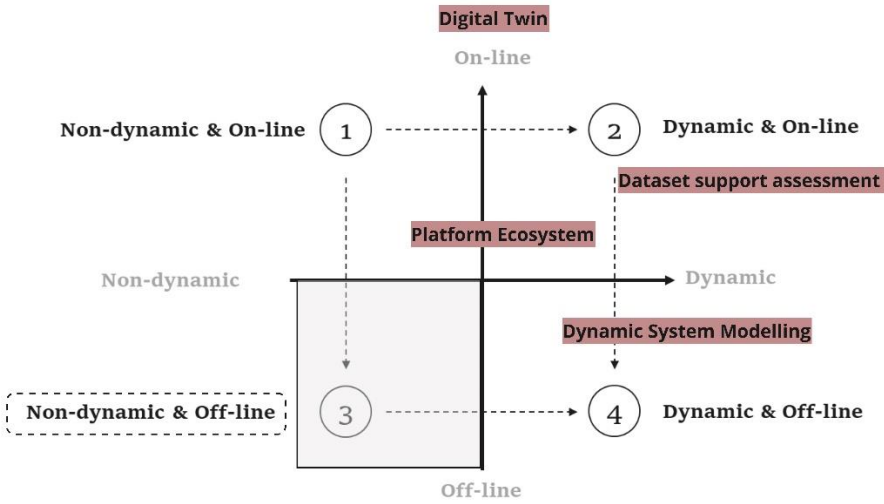
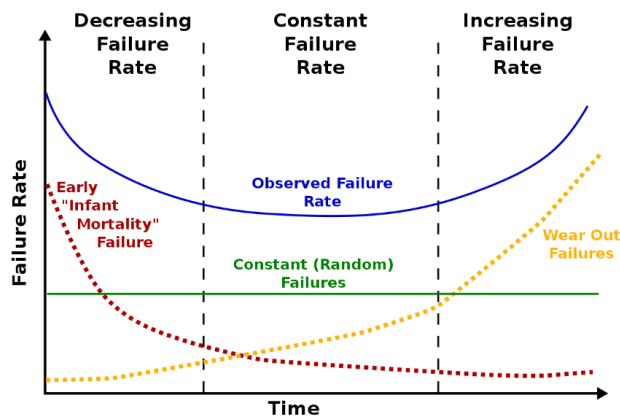


Figure 11.2 Further step on system modelling

Under the support of digital dataset and a real-time platform, the dynamic model can be established to have an interactive API to connect different parts to receive the feedbacks. Based on the dynamic digital environment, a digital twin for freeform structure prefabricated and constructed by robotic automation technique can be built.

11.4.2 Net Zero Target

The robotic automation construction has higher productivity means this technique can reduce the production time and energy consumption. The accuracy of RAC can extend the lifespan which means less construction is needed. Further research would focus on modelling the relationship between carbon emission and the deterioration rate. Based on the deterioration modelling for robotic automation construction, the durability of freeform timber structure would be optimised to achieve longer lifespan to reduce carbon emission to meet the goals of net zero. A more comprehensive sustainability research would be operated on freeform structure and the robotic automation technique to make it more applicable for mass production with longer lifespan.



Source (Lienig & Bruemmer, 2017)

Figure 11.3 'Bathtub Curve' Hazard function

Appendices-1 Figures

Figure A1 1- Figure A1 5 use different charts to illustrate the research categories within every main searching keyword and the top 10 research areas within the searching keywords. There are 8060 results (in English) for “automation construction” keyword searching including articles and reviews and 46 research are in architecture research area which accounts for 0.57% only. 3010 results for the searching “complex design” related to architecture and engineering categories. “Technology” accounts for 25% of the total amount, while “geometry” and “building performance” are of similar proportions. And there are 2905 search results for “robotic fabrication” including 188 papers specializing in “architecture” and 38 specializing in timber material.

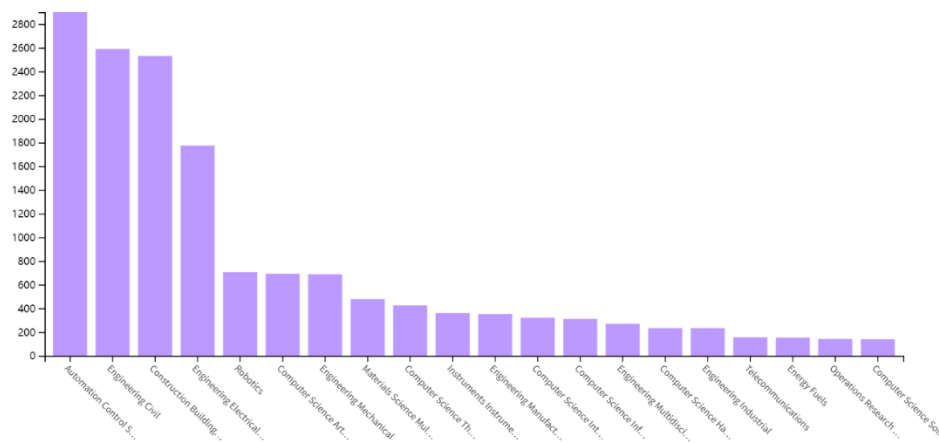


Figure A1 1 Bar chart of WOS categories of “automation construction”

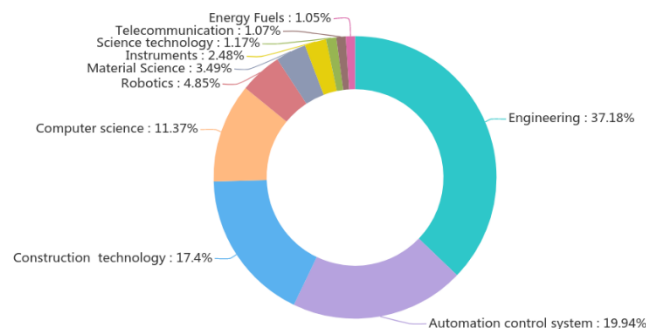


Figure A1 2 Donut chart of top 10 research areas of “automation construction”

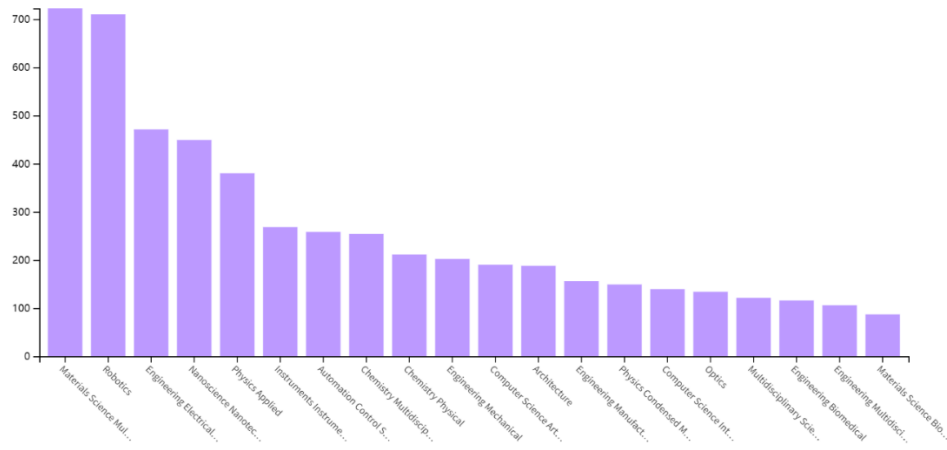


Figure A1 3 Bar chart of WOS categories of “robotic fabrication”

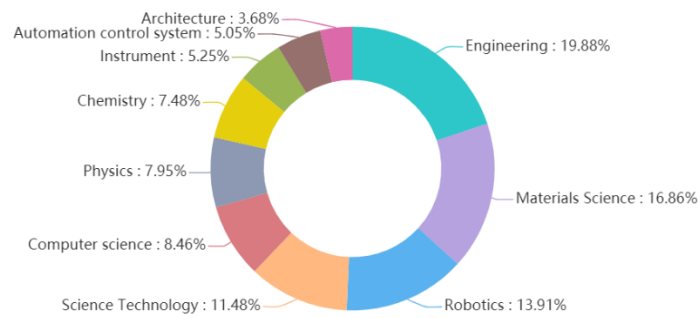


Figure A1 4 Donut chart of top 10 research areas of “robotic fabrication”

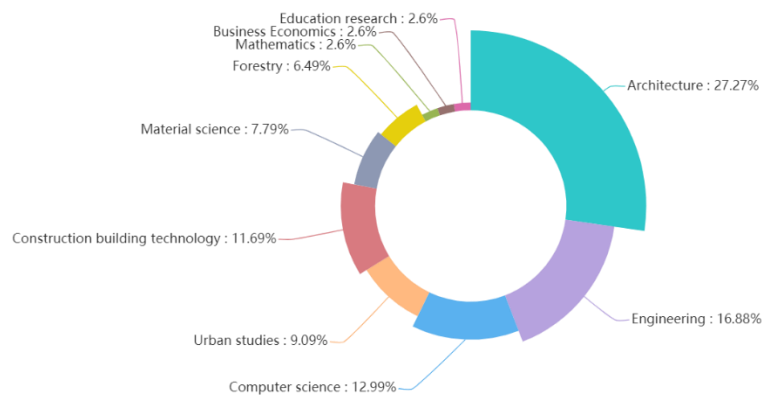


Figure A1 5 Donut chart shows the ratio of research areas within the “robotic timber fabrication” topic

Figure A1 6 summarises the extracted main research areas and categories. Then in the detailed search, the searching takes the combination of keywords for categories and research areas like “complex design” + “rationalisation”. And some keywords include different aspects as there are relatively few relevant studies in each of these areas, e.g., the keyword “component” under the “complex design” category includes the “bar”, “panel” and “lattice”.

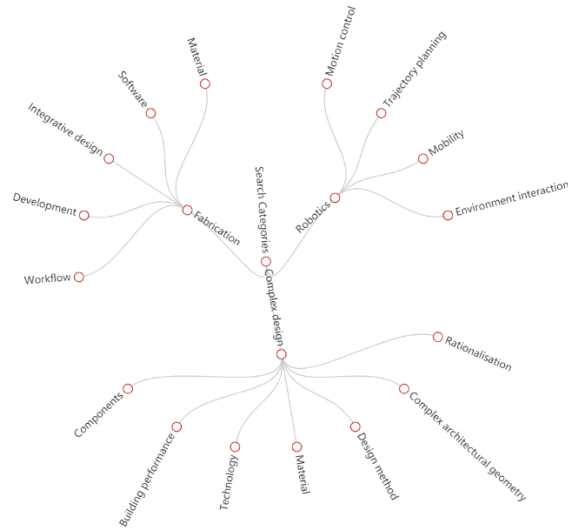


Figure A1 6 Tree map of the relations between the keywords and categories

Figure A1 7 shows the proportion of different research results in each respective research area. Each field of study clearly shows an increasing trend in terms of time horizon. And in each year, the ratio of every research area in its total count can also be compared.

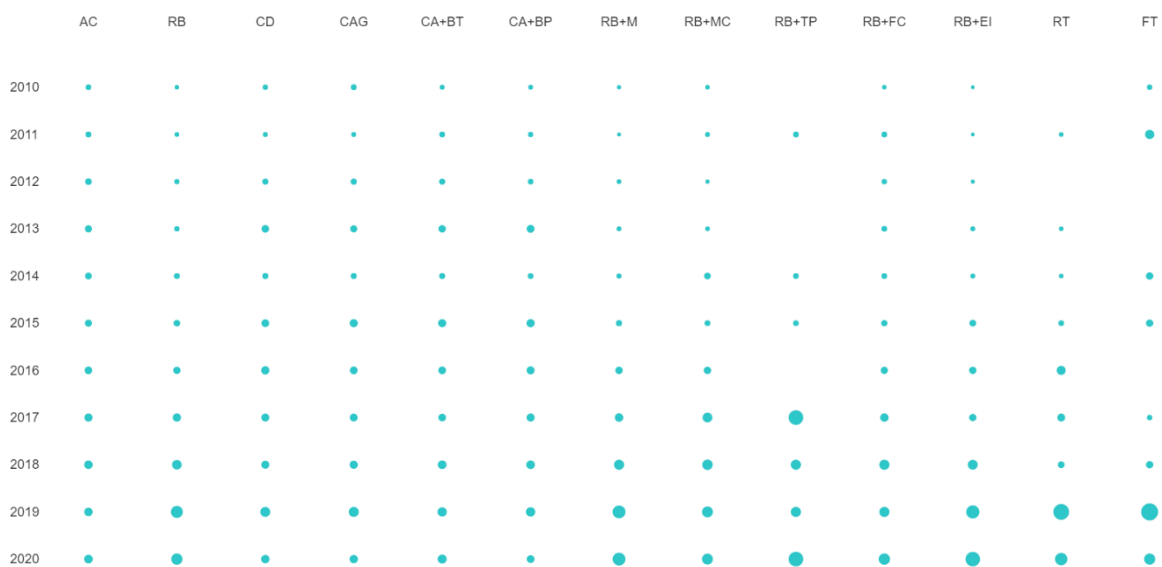


Figure A1 7 Dot chart of the distribution of research in timeline

Figure A1 8 has shown an intersection between different research categories only according to the searching keywords. To obtain a clearer cross-sectional relationship for later impact factor identification, method for analysing and sorting out the complex relations between different factors is needed.

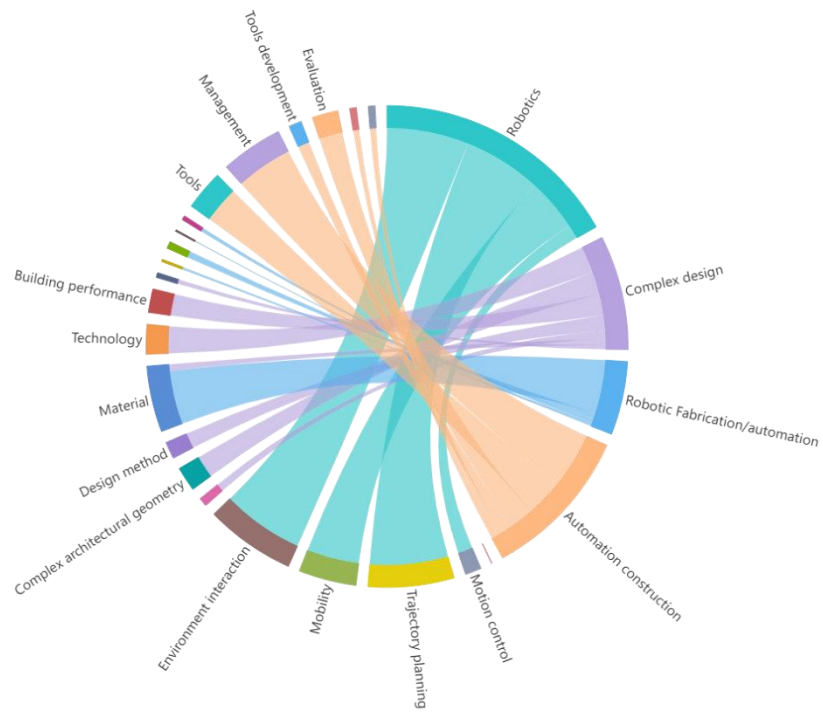


Figure A1 8 Choral graph of keywords

Appendices-2 Tables

Chapter 5

Tables for the literature text dataset

Table A2 1 Summary of rough search details

Source list	Description
Source website	Web of science
Dataset	Core of web of science
Years	2010-2020 (11 years)
Document type	Articles; Reviews; Conference paper; Book chapter
Main categories	Engineering; Construction building technology; Automation control system; Computer science; Robotics; Architecture;
Keyword Searching	“Automation construction”; “robotic fabrication”; “robotic timber”; “freeform timber structure”; “complex design”
Collection size	13775(8060+2636+3079)
Reference size	113691(52038+38969+22684)

Table A2 2A2 2 presents the searching results along the timeline from 2010-2020.

Table A2 2 Searching keywords and Years

Year/ Main Source	2010	2011	2012	2013	2014	2015	2016	2017	2018	2019	2020	Total
Automation	406	438	612	703	647	697	795	891	967	954	1000	8060
Construction												
Robotic fabrication	70	83	117	127	157	216	260	326	423	589	537	2905
Complex design	134	107	196	297	182	317	351	330	335	469	361	3079
Complex architecture geometry	36	22	43	55	38	71	65	67	71	99	74	641
Complex architecture + building technology	27	40	50	72	45	85	77	76	96	106	102	776
Complex architecture + building performance	20	26	31	64	33	70	66	68	76	86	64	618
Robotic fabrication + material	26	17	44	51	60	96	145	184	243	343	340	1549
Robotic fabrication + motion control	7	9	5	8	20	14	24	39	43	46	46	261
Robotic fabrication + trajectory planning	0	1	0	0	1	1	0	5	3	3	5	19
Robotic fabrication + mobility	1	2	3	3	2	7	2	5	5	18	13	61
Robotic fabrication + force control	6	13	11	13	13	17	22	29	39	39	46	248
Robotic fabrication + interaction	2	2	4	9	9	20	23	23	39	59	67	257
Robotic timber	0	1	0	1	1	2	5	4	3	11	8	38
Freeform timber	1	3	0	0	2	2	0	1	2	7	4	22

The RAC-FTS system are divided into three main fields: 1) robotics, 2) complex design, 3) fabrication and the corresponding keywords and the counts are shown in Table A2 3.

Table A2 3 Topics and counts of three main research field

Field	Keywords	Description	Count	
Automation construction	Technology	Different techniques applied in the automation construction process including the development of the tools or the application of it.	1050	
	Management	To fulfil the achievement of the automation construction, every aspect of the whole process needs the transition of management compared to the conventional construction methods.	1634	
	Tools development	Includes the computer-aided tools or the fabrication tools.	332	
	Evaluation	Evaluation for the efficiency of the process, workflow management, etc.	681	
	Off-site	Prefabrication research include the prefabrication, industrialization, modularization.	171	
	On-site	Include the review for this specific application,	177	
	Motion control	Control of the robot arm to execute the instructions.	261	
	Trajectory planning	The path planning and optimisation for the robot arm and the end-effector.	19	
	Robotics	Mobility	The ability of the robot to move to the designated locations.	61
		Environment interaction	Force control of the end-effector to interact with the objects or environment.	505
Rationalisation		Optimize the geometry to achieve rationality for various objectives, e.g., more stable structure, homogenisation of components.	222	
Complex architectural geometry			641	
Design method			443	
Complex design	Material	Different kinds of material used in complex architecture design including timber, glass fibre, concrete.	183	
	Technology	Manufacturing to meet the design demands.	776	
	Building performance	Acoustic, lightning, thermal comfort, energy-saving and other sustainable issues.	618	
	Components	Material in bar, panel, lattice, or other forms. Research focused on the modularization and standardization for different size of components.	122	
	Workflow Development	Development timeline of fabrication methods.	60	
	Integrative design	New or optimal design methods integrate with other disciplines.	182	
Robotic Fabrication/automation	Software	New or optimal design methods integrate with other disciplines.	34	
	Material	Software environment developed for the robotic fabrication or interaction with modelling environment	108	
		Dealing with various materials.	1549	

Table A2 4 - A2 24 are for the same calculation process as Table 5-8-Table 5-12.

Table A2 4 Judgement Matrix of Criterion $U_1 - U_{1i}$ for Fabrication O_2 ($CR = 0.0797$)

	Robotic Motion control u_{11}	Robotic calibration u_{12}	Robotic force control u_{13}	Interactivity u_{14}	W
Robotic Motion control u_{11}	1	3	1/3	2	0.247248
Robotic calibration u_{12}	1/3	1	1/3	1/3	0.093934
Robotic force control u_{13}	3	3	1	3	0.482683
Interactivity u_{14}	1/2	3	1/3	1	0.176135

Table A2 5 Judgement Matrix of Criterion $U_2 - U_{2i}$ for Fabrication O_2 ($CR = 0.0768$)

	Number of equipment u_{21}	Cooperation between robots u_{22}	Number of end- effectors u_{23}	Mobility u_{24}	Real-time feedback u_{25}	W
Number of equipment u_{21}	1	1/2	1	1/3	1/3	0.135614
Cooperation between robots u_{22}	2	1	2	1/2	1/2	0.315263
Number of end- effectors u_{23}	1	1/2	1	1/3	1/3	0.173214
Mobility u_{24}	3	2	3	1	1/2	0.226853
Real-time feedback u_{25}	3	2	3	2	1	0.149056

Table A2 6 Judgement Matrix of Criterion $U_3 - U_{3i}$ for Fabrication O_2 ($CR = 0.0611$)

	Material types u_{31}	Material properties u_{32}	Material dimensions u_{33}	Number of material types u_{34}	W
Material types u_{31}	1	2	3	2	0.419719
Material properties u_{32}	1/2	1	2	3	0.289203
Material dimensions u_{33}	1/3	1/2	1	2	0.167799
Number of material types u_{34}	1/2	1/3	1/2	1	0.123278

Table A2 7 Judgement Matrix of Criterion $U_4 - U_{4i}$ for Fabrication O_2 ($CR = 0.0038$)

	Standard element prefabrication u_{41}	Non-standard element fabrication u_{42}	Assembly on site u_{43}	Construction on site u_{44}	W
Standard element prefabrication u_{41}	1	2	3	4	0.477831
Non-standard element fabrication u_{42}	1/2	1	2	2	0.25612
Assembly on site u_{43}	1/3	1/2	1	1	0.137989
Construction on site u_{44}	1/4	1/2	1	1	0.12806

Table A2 8 Weights of the Impact Level Evaluation Indicators for Fabrication O_2

Criterion U_i	W	Indicator u_{ij}	W
Technology U_1	0.1684	Robotic Motion control u_{11}	0.247248
		Robotic calibration u_{12}	0.093934
		Robotic force control u_{13}	0.482683
		Interactivity u_{14}	0.176135
Environment U_2	0.3857	Number of equipment u_{21}	0.135614
		Cooperation between robots u_{22}	0.315263
		Number of end-effectors u_{23}	0.173214
		Mobility u_{24}	0.226853
		Real-time feedback u_{25}	0.149056
Material U_3	0.2042	Material types u_{31}	0.419719
		Material properties u_{32}	0.289203
		Material dimensions u_{33}	0.167799
		Number of material types u_{34}	0.123278
Application U_4	0.2416	Standard element prefabrication u_{41}	0.477831
		Non-standard element fabrication u_{42}	0.25612
		Assembly on site u_{43}	0.137989

Continue Table A2 8 Weights of the Impact Level Evaluation Indicators for Fabrication O_2

Criterion U_i	W	Indicator u_{ij}	W
		Construction on site	
		u_{44}	0.12806

Table A2 9 Comprehensive values of impact levels for Fabrication O_2

Indicators		Very High	High	Average	Low	Very Low
Technology	u_{11}	42	31	71	3	2
U_1	u_{12}	21	86	7	17	20
	u_{13}	84	13	8	17	29
	u_{14}	13	27	9	47	54
	Environment	u_{21}	90	19	31	3
U_2	u_{22}	20	52	6	53	19
	u_{23}	5	5	42	68	30
	u_{24}	19	31	7	86	7
	u_{25}	27	7	17	16	83
	Material U_3	u_{31}	30	19	10	2
	u_{32}	62	40	28	16	4
	u_{33}	113	16	1	6	13
	u_{34}	10	15	1	41	83
Application	u_{41}	57	4	25	22	43
U_4	u_{42}	19	76	26	10	19
	u_{43}	4	55	3	77	11
	u_{44}	24	5	86	12	22

Table A2 10 Affiliation level for O_2

Indicators		Very High	High	Average	Low	Very Low
Technology	u_{11}	3	19	71	28	29
U_1	u_{12}	12	10	63	39	26
	u_{13}	60	21	8	58	4
	u_{14}	7	10	8	32	93
	Environment	u_{21}	10	20	20	69
U_2	u_{22}	25	59	34	9	22
	u_{23}	46	44	13	25	22
	u_{24}	9	38	40	10	53
	u_{25}	50	3	52	24	21
	Material	u_{31}	55	12	43	20
U_3	u_{32}	18	2	77	26	28
	u_{33}	28	14	12	76	19
	u_{34}	38	61	18	11	21
	Application	u_{41}	12	37	70	16
U_4	u_{42}	10	29	30	9	72
	u_{43}	3	27	59	52	10
	u_{44}	13	26	15	40	57

Table A2 11 Judgement Matrix of Criterion $U_1 - U_{1i}$ for Design O_3 ($CR = 0.0611$)

	Robotic Motion control u_{11}	Robotic calibration u_{12}	Robotic force control u_{13}	Interactivity u_{14}	W
Robotic Motion control u_{11}	1	2	3	1/3	0.259665
Robotic calibration u_{12}	1/2	1	2	1/2	0.178919
Robotic force control u_{13}	1/3	1/2	1	1/3	0.103811
Interactivity u_{14}	3	2	3	1	0.457605

Table A2 12 Judgement Matrix of Criterion $U_2 - U_{2i}$ for Design O_3 ($CR = 0.0161$)

	Number of equipment u_{21}	Cooperation between robots u_{22}	Number of end- effectors u_{23}	Mobility u_{24}	Real-time feedback u_{25}	W
Number of equipment u_{21}	1	1/2	1	1/3	1/3	0.09687
Cooperation between robots u_{22}	2	1	2	1/2	1/2	0.172928
Number of end- effectors u_{23}	1	1/2	1	1/3	1/3	0.09687
Mobility u_{24}	3	2	3	1	1/2	0.27204
Real-time feedback u_{25}	3	2	3	2	1	0.361293

Table A2 13 Judgement Matrix of Criterion $U_3 - U_{3i}$ for Design O_3 ($CR = 0.0382$)

	Material types u_{31}	Material properties u_{32}	Material dimensions u_{33}	Number of material types u_{34}	W
Material types u_{31}	1	1/2	1/3	1	0.139411
Material properties u_{32}	2	1	1/2	3	0.296979
Material dimensions u_{33}	3	2	1	2	0.419234
Number of material types u_{34}	1	1/3	1/2	1	0.144376

Table A2 14 Judgement Matrix of Criterion $U_4 - U_{4i}$ for Design O_3 ($CR = 0.0797$)

	Standard element prefabrication u_{41}	Non-standard element fabrication u_{42}	Assembly on site u_{43}	Construction on site u_{44}	W
Standard element prefabrication u_{41}	1	3	3	2	0.433048
Non-standard element fabrication u_{42}	1/3	1	1/3	1/3	0.093934
Assembly on site u_{43}	1/3	3	1	1/3	0.164523
Construction on site u_{44}	1/2	3	3	1	0.308496

Table A2 15 Weights of the Impact Level Evaluation Indicators for O_3

Criterion U_i	W	Indicator u_{ij}	W
Technology U_1	0.4393	Robotic Motion control u_{11}	0.259665
		Robotic calibration u_{12}	0.178919
		Robotic force control u_{13}	0.103811
		Interactivity u_{14}	0.457605
Environment U_2	0.3107	Number of equipment u_{21}	0.09687
		Cooperation between robots u_{22}	0.172928
		Number of end-effectors u_{23}	0.09687
		Mobility u_{24}	0.27204
		Real-time feedback u_{25}	0.361293
Material U_3	0.1464	Material types u_{31}	0.139411
		Material properties u_{32}	0.296979
		Material dimensions u_{33}	0.419234
		Number of material types u_{34}	0.144376
Application U_4	0.1036	Standard element prefabrication u_{41}	0.433048
		Non-standard element fabrication u_{42}	0.093934
		Assembly on site u_{43}	0.164523
		Construction on site u_{44}	0.308496

Table A2 16 Comprehensive values of impact levels for O_3

Indicators		Very High	High	Average	Low	Very Low
Technology	u_{11}	7	93	34	15	2
U_1	u_{12}	19	21	19	75	16
	u_{13}	33	58	37	7	16
	u_{14}	8	29	53	27	33
	Environment	u_{21}	10	8	5	10
U_2	u_{22}	40	7	52	33	18
	u_{23}	25	71	2	6	46
	u_{24}	29	11	39	52	18
	u_{25}	11	47	34	16	42
	Material U_3	u_{31}	39	45	6	47
	u_{32}	45	9	30	62	4
	u_{33}	4	13	11	56	66
	u_{34}	18	22	87	22	1
Application	u_{41}	6	20	91	13	21
U_4	u_{42}	32	9	73	9	27
	u_{43}	32	18	8	59	33
	u_{44}	33	15	27	17	58

Table A2 17 Affiliation level for O_3

Indicators		Very High	High	Average	Low	Very Low
Technology	u_{11}	3	19	71	28	29
U_1	u_{12}	12	10	63	39	26
	u_{13}	60	21	8	58	4
	u_{14}	7	10	8	32	93
	Environment	u_{21}	10	20	20	69
U_2	u_{22}	25	59	34	9	22
	u_{23}	46	44	13	25	22
	u_{24}	9	38	40	10	53
	u_{25}	50	3	52	24	21
	Material U_3	u_{31}	55	12	43	20
	u_{32}	18	2	77	26	28
	u_{33}	28	14	12	76	19
	u_{34}	38	61	18	11	21
Application	u_{41}	12	37	70	16	15
U_4	u_{42}	10	29	30	9	72
	u_{43}	3	27	59	52	10
	u_{44}	13	26	15	40	57

Table A2 18 Judgement Matrix of Criterion $U_1 - U_{1i}$ for Design O_4 ($CR = 0.0225$)

	Robotic Motion control u_{11}	Robotic calibration u_{12}	Robotic force control u_{13}	Interactivity u_{14}	W
Robotic Motion control u_{11}	1	1/2	1/2	1/3	0.117254
Robotic calibration u_{12}	2	1	1	1/3	0.193875
Robotic force control u_{13}	2	1	1	1/3	0.193875
Interactivity u_{14}	3	3	3	1	0.494997

Table A2 19 Judgement Matrix of Criterion $U_2 - U_{2i}$ for Design O_4 ($CR = 0.0670$)

	Number of equipment u_{21}	Cooperation between robots u_{22}	Number of end-effectors u_{23}	Mobility u_{24}	Real-time feedback u_{25}	W
Number of equipment u_{21}	1	1/2	1	1/4	1/3	0.094849
Cooperation between robots u_{22}	2	1	3	3	2	0.362205
Number of end-effectors u_{23}	1	1/3	1	1/2	1/3	0.092403
Mobility u_{24}	4	1/3	2	1	1/2	0.189613
Real-time feedback u_{25}	3	1/2	3	2	1	0.260929

Table A2 20 Judgement Matrix of Criterion $U_3 - U_{3i}$ for Design O_4 ($CR = 0.0449$)

	Material types u_{31}	Material properties u_{32}	Material dimensions u_{33}	Number of material types u_{34}	W
Material types u_{31}	1	3	1/2	1/2	0.204682
Material properties u_{32}	1/3	1	1/3	1/3	0.096488
Material dimensions u_{33}	2	3	1	2	0.409365
Number of material types u_{34}	2	3	1/2	1	0.289465

Table A2 21 Judgement Matrix of Criterion $U_4 - U_{4i}$ for Design O_4 ($CR = 0.0449$)

	Standard element prefabrication u_{41}	Non-standard element fabrication u_{42}	Assembly on site u_{43}	Construction on site u_{44}	W
Standard element prefabrication u_{41}	1	3	1/2	1/2	0.204682
Non-standard element fabrication u_{42}	1/3	1	1/3	1/3	0.096488
Assembly on site u_{43}	2	3	1	2	0.409365
Construction on site u_{44}	2	3	1/2	1	0.289465

Table A2 22 Weights of the Impact Level Evaluation Indicators for O_4

Criterion U_i	W	Indicator u_{ij}	W
Technology U_1	0.0939	Robotic Motion control u_{11}	0.117254
		Robotic calibration u_{12}	0.193875
		Robotic force control u_{13}	0.193875
		Interactivity u_{14}	0.494997
Environment U_2	0.4509	Number of equipment u_{21}	0.094849
		Cooperation between robots u_{22}	0.362205
		Number of end-effectors u_{23}	0.092403
		Mobility u_{24}	0.189613
		Real-time feedback u_{25}	0.260929
		Material types u_{31}	0.204682
Material U_3	0.2574	Material properties u_{32}	0.096488
		Material dimensions u_{33}	0.409365
		Number of material types u_{34}	0.289465
		Application U_4	0.1978
Non-standard element fabrication u_{42}	0.096488		
Assembly on site u_{43}	0.409365		
Construction on site u_{44}	0.289465		

Table A2 23 Comprehensive values of impact levels for O_4

Indicators		Very High	High	Average	Low	Very Low
Technology	u_{11}	1	25	62	10	52
U_1	u_{12}	12	2	53	77	5
	u_{13}	38	25	33	45	8
	u_{14}	6	2	24	30	88
	Environment	u_{21}	26	10	36	69
U_2	u_{22}	27	68	3	27	26
	u_{23}	4	21	95	18	13
	u_{24}	48	19	6	26	51
	u_{25}	68	9	45	27	2
	Material U_3	u_{31}	11	6	1	72
	u_{32}	75	15	9	11	39
	u_{33}	30	4	54	7	55
	u_{34}	41	27	18	38	26
Application	u_{41}	69	24	8	38	11
U_4	u_{42}	31	9	74	23	14
	u_{43}	23	13	29	14	71
	u_{44}	7	78	8	20	37

Table A2 24 Affiliation level for O_4

Indicators		Very High	High	Average	Low	Very Low
Technology	u_{11}	0	0.107142857	0.371428571	0	0.3
U_1	u_{12}	0.014285714	0	0.307142857	0.478571429	0
	u_{13}	0.2	0.107142857	0.164285714	0.25	0
	u_{14}	0	0	0.1	0.142857143	0.557142857
Environment	u_{21}	0.114285714	0	0.185714286	0.421428571	0
U_2	u_{22}	0.121428571	0.414285714	0	0.121428571	0.114285714
	u_{23}	0	0.078571429	1	0.057142857	0.021428571
	u_{24}	0.271428571	0.064285714	0	0.114285714	0.292857143
	u_{25}	0.414285714	0	0.25	0.121428571	0
Material U_3	u_{31}	0.007142857	0	0	0.442857143	0.357142857
	u_{32}	0.464285714	0.035714286	0	0.007142857	0.207142857
	u_{33}	0.142857143	0	0.314285714	0	0.321428571
	u_{34}	0.221428571	0.121428571	0.057142857	0.2	0.114285714
Application	u_{41}	0.421428571	0.1	0	0.2	0.007142857
U_4	u_{42}	0.15	0	0.457142857	0.092857143	0.028571429
	u_{43}	0.092857143	0.021428571	0.135714286	0.028571429	0.435714286
	u_{44}	0	0.485714286	0	0.071428571	0.192857143

Chapter 10

Results for KPCA are shown in Table A2 25-Table A2 28.

Table A2 25 Sorted Grey Relation Factors

1	2	3	4	5	6	7	8
0.563215	0.601297	0.635894	0.63757	0.652978	0.694428	0.753014	0.804698

Table A2 26 DS Value

0	0.13095	0.243339	0.248642	0.296844	0.421924	0.589046	0.728852
0.13095	0	0.111944	0.117216	0.165095	0.288995	0.453796	0.591038
0.243339	0.111944	0	0.005264	0.053029	0.176341	0.339716	0.475233
0.248642	0.117216	0.005264	0	0.047763	0.171057	0.334379	0.469824
0.296844	0.165095	0.053029	0.047763	0	0.123168	0.286047	0.420895
0.421924	0.288995	0.176341	0.171057	0.123168	0	0.162168	0.295826
0.589046	0.453796	0.339716	0.334379	0.286047	0.162168	0	0.132865
0.728852	0.591038	0.475233	0.469824	0.420895	0.295826	0.132865	0

Table A2 27 ES Value

0	0.067616	0.129044	0.132019	0.159377	0.232972	0.336993	0.42876
0.063334	0	0.057537	0.060324	0.085949	0.154883	0.252316	0.338271
0.114295	0.054407	0	0.002635	0.026866	0.09205	0.184182	0.26546
0.116623	0.056892	0.002628	0	0.024167	0.089179	0.181069	0.262134
0.137468	0.079146	0.026163	0.023597	0	0.063478	0.1532	0.232352
0.188952	0.134112	0.084291	0.081878	0.059689	0	0.084366	0.158793
0.252053	0.20148	0.155535	0.153309	0.132848	0.077802	0	0.068637
0.300092	0.252767	0.209773	0.207691	0.188543	0.137033	0.064228	0

Table A2 28 RG Value

1	0.820334	0.666134	0.658858	0.592723	0.421112	0.191817	0
0.820334	1	0.846411	0.839177	0.773486	0.603493	0.377383	0.189084
0.666134	0.846411	1	0.992778	0.927243	0.758057	0.533902	0.34797
0.658858	0.839177	0.992778	1	0.934468	0.765306	0.541226	0.355391
0.592723	0.773486	0.927243	0.934468	1	0.831011	0.607537	0.422524
0.421112	0.603493	0.758057	0.765306	0.831011	1	0.777502	0.59412
0.191817	0.377383	0.533902	0.541226	0.607537	0.777502	1	0.817707
0	0.189084	0.34797	0.355391	0.422524	0.59412	0.817707	1

Appendices – 3 Equations

Chapter 10

Equations for KPCA

Given data sample x_1, x_2, \dots, x_M , where $x_i \in R^N, i = 1, 2, \dots, M$, M is the total number of samples and N is the total number of indicators. The Mercer kernel function is defined as $K: R^N \times R^N \rightarrow R$. According to Mercer's theorem, there exists a mapping $\Phi: R^N \rightarrow R^F$ such that $K(x_i, x_j) = \Phi(x_i)^T \Phi(x_j)$, F is the kernel space dimension. Noted that PCA is discussed in R^N and KPCA is discussed in the mapped R^F space, i.e., the PCA of the reformed vectors $\Phi(x_1), \Phi(x_2), \dots, \Phi(x_m)$ is discussed in R^F .

The de-averaged covariance matrix of the sample in R^F is:

$$C = \frac{1}{M} \sum_{i=1}^M \left(\Phi(x_i) - \frac{1}{M} \sum_{i=1}^M \Phi(x_i) \right) \left(\Phi(x_i) - \frac{1}{M} \sum_{i=1}^M \Phi(x_i) \right)^T \quad 10.1$$

Define $\Psi(x_i) = \Phi(x_i) - \frac{1}{M} \sum_{i=1}^M \Phi(x_i)$, where $\Psi(x_i)$ is the de-averaged sample in R^F and $\sum_{i=1}^M \Psi(x_i) = 0$.

$$C = \frac{1}{M} \sum_{i=1}^M \Psi(x_i) \Psi(x_i)^T \quad 10.2$$

The eigenvalues of C , λ , can be calculated by $Cv = \lambda v$, where v are the related eigenvectors. Then, v are defined by,

$$v = \frac{1}{\lambda M} \sum_{i=1}^M \Psi(x_i) \Psi(x_i)^T v = \frac{1}{\lambda M} \sum_{i=1}^M \Psi(x_i) (\Psi(x_i)^T v) \quad 10.3$$

where $(\Psi(x_i)^T v)$ is a scalar, which means that there exists $a_i = \frac{1}{\lambda M} (\Psi(x_i)^T v)$, $i = 1, 2, \dots, M$.

Therefore, by

$$v = \sum_{i=1}^M a_i \Psi(x_i) \quad 10.4$$

the eigenvalues of C are defined, which are $\{\Psi(x_1), \Psi(x_2), \dots, \Psi(x_M)\}$.

As $Cv = \lambda v$, then we have $(\Psi | (x_k))^T Cv = \lambda (\Psi(x_k))^T v$. Taking Eq. 10.4 into account gives

$$\lambda \sum_{i=1}^M a_i (\Psi(x_k))^T \Psi(x_i) = \frac{1}{M} \sum_{i=1}^M a_i (\Psi(x_k))^T \left(\sum_{j=1}^M \Psi(x_j) \Psi(x_j)^T \right) \Psi(x_i) \quad 10.5$$

Define a matrix $\bar{K}_{i,j} = \Psi(x_i)^T \times \Psi(x_j)$, then we have $M\lambda \bar{a} = \bar{K} \bar{a}$, where \bar{a} is the eigenvector of $\frac{\bar{K}}{M}$.

Suppose that $I \in R^M \times R^M$, $I_{ij} = E; i, j, k, l \in \{1, 2, \dots, M\}$, then we have

$$\bar{K}_{ij} = \Psi(x_i)^T \Psi(x_j) = K_{ij} - \frac{1}{M} \sum_{l=1}^M I_{il} K_{lj} - \frac{1}{M} \sum_{k=1}^M K_{ik} I_{jk} + \frac{1}{M^2} \sum_{l,k=1}^M I_{il} K_{lk} I_{kj} \quad 10.6$$

where $K_{ij} = \Phi(x_i)^T \Phi(x_j)$, K is the kernel matrix, thus we have

$$\bar{K} = K - I_M K - K I_M + I_M K I_M, I_M = \frac{1}{M} I \quad 10.7$$

By calculating kernel matrix \bar{K} and the eigenvectors \bar{I} , the projection coordinates of the original samples x_j on v are:

$$(v, \Psi(x_j)) = \sum_{i=1}^M a_i (\Psi(x_i), \Psi(x_j)) = \sum_{i=1}^M a_i \bar{K}_{i,j} \quad 10.8$$

Equations for GRA

The essence of grey cluster analysis is the composition of a mapping from a two-dimensional to a one-dimensional space f :

$$f: R^2 \rightarrow R_g \quad 10.10$$

where $R = (r_1, r_2, \dots, r_m)$ is relevance set, and R_g is the set of similarity relations for the evaluation object. From the correlation set R of the analysed system, the correlation difference matrix E between the elements can be solved by

$$E_s = \begin{bmatrix} e_{11} & e_{12} & \cdots & e_{1m} \\ e_{21} & e_{22} & \cdots & e_{2m} \\ \vdots & \vdots & \vdots & \vdots \\ e_{m1} & e_{m2} & \cdots & e_{mm} \end{bmatrix} \quad 10.11$$

where $e_{ij} = \frac{|r_i - r_j|}{r_i}$ ($i = 1, 2, \dots, m$) is the coefficient of variation of X_i relative to X_j

The difference distance matrix Ds is obtained from the E_s

$$D_s = \begin{bmatrix} d_{11} & d_{12} & \cdots & d_{1m} \\ d_{21} & d_{22} & \cdots & d_{2m} \\ \vdots & \vdots & \vdots & \vdots \\ d_{m1} & d_{m2} & \cdots & d_{mm} \end{bmatrix} \quad 10.12$$

where d_{ij} is the difference distance, $d_{ij} = e_{ij} + e_{ji}$. As Ds is a symmetric matrix, the R_g is defined as

$$R_g = \begin{bmatrix} g_{11} & g_{12} & \cdots & g_{1m} \\ g_{21} & g_{22} & \cdots & g_{2m} \\ \vdots & \vdots & \vdots & \vdots \\ g_{m1} & g_{m2} & \cdots & g_{mm} \end{bmatrix} \quad 10.13$$

$$g_{ij} = 1 - \frac{d_{ij}}{\max(Ds)} \quad 10.14$$

where $\max(Ds)$ is the maximum value in Ds . After the above steps, the mapping $f: R^2 \rightarrow R_g$ is completed.

Appendices – 4 Publications

1. Meng Y, Sun Y, Chang W, Morphology of Free-form Timber Structure Determination by LSTM oriented by Robotic Fabrication[C], CDRF 2022
2. Meng Y, Sun Y, Chang W. Optimal trajectory planning of complicated robotic timber joints based on particle swarm optimisation and an adaptive genetic algorithm[J]. Construction Robotics, 2021: 1-16.



Morphology of Free-Form Timber Structure Determination by LSTM Oriented by Robotic Fabrication

Yiping Meng¹(✉), Yiming Sun², and Wen-Shao Chang¹

¹ School of Architecture, University of Sheffield, Sheffield, UK
ymeng16@sheffield.ac.uk

² Department of Automatic Control and System Engineering, University of Sheffield, Sheffield, UK

Abstract. Robotic arms are increasingly being used as an automation tool in non-standardized fabrication and construction, while the mechanical characteristics can also impact the accomplishment or the accuracy of the components. Timber is regularly used in different scales of a non-standard free-form structure fabricated by the robotic arm. The anisotropic mechanical characteristics of timber constrain the structural morphology. Developing a method of determining the morphology that meets the technical restrictions of the robotic arm and the material properties of timber is the aim of this research. In this paper, taking Centre Pompidou-Metz as a geometric case, glue-laminated timber as the main construction material, LSTM is applied for predicting the shape of the element. The geometric data is transformed into the fabrication data to testify to the kinematic singularities. The limitation of the workspace is derived from the Monte-Carlo method based on the DH model of the robotic arm. The experimental results show that the proposed method is effective in predicting the curves that match the characteristics of timber materials and robotic fabrication constraints.

Keywords: Free-form structure · Timber · Morphology · Robotic fabrication

1 Introduction

The design for free-form timber structures fabricated/constructed by robotic automation is a complex and multi-disciplinary system. To clarify the research questions, different factors related to the research field need comprehensive considerations.

Robotic fabrication: Since the 1990s, industrial robots dominated robotics research, and the technical necessities determined areas of investigation for robotics [1]. Efficiency is highly valued to achieve production sustainability and economic growth in the manufacturing industry. Under the notion of “Industry 4.0” calling for a highly automated, autonomous, flexible system, robotic automation as a new technique has been gradually applied to construction in academics and industries.

Free-form timber structure: The current standard form of architecture could not meet the variety of demands of human Aesthetic needs. Non-standard and free-form

© The Author(s) 2023

P. F. Yuan et al. (eds.), *Hybrid Intelligence*, Computational Design and Robotic Fabrication, https://doi.org/10.1007/978-981-19-8637-6_40

architecture becomes more and more acceptable. Based on the attention paid to sustainable environmental design, timber is a perfect building material to meet the measurements for environmental construction efficiency. Freeform structures using timber as the main materials are driven by digital technologies in design methods and product fabrication for irregular geometries [2].

One question for robotic timber fabrication for free-form structure is how to consider the technical aspect and material properties throughout the whole design process. The conventional way of taking a robotic arm as a fabrication method is shown in Fig. 1a–c. The research aims to extract the appropriate features of geometry for the LSTM method and to develop a method to transform the predicted geometry data into robotic information for fabrication.

AQ1

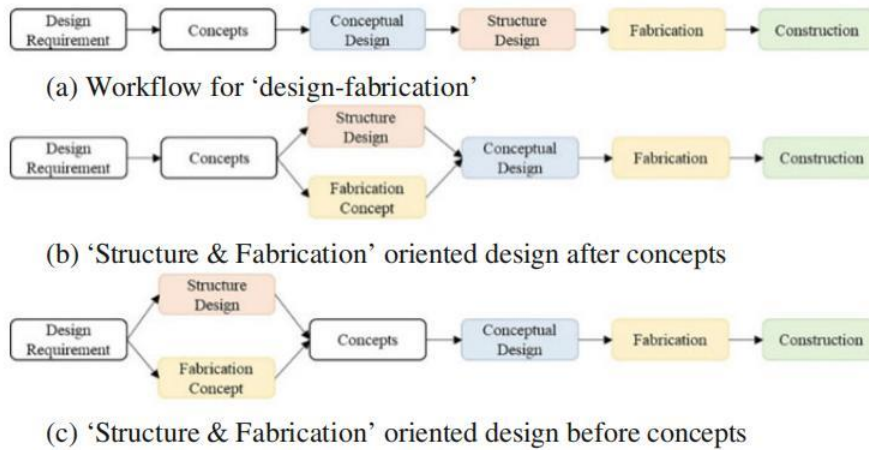


Fig. 1. Fabrication consideration in a different stage of the design process

2 Related Work

Digital fabrication technologies have enabled timber structures become irregular and complex. Compared with Computational Numerical Control (CNC) technique, the mobility, and not high requirements for the working condition of robotic fabrication system are more flexible [3]. And this advantage conforms to the development trend—that is to take the design information as the input to produce construction automatically [4]. Now, the robotic timber fabrication technique has not only been researched in laboratories but also applied in some large-scale construction applications [3, 5–7]. According to different forms of the components designed by different based-factors, different robotic fabrication types are needed such as cutting, milling, sewing, drying on different timber products from natural wood to engineering timber products [8]. More and more cases of using robotic fabrication automation have been demonstrated [9–12]. In summary, robotic fabrication can be applied throughout the whole design process in different phases from preparation to customised fabrication.

The rationality of free-form morphology means the design can be fabricated and constructed which is a complex work for architects and engineers [13]. Machine learning (ML) is derived from statistics, and the quality of an ML system is determined by the low error rate of prediction or classification [14]. ML can generate data which can be applied in generative design work using technique like deep neural networks (DNNs) [15]. One of the DNN model that has demonstrated the ability to be applied in geometry generation is the generative adversarial network (GAN) [16]. The model built through GAN can learn from the existing 2D images and transfer the empirical data into the generative design in 2D form [17]. 2D application of GAN is only limited to the 2D plan or façade generations. In ML area, many attempts have been made to generate 3D objects.

Other machine learning networks has potential to deal with 3D geometry. The data type of the current LSTM applications is in time-sequence, and the results prove the effectiveness and accuracy in predicting time sequential data like wind or air quality [18, 19]. As for the image or 2D data type which is not in sequence technically, one step to transform image into sequence data is needed additionally [20]. As for 3D geometric data, LSTM or other machine learning methods have not been widely used, especially in architectural design field.

In this paper, LSTM method is applied to predict the free-form surface morphology to improve the rationality of free-form structure considering material properties of timber and robotic fabrication. The first step is to transform the geometric data into sequential data types, and the simulation environment for the robotic is set up. The experiment of applying LSTM model to predict the morphology of free-form curves would be taken in to testify the feasibility of the transformed data to be applied in LSTM. After the prediction experiment, the methods of testifying for the singularities and the limitation of the robotic fabrication would be operated. The results of the experiments and the method would be discussed in the discussion and conclusion part.

3 Methodology

3.1 Workflow

To improve the rationality of the free-form morphology design, the impact of characteristics (6 Degree-of-freedom) and constraints (the type of fabrication, the dimensions of working space) of robotics as a technique on architectural geometry design are considered. To generate the initial geometry of free-form timber morphology, this research would discuss using LSTM machine learning to fulfil the constraints of timber material and robotic fabrication in conceptual design.

Based on the morphological design requirements of free-form timber structures, the pathway of machine learning for predicting the curve is developed as follows, shown in Fig. 2:

1. Choose the appropriate input and output.
2. Transform the input and output into a training set (in numbers or figures).
3. Select the training method.
4. Test the training accuracy.

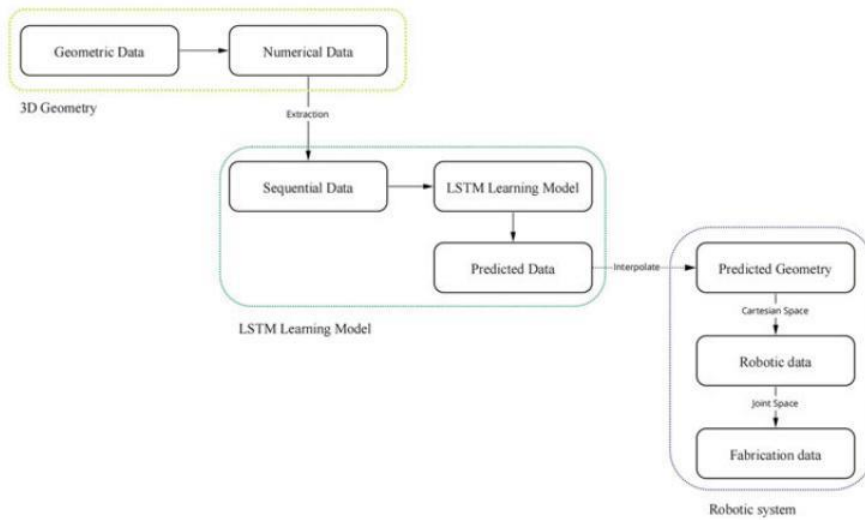


Fig. 2. Workflow of the LSTM prediction and robotic testing

3.2 Data Transformation

To complete the prediction learning task, the appropriate free-form model matters in the learning task. This research takes the Center Pompidou-Metz Model as a case to extract the data for LSTM (Fig. 3).

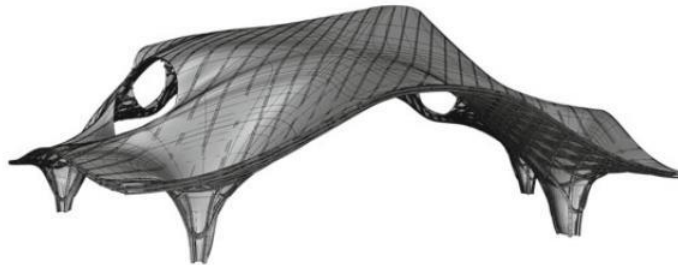


Fig. 3. 3D model of the case

As LSTM works well for the sequential data, the geometric data of the model would be transformed. The main difficulty is the geometric design is stored in a three-dimension form (like 3 dm, obj) while machine learning deals with numbers. If the model is presented in the figures from perspective views, there would be a loss of geometric information. The idea of data transformation is to find the proper way to store geometric information that fits the LSTM method and could be exported to the robot arm to generate fabrication commands (Fig. 4).

For the data transformation in this condition, assuming the number of curves to be analysed in N , every curve has been divided into $(M - 1)$ parts evenly. There are eight

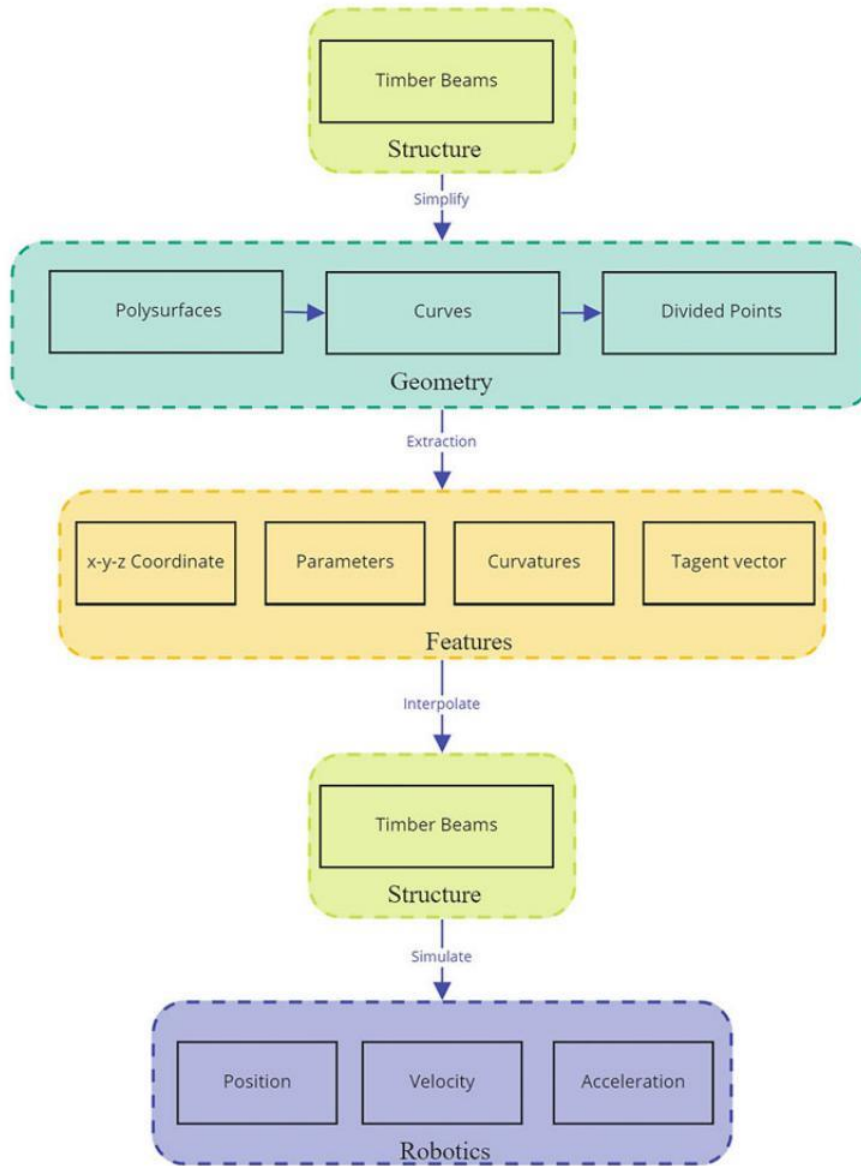


Fig. 4. Data transformation

parameters to describe this curve, the position of the division-point $P(x, y, z)$, curvature K , the position of the point on the curve t_1 , the tangent of the points $T(a, b, c)$. Every curve can be described by a matrix, which is $Q_{m \times 8}$.

The detailed of matrix Q is shown as:

$$Q_{M \times 8} = \begin{bmatrix} x_1 & y_1 & z_1 & t_1 & K_1 & a_1 & b_1 & c_1 \\ x_2 & y_2 & z_2 & t_2 & K_2 & a_2 & b_2 & c_2 \\ \dots & \dots & \dots & \dots & \dots & \dots & \dots & \dots \\ x_M & y_M & z_M & t_M & K_M & a_M & b_M & c_M \end{bmatrix} \quad (1)$$

According to the features of the discrete numbers extracted from the curves of the timber columns and beams, the LSTM training model is selected to predict the six variables of every curve for the best result. The workflow is shown in Fig. 5. After the LSTM learning network, the predicted parameters can interpolate the predicted curve which can be compared with the test one.

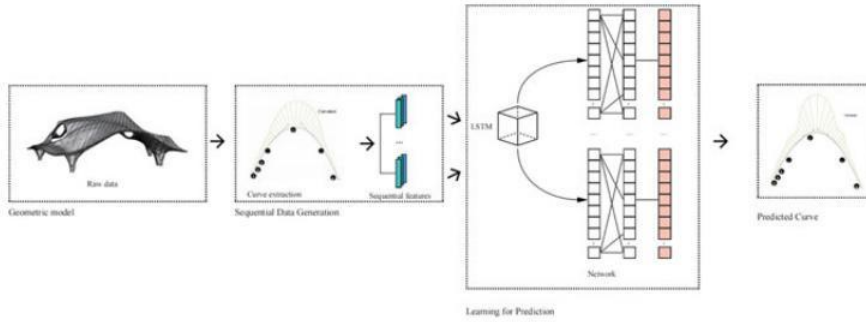


Fig. 5. LSTM learning process

3.3 Robotic Setup

To operate the technical analysis of robotic in both Cartesian space and joint space which is unique for robotic system, DH method is applied to build the model of robotic arm. The x–y–z coordinate of the components can connect the geometry model of the component with robotic arm.

In robot motion control, there is a corresponding matrix mapping between the joint velocity and the corresponding end-effector velocity and angular velocity as in the correspondence of the previous section, and this mapping reflecting the interrelationship between joint velocity and end velocity is known in robotics as the "Jacobi matrix ". It is expressed as follows,

$$V_e = J[q] \cdot \dot{q} \quad (2)$$

Whether $|J[q]| \neq 0$ is the way to testify the singularities.

4 Experiment

4.1 Training

Four timber beams from the geometric model are selected, and 16 curves are extracted to get the division points. In the prediction for 21 divided-points, the geometric information

of 15 curves are selected and one curve is set as the test data and the training process is shown in Fig. 6. Figures 7 and 8 present the prediction error compared with the test data. To further test the prediction accuracy, the predicted tangent vector and the corresponding curvatures of the divided points are applied to fit the curve. The angles between the predicted tangent vector and the original one are shown in Fig. 9a.

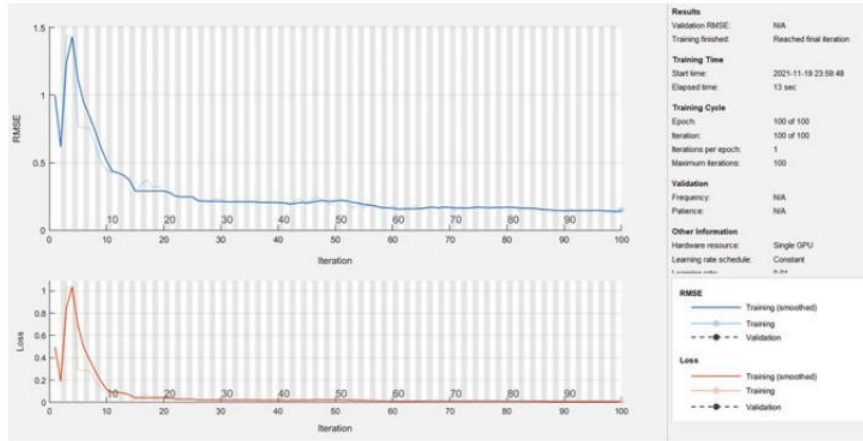


Fig. 6. Training results with 21 points

4.2 Robotic Simulation

Based on the robotic working space cell, the limitation including the obstacles and the range or the movement can be visualised as shown in Fig. 10.

The determination of whether the toolpath of the fabrication of the free-form components satisfies the constraints of the robotic arm is shown in Fig. 11.

5 Discussion and Conclusion

The results of the prediction experiment shows that the transformed 3D geometric data in sequential form fits for the LSTM to operate the prediction learning task. The converged training results illustrates the feasibility of LSTM in predicting the morphology of free-form. By comparing the test and predict datasets, the predicted vectors match the test data sets while the predicted curvature is more oscillatory and deviates to some extent from the test ones. By transforming the predicted curve into 3D model, the predicted geometry can be compared with the test model directly in 3D environment. Figure 9 shows the deviation between the predicted vectors and original vectors where color blue stands for the predicted curve. Based on the predicted curve model, the curve is extended into timber beam which would be fabricated by robotic arm. The robotic work cell case presents the workflow of transforming the predicted timber component information into the fabrication data which can be turned into robotic commands.

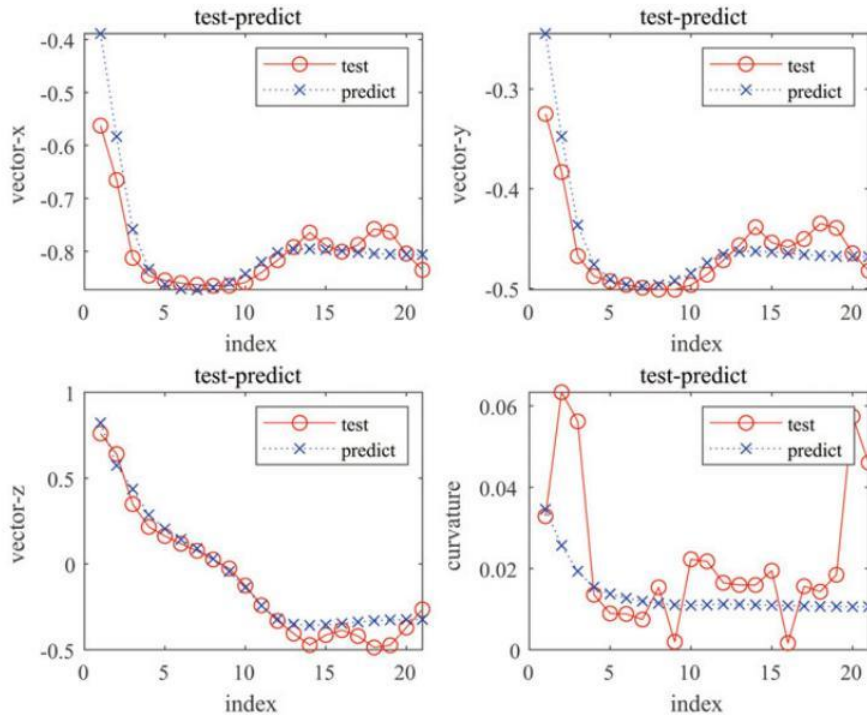


Fig. 7. Test results with 21 points

In conclusion, this research first proposes one method to extract the geometric features to describe the free-form curve which could be transformed into the sequential data for LSTM prediction learning. The experiments demonstrate the workflow of taking LSTM to predict the curve with the curvatures that meet the restrictions of timber properties and the results prove the effectiveness of LSTM taking $\{x, y, z, t, K, a, b, c\}$ as sequential features. When applying the robotic arm to fabricate the structure component which is transformed from the predicted free-form curve, DH method is applied to build the model of robotic arm in Matlab which a process to connect the geometric information in Rhino to the robotic simulation and analysis in Matlab. The working space limit can be computed by Monte Carlo method and the singularities of the robotic arm are derived based on the Jacob matrix to testify the tool path of the predicted free-form structure components.

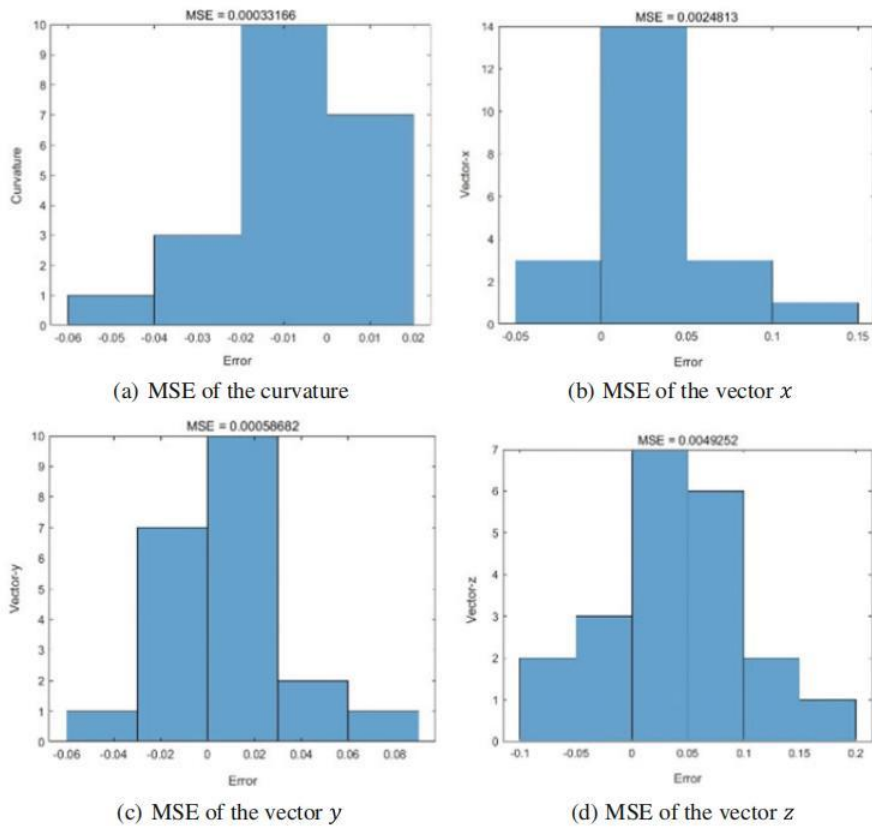


Fig. 8. Histogram of the MSE of the prediction



Fig. 9. Comparison of the generated curve and the tested curve

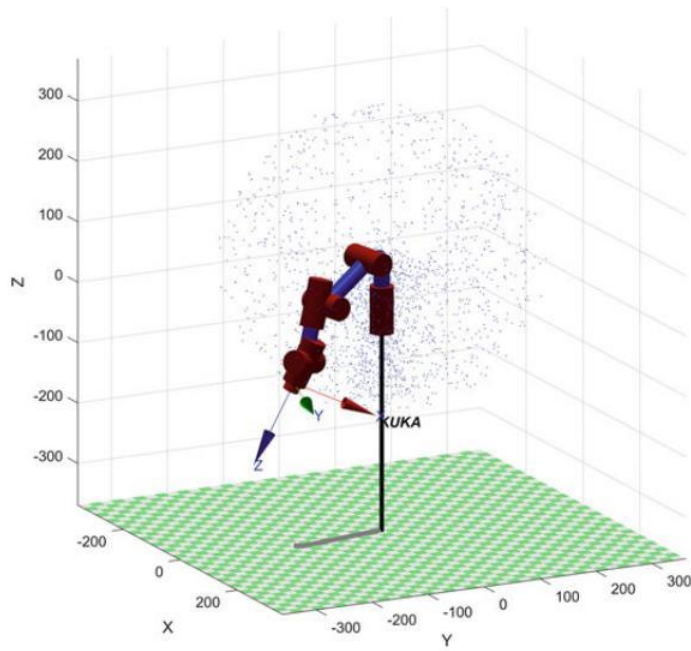


Fig. 10. Robotic working limits

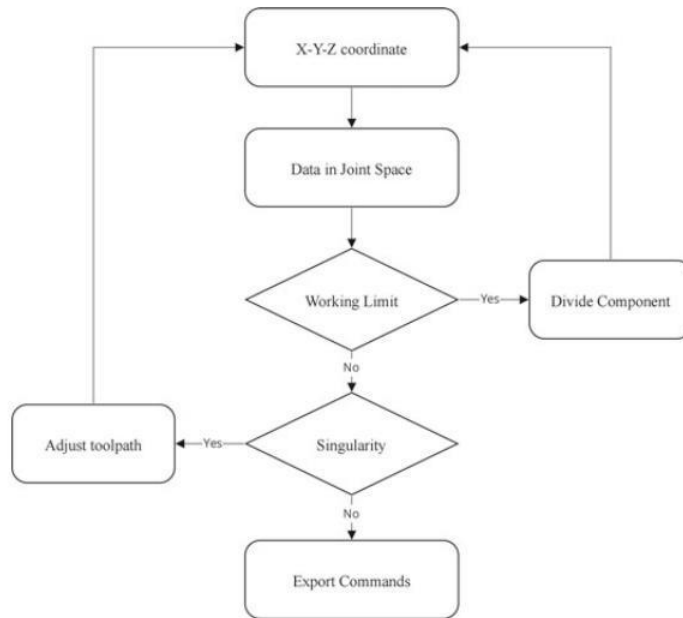


Fig. 11. Workflow of the robotic testification

References

1. Garcia E, Jimenez MA, De Santos PG, Armada M (2007) The evolution of robotics research. *IEEE Robot Automat Magaz* 14(1):90–103
2. Monier V, Bignon JC, Duchanois G (eds) (2013) Use of irregular wood components to design non-standard structures. Trans Tech Publication
3. Willmann J, Knauss M, Bonwetsch T, Apolinarska AA, Gramazio F, Kohler M (2016) Robotic timber construction—expanding additive fabrication to new dimensions. *Autom Constr* 61:16–23
4. Bock T (2015) The future of construction automation: technological disruption and the upcoming ubiquity of robotics. *Automat Constr* 59:113–121
5. Menges A, Schwinn T, Krieg OD (2016) Advancing wood architecture. Taylor & Francis
6. Vercruysse E, Mollica Z, Devadass P (eds) (2018) Altered behaviour: the performative nature of manufacture Chainsaw Choreographies+Bandsaw Manoeuvres. Springer
7. Williams N, Cherrey J (2016) Crafting robustness: rapidly fabricating ruled surface acoustic panels. In: *Robotic fabrication in architecture, art and design 2016*. Springer, pp 294–303
8. Menges A, Schwinn T, Krieg OD (2016) Advancing wood architecture: a computational approach. Routledge
9. Brell-Cokcan S, Braumann J (2013) *Robl Arch 2012: robotic fabrication in architecture, art and design*. Springer Science & Business Media
10. Reinhardt D, Saunders R, Burry J (2016) *Robotic fabrication in architecture, art and design*. Springer
11. Willette A, Brell-Cokcan S, Braumann J (2014) *Robotic fabrication in architecture, art and design 2014*. Springer
12. Willmann J, Block P, Hutter M, Byrne K, Schork T (2018) *Robotic fabrication in architecture, art and design 2018: foreword by Sigrid Brell-Cokcan and Johannes Braumann, association for robots in architecture*. Springer
13. Menna C, Mata-Falcón J, Bos FP, Vantighem G, Ferrara L, Asprone D et al (2020) Opportunities and challenges for structural engineering of digitally fabricated concrete. *Cem Concr Res* 133:106079
14. Hastie T, Tibshirani R, Friedman J (2009) *The elements of statistical learning: data mining, inference, and prediction*. Springer Science & Business Media
15. Larochelle H, Bengio Y, Louradour J, Lamblin P (2009) Exploring strategies for training deep neural networks. *J Mach Learn Res* 10(1):1532–4435
16. Goodfellow IJ, Pouget-Abadie J, Mirza M, Xu B, Warde-Farley D, Ozair S, et al (2014) Generative adversarial networks. *arXiv preprint arXiv:1406.2661*
17. Oh S, Jung Y, Kim S, Lee I, Kang N (2019) Deep generative design: Integration of topology optimization and generative models. *J Mech Design* 141(11):1050–0472.
18. Han S, Qiao Y-H, Yan J, Liu Y-Q, Li L, Wang Z (2019) Mid-to-long term wind and photovoltaic power generation prediction based on copula function and long short term memory network. *Appl Energy* 239:181–191
19. Qin Y, Li K, Liang Z, Lee B, Zhang F, Gu Y et al (2019) Hybrid forecasting model based on long short term memory network and deep learning neural network for wind signal. *Appl Energy* 236:262–272
20. Xie K, Wen Y (eds) (2010) LSTM-MA: A LSTM method with multi-modality and adjacency constraint for brain image segmentation. *IEEE*

Open Access This chapter is licensed under the terms of the Creative Commons Attribution 4.0 International License (<http://creativecommons.org/licenses/by/4.0/>), which permits use, sharing, adaptation, distribution and reproduction in any medium or format, as long as you give appropriate credit to the original author(s) and the source, provide a link to the Creative Commons license and indicate if changes were made.

The images or other third party material in this chapter are included in the chapter's Creative Commons license, unless indicated otherwise in a credit line to the material. If material is not included in the chapter's Creative Commons license and your intended use is not permitted by statutory regulation or exceeds the permitted use, you will need to obtain permission directly from the copyright holder.





Optimal trajectory planning of complicated robotic timber joints based on particle swarm optimization and an adaptive genetic algorithm

Yiping Meng¹ · Yiming Sun² · Wen-shao Chang¹

Received: 5 August 2020 / Accepted: 4 February 2021 / Published online: 11 April 2021
© The Author(s) 2021

Abstract

In this paper, a methodology for path distance and time synthetic optimal trajectory planning is described in order to improve the work efficiency of a robotic chainsaw when dealing with cutting complex timber joints. To demonstrate this approach one specific complicated timber joint is used as an example. The trajectory is interpolated in the joint space by using a quantic polynomial function which enables the trajectory to be constrained in the kinematic limits of velocity, acceleration, and jerk. The particle swarm optimization (PSO) is applied to optimize the path of all cutting surfaces of the timber joint in operating space to achieve the shortest path. Based on the optimal path, an adaptive genetic algorithm (AGA) is used to optimize the time interval of interpolation points of every joint to realize the time-optimal trajectory. The results of the simulation show that the PSO method shortens the distance of the trajectory and that the AGA algorithm reduces time intervals and helps to obtain smooth trajectories, validating the effectiveness and practicability of the two proposed methodology on path and time optimization for 6-DOF robots when used in cutting tasks.

Keywords Optimal trajectory · Time optimization · Robotic fabrication · Particle swarm optimization · Adaptive genetic algorithm · Polynomial interpolation · Chainsaw cutting

1 Introduction

During the past decades, the use of robotic fabrication practices has increased in many fields, especially in architecture. Robotic fabrication shows potential for improving processes across a variety of application, from improving the sustainability of additive manufacturing (Ford and Despeisse 2016), such as reduction in waster and energy saving (Faludi et al. 2015), to its use for the execution of both standardized and customized construction assembly tasks (Keating and

Oxman 2013). Robotic fabrication shows its potential benefits for complex structures in concrete (Agustí-Juan et al. 2017), lightweight timber plates through robotic milling combined with manual assembly work (Krieg et al. 2015), and brick laying using mobile robots (Helm et al. 2012). Compared to CNC technologies, which are used in timber prefabrication predominantly to manufacture standard components like beams and plates (Popovic et al. 2016; Eversmann et al. 2017), robotic fabrication shows its strength in mass customization of movements to make more complicated timber joints due to the potential for complex manipulator trajectories (Jeffers 2016). However, the complexity of the design makes the trajectory more intricate which often increases process time. Robotic chainsaw cutting has a range of applications in timber fabrication industries, however, to achieve an efficient process there are specific aspects of the task which must be taken into consideration. The surfaces in the cutting task are in different surfaces and the cutting order passing through these surfaces has significant impact on working efficiency. When dealing with complex joints, path planning for robotic chainsaw cutting can be

✉ Yiping Meng
ymeng16@sheffield.ac.uk
Yiming Sun
ysun67@sheffield.ac.uk
Wen-shao Chang
w.chang@sheffield.ac.uk

¹ People, Environments and Performance Group, School of Architecture, The University of Sheffield, Sheffield, UK

² Department of Automatic Control and Systems Engineering, The University of Sheffield, Sheffield, UK

time-consuming and manual creation of paths can not guarantee the most efficient solution.

To generate an efficient trajectory requires the satisfaction of specific objectives like time reduction and minimizing of the quick short movements of the robot manipulator. These quick short movements create sudden jerks to the end effector and can reduce the quality of the cut of damage the chainsaw. There are diverse researches on robotic automation construction (Labonnote et al. 2016) and various trajectory optimization techniques (Ata 2007; Jeevamalar and Ramabalan 2012; Ratiu and Prichici 2017), however research on specific trajectory planning optimization methodology applied on a full-scale architecture joint fabrication is rare. Therefore, this study takes the following case as an example to test the feasibility of the trajectory optimization techniques in real practice.

1.1 Case study

In this case, tree trunks are chosen to be the material which would be firstly scanned and then cut by a robot arm equipped with a chainsaw. This case study illustrates the problems within trajectory planning of complicated timber joints in order to test optimization methods for increasing process efficiency. The complicated timber joint was designed and fabricated in a workshop at the international conference: ROBIARCH 2018. The timber joints are designed in Rhino, and the simulation of cutting process using a KUKA robot equipped with a planar cutting tool (chainsaw) uses KUKAlprc. The details of the robotic chainsaw cutting task including the design of the timber joints and the setting work space are shown in Fig. 1.

The first parameter of the process is the shape of the cutting faces as the input surfaces. The cutting tool is always at

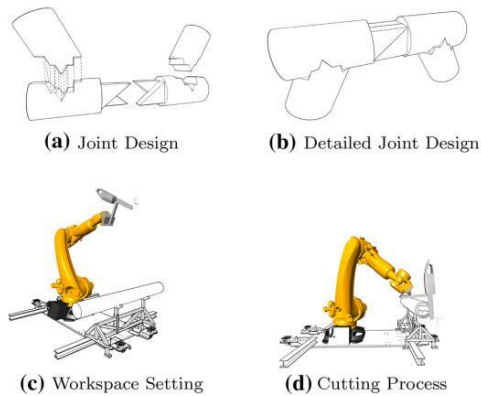


Fig. 1 Diagram of chainsaw cutting

the backside of the input surface, which could be achieved by reversing the normal direction of the input surfaces. This is to align the normal direction of the tool with the normal direction of input surfaces to be in the right offset side. The cutting direction and the cutting order of the four points within one cutting surface is consistent with the drawing order 1, 2, 3, 4, shown in Fig. 2. In this case, the surfaces that have similar orientation are grouped to reduce the amount of re-orientations to save time and avoid collisions.

When planning multiple cuts, the main difficulty is to designate the cutting order of different cutting surfaces to avoid kinematic singularities and at the same time to avoid collisions. The timber joint in this case has been divided into four cutting parts, and every part has more than 10 cutting surfaces; each surface has four cutting points. The cutting order combinations could be $n! \times C_4^n$, where n is the number of cutting surfaces, which means it is impractical to figure out every rational combination. Two parts of the timber joint have been fabricated in the work space (Fig. 3) and the results are shown in Fig. 4a, the same as the initial design in Rhino. During the workshop, the cutting order was set manually. The whole process took considerable time and decreased the degree of automation of robotic fabrication. This also added uncertainty as to whether the manually designed path was the shortest travel distance or not. To tackle the difficulty found during the workshop, one part of the joint (Fig. 4b) is selected to be optimized.

This study took 13 cutting surfaces of the first part as the example for addressing complicated robotic timber joints within trajectory planning and utilizes a multi-objective technique to obtain trajectory planning optimization

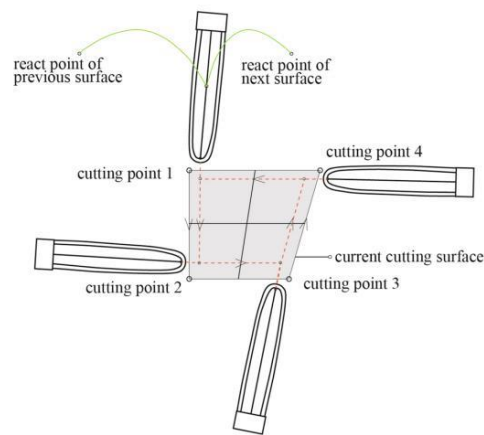


Fig. 2 Movement of chainsaw within one cutting surface

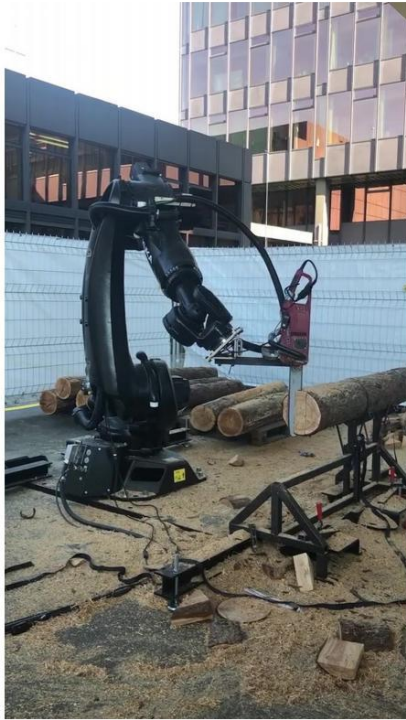
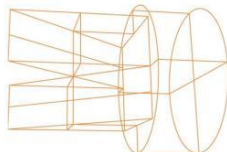


Fig. 3 On-site fabrication



(a) Results of workshop



(b) Example of the Case Study

Fig. 4 Timber joint fabrication

of robot manipulators corresponding to the specific example in this study, to put forward a feasible solution to find the best cutting order automatically to achieve the shortest distance and time.

1.2 Trajectory planning in robotics

The trajectory planning problem in robotics is to find a motion along the given geometric path, taking into account process constraints, to generate inputs for the control system of the manipulator, which ensures the implementation of the planned movement (Gasparetto and Zanotto 2010; Gasparetto et al. 2012). Trajectory planning in robotics is generally carried out in the operating space (Luh and Lin 1981) or joint space (Craig 2009). The trajectory described in the joint space returns the position for each joint of the manipulator, corresponding to the points set by the user.

Though in the operating space, the trajectory of the end-effector can be described directly, it is very difficult to solve the problem analytically due to the highly coupled and highly sub-linear characteristics of robot dynamics equations. In most cases, the trajectory planning is solved in joint space to avoid kinematic singularities or manipulator redundancy (Gasparetto et al. 2015). The most common method is to transform the trajectory function from operating space into joint space, and then to control the manipulator in the joint space.

The trajectories defined in the joint space are constructed by means of interpolation functions such as polynomial, spline, Bezier, and NURBS, etc., which are restricted to kinematic constraints. Conventional polynomial interpolation has developed 343,445 and novel 5455 methods based on different orders polynomial functions (Cook and Ho 1984; Petrínek and Kovacic 2007; Boscaroli et al. 2012). Trajectories interpolated by spline functions shows good performance ensuring the continuity of the acceleration or jerk (derivative of the acceleration), cubic B-spline, quintic B-spline as 7th-order B-spline have been tested to obtain trajectory smoothness (Ramabalan et al. 2009; Gasparetto and Zanotto 2008; Zhu et al. 2010).

Numerous techniques for optimal offline trajectory planning have been developed in the last decades by different researchers in the field. The trajectory planning algorithm takes the geometric path, kinematic and dynamic constraints as inputs and generates the trajectory of the joints, or of the end-effector by means of position, velocity and acceleration expressed in time sequence (Siciliano et al. 2010). The aim of the trajectory planning optimization is to improve the manufacturing productivity and the movement stability, which means the short execution time or smooth path (Huang et al. 2018). Most of the trajectory planning algorithm optimizations are based on an objective function of some parameters to improve: (1) minimum execution time, (2) minimum energy, and (3) minimum jerk, or a combination of these (Gasparetto et al. 2012).

1.3 Optimal techniques

The most common used trajectory planning optimization techniques are minimum-time algorithms, due to the need for increasing productivity in the industrial sector (Gasparetto and Zanotto 2010; Piazzzi and Visioli 1998). A convex optimization for time trajectory planning was put forward by converting time-optimal problem into convex optimal control problem, neglecting the viscous friction (Verscheure et al. 2009). When robot moved at high speed, time-optimal optimization could be non-convex taking the viscous friction of robots into consideration (Shen et al. 2019). To solve this inaccuracy, a new genetic algorithm for time-optimal and collision-free trajectory in complex environments was developed (Abu-Dakka et al. 2015). Also, these algorithms meet torque and acceleration discontinuity required by assuming that robot was a rigid body. To overcome these drawbacks, the actuator jerks were introduced as an additional metric for optimization (Constantinescu and Croft 2000).

Besides time optimization, jerk minimization results in better performance in tracking capacity (Gasparetto et al. 2015; Kyriakopoulos and Saridis 1988), being able to achieve smaller excitation of resonance frequencies (Gasparetto et al. 2015). Squared jerk has also been set as the optimization object using spline interpolation (Gasparetto and Zanotto 2007; Simon 1993; Zanotto et al. 2011).

Minimizing the energy consumption is another alternative optimization objectives, which leads to the smoothness of the trajectory with smaller stresses on the robot manipulator (Field and Stepanenko 1996). Cubic B-spline functions, fifth order B-spline and Lagrange interpolation have been applied to construction trajectories within energy minimization objective (Gasparetto and Zanotto 2007; Sato et al. 2007; Luo et al. 2015).

In addition, hybrid optimizations have also been proposed instead of a single optimization objective function. Time-energy optimal trajectories planning is composed by two terms, the first related to the travel time and the second to energy. The optimal objective is to reduce the stresses of the actuators and to promote the most efficient trajectory tracking (Balkan 1998; Shiller 1996). Similar to time-energy, time-jerk optimal trajectory planning also consists of two parts, time and jerk (third derivative of position) (Gasparetto and Zanotto 2007, 2008; Zanotto et al. 2011). The simulation and experiment results validated the effectiveness of the methods. However, the trade-off between the two criteria is controlled by two weights of the objective function which still requires artificial adjustment. To solve the multi-objective problems, there is an emerging alternative which is to employ evolutionary algorithms such as particle swarm optimization (PSO) and adaptive genetic algorithm (AGA) to solve the above-mentioned drawbacks (Ata and Myo 2005; Saravanan et al. 2008).

PSO was devised in 1995 inspired by the flock of birds' behaviour and has been applied to many fields of optimization problems (Eberhart and Kennedy 1995). As a random-search algorithm, studies have verified the convergence speed of particle swarms by offering the initial behaviour of a population (Reyes-Sierra and Coello 2006; Helwig and Wanka 2008; Trelea 2003). In addition to the performance of PSO on continuous optimization problems, many studies have tested the application of PSO on discrete problems (Kennedy and Eberhart 1997; Wang et al. 2003; Shi et al. 2007), including the optimization of path planning (Hoffmann et al. 2011). PSO shows its potential in finding the shortest collision-free path for mobile robots effectively (Zhao and Yan 2005). More simulation results shows the competence of PSO in path planning in static or dynamic environments (Xu et al. 2008; Hao et al. 2007). PSO could also tackle multi-objective robot path planning with uncertainty in planar surface (Zhang et al. 2013). Apart from travel distance, a multi-objective particle swarm optimization algorithm is applied to minimize the travel time, energy and the distance of the end-effector (Xu et al. 2015).

Genetic algorithm (GA), inspired by natural genetic systems and natural selection (Davis 1991), is viewed as another advantageous evolutionary process to optimize non-linear and complex problems which traditional method could not solve (Davis 1987). The AGA varied the probability of crossover and mutation probability depending on the fitness value of the objective function (Srinivas and Patnaik 1994). The AGA method significantly optimizes the time-intervals between each section of the trajectory so as to raise the efficiency of the robot (Liao et al. 2010). Combing the quintic polynomial function to interpolate the trajectory, time-optimal trajectory planning could be realized by AGA to reduce running time (Zhang et al. 2018). When tackling the same trajectory time-optimal problem, the simulation results show that AGA converge better than GA and reduce the probability of local best solutions to achieve better stability of robot (Fu and Ju 2011).

This study reports two optimal objectives (travel distance and execution time) to obtain smooth and short trajectories of robot manipulators. With respect to most path and time optimal algorithm techniques in scientific literature so far, the PSO along with AGA are selected to deal with the two optimization objectives, respectively.

This paper is organized as follows. In Sect. 2, the trajectory optimization problem is formulated and kinematic singularities are defined; fifth-order polynomial function is chosen to construct the joint trajectory, and Modified Denavit–Hartenberg is chosen to build the robot model. In Sect. 3, the robot arm model is built in MATLAB and the data of the model in Rhino is converted to interpolate the position, velocity and acceleration of the six joints according to the setting points. Section 4, describes the

whole algorithms in detail and describes the execution. Section 5 shows the results of the simulation.

2 Methodology

2.1 Formulation of the optimization objectives

The KUKA robot with six degrees of freedom is considered in this study. The trajectory planning methodology described in this paper assumes that the geometric path is converted from the specific geometry vertices. The path is given as a sequence of points in the operating space, which represent the positions and orientations of the end-effector. The points would be transformed to consecutive points in the joint space through inverse kinematics. Based on the points in the joint space, a trajectory would be constructed and then optimized for the minimization objectives. Obstacle avoidance and collision problems are assumed solved and will not be in the scope of this study.

Considering the uniqueness of this case study, the proposed technique does not set the geometric path as a variable, which is different from the current trajectory planning. The minimization of the travel distance of the end-effector has direct effect on the time minimization. In this study, two objective functions are formulated: the travel distance and the execution time.

The two optimization problems are mathematically defined as follows and the meaning of the symbols are listed in Table 1 and Table 2: Minimize:

Table 1 Meanings of symbols appearing in Eqs. (1) and (2)

Symbol	Meaning
D	Traveling distance objective function
L_i	Distance between two surfaces
$L_{i,j}$	Distance between the two vertices belonging to one surface
p_k	Position of the k th joint
x_e	x coordinate of the end-effector
y_e	y coordinate of the end-effector
z_e	z coordinate of the end-effector
U_j	Position range of the j th joint
U_x	Working space range for x coordinate
U_y	Working space range for y coordinate
U_z	Working space range for z coordinate
$ J[q] $	Determinant of Jacobian matrix
N	Number of surfaces
M	Number of vertices
n	Number of robotic manipulator joints

Table 2 Meanings of symbols appearing in Eqs. (3) and (4)

Symbol	Meaning
T	Traveling time objective function
h_i	Time interval between the i th via-point and $(i + 1)$ th via-point
t_i	i th time node
p_i	Position of the i th joint
\dot{p}_i	Velocity of the i th joint
\ddot{p}_i	Acceleration of the i th joint
$\overset{\cdot\cdot}{p}_i$	Jerk of the i th joint
VC_i	Velocity constraint for the i th joint
WC_i	Acceleration constraint for the i th joint
JC_i	Jerk constraint for the i th joint
$n + 1$	Number of the via-points in the joint space
N	Number of robotic manipulator joints

$$D = \sum_{i=1}^N L_i + \sum_{i=1}^{N-3} \sum_{j=1}^M L_{i,j} \tag{1}$$

Subject to:

$$\begin{cases} p_k(t) \in U_j, k = 1, 2, \dots, n \\ x_e(t) \in U_x \\ y_e(t) \in U_y \\ z_e(t) \in U_z \\ |J[q]| \neq 0. \end{cases} \tag{2}$$

Minimize:

$$T = \sum_{i=1}^{n-1} h_i = \sum_{i=1}^{n-1} (t_{i+1} - t_i) \tag{3}$$

Subject to:

$$\begin{cases} |\dot{p}_i(t)| \leq VC_i, i = 1, 2, \dots, N \\ |\ddot{p}_i(t)| \leq WC_i, i = 1, 2, \dots, N \\ |\overset{\cdot\cdot}{p}_i(t)| \leq JC_i, i = 1, 2, \dots, N. \end{cases} \tag{4}$$

The two objective functions are related. Objectives one would be optimized first to work out the fittest travel path and based on the optimal path travel time would be optimized to get the smooth trajectory. Also, the kinematic constraints for velocity, acceleration and jerk as well as the interpolation conditions for all via-points (vertices of the cutting surfaces) must be met.

2.2 Definition of the trajectory by means of fifth-order polynomial function

To solve the optimization problems above, fifth-order polynomial function is selected to construct the trajectory in joint space. $\theta_i(t)$ denotes the position of six joints in angle. According to the definition of the quintic polynomial function (Thomas et al. 2010), the trajectories of six joints are expressed mathematically as follows, i means the number of joints:

$$\theta_i(t) = a_{i0} + a_{i1}t + a_{i2}t^2 + a_{i3}t^3 + a_{i4}t^4 + a_{i5}t^5 \quad (5)$$

$i = 1, 2, \dots, 6.$

For one of the trajectories, the start time is set to be t_0 and end time to be t_f ; the start point and end point of position, velocity and acceleration constraints are expressed as follows:

$$\begin{cases} \theta_i(0) = \theta_{i0} \\ \theta_i(t_f) = \theta_{if} \end{cases} \quad (6)$$

$$\begin{cases} \dot{\theta}_i(0) = \dot{\theta}_{i0} \\ \dot{\theta}_i(t_f) = \dot{\theta}_{if} \end{cases} \quad (7)$$

$$\begin{cases} \ddot{\theta}_i(0) = \ddot{\theta}_{i0} \\ \ddot{\theta}_i(t_f) = \ddot{\theta}_{if} \end{cases} \quad (8)$$

$$\begin{cases} \ddot{\theta}_i(0) = \ddot{\theta}_{i0} \\ \ddot{\theta}_i(t_f) = \ddot{\theta}_{if} \end{cases} \quad (9)$$

Supposing the initial and ending positions of the 6-DOF robot are known, position constraints, velocity constraints, acceleration constraints of the initial and end points are also included. The 6 parameters of the fifth-degree polynomial uniquely determine a trajectory to meet the constraints. Deriving Eq. (5), the velocity expression $\dot{\theta}_i(t)$ of the trajectory is obtained as

$$\dot{\theta}_i(t) = a_{i1} + 2a_{i2}t + 3a_{i3}t^2 + 4a_{i4}t^3 + 5a_{i5}t^4 \quad (10)$$

$i = 1, 2, \dots, 6.$

Similarly, the acceleration function $\ddot{\theta}_i(t)$ and jerk function $\dddot{\theta}_i(t)$ are expressed as below as the second and third derivative of Eq. (5):

$$\ddot{\theta}_i(t) = 2a_{i2} + 6a_{i3}t + 12a_{i4}t^2 + 20a_{i5}t^3 \quad (11)$$

$i = 1, 2, \dots, 6.$

According to the coefficients, the equation of jerk (third derivative of position) could be formed to get the constrains of the JC_i .

$$\dddot{\theta}_i(t) = 6a_{i3} + 24a_{i4}t + 60a_{i5}t^2 \quad (12)$$

$i = 1, 2, \dots, 6.$

According to Eqs. (6)–(9), the constants of a_{ij} could be conducted, means the j th constant of the i th joint, $i = 1, 2, \dots, 6$, means the number of joint and $j = 0, 1, \dots, 5$, means the index of the constants a :

$$\begin{cases} a_{i0} = \theta_{i0} \\ a_{i1} = \dot{\theta}_{i0} \\ a_{i2} = \frac{\ddot{\theta}_{i0}}{2} \\ a_{i3} = \frac{20\theta_{if} - 20\theta_{i0} - (8\dot{\theta}_{if} + 12\dot{\theta}_{i0})t_f - (3\ddot{\theta}_{i0} - \ddot{\theta}_{if})t_f^2}{2t_f^3} \\ a_{i4} = \frac{30\theta_{i0} - 30\theta_{if} + (14\dot{\theta}_{if} + 16\dot{\theta}_{i0})t_f + (3\ddot{\theta}_{i0} - 2\ddot{\theta}_{if})t_f^2}{2t_f^4} \\ a_{i5} = \frac{12\theta_{if} - 12\theta_{i0} - (6\dot{\theta}_{if} + 6\dot{\theta}_{i0})t_f - (\ddot{\theta}_{i0} - \ddot{\theta}_{if})t_f^2}{2t_f^5} \end{cases} \quad (13)$$

2.3 Modified Denavit–Hartenberg parameters

In 1955, Denavit and Hartenberg proposed a method for systematically describing multi-axis robots, which are now widely used in robotics research and are known as DH parameters (Denavit et al. 1955). The specific definition model of DH parameters is shown in Fig. 5. Z_{i-1} -axis means the rotation axis of the i th joint, and X_{i-1} -axis means the common perpendicular between the joint i and joint $i + 1$. Y_{i-1} is determined by the right-hand rule following Z_{i-1} -axis and X_{i-1} -axis.

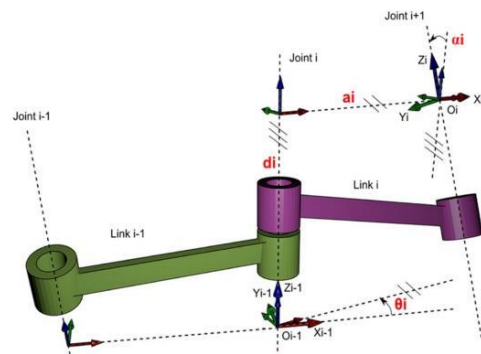


Fig. 5 Standard DH parameters

Besides the DH parameters, there is another definition used widely, which is called modified DH parameters, showing in Fig. 6 (Craig 2009). The difference between these two methods is that the coordinate system is based on the previous joint rather than the next one in standard DH, which means that the frame O_{i-1} is put on joint $i - 1$ not joint i .

2.4 Singularities identification

To identify the singularities, In Robotics, Jacobian matrix is a map that reflects the relationship between joint speed and end-effector speed, shown as Eq. (13):

$$V_e = J[q] \cdot \dot{q} \tag{14}$$

V_e is the velocity of the end-effector, $J[q]$ is the Jacobian matrix, and \dot{q} is the velocity of the joints. To be more specific, V_e includes the linear velocity p_e and angular velocity w_e , the same as $J[q]$:

$$V_e = \begin{bmatrix} p_e \\ w_e \end{bmatrix} = \begin{bmatrix} J_p[q] \\ J_o[q] \end{bmatrix} \cdot \dot{q}. \tag{15}$$

The number of rows in the matrix is the freedom of robot manipulator in operating space, and the number of columns equals the number of joints, so the Jacobian matrix could be divided as

$$\begin{bmatrix} p_e \\ w_e \end{bmatrix} = \begin{bmatrix} J_{P1} J_{P2} J_{P3} J_{P4} J_{P5} J_{P6} \\ J_{W1} J_{W2} J_{W3} J_{W4} J_{W5} J_{W6} \end{bmatrix} \cdot [\dot{q}_1 \dot{q}_2 \dot{q}_3 \dot{q}_4 \dot{q}_5 \dot{q}_6]^T. \tag{16}$$

From above, the p_e and w_e could be mapped from the linear velocity of the joints.

$$\begin{aligned} p_e &= J_{P1} \cdot \dot{q}_1 + J_{P2} \cdot \dot{q}_2 + \dots + J_{P6} \cdot \dot{q}_6 \\ w_e &= J_{W1} \cdot \dot{q}_1 + J_{W2} \cdot \dot{q}_2 + \dots + J_{W6} \cdot \dot{q}_6. \end{aligned} \tag{17}$$

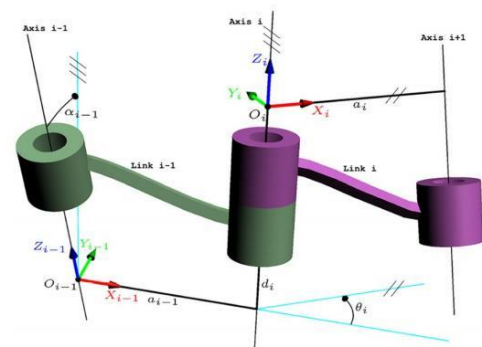


Fig. 6 Modified DH parameters

When the end-effector approaches the kinematic singularities area, the rank of the matrix would decrease, which could conclude that $det(j[q]) = 0$. From Eq. (18), when $|J[q]|$ approaches 0, q could be so large to damage the robot.

$$q = J[q]^{-1} \cdot V_e = \frac{(J[q])^*}{|J[q]|} \cdot V_e. \tag{18}$$

So $|J[q]| = 0$ is the analyzing condition of the singularity zone of the robot manipulator.

3 Experiment setup

3.1 Robot model

The robot manipulator used in the case study is KUKA KR90. The DH parameters of the robot are shown in Table 3. Based on the DH parameter in Table 3, the robot link model could be built in MATLAB2018a using Robotics Toolbox 10.2, shown in Fig. 7.

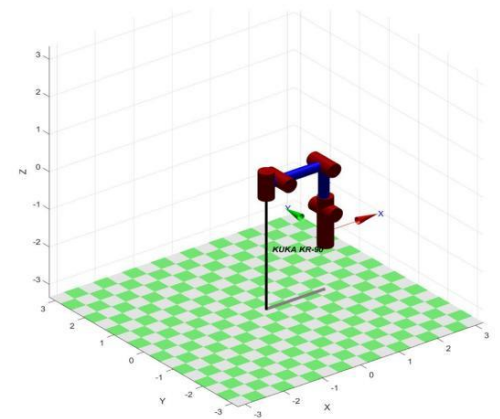


Fig. 7 KUKA-KR90 link model

Table 3 DH parameters of the robot

Link i	θ_i (°)	α_{i-1} (°)	a_{i-1} (m)	d_i (m)
1	0	0	0	0
2	0	90	0.350	0
3	0	0	1.150	0
4	0	90	0.041	1.200
5	0	-90	0	0
6	0	-90	0	0

3.2 Data conversion

In this study, one custom wood joint (Fig. 4b) is selected as the research object, with 13 cutting surfaces. The coordinates of 52 vertices of these 13 cutting surfaces are converted from Rhino (Fig. 8) to Matlab (Fig. 9) to construct the via-points of the geometric path, based on which the trajectory would be interpolated using the fifth-order polynomial function. According to the motion control law of the chainsaw, the end-effector cuts the timber along the cutting surfaces. A total of 66 cutting trajectories are formed: (1) trajectories within the 13 cutting surfaces; (2) trajectories from n th surface to $(n + 1)$ th surface; (3) two additional trajectories adding the start and end points.

3.3 Kinematics constraints

The vertices in form of o -xyz coordinate would be transformed into the points in joint space from operating space using inverse kinematics. The results of the 6 joints in form of angular position, velocity and acceleration are shown in Fig. 10.

In Fig. 10, there are 66 curves representing each of the six joints constructed by 66 fifth-order polynomial functions. The coefficients of the functions could be calculated according to Eq. (18) and the constraints for each joint along every trajectory would be obtained. The overall velocity, acceleration and jerk constraints for the objective function T in Eq. (4) can be obtained by setting as:

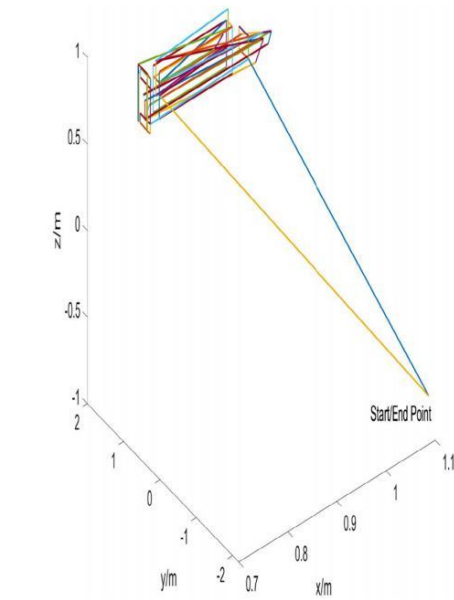


Fig. 9 Trajectory in Matlab

$$\begin{cases} VC_i = \max \{ \max \{ p_{ij} \} \} \\ WC_i = \max \{ \max \{ \dot{p}_{ij} \} \} \\ JC_i = \max \{ \max \{ \ddot{p}_{ij} \} \} \\ i = \text{number of joint} \\ j = \text{number of trajectory.} \end{cases} \quad (19)$$

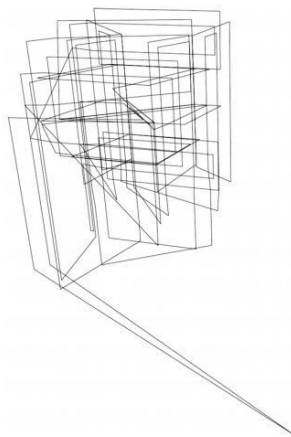


Fig. 8 Trajectory in Rhino

3.4 Working space

The work-space of a robot manipulator represents a set of positions that the end-effector could approach, showing the working range of its accessibility. The working space of the manipulator could be expressed as

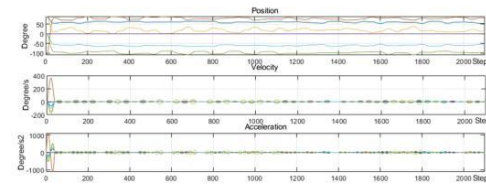


Fig. 10 Full trajectory

Table 4 Angle range of every joint

Joint	Angle range (°)
1	- 185 to 185
2	- 140 to - 5
3	- 120 to 155
4	- 350 to 350
5	- 125 to 125
6	- 350 to 350

$$W = \begin{cases} p_x = p_x(\theta_i) \\ p_y = p_y(\theta_i) \\ p_z = p_z(\theta_i) \end{cases}, \theta_{i\min} \leq \theta_i \leq \theta_{i\max} \quad (20)$$

Monte Carlo method is one discretization method widely used to compute the work space for complex robots (Rashtegar and Fardanesh 1990; Cao et al. 2011). Monte Carlo method gets the approximate work-space by setting the random joint angle of every joints to get the random positions of the end-effector. The angle range of every joint is shown in Table 4.

4 Running the optimization

4.1 Particle swarm optimization for path minimization

Particle swarm optimization is one typical algorithm in swarm intelligence. Eberhard and Kennedy proposed this optimization technique by observing the social behavior of bird flocking (Kennedy and Eberhart 1995). Research has shown the effectiveness of particle swarm optimization in path planning to achieve collision-free trajectories (Hereford 2006; Doctor et al. 2004). Specifically, a group of random particles (random solution) are initialized and the best solution are found through iteration. Within each iteration, the particles update itself by tracking two values: personal best and global best. After finding these two optimal values, the particles update their velocity and position using the following equations.

$$v_i = \omega \times v_i + c_1 \times \text{rand}() \times (p\text{Best}_i - x_i) + c_2 \times \text{rand}() \times (g\text{Best}_i - x_i) \quad (21)$$

$$x_i = x_i + v_i \quad (22)$$

where v_i is the velocity of the i th particle; $\text{rand}()$ is the random number between 0 and 1; x_i is the current position of the particle; c_1 and c_2 are the learning factors, usually equal 2; ω is the inertia weight, which is a positive number, the larger of the number, the better global searching ability and

weaker local searching ability. The common method is to use the linearly decreasing weight strategy to get the dynamic ω .

$$\omega^{(t)} = \frac{(\omega_{\text{ini}} - \omega_{\text{end}})(G_k - g)}{G_k + \omega_{\text{end}}} \quad (23)$$

where ω_{ini} is the initial inertia weight; ω_{end} is the inertia weight of maximum iteration; G_k is the maximum number of iterations. In this study, $\omega_{\text{ini}} = 1$, $\omega_{\text{end}} = 4e^{-5}$. The detailed flow chart is shown as below in Figs. 11 and 12

To combine the algorithm with the parameters in this case, a population of $m \times 13$ particles are created: $\text{swarm} = \{x_1^k, x_2^k, \dots, x_m^k\}$, k means the k th iteration. Within the k th iteration, the i th particle is expressed in a 13-dimension vector: $x_i^k = [(x_{i1}^k), (x_{i2}^k), (x_{i3}^k), \dots, (x_{i13}^k)]$, $i = 1, 2, \dots, m$. Every element of the vector stands for the index of the cutting surface and the index of the vertices within every surface, the j th element of the i th particle is: $x_{ij}^k = (s_{in}^k, \text{ver}_{ip}^k)$, $j = 1, 2, \dots, 13$, $n = 1, 2, \dots, 13$, $p = 1, 2, 3, 4$. Figure 13 explains the detailed layer information, from

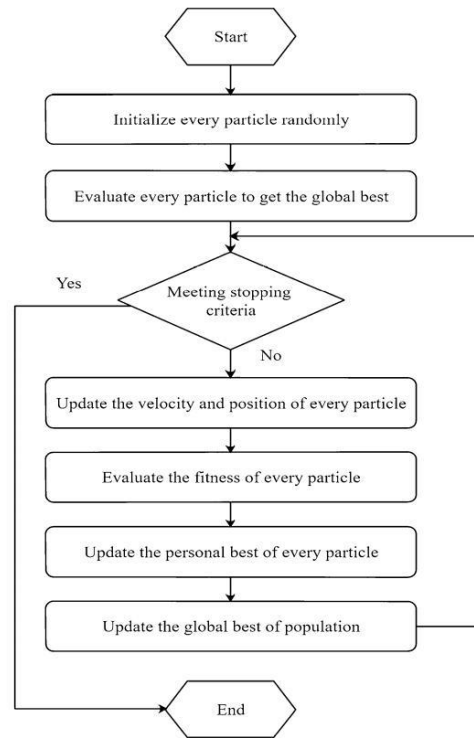
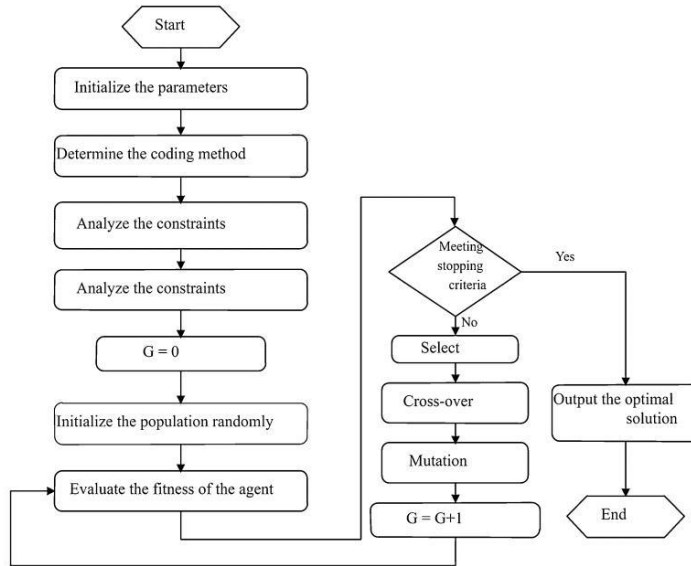


Fig. 11 Flow chart of PSO

Fig. 12 Flow chart of robot time optimization using AGA



every particle to the swarm within every step of iteration.

4.2 Adaptive genetic algorithm for travel time minimization

To validate the adaptive genetic algorithm in this study, one closed surface was chosen as an example to optimize the travel time along four edges, which means four time-intervals. The time optimization of the manipulator could be concluded as the joint optimization. The objective functions of *j*th joint is:

$$f(t) = \min (t_{j1} + t_{j2} + t_{j3} + t_{j4}). \tag{24}$$

According to Eq. (10), the trajectories of the manipulator are constructed by the fifth-order polynomial, the general formula for the trajectories could be expressed as:

$$\begin{cases} h_{ij}(t) = a_{ij5}t_i^5 + a_{ij4}t_i^4 + a_{ij3}t_i^3 + a_{ij2}t_i^2 + a_{ij1}t_i + a_{ij0} \\ i = 1, 2, \dots, N \\ j = 1, 2, \dots, n \end{cases} \tag{25}$$

$h_{ij}(t)$ is the fifth-order polynomial function of the *i*th trajectory of the *j*th joint. In one specific surface optimization, $N = 4$. The four positions of the six joints are known concluded from the inverse kinematics, expressed as $X_{j1}, X_{j2}, X_{j3}, X_{j4}, X_{j5}$, and $A_{j1}, A_{j5}, V_{j1}, V_{j5}$ are also known as 0. Based on the known conditions, the relationship between

the unknown a_{ij} and the known X_{ji} could be derived from A_j (a 24×24 matrix) and b_j (vector constructed from X_{ji}).

$$b_j = [0 \ 0 \ 0 \ 0 \ 0 \ 0 \ 0 \ 0 \ 0 \ 0 \ X_{j5} \ 0 \ 0 \ X_{j1} \ 0 \ 0 \ X_{j2} \ X_{j3} \ X_{j4}]^T \tag{26}$$

$$a_j = \text{inv}(A) \times b_j \tag{27}$$

$$a_j = [a_{ij5} \ a_{ij4} \ a_{ij3} \ a_{ij2} \ a_{ij1} \ a_{ij0}]^T. \tag{28}$$

After integrating the John Holland genetic algorithm, the improvement of the process has developed a lot (Whitley 1994). Adaptive genetic algorithm is one method that adjusts the probability of crossover p_c and probability of mutation p_m dynamically according to the fitness value. The adjustment of the two operators are shown in Eqs. (29) and (30):

$$p_c = \begin{cases} p_{c1} - \frac{(p_{c1} - p_{c2})(f' - f_{avg})}{f_{max} - f_{avg}}, & f' \geq f_{avg} \\ p_{c1}, & f' < f_{avg} \end{cases} \tag{29}$$

$$p_m = \begin{cases} p_{m1} - \frac{(p_{m1} - p_{m2})(f' - f_{avg})}{f_{max} - f_{avg}}, & f' \geq f_{avg} \\ p_{m1}, & f' < f_{avg} \end{cases} \tag{30}$$

where f is the fitness value of the solution; f' is the larger fitness values of the two solutions to cross; f_{max} is the maximum fitness value of the population; f_{avg} is the average fitness value of the population (Srinivas and Patnaik 1994). The parameters of the

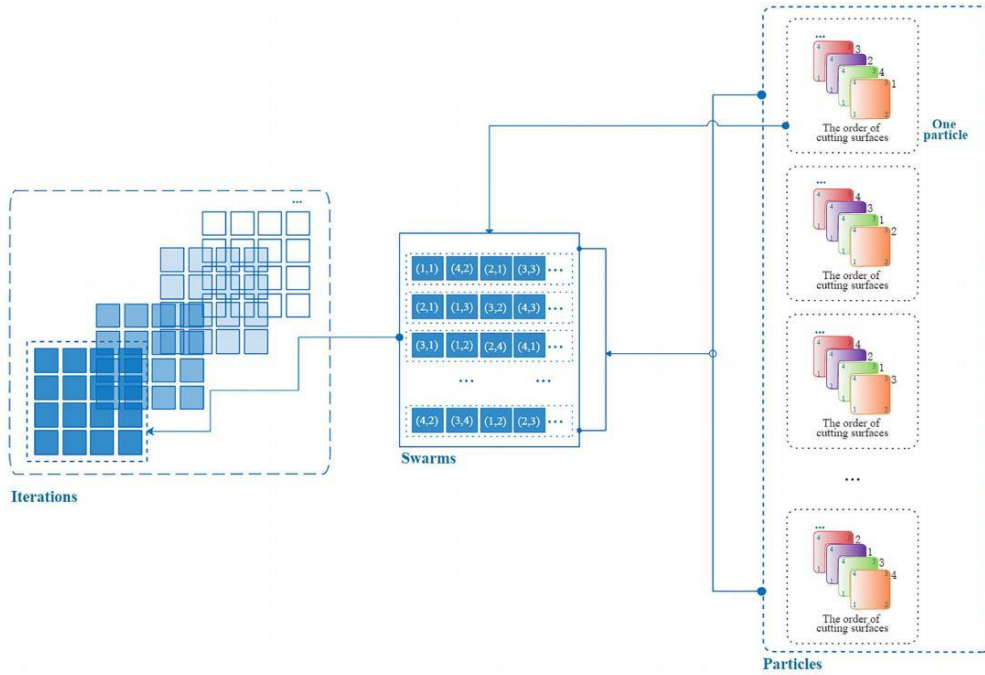


Fig. 13 Layers of iterations PSO

algorithm are selected as follows: population size $M = 100$; $P_{c1} = 0.9, P_{c2} = 0.4, P_{m1} = 0.1, P_{m2} = 0.01$. The $M \times 6$ group of initial combinations of $[t_1 t_2 t_3 t_4]$ as the evolution population would be taken to the algorithm as the independent variables and a_j would be the dependent variables to validate the constraints. After all the optimization for all the joints, the optimized time interval should equal the maximum one within one trajectory to satisfy the kinematics constraints, that is:

$$\begin{cases} t_i = \max \{t_{ji}\} \\ i = 1, 2, \dots, n \\ j = 1, 2, \dots, N. \end{cases} \quad (31)$$

5 Results and analysis

5.1 Distance-optimal simulation

After 300 PSO algorithm iterations, the travel distance decreases from 16.1373 to 15.2010 m. The travel distance

within every cutting surface remain the same, the reduction is diminished by the distance between two cutting surfaces. The trajectories from the start point of n th cutting surface to next start point of $(n + 1)$ th cutting surface are compared in Figs. 14 and 15. The effectiveness of the algorithm in decreasing the distance, from 16.1373 to 15.2010 m (Fig. 16), without singularities in new cutting order, is also validated in KUKA|prc.

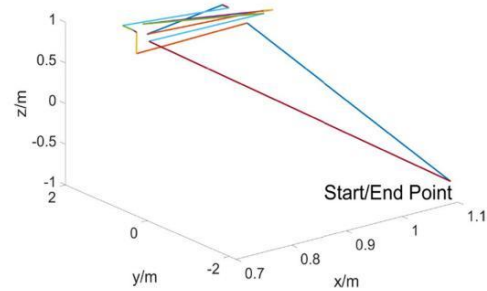


Fig. 14 Initial surface-to-surface trajectory

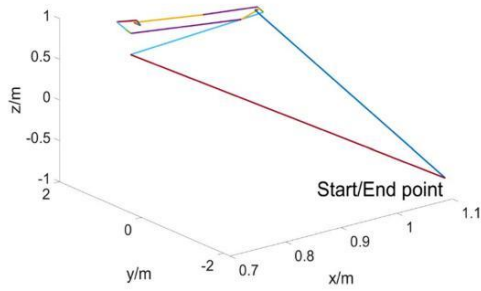


Fig. 15 Optimized the surface to surface trajectory

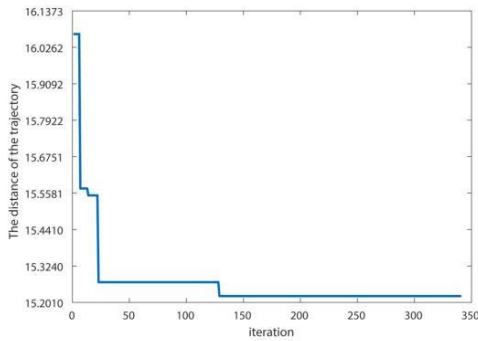


Fig. 16 Convergence of the distance optimization

This optimization process provides a new method in fabricating complicated components, enhancing the degree in automation in robotic fabrication tool path generation instead of setting the cutting order manually. In addition, the shorter distance could save time and energy.

5.2 Time-optimal simulation

As for the decreased in travel distance, the time optimization is operated within the cutting surface. In the optimization process, the trajectories of the six joints are composed of

four fifth polynomial curves, and precision is 0.0001. The results of the first cutting surface are shown in Table 5. From the optimal results, the travel time along the four edges, four points is reduced under the kinematics constraints of joint velocity, and acceleration.

For all the six joints, the initial total time is 54s, the time is shortened at least 33.3% to 36 s. As shown in Fig. 17a–f, the operating time for each joint would converge to the optimized time, and the optimized operating times are stable. Figure 18 shows after the optimization, the curves of the position, velocity and acceleration are smoother compared to the initial ones, which means the smooth transition after every trajectory ends. Furthermore, this leads to energy saving and deviation reduction in motion control.

6 Conclusion

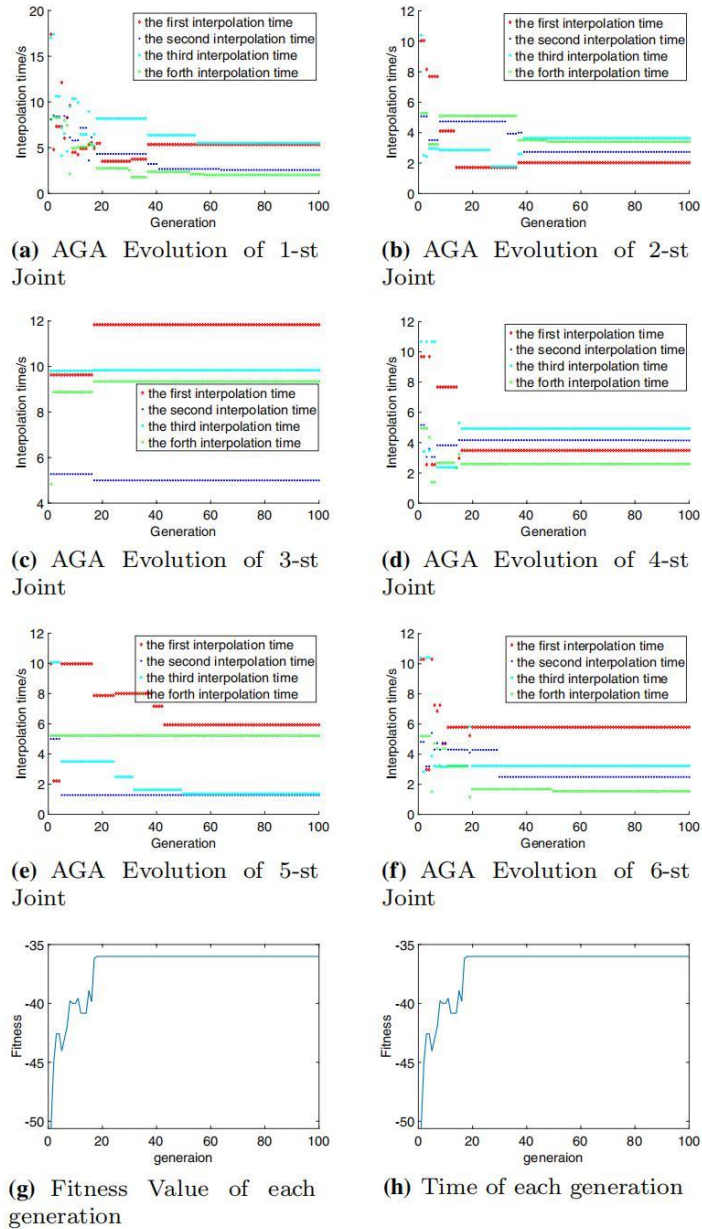
Based on this research’s typical timber joint, this study briefly takes the 6 DOF KUKA-KR90 robot as an example, to convert the geometric information from Rhino into the position information in working space. To implement the objectives functions, the modified DH parameter is chosen to build the link model and the trajectories of the joints are interpolated by fifth-order polynomial functions in joint space. Particle swarm optimization and adaptive genetic algorithm are applied to optimize the path distance and travel time interval respectively.

The two optimization methods achieved the optimal objectives, satisfying the kinematics constraints, and showed effectiveness in decreasing the distance and travel time in the complicated trajectories in this case study. PSO technique improves the automation of robotic trajectory planning in complicated joint fabrication through generating a rational cutting order without singularities. At the same time the trajectory optimized by PSO is also shortened compared to the initial one. The trajectories within one cutting surface optimized by AGA results in time saving and smoother robotic paths, improves the working efficiency and stability by reducing the stress on the actuators in real practice. In real on-site fabrication, this control method could increase working efficiency and improve fabrication accuracy.

Table 5 The optimized time

Time interval	Joint <i>i</i> initial time	1	2	3	4	5	6
		Optimized time					
t_1	18	5.3522	2.0261	11.8355	3.4864	5.9286	5.7879
t_2	9	2.5653	2.7381	4.9952	4.1484	1.2748	2.4834
t_3	18	5.499	3.6438	9.8371	4.9294	1.3568	3.2208
t_4	9	2.0274	3.3993	9.3441	2.5918	5.2089	1.5308
Total times (s)	54	15.4439	11.8074	36.0119	15.1561	13.7691	13.0301

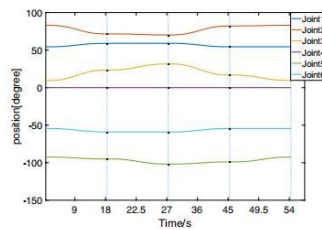
Fig. 17 Convergence of AGA



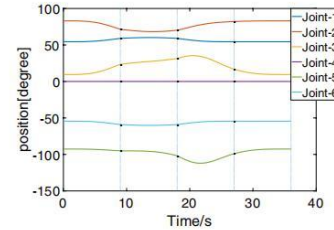
Future work would focus on different combinations of trajectories technique (like fifth-order B-spline, 3-5-3 polynomial interpolation, etc.) and optimal algorithms like grey

wolf optimization (GWO), ant colony optimization (ACO) to choose the best combination to optimize the distance and

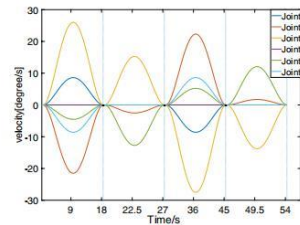
Fig. 18 Comparison of the initial trajectory and AGA time-optimal trajectory



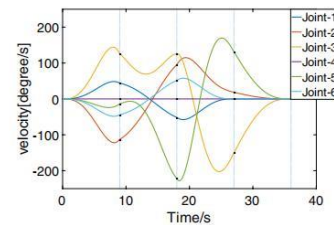
(a) Position of 6 Joints for the Initial Trajectory



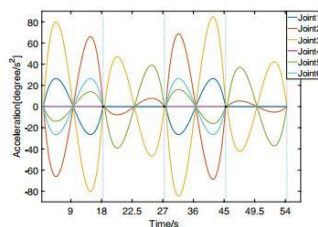
(b) Position of 6 Joints for the AGA Time-Optimal Trajectory



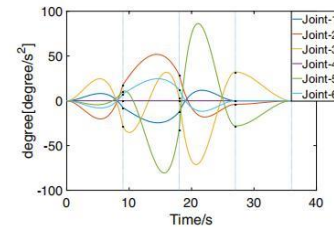
(c) Velocity of 6 Joints for the Initial Trajectory



(d) Velocity of 6 Joints for the AGA Time-Optimal Trajectory



(e) Acceleration of 6 Joints for the Initial Trajectory



(f) Acceleration of 6 Joints for the AGA Time-Optimal Trajectory

time. Validation would also be tested on industrial timber which have similar properties to validate the algorithm.

Acknowledgements The case in this research was completed in the workshop in ROBIARCH 2018 and the presented research builds on the case findings. Thanks to the team member Lynn Masuda together working on the model in Rhino. In particular, the authors would warmly like to thank: Achilleas Xydis, Florian Fend and Yuko Ishizu for their helpful technical support and the organization of ETH Zurich.

Funding Not applicable.

Availability of data and material Not applicable.

Code availability Not applicable.

Declarations

Conflict of interest The authors declare that they have no conflict of interest.

Open Access This article is licensed under a Creative Commons Attribution 4.0 International License, which permits use, sharing, adaptation, distribution and reproduction in any medium or format, as long as you give appropriate credit to the original author(s) and the source, provide a link to the Creative Commons licence, and indicate if changes were made. The images or other third party material in this article are

included in the article's Creative Commons licence, unless indicated otherwise in a credit line to the material. If material is not included in the article's Creative Commons licence and your intended use is not permitted by statutory regulation or exceeds the permitted use, you will need to obtain permission directly from the copyright holder. To view a copy of this licence, visit <http://creativecommons.org/licenses/by/4.0/>.

References

- Abu-Dakka FJ, Valero FJ, Suñer JL, Mata V (2015) A direct approach to solving trajectory planning problems using genetic algorithms with dynamics considerations in complex environments. *Robotica* 33(3):669
- Agusti-Juan I, Müller F, Hack N, Wangler T, Habert G (2017) Potential benefits of digital fabrication for complex structures: environmental assessment of a robotically fabricated concrete wall. *J Clean Prod* 154:330
- Ata AA (2007) Optimal trajectory planning of manipulators: a review. *J Eng Sci Technol* 2(1):32
- Ata AA, Myo TR (2005) Optimal point-to-point trajectory tracking of redundant manipulators using generalized pattern search. *Int J Adv Robot Syst* 2(3):24
- Balkan T (1998) A dynamic programming approach to optimal control of robotic manipulators. *Mech Res Commun* 25(2):225
- Boscariol P, Gasparetto A, Vidoni R (2012) Jerk-continuous trajectories for cyclic tasks. In: International design engineering technical conferences and computers and information in engineering conference, vol 45035. American Society of Mechanical Engineers, pp 1277–1286
- Cao Y, Lu K, Li X, Zang Y (2011) Accurate numerical methods for computing 2d and 3d robot workspace. *Int J Adv Robot Syst* 8(6):76
- Constantinescu D, Croft EA (2000) Smooth and time-optimal trajectory planning for industrial manipulators along specified paths. *J Robot Syst* 17(5):233
- Cook CC, Ho CY (1984) The application of spline functions to trajectory generation for computer-controlled manipulators. *Computing techniques for robots*. Springer, Boston, MA, pp 101–110
- Craig JJ (2009) Introduction to robotics: mechanics and control, 3/E. Pearson Education India
- Davis L (1991) Handbook of genetic algorithms
- Davis L (1987) Genetic algorithms and simulated annealing
- Denavit J, Hartenberg RS, Mooring BW, Tang GR, Whitney DE, Lozinski CA (1955) 54 Kinematic parameter. *J Appl Mech* 77(2):215–221
- Doctor S, Venayagamoorthy GK, Gudise VG (2004) Optimal PSO for collective robotic search applications. In: Proceedings of the 2004 congress on evolutionary computation (IEEE Cat. No.04TH8753), vol 2, pp 1390–1395
- Eberhart R, Kennedy J (1995) A new optimizer using particle swarm theory. In: MHS'95. Proceedings of the sixth international symposium on micro machine and human science. IEEE, pp 39–43
- Eversmann P, Gramazio F, Kohler M (2017) Robotic prefabrication of timber structures: towards automated large-scale spatial assembly. *Constr Robot* 1(1–4):49
- Faludi J, Bayley C, Bhogal S, Iribarne M (2015) Comparing environmental impacts of additive manufacturing vs traditional machining via life-cycle assessment. *Rapid Prototyp J* 21(1):14–33
- Field G, Stepanenko Y (1996) Iterative dynamic programming: An approach to minimum energy trajectory planning for robotic manipulators. In: Proceedings of IEEE international conference on robotics and automation, vol 3. IEEE, Minneapolis, pp 2755–2760
- Ford S, Despeisse M (2016) Additive manufacturing and sustainability: an exploratory study of the advantages and challenges. *J Clean Prod* 137:1573
- Fu R, Ju HH (2011) Time-optimal trajectory planning algorithm based on AGA for manipulator. *Jisuanji Yingyong Yanjiu* 28(9):3275
- Gasparetto A, Zanotto V (2007) A new method for smooth trajectory planning of robot manipulators. *Mech Mach Theory* 42(4):455
- Gasparetto A, Zanotto V (2008) A technique for time-jerk optimal planning of robot trajectories. *Robot Comput Integr Manuf* 24(3):415
- Gasparetto A, Zanotto V (2010) Optimal trajectory planning for industrial robots. *Adv Eng Softw* 41(4):548
- Gasparetto A, Boscariol P, Lanzutti A, Vidoni R (2012) Trajectory planning in robotics. *Math Comput Sci* 6(3):269
- Gasparetto A, Boscariol P, Lanzutti A, Vidoni R (2015) Path planning and trajectory planning algorithms: A general overview. Motion and operation planning of robotic systems. Springer, pp 3–27
- Hao Y, Zu W, Zhao Y (2007) Real-time obstacle avoidance method based on polar coordination particle swarm optimization in dynamic environment. In: 2007 2nd IEEE conference on industrial electronics and applications, pp 1612–1617
- Helm V, Ercan S, Gramazio F, Kohler M (2012) Mobile robotic fabrication on construction sites: DimRob. In: 2012 IEEE/RSJ international conference on intelligent robots and systems, pp 4335–4341
- Helwig S, Wanka R (2008) Theoretical analysis of initial particle swarm behavior. In: Parallel problem solving from nature – PPSN X. Lecture notes in computer science, vol 5199. Springer, Berlin, Heidelberg, pp 889–898
- Hereford JM (2006) A distributed particle swarm optimization algorithm for swarm robotic applications. In: 2006 IEEE international conference on evolutionary computation. IEEE, Vancouver, pp 1678–1685
- Hoffmann M, Mühlenthaler M, Helwig S, Wanka R (2011) Discrete particle swarm optimization for TSP: theoretical results and experimental evaluations. In: Adaptive and intelligent systems. Lecture notes in computer science, vol 6943. Springer, Berlin, Heidelberg, pp 416–427
- Huang J, Hu P, Wu K, Zeng M (2018) Optimal time-jerk trajectory planning for industrial robots. *Mech Mach Theory* 121:530
- Jeevamalar J, Ramabalan S (2012) Optimal trajectory planning for autonomous robots - A review. In: IEEE-International conference on advances in engineering, science and management (ICAESM-2012), pp 269–275
- Jeffers M (2016) Autonomous robotic assembly with variable material properties. *Robotic fabrication in architecture, art and design 2016*. Springer, Cham, pp 48–61
- Keating S, Oxman N (2013) Compound fabrication: a multi-functional robotic platform for digital design and fabrication. *Robot Comput Integr Manuf* 29(6):439
- Kennedy J, Eberhart R (1995) Particle swarm optimization. In: Proceedings of ICNN'95-international conference on neural networks, vol 4. IEEE, pp 1942–1948
- Kennedy J, Eberhart RC (1997) A discrete binary version of the particle swarm algorithm. In: 1997 IEEE international conference on systems, man, and cybernetics. Computational cybernetics and simulation, vol 5, pp 4104–4108
- Krieg OD, Schwinn T, Menges A, Li JM, Knippers J, Schmitt A, Schwieger V (2015) Biomimetic lightweight timber plate shells: computational integration of robotic fabrication, architectural geometry and structural design. *Advances in architectural geometry 2014*. Springer, Cham, pp 109–125
- Kyriakopoulos KJ, Saridis GN (1988) Minimum jerk path generation. In: Proceedings. 1988 IEEE international conference on robotics and automation. IEEE, pp 364–369
- Labonnote N, Rönquist A, Manum B, Rütther P (2016) Additive construction: state-of-the-art, challenges and opportunities. *Autom Constr* 72:347

- Liao X, Wang W, Lin Y, Gong C (2010) Time-optimal trajectory planning for a 6R jointed welding robot using adaptive genetic algorithms. In: 2010 International conference on computer, mechatronics, control and electronic engineering, vol 2. IEEE, pp 600–603
- Luh JYS, Lin CS (1981) Optimum path planning for mechanical manipulators. *J Dyn Syst Meas Control* 103(2):142. <https://doi.org/10.1115/1.3139654>
- Luo LP, Yuan C, Yan RJ, Yuan Q, Wu J, Shin KS, Han CS (2015) Trajectory planning for energy minimization of industry robotic manipulators using the Lagrange interpolation method. *Int J Precis Eng Manuf* 16(5):911
- Petrinec K, Kovacic Z (2007) Trajectory planning algorithm based on the continuity of jerk. In: 2007 Mediterranean conference on control & automation, pp 1–5
- Piazzzi A, Visioli A (1998) Global minimum-time trajectory planning of mechanical manipulators using interval analysis. *Int J Control* 71(4):631
- Popovic D, Fast-Berglund Å, Winroth M (2016) Production of customized and standardized single family timber houses—A comparative study on levels of automation. In: 7th Swedish production symposium
- Ramabalan S, Saravanan R, Balamurugan C (2009) Multi-objective dynamic optimal trajectory planning of robot manipulators in the presence of obstacles. *Int J Adv Manuf Technol* 41(5–6):580
- Rastegar J, Fardanesh B (1990) Manipulation workspace analysis using the Monte Carlo method. *Mech Mach Theory* 25(2):233
- Ratiu M, Adriana Prichici M (2017) Industrial robot trajectory optimization- a review. *MATEC web of conferences*, vol 126, p 2005
- Reyes-Sierra M, Coelho CC et al (2006) Multi-objective particle swarm optimizers: a survey of the state-of-the-art. *Int J Comput Intell Res* 2(3):287
- Saravanan R, Ramabalan S, Balamurugan C (2008) Evolutionary optimal trajectory planning for industrial robot with payload constraints. *Int J Adv Manuf Technol* 38(11–12):1213
- Sato A, Sato O, Takahashi N, Kono M (2007) Trajectory for saving energy of a direct-drive manipulator in throwing motion. *Artif Life Robot* 11(1):61
- Shen J, Kong M, Zhu Y (2019) Trajectory optimization algorithm based on robot dynamics and convex optimization. In: 2019 IEEE 3rd advanced information management, communicates, electronic and automation control conference (IMCEC). IEEE, pp 1583–1588
- Shi XH, Liang YC, Lee HP, Lu C, Wang Q (2007) Particle swarm optimization-based algorithms for TSP and generalized TSP. *Inf Process Lett* 103(5):169
- Shiller Z (1996) Time-energy optimal control of articulated systems with geometric path constraints. *J Dyn Syst Meas Control* 118(1):139. <https://doi.org/10.1115/1.2801134>
- Siciliano B, Sciavicco L, Villani L, Oriolo G (2010) *Robotics: modeling, planning and control*. Springer Science & Business Media
- Simon D (1993) The application of neural networks to optimal robot trajectory planning. *Robot Auton Syst* 11(1):23
- Srinivas M, Patnaik LM (1994) Adaptive probabilities of crossover and mutation in genetic algorithms. *IEEE Trans Syst Man Cybern* 24(4):656
- Thomas GB, Weir MD, Hass J, Giordano FR, Korkmaz R (2010) *Thomas' calculus*. Pearson, Boston
- Trelea IC (2003) The particle swarm optimization algorithm: convergence analysis and parameter selection. *Inf Process Lett* 85(6):317
- Verschuere D, Demeulenaere B, Swevers J, De Schutter J, Diehl M (2009) Time-optimal path tracking for robots: a convex optimization approach. *IEEE Trans Autom Control* 54(10):2318
- Wang K-P, Huang L, Zhou C-G, Pang W (2003) Particle swarm optimization for traveling salesman problem. In: Proceedings of the 2003 international conference on machine learning and cybernetics (IEEE Cat. No.03EX693), vol 3, pp 1583–1585
- Whitley D (1994) A genetic algorithm tutorial. *Stat Comp* 4(2):65
- Xu W, Li C, Liang B, Liu Y, Xu Y (2008) The Cartesian path planning of free-floating space robot using particle swarm optimization. *Int J Adv Robot Syst* 5(3):27
- Xu Z, Li S, Chen Q, Hou B (2015) MOPSO based multi-objective trajectory planning for robot manipulators. In: 2015 2nd international conference on information science and control engineering. IEEE, pp 824–828
- Zanotto V, Gasparetto A, Lanzutti A, Boscariol P, Vidoni R (2011) Experimental validation of minimum time-jerk algorithms for industrial robots. *J Intell Robot Syst* 64(2):197
- Zhang Y, Gong DW, Zhang JH (2013) Robot path planning in uncertain environment using multi-objective particle swarm optimization. *Neurocomputing* 103:172
- Zhang J, Meng Q, Feng X, Shen H (2018) A 6-DOF robot-time optimal trajectory planning based on an improved genetic algorithm. *Robot Biomim* 5(1):1
- Zhao Q, Yan S (2005) Collision-free path planning for mobile robots using chaotic particle swarm optimization. In: Wang L, Chen K, Ong YS (eds) *Advances in natural computation*. ICNC 2005. Lecture notes in computer science, vol 3612. Springer, Berlin, Heidelberg. https://doi.org/10.1007/11539902_77
- Zhu S, Liu S, Wang X, Wang H (2010) Time-optimal and jerk-continuous trajectory planning algorithm for manipulators. *J Mech Eng* 46(3):47

Publisher's Note Springer Nature remains neutral with regard to jurisdictional claims in published maps and institutional affiliations.

References

- Aas, K., & Eikvil, L. (1999). *Text categorisation: A survey*. Retrieved from
- Abderrahim, M., Khamis, A., Garrido, S., & Moreno, L. (2006). Accuracy and Calibration Issues of Industrial Manipulators, *Industrial Robotics: Programming, Simulation and Application. Advanced Robotic Systems International & Pro Literatur Verlag*, 131146.
- Abtahi, M., Pendar, H., Alasty, A., & Vossoughi, G. (2010). Experimental kinematic calibration of parallel manipulators using a relative position error measurement system. *Robotics and Computer-Integrated Manufacturing*, 26(6), 799-804.
- Adeli, H., & Cheng, N.-T. (1993). Integrated genetic algorithm for optimization of space structures. *Journal of Aerospace Engineering*, 6(4), 315-328 0893-1321.
- Adriaenssens, S., Gramazio, F., Kohler, M., Menges, A., & Pauly, M. (2016). *Advances in architectural geometry 2016*: vdf Hochschulverlag AG.
- Aggarwal, C. C., & Zhai, C. (2012). A survey of text clustering algorithms. In *Mining text data* (pp. 77-128): Springer.
- Agirbas, A. (2018). Performance-based design optimization for minimal surface based form. *Architectural Science Review*, 61(6), 384-399 0003-8628.
- Aish, R. (2013). First build your tools. *Inside Smartgeometry: Expanding the Architectural Possibilities of Computational Design*, 36-49.
- Aksöz, Z., & Preisinger, C. (2019). *An Interactive Structural Optimization of Space Frame Structures Using Machine Learning*.
- Aldersey-Williams, H. (2003). *Zoomorphic: new animal architecture*: Laurence King London.
- Alexandridis, G., Tzetzis, D., & Kyratsis, P. (2016). *Biomimicry in Product Design through Materials Selection and Computer Aided Engineering*.
- Alfaris, A. A. F. (2009). *Emergence through conflict: the Multi-Disciplinary Design System (MDDS)*. Massachusetts Institute of Technology,
- Altshuller, G. S. (1984). *Creativity as an exact science: the theory of the solution of inventive problems*: Gordon and Breach.
- Angra, S., & Ahuja, S. (2017). *Machine learning and its applications: A review*.
- Ansell, M. P., & Smedley, D. X. (2007). Briefing: Bonded-in technology for structural timber. In: Thomas Telford Ltd.
- Ardiny, H., Witwicki, S., & Mondada, F. (2015a). Are autonomous mobile robots able to take over construction? a review.
- Ardiny, H., Witwicki, S., & Mondada, F. (2015b). *Construction automation with autonomous mobile robots: A review*.
- Arens, E. A., & Williams, P. B. (1977). The effect of wind on energy consumption in buildings. *Energy and Buildings*, 1(1), 77-84.
- Arslan, G. Y. (2014). Biomimetic Architecture A New Interdisciplinary Approach to Architecture. *ALAM CIPTA, International Journal of Sustainable Tropical Design Research and Practice*, 7(2), 29-36 2289-3687.
- As, I., Pal, S., & Basu, P. (2018). Artificial intelligence in architecture: Generating conceptual design via deep learning. *International Journal of Architectural Computing*, 16(4), 306-327 1478-0771.
- Au, C. K., & Yuen, M. M.-F. (1995). Unified approach to NURBS curve shape modification. *Computer-Aided Design*, 27(2), 85-93 0010-4485.
- Azariadis, P. N., & Aspragathos, N. A. (2005). Obstacle representation by Bump-surfaces for optimal motion-planning. *Robotics and Autonomous Systems*, 51(2-3), 129-150.
- Badarnah, L., & Kadri, U. (2015). A methodology for the generation of biomimetic design concepts. *Architectural Science Review*, 58(2), 120-133 0003-8628.
- Bagnéris, M., Marty, A., Maurin, B., Motro, R., & Pauli, N. (2010). Pascalian Forms as Morphogenetic Tool. *Journal of the International Association for Shell and Spatial Structures*, 51(3), 165-181.
- Bainbridge, R., Mettem, C., Harvey, K., & Ansell, M. (2002). Bonded-in rod connections for timber structures—development of design methods and test observations. *International journal of adhesion and adhesives*, 22(1), 47-59 0143-7496.
- Balaguer, C., Abderrahim, M., Navarro, J. M., Boudjabeur, S., Aromaa, P., Kahkonen, K., . . . Wing, R. (2002). FutureHome: An integrated construction automation approach. *IEEE Robotics & Automation Magazine*, 9(1), 55-66 1070-9932.
- Balaguer, C., Gambao, E., Barrientos, A., Puente, E. A., & Aracil, R. (1996). *Site assembly in construction industry by means of a large range advanced robot*.

- Balmond, C. (1997). New structure and the informal. *Assemblage*(33), 47-57 0889-3012.
- Baron, P., Fisher, R., Tuson, A., Mill, F., & Sherlock, A. (1999). A Voxel Based Representation for Evolutionary Shape Optimization. *Ai Edam*, 13(3), 145-156 0890-0604.
- Bathon, L., Bletz-Mühldorfer, O., Schmidt, J., & Diehl, F. (2014). *Fatigue design of adhesive connections using perforated steel plates*.
- Baumeister, D., Tocke, R., Dwyer, J., Ritter, S., & Benyus, J. M. (2014). *Biomimicry*.
- Belém, C., Santos, L., & Leitão, A. (2019). On the Impact of Machine Learning: Architecture without Architects?
- Benyus, J. M. (1997). *Biomimicry: Innovation inspired by nature*: Morrow New York.
- Bernal, M., Haymaker, J. R., & Eastman, C. (2015). On the role of computational support for designers in action. *Design Studies*, 41, 163-182 0142-0694X.
- Bishop, C. M. (2006). *Pattern recognition and machine learning*: springer.
- Bitar, A., & Cobucci Paolucci, P. (2020). Connections in Large Timber Beams Free-Form Structures.
- Block, P., Knippers, J., Mitra, N. J., & Wang, W. (2015). *Advances in architectural geometry 2014*: Springer.
- Bobenko, A. I., Sullivan, J. M., Schröder, P., & Ziegler, G. (2008). *Discrete differential geometry* (Vol. 38): Springer.
- Bock, & Linner. (2015). *Robot-Oriented Design: design and management tools for the deployment of automation and robotics in construction*: Cambridge University Press.
- Bock, T. (2007). Construction robotics. *Autonomous Robots*, 22(3), 201-209 1573-7527.
- Bock, T. (2015). The future of construction automation: Technological disruption and the upcoming ubiquity of robotics. *Automation in Construction*, 59, 113-121 0926-5805.
- Bock, T., & Linner, T. (2015). *Robot oriented design*: Cambridge university press.
- Bock, T., & Linner, T. (2016). *Construction Robots: Volume 3: Elementary Technologies and Single-task Construction Robots*: Cambridge University Press.
- Bofang, Z. (2018). *The finite element method theory and applications, 4th edition* (4 ed.): China Water Power Press.
- Bommes, D., Zimmer, H., & Kobbelt, L. (2009). Mixed-integer quadrangulation. *ACM Transactions on Graphics (TOG)*, 28(3), 1-10 0730-0301.
- Bonahon, F. (2002). Geometric structures on 3-manifolds. *Handbook of geometric topology*, 93164.
- Bonola, R. (1955). *Non-Euclidean geometry: A critical and historical study of its development*: Courier Corporation.
- Bonwetsch, T., Gramazio, F., & Kohler, M. (2012). ROB: Towards a Bespoke Building Process. *Manufacturing the Bespoke: Making and Prototyping Architecture*, 78-87.
- Brandner, R. (2013). *Production and Technology of Cross Laminated Timber (CLT): A state-of-the-art Report*.
- Brandner, R., Flatscher, G., Ringhofer, A., Schickhofer, G., & Thiel, A. (2016). Cross laminated timber (CLT): overview and development. *European Journal of Wood and Wood Products*, 74(3), 331-351 0018-3768.
- Brell-Cokcan, S., & Braumann, J. (2013). *Rob/ Arch 2012: Robotic fabrication in architecture, art and design*: Springer Science & Business Media.
- Brent, A. C., & Pretorius, M. W. (2008). Sustainable development: A conceptual framework for the technology management field of knowledge and a departure for further research. *South African Journal of Industrial Engineering*, 19(1), 31-52 2224-7890.
- Brent, A. C., Van Erck, R. P. G., & Labuschagne, C. (2006). Sustainability cost accounting-part 1: a monetary procedure to evaluate the sustainability of technologies in the South African process industry. *South African Journal of Industrial Engineering*, 17(2), 35-51 1012-1277X.
- Brogårdh, T. (2009). Robot control overview: An industrial perspective. *Modeling, Identification and Control*, 30(3), 167.
- Brujic, D., Ainsworth, I., & Ristic, M. (2011). Fast and accurate NURBS fitting for reverse engineering. *The International Journal of Advanced Manufacturing Technology*, 54(5-8), 691-700 0268-3768.
- Buchanan, A. H. (2000). Fire performance of timber construction. *Progress in structural engineering and materials*, 2(3), 278-289 1365-0556.
- Buchanan, R. (2001). Design research and the new learning. *Design issues*, 17(4), 3-23 0747-9360.
- Buell, T. W., & Saadatmanesh, H. (2005). Strengthening timber bridge beams using carbon fiber. *Journal of structural engineering*, 131(1), 173-187 0733-9445.
- Burkhardt, B. (2016). Natural structures-the research of Frei Otto in natural sciences. *International journal of space structures*, 31(1), 9-15 0266-3511.

- Burry, M. (2011). *Scripting cultures: Architectural design and programming*: John Wiley & Sons.
- Buyle, M., Braet, J., & Audenaert, A. (2013). Life cycle assessment in the construction sector: A review. *Renewable and Sustainable Energy Reviews*, 26, 379-388 1364-0321.
- Caetano, I., Santos, L., & Leitão, A. (2020). Computational design in architecture: Defining parametric, generative, and algorithmic design. *Frontiers of Architectural Research* 2095-2635.
- Caldas, L. (2006). *GENE_ARCH: an evolution-based generative design system for sustainable architecture*.
- Caldas, L. (2008). Generation of energy-efficient architecture solutions applying GENE_ARCH: An evolution-based generative design system. *Advanced Engineering Informatics*, 22(1), 59-70 1474-0346.
- Carll, C., & Wiedenhoef, A. C. (2009). Moisture-related properties of wood and the effects of moisture on wood and wood products. *Moisture control in buildings: the key factor in mold prevention, 2nd ed. West Conshohocken, PA: ASTM International*, 54-79.
- Castro-Lacouture, D. (2009). Construction automation. In *Springer handbook of automation* (pp. 1063-1078): Springer.
- Cavalliere, C., Dell'Osso, G. R., Favia, F., & Lovicario, M. (2019). BIM-based assessment metrics for the functional flexibility of building designs. *Automation in Construction*, 107, 102925 100926-105805.
- Ceccato, C., Hesselgren, L., Pauly, M., Pottmann, H., & Wallner, J. (2016). *Advances in Architectural Geometry 2010*: Birkhäuser.
- Celniker, G., & Gossard, D. (1991). *Deformable curve and surface finite-elements for free-form shape design*.
- Celniker, G., & Welch, W. (1992). *Linear constraints for deformable non-uniform b-spline surfaces*.
- Cf, O. (2015). Transforming our world: the 2030 Agenda for Sustainable Development.
- Chai, H., So, C., & Yuan, P. F. (2021). Manufacturing double-curved glulam with robotic band saw cutting technique. *Automation in Construction*, 124, 103571 100926-105805.
- Chai, H., & Yuan, P. F. (2018). *Investigations on potentials of robotic band-saw cutting in complex wood structures*.
- Chaszar, A., & Joyce, S. C. (2016). Generating freedom: Questions of flexibility in digital design and architectural computation. *International Journal of Architectural Computing*, 14(2), 167-181 1478-0771.
- Chen, H., Ooka, R., & Kato, S. (2008). Study on optimum design method for pleasant outdoor thermal environment using genetic algorithms (GA) and coupled simulation of convection, radiation and conduction. *Building and Environment*, 43(1), 18-30 0360-1323.
- Chettibi, T., Lehtihet, H., Haddad, M., & Hanchi, S. (2004). Minimum cost trajectory planning for industrial robots. *European journal of mechanics. A, Solids*, 23(4), 703-715.
- Chilton, J. (2007). *Space grid structures*: Routledge.
- Chivate, P. N., & Jablow, A. G. (1995). Review of surface representations and fitting for reverse engineering. *Computer Integrated Manufacturing Systems*, 8(3), 193-204 0951-5240.
- Chong, Y. T., Chen, C.-H., & Leong, K. F. (2009). A heuristic-based approach to conceptual design. *Research in Engineering Design*, 20(2), 97-116 0934-9839.
- Colglazier, W. (2015). Sustainable development agenda: 2030. *Science*, 349(6252), 1048-1050 0036-8075.
- Conte, S. D., & De Boor, C. (2017). *Elementary numerical analysis: an algorithmic approach*: SIAM.
- Cousineau, L., & Miura, N. (1998). *Construction robots: the search for new building technology in Japan*: ASCE Publications.
- Craig, J. J. (2005). *Introduction to robotics: mechanics and control* (Vol. 3): Pearson/Prentice Hall Upper Saddle River, NJ, USA:.
- Craig, J. J. (2009). *Introduction to robotics: mechanics and control, 3/E*: Pearson Education India.
- Cramer-Petersen, C. L., Christensen, B. T., & Ahmed-Kristensen, S. (2019). Empirically analysing design reasoning patterns: Abductive-deductive reasoning patterns dominate design idea generation. *Design Studies*, 60, 39-70 0142-0694X.
- Crane, K. (2018). Discrete differential geometry: An applied introduction. *Notices of the AMS, Communication*, 1153-1159.
- Crane, K., & Wardetzky, M. (2017). A glimpse into discrete differential geometry. *Notices of the AMS*, 64(10).
- Cross, N. (2011). *Design thinking: Understanding how designers think and work*: Berg.
- Cudzik, J., & Radziszewski, K. (2018). Artificial intelligence aided architectural design.

- D'CRUZ, N., RADFORD, A. D., & GERO, J. S. (1983). A Pareto optimization problem formulation for building performance and design. *Engineering optimization*, 7(1), 17-33.
- da Graça Marcos, M., Machado, J. A. T., & Azevedo-Perdicoulis, T. P. (2012). A multi-objective approach for the motion planning of redundant manipulators. *Applied Soft Computing*, 12(2), 589-599 1568-4946.
- Danhaive, R., & Mueller, C. (2018). *Structural metamodelling of shells*.
- Das, S. (2018). Interactive Artificial Life Based Systems, Augmenting Design Generation and Evaluation by Embedding Expert Opinion-A Human Machine dialogue for form finding.
- De Berg, M., Van Kreveld, M., Overmars, M., & Schwarzkopf, O. (1997). Computational geometry. In *Computational geometry* (pp. 1-17): Springer.
- De Boor, C. (1972). On calculating with B-splines. *Journal of Approximation theory*, 6(1), 50-62 0021-9045.
- De Boor, C., & De Boor, C. (1978). *A practical guide to splines* (Vol. 27): springer-verlag New York.
- De Schutter, G., Lesage, K., Mechtcherine, V., Nerella, V. N., Habert, G., & Agusti-Juan, I. (2018). Vision of 3D printing with concrete—technical, economic and environmental potentials. *Cement and Concrete Research*, 112, 25-36 0008-8846.
- de Soto, B. G., Agustí-Juan, I., Hunhevicz, J., Joss, S., Graser, K., Habert, G., & Adey, B. T. (2018). Productivity of digital fabrication in construction: Cost and time analysis of a robotically built wall. *Automation in Construction*, 92, 297-311 0926-5805.
- Decenciere, E., Cazuguel, G., Zhang, X., Thibault, G., Klein, J. C., Meyer, F., . . . Danno, R. (2013). TeleOphta: Machine learning and image processing methods for teleophthalmology. *Irbm*, 34(2), 196-203 1959-0318.
- Delgado, J. M. D., Oyedele, L., Ajayi, A., Akanbi, L., Akinade, O., Bilal, M., & Owolabi, H. (2019). Robotics and automated systems in construction: Understanding industry-specific challenges for adoption. *Journal of Building Engineering*, 26, 100868 102352-107102.
- Denzler, J. K., & Weidenhiller, A. (2014). New perspectives in machine strength grading: or how to identify a top rupture. In *Materials and joints in timber structures* (pp. 761-771): Springer.
- Diakaki, C., Grigoroudis, E., Kabelis, N., Kolokotsa, D., Kalaitzakis, K., & Stavrakakis, G. (2010). A multi-objective decision model for the improvement of energy efficiency in buildings. *Energy*, 35(12), 5483-5496 0360-5442.
- Ding, M., Xiao, Y., Peng, J., Schomburg, D., Krebs, B., & Wahl, F. M. (2003). 3D reconstruction of free-formed line-like objects using NURBS representation. *Pattern Recognition*, 36(6), 1255-1268 0031-3203.
- Dinwoodie, J. M. (2000). *Timber: its nature and behaviour*: CRC Press.
- Douthe, C., Baverel, O., & Caron, J. F. (2006). Form-finding of a grid shell in composite materials. *journal of the International Association for Shell and Spatial Structures*, 47(1), 53-62 1028-1365X.
- Drouet, P., Dubowsky, S., Zegloul, S., & Mavroidis, C. (2002). Compensation of geometric and elastic errors in large manipulators with an application to a high accuracy medical system. *Robotica*, 20(3), 341-352.
- du Plessis, A., Broeckhoven, C., Yadroitsava, I., Yadroitsev, I., Hands, C. H., Kunju, R., & Bhate, D. (2019). Beautiful and functional: a review of biomimetic design in additive manufacturing. *Additive Manufacturing*, 27, 408-427 2214-8604.
- Dunn, N. (2012). *Digital fabrication in architecture*: Laurence King Publishing.
- Dyvik, S. H., Luczkowski, M., Mork, J. H., Ronnquist, A., & Manum, B. (2019). *Design of freeform gridshell structure-Simplifying the parametric workflow*.
- Eggert, R. X. (2005). *Engineering design*: Pearson/Prentice Hall.
- Eisenhart, L. P. (1997). *Riemannian geometry* (Vol. 51 0691023530): Princeton university press.
- El Ahmar, S. A. S. (2011). Biomimicry as a tool for sustainable architectural design. *Unpublished Master of Science Thesis, Alexandria University, Alexandria*.
- Ercan, B., & Elias-Ozkan, S. T. (2015). Performance-based parametric design explorations: A method for generating appropriate building components. *Design Studies*, 38, 33-53 0142-0694X.
- Espinoza, O., Trujillo, V. R., Mallo, M. F. L., & Buehlmann, U. (2016). Cross-laminated timber: Status and research needs in Europe. *BioResources*, 11(1), 281-295 1930-2126.
- Eversmann, P., Gramazio, F., & Kohler, M. (2017). Robotic prefabrication of timber structures: towards automated large-scale spatial assembly. *Construction Robotics*, 1(1), 49-60 2509-8780.
- Färg, F. E. M. B. (2015). COUTURE Armchair. Retrieved from <http://fargblanche.com/COUTURE-armchair-produced-by-B-D-BARCELONA-DESIGN>

- Farin, G. (1992). From conics to NURBS: A tutorial and survey. *IEEE Computer Graphics and Applications*, 12(5), 78-86 0272-1716.
- Farin, G. E. (1995). *NURB curves and surfaces: from projective geometry to practical use*: AK Peters, Ltd.
- Ficca, J. (2009). Inclusion of performative surfaces material and fabrication research. *Digital Fabrications: Architectural and Material Techniques*. Princeton Architectural Press, New York.
- Figueredo, L., Adorno, B. V., Ishihara, J. Y., & Borges, G. A. (2013). *Robust kinematic control of manipulator robots using dual quaternion representation*. Paper presented at the Robotics and Automation (ICRA), 2013 IEEE International Conference on.
- Filz, G. H. (2013). Minimal-Surface-T-Connections in Architecture. In: ICOSA.
- Fleischmann, M., Knippers, J., Lienhard, J., Menges, A., & Schleicher, S. (2012). Material behaviour: embedding physical properties in computational design processes. *Architectural design*, 82(2), 44-51 0003-8504.
- Fleischmann, M., & Menges, A. (2011). Icd/itke research pavilion: A case study of multi-disciplinary collaborative computational design. In *Computational Design Modelling* (pp. 239-248): Springer.
- Floater, M. S. (1997). Parametrization and smooth approximation of surface triangulations. *Computer aided geometric design*, 14(3), 231-250 0167-8396.
- Foley, J. D., Van, F. D., Van Dam, A., Feiner, S. K., Hughes, J. F., Angel, E., & Hughes, J. (1996). *Computer graphics: principles and practice* (Vol. 12110 0201848406): Addison-Wesley Professional.
- Fuhrmann, L., Moosavi, V., Ohlbrock, P. O., & D'acunto, P. (2018). *Data-driven design: Exploring new structural forms using machine learning and graphic statics*.
- Gálvez, A., & Iglesias, A. (2012). Particle swarm optimization for non-uniform rational B-spline surface reconstruction from clouds of 3D data points. *Information sciences*, 192, 174-192 0020-0255.
- Gamage, A., & Hyde, R. (2012). A model based on Biomimicry to enhance ecologically sustainable design. *Architectural Science Review*, 55(3), 224-235 0003-8628.
- Gamage, A. U., & Wickramanayake, R. S. D. (2005). Parallels between nature and design teaching through nature studies. *Built Environment Sri Lanka*, 5(2), 1-12.
- Garcia, E., Jimenez, M. A., De Santos, P. G., & Armada, M. (2007). The evolution of robotics research. *IEEE Robotics & Automation Magazine*, 14(1), 90-103 1070-9932.
- Gardner, D. J. (2006). Adhesion mechanisms of durable wood adhesive bonds. *Characterization of the cellulosic cell wall*, 254-265.
- Gawell, E. (2013). Non-euclidean geometry in the modeling of contemporary architectural forms. *Journal Biuletyn of Polish Society for Geometry and Engineering Graphics*, 24 1644-9363.
- Gerber, D. J., & Pantazis, E. (2016). A multi-agent system for facade design: a design methodology for design exploration, analysis and simulated robotic fabrication.
- Gholizadeh, S. (2013). Layout optimization of truss structures by hybridizing cellular automata and particle swarm optimization. *Computers & Structures*, 125, 86-99 0045-7949.
- Gibson, I. (2005). Rapid Prototyping: a tool for product development. *Computer-Aided Design and Applications*, 2(6), 785-793 1686-4360.
- Gibson, L. J., Ashby, M. F., & Harley, B. A. (2010). *Cellular materials in nature and medicine*: Cambridge University Press.
- Gilfillan, J. R., Gilbert, S. G., & Patrick, G. R. H. (2003). The use of FRP composites in enhancing the structural behavior of timber beams. *Journal of reinforced plastics and composites*, 22(15), 1373-1388 0731-6844.
- Glymph, J., Shelden, D., Ceccato, C., Mussel, J., & Schober, H. (2004). A parametric strategy for free-form glass structures using quadrilateral planar facets. *Automation in Construction*, 13(2), 187-202 0926-5805.
- Goodfellow, I. J., Pouget-Abadie, J., Mirza, M., Xu, B., Warde-Farley, D., Ozair, S., . . . Bengio, Y. (2014). Generative adversarial networks. *arXiv preprint arXiv:1406.2661*.
- Gordon, W. J., & Riesenfeld, R. F. (1974). B-spline curves and surfaces. In *Computer aided geometric design* (pp. 95-126): Elsevier.
- Gramazio, F., & Yoon, J. M. (2018). *Digital materiality in architecture*.
- Greicius, M. D., Supekar, K., Menon, V., & Dougherty, R. F. (2009). Resting-state functional connectivity reflects structural connectivity in the default mode network. *Cerebral cortex*, 19(1), 72-78 1047-3211.

- Greil, P., Lifka, T., & Kaindl, A. (1998). Biomorphic cellular silicon carbide ceramics from wood: I. Processing and microstructure. *Journal of the European Ceramic Society*, 18(14), 1961-1973 0955-2219.
- Gruber, P., & Jeronimidis, G. (2012). Has biomimetics arrived in architecture? *Bioinspiration & biomimetics*, 7(1), 010201 011748-013190.
- Hajela, P., & Berke, L. (1991). Neural network based decomposition in optimal structural synthesis. *Computing Systems in Engineering*, 2(5-6), 473-481 0956-0521.
- Hamby, D. M. (1994). A review of techniques for parameter sensitivity analysis of environmental models. *Environmental monitoring and assessment*, 32(2), 135-154.
- Hamdy, M., Hasan, A., & Siren, K. (2011). Applying a multi-objective optimization approach for design of low-emission cost-effective dwellings. *Building and Environment*, 46(1), 109-123 0360-1323.
- Harris, R., Haskins, S., & Roynon, J. (2008). The Savill Garden gridshell: design and construction. *The Structural Engineer*, 86(17), 27-34 1466-5123.
- Hastie, T., Tibshirani, R., & Friedman, J. (2009). *The elements of statistical learning: data mining, inference, and prediction*: Springer Science & Business Media.
- Haygreen, J. G., & Bowyer, J. L. (1996). *Forest products and wood science: an introduction*: Iowa state university press.
- Heintze, J., Teerhuis, P. C., & Weiden, A. (1996). Controlled hydraulics for a direct drive brick laying robot. *Automation in Construction*, 5(1), 23-29 0926-5805.
- Helm, V., & Knauss, M. (2015). Additive robotic fabrication of complex timber structures.
- Helms, M., Vattam, S. S., & Goel, A. K. (2009). Biologically inspired design: process and products. *Design Studies*, 30(5), 606-622 0142-0694X.
- Helms, M. E., Vattam, S., & Goel, A. (2008). *Compound analogical design, or how to make a surfboard disappear*.
- Hillier, B. (2007). *Space is the machine: a configurational theory of architecture*: Space Syntax.
- Hirz, M., Dietrich, W., Gfrerrer, A., & Lang, J. (2013). Integrated computer-aided design in automotive development. *Springer-Verlag, Berlin-Heidelberg, DOI, 10*, 978-973.
- Holgate, A. (1997). *The art of structural engineering: the work of Jörg Schlaich and his team*: Edition Axel Menges.
- Hollerbach, J. M., & Wampler, C. W. (1996). The calibration index and taxonomy for robot kinematic calibration methods. *The international journal of robotics research*, 15(6), 573-591.
- Hollerbach, J. M., & Wampler, C. W. (1996). The calibration index and taxonomy for robot kinematic calibration methods. *The international journal of robotics research*, 15(6), 573-591 0278-3649.
- Hong, J., Shen, G. Q., Mao, C., Li, Z., & Li, K. (2016). Life-cycle energy analysis of prefabricated building components: an input-output-based hybrid model. *Journal of Cleaner Production*, 112, 2198-2207.
- Hopkinson, N., & Dickens, P. (2006). Emerging rapid manufacturing processes. *Rapid manufacturing: an industrial revolution for the digital age, 1938(1930)*, 55 0470016132.
- Horváth, I. (2004). On some crucial issues of computer support of conceptual design. In *Product engineering* (pp. 123-142): Springer.
- Hu, S. M., Li, Y. F., Ju, T., & Zhu, X. (2001). Modifying the shape of NURBS surfaces with geometric constraints. *Computer-Aided Design*, 33(12), 903-912 0010-4485.
- Huang, H., Kalogerakis, E., & Marlin, B. (2015). *Analysis and synthesis of 3D shape families via deep - learned generative models of surfaces*.
- Huang, S.-H., Ke, H.-R., & Yang, W.-P. (2008). Structure clustering for Chinese patent documents. *Expert Systems with Applications*, 34(4), 2290-2297.
- Huang, W., & Zheng, H. (2018). Architectural drawings recognition and generation through machine learning.
- Huang, Y. (2016). Creep behavior of wood under cyclic moisture changes: interaction between load effect and moisture effect. *Journal of Wood Science*, 62(5), 392-399 1611-4663.
- Humppi, H., & Österlund, T. (2016). Algorithm-aided BIM.
- Hurmekoski, E., Jonsson, R., & Nord, T. (2015). Context, drivers, and future potential for wood-frame multi-story construction in Europe. *Technological Forecasting and Social Change*, 99, 181-196 0040-1625.
- Isa, D., Kallimani, V., & Lee, L. H. (2009). Using the self organizing map for clustering of text documents. *Expert Systems with Applications*, 36(5), 9584-9591.
- Jabi, W. (2013). *Parametric design for architecture*: Laurence King Publishing.

- Jabi, W., Soe, S., Theobald, P., Aish, R., & Lannon, S. (2017). Enhancing parametric design through non-manifold topology. *Design Studies*, 52, 96-114 0142-0694X.
- James, K. R., Haritos, N., & Ades, P. K. (2006). Mechanical stability of trees under dynamic loads. *American journal of Botany*, 93(10), 1522-1530 0002-9122.
- Jiang, J., & Scott, P. (2020). *Advanced Metrology: Freeform Surfaces*: Academic Press Inc.
- Johns, R. L., & Foley, N. (2014). Bandsawn bands. In *Robotic fabrication in architecture, art and design 2014* (pp. 17-32): Springer.
- Johnson-Laird, P. N. (2006). *How we reason*: Oxford University Press, USA.
- Kaltenbach, F. (2010). Teaching by Doing-A Research Pavilion in Stuttgart. *Detail. Review of Architecture, Timber Construction*(10), 994-995.
- Kaveh, A., Hassani, B., Shojaei, S., & Tavakkoli, S. M. (2008). Structural topology optimization using ant colony methodology. *Engineering Structures*, 30(9), 2559-2565 0141-0296.
- Kelly, G. (2005). Load transfer in hybrid (bonded/bolted) composite single-lap joints. *Composite Structures*, 69(1), 35-43 0263-8223.
- Khean, N., Fabbri, A., & Haeusler, M. H. (2018). Learning Machine Learning as an Architect, How to?- Presenting and evaluating a Grasshopper based platform to teach architecture students machine learning.
- Kim, J. H., & Joo, C. B. (2013). Optimal motion planning of redundant manipulators with controlled task infeasibility. *Mechanism and Machine Theory*, 64, 155-174.
- Knight, T., & Stiny, G. (2015). Making grammars: from computing with shapes to computing with things. *Design Studies*, 41, 8-28 0142-0694X.
- Knopf, G. K., & Kofman, J. (2001). Adaptive reconstruction of free-form surfaces using Bernstein basis function networks. *Engineering Applications of Artificial Intelligence*, 14(5), 577-588 0952-1976.
- Kodama, T., Li, X., Nakahira, K., & Ito, D. (2005). Evolutionary computation applied to the reconstruction of 3-D surface topography in the SEM. *Journal of electron microscopy*, 54(5), 429-435 2050-5701.
- Koenderink, J. J., & Van Doorn, A. J. (1992). Surface shape and curvature scales. *Image and vision computing*, 10(8), 557-564 0262-8856.
- Kohler, M., Gramazio, F., & Willmann, J. (2014). The robotic touch: how robots change architecture. In: Park Books Zurich.
- Kohlhammer, T., Apolinarska, A. A., Gramazio, F., & Kohler, M. (2017). Design and structural analysis of complex timber structures with glued T-joint connections for robotic assembly. *International journal of space structures*, 32(3-4), 199-215 0266-3511.
- Kohonen, T., Kaski, S., Lagus, K., Salojärvi, J., Honkela, J., Paatero, V., & Saarela, A. (2000). Self organization of a massive document collection. *IEEE Transactions on neural networks*, 11(3), 574-585.
- Kolarevic, B. (2004). *Architecture in the digital age: design and manufacturing*: Taylor & Francis.
- Kolev, K., Klodt, M., Brox, T., & Cremers, D. (2009). Continuous global optimization in multiview 3d reconstruction. *International Journal of Computer Vision*, 84(1), 80-96 0920-5691.
- Kotsiantis, S. B., Kanellopoulos, D., & Pintelas, P. E. (2006). Data preprocessing for supervised learning. *International Journal of Computer Science*, 1(2), 111-117 1306-4428.
- Krause, J. (2003). *Reflections: the creative process of generative design in architecture*.
- Krieg, O. D., & Lang, O. (2019). *Adaptive automation strategies for robotic prefabrication of parametrized mass timber building components*.
- Krieg, O. D., & Menges, A. (2013). *Potentials of robotic fabrication in wood construction: elastically bent timber sheets with robotically fabricated finger joints*.
- Krieg, O. D., Schwinn, T., Menges, A., Li, J.-M., Knippers, J., Schmitt, A., & Schwieger, V. (2015). Biomimetic lightweight timber plate shells: Computational integration of robotic fabrication, architectural geometry and structural design. In *Advances in architectural geometry 2014* (pp. 109-125): Springer.
- Kumar, N., Hack, N., Doerfler, K., Walzer, A. N., Rey, G. J., Gramazio, F., . . . Buchli, J. (2017). *Design, development and experimental assessment of a robotic end-effector for non-standard concrete applications*.
- Kumbhakar, S. C., & Lai, H.-p. (2021). A multi-output multi-input stochastic frontier system with input- and output-specific inefficiency. *Economics Letters*, 201, 109807.
- Kunic, A., Naboni, R., Kramberger, A., & Schlette, C. (2021). Design and assembly automation of the Robotic Reversible Timber Beam. *Automation in Construction*, 123, 103531 100926-105805.

- Labuschagne, C., Brent, A. C., & Van Erck, R. P. G. (2005). Assessing the sustainability performances of industries. *Journal of Cleaner Production*, 13(4), 373-385 0959-6526.
- Lam, F. (2001). Modern structural wood products. *Progress in structural engineering and materials*, 3(3), 238-245 1365-0556.
- Larochelle, H., Bengio, Y., Louradour, J., & Lamblin, P. (2009). Exploring strategies for training deep neural networks. *Journal of machine learning research*, 10(1 1532-4435).
- Larsen, H. J., & Munch-Andersen, J. (2011). The sad story of glued-in bolts in Eurocode 5. *Essay*, 4, 1-43.
- Lasi, H., Fettke, P., Kemper, H.-G., Feld, T., & Hoffmann, M. (2014). Industry 4.0. *Business & Information Systems Engineering*, 6(4), 239-242.
- Lee, S., Pan, W., Linner, T., & Bock, T. (2015). *A framework for robot assisted deconstruction: process, sub-systems and modelling*.
- Lepora, N. F., Verschure, P., & Prescott, T. J. (2013). The state of the art in biomimetics. *Bioinspiration & biomimetics*, 8(1), 013001 011748-013190.
- Li, J.-M., & Knippers, J. (2015). Segmental timber plate shell for the landesgartenschau exhibition hall in schwäbisch gmünd—the application of finger joints in plate structures. *International journal of space structures*, 30(2), 123-139 0266-3511.
- Li, J., Hua, C., Qian, J., & Guan, X. (2021). Low-rank based Multi-Input Multi-Output Takagi-Sugeno fuzzy modeling for prediction of molten iron quality in blast furnace. *Fuzzy Sets and Systems*, 421, 178-192.
- Li, X., Wu, Y., & Cao, Z. (2011). Computational Morphogenesis Method for Freeform Structures Generated by Translating B-Spline Curves. *Advanced Science Letters*, 4(8-9), 2727-2732 1936-6612.
- Liddell, I. (2015). Frei Otto and the development of gridshells. *Case Studies in Structural Engineering*, 4, 39-49 2214-3998.
- Lienig, J., & Bruemmer, H. (2017). *Fundamentals of electronic systems design*: Springer.
- Liew, A., Avelino, R., Moosavi, V., Van Mele, T., & Block, P. (2019). Optimising the load path of compression-only thrust networks through independent sets. *Structural and Multidisciplinary Optimization*, 60(1), 231-244 1615-1488.
- Linderoth, M., Stolt, A., Robertsson, A., & Johansson, R. (2013). *Robotic force estimation using motor torques and modeling of low velocity friction disturbances*. Paper presented at the Intelligent Robots and Systems (IROS), 2013 IEEE/RSJ International Conference on.
- Linner, T. (2013). *Automated and robotic construction: Integrated automated construction sites*. Technische Universität München,
- Linner, T., & Bock, T. (2012). Evolution of large - scale industrialisation and service innovation in Japanese prefabrication industry. *Construction Innovation* 1471-4175.
- Liu, D., Wang, W., & Liu, J. (2017). Sensitivity analysis of meteorological parameters on building energy consumption. *Energy Procedia*, 132, 634-639.
- Liu, L., Chen, I. M., Kayacan, E., Tiong, L. K., & Maruvanchery, V. (2015). *Automated construction quality assessment: A review*.
- Liu, Y.-c., Wu, C., & Liu, M. (2011). Research of fast SOM clustering for text information. *Expert Systems with Applications*, 38(8), 9325-9333.
- Liu, Y., Pottmann, H., Wallner, J., Yang, Y.-L., & Wang, W. (2006). Geometric modeling with conical meshes and developable surfaces. In *ACM SIGGRAPH 2006 Papers* (pp. 681-689).
- Liu, Y., Xu, W., Wang, J., Zhu, L., Guo, B., Chen, F., & Wang, G. (2011). General planar quadrilateral mesh design using conjugate direction field. *ACM Transactions on Graphics (TOG)*, 30(6), 1-10 0730-0301.
- López, M., Rubio, R., Martín, S., & Croxford, B. (2017). How plants inspire façades. From plants to architecture: Biomimetic principles for the development of adaptive architectural envelopes. *Renewable and Sustainable Energy Reviews*, 67, 692-703 1364-0321.
- Lotz, M., Bruhm, H., & Czinki, A. (2014). An new force control strategy improving the force control capabilities of standard industrial robots. *Journal of Mechanics Engineering and Automation*, 4(2014), 276-283.
- M Rocker, I. (2006). When code matters. *Architectural design*, 76(4), 16-25 0003-8504.
- Madhoushi, M., & Ansell, M. P. (2004). Experimental study of static and fatigue strengths of pultruded GFRP rods bonded into LVL and glulam. *International journal of adhesion and adhesives*, 24(4), 319-325 0143-7496.

- Madhoushi, M., & Ansell, M. P. (2008). Behaviour of timber connections using glued-in GFRP rods under fatigue loading. Part I: In-line beam to beam connections. *Composites Part B: Engineering*, 39(2), 243-248 1359-8368.
- Magna, R. L., Gabler, M., Reichert, S., Schwinn, T., Waimer, F., Menges, A., & Knippers, J. (2013). From nature to fabrication: biomimetic design principles for the production of complex spatial structures. *International journal of space structures*, 28(1), 27-39 0266-3511.
- Magnier, L., & Haghghat, F. (2010). Multiobjective optimization of building design using TRNSYS simulations, genetic algorithm, and Artificial Neural Network. *Building and Environment*, 45(3), 739-746 0360-1323.
- Mandelbrot, B. B., & Mandelbrot, B. B. (1982). *The fractal geometry of nature* (Vol. 1): WH freeman New York.
- Marinho, M., Figueredo, L., & Adorno, B. V. (2015). *A dual quaternion linear-quadratic optimal controller for trajectory tracking*. Paper presented at the Intelligent Robots and Systems (IROS), 2015 IEEE/RSJ International Conference on.
- Markus, E. D., Agee, J. T., & Jimoh, A. A. (2017). Flat control of industrial robotic manipulators. *Robotics and Autonomous Systems*, 87, 226-236.
- Markus, E. D., Yskander, H., Agee, J. T., & Jimoh, A. A. (2016). Coordination control of robot manipulators using flat outputs. *Robotics and Autonomous Systems*, 83, 169-176.
- Martinec, T., Mlýnek, J., & Petrů, M. (2015). Calculation of the robot trajectory for the optimum directional orientation of fibre placement in the manufacture of composite profile frames. *Robotics and Computer-Integrated Manufacturing*, 35, 42-54.
- Mattheck, C., & Tesari, I. (2004). The mechanical self-optimisation of trees. *WIT Transactions on Ecology and the Environment*, 73 1853127213.
- Mazzoleni, I. (2013). *Architecture follows nature-biomimetic principles for innovative design* (Vol. 2 1466506075): Crc Press.
- McCormack, J., Dorin, A., & Innocent, T. (2004). Generative Design: A Paradigm for Design Research.
- Menges, A. (2006). Manufacturing diversity. *Architectural design*, 76(2), 70-77 0003-8504.
- Menges, A. (2012a). Biomimetic design processes in architecture: morphogenetic and evolutionary computational design. *Bioinspiration & biomimetics*, 7(1), 015003 011748-013190.
- Menges, A. (2012b). *Material computation: Higher integration in morphogenetic design*: John Wiley & Sons.
- Menges, A., & Schwinn, T. (2012). Manufacturing reciprocities. *Architectural design*, 82(2), 118-125 0003-8504.
- Menges, A., Schwinn, T., & Krieg, O. D. (2016). *Advancing wood architecture: a computational approach*: Routledge.
- Meredith, M., & Sasaki, M. (2008). *From control to design: parametric/algorithmic architecture*: Actar-D.
- Messay, T., Ordóñez, R., & Marcil, E. (2016). Computationally efficient and robust kinematic calibration methodologies and their application to industrial robots. *Robotics and Computer-Integrated Manufacturing*, 37, 33-48.
- Mitchell, W. J. (1975). The theoretical foundation of computer-aided architectural design. *Environment and planning b: planning and design*, 2(2), 127-150 0265-8135.
- Monier, V., Bignon, J. C., & Duchanois, G. (2013). *Use of irregular wood components to design non-standard structures*.
- Moretti, L. (1971). Ricerca matematica in architettura e urbanistica. In *Moebius* (Vol. 4, pp. 30-53).
- Mork, J. H., Luczkowski, M., Dyvik, S., Manum, B., & Rønnquist, A. (2017). *A parametric toolkit for advanced timber structures*.
- Morlier, P. (1994). *Creep in timber structures*: CRC Press.
- Mumford, L. (2010). *Technics and civilization*: University of Chicago Press.
- Myers, W. (2012). *Bio design*: Museum of Modern Art.
- Naicu, D., Harris, R., & Williams, C. (2014). *Timber gridshells: Design methods and their application to a temporary pavilion*.
- Nasir, V., & Cool, J. (2020). A review on wood machining: characterization, optimization, and monitoring of the sawing process. *Wood Material Science & Engineering*, 15(1), 1-16 1748-0272.
- Neelamkavil, J. (2009). *Automation in the prefab and modular construction industry*.
- Newton, D. (2019). Generative deep learning in architectural design. *Technology| Architecture+ Design*, 3(2), 176-189 2475-1448.

- Nguyen, A. C., Vestartas, P., & Weinand, Y. (2019). Design framework for the structural analysis of free-form timber plate structures using wood-wood connections. *Automation in Construction*, *107*, 102948 100926-105805.
- Nicholas, P., Zwierzycki, M., Stasiuk, D., & Thomsen, M. R. (2016). *Concepts and Methodologies for Multi-scale Modelling: a Mesh-based Approach for Bi-directional Information Flows*.
- Nof, S. Y. (1999). *Handbook of industrial robotics*: John Wiley & Sons.
- Nubiola, A., & Bonev, I. A. (2013). Absolute calibration of an ABB IRB 1600 robot using a laser tracker. *Robotics and Computer-Integrated Manufacturing*, *29*(1), 236-245.
- Nubiola, A., & Bonev, I. A. (2014). Absolute robot calibration with a single telescoping ballbar. *Precision Engineering*, *38*(3), 472-480.
- Oh, S., Jung, Y., Kim, S., Lee, I., & Kang, N. (2019). Deep generative design: Integration of topology optimization and generative models. *Journal of Mechanical Design*, *141*(11 1050-0472).
- Ohmori, H., & Hamada, H. (2006). Computational morphogenesis of shells with free curved surface considering both designer's preference and structural rationality. *Proceeding of IASS-APCS*.
- Ooka, R., & Komamura, K. (2009). Optimal design method for building energy systems using genetic algorithms. *Building and Environment*, *44*(7), 1538-1544 0360-1323.
- Orlowski, K. (2019). Assessment of manufacturing processes for automated timber-based panelised prefabrication. *Buildings*, *9*(5), 125.
- Otto, F., Trostel, R., & Schleyer, F. K. (1973). *Tensile structures; design, structure, and calculation of buildings of cables, nets, and membranes*.
- Oxman, R. (2008). Digital architecture as a challenge for design pedagogy: theory, knowledge, models and medium. *Design Studies*, *29*(2), 99-120 0142-0694X.
- Oxman, R. (2017). Thinking difference: Theories and models of parametric design thinking. *Design Studies*, *52*, 4-39 0142-0694X.
- Özgür, E., & Mezouar, Y. (2016). Kinematic modeling and control of a robot arm using unit dual quaternions. *Robotics and Autonomous Systems*, *77*, 66-73.
- Pahl, G., & Beitz, W. (2013). *Engineering design: a systematic approach*: Springer Science & Business Media.
- Palmieri, G., Palpacelli, M.-C., Carbonari, L., & Callegari, M. (2018). Vision-based kinematic calibration of a small-scale spherical parallel kinematic machine. *Robotics and Computer-Integrated Manufacturing*, *49*, 162-169.
- Pan, M., Linner, T., Pan, W., Cheng, H., & Bock, T. (2018a). A framework of indicators for assessing construction automation and robotics in the sustainability context. *Journal of Cleaner Production*, *182*, 82-95 0959-6526.
- Pan, M., Linner, T., Pan, W., Cheng, H., & Bock, T. (2018b). A framework of indicators for assessing construction automation and robotics in the sustainability context. *Journal of Cleaner Production*, *182*, 82-95.
- Pan, R., & Skala, V. (2011). Continuous global optimization in surface reconstruction from an oriented point cloud. *Computer-Aided Design*, *43*(8), 896-901 0010-4485.
- Pan, W., & Ning, Y. (2014). Dialectics of sustainable building: Evidence from empirical studies 1987–2013. *Building and Environment*, *82*, 666-674 0360-1323.
- Paukkeri, M.-S., García-Plaza, A. P., Fresno, V., Unanue, R. M., & Honkela, T. (2012). Learning a taxonomy from a set of text documents. *Applied Soft Computing*, *12*(3), 1138-1148.
- Pawlyn, M. (2019). *Biomimicry in architecture*: Routledge.
- Pedrocchi, N., Villagrossi, E., Vicentini, F., & Tosatti, L. M. (2014). *Robot-dynamic calibration improvement by local identification*. Paper presented at the Robotics and Automation (ICRA), 2014 IEEE International Conference on.
- Phaal, R., Farrukh, C. J. P., & Probert, D. R. (2004). A framework for supporting the management of technological knowledge. *International Journal of Technology Management*, *27*(1), 1-15 0267-5730.
- Pham, H., Adorno, B., Perdereau, V., & Fraise, P. (2017). Set-point control of robot end-effector pose using dual quaternion feedback. *Robotics and Computer-Integrated Manufacturing*.
- Piegl, L. (1989a). Modifying the shape of rational B-splines. part 1: curves. *Computer-Aided Design*, *21*(8), 509-518 0010-4485.
- Piegl, L. (1989b). Modifying the shape of rational B-splines. part 2: surfaces. *Computer-Aided Design*, *21*(9), 538-546 0010-4485.
- Piegl, L., & Tiller, W. (1996). *The NURBS book*: Springer Science & Business Media.
- Pigram, D., & McGee, W. (2011). Formation Embedded Design: A methodology for the integration of fabrication constraints into architectural design.

- Poinet, P., Nicholas, P., Tamke, M., & Thomsen, M. R. (2016). *Multi-scalar modelling for free-form timber structures*.
- Pons, O., & Aguado, A. (2012). Integrated value model for sustainable assessment applied to technologies used to build schools in Catalonia, Spain. *Building and Environment*, *53*, 49-58 0360-1323.
- Popovic, D. (2018). *Off-site manufacturing systems development in timber house building: Towards mass customization-oriented manufacturing*. Jönköping University, School of Engineering,
- Pottmann, H. (2007). *Architectural geometry* (Vol. 10 193449304X): Bentley Institute Press.
- Pottmann, H., Eigensatz, M., Vaxman, A., & Wallner, J. (2015). Architectural geometry. *Computers & graphics*, *47*, 145-164 0097-8493.
- Presley, A., & Meade, L. (2010). Benchmarking for sustainability: an application to the sustainable construction industry. *Benchmarking: an international Journal* 1463-5771.
- Qian, Z. C. (2009). *Design patterns: augmenting design practice in parametric CAD systems*. School of Interactive Arts & Technology-Simon Fraser University,
- Queiroz, N., Dantas, N., Nome, C., & Vaz, C. (2015). *Designing a Building envelope using parametric and algorithmic processes*.
- Rad, A. R., Burton, H., Rogeau, N., Vestartas, P., & Weinand, Y. (2021). A framework to automate the design of digitally-fabricated timber plate structures. *Computers & Structures*, *244*, 106456 100045-107949.
- Radford, A. D., & Gero, J. S. (1980). Tradeoff diagrams for the integrated design of the physical environment in buildings. *Building and environment*, *15*(1), 3-15.
- Radkau, J. (2012). *Wood: a history*: Polity.
- Ramage, M. H., Burrige, H., Busse-Wicher, M., Fereday, G., Reynolds, T., Shah, D. U., . . . Densley-Tingley, D. (2017). The wood from the trees: The use of timber in construction. *Renewable and Sustainable Energy Reviews*, *68*, 333-359 1364-0321.
- Rasch, B., & Otto, F. (1996). Finding Form. In: Axel Menges.
- Reap, J., Baumeister, D., & Bras, B. (2005). *Holism, biomimicry and sustainable engineering*.
- Reddi, S., Jain, A. K., Yun, H.-B., & Reddi, L. N. (2012). Biomimetics of stabilized earth construction: Challenges and opportunities. *Energy and Buildings*, *55*, 452-458 0378-7788.
- Reinhardt, D., Saunders, R., & Burry, J. (2016). *Robotic fabrication in architecture, art and design 2016*: Springer.
- Renner, G., & Ekárt, A. (2003). Genetic algorithms in computer aided design. *Computer-Aided Design*, *35*(8), 709-726 0010-4485.
- Rian, I. M., & Asayama, S. (2016). Computational Design of a nature-inspired architectural structure using the concepts of self-similar and random fractals. *Automation in Construction*, *66*, 43-58 0926-5805.
- Rian, I. M., & Sassone, M. (2014). Tree-inspired dendriforms and fractal-like branching structures in architecture: A brief historical overview. *Frontiers of Architectural Research*, *3*(3), 298-323 2095-2635.
- Rian, I. M., Sassone, M., & Asayama, S. (2018). From fractal geometry to architecture: Designing a grid-shell-like structure using the Takagi–Landsberg surface. *Computer-Aided Design*, *98*, 40-53 0010-4485.
- Robeller, C. (2015). Integral mechanical attachment for timber folded plate structures. In: EPFL.
- Robeller, C., Gamarro, J., & Weinand, Y. (2017). Théâtre vidy lausanne—a double-layered timber folded plate structure. *journal of the International Association for Shell and Spatial Structures*, *58*(4), 295-314 1028-1365X.
- Robeller, C., Konakovic, M. A., Dedijer, M., Pauly, M., & Weinand, Y. (2016). A double-layered timber plate shell-computational methods for assembly, prefabrication, and structural design. *Advances in Architectural Geometry 2016*, *5*(CONF), 104-122 3728137782.
- Robeller, C., Stitic, A., Mayencourt, P., & Weinand, Y. (2015). Interlocking folded plate: integrated mechanical attachment for structural wood panels. In *Advances in architectural geometry 2014* (pp. 281-294): Springer.
- Robeller, C., & Weinand, Y. (2016). Fabrication-aware design of timber folded plate shells with double through tenon joints. In *Robotic fabrication in architecture, art and design 2016* (pp. 166-177): Springer.
- Roche, S., Gamarro, J., & Weinand, Y. (2016). *Multiple tab-and-slot joint: Improvement of the rotational stiffness for the connection of thin structural wood panels*.

- Rohden, A. B., & Garcez, M. R. (2018). Increasing the sustainability potential of a reinforced concrete building through design strategies: Case study. *Case Studies in Construction Materials*, 9, e00174 02214-05095.
- Rosenfeld, B. A. (2012). *A history of non-Euclidean geometry: evolution of the concept of a geometric space* (Vol. 12 1441986804): Springer Science & Business Media.
- Rossin, K. J. (2010). Biomimicry: nature's design process versus the designer's process. *WIT Transactions on Ecology and the Environment*, 138, 559-570 1845644549.
- Roveda, L., Iannacci, N., Vicentini, F., Pedrocchi, N., Braghin, F., & Tosatti, L. M. (2016). Optimal impedance force-tracking control design with impact formulation for interaction tasks. *IEEE Robotics and Automation Letters*, 1(1), 130-136.
- Roy, R. (2013). Exploring the boundary conditions of disruption: large firms and new product introduction with a potentially disruptive technology in the industrial robotics industry. *IEEE Transactions on Engineering Management*, 61(1), 90-100 0018-9391.
- Russell, S., & Norvig, P. (2002). *Artificial intelligence: a modern approach*.
- Ryan, P. J. (1986). *Euclidean and non-Euclidean geometry: an analytic approach*: Cambridge university press.
- Salazar, J., & Meil, J. (2009). Prospects for carbon-neutral housing: the influence of greater wood use on the carbon footprint of a single-family residence. *Journal of Cleaner Production*, 17(17), 1563-1571 0959-6526.
- Salman, M., Mansor, A., & Pinang, S. P. S. P. (2006). Free-Form Surface Models Generation Using Reverse Engineering Technique-An Investigation.
- Salvadori, M. (2015). Can There Be Any Relationships Between Mathematics and Architecture? In *Architecture and Mathematics from Antiquity to the Future* (pp. 25-29): Springer.
- Sanchez-Reyes, J. (1997). A simple technique for NURBS shape modification. *IEEE Computer Graphics and Applications*, 17(1), 52-59 0272-1716.
- Sánchez-Sánchez, J., Pallarés, F. E., & Rodríguez-León, M. T. (2014). Reciprocal tree-like fractal structures. *Nexus Network Journal*, 16(1), 135-150 1522-4600.
- Santolaria, J., & Ginés, M. (2013). Uncertainty estimation in robot kinematic calibration. *Robotics and Computer-Integrated Manufacturing*, 29(2), 370-384 0736-5845.
- Sarfraz, M., Raza, S. A., & Baig, M. H. (2005). *Computing optimized curves with NURBS using evolutionary intelligence*.
- Saridakis, K. M., & Dentsoras, A. J. (2006). Integration of fuzzy logic, genetic algorithms and neural networks in collaborative parametric design. *Advanced Engineering Informatics*, 20(4), 379-399 1474-0346.
- Sauer, R. (1970). *Differenzgeometrie*: Springer.
- Scheer, D. R. (2014). *The death of drawing: architecture in the age of simulation*: Routledge.
- Scheible, F., & Dimcic, M. (2011). *Parametric Engineering Everything is Possible*.
- Scheurer, F., Schindler, C., & Braach, M. (2005). *From design to production: Three complex structures materialised in wood*.
- Schober, K.-U., Drass, M., & Becker, W. (2013). *Adhesive strength of timber joints with unconventional glued-in steel rods*.
- Schober, K.-U., & Tannert, T. (2016). Hybrid connections for timber structures. *European Journal of Wood and Wood Products*, 74(3), 369-377 0018-3768.
- Schodek, D. L. (2005). *Digital design and manufacturing*.
- Schumacher, P. (2008). Parametricism as style-Parametricist manifesto. *11th Architecture Biennale, Venice*, 14.
- Schumacher, P. (2016). *Parametricism 2.0: Rethinking Architecture's Agenda for the 21st Century*: John Wiley & Sons.
- Schwinn, T., Krieg, O. D., & Menges, A. (2013). Robotically fabricated wood plate morphologies. In *Rob/Arch 2012* (pp. 48-61): Springer.
- Schwinn, T., Krieg, O. D., & Menges, A. (2014). Behavioral strategies: synthesizing design computation and robotic fabrication of lightweight timber plate structures.
- Schwinn, T., Krieg, O. D., & Menges, A. (2016). Robotic sewing: A textile approach towards the computational design and fabrication of lightweight timber shells.
- Sebe, N., Cohen, I., Garg, A., & Huang, T. S. (2005). *Machine learning in computer vision* (Vol. 29 1402032749): Springer Science & Business Media.
- Seraphin, M. (2003). *On the origin of modern timber engineering*.
- Shelden, D. R. (2002). *Digital surface representation and the constructibility of Gehry's architecture*. Massachusetts Institute of Technology,

- Siciliano, B., Sciavicco, L., Villani, L., & Oriolo, G. (2010). *Robotics: modelling, planning and control*: Springer Science & Business Media.
- Sjoberg, C., Beorkrem, C., & Ellinger, J. (2017). Emergent Syntax: Machine Learning for the Curation of Design Solution Space.
- Son, H., Kim, C., Kim, H., Han, S. H., & Kim, M. K. (2010). Trend analysis of research and development on automation and robotics technology in the construction industry. *KSCE Journal of Civil Engineering*, 14(2), 131-139 1226-7988.
- Spong, M. W., Hutchinson, S., & Vidyasagar, M. (2006). *Robot modeling and control* (Vol. 3): Wiley New York.
- Ståhl, M., Granström, K., Berghel, J., & Renström, R. (2004). Industrial processes for biomass drying and their effects on the quality properties of wood pellets. *Biomass and Bioenergy*, 27(6), 621-628 0961-9534.
- Struková, Z., & Liška, M. (2012). Application of automation and robotics in construction work execution. *AD ALTA: Journal of Interdisciplinary Research*, 2(2), 121-125.
- Sugiarto, I., & Conradt, J. (2017). A model-based approach to robot kinematics and control using discrete factor graphs with belief propagation. *Robotics and Autonomous Systems*, 91, 234-246.
- Svilans, T., Poinet, P., Tamke, M., & Thomsen, M. R. (2018). A multi-scalar approach for the modelling and fabrication of free-form glue-laminated timber structures. In *Humanizing Digital Reality* (pp. 247-257): Springer.
- Svilans, T., Tamke, M., Thomsen, M. R., Runberger, J., Strehlke, K., & Antemann, M. (2019). New workflows for digital timber. In *Digital Wood Design* (pp. 93-134): Springer.
- Tamke, M., Nicholas, P., & Zwierzycki, M. (2018). Machine learning for architectural design: Practices and infrastructure. *International Journal of Architectural Computing*, 16(2), 123-143 1478-0771.
- Technologies, A. C. F. o. A. M., & Terminology, A. C. F. o. A. M. T. S. F. o. (2012). *Standard Terminology for Additive Manufacturing Technologies*: ASTM International.
- Tenu, V. (2009). *Minimal surfaces as self-organizing systems: a particle-spring system simulation for generating triply periodic minimal surface tensegrity structure*. UCL (University College London),
- Terzidis, K. (2004). algorithmic design: A Paradigm Shift in Architecture?
- Terzopoulos, D., & Qin, H. (1994). Dynamic NURBS with geometric constraints for interactive sculpting. *ACM Transactions on Graphics (TOG)*, 13(2), 103-136 0730-0301.
- Tessmann, O., & Rossi, A. (2019). Geometry as Interface: Parametric and Combinatorial Topological Interlocking Assemblies. *Journal of Applied Mechanics*, 86(11 0021-8936).
- Thurston, W. P. (1997). *Three-dimensional geometry and topology*: Princeton university press.
- Tian, L., & Collins, C. (2004). An effective robot trajectory planning method using a genetic algorithm. *Mechatronics*, 14(5), 455-470.
- Tlustochowicz, G., Serrano, E., & Steiger, R. (2011). State-of-the-art review on timber connections with glued-in steel rods. *Materials and structures*, 44(5), 997-1020 1871-6873.
- Tolszczuk-Leclerc, Z., Bernier-Lavigne, S., Salenikovich, A., & Potvin, A. (2016). *Design process of a free-form structure using CLT panels—Analysis of an architectural large scale structure*.
- Turing, A. M. (2009). Computing machinery and intelligence. In *Parsing the turing test* (pp. 23-65): Springer.
- Turlock, M., & Steinfeld, K. (2019). *Necessary Tension*.
- Turner, J. S., & Soar, R. C. (2008). *Beyond biomimicry: What termites can tell us about realizing the living building*.
- Turrin, M., Von Buelow, P., & Stouffs, R. (2011). Design explorations of performance driven geometry in architectural design using parametric modeling and genetic algorithms. *Advanced Engineering Informatics*, 25(4), 656-675 1474-0346.
- Tušar, T., & Filipič, B. (2014). Visualization of Pareto front approximations in evolutionary multiobjective optimization: A critical review and the prosection method. *IEEE Transactions on Evolutionary Computation*, 19(2), 225-245.
- Vallée, T., Tannert, T., & Hehl, S. (2011). Experimental and numerical investigations on full-scale adhesively bonded timber trusses. *Materials and structures*, 44(10), 1745-1758 1871-6873.
- Vallée, T., Tannert, T., Meena, R., & Hehl, S. (2013). Dimensioning method for bolted, adhesively bonded, and hybrid joints involving Fibre-Reinforced-Polymers. *Composites Part B: Engineering*, 46, 179-187 1359-8368.
- Van der Zee, A., & De Vries, B. (2008). *Design by computation*.
- van Gassel, F. J. M. (1993). *Design of a machine which rotates hoist elements around its vertical axis*.

- Van Kaick, O., Zhang, H., Hamarneh, G., & Cohen - Or, D. (2011). *A survey on shape correspondence*.
- Vattam, S. S., Helms, M. E., & Goel, A. K. (2008). Compound analogical design: interaction between problem decomposition and analogical transfer in biologically inspired design. In *Design computing and cognition'08* (pp. 377-396): Springer.
- Vercruyssen, E., Mollica, Z., & Devadass, P. (2018). *Altered behaviour: the performative nature of manufacture Chainsaw Choreographies+ Bandsaw Manoeuvres*.
- Versprille, K. J. (1975). Computer-aided design applications of the rational B-spline approximation form.
- Vesanto, J., & Alhoniemi, E. (2000). Clustering of the self-organizing map. *IEEE Transactions on neural networks*, 11(3), 586-600.
- Villagrossi, E., Simoni, L., Beschi, M., Pedrocchi, N., Marini, A., Tosatti, L. M., & Visioli, A. (2018). A virtual force sensor for interaction tasks with conventional industrial robots. *Mechatronics*, 50, 78-86.
- Vincent, J. F. V., Bogatyreva, O. A., Bogatyrev, N. R., Bowyer, A., & Pahl, A.-K. (2006). Biomimetics: its practice and theory. *Journal of the Royal Society Interface*, 3(9), 471-482 1742-5689.
- Wagner, H. J., Alvarez, M., Groenewolt, A., & Menges, A. (2020). Towards digital automation flexibility in large-scale timber construction: integrative robotic prefabrication and co-design of the BUGA Wood Pavilion. *Construction Robotics*, 4(3), 187-204 2509-8780.
- Wagner, H. J., Alvarez, M., Kyjaneck, O., Bhiri, Z., Buck, M., & Menges, A. (2020). Flexible and transportable robotic timber construction platform—TIM. *Automation in Construction*, 120, 103400 100926-105805.
- Wagner, T., Michelitsch, T., & Sacharow, A. (2007). *On the design of optimisers for surface reconstruction*.
- Walker, J. C. F. (2006). *Primary wood processing: principles and practice*: Springer Science & Business Media.
- Wallner, J., & Pottmann, H. (2011). Geometric computing for freeform architecture. *Journal of Mathematics in Industry*, 1(1), 1-19 2190-5983.
- Wallner, J., Schiftner, A., Kilian, M., Flöry, S., Höbinger, M., Deng, B., . . . Pottmann, H. (2010). Tiling freeform shapes with straight panels: Algorithmic methods. *Advances in architectural geometry*, 2010, 73-86.
- Wang, J. (2001). Ranking engineering design concepts using a fuzzy outranking preference model. *Fuzzy sets and systems*, 119(1), 161-170 0165-0114.
- Wang, J. (2002). Improved engineering design concept selection using fuzzy sets. *International Journal of Computer Integrated Manufacturing*, 15(1), 18-27 0951-0192X.
- Wang, Q.-s., Ye, J., Wu, H., Gao, B.-q., & Shepherd, P. (2019). A triangular grid generation and optimization framework for the design of free-form gridshells. *Computer-Aided Design*, 113, 96-113 0010-4485.
- Wang, W., Zmeureanu, R., & Rivard, H. (2005). Applying multi-objective genetic algorithms in green building design optimization. *Building and Environment*, 40(11), 1512-1525 0360-1323.
- Weinan, E. (2011). *Principles of multiscale modeling*: Cambridge University Press.
- Weinand, Y. (2009). Innovative timber constructions. *Journal of the International Association for Shell and Spatial Structures*, 50(2), 111-120 1028-1365X.
- Weinand, Y., & Hudert, M. (2010). Timberfabric: Applying textile principles on a building scale. *Architectural design*, 80(4), 102-107 0003-8504.
- Weizmann, M., Amir, O., & Grobman, Y. J. (2016). Topological interlocking in buildings: A case for the design and construction of floors. *Automation in Construction*, 72, 18-25 0926-5805.
- Weyer, S., Schmitt, M., Ohmer, M., & Gorecky, D. (2015). Towards Industry 4.0-Standardization as the crucial challenge for highly modular, multi-vendor production systems. *Ifac-Papersonline*, 48(3), 579-584 2405-8963.
- Wibranek, B., Wietschorke, L., Glatzer, T., & Tessmann, O. (2020). Sequential Modular Assembly-Robotic Assembly of Cantilevering Structures through Differentiated Load Modules.
- Willette, A., Brell-Cokcan, S., & Braumann, J. (2014). *Robotic fabrication in architecture, art and design 2014*: Springer.
- Williams, C. (2013). *Origins of Form: The Shape of Natural and Man-made Things—Why They Came to Be the Way They Are and How They Change*: Architectural Book Publishing.
- Williams, N., & Cherrey, J. (2016). Crafting robustness: Rapidly fabricating ruled surface acoustic panels. In *Robotic fabrication in architecture, art and design 2016* (pp. 294-303): Springer.

- Willmann, J., Block, P., Hutter, M., Byrne, K., & Schork, T. (2018). *Robotic Fabrication in Architecture, Art and Design 2018: Foreword by Sigrid Brell-Çokcan and Johannes Braumann, Association for Robots in Architecture*: Springer.
- Willmann, J., Gramazio, F., Kohler, M., & Langenberg, S. (2013). Digital by material. In *Rob/ Arch 2012* (pp. 12-27): Springer.
- Willmann, J., Knauss, M., Bonwetsch, T., Apolinarska, A. A., Gramazio, F., & Kohler, M. (2016). Robotic timber construction—Expanding additive fabrication to new dimensions. *Automation in construction*, *61*, 16-23 0926-5805.
- Wolfram, S. (2002). *A new kind of science* (Vol. 5): Wolfram media Champaign, IL.
- Woodbury, R. (2010). Elements of parametric design.
- Wortmann, T., & Tunçer, B. (2017). Differentiating parametric design: Digital workflows in contemporary architecture and construction. *Design Studies*, *52*, 173-197 0142-0694X.
- Wu, J., Zhang, C., Xue, T., Freeman, W. T., & Tenenbaum, J. B. (2016). Learning a probabilistic latent space of object shapes via 3d generative-adversarial modeling. *arXiv preprint arXiv:1610.07584*.
- Wu, Y., Klimchik, A., Caro, S., Furet, B., & Pashkevich, A. (2015). Geometric calibration of industrial robots using enhanced partial pose measurements and design of experiments. *Robotics and Computer-Integrated Manufacturing*, *35*, 151-168.
- Xie, W.-C., Zou, X.-F., Yang, J.-D., & Yang, J.-B. (2012). Iteration and optimization scheme for the reconstruction of 3D surfaces based on non-uniform rational B-splines. *Computer-Aided Design*, *44*(11), 1127-1140 0010-4485.
- Xu, R., & Wunsch, D. (2005). Survey of clustering algorithms. *IEEE Transactions on neural networks*, *16*(3), 645-678.
- Yang, X., Wu, H., Li, Y., & Chen, B. (2017). A dual quaternion solution to the forward kinematics of a class of six-DOF parallel robots with full or reductant actuation. *Mechanism and Machine Theory*, *107*, 27-36.
- Yang, Y., Pan, M., & Pan, W. (2019). ‘Co-evolution through interaction’ of innovative building technologies: The case of modular integrated construction and robotics. *Automation in Construction*, *107*, 102932 100926-105805.
- Yetkin, O., & Göneng Sorguç, A. (2019). Design Space Exploration of Initial Structural Design Alternatives via Artificial Neural Networks.
- Yin, X., & Pan, L. (2018). Enhancing trajectory tracking accuracy for industrial robot with robust adaptive control. *Robotics and Computer-Integrated Manufacturing*, *51*, 97-102.
- Yu, C., & Xi, J. (2018). Simultaneous and on-line calibration of a robot-based inspecting system. *Robotics and Computer-Integrated Manufacturing*, *49*, 349-360. doi:10.1016/j.rcim.2017.08.006
- Yu, R., Gero, J. S., Ikeda, Y., Herr, C. M., Holzer, D., Kaijima, S., . . . Schnabel, A. (2015). *An empirical foundation for design patterns in parametric design*.
- Yuan, Y., Yu, X., Yang, X., Xiao, Y., Xiang, B., & Wang, Y. (2017). Bionic building energy efficiency and bionic green architecture: A review. *Renewable and Sustainable Energy Reviews*, *74*, 771-787 1364-0321.
- Zacharia, P. T., & Aspragathos, N. (2005). Optimal robot task scheduling based on genetic algorithms. *Robotics and Computer-Integrated Manufacturing*, *21*(1), 67-79.
- Zacharia, P. T., Xidias, E. K., & Aspragathos, N. A. (2013). Task scheduling and motion planning for an industrial manipulator. *Robotics and Computer-Integrated Manufacturing*, *29*(6), 449-462.
- Zadavec, M., Schiffner, A., & Wallner, J. (2010). *Designing quad - dominant meshes with planar faces*.
- Zäh, M. F., Beetz, M., Shea, K., Reinhart, G., Bender, K., Lau, C., . . . Engelhard, M. (2009). The cognitive factory. In *Changeable and reconfigurable manufacturing systems* (pp. 355-371): Springer.
- Zapata, P., & Gambatese, J. A. (2005). Energy consumption of asphalt and reinforced concrete pavement materials and construction. *Journal of infrastructure systems*, *11*(1), 9-20 1076-0342.
- Zari, M. P. (2007). *Biomimetic approaches to architectural design for increased sustainability*.
- Zari, M. P. (2010). Biomimetic design for climate change adaptation and mitigation. *Architectural Science Review*, *53*(2), 172-183 0003-8628.
- Zavoleas, Y., & Taylor, M. (2019). From Cartesian to Topological Geometry: Challenging Flatness in Architecture. *Nexus Network Journal*, *21*(1), 5-18 1522-4600.
- Zboinska, M. A. (2015). Hybrid CAD/E platform supporting exploratory architectural design. *Computer-Aided Design*, *59*, 64-84 0010-4485.

- Zhang, Q., Yang, X., Li, P., Huang, G., Feng, S., Shen, C., . . . Xu, F. (2015). Bioinspired engineering of honeycomb structure—Using nature to inspire human innovation. *Progress in Materials Science*, 74, 332-400 0079-6425.
- Zhang, X., Wang, J., Yamazaki, K., & Mori, M. (2004). A surface based approach to recognition of geometric features for quality freeform surface machining. *Computer-Aided Design*, 36(8), 735-744 0010-4485.
- Zhao, J., Zhao, X., Jiang, Z., Li, Z., Fan, X., Zhu, J., . . . Pan, F. (2014). Biomimetic and bioinspired membranes: Preparation and application. *Progress in polymer science*, 39(9), 1668-1720 0079-6700.
- Zhao, Z.-Y., Zhao, X.-J., Davidson, K., & Zuo, J. (2012). A corporate social responsibility indicator system for construction enterprises. *Journal of Cleaner Production*, 29, 277-289 0959-6526.
- Zheng, H. (2019). *Form Finding and Evaluating Through Machine Learning: The Prediction of Personal Design Preference in Polyhedral Structures*.
- Zheng, H., Moosavi, V., & Akbarzadeh, M. (2020). Machine learning assisted evaluations in structural design and construction. *Automation in Construction*, 119, 103346 100926-105805.
- Zhu, J.-Y., Park, T., Isola, P., & Efros, A. A. (2017). *Unpaired image-to-image translation using cycle-consistent adversarial networks*.
- Zobel, B. J., & Van Buijtenen, J. P. (2012). *Wood variation: its causes and control*: Springer Science & Business Media.